

Electronic Thesis and Dissertation Repository

12-14-2020 2:00 PM

Geometallurgy and Gold Mineralization of the Monument Bay Project, Stull Lake Greenstone Belt, Manitoba, Canada

Chunyi Hao, *The University of Western Ontario*

Supervisor: Banerjee, Neil R., *The University of Western Ontario*

Co-Supervisor: Van Loon, Lisa L., *The University of Western Ontario*

A thesis submitted in partial fulfillment of the requirements for the Master of Science degree in Geology

© Chunyi Hao 2020

Follow this and additional works at: <https://ir.lib.uwo.ca/etd>



Part of the [Geochemistry Commons](#), and the [Geology Commons](#)

Recommended Citation

Hao, Chunyi, "Geometallurgy and Gold Mineralization of the Monument Bay Project, Stull Lake Greenstone Belt, Manitoba, Canada" (2020). *Electronic Thesis and Dissertation Repository*. 7524.
<https://ir.lib.uwo.ca/etd/7524>

This Dissertation/Thesis is brought to you for free and open access by Scholarship@Western. It has been accepted for inclusion in Electronic Thesis and Dissertation Repository by an authorized administrator of Scholarship@Western. For more information, please contact wlsadmin@uwo.ca.

Abstract

The Monument Bay Project is located in the Archean Stull Lake Greenstone Belt, in Northern Manitoba, Canada. This thesis focuses on the geometallurgy and gold mineralization of the Monument Bay Deposit in order to better understand the multiple gold mineralizing events and provide a pathfinder to gold mineralization. Traditional microscopy is used in combination with geochemical and mineralogical analytical techniques (Electron Probe Microanalysis (EPMA) and Energy-dispersive X-ray Spectroscopy (EDS)/(WDS) element map) and synchrotron geochemical techniques (synchrotron X-ray Diffraction (SR-XRD), synchrotron micro X-ray fluorescence (SR- μ XRF) mapping, X-ray Absorption Near-edge Structure (XANES) Spectroscopy). Metallic gold (Au^0) exists as free gold and inclusion gold, and no refractory gold (Au^{+1}) has been found in the selected samples. As^{-1} , which is the non-toxic form of arsenic, occurs in arsenopyrite and is the only form of arsenic in the samples. Free gold and inclusion gold have been found in porphyritic dacite and metasediments. Only free gold exhibit in metavolcanic rocks. Microscopic gold distribution is related to sulphide morphology. There is evidence for four sulphide generations identified from microscopy and EDS/WDS element maps: I. Arsenopyrite 1 (Apy_1); II. Pyrite 1 (Py_1) and Arsenopyrite 2 (Apy_2); III. Chalcopyrite (Ccp), Galena (Gn), and Sphalerite (Sp); IV. Pyrite 2 (Py_2) and Arsenopyrite 3 (Apy_3). The various Au/Ag and Au/Sb ratios identified using EDS point analysis suggest an episode of Au remobilization during sulphide formation because of changes in temperature and pressure. The spatial distribution of different types of sulphides in different veining events suggests there were three main gold mineralizing events. The majority of the gold was deposited as metallic gold in episode II. This information is being applied by Yamana to understand the multi-episodic fluid history and environmental characterization of the Monument Bay project and will lead to a better understanding of the mineralogical expression of gold mineralization and geometallurgy at the Monument Bay Project.

Keywords

Monument Bay Project, Stull Lake Greenstone Belt, gold mineralization, sulphide morphology, sulphide generations, arsenic and gold speciation

Summary for Lay Audience

Because of the appearance and properties of gold, it is a store of value and widely used in various fields, like technology, manufacturing, jewellery, and investment. The main source of gold supply is mine production. Canada has a rich gold endowment and was the fifth largest producer of gold worldwide in 2019. Orogenic gold deposits make up 35% of world gold production and are the most typical gold deposit type in Canada. One such deposit is the Monument Bay Project which is located in northeastern Manitoba.

Nowadays, more and more geoscientists are trying to apply new techniques to be more efficient and effective at exploration in order to locate gold deposits and figure out how gold formed. Synchrotron X-ray technology is one of the cutting-edged techniques. Although this technique is well established in environmental sciences, the applications for mineral exploration and production are underdeveloped. This research combines traditional geological methods with innovative synchrotron techniques to enhance the understanding of the gold formation, type, location, and distribution of possible toxic elements in rocks.

Generally, gold is strongly associated with sulphides in orogenic gold deposits. The typical and common sulphides are pyrite and arsenopyrite. The characteristics and distribution of sulphids can reflect the history of gold formation. Apart from that, Au presents as metallic gold (Au^0) and refractory gold (Au^{+1}) in gold deposits. Metallic gold is easier to extract, and the process is more environmentally friendly. But the refractory gold is the opposite. Arsenic has three possible oxidation states: -1, +3, and +5. -1 and +5 are not toxic, but +3 is toxic and harmful to the environment. As a result, confirming the types of gold and arsenic is important in making decision on looking for gold and producing gold.

Acknowledgments

I would like to thank the following people, without whom I would not have completed my master's degree in this uncertain COVID-19 pandemic time!

Firstly, I would like to give my sincerest and deepest thanks to my supervisor Dr. Neil R. Banerjee and my co-supervisor Dr. Lisa L. Van Loon. Thank you to them to provide this great opportunity so that I could come to Canada to do my master's and take this scientific adventure at Western University. Their enthusiasm and insightful suggestions were invaluable to my success in this research and encourage me to keep the passion of being a professional geologist in the future.

I would like to thank Yamana Gold Inc. for its financial and technical support. Thank you to the geologists from the Monument Bay Project, Duncan Mackay, Hannah Cavallin, Duncan McBean, Richard Mann, Katie Turner for sharing your knowledge, providing insightful rock and geology information and dataset, and giving me invaluable feedback on my research.

I would like to thank the generous assistance of the beamline technicians and Western technicians. I gave my thanks to Renfei Feng and Peter Blanchard from VEPSERS Beamline at the Canadian Light Source (CLS), Zou Finfrock and Debora Motta Meira from the 20ID Beamline at the Advanced Photon Source (APS), and Evan R. Maxey from the 8BM Beamline at the APS for support in conducting the synchrotron experiments in the past two years. Thank you to Marc Beauchamp for sharing his knowledge and assistance with EPMA.

I would like to thank all my amazing teammates in Banerjee Research Team (Juliana, Zohreh, Ramjay, Claire, and James). Your enthusiasm, hard-working, knowledge, and support helped me to overcome all the difficulties in my research.

I would like to give my biggest thanks to my family and my friends both in China and Canada. Thank you to my parents Yu Hao and Xia Wang for your unconditional love, encouragement, and support all the time, even though we have a thirteen-hour time difference. I would like to thank my father for giving me insightful opinions as an experienced geologist. I am so grateful we had a lot of opinions and knowledge to discuss and share with each other because of

geology. I would like to thank my peers, classmates, mentors, and friends in Canada. Thank you for sharing knowledge, support, friendship, and kindness, which make my experience at Western University to be memorable. I am looking forward to seeing you again in industry and conferences in the future.

Table of Contents

Abstract	ii
Summary for Lay Audience	iii
Acknowledgments	iv
Table of Contents	vi
List of Tables	ix
List of Figures	x
List of Appendices	xx
Chapter 1	1
1 Introduction	1
1.1 Project Scope	1
1.2 Archean Orogenic Gold Deposits	2
1.3 Sulphide Geochemistry	6
1.4 Gold Solubility and Speciation	7
1.5 Arsenic Solubility and Speciation	7
1.6 Synchrotron Radiation (SR)	8
1.6.1 Application of Synchrotron Radiation Technology	10
Chapter 2	12
2 Regional and Local Geology	12
2.1 The Superior Province	12
2.2 Stull Lake Greenstone Belt	16
2.3 Study Area	17
2.3.1 Location	17
2.3.2 Exploration and Research History	18

2.3.3	Geology and Deposit Type	19
2.3.4	Mineralization	21
2.3.5	Metallurgy	22
Chapter 3	23
3	Methods	23
3.1	Sampling Program	23
3.2	Optical Microscopy	26
3.3	Synchrotron X-ray Diffraction (SR-XRD)	27
3.3.1	SR-XRD Sample Preparation	28
3.3.2	Experiment Setup and Remote-Controlled Data collection at the CMCF	29
3.3.3	SR-XRD Data Processing	33
3.4	Synchrotron Micro X-Ray Fluorescence (SR- μ XRF) mapping	33
3.4.1	SR-XRF Sample Preparation	34
3.4.2	SR-XRF Data Collection	34
3.4.3	SR- μ XRF Mapping Data Processing	43
3.5	X-ray Absorption Near-edge Structure (XANES) Spectroscopy	47
3.5.1	Micro-XANES Spectroscopy	48
3.5.2	Bulk-XANES Spectroscopy	49
3.5.3	Data Processing and Interpretation	50
3.6	Electron Probe Micro-Analysis (EPMA)	51
Chapter 4	53
4	Results	53
4.1	Petrology	53
4.1.1	Porphyritic Dacite	53
4.1.2	Metavolcanic Rocks	57
4.1.3	Metasedimentary Rocks	60

4.2	Synchrotron X-ray Diffraction.....	64
4.3	Synchrotron Micro X-Ray Fluorescence (SR- μ XRF) mapping	69
4.3.1	Porphyritic Dacite	70
4.3.2	Intermediate Metatuff	73
4.3.3	Felsic Metatuff	74
4.3.4	Metasediment	77
4.4	X-ray Absorption Near-edge Structure (XANES) Spectroscopy	80
4.5	Electron Probe Micro-Analysis (EPMA).....	84
4.5.1	Energy-dispersive X-ray spectroscopy (EDS) point analysis.....	85
4.5.2	EDS/WDS Element Mapping	89
	Chapter 5.....	91
5	Discussion	91
5.1	Element Distribution and Mineral Distribution	91
5.2	Sulphide Morphology and Gold Distribution	95
5.3	Arsenic and Gold Speciation	104
	Chapter 6.....	107
6	Conclusion	107
	References.....	109
	Appendices.....	119
	Curriculum Vitae	396

List of Tables

Table 3-1. High Gold Grade Drill Core Sample Selection at the Monument Bay Project	25
Table 3-2. SR- μ XRF Mapping Data Collection	36
Table 3-3. Parameters for SR-XRF Mapping (Beam energy was set to allow excitation of elements of interest).....	38
Table 3-4. XANES Data Collection.....	47
Table 3-5. Sample analysis parameters for XANES.....	49
Table 4-1 Petrology of Different Rock Types	53
Table 4-2. Synchrotron X-ray Diffraction Data collected at CMCF Beamline, CLS.....	67
Table 4-3. EPMA Dataset of the Monument Bay Project	84
Table 5-1. Summary of the sulphide morphology, microscopic gold, and locations at the Monument Bay Project	97

List of Figures

- Figure 1-1. Map illustrating the orogenic gold deposit distribution in the gold metallogenic provinces in North America, including the age of the crust (Modified after Goldfarb et al., 2001). 3
- Figure 1-2. Schematic illustrating three types of orogenic gold deposits formed in various depths and a compressional/transpressional crustal environment. Au transported in the fluid along with the fractures in faults and shear zone, and deposited when temperature and pressure changed. The mineralization is continuously from granulite facies to prehnite-pumpellyite facies (modified after Gebre-Mariam et al., 1995; Goldfarb et al., 2001; Goldfarb & Groves, 2015; Groves, 2003; Groves et al., 1998). 4
- Figure 1-3. Schematic planar view of a general synchrotron radiation facility. The arrows show the direction of the beam in a synchrotron radiation facility. The linac is a linear accelerator where the electrons are accelerated. The booster is the place that the electrons gain high energy. The electrons are injected into the circular accelerator, the storage ring after gaining energy. Finally, the electrons are forced to follow the circumference forced by bending magnets and the radiation captured by very narrow beamlines (Balerna and Mobilio, 2015). The storage ring of the Canadian Light Source (CLS) is 170.88m in circumference, while the storage ring of the Advanced Photon Source (APS) is 1104 m in circumference (Advanced Photon Source, 2020; Canadian Light Source, 2020). 9
- Figure 1-4. Schematic of the VESPERS beamline at the CLS (KB –Kirkpatrick-Baez) (Modified from the Canadian Light Source). 10
- Figure 2-1. Mosaic map of the Superior Province illustrating major tectonic elements and gold deposits. Phanerozoic: Ph: Platform Sediments; Proterozoic: Kw: Keweenawan, Th: Trans-Hudson Orogen; Archean: VII: Douglas Harbour Domain, VI: Utsalik Domain, V: Goudalie Domain, IV: L. Minto Domain, II: Tikkerutuk Domain, I: Inukjuak Domain, BS: Bienville Subprovince, LG: La Grande Subprovince, OnS: Opinaca Subprovince, AC: Ashuanipi Complex, OcS: Opatca Subprovince, PT: Pontiac Terrane, AT: Abitibi Terrane, KU: Kapuskasing Uplift, WT: Wawa Terrane, QT: Quetico Terrane, EWT: E. Wabigoon Terrane, WWS: W. Wabigoon Terrane, WRT: Winnipeg R. Terrane, ERT: English R. Terrane, NCS:

North Caribou Superterrane, OSD: Oxford-Stull Domain, NSS: Northern Superior Superterrane, MT: Marmion Terrane, BR: Bird R. Subprovince, MLD: Molson L. Domain, ILD: Island L. Domain. The numbers represent the locations of major mineral districts: 1: Red Lake; 2: Confederation Lake; 3: Sturgeon Lake; 4: Timmins; 5: Kirkland Lake; 6: Cadillac; 7: Noranda; 8: Chibougamau; 9: Casa Berardi; 10: Normémetal. The yellow squares represent gold deposits and the symbol sizes are proportional to deposit size (Modified from Percival, 2007).

..... 14

Figure 2-2. Regional geologic setting and major subdivisions in the Stull Lake–Edmund Lake greenstone belt, Oxford Lake–Stull Lake terrane. The red box shows the location of the Monument Bay Project and Stull Lake Property (Modified from Skulski et al., 2000). 17

Figure 2-3. Regional geology map with major structures and claim outlines of Monument Bay Property and Stull Lake Property (the red box in Figure 2-2). The red stars indicate the geographical distribution of the 7 different targets in the Twin Lakes Deposit..... 18

Figure 3-1. Satellite image of geographical locations of targets and selected samples in the Monument Bay Project. The white points are the new sample section and green points are the previous sample section (modified from Google Earth by Casali and Hao in 2019). 24

Figure 3-2. The Nikon LV100POL microscope mounted with Nikon DS-Ri1 digital camera used for petrographic analysis in the Earth and Planetary Materials Analysis Laboratory at Western University. 27

Figure 3-3. Illustrating SR-XRD sample preparation at Laboratory for Stable Isotope Science at Western University. A. The author was filling powder sample in capillary tubes. B&C. MiTeGen B3S ALS-style reusable bases and SSRL-style sample cassette required at the CMCF for SR-XRD data collection..... 29

Figure 3-4. Showing typical control panel of Setup tab in MxDC remotely controlled via No machine. The Setup is used to set up experiment parameters..... 31

Figure 3-5. The typical experimental setup inside the hutch of CMCF-BM Beamline. A. The robotic arm (1) moves capillary sample and its base from the cassette (2) and mounts it close to the beam (3). B. The capillary sample (4) is examined close to the beam (5). The arrow

shows the direction of beam and the signal is collected by the Rayonix MX300HE CCD X-ray detector (6).....	31
Figure 3-6. Showing typical control panel of Samples tab in MxDC remotely controlled via No machine. The capillary of LaB6_D1_C2 is centering on the left and the sample list was listed on the right in the order of port cord.....	32
Figure 3-7. Showing typical control panel of Data tab in MxDC remotely controlled via No machine. The left side shows a frame of the dataset and the right side shows the data collection settings.	32
Figure 3-8. Experimental station setup in the hutch at APS 20ID beamline. (1) XSP3 four-element detector; (2) Beam Source; (3) Camera; (4) Half drill core samples mounted on the wooden sample holder (February 2019).	39
Figure 3-9. ROI Setup in APS 20ID beamline (February 2019).	40
Figure 3-10. ROI Setup in APS 20ID beamline (July 2019).	40
Figure 3-11. The monitors in experimental hall outside the APS 20ID hutch. The author was using cursor in the top monitor to locate the left bottom corner of a sample and setting up an analysis workflow. The left monitor shows beamline conditions. The middle monitor shows the SR- μ XRF mapping software.....	41
Figure 3-12. The end station setup in the hutch of 8BM-B beamline. (March,2019).	42
Figure 3-13. Offcuts mounted on the sample stage in the hutch of VESPERS at CLS. (February 2019).	43
Figure 3-14. Example of an SR-XRF MCA Spectrum of a metasandstone (2831) showing the peak fitting and relative intensity of the elements. Fe K was used to adjust Max energy. The light green spectrum is the actual raw spectrum. The darker green ones show the fitted element spectrum after peak fitting. The blue one is spectrum of Fe K in the samples. Collected at 20ID Beamline at APS (July 2019).....	44

Figure 3-15. Example of Ar normalization. A. The cursor was used to check the Ar channel at the bottom of the window. In this sample, the Ar channel is 294. B. Ar trace element map before Ar normalization shows the texture of the rock sample because of the uneven surface of the sample C. Ar trace element map after Ar normalization is much smoother with lower relative intensity..... 46

Figure 3-16 A. Illustrating sample preparation for bulk-XANES in Teflon washers in Laboratory for Stable Isotope Science at Western University. B. Well-sealed samples and sample holder before mounting at 20BM beamline, APS. 49

Figure 3-17. Illustrating As K-edge XANES spectrums before (A) and after normalization (B) using Athena. Pre-edge line and post-edge line became relatively horizontal after normalization. The raw data was collected on 2820 offcut at CLS VESPERS Beamline in February 2019. 50

Figure 3-18. The JEOL JXA-8530F field-emission electron microprobe, at the Earth and Planetary Materials Analysis Laboratory, at Western University. 52

Figure 4-1. Photomicrographs of metatuff. Ms=muscovite, Qtz=quartz, Cb=carbonate, Ser=sericite, Fsp=feldspar, Pl=plagioclase, Kfs=K-feldspar, Asp=arsenopyrite, Py=pyrite. A. The groundmass is porphyritic textured with feldspar and quartz phenocrysts. Quartz is recrystallized in the vein and the fine-grained arsenopyrite grains on the edge (2827, XPL, 500 μm). B. Needle arsenopyrite in the quartz vein and the discontinuous very fine muscovite vein crosscut the quartz veins (2824, XPL, 500 μm). C. Fractured subhedral coarse-grained arsenopyrite in the quartz vein with chlorite and carbonate alteration in the groundmass. Quartz recrystallized surrounding the sulphides grains (2841, PPL, 500 μm). D. Corroded medium-grained and euhedral medium to fine-grained arsenopyrite surrounding the plagioclase phenocrysts (2841, RL, 500 μm). E. Coarse-grained fractured arsenopyrite in the middle of the quartz vein and fine-grained arsenopyrite on the edge of the vein (2827, RL, 500 μm). F. Euhedral to subhedral fine-grained needle arsenopyrite in the quartz vein. (2853, RL, 500 μm). 56

Figure 4-2. Photomicrographs of metatuff. Ms=muscovite, Qtz=quartz, Cb=carbonate, Fsp=feldspar, Kfs=potassium feldspar, Ser=sericite, Pl=plagioclase, Apy=arsenopyrite,

Py=pyrite, Ccp=chalcopyrite, Au=gold, Sp=sphalerite. A. Decussate texture quartz-dominant matrix and sericite veinlets throughout. Some veins are filled with arsenopyrite and pyrite. (1519, XPL, 500 μm) B. Pressure shadow texture around potassium feldspar fragments in foliation (2834, XPL, 500 μm). C. Fractured plagioclase grains with polysynthetic twinning with the same direction of the foliation (2834, XPL, 500 μm) D. Corroded subhedral-euhedral coarse-grained pyrite grains and disseminated euhedral fine-grained arsenopyrite in carbonate vein (2834, RL, 500 μm). E. Euhedral arsenopyrite, corroded euhedral pyrite and disseminated anhedral boudinaged sphalerite in the matrix (2858, RL, 200 μm) F. Inclusion gold on the edge of subhedral pyrite and near euhedral disseminated arsenopyrite (1543A, RL, 100 μm). 59

Figure 4-3. Photomicrographs of metasandstone sample (2831). Ms= muscovite, Qtz=quartz, Cb=carbonate, Fsp=feldspar, Pl=plagioclase, Apy=arsenopyrite, Py=pyrite, Ccp=chalcopyrite, Au=gold. A. Intensive foliation formed by recrystallized muscovite with oriented quartz-rich clasts and carbonate (XPL, 500 μm). B. Feldspar-rich clasts and quartz-rich clasts in the felspar + quartz + muscovite + carbonate matrix (XPL, 500 μm). C. Euhedral medium-grained arsenopyrite in the quartz vein and quartz are recrystallized surrounding arsenopyrite grains (XPL, 200 μm). D. Inclusion gold with chalcopyrite in the quartz vein with disseminated arsenopyrite and sphalerite inside (RL, 100 μm)..... 61

Figure 4-4. Photomicrographs of metasiltstone (A&B) and metaconglomerate (C&D) samples. Ms= muscovite, Ser= sericite, Chl=chlorite, Asp=arsenopyrite, Py=pyrite, Au=gold. A. Chlorite and fine-grained sericite interbedded, and crosscutting quartz-carbonate-pyrite fine veins (1536A, XPL, 500 μm). B. Pyrite and arsenopyrite segregated in different zones within sheared area (1535B, RL, 500 μm). C. Sericite-chlorite band with coarse-grained euhedral arsenopyrite grains (1544A, XPL, 500 μm). D. Free gold near coarse-grained euhedral arsenopyrite grains in the sericite-chlorite band (1544A, RL, 100 μm). 63

Figure 4-5. X-ray diffractogram of sample 1541 from Twin Lakes West. The host rock lithology is feldspar porphyry (FP). The major mineral phases are quartz, albite, microcline, and orthoclase. The minor mineral phases are muscovite, ankerite, calcite, dolomite, pyrite, arsenopyrite, and chalcopyrite. The trace mineral phase is sphalerite..... 65

Figure 4-6. X-ray diffractogram of sample 1536 from Twin Lakes West. The host rock lithology is metasiltstone. The major mineral phases are quartz, albite, kaolinite, muscovite,

and chlorite. The minor mineral phases are ankerite, calcite, pyrite, arsenopyrite, chalcopyrite, and sphalerite. 65

Figure 4-7. X-ray diffractogram of sample 1542 from Twin Lakes West. The host rock lithology is felsic lapilli meta-tuff. The major mineral phases are quartz, albite, and muscovite. The minor mineral phases are calcite, dolomite, pyrite, arsenopyrite, chalcopyrite, galena and sphalerite. 66

Figure 4-8. MCA spectrum of 2834 (lapilli metauff), 2858 (lapilli metauff), 2853 (porphyritic dacite), and 2841 (porphyritic dacite) half-core sample. The peaks were fitted with Fe K, Ca K, As K, Cu K, Mn K, Au L, Zn K, K K, W L, Ti K interpreted via Peakaboo Software. A. Au peak on the As shoulder on the MCA Spectrum, but higher than the shoulder; B. real Au peak, much higher than As shoulder; C. Au peak and W peak are overlapped, but Au peak is much higher than As shoulder and W peak; D. False Au signal caused by overlapped high-intensity W peak. 70

Figure 4-9. A. MCA spectrum of 2819 half-core sample B. Photograph of 2819 half-core sample and corresponding large-scale 2D μ XRF trace element maps of Au, As, W, Fe, Cu, Zn, Mn, Ti, K, Ca and Ar. The red circles correspond to high-intensity Au spot. (Data collected in APS 20ID Beamline in February 2019 with the beam size of 800 μ m x 800 μ m and interpreted by Peakaboo). C-E. Higher-resolution Au 2D μ XRF trace element maps of Au spot No. 1-3 in Figure 4-9B. F. MCA spectrum of gold spot No.1 in Figure 4-9C: Au peak on the As shoulder on the MCA Spectrum, but higher than the shoulder (Data collected in APS 20ID Beamline in July 2019 with the beam size of 60 μ m x 60 μ m and interpreted by Peakaboo). 72

Figure 4-10. A. MCA spectrum of 2858 half-core sample B. Photograph of 2834 half-core sample and corresponding large-scale 2D μ XRF trace element maps of Au, As, W, Fe, Cu, Zn, Mn, Ti, K, Ca and Ar. The red circles correspond to high-intensity Au spot. C. MCA spectrum of gold spot No.1: real Au peak, much higher than As shoulder (Data collected in APS 20ID Beamline in February 2019 with the beam size of 800 μ m x 800 μ m and interpreted by Peakaboo). 74

Figure 4-11. A. MCA spectrum of 2854 half-core sample B. Photograph of 2854 half-core sample and corresponding large-scale 2D μ XRF trace element maps of Au, As, W, Fe, Cu, Zn,

Mn, Ti, K, Ca and Ar. The red circles correspond to high-intensity Au spot. C-D. MCA spectrum of gold spot No.1&4: No 1. is a real Au peak, much higher than As shoulder; No 4. is a false Au signal caused by overlapped high-intensity W peak (Data collected in APS 8BM Beamline in March 2019 with the beam size of 500 μm x 500μm and interpreted by Peakaboo).

..... 76

Figure 4-12. A&B. Higher-resolution Au 2D μXRF trace element maps of Au spot No. 1&2 in Figure 4-11A. C. MCA spectrum of gold spot No.8 in Figure 4-12A: Au peak on the As shoulder on the MCA Spectrum, but higher than the shoulder (Data collected in APS 20ID Beamline in July 2019 with the beam size of 60 μm x 60μm and interpreted by Peakaboo). 77

Figure 4-13. A. MCA spectrum of 2831 half-core sample B. Photograph of 2831 half-core sample and corresponding large-scale 2D μXRF trace element maps of Au, As, W, Fe, Cu, Zn, Mn, Ti, K, Ca and Ar. The red circles correspond to high-intensity Au spot. (Data collected in APS 20ID Beamline in February 2019 with the beam size of 800 μm x 800μm and interpreted by Peakaboo). C-E. Higher-resolution Au 2D μXRF trace element maps of Au spot No. 1-3 in Figure 4-13B. F. MCA spectrum of gold spot No.6 in Figure 4-13E: Au peak on the As shoulder on the MCA Spectrum, but higher than the shoulder (Data collected in APS 20ID Beamline in July 2019 with the beam size of 60 μm x 60μm and interpreted by Peakaboo). 79

Figure 4-14. A. As K-edge micro-XANES spectrum collected directly on 2854 offcut analysed at CLS VESPERS Beamline in February 2019. B. As K-edge bulk-XANES spectrum collected directly on 2853 rock powder sample analysed at APS 20BM Beamline in July 2019. 80

Figure 4-15. A-C. Standard As K-edge XANES spectrum of As³⁺ dissolved in water, As₂O₅ powder on Kapton tape, and As⁵⁺ dissolved in water accessed from Hephaestus software (Ravel & Newville, 2005). D. Normalized standard As K-edge XANES spectra of arsenopyrite (blue line), As₂O₃ (red line) and H₃AsO₄ (As³⁺, purple line) (Wang et al., 2013)..... 81

Figure 4-16. A-C. Au L₃-edge micro-XANES spectrum collected directly on gold foil as a standard and 2831 and 2819 half drill core samples examined at APS 20ID Beamline in July 2019. B. As K-edge bulk-XANES spectrum collected directly on 1533 rock powder sample collected at APS 20BM Beamline in July 2019..... 82

Figure 4-17. A-C. Standard Au L₃-edge XANES spectrum of gold foil (represents metallic gold, Au⁰), gold hydroxide powder (represents refractory gold, Au¹⁺), and gold sulphide powder (represents Au³⁺) accessed from Hephaestus software (Ravel & Newville, 2005). .. 83

Figure 4-18. Back-scattered images of sulphide morphologies in the Monument Bay Project: A. Anhedral scheelite, subhedral arsenopyrite, hematite, and monazite inclusions in a needle-shaped corroded pyrite grain. B. Fractured euhedral arsenopyrite with galena filled in fractures and as inclusions. C. Fractured subhedral arsenopyrite with zircon and chalcopyrite on the edge and fine-grained pyrite inside. D. Corroded anhedral chalcopyrite grain with pyrite inside, and fine-grained subhedral arsenopyrite grains in chlorite matrix E. Combination of chalcopyrite + galena + antimony in the matrix.F. Combination of sphalerite + chalcopyrite and stibnite in matrix. 86

Figure 4-19. A-C. Spectra collected by EDS point analysis on microscopic gold represent: Au + Ag, pure gold, and Au + Sb. D&E. Au/Ag ratio and Au/Sb ratio of microscopic gold. 87

Figure 4-20. Back-scatted images of inclusion gold within sulphides: A. Inclusion gold (Au +Ag) and chalcopyrite in fractured pyrite; B. Inclusion gold (Au +Ag) in corroded subhedral arsenopyrite and arsenopyrite + Pyrite grains; C. Inclusion gold (pure gold) in the combination of pyrite + Arsenopyrite. D. Inclusion gold (Au +Ag) in galena grain, E. Pure gold and Au + Sb in rutile grain; F. Inclusion gold with sphalerite and pyrite in quartz vein. 88

Figure 4-21. Back-scatted images of different types of free gold: A. Free gold near corroded euhedral pyrite; B. Free gold near disseminated arsenopyrite; C. Free gold in the matrix; D. Free gold near corroded anhedral pyrite, fine-grained chalcopyrite, fine-grained scheelite and arsenopyrite. 89

Figure 4-22. A. Back-scatted images and EDS/WDS-EPMA 2D element maps show euhedral arsenopyrite grains and quartz inclusions inside corroded needle-shaped pyrite grains and gold along with the fractures; B&C. Back-scatted images and EDS/WDS-EPMA 2D element maps show zoning texture in corroded euhedral to subhedral pyrite grains without fractures. No high-intensity gold spots in pyrite. 90

Figure 5-1. A. The SR-XRD diffractogram of a typical porphyritic dacite sample (2824). B. Fine-grained chalcopyrite and arsenopyrite disseminated in the groundmass (RL, X20) C.

Carbonate (ankerite) grains and albite phenocrysts and subhedral arsenopyrite inside feldspar + quartz + sericite/muscovite groundmass (XPL, X5). D. Needle arsenopyrite in the quartz vein and the discontinuous very fine muscovite vein crosscut the quartz veins (XPL, X5). E. The pie chart shows the modal percentages of minerals..... 93

Figure 5-2. A. The SR-XRD diffractogram of a typical metatuff sample (1543). B. Pyrite grain exhibiting quartz pressure shadows on both sides within muscovite-rich groundmass (XPL, X10). C. Carbonate and albite phenocrysts and subhedral arsenopyrite inside feldspar + quartz + sericite/muscovite groundmass (XPL, X5). D. Euhedral pyrite, euhedral arsenopyrite, and fine-grained anhedral sphalerite in the matrix (XPL, X5). E. The pie chart shows the modal percentages of minerals..... 94

Figure 5-3. A. The SR-XRD diffractogram of a typical metasiltstone sample (1536). B. Chlorite occurring within fine-grained sericite, and crosscutting quartz-carbonate-pyrite veinlet (XPL, X10). C. Recrystallized muscovite crosscut by quartz-carbonate vein, and exhibiting kinematic indicators in the bent muscovite (XPL, X5). D. Coarse to fine-grained euhedral pyrite and fine-grained disseminated in the matrix (XPL, X5). E. The pie chart shows the modal percentages of minerals..... 95

Figure 5-4 A. Arsenopyrite (Apy_1), apatite, plagioclase inside a euhedral pyrite grain (Py_1) and euhedral arsenopyrite (Apy_1) in quartz veins and ankerite matrix; B. Fractured subhedral arsenopyrite (Apy_2) with zircon and chalcopyrite (Ccp) on the edge and fine-grained pyrite (Py_2) inside fractures; C. Combination of sphalerite (Sp) + chalcopyrite (Ccp) in matrix; D. Combination of chalcopyrite (Ccp) + galena (Gn) + antimony in the matrix; E. Corroded anhedral chalcopyrite (Ccp) grain with pyrite (Py_2) inside, and fine-grained subhedral arsenopyrite grains in chlorite matrix; F. Scheelite with anhedral pyrite (Py_2) inside chalcopyrite (Ccp)..... 100

Figure 5-5. A. Inclusion gold I (Au + Ag) in corroded subhedral arsenopyrite (Apy_2) and arsenopyrite + Pyrite grains (Apy_2+Py_1); B. Inclusion gold I (Au + Ag) on the edge of subhedral pyrite (Py_1); C. Free gold I (Au + Ag) near pyrite (Py_1) in quartz vein; D. Inclusion gold II (Au + Ag) and chalcopyrite (Ccp) in fractured pyrite (Py_1); E. Inclusion gold III (Au

+ Sb) and Inclusion gold IV (Pure gold) with rutile; F. Free gold II (Pure gold) in the matrix.
..... 101

Figure 5-6. Boxplot illustrating the Au/Ag ratio of different types of microscopic gold using EDS point analysis at Western University (Free Gold I (n=4), Free Gold II (n=6), Inclusion Gold I (n=3), Inclusion Gold II (n=16)). 103

Figure 5-7. A. Photo of 2831 Metasandstone B-D. SR- μ XRF elemental maps collected in Advanced Photon Source (APS) 20ID Beamline with the resolution of 800 μ m. The red squares are the regions of interests with high Au intensity for higher resolution SR- μ XRF mapping. E. A representative SR- μ XRF Au map (the top square in Figure X-5A & B) was collected in APS 20ID Beamline with the resolution of 60 μ m. The red circles are the regions of interests with high Au intensity for XANES spectroscopy. F & G. Au L₃-edge micro-XANES spectrum collected on the spots in Figure X-5E examined at APS 20ID Beamline in July 2019..... 105

List of Appendices

Appendix A: Petrographic Description.....	119
Appendix B: Low Gold Grade Drill Core Samples (<1 ppm) at the Monument Bay Project	183
Appendix C: Synchrotron X-ray Diffraction (SR-XRD).....	185
Appendix D: Synchrotron Micro-X-ray Fluorescence Data Processing and Maps	201
Appendix E: X-ray Absorption Near-edge Structure (XANES) Spectroscopy	307
Appendix F: EPMA (EDS Point Analysis & EDS/WDS Element Maps).....	320

Chapter 1

1 Introduction

1.1 Project Scope

The research area is the Monument Bay Project, which occurs in the Archean Stull Lake Greenstone Belt, located in Northern Manitoba, Canada. Owing to a series of complex geological events over its history, the Stull Lake Greenstone Belt hosts a number of high-grade orogenic gold deposits. The mineral exploration of the Monument Bay Project started with geophysical exploration and drilling in 1987 by Noranda Inc. (McCracken & Thibault, 2016). After the property became 100%-owned by Yamana Gold Inc. in 2015, more than 400 diamond drills have been conducted in the property (McCracken & Thibault, 2016). The property contains three gold-tungsten mineralized shear zones: The Twin Lakes, Mid-East, and AZ Zones with three main types of gold mineralization. Resource estimation and metallurgical testing for both gold and tungsten recovery was completed on the Twin Lakes, Mid-East and AZ Zones (McCracken & Thibault, 2016). Hannah Cavallin initiated academic research in this area with Yamana Gold Inc. that represents some of the first academic work completed on this deposit and she determined the initial relationship among lithology, alteration, geochemistry, and gold mineralization (Cavallin et al., 2019; Cavallin, 2017). Owing to the existence of metamorphism and deformation overprinting and remobilizing process, the genesis of an orogenic gold deposit is difficult to determine, and transitional forms exist (Phillips & Powell, 2010; Poulsen et al., 2000). In this research, the author used multiple geochemical and mineralogical analytical techniques to have a better understanding on gold distribution, gold speciation, timing relationships, sulphide paragenesis, deleterious element characterization, and ore-forming fluid events in the Monument Bay Project.

The overall objective of this thesis is to characterize gold mineralization and geometallurgy at the Monument Bay Project. In order to achieve this goal, traditional microscopy was used combining with geochemical and mineralogical analytical techniques (Synchrotron X-ray Diffraction (SR-XRD), X-ray Absorption Near-edge Structure (XANES) Spectroscopy, and Electron Probe Microanalysis (EPMA)) and geochemical mapping techniques (Synchrotron Micro X-Ray Fluorescence (SR- μ XRF) mapping). To be more specific, this work can be divided into the

following objectives: The first objective is to determine the relationships between sulphide and gold distribution. Optical microscopy, XRD, and EPMA-point analysis were used to characterize host rock types, mineralogy, texture, microstructures, sulphide morphology, and microscopic gold distribution in different rock types in Monument Bay Project. The second objective is to predict the ore-forming fluid events associated with gold mineralization. Optical microscopy and EPMA EDS/WDS trace element mapping provided the overprinting and progressive zonation of sulphides grains, which indicated multiple fluid events. The third objective is to determine the spatial relationship among the microscopic gold, sulphides, and trace element distribution by SR- μ XRF mapping and optical microscopy. After SR- μ XRF mapping, the speciation of As and Au could be identified on the specific spots on drill core samples using Au L₃-edge micro-XANES spectroscopy and As K-edge XANES spectroscopy, and Au L₃-edge bulk-XANES spectroscopy on powdered rock samples.

The combination of traditional microscopy and novel synchrotron techniques provide insight into gold mineralization, geometallurgy, and deleterious element characterization. This information is being used by Yamana to understand the complex auriferous fluid history, geometallurgical characteristics, and environmental characterization of the Monument Bay deposit. Additional future research of the project will lead to a better understanding of the mineralogical expression of gold mineralization in a portion of the Stull Lake Greenstone Belt and this knowledge will be applied to discover and explore other greenstone-hosted gold deposits in northern Canada. The techniques can be used not only in exploration but also in extractive metallurgy and even tailings remediation.

1.2 Archean Orogenic Gold Deposits

Canada has a rich gold endowment and was the fifth largest producer of gold worldwide in 2019 (Poulsen et al., 2000). In 2004, Archean orogenic gold deposits contributed 77% of the gold produced in Canada (Lydon, 2007). Most gold deposits are located in the orogenic belts in Canada, especially in the Superior Province and Slave Province. These two geological provinces host more than 220 gold deposits containing between 400,000-10,000,000 t of ore with the Au grades of 4-12ppm. There are 14 'world-class' gold deposits among them and each of them contains more than 100 t Au (Poulsen et al., 2000; Robert & Poulsen, 1997). The majority of gold deposits are

concentrated in Southern Superior Province, which makes the Superior Craton the second-largest Archean gold producer in the world, just after Kaapvaal Craton in South Africa.

The Archean deposits and their host districts have many similar characteristics:

Timing: The majority of global gold resources are in Archean terranes. Only a few small gold systems formed in the Middle Archean (ca. 3.4–3.0 Ga). The most favorable period for orogenic gold-vein formation is the Late Archean (ca. 3.0–2.5 Ga) which hosts a large proportion of the global gold resource. Only a few deposits are found in Proterozoic and Phanerozoic terranes. In Canada, the world-class gold deposits in the Superior province and the Slave province are both former in the latter half of the Late Archean (ca. 2.8-2.5 Ga). There is no unequivocal evidence of a significantly large gold-vein system younger than about 55 Ma (Figure 1-1, (Goldfarb et al., 2001)). The most important ones occur in the Archean cratons of the Canadian Shield with fewer and in some cases smaller, deposits in Proterozoic and Phanerozoic terranes.

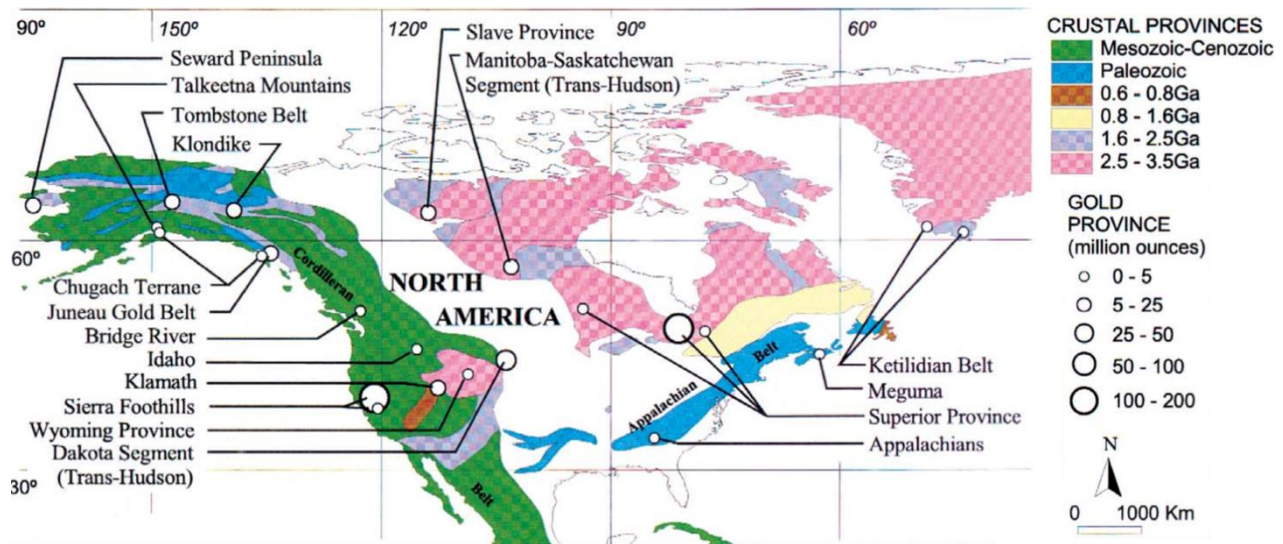


Figure 1-1. Map illustrating the orogenic gold deposit distribution in the gold metallogenic provinces in North America, including the age of the crust (Modified after Goldfarb et al., 2001).

Host terrane geology: In general, the goldfields experienced accretionary orogenic events and the gold deposits are all restricted to the complex compressional/ transpressional environments in the fore-arc or back-arc in deformed metamorphic greenstone terranes (Goldfarb & Groves, 2015; Groves et al., 1998). The orogenic gold deposits are commonly associated with brittle-ductile structure, but have various types: 1) brittle-ductile shear zones with a low-high reverse motion to

strike/oblique-slip motion; 2) fold hinges in ductile turbidite sequences; 3) fracture arrays, stockwork networks, or breccia zones; 4) foliated zones (Groves et al., 1998; Poulsen et al., 2000). As orogenic gold deposits formed continuously at various depth, they can be divided into three types vertically: epizonal (<6 km), mesozonal (6–12 km), and hypozonal (12 km) (Figure 1-2, (Groves, 2003; Groves et al., 1998)). In both provinces, gold deposits are hosted mainly by supracrustal sequences and coeval intrusions. The majority of them occur within, or immediately adjacent to, greenstone belts, commonly in spatial association with crustal-scale fault zones marking major lithological boundaries (Card et al., 1989; Robert & Poulsen, 1997). Only a few deposits, such as those in central Slave Province, are hosted by sedimentary sequences (Padgham, 1992).

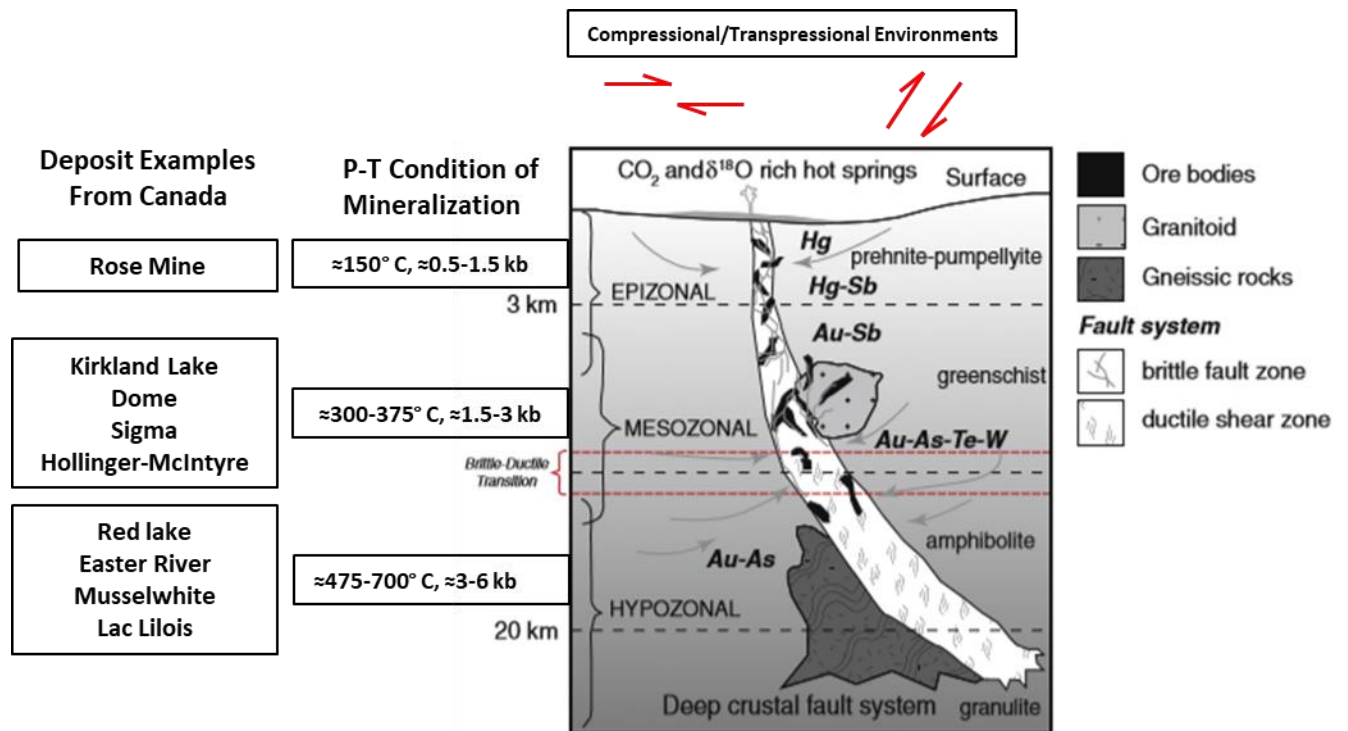


Figure 1-2. Schematic illustrating three types of orogenic gold deposits formed in various depths and a compressional/transpressional crustal environment. Au transported in the fluid along with the fractures in faults and shear zone, and deposited when temperature and pressure changed. The mineralization is continuously from granulite faces to prehnite-pumpellyite faces (modified after Gebre-Mariam et al., 1995; Goldfarb et al., 2001; Goldfarb & Groves, 2015; Groves, 2003; Groves et al., 1998).

Mineralization and Alteration: The orogenic deposits in North America are typically in a quartz-dominated vein system in greenschist-facies host rocks with 3-5% sulphides and 5-15% carbonate

minerals (Dubé & Gosselin, 2007; Groves et al., 1998; R. Kerrich et al., 2000). Gold commonly has a strong association with veins and sulphidized wallrocks. Ore minerals are mainly gold, pyrite, arsenopyrite, pyrrhotite, sphalerite, chalcopyrite, and a trace amount of galena, bismuth, tellurides, molybdenite. Albite, white mica, chlorite, scheelite, tourmaline, calcite, dolomite, ankerite, and graphite show as gangue minerals in veins. (Dubé & Gosselin, 2007; Groves et al., 1998; R. Kerrich et al., 2000). Wall-rock alteration haloes exhibit lateral zonation of alteration assemblages. Ankerite, dolomite, and calcite represent carbonatization; pyrite, arsenopyrite, chalcopyrite, and pyrrhotite represent sulphidization; muscovite, illite, and paragonite represent sericitization (Groves, 2003; Groves et al., 1998). The mineral assemblages of ore and gangue minerals reflect fluid composition. For instance, arsenopyrite and pyrrhotite present in both hypothermal and mesothermal deposits, but not in epithermal deposits; tourmaline and scheelite are the sign of hypothermal deposits (Poulsen et al., 2000).

Ore forming fluid and geochemical enrichments: Ores were deposited from H₂O-CO₂ (\pm N₂, H₂S, CH₄)-rich, and low-moderate salinity mixed aqueous-carbonic fluids, transporting gold as AuHS (H₂S)₃ complex. The temperature and pressure conditions are 220-500 °C, 0.5-4 kb (Goldfarb & Groves, 2015; Groves et al., 1998; Phillips & Powell, 2010). The destabilization of the Au-S complex in the fluid is an efficient way to remove gold from the solution and form a gold orebody. The destabilization can be achieved by fluid mixing, fluid-wallrock reactions, and a large-scale decrease in temperature and pressure in the fluid system (Goldfarb et al., 1988; Kerrich et al., 2000). Compared to background abundances, Orogenic gold deposits share the common trace element inventory with the high enrichments of Au, Ag, As, Sb, Te, W, Mo, Bi, B, and low enrichments of Cu, Pb, Zn, Hg, and Tl (Goldfarb & Groves, 2015; Kerrich et al., 2000; Kerrich & Cassidy, 1994). “Metamorphic devolatilization” and “fluid release from felsic intrusive rocks” are the two genetic models of the auriferous fluid—metamorphic devolatilization, and fluid release from felsic intrusive rocks (Phillips & Powell, 2010). Metamorphic devolatilization operates on hydrated and carbonated greenschist facies rocks across the upper greenschist facies and middle amphibolite facies. H₂O, CO₂, and S were extracted first. The H₂CO₃ formed weak acid, as a result, Au complex with reduced S in the fluid. The low salinity guaranteed the low enrichment of base metals, and the geometry of the shear zones, as the ore fluid migration paths, limited the volume of gold deposition. The gold deposition must experience the destabilization of the Au-S complex, accompanied by carbonation, sulphidization, and muscovite/biotite alteration. This

genetic model explained most Archean orogenic gold deposits in greenstone belts and slate-belts (Ridley and Diamond, 2000; Phillips & Powell, 2010; Powell et al., 1991). The magmatic fluids genetic model explains the auriferous fluid generated from the granitic with low CO₂-solubility. The solubility of CO₂ rapidly rises with a relatively high depth and the increasing pressure of crystallization in fluid-wallrock reactions (Ridley and Diamond, 2000).

Poulsen et al. (2000) compared several well-established classification schemes and pointed out 16 typical types of gold deposits in Canada: paleoplacer (Witwatersrand-type) deposits, submarine Au-rich massive-sulphide (VMS-type) deposits, hot spring deposits, low-sulfidation epithermal deposits, high-sulfidation epithermal deposits, porphyry gold deposits, breccia-pipe deposits, skarn deposits, carbonate-replacement (Manto-type) deposits, sediment-hosted micron gold (Carlin-type) deposits, noncarbonate stockwork-disseminated deposits, Cu-Au sulphide-rich vein deposits, batholith-associated quartz-vein (Korean-type) deposits, greenstone-hosted quartz-carbonate vein (Mother-Load-type) deposits, turbidite-hosted quartz-carbonate-vein (Bendigo-type) deposits, and iron-formation-hosted vein and disseminated (Homestake-type) deposits. The three deposits in the Monument Bay project are one of the subtypes of greenstone-hosted quartz-carbonate vein (Mother-Load-type) deposits. They are defined as Archean greenstone belt shear-hosted, mesothermal gold-quartz vein deposits (Hannah Evy Cavallin, 2017).

1.3 Sulphide Geochemistry

Gold mineralization was generally due to the sulfidation reaction between auriferous fluid and Fe-rich wallrocks, and the great change of temperature and pressure conditions caused gold deposition. Goldfarb et al., (2005) mentioned that according to the sulfur isotope measurements on ore-related sulphide minerals, $\delta^{34}\text{S}$ values have a large fluctuation from -20 to +25, which indicates the various sulfur source and multiple fluid events. Because of the refractory nature of sulphides, the temperature of sulphide formation has a wide range, from ~30 to ~600 °C (Deditius et al., 2014). As in most orogenic gold deposits, the orebodies formed under the temperature of 325-400 °C, the sulphide morphology and its trace elements distribution is a record of the variations in fluid compositions and P-T conditions (Deditius et al., 2014; Del Real et al., 2019; Ross-Lindeman & Kirste, 2019; Stromberg, Barr, et al., 2019; Stromberg, Van Loon, et al., 2019; Yang et al., 2016). Pyrite, arsenopyrite, and arsenian pyrite are generally dominant sulphide minerals and can be divided into several generations based on the zonation, texture, and

composition of sulphide. And each generation of sulphides corresponds to a regional deformation event (Deditius et al., 2014). Thus, the temporal and spatial relationship between gold and sulphide is useful to deduct the gold forming event.

1.4 Gold Solubility and Speciation

Gold in gold deposits is present as visible native gold, microscopic gold, lattice-bound gold, and nanoparticulate gold (<250 nm). As lattice-bound gold and nanoparticulate gold are incorporated in sulphide grains and difficult to recognize even under an optical microscope, these types of gold are referred to as “invisible gold” in some published studies (Cook et al., 2013; Deditius et al., 2014; Fleet & Mumin, 1997; Reich et al., 2005; Sung et al., 2009).

There are three types of gold speciation in gold deposits: Au^0 , Au^{1+} , and Au^{3+} . Au^0 and Au^{1+} are the typical speciations representing metallic gold and refractory gold, respectively. Spectroscopic technology proved that the valence of Au in lattice-bound gold is +1 and that invisible native gold, microscopic gold, and nanoparticulate gold the valence is 0 (Banerjee et al., 2018; Cabri et al., 2000; Deditius et al., 2014; Reich et al., 2005). Maddox et al. (1998) measured open-circuit potentials of pyrite and arsenopyrite. They found that larger but fewer Au^0 particles grow on the pyrite surface than the arsenopyrite surface in Au^{3+} chloride solution and the rate of Au reduction is controlled by the rate of arsenopyrite oxidation. Some scientists suggested a substitution mechanism in arsenopyrite: $2\text{As} [\text{Fe}] \Leftrightarrow (\text{Au}, \text{Sb}) + \text{Fe}$ (Cabri et al., 2000; Deditius et al., 2014; Reich et al., 2005). Considering the existence of nonpolar-state Fe^{3+} in arsenopyrite structure, they suggested gold was possibly present as Au^{3+} . The charged species were likely to be deposited with arsenic as a solid solution instead of pyrite/arsenopyrite. This hypothesis is consistent with the unusual oxidation environment during the formation of some gold deposits (Arehart et al., 1993; Chouinard et al., 2005; Johan et al., 1989). However, there is no spectroscopic evidence for the natural existence of Au^{3+} in minerals.

1.5 Arsenic Solubility and Speciation

Arsenic is a potentially toxic element in gold extraction, and it can enter the biosphere through natural and anthropogenic processes. As_2O_3 is one of the most easily bioavailable and toxic forms of arsenic. In order to reduce the harm to public health and the environment, it is essential to study

the speciation and distribution of arsenic (Van Den et al., 2018). As presents in synthesized minerals in gold deposits, mainly in arsenian pyrite (FeS_2), arsenopyrite (FeAsS), and löllingite (FeAs_2) (Trigub et al., 2017). Many studies showed a positive correlation between the concentration of Au and As in pyrite (Deditius et al., 2014; Reich et al., 2005; Trigub et al., 2017). And Arsenic solubility in pyrite increases with decreasing temperature (Deditius et al., 2014). The concentration of As in pyrite with As^{1-} species is ≤ 19 wt.% (Reich et al., 2005) and that in pyrite with As^{3+} species is ≤ 5.5 wt.% (Deditius et al., 2008). XANES analyses and cross-sectional X-ray photoelectron spectroscopy (XPS) analysis confirmed the dominant oxidation state of As in arsenian pyrite was +2. And the more oxidized forms, As^{3+} and As^{5+} , were the possible evidence of weathering on the surface of arsenian pyrite (Qian et al., 2013). Arsenic can also present as As^0 in As-Fe-S nanoparticles aggregates in arsenian pyrite (Deditius et al., 2009). Anomalous Au concentrations were found in the fractures, grain margins, and porous parts of sulphide grains, especially As-rich, Fe-poor sulphides, and sulphide core are Au-poor (Cook et al., 2013; Fleet & Mumin, 1997). Fleet and Mumin (1997) suggested a large portion of Au was removed from ore fluids during metamorphism by absorption of sulphides, and then Au incorporated in a metastable solid solution. In the metamorphism process, the refractory property of host sulphides decreased due to pressure and temperature changes, and Au nanoparticles were forced out of the lattice and deposited.

1.6 Synchrotron Radiation (SR)

Synchrotron Radiation (SR) is electromagnetic radiation that relativistic electrons or other kinds of charged particles emit when they are forced by applied magnetic fields to move along curved trajectories. This extraordinary intense radiation covers a wide and continuous spectral range of the electromagnetic spectrum including infrared (IR), the visible light, ultraviolet (UV), and soft and hard X-ray. Since the late 1960s when scientists realized synchrotron radiation could be helpful in condensed matter research, the electron storage rings and facilities were built and became a powerful research tool in many scientific fields, like material science, biology, chemistry, environmental science, and earth science (Balerna & Mobilio, 2015).

A basic synchrotron radiation facility is a high-energy electron circular accelerator, consisting of linac, booster, storage ring, and beamlines. The electrons are accelerated by a linear accelerator, called linac, and then by a booster ring to gain high energy. After the energy of electrons boosts

into Giga electron volts (GeV), the electrons are injected into the circular accelerator, the storage ring. The storage ring is made by circular evacuated pipes and magnets placed along the circular paths (bending magnets). In this way, when the electrons are forced to follow the circumference forced by bending magnets, in each turn, they lose part of their energy and emit synchrotron radiation (Balerna & Mobilio, 2015, Figure 1-3). The radiation is finally captured by very narrow beamlines, which are aligned to the velocity of the electrons moving around the ring (Margaritondo, 2015). A standard beamline has the optical section and the experimental station. The optical section is commonly composed of filters, slits, photon shutters, monochromators, and mirrors (Aquilanti et al., 2015). Figure 1-4 shows a schematic of the VESPERS beamline at the CLS.

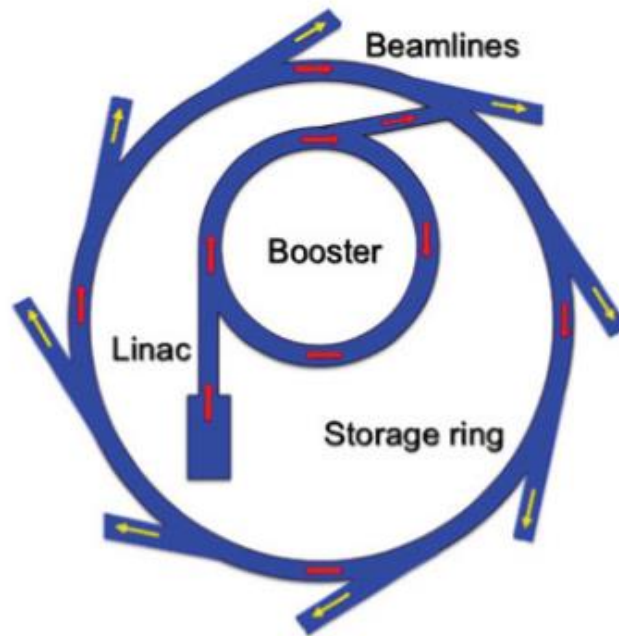


Figure 1-3. Schematic planar view of a general synchrotron radiation facility. The arrows show the direction of the beam in a synchrotron radiation facility. The linac is a linear accelerator where the electrons are accelerated. The booster is the place that the electrons gain high energy. The electrons are injected into the circular accelerator, the storage ring after gaining energy. Finally, the electrons are forced to follow the circumference forced by bending magnets and the radiation captured by very narrow beamlines (Balerna and Mobilio, 2015). The storage ring of the Canadian Light Source (CLS) is 170.88m in circumference, while the storage ring of the Advanced Photon Source (APS) is 1104 m in circumference (Advanced Photon Source, 2020; Canadian Light Source, 2020).

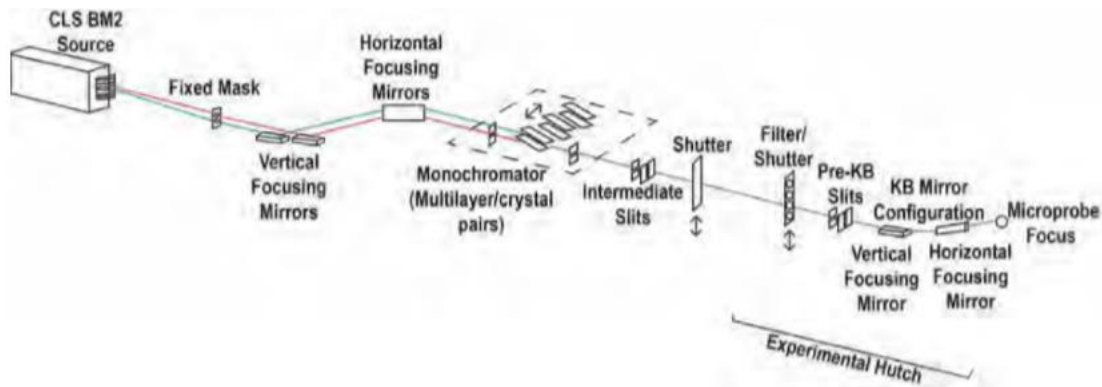


Figure 1-4. Schematic of the VESPERS beamline at the CLS (KB –Kirkpatrick-Baez) (Modified from the Canadian Light Source).

In many decades, scientists and engineers are making every effort to improve source size and divergence to gain high peak intensity and brightness and meet the requirements of various kinds of scientific experiments. Currently, there are a number of third-generation synchrotron facilities around the world including Advanced Photon Source (APS) in Chicago, USA and the Canadian Light Source (CLS), Saskatchewan, Canada. Because of the optimization of insertion devices, APS became one of the few of third-generation synchrotrons in the world operating in the high-energy range of electron beams (7 GeV).

1.6.1 Application of Synchrotron Radiation Technology

Synchrotron Radiation technology is widely applied in various fields, including material science, biology, medical science, geoscience, environmental science, and even art and archaeology heritage (Balerna & Mobilio, 2015). In earth science studies, SR techniques can provide information at an atomic level in mineralogy, petrology, and geochemistry with the energy range of hard X-ray mostly. Single-crystal X-ray diffraction, X-ray powder diffraction, Small-angle and wide-angle synchrotron X-ray scattering (SAXS/WAXS), X-ray absorption spectroscopy, X-ray fluorescence microanalysis, infrared and Raman spectroscopy, synchrotron Mössbauer spectroscopy, and X-ray topography and microtomography are the most popular SR-based methods applied in geoscience (Quartieri, 2015). X-ray powder diffraction (XRD), Synchrotron micro X-ray fluorescence (SR- μ XRF) mapping, and X-ray Absorption Near-edge Structure (XANES) Spectroscopy are the three SR techniques used in the geometallurgy study of the Monument Bay Project. XRD is used to identify the minerals; SR- μ XRF mapping provides high-

resolution trace elemental variation maps of regions of interest for defining the mineralizing system and understanding the spatial relationships between key trace elements. XANES Spectroscopy is used to identify the redox, speciation, and coordination of key elements by investigating local electronic structures in geological material.

A number of studies show the advantages of SR techniques compared to conventional source X-ray methods. Stromberg et al. (2019) determined the trace element distribution of different stages of pyrite by SR- μ XRF mapping on regions of interest and assumed three auriferous fluid events resulted in gold mineralization at the Dome Mine in Timmins, Ontario. Cabri et al. (2000) used XANES spectroscopy of Au on gold-rich arsenopyrite from four gold deposits. They found two kinds of Au speciation (Au^0 and Au^{1+}) which illustrated the invisible gold were metallic gold and lattice-bound gold. Furthermore, the correlation between arsenopyrite growth zoning and gold concentration represents the changes in the environmental condition during recrystallization. Yang et al. (2014) identified Cu and Fe distribution and speciation by combining multiple SR techniques, including bulk-extended X-ray absorption fine structure (EXAFS) and (scanning transmission X-ray microscopy (STXM) nanoanalysis, and nano-XANES for Fe, and μ -XANES and bulk-XANES for Cu. Brugger et al. (2010) synchrotron-based XRD, XRF, XANES, and particle-induced X-ray emission (PIXE) can support mining and exploration in the modeling of transportation and deposition of ore-forming fluid, predicting the potential of ore-forming and vectoring to the geochemical footprint of buried deposits. However, there are several challenges when SR techniques are applied in geosciences: 1) owing to the low concentration of elements of interest and complexity of geological materials, the detection limits and beam sensitivity make the analysis not accurate enough to identify redox in some cases; 2) extreme environment for in-situ analysis on fluid inclusions (Brugger et al., 2010). Therefore, the application of SR techniques in geosciences is challenging and the requirements of the environment and samples are strict.

Chapter 2

2 Regional and Local Geology

2.1 The Superior Province

The Superior Province is the nucleus of the Canadian Shield, beneath which lies part of the thickest lithosphere in the North American continent with a thickness of 200-250 km (Percival et al., 2006; Percival et al., 2012; van der Lee & Frederiksen, 2005). As Canada's metallogenic and mining heartland, the Superior Province hosts vast mineral deposits including the largest Archean orogenic lode gold camp in the world, Timmins gold camp (Percival, 2007; Percival et al., 2012). The successive docking of continental fragments and the oceanic crust between the oceanic terranes formed the Superior Province during five progressive accretionary and collisional events between 2720 and 2680 Ma. These events and subsequent post-orogenic effects resulted in the suspension of subduction magmatism and the crustal-scale imbricated terranes (Percival et al., 2006; Percival, 2007; Percival et al., 2012). Most parts of the Superior Province have remained relatively tectonically stable since 2.6 Ga, although some diabase dyke swarms occasionally emplace. After the Proterozoic era, the craton experienced rifting, failed lifting, compressional reactivation, and large-scale rotation. The ductile deformation only happened to the northeastern and northwestern margins of the cratons (Buchan & Ernst, 2004; Percival et al., 2006; Percival, 2007). The deformation events in the southern and northern were different across the Superior Province. For example, when Wabigoon and Wawa-Abitibi terranes in the south underwent the submarine volcanism, the deformation was in progress in Hudson Bay and North Caribou terranes in the north. The different orogenies and large-scale transpressive faults between the boundaries are the evidence of consecutive assembly of crust fragments and horizontal tectonism.

The terms "terranes", "domains", "superterranes", "subprovince" are generally used to identify the regions with different tectonic, lithological, geological, and geophysical characteristics (Percival, 2007; Percival et al., 2012; Stott et al., 2010). The most distinctive feature of the Superior Province is the linear subprovinces dominated by granite-greenstone and gneissic terranes, which can be distinguished by transpressive subparallel faults on the boundary (Figure 2-1; Card & Ciesielski, 1986; John A Percival et al., 2012). The Superior Province is composed of three regions: southern, northwestern, and northeastern. These parts are characterized by different rock types: metavolcanic

and metasediments in the south, high-grade gneiss in the northwest, and granulite in the northeast (Card, 1986; Mints, 2017). The trend of the Southern Superior Province is normally E-W, that of Northwestern Superior Province is commonly W-NW, and that of Northeastern Superior Province is NW (Mints, 2017; J.A. Percival, 2007).

The Northwestern Superior Province is more difficult to access and less understood than the Southern Superior Province. It is regarded as an assemblage of small continental blocks and intervening tracts of oceanic plates with a complex history between 2.72 and 2.68 Ga (Figure 2-1, (Parks et al., 2006; J. A. Percival et al., 2004)). From the south to north, they are the North Caribou Superterrane (NCS), the Oxford-Stull Domain (OSD), and the Northern Superior Superterrane (NSS) (Lin, 2005; Parks et al., 2006; Skulski et al., 2000). However, there is no accurately defined boundary between them in the literature. The NCS is referred to as an Archean micro-continent with a 3.0 Ga basement. And the volcanic sequences conformable contact with the underlying quartz-rich metasediments and platformal carbonate near the base (Lin, 2005; Percival et al., 2004; Skulski et al., 2000). The NSS is characterized by granitoid, gneiss, and few greywackes, iron formation, and mafic-intermediate volcanic intrusions with a recorded age of ~3.9 Ga (Lin, 2005; Skulski et al., 2000). The OSD is between the NCS and the NSS, dominated by metavolcanic rocks and subvolcanic (2.83-2.69 Ga) (Lin, 2005; Parks et al., 2006; Skulski et al., 2000). These terranes formed the Sachigo Subprovince, and the Berens Subprovince, and the Uchi Subprovince (Card & Ciesielski, 1986).

Most mineral deposits of the Superior Province are associated with mafic-ultramafic intrusions which formed between 2.76 and 2.74 Ga during the magmatic arc and collisional stages of orogenesis. These deposits typically exhibit syn- to very late deformation with mineralization usually hosted within post-peak greenschist facies or local syn-peak amphibolite facies metamorphic rocks (Dubé & Gosselin, 2007; Goldfarb & Groves, 2015).

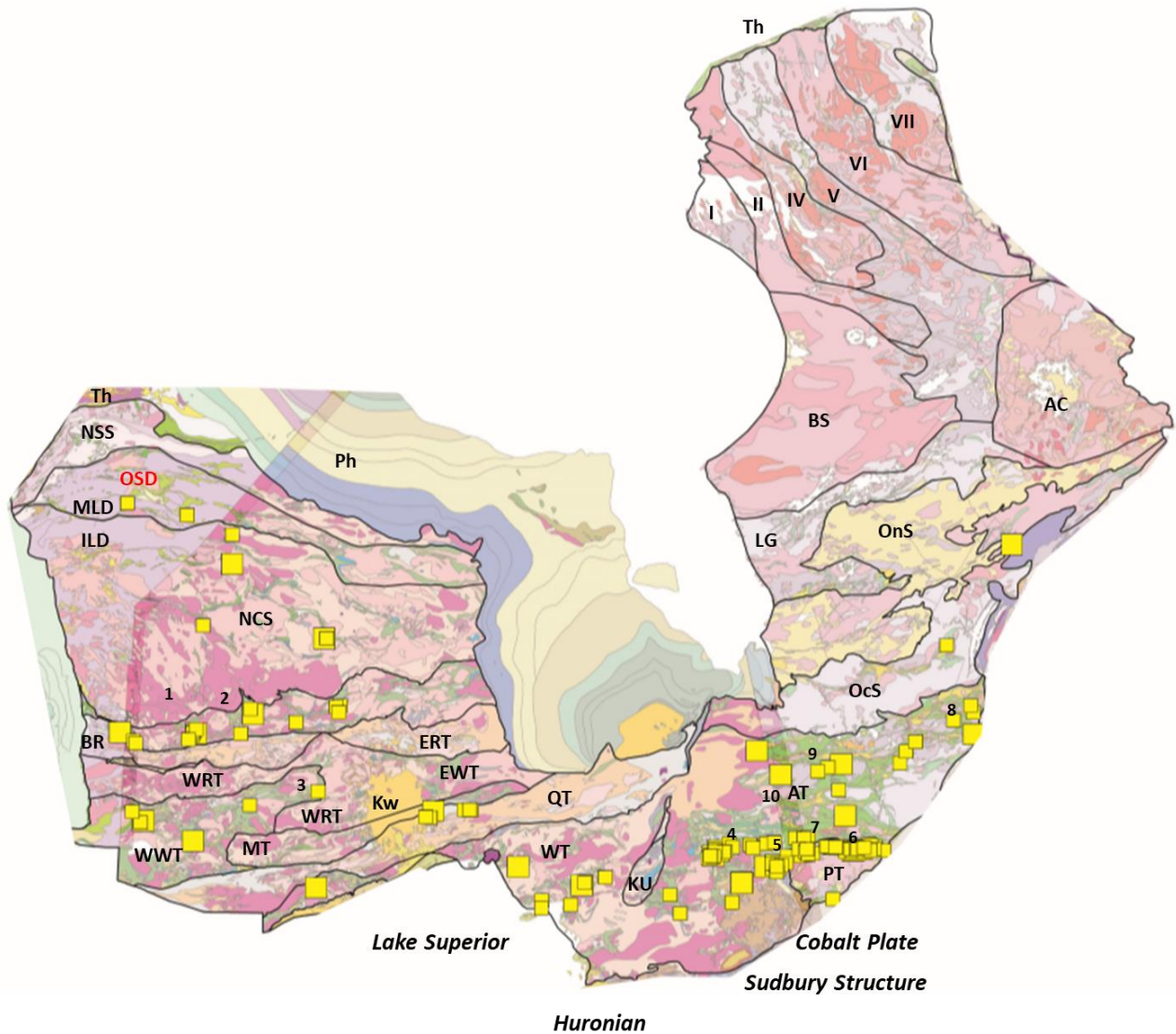


Figure 2-1. Mosaic map of the Superior Province illustrating major tectonic elements and gold deposits. Phanerozoic: Ph: Platform Sediments; Proterozoic: Kw: Keweenawan, Th: Trans-Hudson Orogen; Archean: VII: Douglas Harbour Domain, VI: Utsalik Domain, V: Goudalie Domain, IV: L. Minto Domain, II: Tikkerutuk Domain, I: Inukjuak Domain, BS: Bienville Subprovince, LG: La Grande Subprovince, OnS: Opinaca Subprovince, AC: Ashuanipi Complex, OcS: Opatoca Subprovince, PT: Pontiac Terrane, AT: Abitibi Terrane, KU: Kapuskasing Uplift, WT: Wawa Terrane, QT: Quetico Terrane, EWT: E. Wabigoon Terrane, WWS: W. Wabigoon Terrane, WRT: Winnipeg R. Terrane, ERT: English R. Terrane, NCS: North Caribou Superterrane, OSD: Oxford-Stull Domain, NSS: Northern Superior Superterrane, MT: Marmion Terrane, BR: Bird R. Subprovince, MLD: Molson L. Domain, ILD: Island L. Domain. The numbers represent the locations of major mineral districts: 1: Red Lake; 2: Confederation Lake; 3: Sturgeon Lake; 4: Timmins; 5: Kirkland Lake; 6: Cadillac; 7: Noranda; 8: Chibougamau; 9: Casa Berardi; 10: Normétal. The yellow squares represent gold deposits and the symbol sizes are proportional to deposit size (Modified from Percival, 2007).

The Oxford-Stull Domain (OSD) is one of the superterrane in the Northwestern Superior Province, which hosts abundant lode gold along with major and minor structures in faults and shear zones of large greenstone belts, e.g. the Knee Lake-Gods Lake Greenstone Belt and Stull Lake Greenstone Belt (Corkery et al., 2000; Corkery & Skulski, 1998; Percival, 2007). The OSD is a granite-greenstone terrane with a trend of east-west located between the North Caribou Terrane (NCT) and the Hudson Bay Terrane (HBT). The plutonic rocks and greenstone belts in the OSD are the significant evidence of collision and subduction between the NCT and the HBT and magmatism, sedimentation, and deformation (Stone, 2005). The OSD is a mature volcanic arc, which is younger than the basement terranes, NCT (~3.7 Ga) and the HBT (~3.0 Ga). The dominant lithology of the OSD is six types of felsic plutonic rocks and a few superacrustal rocks in the greenstone belts. The felsic plutonic rocks indicate the magmatism during ~2.86-2.69 Ga and melt of tectonic subducted slabs (Stone, 2005). Based on the lithological, geochronological, and structural study, another two significant supracrustal sequences have been identified: a fault-bounded sequence of volcanic rocks and sandstones formed in later-stage plutonium with an age of ~2.72 Ga, and alkaline volcanic rocks and conglomerate of the Oxford Lake Group with an age of ~2.71 Ga (Lin et al., 2006; Stone, 2005). The sign of the subsiding of subduction and the beginning of continental collision is considered to be the transition from the melting of the subducted slab into the partial melting of the mantle (Stone, 2005).

The OSD recored four main deformation events. Layer parallel foliation (S1) was conserved in the older mafic sequences, resulting from the thrusting in the Hayes River Group before the volcanism before the Oxford Lake Group (Skulski et al., 2000). The regional S2 fabric led to reverse displacements and dip-slip movement in D2 shear zones. Because of the reactivation of D2 structures at the same time as D3 shearing, D2 structures have been partially overprinted (Jiang & Corkery, 1998). D3 structures present as pervasive dextral transcurrent mylonitic shear zones. Extensional basins developed along with D3 structures. The extensional basins had Cross Lake Group sediments deposited in (Stone, 2005). D4 is the last deformation event. D4 refolded D3 shear zones and produce brittle faults, resulting in the north-south shortening (Jiang & Corkery, 1998).

2.2 Stull Lake Greenstone Belt

The Stull Lake Greenstone Belt is a portion of a group of greenstone belts, Stull Lake–Edmund Lake greenstone belt in Wolf Bay–Stull–Wunnumman Shear Zone (Figure 2-2). The Stull Lake Greenstone Belt consists of three volcanic-sedimentary assemblages and four selections of internal plutonic rocks, preserving complex ductile deformation history and tectonic segmentation (Skulski et al., 2000).

The Hayes River Assemblage (~2.85-2.83 Ga) is the oldest assemblage, mainly formed by a thick sequence of tholeiitic basalt aphyric with pillowed and massive flows intruded by gabbro sills (Skulski et al., 2000). The pillow structures and graded bedding illustrated a stratigraphic succession with mafic volcanic rocks, intermediate to felsic volcanic, and volcanogenic sedimentary rocks from the bottom to top (Corfu & Lin, 2000). The Rapson Bay felsic complex has the thickest and best-preserved part of this sequence (Skulski et al., 2000). The Oxford Lake Assemblage (~2.73-2.71 Ga) overlapped on the Hayes River Assemblage (Corkery et al., 2000). The White House tonalite and Margaret Lake granite are typical synvolcanic during the Oxford Lake volcanism (Skulski et al., 2000). The Oxford Lake Assemblage is composed of the lower Oxford Lake Volcanic Assemblage and the upper Oxford Lake Sedimentary Assemblage (Stone, 2005). The lower Oxford Lake Volcanic Assemblage is dominated by intermediate to felsic volcanic rocks with the calc-alkalic grading to alkalic compositions related to the feldspar- and hornblende-phyric lavas (Stone, 2005). The upper Oxford Lake Sedimentary Assemblage and unconformably overlying the Cross Lake Assemblage (~2.71 Ga) are the clastic sedimentary sequences dominated by conglomerate, pebbly sandstone, and sandstone with massive to thick-bedded and locally graded and cross-bedded (Ketchum & Davis, 2001).

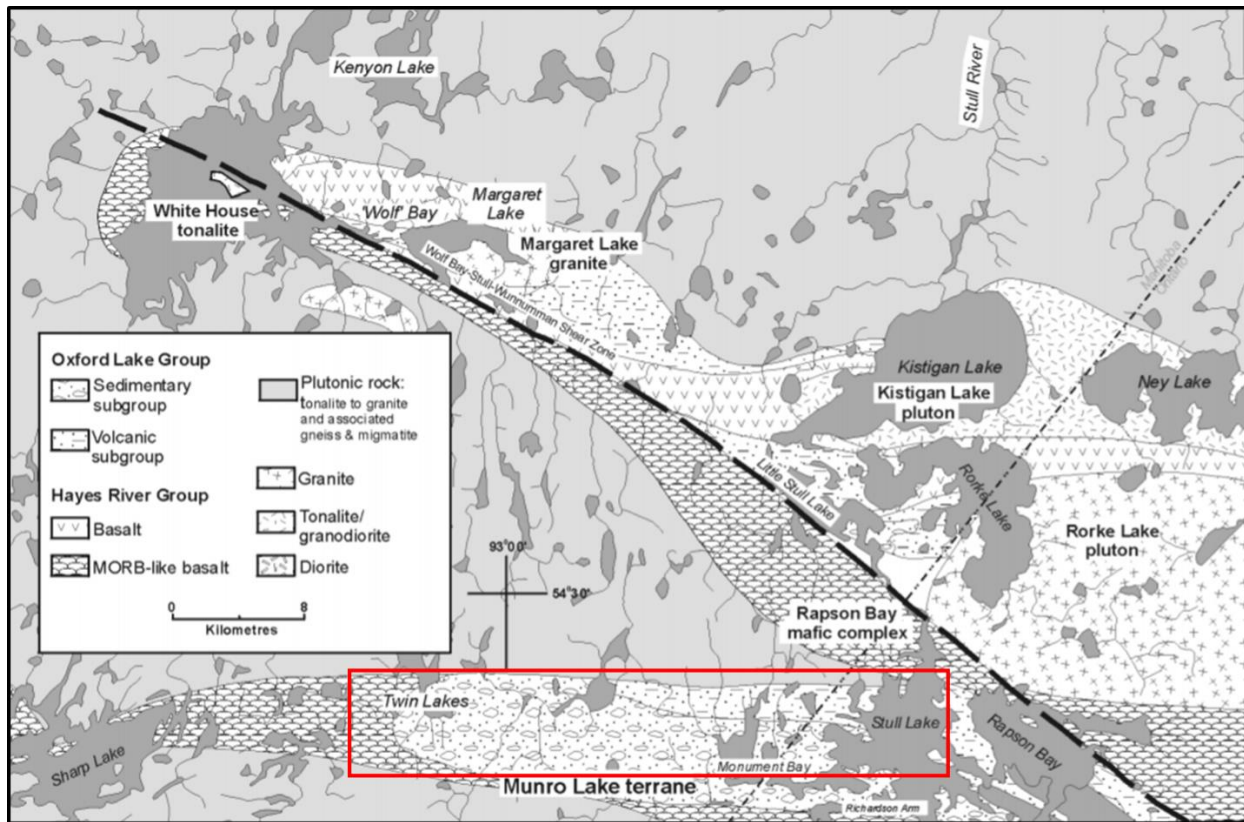


Figure 2-2. Regional geologic setting and major subdivisions in the Stull Lake–Edmund Lake greenstone belt, Oxford Lake–Stull Lake terrane. The red box shows the location of the Monument Bay Project and Stull Lake Property (Modified from Skulski et al., 2000).

2.3 Study Area

2.3.1 Location

The Monument Bay Project is in a gold-bearing shear system located within the Oxford-Stull Domain of the Northwestern Superior Province, in northeastern Manitoba and along the border of Ontario (McCracken & Thibault, 2016). The 31250-hectare property consists of 136 contiguous mining claims in Manitoba and 14 claims in Ontario, which are currently 100% owned by Yamana Gold Inc (McCracken & Thibault, 2016). The property has rare outcrops because of 1-30 m till cover on the bedrock. The area is low topographic relief covered mainly by spruce forest, underbrush, and thick moss (McCracken & Thibault, 2016). The exploration camp is located at the central area of the property on the shore in the southwest area in the Twin Lake Zone. The exploration camp can be accessible by snowmobile and bulldozers in wintertime and by floatplane and helicopter in unfrozen months. The Monument Bay Project is composed of three individual deposits: Twin Lakes Deposit, Mid-East Deposit, and AZ Deposit, which are all located in steeply

north-dipping shear zones within the Stull-Wunnummin Shear Zone (SWSZ). Yamana Gold Inc. has drilled in seven targets: Twin Lakes (TL), Twin Lakes West (TLW), Twin Lakes East (TLE), Mid-East (ME), South Limb Shear (SLS), and AZ (Figure 2-3).

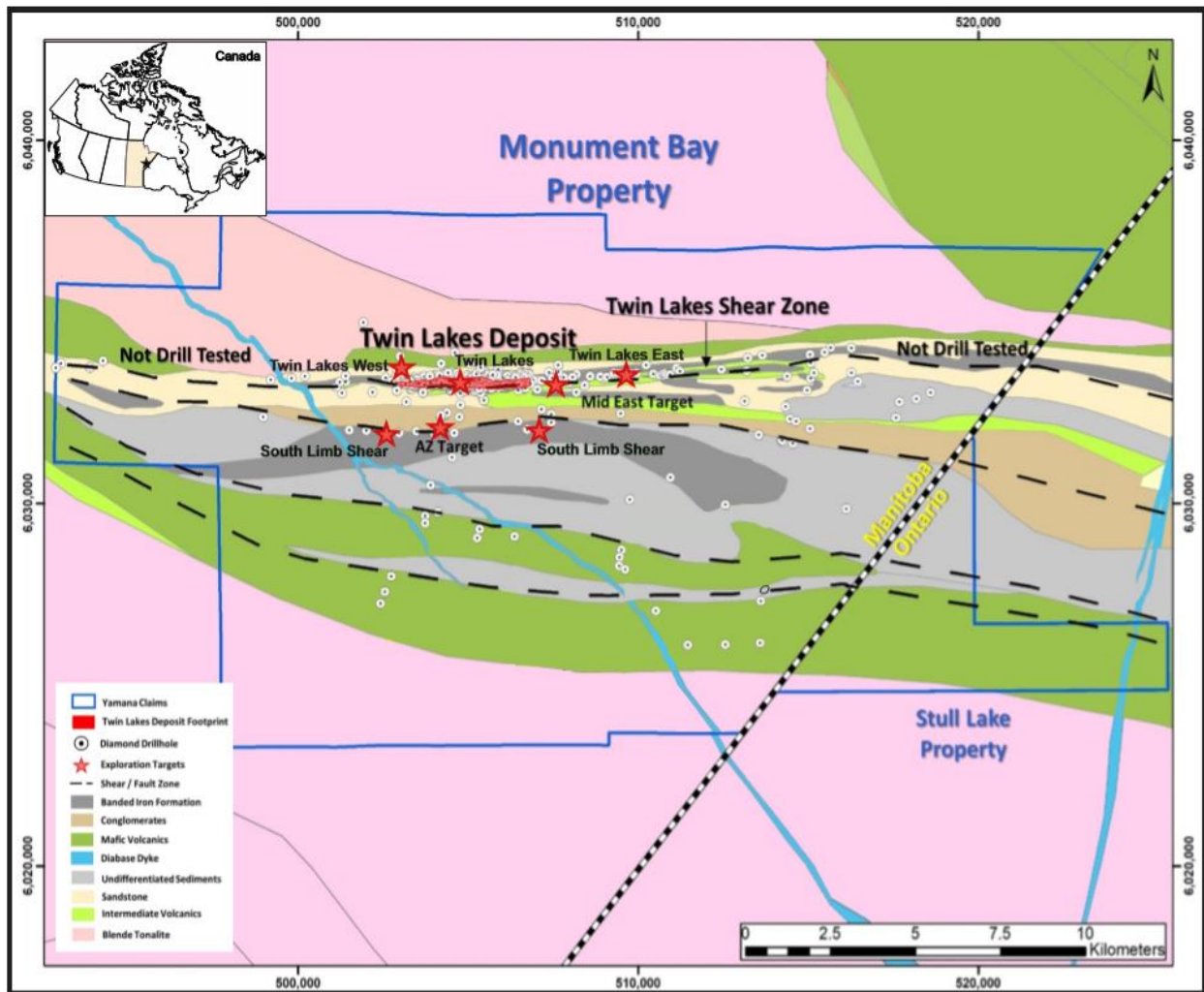


Figure 2-3. Regional geology map with major structures and claim outlines of Monument Bay Property and Stull Lake Property (the red box in Figure 2-2). The red stars indicate the geographical distribution of the 7 different targets in the Twin Lakes Deposit.

2.3.2 Exploration and Research History

The mineral exploration of the Monument Bay Project started with geophysical exploration and more than 30,000m of diamond drilling since 1987 by Noranda Inc. Following the 7-year dormancy period (1991-1998), the property became 100%-owned by Yamana Gold Inc. in 2015. Currently, 628 boreholes have been drilled by Forthright Drilling Services Inc. on the Monument

Bay project. All drilling was completed using a 3-m core tube with a core diameter of 47.5 mm (McCracken & Thibault, 2016). The 2014 drill program completed 1652 m in six drill holes and the 2015 drill program completed 3472 m in twelve drill holes. Up to the first six months of 2018, approximately 10,560 m of drilling was completed. In 2019, more groundwork was conducted to generate prospects (Yamana, 2018). The total Measured and Indicated Mineral Resources is 1.787 million ounces gold contained in 36.581 million tonnes with an average gold grade of 1.52 g/t. The total Inferred Mineral Resources is 1.781 million ounces gold in 41.946 million tonnes with an average gold grade of 1.32 g/t (Yamana, 2018).

In 2017, Cavallin initiated research in gold mineralization that represented some of the first academic work completed on this deposit. After collecting samples and using traditional microscopy combined with geochemical and mineralogical analytical techniques (XRD and ICP + XRF geochemical data analysis) and geochemical mapping techniques (synchrotron micro X-ray fluorescence (μ XRF) mapping), Cavallin determined the initial relationships among lithology, alteration, geochemistry, and gold mineralization. Porphyritic felsic intrusive unit was determined as the major host rock of the Twin Lakes Deposit. Tungsten mineralization is not directly correlated with gold mineralization, and a late, hot ore-forming fluid resulting in the gold deposition. Brecciated and silicified structure, varied textures of sulphides, and pervasive alteration indicate the multi-episodic fluid events and potential fluid mixing in the Monument Bay Project (Cavallin et al., 2019). This project was built on Cavallin's observation and results of petrography, mineralogy, and geochemistry. This research expanded the study to more samples from a greater geographic distribution to specifically characterize the gold mineralization, including links to the geometallurgy and mineralization model. Thus, the more detailed and more deeply analysis and interpretation in this research will lead to a better understanding of gold mineralizing fluid events and geometallurgy at the Monument Bay Project.

2.3.3 Geology and Deposit Type

Three mineralized zones with gold and tungsten mineralization have been delineated by Yamana including the Twin Lakes Deposit, the Mid-East Deposit, and the AZ Deposit. These deposits all occur within steeply northern dipping, dextral strike-slip mylonitic shear zones, resulting in the deformation of sedimentary rock and volcanic rock in the Stull Lake Greenstone Belt. These three deposits are interpreted as a splay of the Stull-Wunnumin Fault Zone (Skulski et al., 2000). The

Twin Lakes Deposit and the Mid-East deposit are located in the Twin Lakes Shear Zone in the northern SWFZ, and the AZ deposit is situated in the AZ Shear Zone in the southern SWFZ. The Twin Lakes Shear Zone and the AZ Shear Zone are east-west trendings with a length of ~40 km and a width of ~200 m. The Twin Lakes Shear Zone and the AZ Shear Zone are parallel to each other (McCracken & Thibault, 2016).

The stratigraphy of the Monument Bay Project consists of three groups of rock: the Hayes River Group, the Oxford Lake Group, and the Cross Lake Group. The Hayes River Group is the oldest rock assemblages in the south of the property (2830 Ma), including gabbro, mafic volcanic rock, siltstone with minor oxide facies iron formation, and greywacke/siltstone (McCracken & Thibault, 2016). The Oxford Lake Group rocks, which is the host rock of Twin Lakes Deposit (2717-2726 Ma), comprised of felsic feldspar porphyritic dyke, felsic-intermediate tuff and intercalated sediments, intermediate feldspar phyric volcanic flow, and felsic tuff. It has been found that intermediate feldspar phyric volcanic flow and felsic tuff was crosscut by felsic feldspar porphyritic dyke. The Cross Lake Group is composed of conglomerate and intrusive rocks (McCracken & Thibault, 2016). The property presents variable and pervasive alteration including carbonatization, silicification, sericitization, and chloritization. Mineralization and alteration overprints make the identification of rocks and mineral difficult. The silica-rich fluid intruded in the Twin Lakes Shear Zone, which formed quartz veining and silicic rocks along with the strikes afterward. The silicified rocks, strong and continuous deformation, and brecciation became an ideal place for the deposition of subsequent hydrothermal fluid and mineralization. Sericitization formed a halo surrounding the mineralized core and the host rock has been pervasively altered into sericite. Carbonatization and chloritization are weaker than sericitization and silicification, but minor-moderate in some sedimentary rocks.

The deposits in the Monument Bay Project are defined as Archean greenstone belt shear-hosted, mesothermal gold-quartz vein deposits (Goldfarb & Groves, 2015). The tectonic setting of this type of gold deposit is crustal deformation in fault zones within stable cratons and collision boundaries between terranes. The host rocks are granite, felsic volcanic rocks, intermediate-felsic intrusive rocks, intermediate-felsic sedimentary rock, and relative metamorphic rock (shale and schist). Deposits formed thick fissure veins in competent host rocks and veinlets in less competent host rocks. Veins sharply intruded in wallrocks with massive, ribboned, and/or banded texture, and

silicification, pyritization, carbonatization, and potassium alteration exhibit within veins and wallrocks. The ore mineralogy, gangue assemblages, and alteration assemblages are similar in this type of gold deposits.

2.3.4 Mineralization

Gold and tungsten mineralization in the Monument Bay Project exhibits in the Twin Lakes Shear Zone and the AZ Shear Zone, which are splays of the crustal-scale Stull-Wunnumin Fault Zone. The mineralization event occurred during ~2706--2696 Ma with the main mineralization mechanism by cooling reduced mineralizing fluid. The observable tungsten mineralization reveals intrusion-related mineralization. In 2016, McCracken and Thibault summarized three modes of gold mineralization in this area in the technical report: 1) Quartz-tourmaline±pyrite-arsenopyrite-pyrrhotite veins; 2) Smoky quartz±pyrite-pyrrhotite-arsenopyrite-chalcopyrite veins; 3) Quartz-albite-ankerite-scheelite±pyrite-arsenopyrite-sphalerite-chalcopyrite-galena-stibnite veins. The first type of vein is typically concentrated on the quartz-feldspar porphyritic dyke and the trend of the high-grade gold-tungsten mineralization zone is subparallel to parallel with the trend of surrounding volcanic and sedimentary rocks. The porphyritic dyke with brecciated structure and filled with quartz veins formed the core of the Twin Lakes Deposit. Thus, it became the more competent rock compared with volcanic and sedimentary rocks and speeded up the brittle deformation. Surrounding rocks have a similar structure to the dyke, and silicification and brecciation are typical. The second type generally has higher sulphide content, but lower gold content than the first type. The shear veins typically appear on the more ductile contacts contrasted with the broad brecciated dykes. Alteration is less intense than the first type but more adjacent to the veins. The third type is high-grade intense veins, which is the most common and dominant mineralization form in the intermediate-felsic intrusive quartz-feldspar porphyry rocks in the Monument Bay Project. Alteration is also proximal to the veins.

The gold-tungsten mineralization in the Twin Lakes Deposit is mainly hosted in quartz-carbonate-albite-scheelite veins in a strong sericite altered and silicified rock (McCracken & Thibault, 2016). The mineralization spreads into felsic-intermediate tuff and intermediate feldspar phyric volcanic flow in the Oxford Lake Group. U-Pb dating indicated the age of the host porphyry in the Twin Lakes Deposit is 2706 ± 2.8 Ma and the age of gold tungsten mineralization is 2706-2696 Ma (McCracken & Thibault, 2016). The Mid-East Deposit has similar mineralization characteristics

and host rock to the Twin Lakes Deposit, but the gold grade is lower and tungsten mineralization is less. As for the AZ Deposit, there is no tungsten mineralization observed. The gold mineralization of the AZ Deposit has the same vein style as the other two deposits, but the host rock is conglomerates of the Cross Lake Group. The sulphide content in the AZ Deposit is commonly lower compared with the other two deposits and declines with increasing silicification. The sulphide content drops to trace amounts in some regions of the AZ deposit (McCracken & Thibault, 2016).

2.3.5 Metallurgy

Bema Gold Corporation accomplished a metallurgical test program to recover gold from varied targets within the Twin Lakes Deposit in 2005. Mega started additional metallurgical testing for both gold and tungsten recovery from gold zones and gold-tungsten zones in the deposit in 2013 and 2015. The study of gold deportment illustrated that gold in the Twin Lakes Deposit dominantly presents as native gold with trace electrum and kustelite. They used pre-concentration by flotation, direct cyanidation of the ore, cyanidation of flotation concentrate, and pressure oxidation of flotation concentrate to evaluate the extraction of gold. 80% of gold grains are finer than 50 μm and the size of the coarsest gold grain is 62 μm . In the test samples, gold generally occurs as visible gold exposed or attached on non-sulphides (50.7%, mainly silicates), free gold (21.8%), visible gold locked in non-sulphides (12.7%), visible gold exposed or attached on sulphides (9.9%, e.g. pyrite and arsenopyrite), visible gold locked in sulphides (2.9%), and refractory gold (2.0%). 94% visible gold locked in non-sulphides can be extracted by grinding to <8 μm , while 76% visible gold locked in sulphides can be extracted by grinding to <8 μm . There However, as the grains of scheelite are too fine, gravity recovery cannot be used. Thus, for the gold-tungsten zone, bulk sulphide flotation can be used to concentrate gold + sulphides, and then apply pressure oxidation and cyanidation to recover gold. Afterward, tungsten recovery has the best performance using flotation after sulphide flotation. is a strong positive correlation between the concentration of refractory gold and the concentration of arsenic. In the samples with both gold and tungsten, scheelite is the form of tungsten. However, as the grains of scheelite are too fine, gravity recovery cannot be used. Thus, for the gold-tungsten zone, bulk sulphide flotation can be used to concentrate gold + sulphides, and then apply pressure oxidation and cyanidation to recover gold. Afterward, tungsten recovery has the best performance using flotation after sulphide flotation.

Chapter 3

3 Methods

3.1 Sampling Program

In October 2016, Cavallin collected forty quartered drill core samples with a length ~25cm from sixteen drill holes. The samples were collected across three main mineralized zones including the Twin Lakes (TL) Zone, the AZ Zone, and the Mideast (ME) Zone. In order to make the sample selection more comprehensive, another sampling program in October 2018 was aimed to get a real distribution across the property and not only limited to mineralized zones but also the surrounding area without mineralization. Casali made a pre-sampling plan based on Yamana's logging database and conducted one-week sampling at the Monument Bay campsite. The core log and assay database include drill core ID, sample ID, location (mineralized zones), gold and tungsten concentration, and lithological characteristics. The samples were collected to ensure at least one sample across different mineralized zones, with different alteration and rock types, a variety of gold grade, and the presence of sulphides and veining. According to the pre-sampling plan, seventy half drill core samples with the length ~25cm from twenty drill holes were collected by Casali at the Twin Lakes (TL) Zone, the Twin Lakes West (TLW) Zone, the Twin Lakes East (TLE) Zone, the Mideast (ME) Zone, the South Limb Shear (SLS) Zone, and the AZ Zone.

After the new sample selection was transported to Western University, the author carefully looked into all of the samples and core logs of both Cavallin's previous sample selection and Casali's new sample selection. Considering the main goal of this research is about gold mineralization and geometallurgy, the author decided to focus on the analytical program on high gold grade samples (>1 ppm). In addition, the low gold grade samples are all located outside mineralization. Thus, low gold grade samples are not appropriate for the study. As a result, 31 drill core samples with high gold grade (>1 ppm) were selected from 17 different drill holes. There are 13 samples from the Twin Lakes (TL) Zone, 14 samples from the Twin Lakes West (TLW) Zone, 2 samples from Mid-East (ME) Zone, 2 samples from South Limb Shear (SLS) Zone, 1 sample from AZ Zone (Figure 3-1). The average gold grade is 3.316 g/t.

The drill core samples were photographed with a scale, systematically described and classified according to rock types at the Laboratory for Stable Isotope Science (LSIS). The description included color, texture, structure, alteration type, and major ore minerals observed using a 20X magnifying hand lens. All samples were tested using hydrochloric acid (HCl) to determine if they contained carbonate minerals. Table 3-1 summarizes the locations of each sample, gold and tungsten grades, and lithology identified in the mining log. The detailed drill core photos and descriptions are shown in Appendix A. Low gold grade samples are listed in Appendix B as well.

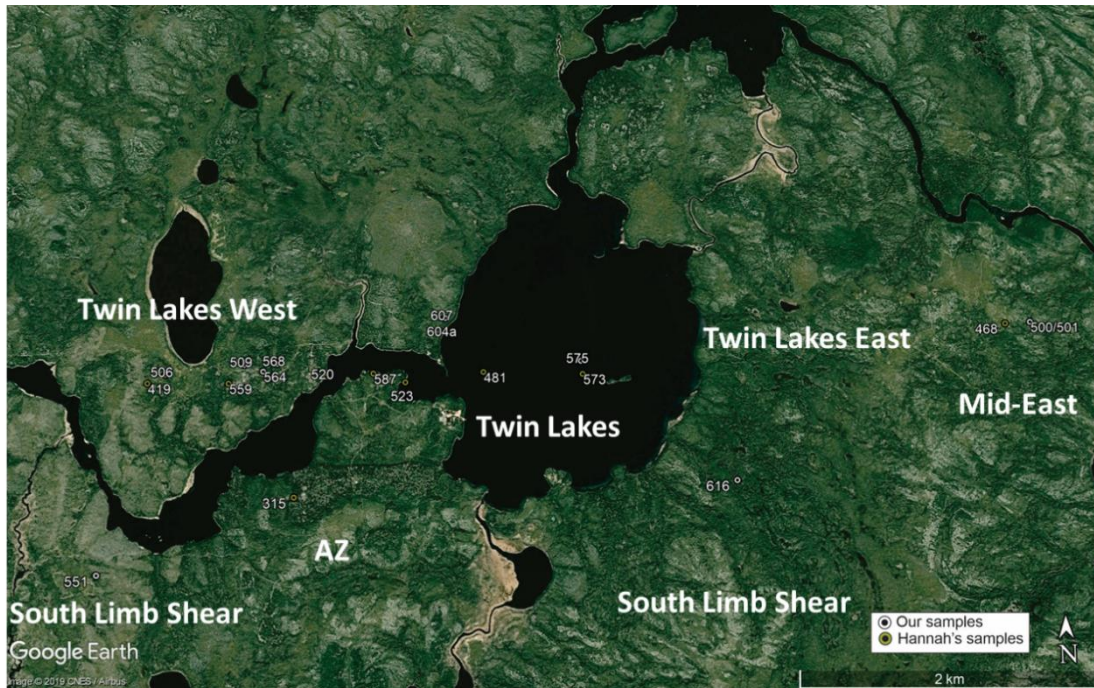


Figure 3-1. Satellite image of geographical locations of targets and selected samples in the Monument Bay Project. The white points are the new sample section and green points are the previous sample section (modified from Google Earth by Casali and Hao in 2019).

Table 3-1. High Gold Grade Drill Core Sample Selection at the Monument Bay Project

Hole ID	Western Sample ID	Sampled From	Sampled To	Target	Au Grade (ppm)	W Grade (ppm)	Lithology (by Yamana)
TL-03-160	E5551530	180.1	181.1	ME	2.61	50	Felsic Metavolcanics: Heterolithic Tuff
TL-06-315	E5551544	125.7	126.39	AZ	2.86	NA	Clastic Metasediments: Conglomerate
TL-11-419	E5551535	83	84	TLW	4.969	NA	Clastic Metasediments: Siltstone
TL-11-419	E5551536	84	85	TLW	3.435	NA	Clastic Metasediments: Siltstone
TL-11-419	E5551540	88	89	TLW	1.556	NA	Intermediate-Felsic Intrusives: Feldspar Porphyry
TL-11-419	E5551541	89	90	TLW	2.816	NA	Intermediate-Felsic Intrusives: Feldspar Porphyry
TL-11-419	E5551542	90	91	TLW	3.541	NA	Felsic Metavolcanics: Lapilli Tuff
TL-11-419	E5551543	91	92	TLW	4.135	NA	Felsic Metavolcanics: Lapilli Tuff
TL-12-468	E5551526	243	244	ME	1.112	NA	Intermediate Metavolcanics: Ash Tuff
TL-12-481	E5551532	90	91	TL	3.463	NA	Intermediate-Felsic Intrusives: Feldspar Porphyry
TL-12-481	E5551533	99	100.1	TL	13.22	NA	Intermediate-Felsic Intrusives: Feldspar Porphyry
TL-13-500	E5552834	195.76	196	ME	5.21	50	Intermediate Metavolcanics: Lapilli Tuff
TL-13-504	E5552841	190.5	190.78	TLW	25.2	520	Intermediate-Felsic Intrusives: Feldspar Porphyry
TL-13-506	E5551515	164	164.7	TLW	1.533	50	Intermediate-Felsic Intrusives: Feldspar Porphyry
TL-13-506	E5551516	164.7	165.6	TLW	4.96	320	Chemical Metasediments: Oxide Facies IF
TL-13-509	E5552845	235.6	235.86	TLW	1.13	50	Intermediate-Felsic Intrusives: Quartz-Feldspar Porphyry
TL-14-520	E5551521	59	60	TLW	6.597	NA	Intermediate-Felsic Intrusives: Feldspar Porphyry
TL-14-523	E5551513	101	102.05	TL	7.568	2140	Intermediate Metavolcanics: Undifferentiated
TL-14-523	E5551514	105.42	106	TL	5.702	2240	Intermediate-Felsic Intrusives: Feldspar Porphyry
TL-15-551	E5552831	96.8	97	SLS	2.26	NA	Clastic Metasediments: Sandstone
TL-15-559	E5551523	114.4	115.1	TLW	1.6	315	Intermediate-Felsic Intrusives: Feldspar Porphyry
TL-15-564	E5552827	183	183.23	TL	close to 9 - ~0.6	124	Intermediate-Felsic Intrusives: Quartz-Feldspar Porphyry
TL-15-568	E5552824	200.62	200.82	TLW	1.91- ~8.25	50	Intermediate-Felsic Intrusives: Feldspar Porphyry
TL-16-573	E5551517	49	50	TL	8.457	145	Intermediate-Felsic Intrusives: Feldspar Porphyry
TL-16-573	E5551518	56	57	TL	5.372	50	Intermediate-Felsic Intrusives: Feldspar Porphyry
TL-16-573	E5551519	57.7	59	TL	1.79	50	Intermediate Metavolcanics: Lapilli Tuff
TL-16-575	E5552819	154.1	154.32	TL	7.21	50	Intermediate-Felsic Intrusives: Feldspar Porphyry
TL-16-575	E5552821	183.78	184.06	TL	3.38	50	Intermediate Metavolcanics: Ash Tuff
TL-16-587	E5551511	252.6	253.4	TL	2.289	50	Intermediate-Felsic Intrusives: Feldspar Porphyry
TL-16-604A	E5552853	643.96	644.24	TL	7.73	442	Intermediate-Felsic Intrusives: Feldspar Porphyry
TL-16-604A	E5552854	729.02	729.2	TL	10.49	2705	Felsic Metavolcanics: Undifferentiated Tuff
TL-16-607	E5552857	718.4	718.66	TL	2.16	1055	Intermediate-Felsic Intrusives: Feldspar Porphyry
TL-16-607	E5552858	817.4	817.6	TL	2.45	50	Intermediate Metavolcanics: Lapilli Tuff
TL-17-616	E5552360	148.6	148.8	SLS	1.2-0.01	NA	Intermediate Metavolcanics: Lapilli Tuff

*Samples in Table 3-1 are listed by the Hole ID. “Intermediate-Felsic Intrusives: Feldspar Porphyry” samples are labeled in blue, “Intermediate-Felsic Intrusives: Quartz-Feldspar Porphyry” samples are labeled in yellow, “Intermediate Metavolcanics” are labeled in green, “Felsic Metavolcanics” are labeled in pink, and “Clastic Metasediments” are labeled in purple. TW=Twin Lakes, TLE=Twin Lakes East, TLW=Twin Lakes West, SLS=South Limb Shear, ME=Mideast.

3.2 Optical Microscopy

Based on the drill core sample descriptions, 11 high gold grade drill core samples from the new sample group were chosen for petrographic analysis. The selection of regions of interest on drill core samples aimed to analyze the representative area of each high gold grade samples with typical foliation, veins, alteration, and/or sulphide distribution. When possible, the regions of interest were selected to avoid destroying the integrity of the drill core samples. In this way, the rest of the drill core samples after cutting could be used in Synchrotron Micro X-Ray Fluorescence (SR- μ XRF) mapping. A water-cooled Mk Diamond Tipped Tile Saw was used to cut the offcuts from the drill core samples in the Rock Preparation Laboratory at Western University. Polished thin sections and polished offcuts were prepared by Stephen Wood in the same laboratory.

46 polished thin sections (11 samples from new sample group and 35 from previous group) were observed under plane-polarized transmitted light (PPL), cross-polarized transmitted light (XPL), and reflected light (RL) using an optical Nikon LV100POL microscope in the Earth and Planetary Materials Analysis Laboratory at Western University. The optical microscope was equipped with five objective lenses (2.5x, 5X, 10X, 20X, and 50X) and a 10x optical eyepiece. The observation under PPL and XPL was used to identify the minerals and their modal percentages, veining, textures, and alteration, whereas the observation under RL could provide information about sulphide morphology and gold mineralization. Regions of interest including various sulphide morphologies and microscopic gold grains were marked and photographed under RL for EPMA. The photomicrographs were taken by a Nikon DS-Ri1 digital camera mounted on the microscope via the imaging software Nikon NIS-Elements D3.2 (Figure 3-2). The detailed petrographic descriptions for each polished thin section are shown in Appendix A.



Figure 3-2. The Nikon LV100POL microscope mounted with Nikon DS-Ri1 digital camera used for petrographic analysis in the Earth and Planetary Materials Analysis Laboratory at Western University.

3.3 Synchrotron X-ray Diffraction (SR-XRD)

X-ray Diffraction technique is based on Thomson scattering, which can be regarded as an elastic interaction between electromagnetic radiation and electrons. A scattering of X-rays by the atoms of a crystal produces an interference effect so that the diffraction pattern gives information on the structure of the crystal or the identity of a crystalline substance. By searching/matching the diffraction pattern with the crystallographic databases, the mineral phase can be identified (Lavina et al., 2014). Synchrotron X-ray Diffraction (SR-XRD) is useful in identifying the crystalline structure of minerals in powder rock samples and pulps and quantifying the proportions of different minerals (Pecharesky & Zavalij, 2005). SR-XRD can provide more information about gangue and alteration assemblages, which are hard to identify using an optical microscope.

3.3.1 SR-XRD Sample Preparation

SR-XRD studies were performed on pulps and powder rock samples. 83 Pulp rejects were supplied by Yamana Gold Inc. and shipped to Western University. And five half drill core samples in the new sample selection were ground into powder at Rock Cutting and Thin Section Laboratory at Western University. Pulps and powder rock samples were prepared at Laboratory for Stable Isotope Science at Western University (Figure 3-3A). Before preparing each sample, the mortar and pestle were cleaned using acetone to avoid cross-contamination between samples. Each sample was packed in 2 cm-long polyimide capillary tubes with an outside diameter of 5.5 mm and an inside diameter of 5.0 mm. Capillary tubes were filled carefully by poking the capillary tubes into a little powder sample in the mortar. After making sure there was no empty space in the capillary tubes checked under light, a little quick-drying epoxy was used to seal both sides of the capillary tubes. The quick-drying epoxy was not allowed to coat the outside of capillary tubes or the capillary would not fit into the base. The quick-drying epoxy on the capillaries which is not dried enough might ruin the reusable bases. Filled and sealed capillaries were tightly mounted inside MiTeGen B3S ALS-style reusable bases (Figure 3-3B). Unsecured capillaries might slide out from the bases or cause centering problems in the experiment. The SSRL-style sample cassette with 8X12 sample slots was used as a container to store the samples, and each slot has a unique code with a capital letter and a number (e.g. A1) for labeling (Figure 3-3C). Generally, three lanthanum hexaboride (LaB_6) standards were loaded in the cassette along with eighty to ninety-three duplicates of pulps and powder rock samples. In the filling and mounting steps, capillary tubes were treated gently, and any rusted or bent sample mounts needed to be avoided. Otherwise, it would cause a bad quality of data collection. A spreadsheet was made for recording sample code and sample ID and uploaded via MxLIVE (<https://mxlive.lightsources.ca/login/?next=/>). The filled cassettes were well-packed with bubble paper in a box and shipped to the CMCF at least one week before the SR-XRD experiments.

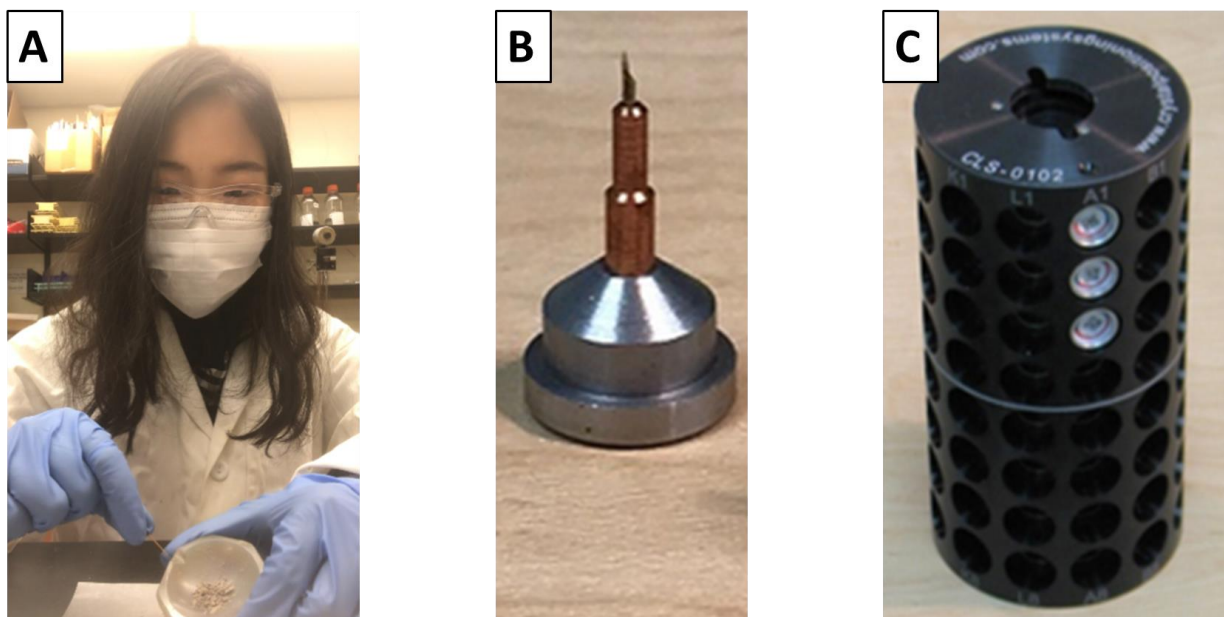


Figure 3-3. Illustrating SR-XRD sample preparation at Laboratory for Stable Isotope Science at Western University. A. The author was filling powder sample in capillary tubes. B&C. MiTeGen B3S ALS-style reusable bases and SSRL-style sample cassette required at the CMCF for SR-XRD data collection.

3.3.2 Experiment Setup and Remote-Controlled Data collection at the CMCF

In this research, SR-XRD on powder rock samples were examined at the Canadian Macromolecular Crystallography Facility (CMCF) at the Canadian Light Source (CLS) in Saskatoon, Saskatchewan, in July 2019, August 2019, and March 2020. CMCF operates two beamline, 08ID-1 (CMCF-ID) and 08B1-1 (CMCF-BM), providing high-resolution macromolecular crystallography experiments (Fodje et al., 2020). Both beamlines now operate automatically and manually together, and data collection is controlled remotely by users via MxLIVE (Mx Laboratory Information Virtual Environment), the CMCF online sample, and data management software. CMCF-BM was the beamline used for this research.

At the beginning of the beamtime, the cassettes were loaded into the automounting robot by the beamline scientist responsible for supporting the beamtime. Once the cassettes were loaded, all handling and data collection was done remotely from UWO. MxDC is the operating system at the CMCF for experiment setup and data collection, remotely controlled by NoMachine software (<https://www.nomachine.com/>). In the Setup tab of MxDC, the parameters of the SR-XRD experiment could be set up and the camera inside the hutch could be used to check the status of

the machine and make sure no one inside the hutch before turning on the beam (Figure 3-4). A Rayonix MX300HE CCD X-ray detector was used to collect data. The experimental parameters were set up with the beam energy of 18 keV and the detector distance of 250 mm (Figure 3-5). The detector pixel size of 0.732 μm . In the Samples tab of MxDC, the sample list loaded before the experiment showed up (Figure 3-6). Samples could be remotely mounted, dismounted, and centered, and the Epson robotic arm would follow the request and mount samples from the cassettes. In the Data tab, the mounted sample would be automatically displayed, and the total frame was set as 24 (Figure 3-7). The resolution of the experiments in August and March were 1.29 \AA with a beam aperture of 150 μm , while the resolution of the experiment in July was 1.6 \AA resolution with a beam aperture of 250 μm . The sample was rotated 180° in each frame and the exposure time for each frame was 5 seconds. The parameter setting was important in collecting representative peaks for each side of the powder sample in capillaries. All data was calibrated using a standard for powder diffraction, lanthanum hexaboride (LaB_6) from US Research Nanomaterials, Inc. The LaB_6 standard provides the correct experimental parameters including detector distance. LaB_6 was analysed several times at the beginning, the middle, and the end of each beamtime. The data was calibrated automatically by MxDC live software using one frame of LaB_6 . Sometimes automatic data calibration was not proper, the data needed to be recalibrated manually using GSAS-II (Toby & Von Dreele, 2013).

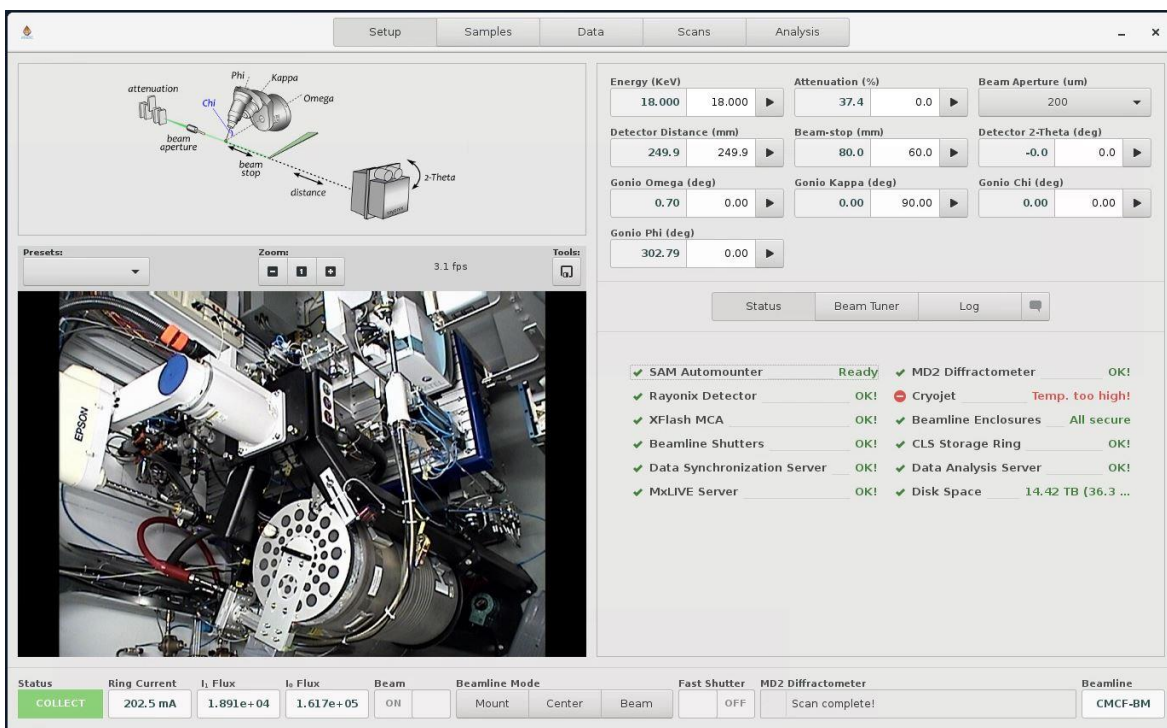


Figure 3-4. Showing typical control panel of Setup tab in MxDC remotely controlled via No machine. The Setup is used to set up experiment parameters.

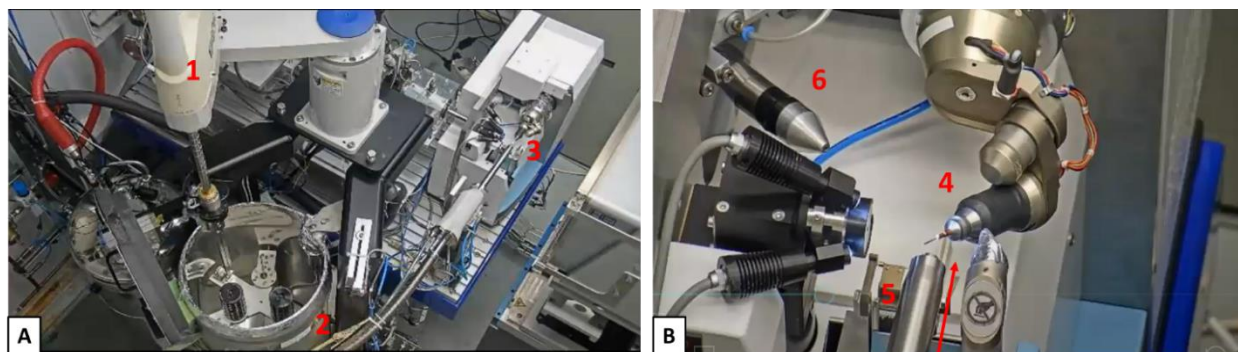


Figure 3-5. The typical experimental setup inside the hutch of CMCF-BM Beamline. A. The robotic arm (1) moves capillary sample and its base from the cassette (2) and mounts it close to the beam (3). B. The capillary sample (4) is examined close to the beam (5). The arrow shows the direction of beam and the signal is collected by the Rayonix MX300HE CCD X-ray detector (6).

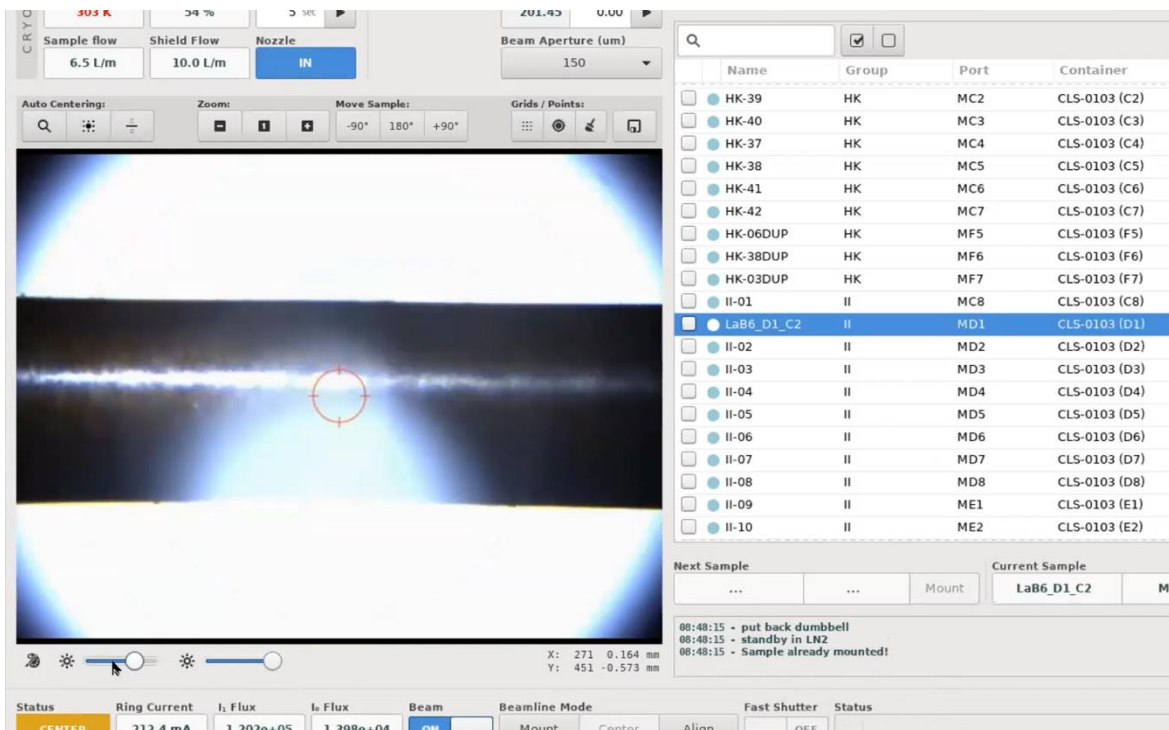


Figure 3-6. Showing typical control panel of Samples tab in MxDC remotely controlled via No machine. The capillary of LaB6_D1_C2 is centering on the left and the sample list was listed on the right in the order of port cord.

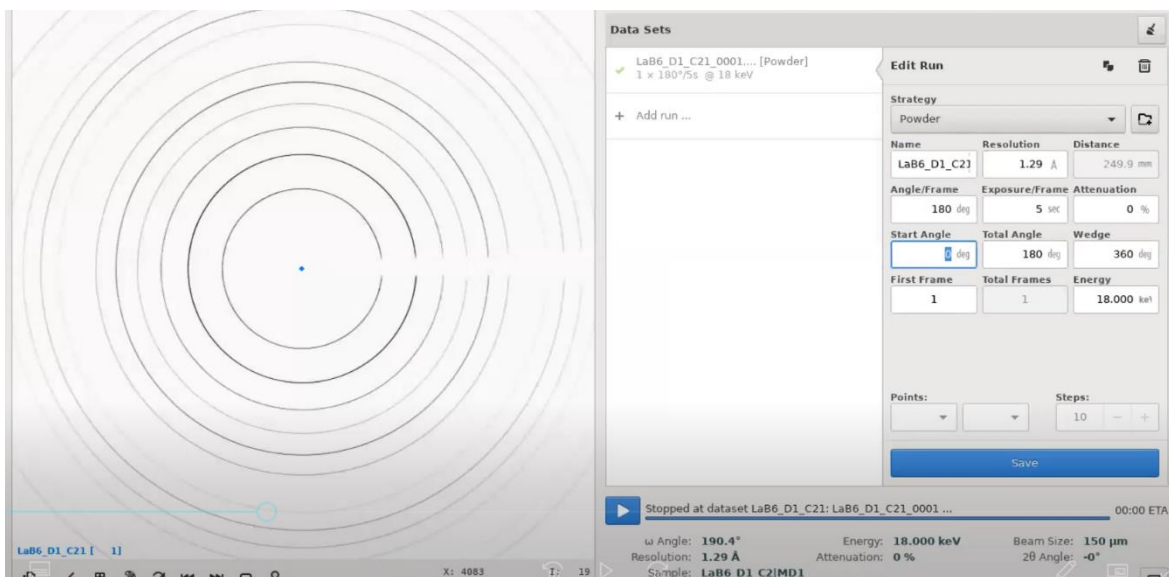


Figure 3-7. Showing typical control panel of Data tab in MxDC remotely controlled via No machine. The left side shows a frame of the dataset and the right side shows the data collection settings.

3.3.3 SR-XRD Data Processing

Once the SR-XRD data has been collected in the beamline, raw data files can be downloaded from MXLive data storage site. LaB₆ standard processed the same day as the other data (under the same conditions) was used for manual calibration using GSAS-II (Toby & Von Dreele, 2013). LaB₆.tar file including the images of all frames need to be extracted into img. Files. One of the frames was converted from .img data to .tiff file in calibration. After loading calibration controls, copying controls, and integrating all data in GSAS-II, .XDI files can be exported and processed by DIFFRAC.EVA software (Bruker, 2018). DIFFRAC.EVA is a common software for peak evaluation on diffractograms and quantitative analysis of mineral abundance. The background subtraction was used before peak matching to remove interferences and noise and enhance the accuracy of peak matching. The International Centre for Diffraction Data's PDF-2001 database was applied in all samples to identify minerals present in the bulk samples. In peak matching, the subfile called "Mineral" was the only selected subfile. After peak fitting, semi-quantitative mineralogical pie charts can be automatically generated by DIFFRAC.EVA. Major mineral phases were identified according to the best matches to the peaks, while minor mineral phases were selected based on both the peak fitting and the mineralogy information from microscopy and EPMA experiments. The detailed SR-XRD data diffractograms and descriptions are shown in Appendix C.

3.4 Synchrotron Micro X-Ray Fluorescence (SR- μ XRF) mapping

When a normal temperature material is irradiated by X-ray, the electrons on the surface enter the excited state after absorbing the light energy, and immediately deexcite and release energy. The de-excitation process is X-Ray Fluorescence (XRF) and the release of energy in the form of a fluorescent X-ray (Eichert, 2015). Conventional XRF has been widely used in geochemical studies. However, SR-XRF has faster analysis and more sensitive, because SR X-ray is more intense, highly collimated, and linearly polarized (Quartieri, 2015). As the geological materials are inorganic and limited interacted with hard X-rays, SR-XRF causes no damage to rock samples at all during the experiments (Quartieri, 2015). Thus, SR-XRF is a cutting-edge geochemical analytical method in Earth Sciences.

SR-XRF mapping provides rapid simultaneous spectro-chemical identification of multiple trace elements and mapping of minerals at scales ranging from centimeters to sub-micron and at ppm (10^{-6}) levels (Buffiere & Baruchel, 2015). Full-spectra MCA SR- μ XRF raw data were collected on regions of interest. The raw data can be processed into XRF spectrums and trace elemental maps using Peakaboo (Van Loon et al., 2019). The pixels obtained from the ensemble of pixel collections represent contrasts and the relevant higher and lower detected signal intensity result in the distinguishable distribution in trace element maps (Buffiere & Baruchel, 2015).

3.4.1 SR-XRF Sample Preparation

Before each beamtime, a General User Proposal (GUP) was needed to explain the purpose and importance of the research, reasons for the specific beamline, requested instruments, previous experience with synchrotron radiation and results, description of experiments, the estimated amount of beamtime, number of visits, and number of shifts. After the approval, the beamline scientists helped to schedule beamtime and shifts. Each shift was 8 hours and there were three shifts per day. Typically, an SR-XRF mapping GUP was given 9 shifts (3 days). Based on the number of shifts received, a detailed plan was drawn up based on map size, spot size, dwell time, and estimation of mapping time. Samples with high gold grades and good integrity were the priority. For half drill core samples, the sizes of maps were 10 cm x 3.5 cm, 8cm x 3.5 cm, 4 cm x 3.5 cm, and 3 cm x 3.5 cm depending on the length of the drill cores. And mapping areas were marked on the surface.

3.4.2 SR-XRF Data Collection

Synchrotron Micro X-Ray Fluorescence (SR- μ XRF) mapping is a powerful method to provide high-resolution trace elemental variation maps of the flat surface of half drill core samples and a subset of the rock offcuts that were left after making thin sections. Synchrotron Micro X-Ray Fluorescence (SR- μ XRF) raw data was collected at 20ID and 8BM beamlines at the Argonne National Laboratory (APS) in Chicago, USA, and the VESPERS beamline at the Canadian Light Source (CLS) in Saskatoon, Canada. 24 samples have been analyzed in total, including 11 offcuts and 13 drill-core samples. The aim of each experiment was slightly different: 1) the experiments in February 2019 at the 20ID Beamline at the APS and March 2019 at the 8BM Beamline at the APS were to do large-scale SR-XRF mapping on the surface of drill core samples; 2) the

experiment in February 2019 at the VESPERS beamline at the CLS was to do small-scale higher-resolution SR-XRF mapping of select sulphides grains; 3) the experiment in July 2019 at the 20ID Beamline at the APS was to do small-scale higher-resolution SR-XRF mapping of high-intensity gold spots which were identified from previous large-scale SR-XRF element maps. Eight raw data collected on offcuts from previous sample selection by Cavallin in 2015 at CLS IDEAS Beamline has been reprocessed and reanalyzed as well (Table 3-2). The parameters for SR-XRF mapping were listed in Table 3-3.

Table 3-2. SR- μ XRF Mapping Data Collection

Hole ID	Western Sample ID	Lithology (by Yamana)	Au Grade (ppm)	Target	800 μ m 20ID APS Feb 2019	300 μ m 20ID APS Feb 2019	10 μ m VESPERS CLS Feb 2019	100 μ m VESPERS CLS Feb 2019	500 μ m 8BM March 2019	60 μ m APS July 2019	Cavillin's - CLS IDEAS
TL-16-575	E5552819	Intermediate-Felsic Intrusives: Feldspar Porphyry	7.21	TL	Core & Offcut	Offcut			Core & Offcut	Core: ABC	
TL-15-568	E5552824	Intermediate-Felsic Intrusives: Feldspar Porphyry	1.91-~8.25	TLW	Offcut	Offcut	Offcut	Offcut			
TL-13-504	E5552841	Intermediate-Felsic Intrusives: Feldspar Porphyry	25.2	TLW	Core & Offcut	Offcut	Offcut	Offcut	Core & Offcut		
TL-16-604A	E5552853	Intermediate-Felsic Intrusives: Feldspar Porphyry	7.73	TL	Core & Offcut	Offcut			Core & Offcut		
TL-16-607	E5552857	Intermediate-Felsic Intrusives: Feldspar Porphyry	2.16	TL	Core & Offcut	Offcut		Offcut	Core & Offcut		
TL-15-564	E5552827	Intermediate-Felsic Intrusives: Quartz-Feldspar Porphyry	close to 9 - ~0.6	TLW	Core & Offcut	Offcut	Offcut	Offcut	Core		
TL-13-509	E5552845	Intermediate-Felsic Intrusives: Quartz-Feldspar Porphyry	1.13	TLW	Core & Offcut	Offcut	Offcut	Offcut	Offcut		
TL-16-587	E5551511	Intermediate-Felsic Intrusives: Quartz-Feldspar Porphyry	2.289	AZ							Offcut
TL-16-573	E5551517 A	Intermediate-Felsic Intrusives: Quartz-Feldspar Porphyry	8.457	TL							Offcut
TL-15-559	E5551523	Intermediate-Felsic Intrusives: Quartz-Feldspar Porphyry	1.6	TLW							Offcut

Hole ID	Western Sample ID	Lithology (by Yamana)	Au Grade (ppm)	Target	800µm 20ID APS Feb 2019	300µm 20ID APS Feb 2019	10µm VESPERS CLS Feb 2019	100µm VESPERS CLS Feb 2019	500µm 8BM March 2019	60 µm APS July 2019	Cavillin's - CLS IDEAS
TL-16-573	E5551518	Intermediate-Felsic Intrusives: Quartz-Feldspar Porphyry	5.372	TL							Offcut
TL-12-481	E5551533 A	Intermediate-Felsic Intrusives: Quartz-Feldspar Porphyry	13.22	TL							Offcut
TL-12-481	E5551533 B	Intermediate-Felsic Intrusives: Quartz-Feldspar Porphyry	13.22	TL							Offcut
TL-13-500	E5552834	Intermediate Metavolcanics: Lapilli Tuff	5.21	ME	Core & Offcut	Offcut	Offcut	Offcut	Offcut		
TL-16-575	E5552821	Intermediate Metavolcanics: Ash Tuff	3.38	TL	Core						
TL-16-607	E5552858	Intermediate Metavolcanics: Lapilli Tuff	2.45	TL	Core & Offcut	Offcut					
TL-17-616	E5552360	Intermediate Metavolcanics: Lapilli Tuff	1.2 - 0.01	TLE					Core		
TL-16-604A	E5552854	Felsic Metavolcanics: Undifferentiated Tuff	10.49	TL	Core & Offcut	Offcut	Offcut	Offcut	Core & Offcut	Core: AB	
TL-15-551	E5552831	Clastic Metasediments: Sandstone	2.26	SLS	Core & Offcut	Offcut			Core & Offcut	Core: ABC	
TL-13-506	E5551516 A	Chemical Metasediments: Oxide Facies IF	4.96	TLW							Offcut
TL-06-315	E5551544 A	Clastic Metasediments: Conglomerate	2.86	SLS							Offcut

* “Intermediate-Felsic Intrusives: Feldspar Porphyry” samples are labeled in blue, “Intermediate-Felsic Intrusives: Quartz-Feldspar Porphyry” samples are labeled in yellow, “Intermediate Metavolcanics” are labeled in green, “ Felsic Metavolcanics” are labeled in pink, and “Clastic Metasediments” are labeled in purple.

Table 3-3. Parameters for SR-XRF Mapping (Beam energy was set to allow excitation of elements of interest).

Beamline	APS-20ID	APS-8BM	CLS-VESPERS
Energy (keV)	27	15	13
Map Resolution (µm)	500 and 300	800	100 and 10
Type of sample	Half Drill Core & Offcuts	Half Drill Core & Offcuts	Offcuts
Spot Size (µm)	500	500	Pink Beam: 5-6 µm MonoBeam: 10-12 µm
Dwell time (msec)	250	200, 150, 100, 250	1000, 2000
Map Sizes (cm)	10X3.5 to 4X3.5, and offcuts 3X4 cm	10X4 to 10X7 and offcuts 3X4 cm	3X3, 2X4, and random size on visible sulfide grains on offcuts
Detector	XSP3 four- element detector (February) and Vortex four- element Si drift detector (July)	Vortex four-element Silicon Drift Detector	Vortex four-element silicon drift detector

3.4.2.1 Data collection at APS 20ID beamline in February and July 2019

As a third-generation light source with optimized insertion devices, APS provides high-intensity X-ray with energy up to 7 GeV. 20ID beamline provides a microprobe setup using Kirkpatrick–Baez (KB) mirror-based X-ray microprobe and Si (111) monochromator (Heald et al., 2007). At the end station, a 4-element silicon drift detector (the XSP3 detector in February 2019 or the Vortex-ME4 detector in July 2019) was used to collect the fluorescent signal during the SR-XRF mapping experiment. The sample was positioned approximately 15 cm to the incident beam. The detector was positioned at ~ 45 degrees to the sample. The experiment was conducted in an open-air environment (Figure 3-8).

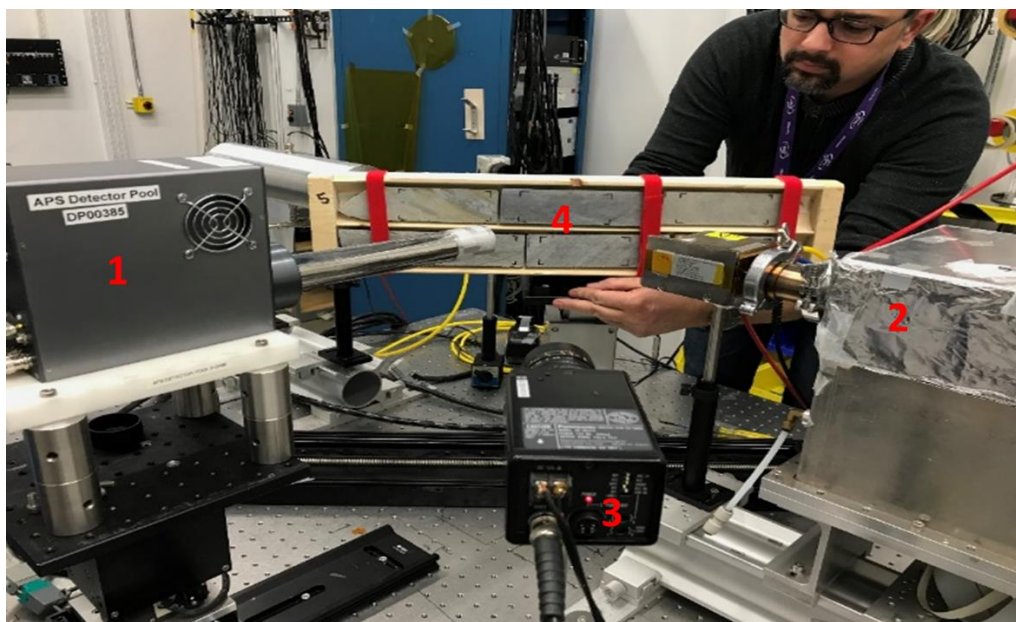


Figure 3-8. Experimental station setup in the hutch at APS 20ID beamline. (1) XSP3 four- element detector; (2) Beam Source; (3) Camera; (4) Half drill core samples mounted on the wooden sample holder (February 2019).

In February, the incident energy was set to 27 keV. The data was collected in the two-dimensional Quick-Scan mode with a spot size of $800\mu\text{m} \times 800\mu\text{m}$ and $300\mu\text{m} \times 300\mu\text{m}$, a step size of $800\mu\text{m}$, and dwell times of 250 msec. Before analysing samples, NIST SRM 610, 612, and 614 were used to ensure that the conditions were the same in different beamtimes. Trace element maps were produced to follow in real-time by setting specific ROIs for the elements of interest: K $K\alpha$, Ca $K\alpha$, Ti $K\alpha$, Cr $K\alpha$, Mn $K\alpha$, Fe $K\alpha$, Ni $K\alpha$, Cu $K\alpha$, Zn $K\alpha$, Au $L\alpha$, As $K\alpha$, Se $K\alpha$, Mo $K\alpha$, Pd $K\alpha$, Ag $K\alpha$ and total sum (Figure 3-9). To be noted, the ROI's were set to check if the data collection was proper and did not exceed the detection limits, but the raw data was collected as full spectrum MCA data and analyzed later.

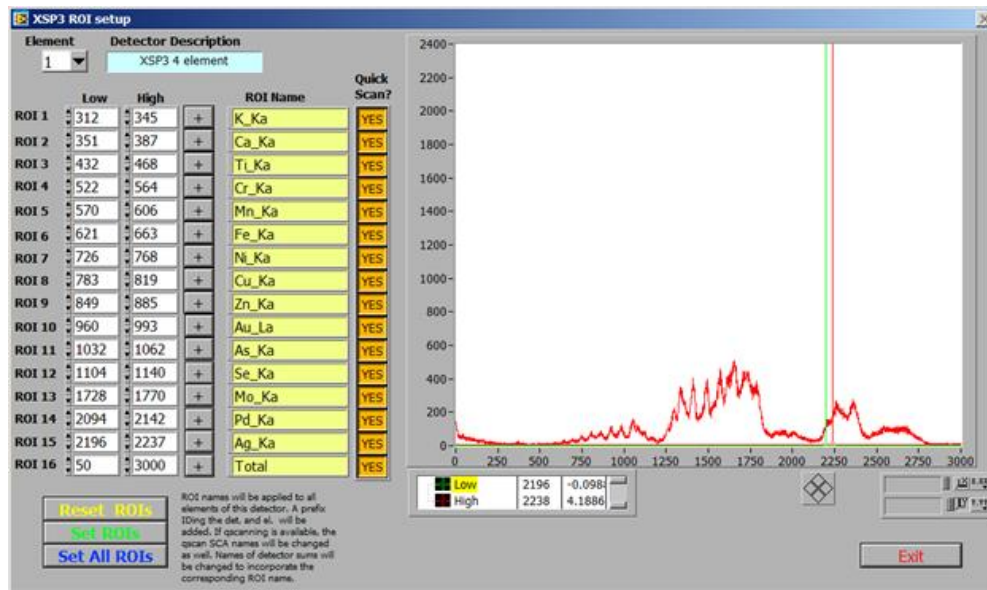


Figure 3-9. ROI Setup in APS 20ID beamline (February 2019).

In July, the incident energy was set to 13 KeV. The data was collected in the two-dimensional Quick-Scan mode with a spot size of 60 μm x 60 μm , a step size of 150 μm , and dwell times of 200 msec. Trace element maps were produced on the monitors in the beamline by setting specific ROIs for the elements of interest: K $\text{K}\alpha$, Ca $\text{K}\alpha$, Ti $\text{K}\alpha$, Cr $\text{K}\alpha$, Mn $\text{K}\alpha$, Fe $\text{K}\alpha$, Ni $\text{K}\alpha$, Cu $\text{K}\alpha$, Zn $\text{K}\alpha$, Au $\text{L}\alpha$, As $\text{K}\alpha$, Se $\text{K}\alpha$, and total sum (Figure 3-10).

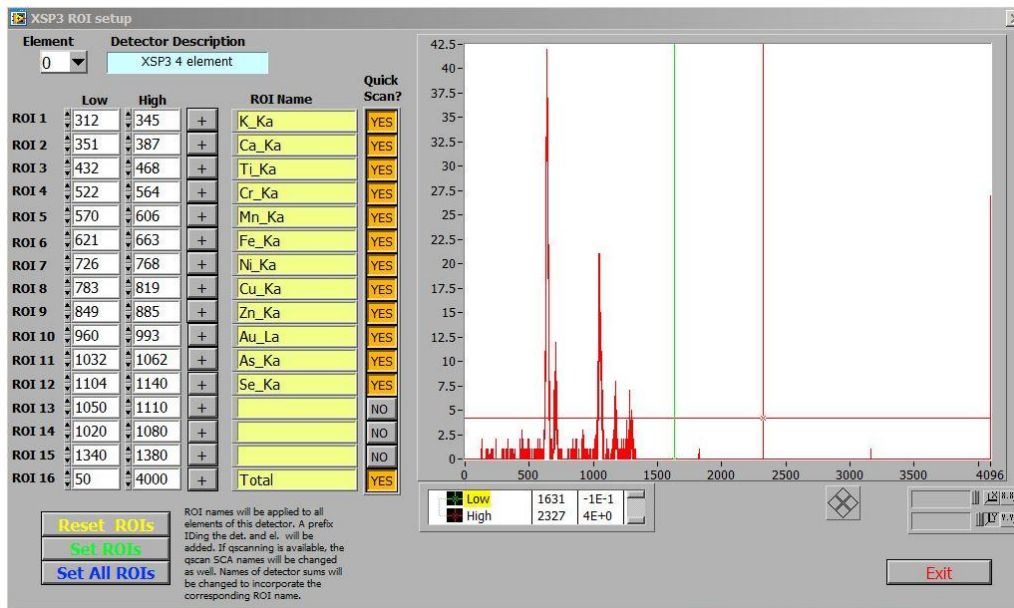


Figure 3-10. ROI Setup in APS 20ID beamline (July 2019).

11 half drill core samples and 11 offcuts were chosen for large beam SR- μ XRF mapping in February 2019. SR- μ XRF mapping was done by rastering across the sample at APS 20ID in February 2019. For half drill core samples, the map dimensions were set to map sections of the samples with complex texture and visible sulphides. The sizes of maps were 10 cm x 3.5 cm, 8cm x 3.5 cm, 4 cm x 3.5 cm, and 3 cm x 3.5 cm depending on the length of the drill cores with the beam spot size of 800 μ m x 800 μ m. Offcuts were analyzed twice: once with the beam spot size of 800 μ m x 800 μ m, once of 300 μ m x 300 μ m. In July, based on the trace element maps collected in February, 1 cm x 1 cm regions of interest with high intensity of Au were identified for additional high-resolution SR- μ XRF mapping with a 60 μ m spot size. An assemblage of samples was mounted on a wooden sample holder with tape and Velcro tapes were used to tightly bound samples avoid falling from the holder (Figure 3-8B). A piece of photosensitive paper was glued on a corner of a sample, the place where didn't need to be analysed, in order to make sure the beam was right in the middle of the cursor on the top monitor, with the hutch closed and the beam turned on. Once the samples were mounted in the hutch, the beam was turned on when the hutch was closed, and no one was inside. The cursor was used to find the xyz coordinates of the left bottom corner of each sample, a workflow could be set and collect data automatically (Figure 3-11).

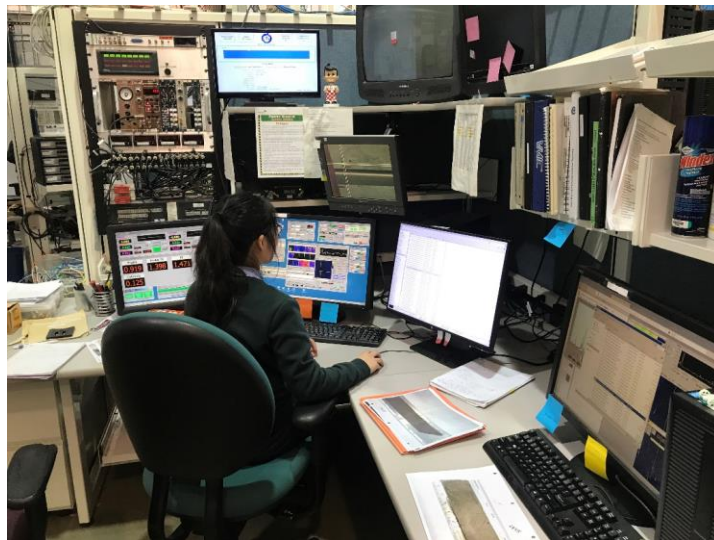


Figure 3-11. The monitors in experimental hall outside the APS 20ID hutch. The author was using cursor in the top monitor to locate the left bottom corner of a sample and setting up an analysis workflow. The left monitor shows beamline conditions. The middle monitor shows the SR- μ XRF mapping software.

3.4.2.2 Data collection at APS 8BM Beamline in March 2019

APS 8BM Beamline is an X-ray Microscopy beamline equipped with a Vortex four-element silicon drift detector (SII Nanotechnology) and Si (111) monochromator. In March 2019, SR-XRF mapping had been done on 8 half-drill core samples and 8 offcuts in the mode of Fly Scan XRF with an incident energy of 15.36 KeV. The beam spot size was 500 μm x 500 μm and the step size was 500 μm . The sizes of maps were 10 cm x 3.5 cm and 8cm x 3.5 cm. The dwell time was set to 0.1- 0.25 sec to figure out the best dwell time in SR-XRF data collection. An assemblage of samples was mounted on a wooden sample holder with tape. A piece of photosensitive paper was glued on a corner of a sample, the place where didn't need to be analysed, in order to make sure the beam was right in the middle of the cursor on the top monitor, with the hutch closed and the beam turned on (Figure 3-12). Once the samples were mounted in the hutch, the beam was turned on when the hutch was closed, and no one was inside. The cursor was used to find the xyz coordinates of the left bottom corner and right top of each sample. A workflow could be set using the coordinates of the center of each sample and collect data automatically.

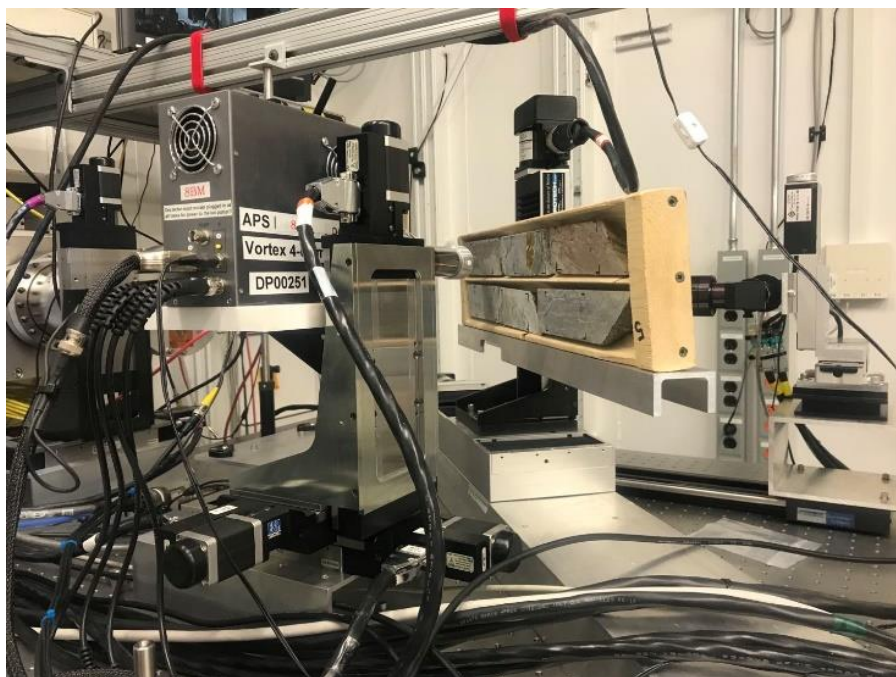


Figure 3-12. The end station setup in the hutch of 8BM-B beamline. (March,2019).

3.4.2.3 Data collection at CLS VESPERs Beamline in February 2019

CLS is a third-generation synchrotron facility with a 2.9 GeV storage ring (Cutler et al., 2007). Vespers Beamline at CLS is a sensitive elemental and structural probe beamline with multi-bandpass (monochromatized) and pink (polychromatic) beam capabilities (McIntyre et al., 2010). In February 2019, SR-XRF mapping was done on selected sulphide spots on 7 offcuts in the mode of the mono beam, with an incident energy of 13 keV. The map size was varied from 0.2 mm x 0.3 mm to 3 mm x 3 mm depending on the size of sulphide grains. The beam spot sizes were 100 μm x 100 μm and 10 μm x 10 μm . The dwell time was set to 1-2 sec. An assemblage of offcuts was mounted on a wooden sample holder with tapes (Figure 3-13).

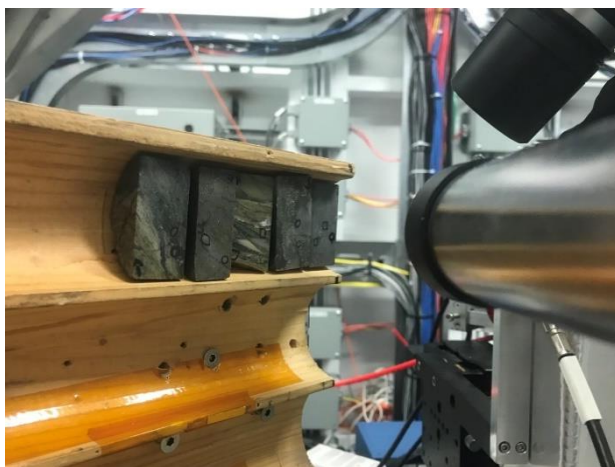


Figure 3-13. Offcuts mounted on the sample stage in the hutch of VESPERs at CLS. (February 2019).

3.4.3 SR- μ XRF Mapping Data Processing

Peakaboo, a powerful software program developed at the University of Western Ontario, is used to analyze complex full spectrum SR- μ XRF mapping Data (Van Loon et al., 2019). The software can be downloaded at <https://www.peakaboo.org/>. Each element has its unique peak shape, energy, and relative intensity. Peakaboo can help to identify elements by overlaying an unknown peak with the expected spectrum of the element. Considering the ROI setup in each beamtime was based on previous knowledge of the samples, the full MCA spectrum is more representative and can be more certain to figure out the potential unknown trace elements.

Each beamline has different software to collect SR-XRF data, the file format of the exported data is different: The 20ID Beamline and 8BM Beamline at APS use “h5.” File formats and VESPERs

Beamline at CLS uses a text “dat.” file. Before processing the raw data file, a proper plugin was needed depending on the beamline. All plugins can be found at <https://github.com/nsherry4/PeakabooPlugins/releases/tag/v5.4.0>. In this research, three plugins were used: “APS-8BM Format”, “APS Sector 20”, and “VESPERS CLS Data Acquisition Format”.

After opening the raw SR- μ XRF Mapping data file in Peakaboo, max energy is used to calibrate the energy range of SR- μ XRF full spectrum. Generally, the max energy was set by observing the peak of Fe K, because iron is the typical trace elements in rock samples with distinct peak according to the previous knowledge of the samples (Figure 3-14). In Peakaboo, the light green spectrum is the actual raw spectrum collected in the beamlines. The darker green ones show the fitted element spectrum after peak fitting. The selected element spectrum is labelled as blue.

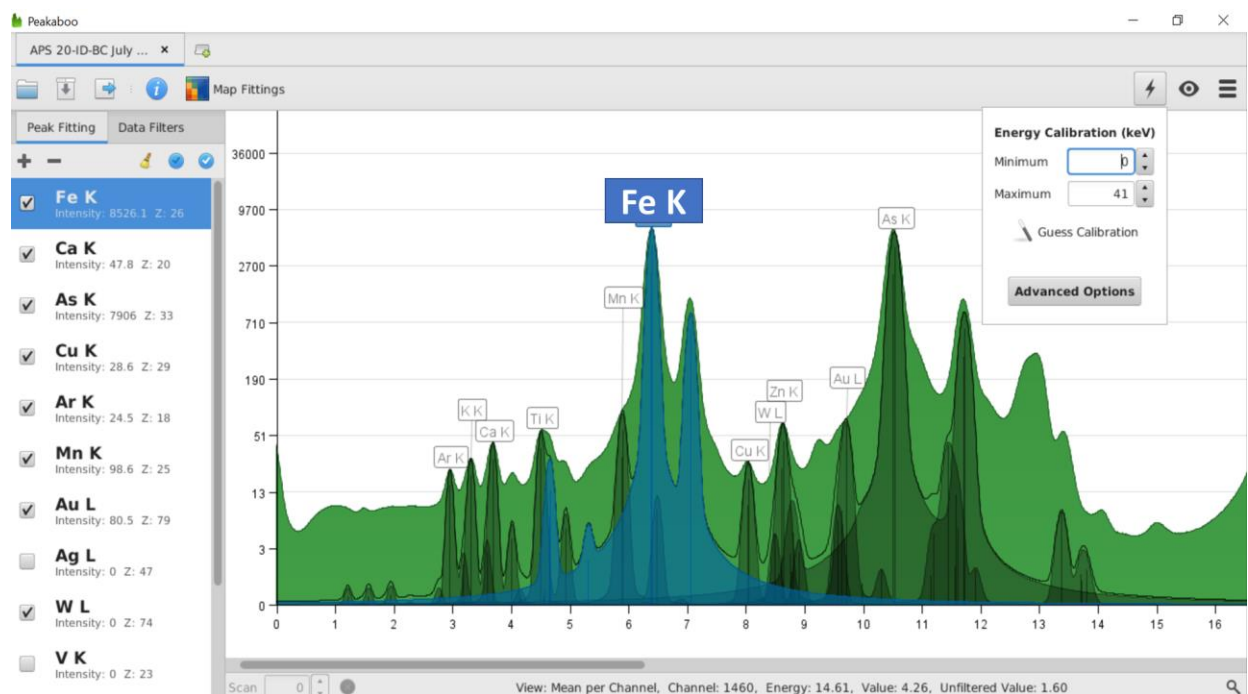


Figure 3-14. Example of an SR-XRF MCA Spectrum of a metasandstone (2831) showing the peak fitting and relative intensity of the elements. Fe K was used to adjust Max energy. The light green spectrum is the actual raw spectrum. The darker green ones show the fitted element spectrum after peak fitting. The blue one is spectrum of Fe K in the samples. Collected at 20ID Beamline at APS (July 2019).

After opening the raw SR- μ XRF Mapping data file in Peakaboo, the range of energy must be determined to calibrate energy range of SR- μ XRF full spectrum. Generally, the max energy was

set by observing the peak of Fe K, because iron is the typical and most common major element in rock samples with distinct peak according to the previous knowledge of the samples (Figure 3-14). The peak shape is usually defined as a pseudo-Voigt function that models the Lorentzian shape expected from a primary fluorescence process and scattered X-rays associated. In this way, the overlapping spectral peaks are easy to be identified by the characteristic K, L, and M element patterns and summation and escape peaks present in the spectrum. “Guided peak fitting” and “element lookup peak fitting” can be used to identify a peak on the spectrum. Fe K, Ca K, As K, Cu K, Ar K, Mn K, Au L, Zn K, K K, W L, and Ti K are the elements selected for peak fitting in the samples of the Monument Bay Project. The peak intensities in MCA spectrum are positively correlated with element abundance.

By clicking “Map Fittings”, 2D trace element SR- μ XRF maps can be automatically created based on the fittings of the MCA spectra. 2D trace element SR- μ XRF maps usually contain thousands of pixels and can be displayed as composite maps, overlaid maps, and ratio maps. Composite maps had been used the most to represent single element spatial distribution. And SR- μ XRF element maps display the intensity via a color spectrum: red represents high intensity, and blue represents low intensity. For each pixel, the MCA spectrum can be examined to check if the hot spots are real signals of elements, especially gold. Some element maps could be hard to identify the texture because of relatively low abundance. To avoid this problem, the “visible” button needs to be checked.

Ar normalization was applied to mitigate the distortion caused by detector saturation, not vertical sample mounting, and uneven surface of samples. Because the samples were collected in air, the Ar peak was selected as the normalizing channel. The cursor was used to check the Ar channel at the bottom of the window (Figure 3-15A). The different datasets had different Ar channels. The channel range of Ar normalization was related to the Ar channel of the beamline. Click “Data Filter” → “Advanced” → “Normalizer” to set the channel range of Ar normalization and normalized intensity (Figure 3-15A). The same beamtime usually has the same Ar normalizing channel range. The best Ar normalizing channel range is where Ar has the lowest intensity and Ar map looks smoothly without any rock texture (Figure 3-15B&C). The details of Ar normalization, XRF maps, and descriptions are shown in Appendix D.

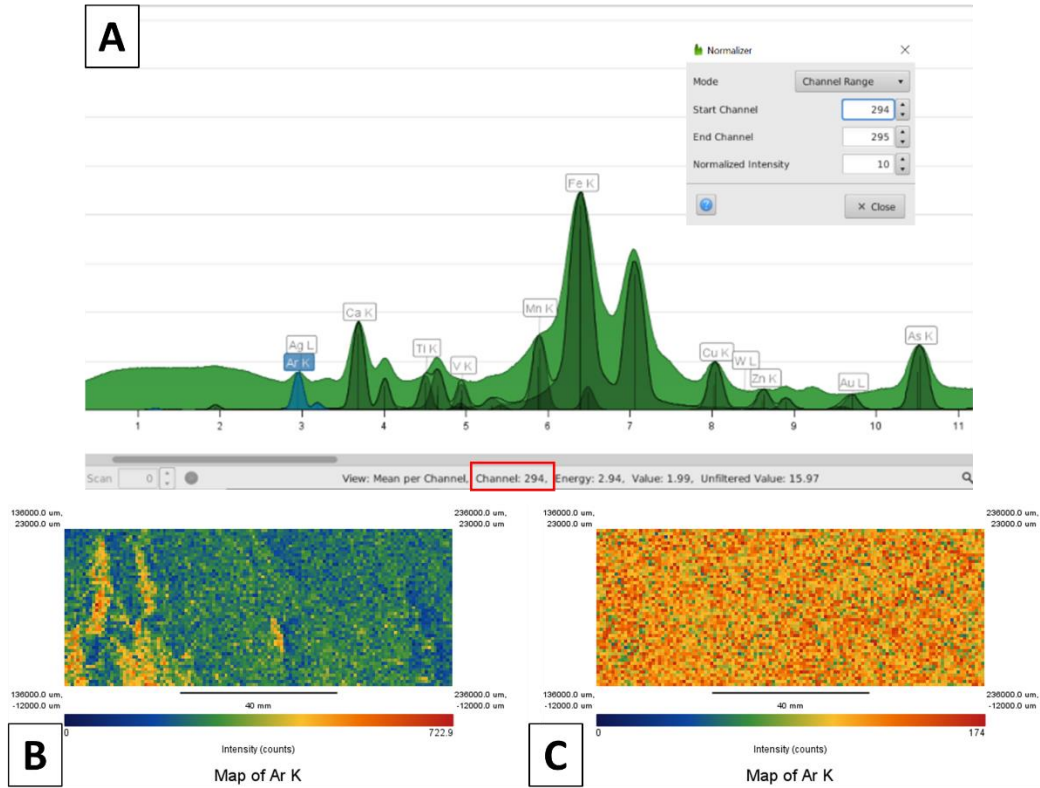


Figure 3-15. Example of Ar normalization. A. The cursor was used to check the Ar channel at the bottom of the window. In this sample, the Ar channel is 294. B. Ar trace element map before Ar normalization shows the texture of the rock sample because of the uneven surface of the sample. C. Ar trace element map after Ar normalization is much smoother with lower relative intensity.

3.5 X-ray Absorption Near-edge Structure (XANES) Spectroscopy

Two types of XANES spectroscopy analysis have been applied in this research: micro-XANES and bulk-XANES (Table 3-4). Micro-XANES spectroscopy was applied in the regions of interest on the half drill core samples and offcuts after SR-XRF mapping, while bulk-XANES spectroscopy was used to examine the rock power samples.

Table 3-4. XANES Data Collection

Hole ID	Western Sample ID	Lithology (by Yamana)	Au Grade (ppm)	Target	XANES Spectroscopy Type	Beamline
TL-16-583	2812A-As 1	Intermediate-Felsic Intrusives: Quartz-Feldspar Porphyry	0.98	TL	As K-edge Micro-XANES	CLS-VESPERS
TL-16-583	2812A-As 2	Intermediate-Felsic Intrusives: Quartz-Feldspar Porphyry	0.98	TL	As K-edge Micro-XANES	CLS-VESPERS
TL-16-583	2812A-As Rerun 1	Intermediate-Felsic Intrusives: Quartz-Feldspar Porphyry	0.98	TL	As K-edge Micro-XANES	CLS-VESPERS
TL-16-583	2812A-As Rerun 2	Intermediate-Felsic Intrusives: Quartz-Feldspar Porphyry	0.98	TL	As K-edge Micro-XANES	CLS-VESPERS
TL-16-583	2812A-Au	Intermediate-Felsic Intrusives: Quartz-Feldspar Porphyry	0.98	TL	Au L3-edge Micro-XANES	CLS-VESPERS
TL-12-481	1533	Intermediate-Felsic Intrusives: Quartz-Feldspar Porphyry	13.22	TL	Au L3-edge Bulk-XANES	APS-20BM
TL-16-575	2820A-As	Intermediate-Felsic Intrusives: Feldspar Porphyry	0.75	TL	As K-edge Micro-XANES	CLS-VESPERS
TL-16-575	2820B-As 1	Intermediate-Felsic Intrusives: Feldspar Porphyry	0.75	TL	As K-edge Micro-XANES	CLS-VESPERS
TL-16-575	2820B-As 2	Intermediate-Felsic Intrusives: Feldspar Porphyry	0.75	TL	As K-edge Micro-XANES	CLS-VESPERS
TL-16-575	2819 A-A	Intermediate-Felsic Intrusives: Feldspar Porphyry	7.21	TL	Au L3-edge Micro-XANES	APS-20ID
TL-16-575	2819 A-B	Intermediate-Felsic Intrusives: Feldspar Porphyry	7.21	TL	Au L3-edge Micro-XANES	APS-20ID
TL-16-575	2819 B-A	Intermediate-Felsic Intrusives: Feldspar Porphyry	7.21	TL	Au L3-edge Micro-XANES	APS-20ID
TL-16-575	2819 C-A	Intermediate-Felsic Intrusives: Feldspar Porphyry	7.21	TL	Au L3-edge Micro-XANES	APS-20ID
TL-13-604	2853-As	Intermediate-Felsic Intrusives: Feldspar Porphyry	7.73	TL	As K-edge Bulk-XANES	APS-20BM

Hole ID	Western Sample ID	Lithology (by Yamana)	Au Grade (ppm)	Target	XANES Spectroscopy Type	Beamline
TL-13-604	2853-Au	Intermediate-Felsic Intrusives: Feldspar Porphyry	7.73	TL	Au L3-edge Bulk-XANES	APS-20BM
TL-17-616	2360	Intermediate Metavolcanics: Lapilli Tuff	12-0.01	TLE	Au L3-edge Bulk-XANES	APS-20BM
TL-16-604A	2854A-As 1	Felsic Metavolcanics: Undifferentiated Tuff	10.49	TL	As K-edge Micro-XANES	CLS-VESPERS
TL-16-604A	2854A-As 2	Felsic Metavolcanics: Undifferentiated Tuff	10.49	TL	As K-edge Micro-XANES	CLS-VESPERS
TL-06-315	2367A-As 1	Clastic Metasediments: Conglomerate	0.04	AZ	As K-edge Micro-XANES	CLS-VESPERS
TL-06-316	2367A-As 2	Clastic Metasediments: Conglomerate	0.04	AZ	As K-edge Micro-XANES	CLS-VESPERS
TL-06-317	2367B-As 1	Clastic Metasediments: Conglomerate	0.04	AZ	As K-edge Micro-XANES	CLS-VESPERS
TL-06-318	2367B-As 2	Clastic Metasediments: Conglomerate	0.04	AZ	As K-edge Micro-XANES	CLS-VESPERS
TL-15-551	2831 A-A	Clastic Metasediments: Sandstone	2.26	SLS	Au L3-edge Micro-XANES	APS-20ID

*“Intermediate-Felsic Intrusives: Feldspar Porphyry” samples are labeled in blue, “Intermediate-Felsic Intrusives: Quartz-Feldspar Porphyry” samples are labeled in yellow, “Intermediate Metavolcanics” are labeled in green, “Felsic Metavolcanics” are labeled in pink, and “Clastic Metasediments” are labeled in purple.

3.5.1 Micro-XANES Spectroscopy

After the full-spectra MCA SR- μ XRF data on the half drill core samples were processed using Peakaboo 5.3.0 to create element maps, 1 cm x 1 cm and <1 mm x 1 mm regions of interest were identified for additional high-resolution SR- μ XRF mapping, and the high-intensity spots corresponding to Au and As were marked for XANES. For micro-XANES spectroscopy, the detector settings were the same as SR- μ XRF mapping and the beam was switched to the mono beam, refocusing on the Au/As spot. Before analyzing samples, the gold foil (~ 5 microns thick, EXAFS Materials, Inc.) was analyzed first in transmission mode to calibrate the energy and also used as the metallic gold standard. The scan bounds of the XANES spectra were from -60 to -30 eV with 0.5 eV steps, -30 to 60 eV with 10 eV steps, and 60 to 9000 eV with 500 eV steps. These parameters were defined by the edge of interest (11919 eV for Au L₃-edge and 11867 eV for As

K-edge). The collection time was 1-3 seconds and two scans were collected for each spot. The detailed parameters of Micro XANES are shown in table 3-5.

Table 3-5. Sample analysis parameters for XANES

Electron Energy Range Relative to Au L ₃ -edge (11919 eV) and As K-edge (11867 eV) (eV)	Step Size (eV)	Collection time
-60 to -30	0.5	1-3 Sec
-30 to 60	10	1-3 Sec
60 to 9000	500	1-3 Sec

3.5.2 Bulk-XANES Spectroscopy

Rock powder samples supplied by Yamana were examined using Au L₃-edge bulk-XANES. Before the beamtime, rock powder samples were firmly packed in Teflon washers, sealed firmly with a single layer of Kapton tape without any bunching or bubbles (Figure 3-16A). After sealing, the samples were checked again to make sure there were no pinholes through the sample by lifting them and looking at with light shining from the backside. The well-sealed samples were mounted into holders at the 20BM beamline in APS (Figure 3-16B). The energy range for pre-edge, edge, and post-edge were -200 to -20 eV, -20 to 30 eV, and 30 to 8980 eV respectively, which is relative to the edge of interest (11919 eV for Au L₃-edge and 11867 eV for As K-edge). And the integration time was 1-3 seconds and two scans were collected for each spot.

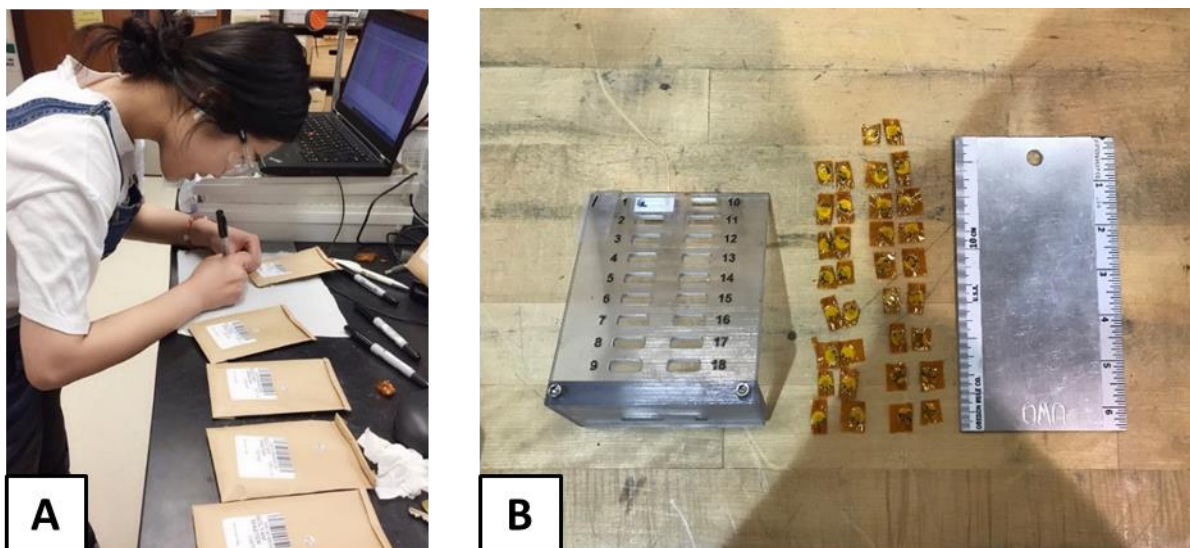


Figure 3-16 A. Illustrating sample preparation for bulk-XANES in Teflon washers in Laboratory for Stable Isotope Science at Western University. B. Well-sealed samples and sample holder before mounting at 20BM beamline, APS.

3.5.3 Data Processing and Interpretation

XANES raw data was processed using Athena (Ravel and Newville, 2005), which converts raw data to $\mu(E)$ spectrum for further interpretation. Athena is an interactive graphical software for energy calibration and X-ray absorption spectroscopy data processing. Pre-edge and post-edge of XANES spectrum were normalized to be relatively horizontal by changing the “pre-edge range” and “normalization range” parameters (Figure 3-17). Comparing normalized Au XANES spectrum with gold foil standard spectrum, the behavior of Au L3-edge was identified to differentiate the oxidation state of gold. The detailed XANES spectra and descriptions are shown in Appendix E.

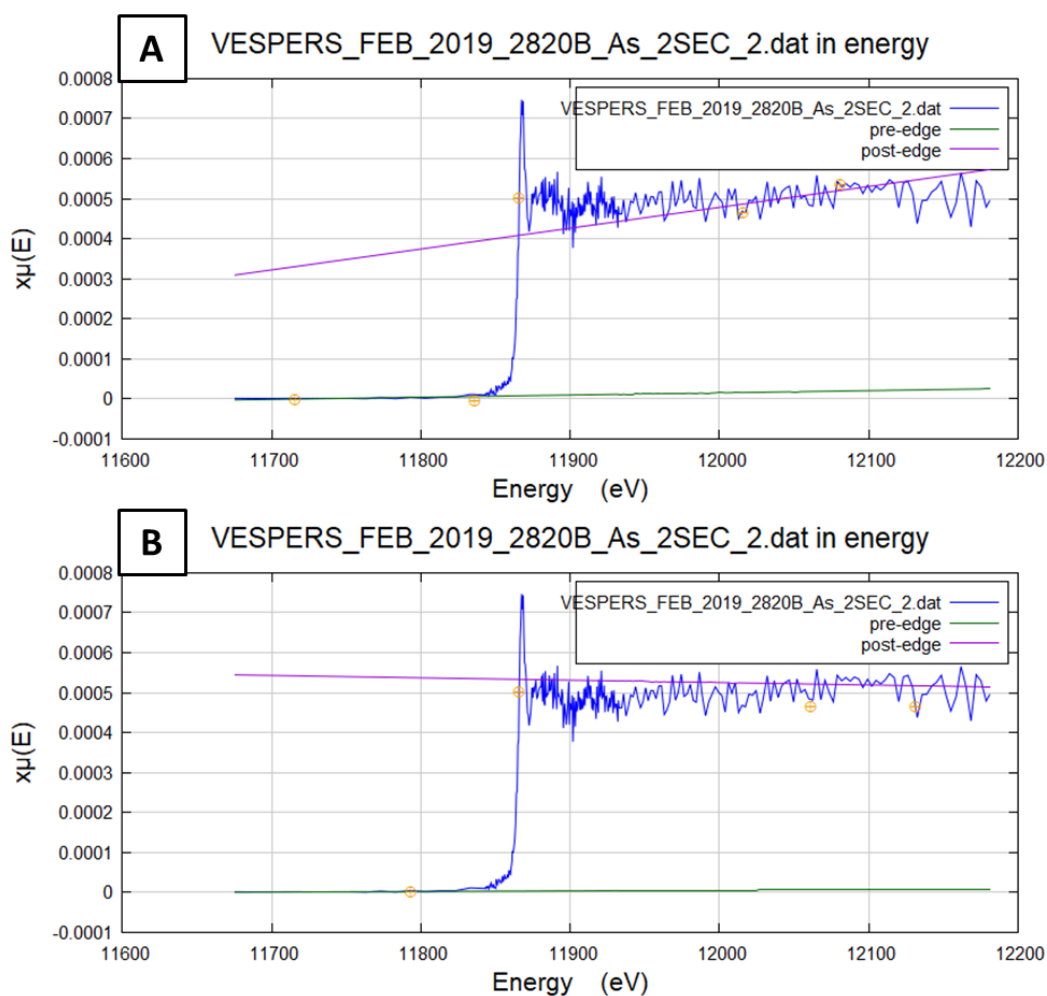


Figure 3-17. Illustrating As K-edge XANES spectrums before (A) and after normalization (B) using Athena. Pre-edge line and post-edge line became relatively horizontal after normalization. The raw data was collected on 2820 offcut at CLS VESPERS Beamline in February 2019.

3.6 Electron Probe Micro-Analysis (EPMA)

EPMA is an in situ, non-destructive, chemical analysis of minute solid samples at small spatial scales (microns), that provides compositional information by energy-dispersive spectroscopy (EDS) and wavelength-dispersive spectroscopy (WDS). EPMA can help to confirm the results of optical petrology and morphological observations and identify microscopic gold distribution in sulphide phases. EDS/WDS X-ray 2D element maps have also been used to analyze trace element spatial distributions in sulphide minerals, which are helpful in determining mineral paragenesis and corresponding mineralizing fluid events.

Based on detailed petrographic description under an optical microscope, regions of interest of sulphide grains with different morphology and microscopic gold grains were selected for EPMA. Generally, thin sections include silicate minerals, which are electrical insulators and can lead to electrical charging if irradiated with the X-ray directly. As a result, prior to EPMA experiments, thin sections need to be coated with a thin layer of a conducting material (i.e. carbon). Selected thin sections were carbon-coated (~25 nm in thickness) using a JEE-420T vacuum evaporator by Marc Beauchamp at the Earth and Planetary Materials Analysis Laboratory in Western University. A JEOL JXA-8530F field-emission electron microprobe was used for EPMA with a 20 keV accelerating voltage and a beam current of 200 nA (Figure 3-18). The beam size was set to 110 μm with a dwell time of 10 msec per spot. A group of four thin sections was placed in a holder with electrical contact using conductive tape. Then the group of samples was mounted on the sample stage the sample chamber in the sample chamber, and a vacuum interlock made the chamber become high-vacuumed ($\sim 4 \times 10^{-5}$ Pa).



Figure 3-18. The JEOL JXA-8530F field-emission electron microprobe, at the Earth and Planetary Materials Analysis Laboratory, at Western University.

Point EDS analysis was done on regions of interest (gold and sulphide grains), providing both a spectrum and average counts of trace elements at each point. EDS analysis is much quicker than WDS analysis but has lower spectral resolution and lower detection limit. In the EPMA experiment in October 2019, EPMA X-ray 2D element maps were collected for the first time on some regions of corroded pyrite by EDS, the zoning in As EDS elemental map was not obvious and could not meet the requests for identifying sulphide generations. Thus, in the EPMA experiment in February 2020, EPMA X-ray 2D element maps were collected on selected sulphide grains for As, Au, Ag, W, and Si by WDS, while S, Fe, Cu, Zn, Pb, Ni, Co, Al, Mg, Ca, Ti, Na and K were collected by EDS. Based on EPMA X-ray 2D element maps on sulphides, EDS point analysis was used to characterize any zoning and remobilization along with fractures observed for quantitative analysis of sulphide composition. The detailed EPMA data and descriptions are shown in Appendix F.

Chapter 4

4 Results

4.1 Petrology

Thirty-four drill core samples and forty-five thin sections have been observed and described. The samples have been classified into three main types: porphyritic dacite, metatuff, and metasedimentary rocks. The texture, mineralogy, veining, alteration, sulphide types, and microscopic gold types are summarized in Table 4-1.

Table 4-1 Petrology of Different Rock Types

Rock Type	Porphyritic Dacite	Metavolcanic Rocks (Intermediate Metatuff &Felsic Metatuff)	Metasedimentary Rocks (metasandstone, metasilstone, and metaconglomerate)
Texture	Porphyritic texture, foliation, quartz recrystallization, pressure shadow	Foliation, decussate texture, quartz recrystallization, pressure shadow	Foliation, stretched clasts, pressure shadow, quartz recrystallization
Mineralogy	Quartz, Albite, K-Feldspar, Ankerite, Muscovite, Chlorite	Quartz, Albite, K-Feldspar, Ankerite, Muscovite, Chlorite	Quartz, Albite, K-Feldspar, Ankerite, Muscovite, Chlorite
Veining	Quartz veins, carbonate veins, sericite/muscovite veinlets	Smoky quartz veins, carbonate veins, carbonate-quartz veins, carbonate-chlorite veins	carbonate ± quartz veins
Alteration	30% to 85% carbonate alteration & sericitization, chlorite alteration	60% to 90%, Sericitization, carbonate alteration, chlorite alteration	70% to 90%, Sericitization, carbonate alteration, chlorite alteration
Sulphides	Arsenopyrite, pyrite, sphalerite, and chalcopyrite	Arsenopyrite, Pyrite, Chalcopyrite, Sphalerite, Galena	Arsenopyrite, Pyrite, Chalcopyrite, Sphalerite, Galena
Microscopic Gold	Free gold & inclusion gold	Free gold	Free gold & inclusion gold

4.1.1 Porphyritic Dacite

Most high gold grade samples are porphyritic dacite, which was classified into “intermediate-felsic intrusive: Quartz-Feldspar Porphyry/ Feldspar Porphyry” in Yamana mining log. The color of porphyritic dacite is various from mauve-green, light yellowish-green, and to dark grey. The color depends on the intensity of carbonate alteration and sericitization. Samples with intensive carbonate alteration are mauve to light pink, while samples with intensive sericitization are generally yellowish green. The observation under the optical microscope shows the alteration intensity of porphyritic dacite is from 30% to 85%. The alteration styles are fine-grained and

cryptocrystalline. The cryptocrystalline alteration style is more common. However, there are coarse-grained calcite grains recrystallized in the veins and muscovite grains within foliation.

Porphyritic dacite typically has massive veinlets including quartz veins and carbonate veins. Quartz veins are more common than carbonate veins. The hand samples with massive quartz veins show a color gradient: the color changed from dark grey, light grey, and to yellowish-green from the inside of veins to the host rock. Subhedral-euhedral medium to fine-grained sulphides (pyrite and arsenopyrite) are filled in the quartz veins. The discontinuity of the veining system in some samples shows a brittle system. Carbonate veins are generally white and sometimes were altered into orange to dark red because of the oxidation of ankerite. A few carbonate veins reflect blue under UV light as a result of scheelite. In the thin sections, there are three groups of veins: quartz veins, quartz + carbonate veins, and sericite/muscovite veins. Quartz veins are composed of fine to very fine-grained recrystallized quartz. Feldspars and sulphides within quartz veins are the secondary minerals. Quartz + carbonate veins are commonly thicker than quartz veins, with more fractured and corroded sulphides and sericite and feldspar are filled between the grains (Figure 4-1A). Sericite/muscovite fine veins crosscut the quartz veins, showing the mechanical reworking and recrystallization were later than the formation of quartz veins (Figure 4-1B).

According to the observation under the optical microscope, porphyritic dacite shows a typical porphyritic texture with strong foliation. The groundmass is typically fine to medium-grained feldspar + quartz + sericite/muscovite \pm chlorite (Figure 4-1C). The phenocrysts are medium to coarse-grained plagioclase with polysynthetic twinning, quartz with subgrain boundaries and undulatory extinction, and K-feldspar with Carlsbad twinning under cross-polarized light. All phenocrysts exhibit various degrees of fracturing, recrystallization, and sericitization. Very fine to fine-grained quartz has commonly infilled and recrystallized between larger grains and along with fractures and micro-faults.

Sulphides occur either within veins or in the groundmass. There are five types of sulphide minerals within porphyritic dacite thin sections: arsenopyrite, pyrite, sphalerite, and chalcopyrite. Arsenopyrite is the major sulphide. In the quartz \pm carbonate veins, arsenopyrite is coarse to medium-grained, corroded, mainly subhedral to anhedral, and with fractures. As for pyrite, the ones in veins are coarser, more corroded, and more fractured than arsenopyrite (Figure 4-1D-F).

Euhedral-subhedral, fine to medium-grained, arsenopyrite and pyrite grains are disseminated in the groundmass and surrounding the coarse-grained plagioclase phenocrysts. The disseminated arsenopyrite grains are mostly needle, diamond, and/or square-shaped. Sphalerite and chalcopyrite commonly present as inclusions in sieved-textured coarse-grained pyrite and arsenopyrite. A few anhedral, fine-grained, and boudinaged sphalerites are disseminated in groundmass.

Two types of microscopic gold have been observed. One type is free gold within the groundmass and usually proximal to disseminated sulphides. The other type is inclusion gold within coarse-grained, corroded pyrite and needle arsenopyrite.

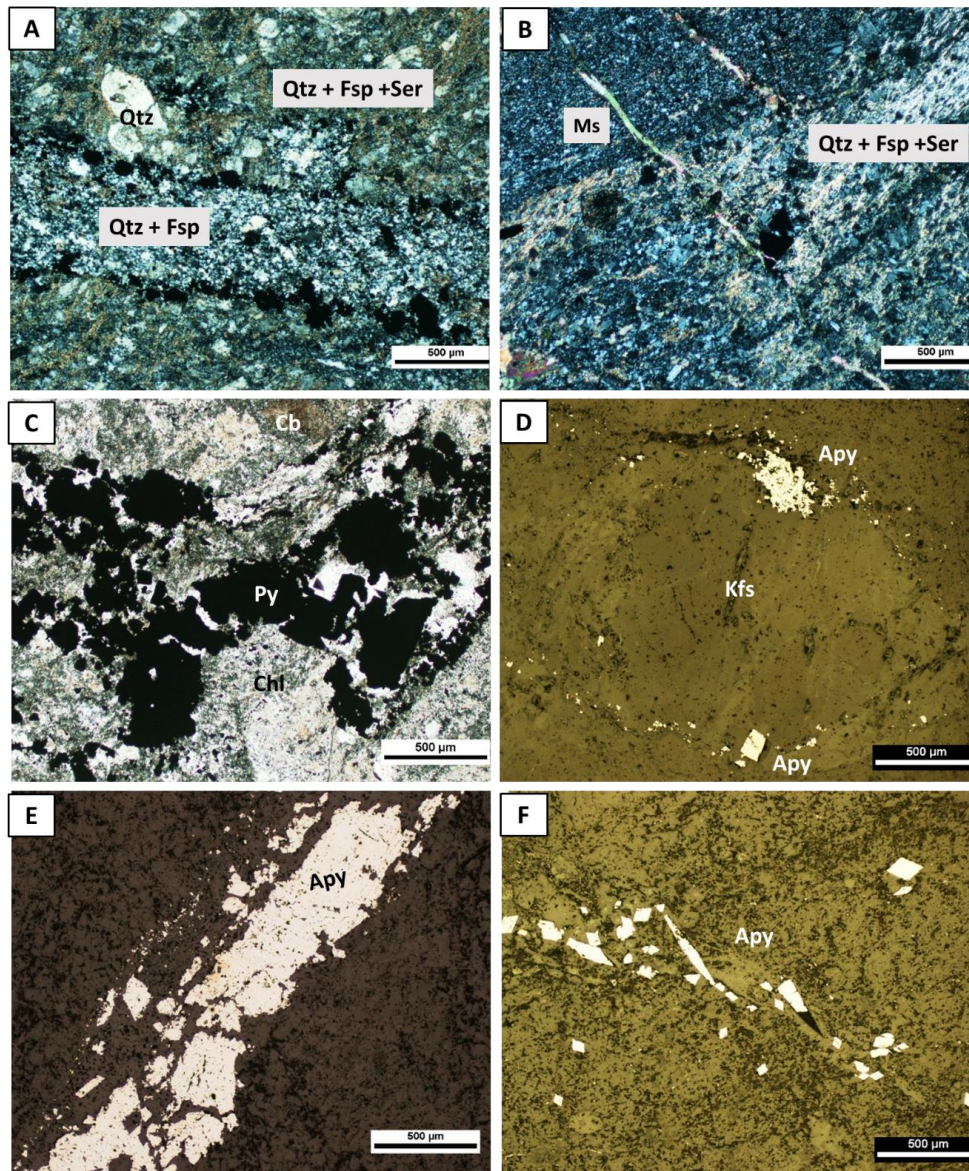


Figure 4-1. Photomicrographs of metatuff. Ms=muscovite, Qtz=quartz, Cb=carbonate, Ser=sericite, Fsp=feldspar, Pl=plagioclase, Kfs=K-feldspar, Asp=arsenopyrite, Py=pyrite. A. The groundmass is porphyritic textured with feldspar and quartz phenocrysts. Quartz is recrystallized in the vein and the fine-grained arsenopyrite grains on the edge (2827, XPL, 500 µm). B. Needle arsenopyrite in the quartz vein and the discontinuous very fine muscovite vein crosscut the quartz veins (2824, XPL, 500 µm). C. Fractured subhedral coarse-grained arsenopyrite in the quartz vein with chlorite and carbonate alteration in the groundmass. Quartz recrystallized surrounding the sulphides grains (2841, PPL, 500 µm). D. Corroded medium-grained and euhedral medium to fine-grained arsenopyrite surrounding the plagioclase phenocrysts (2841, RL, 500 µm). E. Coarse-grained fractured arsenopyrite in the middle of the quartz vein and fine-grained arsenopyrite on the edge of the vein (2827, RL, 500 µm). F. Euhedral to subhedral fine-grained needle arsenopyrite in the quartz vein. (2853, RL, 500 µm).

4.1.2 Metavolcanic Rocks

According to the felsic mineral composition, metavolcanic Rocks in the Monument Bay Project can be divided into intermediate and felsic metatuff. The appearances of intermediate and felsic metatuff hand samples are quite similar. Both intermediate and felsic metatuff show intensive foliation, composed of volcanic ash and lapilli. The color of metatuff is various from mauve-grey, yellowish-green, dark green, to dark grey. Samples with strong sericitization are yellowish-green, while samples with slight sericitization are mauve-grey. Samples also show intensive carbonate alteration and chlorite alteration. The observation under the optical microscope shows strong, pervasive sericitization commonly throughout the entire samples, and is most intense within sericite bands within foliation. Sericite intensifies with arsenopyrite fracture-fill veinlets, especially where veinlets crosscut. Sericite is also flooded with fine-grained silica material and within the foliation as well. Some samples show recrystallized muscovite in the foliation. Some samples exist chlorite alteration where a fine-grained matrix exists between relict clasts. Chlorite occurs as both green masses with arsenopyrite in carbonate veins and with intense sericite in foliations.

Metatuffs in the Monument Bay Project are with intensive veinlets and most of them are strongly altered and reworked. There are two types of folded veins have been observed in the hand samples. Smoky grey veins are formed of smoky quartz with coarse-grained subhedral pyrite and fine-grained disseminated arsenopyrite. White veins are comprised of carbonate and a few are oxidized into a brown color. Carbonate veins are cut by quartz veins which illustrates quartz veins are younger than carbonate veins younger than foliation formation. Some fine-grained arsenopyrite grains are disseminated in the finer carbonate veins and only a few are in the bedded layers. According to the observation under the optical microscope, most relict quartz veinlets have been extremely altered and reworked. The veinlets are consequently infilled with sericite-pyrite-arsenopyrite, quartz-feldspar, or quartz-scheelite within the clast and sericite-chlorite matrix area. At the same time, only a few thin wispy quartz veins have left. Within the wispy quartz veins, small strained grains recrystallize to grow larger, more euhedral grains. In one thin section, a carbonate-chlorite vein crosscuts the foliation and contains remobilized masses including massive corroded pyrite.

Pressure shadows were observed surrounding coarse fragments in the hand samples. There are two groups of fragments in metatuff: fine-grained fragments and crystals in the strongly altered areas and medium to coarse-grained fragments in the less altered areas. Most fragments are dark-colored and oriented along with the foliation. According to the observation under the optical microscope, crystal fragments are mainly skeletal-textured feldspar (~0.5 mm) which partly altered into sericite. Lapilli consists of K-feldspar, plagioclase, quartz, and sericite. Coarse-grained feldspar fragments are strongly fractured with skeletal texture, which indicates brittle deformation (Figure 4-2C). Coarse-grained plagioclase fragments have polysynthetic twinning and micro-boudinage texture. Feldspar-dominate volcanic ash and lapilli within the matrix. Most thin sections show a moderate to intensive foliated quartz + feldspar and sericite \pm muscovite interbedded matrix, and the foliation in the matrix is wiggly oriented. A few thin sections exhibit a decussate texture quartz-dominant matrix (Figure 4-2A). The matrix is composed of disordered fine-grained, lath-shaped quartz grains. Quartz pressure shadows are observed around some sulphide grains in the fine-grained recrystallized quartz veins, which indicates ductile deformation (Figure 4-2B). Some recrystallized quartz has subgrain boundaries.

The majority of sulphides are arsenopyrite and pyrite. Trace chalcopyrite, sphalerite, and galena are disseminated in the fine-grained feldspar-sericite-quartz(-chlorite) matrix. Arsenopyrite is fine- to medium-grained, corroded and fractured, euhedral to subhedral mainly within strongly altered, reworked, and sericitized relict quartz veinlets and carbonate veins (Figure 4-2D). Pyrite grains are less abundant than arsenopyrite grains, medium-grained, corroded, fractured, euhedral-subhedral (Figure 4-2E). Pyrite grains commonly occur as lone grains near veins infilled by arsenopyrite. In a few thin sections, coarse-grained pyrite is surrounded by chlorite. Combinations of pyrite + arsenopyrite and pyrite + sphalerite were observed in quartz veins locally. Subhedral to anhedral sphalerite occurs as inclusions in strongly fractured arsenopyrite and pyrite grains.

Microscopy gold was observed in almost every metatuff thin section. Inclusion gold occurs within large scheelite grain in slightly altered quartz veinlets. Free gold was observed near the fine-grained euhedral disseminated arsenopyrite in the matrix and near the medium-grained subhedral pitted pyrite grains in the slightly altered carbonate-quartz vein (Figure 4-2F).

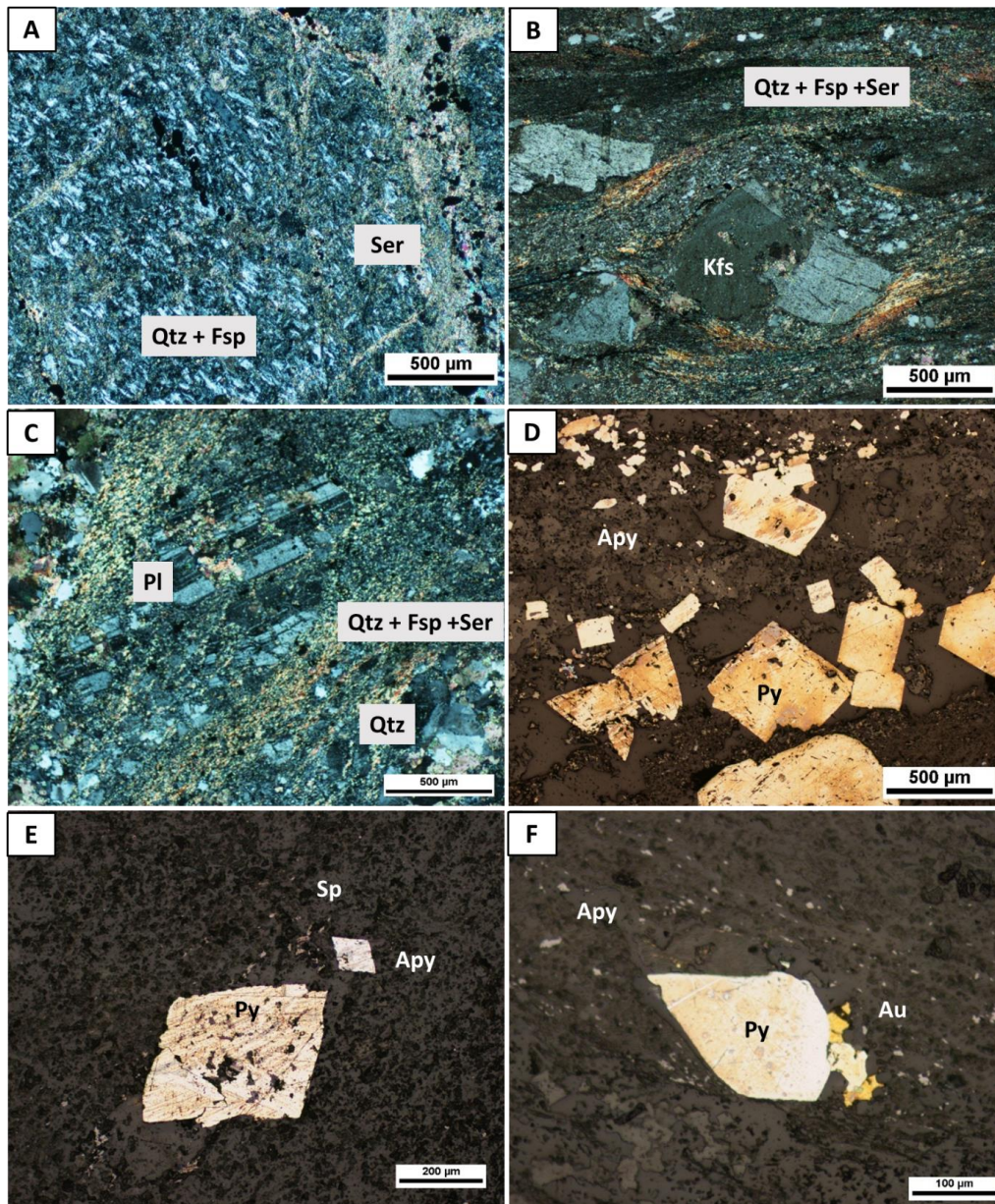


Figure 4-2. Photomicrographs of metatuff. Ms= muscovite, Qtz=quartz, Cb=carbonate, Fsp=feldspar, Kfs=potassium feldspar, Ser=sericite, Pl=plagioclase, Apy=arsenopyrite, Py=pyrite, Ccp=chalcopyrite, Au=gold, Sp=sphalerite. A. Decussate texture quartz-dominant matrix and sericite veinlets throughout. Some veins are filled with arsenopyrite and pyrite. (1519, XPL, 500 μm) B. Pressure shadow texture around potassium feldspar fragments in foliation (2834, XPL, 500 μm). C. Fractured plagioclase grains with polusynthetic twinning with the same direction of the foliation (2834, XPL, 500 μm) D. Corroded subhedral-euhedral coarse-grained pyrite grains and disseminated euhedral fine-grained arsenopyrite in carbonate vein (2834, RL, 500 μm). E. Euhedral arsenopyrite, corroded euhedral pyrite and disseminated anhedral boudinaged sphalerite in the matrix (2858, RL, 200 μm) F. Inclusion gold on the edge of subhedral pyrite and near euhedral disseminated arsenopyrite (1543A, RL, 100 μm).

4.1.3 Metasedimentary Rocks

Metasedimentary rocks can be divided into metasandstone, metasilstone, and metaconglomerate. All metasedimentary rocks show intensive foliation.

4.1.3.1 Metasandstone

2831 is the only high gold grade metasandstone with yellowish green and dark green interbedded layers. It is composed of well-sorted medium-grained clasts (sand-size) with pressure shadow. Pyrite and arsenopyrite were disseminated throughout the sample along with the foliation. The carbonate \pm quartz veins have the same direction as the foliation. The area with strong sericitization is yellowish-green, while the area with chlorite alteration is dark green. Sericitization is more common than chlorite and carbonate alteration.

Feldspar-rich clasts and quartz-rich clasts were observed under the optical microscope. The thin section shows intensive foliation and orientation. The matrix is composed of oriented cryptocrystalline muscovite, quartz, feldspar, and carbonate minerals (Figure 4-3A). The plagioclase-rich clasts are anhedral, exhibiting typical polysynthetic twinning. Quartz-rich clasts are with undulate extinction and along with the foliation (Figure 4-3B). Quartz recrystallized in the carbonate \pm quartz veins, surrounding sulphide grains, and filled the fractures in the clasts (Figure 4-3C).

Sulphides occur in the matrix and in the carbonate \pm quartz veins. In the matrix, subhedral to anhedral fine-grained arsenopyrite, sphalerite, and a few chalcopyrite and galena are disseminated in the groundmass. Sulphides within veins are coarser and more fractured. Pyrite grains are fine to medium-grained, euhedral to subhedral in the carbonate \pm quartz veins. Quartz strain fringes recrystallized surrounding pyrite and arsenopyrite grains in veins. Two types of microscopic gold have been observed in 2831: free gold in the matrix and inclusion gold within galena and chalcopyrite (Figure 4-3D).

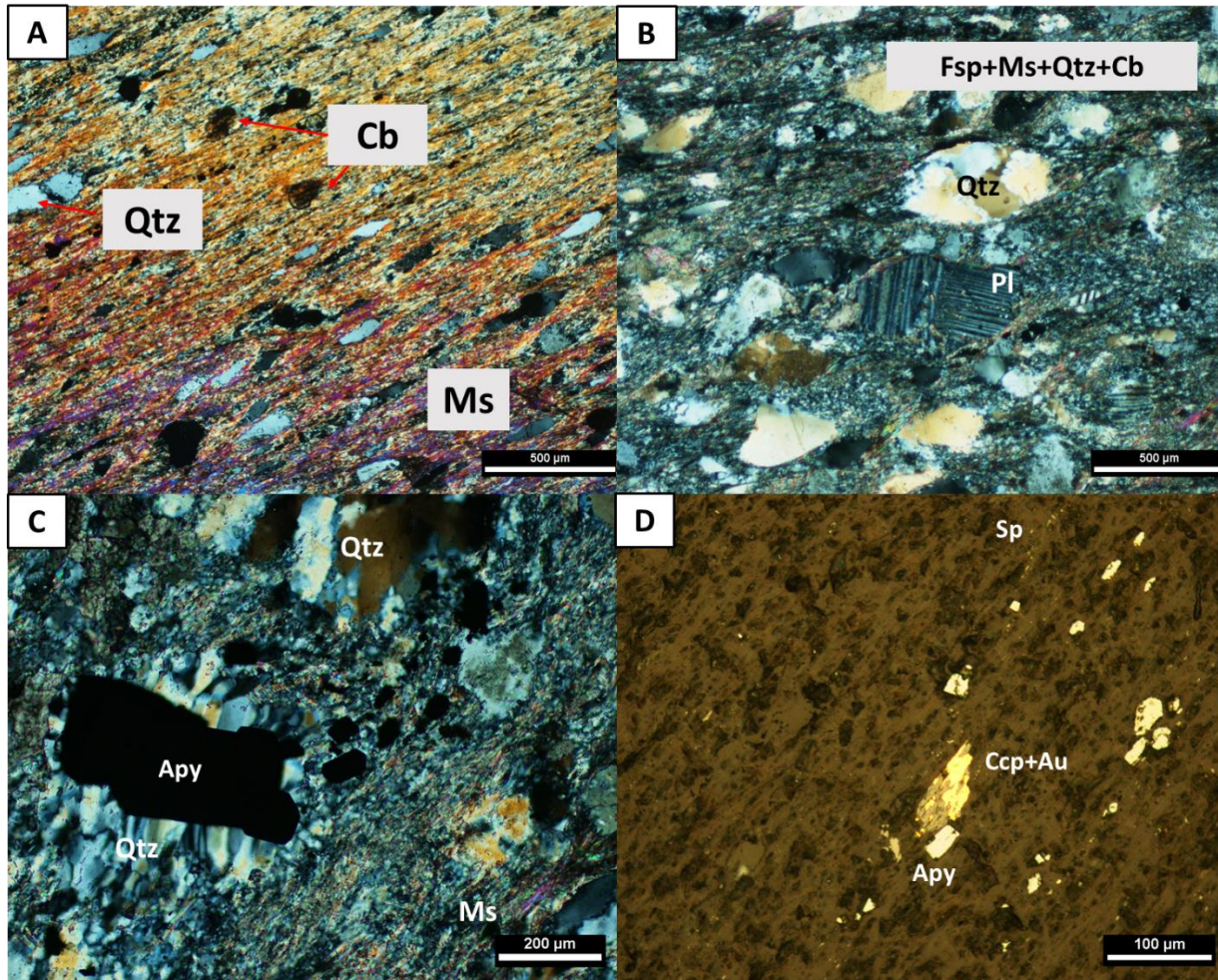


Figure 4-3. Photomicrographs of metasandstone sample (2831). Ms=muscovite, Qtz=quartz, Cb=carbonate, Fsp=feldspar, Pl=plagioclase, Apy=arsenopyrite, Py=pyrite, Ccp=chalcopyrite, Au=gold. A. Intensive foliation formed by recrystallized muscovite with oriented quartz-rich clasts and carbonate (XPL, 500 μ m). B. Feldspar-rich clasts and quartz-rich clasts in the feldspar + quartz + muscovite + carbonate matrix (XPL, 500 μ m). C. Euhedral medium-grained arsenopyrite in the quartz vein and quartz are recrystallized surrounding arsenopyrite grains (XPL, 200 μ m). D. Inclusion gold with chalcopyrite in the quartz vein with disseminated arsenopyrite and sphalerite inside (RL, 100 μ m).

4.1.3.2 Metasiltstone

1535 and 1536 are metasiltstone samples. They are both dark-to-medium grey, fine-grained (silt-size), bedded rock. Carbonate veins are along with the foliation and a few are folded. Weathered surfaces show that carbonate veins are oxidized (ankerite), generally at the outer selvages of the veins. Both of them are moderately silicified throughout, with regions that exhibit a more significant, light grey silica overprint. Mylonitized quartz eyes occur in some carbonate-rich layers. Significant Sulphides throughout the hand samples: Coarse to medium-grained euhedral to

subhedral pyrite and arsenopyrite are disseminated within most layers; fine-grained pyrite and arsenopyrite are filled within >20mm smoky quartz veins in bedding. Coarse-grained sulphides are often fractured and boudinaged. The area with strong sericitization is yellowish-green, while the area with chlorite alteration is dark green. Sericitization is more common than chlorite alteration. Carbonate alteration displays as dark-grey color, but less common in metasilstone.

The entire thin section is intensely sericitized and moderately chloritized, occurring as recrystallized schistose muscovite and chlorite filled in the fractures. The matrix is dominant with recrystallized muscovite, quartz, feldspar, chlorite, and carbonate minerals. Fine-grained quartz-rich clasts were observed under the optical microscope. Quartz in these two samples is recrystallized, within both veins and clasts. All primary textures have been obliterated by alteration overprint (Figure 4-4A).

Sulphides occur as dominantly within quartz veins and minor fine grains are sparsely disseminated throughout muscovite matrix. Pyrite is medium to coarse-grained, subhedral, sieved textured, and fractured. Pyrite located primarily located within fine quartz vein or shear band structures and sometimes intergrown with arsenopyrite (Figure 4-4B). Arsenopyrite occurs as subhedral, pitted, fractured, needle or diamond-shaped, and generally finer-grained than the pyrite. A considerable number of gold inclusions are found within pyrite grains, but none within arsenopyrite. No free gold has been observed.

4.1.3.3 Metaconglomerate

1544 is the only Metaconglomerate sample. It is a fine-grained, siliceous, fractured, and brecciated rock with the color of brown-mauve-white. It is highly fractured and brecciated with white breccias filled in the fractures. The mauve clasts are fractured and crosscut by quartz fine veins. Sulphides are mainly arsenopyrite, which occurs as fine-grained fracture-fill and locally fine and coarse euhedral to subhedral disseminations. Pyrite is only disseminated in unbrecciated area as coarse euhedral to subhedral grains within the Mauve clasts. The area with strong sericitization is yellowish-green, while the area with carbonate alteration is dark-grey. Sericitization is more common than carbonate alteration. The area with less sericitization and carbonate alteration shows mauve color. According to thin section observation, patchy sericitization is throughout the thin section.

A large band of sericite-chlorite across the thin section containing coarse-grained (1-3 mm) euhedral arsenopyrite grains. Muscovite recrystallized in the sericite-chlorite band. Wispy chlorite within sericite bends surrounds sulphide grains. Sericite band has very fine-grained recrystallized quartz and coarser-grained quartz and feldspar (Figure 4-4C).

Large, coarse grains of euhedral arsenopyrite occurs within the sericite-chlorite band. These grains are strongly fractured and corroded. Free gold has been observed as inclusion in the arsenopyrite grains. Rounded pyrite grains also occur within the sericite chlorite band, but do not have gold associated with them. Fine-grained, anhedral, remobilized arsenopyrite also occurs within carbonate veins, but no microscopic gold is associated with this type of vein (Figure 4-4D).

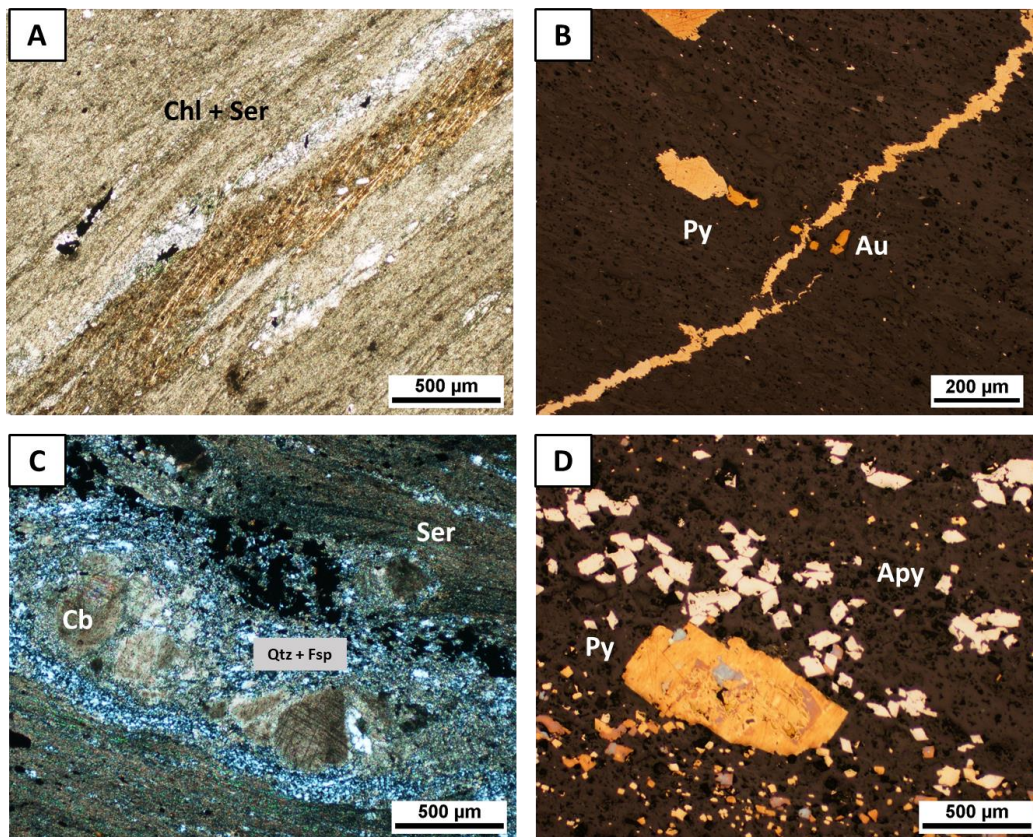


Figure 4-4. Photomicrographs of metasilstone (A&B) and metaconglomerate (C&D) samples. Ms=muscovite, Ser= sericite, Chl=chlorite, Asp=arsenopyrite, Py=pyrite, Au=gold. A. Chlorite and fine-grained sericite interbedded, and crosscutting quartz-carbonate-pyrite fine veins (1536A, XPL, 500 µm). B. Pyrite and arsenopyrite segregated in different zones within sheared area (1535B, RL, 500 µm). C. Sericite-chlorite band with coarse-grained euhedral arsenopyrite grains (1544A, XPL, 500 µm). D. Free gold near coarse-grained euhedral arsenopyrite grains in the sericite-chlorite band (1544A, RL, 100 µm).

4.2 Synchrotron X-ray Diffraction

Sixteen representative high gold grade core pulps and powdered rock samples were analyzed using Synchrotron X-ray Diffraction (SR-XRD) to identify mineral phases and assemblages. By comparing diffractograms of each sample, the lithology, alteration mineralogy, and sulphide mineralogy can support the petrology in microscopy and trace element distribution in SR-XRF maps. Based on the concentration of minerals, the mineral phases can be classified into major (>5%), minor (1-5%), and trace mineral phases (<1%).

The sulphide minerals observed include pyrite, arsenopyrite, chalcopyrite, sphalerite, and galena. Arsenopyrite is generally the most abundant as a major mineral phase. The other types of sulphides are minor to trace mineral phases. The major gangue minerals include quartz, albite, microcline, and muscovite. Minor minerals include anorthite, chlorite. Only a few samples have orthoclase, kaolinite, and/or andesine. The carbonate minerals in the Monument Bay Project are calcite, ankerite, and dolomite. Calcite exhibits in most samples with major to minor concentrations, while ankerite and dolomite are rare with minor concentrations. The high concentration of muscovite represents the pervasive sericitization. And the appearance of chlorite proved the chlorite alteration in a few samples.

For different remnant host rock lithology, the mineral phases and their concentration are slightly different. Andesine and orthoclase only present in feldspar porphyry (FP, Figure 4-5). Kaolinite only presents in metasilstone (Figure 4-6). Metasediments commonly have a higher concentration of sulphides than other rock types (Figure 4-6). Felsic to intermediate meta-tuff has a higher concentration of carbonates than other rocks sample (Figure 4-7). The summary of XRD data is listed in Table 4-2, and the detailed XRD diffractograms are shown in Appendix B.

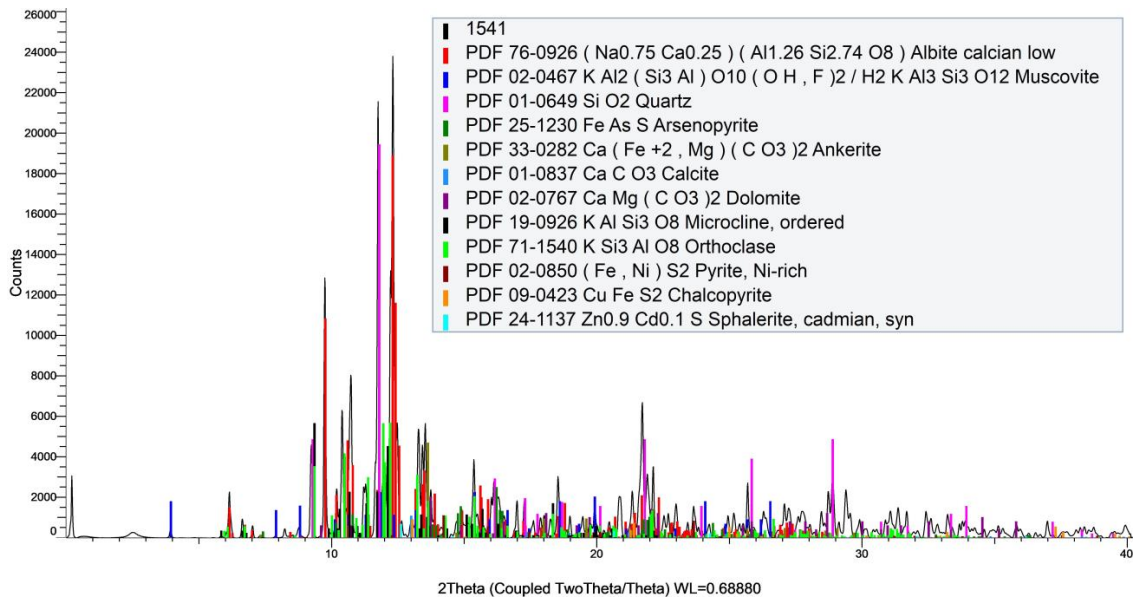


Figure 4-5. X-ray diffractogram of sample 1541 from Twin Lakes West. The host rock lithology is feldspar porphyry (FP). The major mineral phases are quartz, albite, microcline, and orthoclase. The minor mineral phases are muscovite, ankerite, calcite, dolomite, pyrite, arsenopyrite, and chalcopyrite. The trace mineral phase is sphalerite.

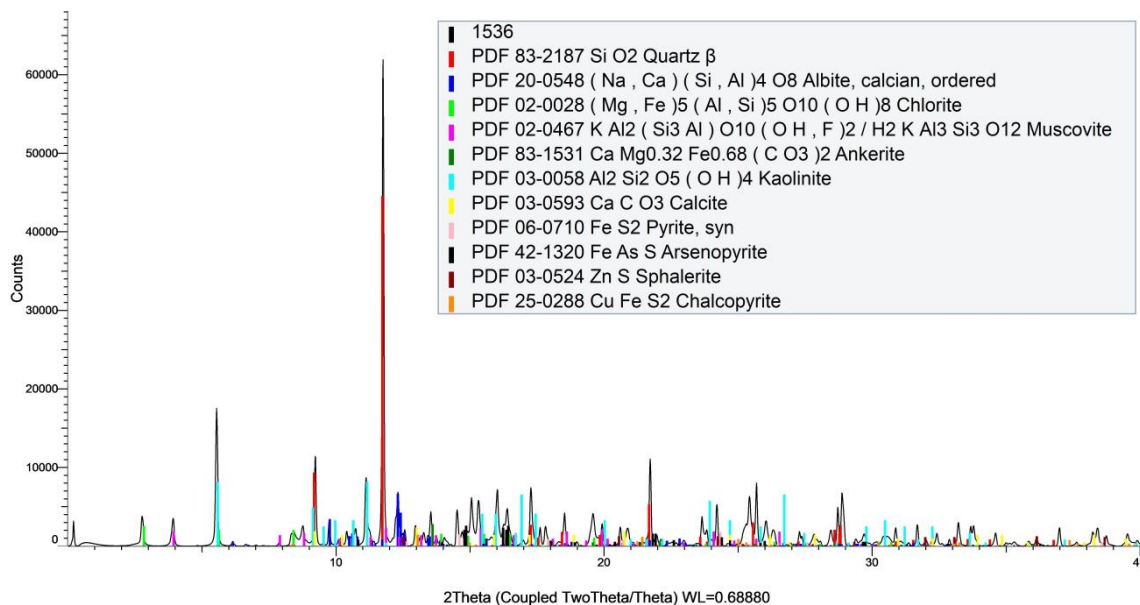


Figure 4-6. X-ray diffractogram of sample 1536 from Twin Lakes West. The host rock lithology is metasiltstone. The major mineral phases are quartz, albite, kaolinite, muscovite, and chlorite. The minor mineral phases are ankerite, calcite, pyrite, arsenopyrite, chalcopyrite, and sphalerite.

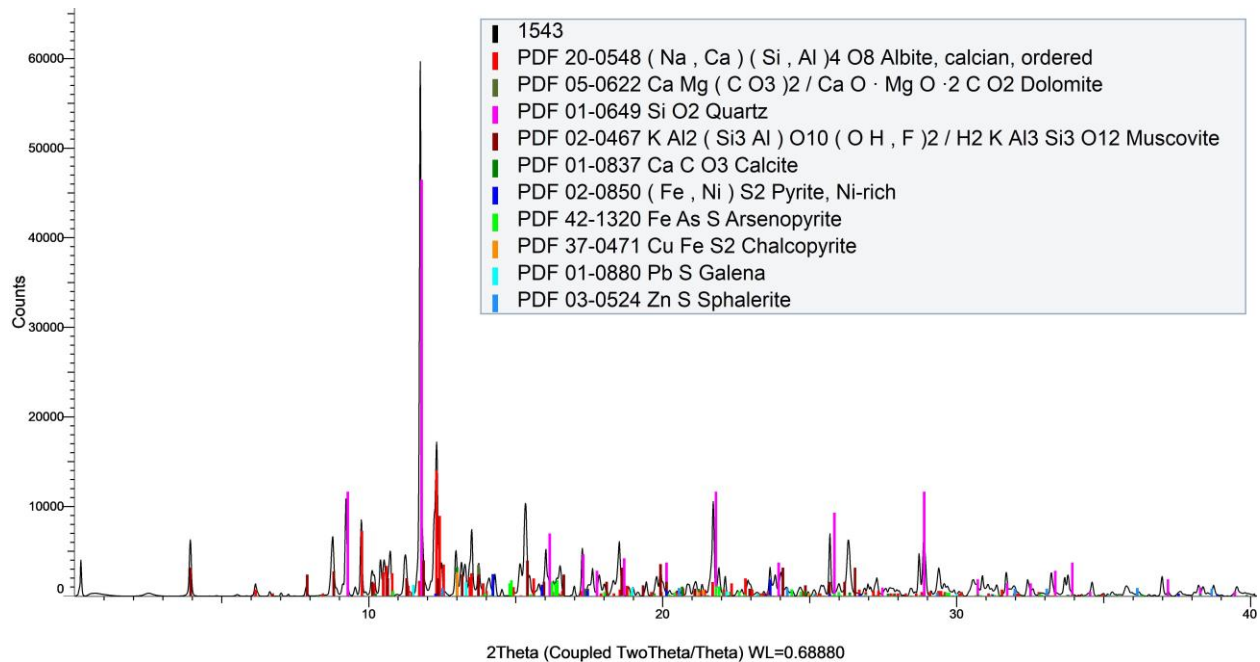


Figure 4-7. X-ray diffractogram of sample 1542 from Twin Lakes West. The host rock lithology is felsic lapilli meta-tuff. The major mineral phases are quartz, albite, and muscovite. The minor mineral phases are calcite, dolomite, pyrite, arsenopyrite, chalcopyrite, galena and sphalerite.

Table 4-2. Synchrotron X-ray Diffraction Data collected at CMCF Beamline, CLS

Hole ID	TL-13-509	TL-16-575	TL-15-568	TL-14-520	TL-12-481	TL-11-419	TL-11-419
Western Sample ID	E5552845	E5552819	E5552824	E5551521	E5551532	E5551540	E5551541
Lithology (by Yamana)	Intermediate-Felsic Intrusives: Quartz-Feldspar Porphyry	Intermediate-Felsic Intrusives: Feldspar Porphyry					
Au Grade	1.13	7.21	1.91- ~8.25	6.597	3.463	1.556	2.816
Target	TLW	TL	TLW	TLW	TL	TLW	TLW
CMCF Feb 2019				√	√	√	√
CMCF July 2019	√	√	√				
Quartz	16.5%	33.8%	16.1%		25.6%	16.4%	25.3%
Albite	39.2%	28.4%	30.3%	26.0%	41.0%	38.5%	42.3%
Muscovite	26.8%		33.0%	22.6%	3.9%	28.3%	2.9%
Microcline	13.3%	15.9%	10.5%				7.4%
Andesine				35.7%			
Anorthite		15.2%			16.9%		
Ankerite	2.3%	1.5%	2.0%			3.2%	2.2%
Orthoclase							10.0%
Calcite				4.2%		3.5%	1.4%
Dolomite							2.6%
Kaolinite							
Pyrite				1.6%	0.5%	1.4%	1.4%
Arsenopyrite		5.2%	6.5%	4.5%	5.7%	6.5%	3.2%
Chalcopyrite	1.9%		1.6%	3.8%	2.5%	0.8%	1.2%
Sphalerite				1.6%	1.5%	1.4%	0.1%
Galena					2.4%		

Hole ID	TL-16-575	TL-17-616	TL-12-468	TL-03-160	TL-11-419	TL-11-419	TL-13-506	TL-11-419	TL-11-419
Western Sample ID	E5552821	E5552360	E5551526	E5551530	E5551542	E5551543	E5551516	E5551535	E5551536
Lithology (by Yamana)	Intermediate Metavolcanics: Ash Tuff	Intermediate Metavolcanics: Lapilli Tuff	Intermediate Metavolcanics: Ash Tuff	Felsic Metavolcanics: Heterolithic Tuff	Felsic Metavolcanics: Lapilli Tuff	Felsic Metavolcanics: Lapilli Tuff	Chemical Metasediments: Oxide Facies IF	Clastic Metasediments: Siltstone	Clastic Metasediments: Siltstone
Au Grade	3.38	1.2 -0.01	1.112	2.61	3.541	4.135	4.96	4.969	3.435
Target	TL	TLE	ME	ME	TLW	TLW	TLW	TLW	TLW
CMCF Feb 2019			√	√	√	√	√	√	√
CMCF July 2019	√	√							
Quartz	10.2%	18.1%	20.4%	37.5%	14.0%	57.9%	24.3%	27.5%	32.7%
Albite	28.5%	39.6%	14.3%	43.5%	28.3%	17.4%	13.4%	15.2%	14.9%
Muscovite	27.9%	28.3%	28.0%	6.9%	7.6%	4.9%	38.8%	5.2%	5.1%
Microcline	25.2%		17.6%		13.0%				
Andesine									
Anorthite								12.6%	
Ankerite	3.8%	11.0%						13.1%	2.0%
Chlorite		3.0%						2.6%	5.7%
Orthoclase									
Calcite			9.5%		11.4%	4.0%	6.9%	7.1%	5.3%
Dolomite						4.3%			
Kaolinite									18.5%
Pyrite	2.5%		3.7%	0.7%	1.2%	3.0%	4.4%	3.8%	3.9%
Arsenopyrite			4.4%	5.0%	7.0%	2.2%	8.7%	7.7%	5.8%
Chalcopyrite	1.9%		1.3%	4.8%	11.1%	3.3%	1.1%	1.7%	3.3%
Sphalerite			0.8%	1.6%	4.6%	1.1%	2.4%	3.5%	2.8%
Galena					1.8%	1.9%			

* “Intermediate-Felsic Intrusives: Feldspar Porphyry” samples are labeled in blue, “Intermediate-Felsic Intrusives: Quartz-Feldspar Porphyry” samples are labeled in yellow, “Intermediate Metavolcanics” are labeled in green, “ Felsic Metavolcanics” are labeled in pink, and “Clastic Metasediments” are labeled in purple.

4.3 Synchrotron Micro X-Ray Fluorescence (SR- μ XRF) mapping

Thirty-one half drill core samples and offcuts have been analyzed in five beamtimes in the APS and CLS. The raw SR- μ XRF dataset of eight offcuts which were analyzed by Cavallin in 2015 at CLS IDEAS Beamline has also been reprocessed by the author using Peakaboo. The relative intensity of elements in the SR- μ XRF element maps reflects the elemental compositions and concentration of different minerals on the surface of the sample. As a result, SR- μ XRF is an intuitive method to identify the spatial relationship between textures, alteration, and ore mineral distribution. The samples with the same petrology generally show the same results of trace element spatial distribution, but also have slightly differences between different targets.

SR-XRF MCA full-spectrums illustrate the relative intensities of all elements identified on the mapping area. Gold (Au) is the key element to understanding the gold mineralization at the Monument Bay Project. However, because of the relatively low concentration of Au comparing to other elements, peak overlap on SR-XRF MCA full-spectrums is the most challenging difficulty in data interpretation. Peak overlap is referred to the interference of neighboring elemental peaks with close emission-line energy and the spectra of the element with relatively higher intensity can overlap the spectra of the element with lower intensity. The common peak overlaps in the samples of the Monument Bay Project are As(K α), Au(L α), and W(L α). The emission-line energies of As(K α), Au(L α), and W(L α) are 10.5 keV, 9.44 keV, and 8.3 keV. In order to obtain the accurate gold distribution, the author checked every high-intensity pixel in Au SR-XRF map and divided the gold peaks into four types (Figure 4-8): 1) Au peak on the As shoulder on the MCA Spectrum, but higher than the shoulder; 2) real Au peak, much higher than As shoulder; 3) Au peak and W peak are overlapped, but Au peak is much higher than As shoulder and W peak; 4) False Au signal caused by overlapped high-intensity W peak.

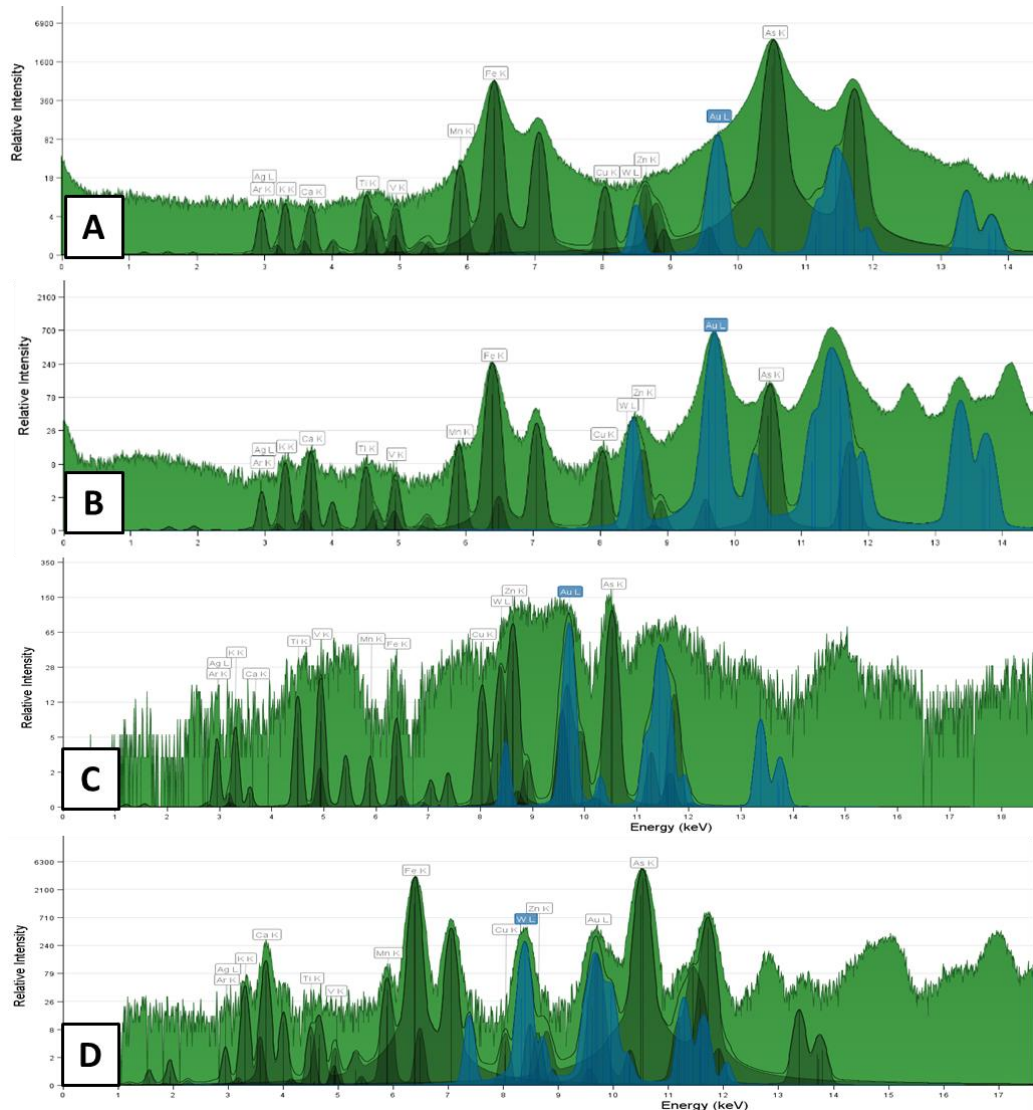


Figure 4-8. MCA spectrum of 2834 (lapilli metauff), 2858 (lapilli metauff), 2853 (porphyritic dacite), and 2841 (porphyritic dacite) half-core sample. The peaks were fitted with Fe K, Ca K, As K, Cu K, Mn K, Au L, Zn K, K K, W L, Ti K interpreted via Peakaboo Software. A. Au peak on the As shoulder on the MCA Spectrum, but higher than the shoulder; B. real Au peak, much higher than As shoulder; C. Au peak and W peak are overlapped, but Au peak is much higher than As shoulder and W peak; D. False Au signal caused by overlapped high-intensity W peak.

4.3.1 Porphyritic Dacite

13 porphyritic dacite samples have been mapped by SR- μ XRF, including seven samples from TL target (2819, 2853, 2857, 1517A, 1518, 1533A, and 1533B), five samples from TLW target (2824, 2827, 2841, 2845, and 1523), and one sample from AZ target (1511). In most data, the peaks in the full MCA spectrum were fitted with Fe K, Ca K, As K, Cu K, Mn K, Au L, Zn K, K K, W L,

Ti K using Peakaboo. The trace element spatial distributions of porphyritic dacite samples are listed as follow:

Ti and K generally distribute as random low-intensity spots cross the sample except in the veins and along with the foliation. They have relatively higher intensity in the white intrusions and light grey or light green layers of foliation, and lower intensity in the yellow-green or dark green layers of foliation. Thus, Ti and K maps are good for identifying the vein cutting (2827, 2845, 2853, and 1523), foliation (1518 and 1533 A&B), and intrusion structures (1511 and 1523) in porphyritic dacite samples. 2853 is a unique sample with two types of veins: white veins with high intensities of Au, W, and Cu and orange veins with high intensities of Fe, Mn, and Ca. As of 2853 is disseminated surrounding the white veins.

As and Fe have the same distribution along with the veins and have much higher intensities than that in other rock types. In samples of typical vein cutting textures, the thick dark-colored ones have much higher As and Fe intensities than the fine light-colored ones (e.g. 2845). Au, Cu, Zn, and W are commonly disseminated in the veins with high As and Fe intensity. However, Cu signals in 1511 and 1523 are super weak, and the W peak in 1511 is not obvious compared to other porphyritic dacite samples. High-intensity Au spots are always next to high-intensity W and/or As spots in veins and fractures. According to high-intensity Au spot testing by replotting into MCA spectrum, there are four types of Au spots in porphyritic dacite samples: 1. All samples have the kind of Au spot with Au peak on the As shoulder on the MCA Spectrum, but higher than the shoulder; 2. real Au peak, much higher than As shoulder (2819, 2853, 2857, 2841, 1511 and 1533 A&B); 3. Au peak and W peak are overlapped, but Au peak is much higher than As shoulder and W peak (2819, 2853, 2857, 2841, 2845 and 1523); 4. false Au signal caused by overlapped high-intensity W peak (2827, 2853, and 2857). Fe, Mn, and Ca distribute along with the foliation texture and intrusive structures. Mn and Ca assemble in the white intrusions and along with veins, but not inside the veins. Mn intensity is usually higher than Ca. Higher-resolution mapping on the regions of interest on 2819 core sample showed the same trace element distributions as large-scale maps. By testing the Au spots in the Au maps, the Au type is the same as the large-scale Au map and specific Au spots were selected for XANES analysis (Figure 4-9).

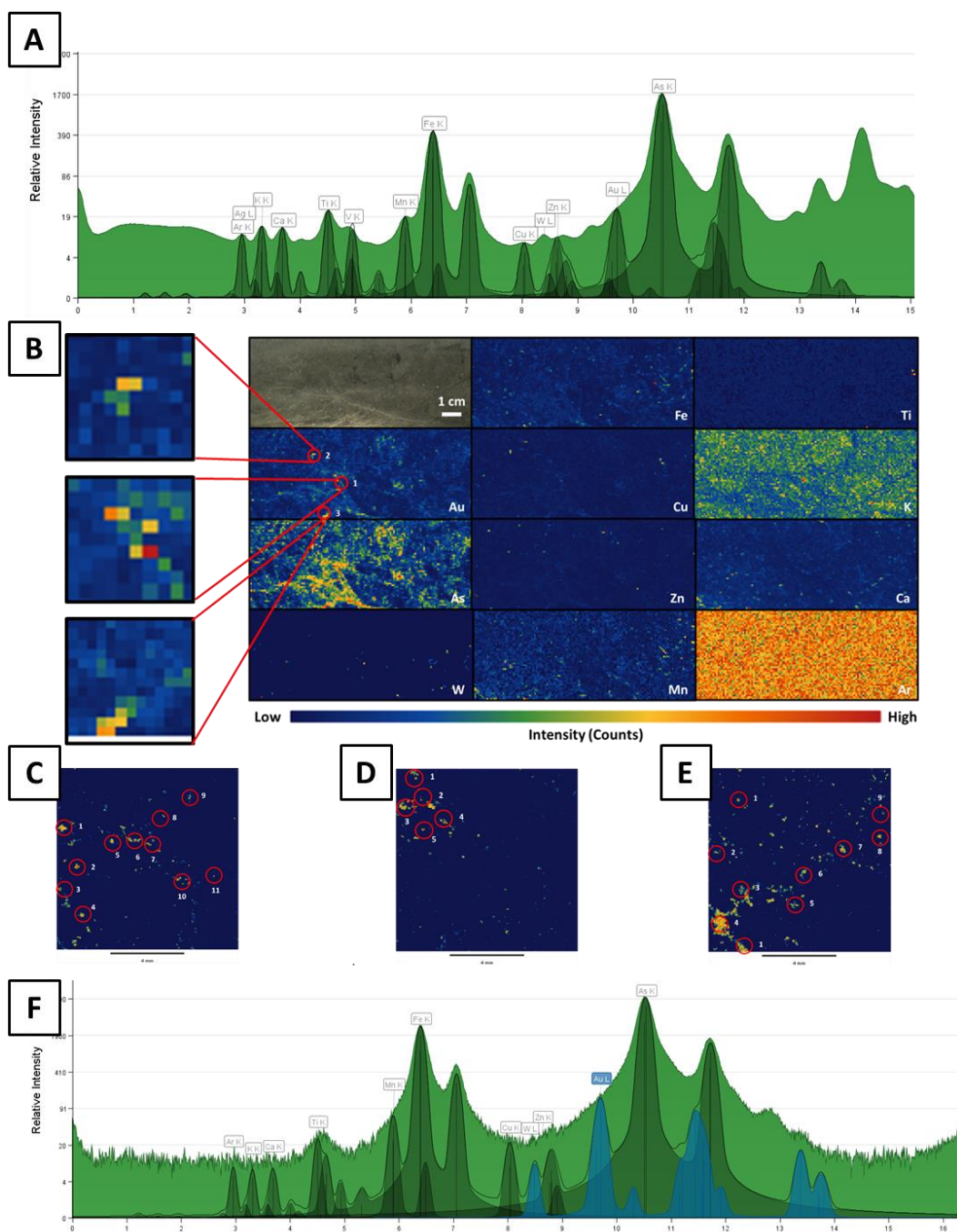


Figure 4-9. A. MCA spectrum of 2819 half-core sample B. Photograph of 2819 half-core sample and corresponding large-scale 2D μ XRF trace element maps of Au, As, W, Fe, Cu, Zn, Mn, Ti, K, Ca and Ar. The red circles correspond to high-intensity Au spot. (Data collected in APS 20ID Beamline in February 2019 with the beam size of 800 μ m x 800 μ m and interpreted by Peakaboo). C-E. Higher-resolution Au 2D μ XRF trace element maps of Au spot No. 1-3 in Figure 4-9B. F. MCA spectrum of gold spot No.1 in Figure 4-9C: Au peak on the As shoulder on the MCA Spectrum, but higher than the shoulder (Data collected in APS 20ID Beamline in July 2019 with the beam size of 60 μ m x 60 μ m and interpreted by Peakaboo).

4.3.2 Intermediate Metatuff

2834, 2858, 2821, and 2360 are four high gold grade intermediate tuff samples chosen for SR- μ XRF mapping. 2821 is an ash metatuff, the others are lapilli metatuff. 2821 and 2858 are from TL target. 2834 and 2360 are from ME and TLE targets individually. In general, the peaks in most data in the full MCA spectrum were fitted with Fe K, Ca K, As K, Cu K, Mn K, Au L, Zn K, K K, W L, Ti K using Peakaboo Software. 2834, 2821, and 2858 have the same trace element spatial distribution, while 2360 is different from them. The High-resolution maps always show more accurate Au spots and less background noise. However, in CLS VESPERS Beamline in February 2019, as the sulphide grains in offcuts are smaller than the beam size, the regions of interest in 2834 offcut has no ideal trace element map in sulphides, and element distributions in sulphide grains are hard to interpret. The trace element spatial distributions in Lapilli tuff are listed as follow:

Au spots are disseminated in veinlets and mostly overlaying with As. The sample without veins (2360) has a weak Au signal and no real Au peak. According to high-intensity Au spot testing by replotting into MCA spectrum, there are two gold types: 1. Au peak on the As shoulder on the MCA Spectrum, but higher than the shoulder (2834); 2. real Au peak, much higher than As shoulder (2858 and 2821). The Au signal is strong. As assembles in some veinlets with strong signals, while in the sample without veins, As is disseminated with much lower intensity. Ti and K usually have the same distribution opposite to the veins. Ti and K maps are totally different from the element maps of other elements. Ti is disseminated in the sample lacking veins with higher intensity. K distributing in the light green foliated layers has higher intensity. Fe, Ca, and Mn commonly have the same distribution next to veinlets and fractures in the dark green foliated layers. Ca sometimes distributes in veins. In a few maps, Mn and Ti are disseminated with less than ten spots with high-intensity spots. W, Cu, and Zn are all disseminated in the mapping areas, especially in the veinlets (Figure 4-10).

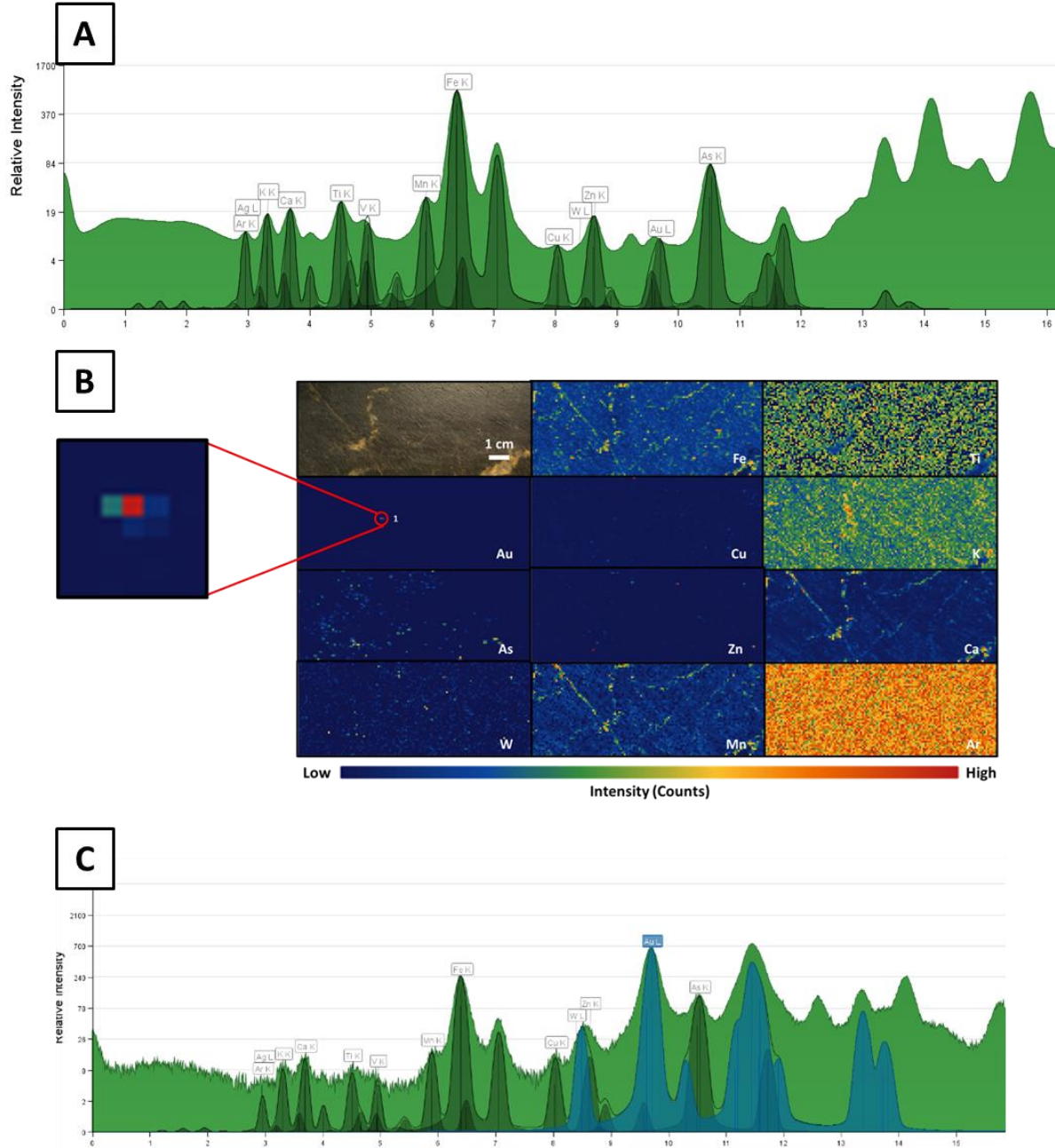


Figure 4-10. A. MCA spectrum of 2858 half-core sample B. Photograph of 2834 half-core sample and corresponding large-scale 2D μ XRF trace element maps of Au, As, W, Fe, Cu, Zn, Mn, Ti, K, Ca and Ar. The red circles correspond to high-intensity Au spot. C. MCA spectrum of gold spot No.1: real Au peak, much higher than As shoulder (Data collected in APS 20ID Beamline in February 2019 with the beam size of 800 μ m x 800 μ m and interpreted by Peakaboo).

4.3.3 Felsic Metatuff

2854 is the only felsic metavolcanics tuff from TL target. 2854 offcut was done SR- μ XRF Mapping with the beam spot size of 800 μ m x 800 μ m in APS 20ID Beamline in February 2019

and 500 μm x 500 μm in APS 8BM Beamline in March 2019. Two regions of interest of sulphide (3mm x 3 mm) on 2854 offcut were examined with the beam size of 100 μm x 100 μm and 10 μm x 10 μm in CLS VESPERS Beamline in February 2019. 2854 half core sample was analyzed with the resolution of 800 μm x 800 μm in APS 20ID Beamline in February 2019; 500 μm x 500 μm in APS 8BM Beamline in March 2019. After the raw data was interpreted by Peakaboo, two 1 cm x 1 cm regions of interest were identified for additional high-resolution SR- μXRF mapping with a 60 μm spot size and the high-intensity spots corresponding to Au and As were marked for XANES in APS 20ID in July 2019.

The peaks in the full MCA spectrum were fitted with Fe K, Ca K, As K, Cu K, Mn K, Au L, Zn K, K K, W L, Ti K interpreted via Peakaboo Software (Figure 4-11A) The trace element spatial distributions of felsic metavolcanic tuff are listed as follow:

Au, W, and Cu have the same distribution in sulphide grains. As, Fe, and Ti are disseminated along with intrusions and have higher intensity on the edge of intrusions. K distributes with relatively higher intensity in the dark-green areas of foliation next to the intrusions. Ca and Mn are disseminated in the same area as high-intensity K (Figure 4-11B). When 3854 core was mapped in 500 μm x 500 μm in APS 8BM Beamline in March 2019, there are two types of Au spots: 1. Real Au peak, much higher than As shoulder (Figure 4-11C); 2. False Au signal caused by overlapped high-intensity W peak (Figure 4-11D). However, when it was examined in APS 20ID in July 2019 (Figure 4-12 A&B), there is only one type of Au which the Au spots with Au peak on the As shoulder of the MCA Spectrum, but higher than the shoulder (Figure 4-12C).

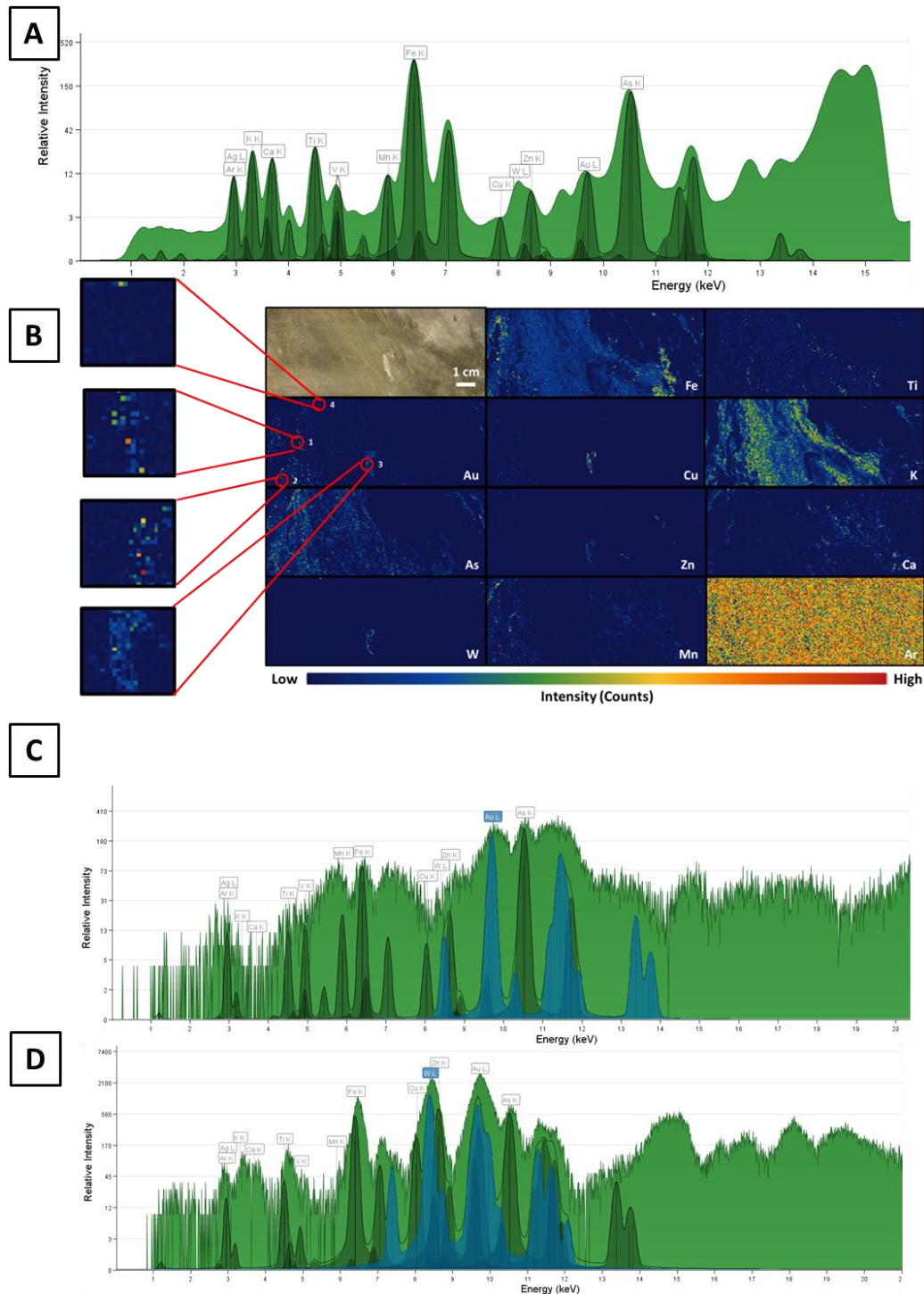


Figure 4-11. A. MCA spectrum of 2854 half-core sample B. Photograph of 2854 half-core sample and corresponding large-scale 2D μ XRF trace element maps of Au, As, W, Fe, Cu, Zn, Mn, Ti, K, Ca and Ar. The red circles correspond to high-intensity Au spot. C-D. MCA spectrum of gold spot No.1&4: No 1. is a real Au peak, much higher than As shoulder; No 4. is a false Au signal caused by overlapped high-intensity W peak (Data collected in APS 8BM Beamline in March 2019 with the beam size of 500 μ m x 500 μ m and interpreted by Peakaboo).

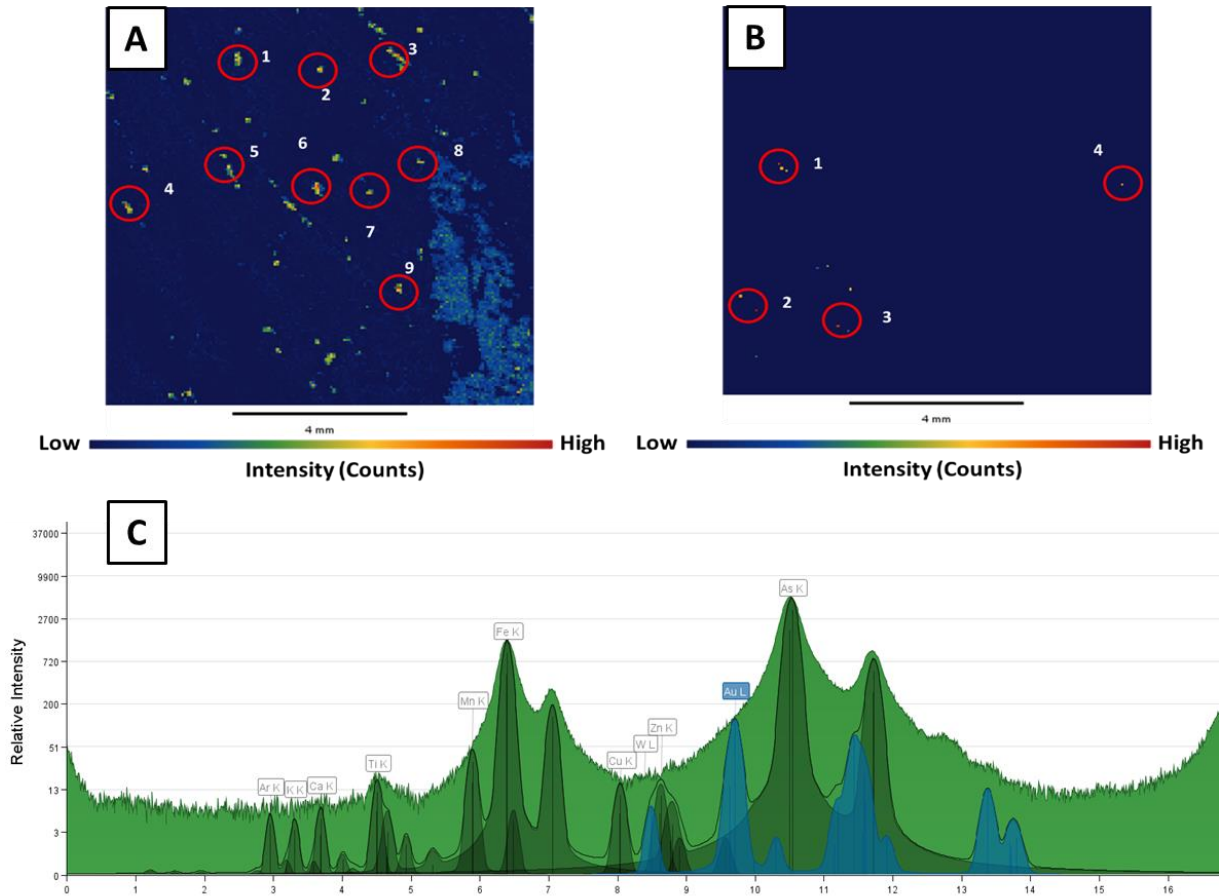


Figure 4-12. A&B. Higher-resolution Au 2D μ XRF trace element maps of Au spot No. 1&2 in Figure 4-11A. C. MCA spectrum of gold spot No.8 in Figure 4-12A: Au peak on the As shoulder on the MCA Spectrum, but higher than the shoulder (Data collected in APS 20ID Beamline in July 2019 with the beam size of $60\ \mu\text{m} \times 60\ \mu\text{m}$ and interpreted by Peakaboo).

4.3.4 Metasediment

2831, 1516A, and 1544A are metasediment samples that were selected for SR- μ XRF Mapping. 2831 is a metasandstone from SLS Target with a half-drill core sample and an offcut. The core was analysed with the beam spot size of $800\ \mu\text{m} \times 800\ \mu\text{m}$ in APS 20ID Beamline in February 2019 and $500\ \mu\text{m} \times 500\ \mu\text{m}$ in APS 8BM Beamline in March 2019. Three $1\ \text{cm} \times 1\ \text{cm}$ regions of interest on cores were analyzed in APS 20ID Beamline in July 2019 for additional high-resolution SR- μ XRF mapping ($60\ \mu\text{m} \times 60\ \mu\text{m}$). The offcut was analysed with the resolution of $800\ \mu\text{m} \times 800\ \mu\text{m}$ and $300\ \mu\text{m} \times 300\ \mu\text{m}$ in APS 20ID Beamline in February 2019 and $500\ \mu\text{m} \times 500\ \mu\text{m}$ in APS 8BM Beamline in March 2019. 1516A and 1544A are metasiltstone from TLW Target and metaconglomerate from SLS Target individually. The raw SR- μ XRF dataset of these two offcuts

was analyzed by Cavallin in 2015 at CLS IDEAS Beamline has also been reprocessed by the author using Peakaboo.

The peaks in the full MCA spectrum were fitted with Fe K, Ca K, As K, Cu K, Mn K, Au L, Zn K, K K, W L, Ti K interpreted via Peakaboo Software (Figure 12A, 13A, and 14A); and the trace element intensity order (from high to low) is As>Fe>Zn>Ti>Cu>Ca>Au>Mn>W>K. The trace element spatial distributions of metasediment are listed as follow:

Mn, Ca, K, and Ti commonly distribute along with foliation: Mn and Ca occur in dark grey or dark green layers, while K and Ti accurate in light green layers. Au, As, and Fe have the same distribution along with the sulphide veins and grains. W, Zn, and Cu are disseminated as high-intensity spots in a few sulphide grains (Figure 4-13). In sample 1544A, Mn and Ca also have high intensity in white intrusions. There are two types of sulphide grains in 1544A: fine-grained ones in veins with high-intensity of Au, As, and Fe and low W, Zn, and Cu signals; coarse-grained ones in intrusions with high intensity of Au, As, Fe, W, Zn, and Cu (Figure 4-13B). According to high-intensity Au spot testing by replotting into MCA spectrum, there are two types of Au spots in metasediment samples: 1. All samples have the Au spots with Au peak on the As shoulder of the MCA Spectrum, but higher than the shoulder; 2. real Au peak, much higher than As shoulder. Higher-resolution mapping on the regions of interest on 2831 core sample showed the same trace element distributions as large-scale maps. By testing the Au spots in the Au maps, the Au type is the same as the large-scale Au map and specific Au spots were selected for XANES analysis (Figure 4-13).

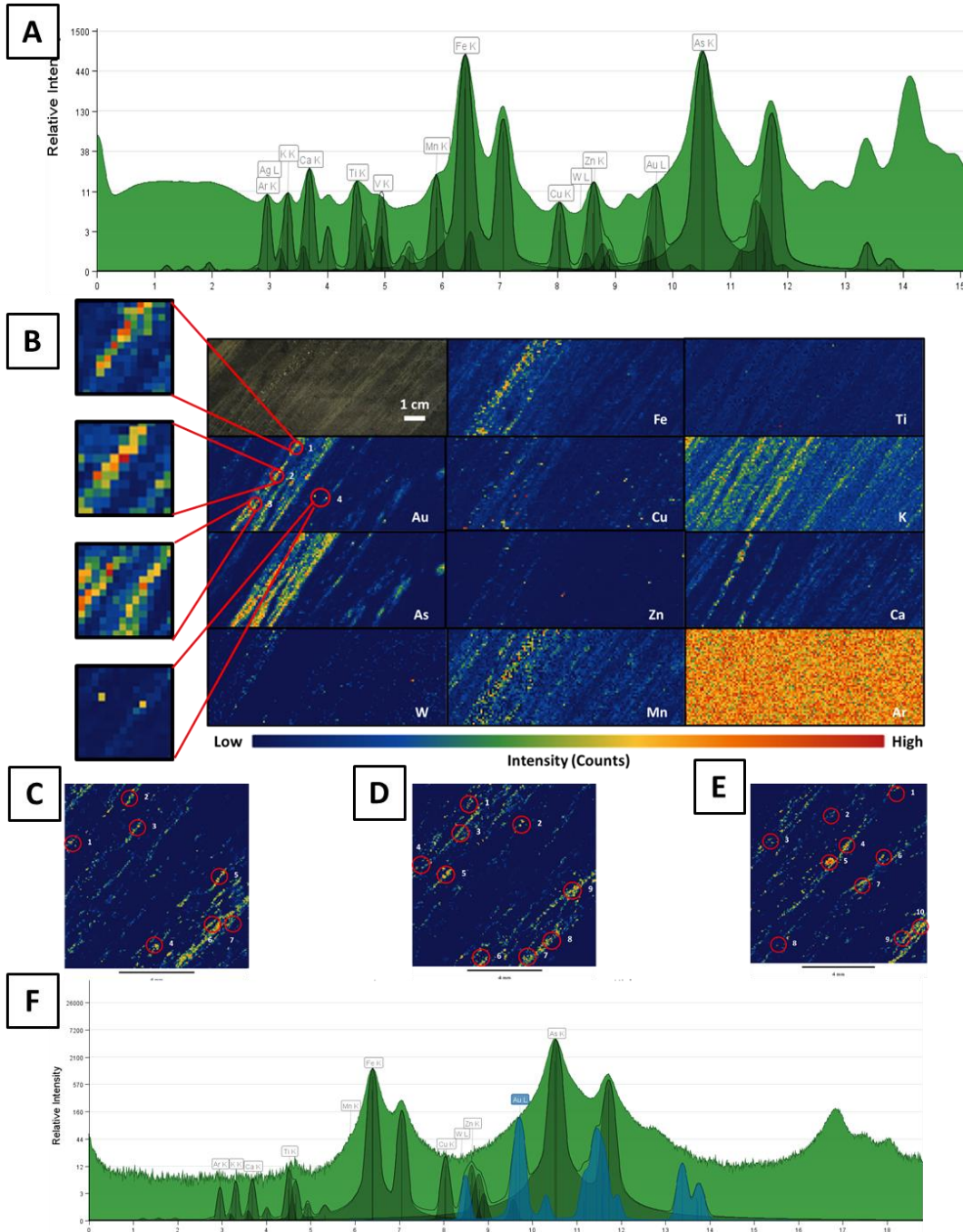


Figure 4-13. A. MCA spectrum of 2831 half-core sample B. Photograph of 2831 half-core sample and corresponding large-scale 2D μ XRF trace element maps of Au, As, W, Fe, Cu, Zn, Mn, Ti, K, Ca and Ar. The red circles correspond to high-intensity Au spot. (Data collected in APS 20ID Beamline in February 2019 with the beam size of 800 μ m x 800 μ m and interpreted by Peakaboo). C-E. Higher-resolution Au 2D μ XRF trace element maps of Au spot No. 1-3 in Figure 4-13B. F. MCA spectrum of gold spot No.6 in Figure 4-13E: Au peak on the As shoulder on the MCA Spectrum, but higher than the shoulder (Data collected in APS 20ID Beamline in July 2019 with the beam size of 60 μ m x 60 μ m and interpreted by Peakaboo).

4.4 X-ray Absorption Near-edge Structure (XANES) Spectroscopy

XANES spectroscopy provided insights into the speciation of As and Au in half drill core samples offcuts, and rock powder samples. The information was applied to analyse the relationship between As and Au in the Monument Bay Project. Because of the low concentration of As and Au in rock powder samples, the spectrums of micro-XANES generally have more obvious edge features than that of bulk-XANES.

As K-edge micro-XANES spectroscopy and bulk XANES spectroscopy identified only As^{1-} in the samples (Figure 4-14), which corresponds to arsenopyrite grains observed in the thin sections and the common association of As and Fe in the SR- μ XRF maps. No other speciation of As was identified (i.e. As^{3+} , As^{5+} , As_2O_3 , and H_3AsO_4 (Figure 4-15)).

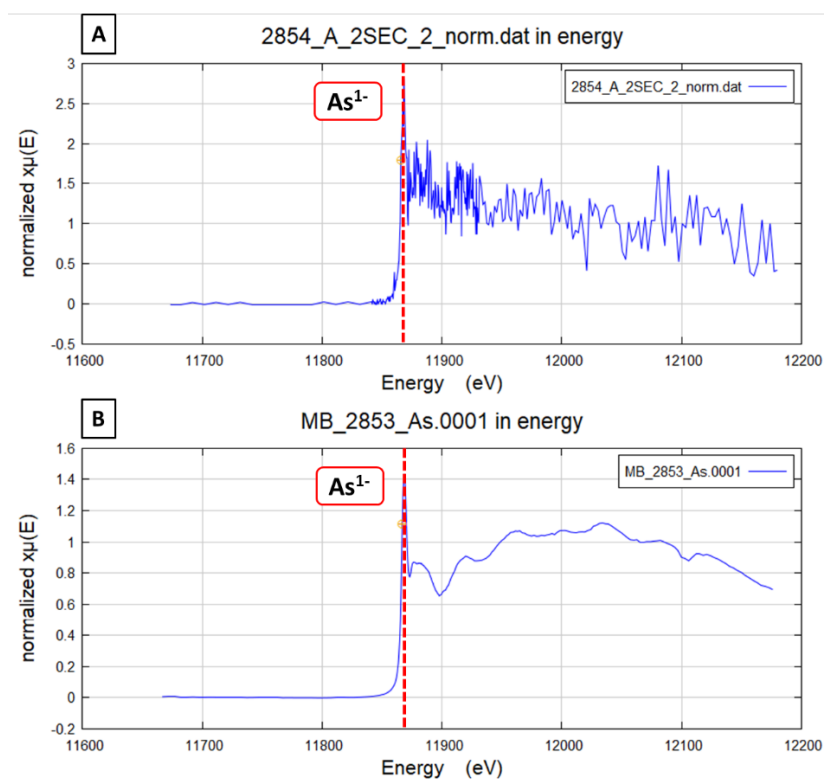


Figure 4-14. A. As K-edge micro-XANES spectrum collected directly on 2854 offcut analysed at CLS VESPERS Beamline in February 2019. B. As K-edge bulk-XANES spectrum collected directly on 2853 rock powder sample analysed at APS 20BM Beamline in July 2019.

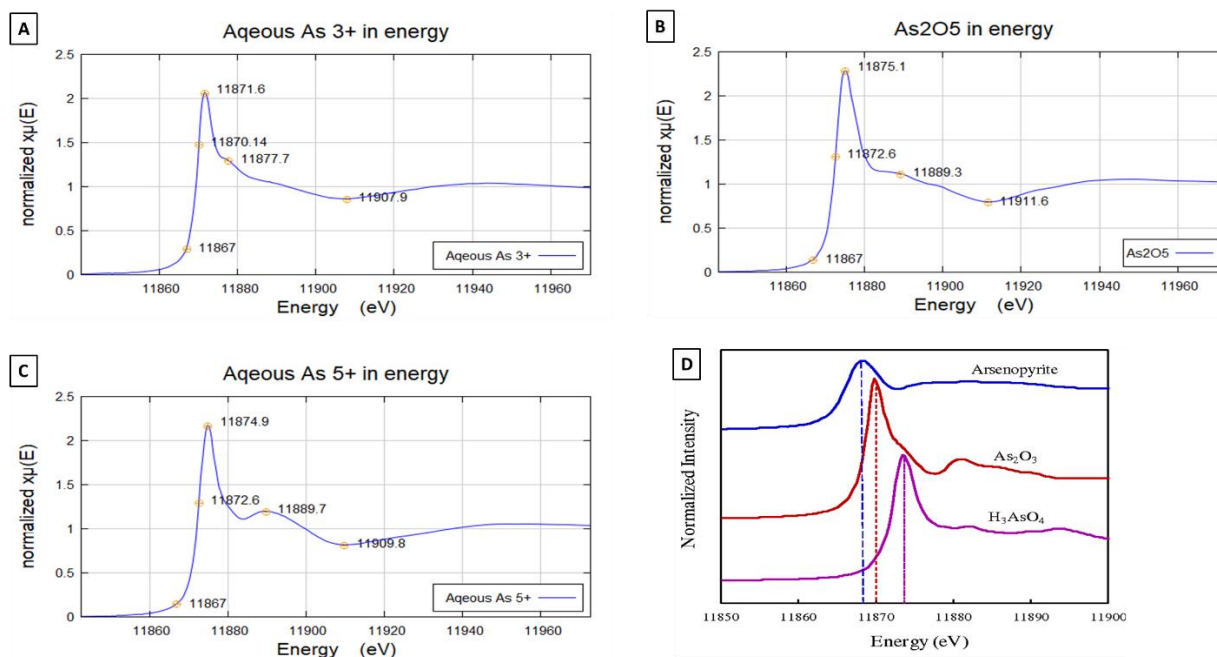


Figure 4-15. A-C. Standard As K-edge XANES spectrum of As^{3+} dissolved in water, As_2O_5 powder on Kapton tape, and As^{5+} dissolved in water accessed from Hephastus software (Ravel & Newville, 2005). D. Normalized standard As K-edge XANES spectra of arsenopyrite (blue line), As_2O_3 (red line) and H_3AsO_4 (As^{3+} , purple line) (Wang et al., 2013).

As K-edge (11867 eV) and Au L_3 -edge (11919 eV) are close to each other and the concentration of As is much higher than Au in most samples. As a result, Au L_3 -edge is easy to be overlapped by the post-edge of As K-edge spectrum, and it is difficult to identify the oxidation of Au (Figure 4-16C). Only one sample (2831) shows a precise Au L_3 -edge micro XANES spectroscopy, in which the Au L_3 -edge is higher than As post-edge. Compared with the spectrum of gold foil, the Au L_3 -edge micro-XANES spectrum identified only metallic gold (Au^0) in the samples, meaning that gold at the Monument Bay deposit is not bound in sulphide lattice structures (Figure 4-16A&B). No other speciation of As were identified (i.e. Au^{3+} and Au^{1+} (Figure 4-17)). There was no clear and distinguishable Au L_3 -edge bulk XANES spectrum, even in the highest gold grade powder sample (1533 with the gold grade of 13.22 pm, Figure 4-16D).

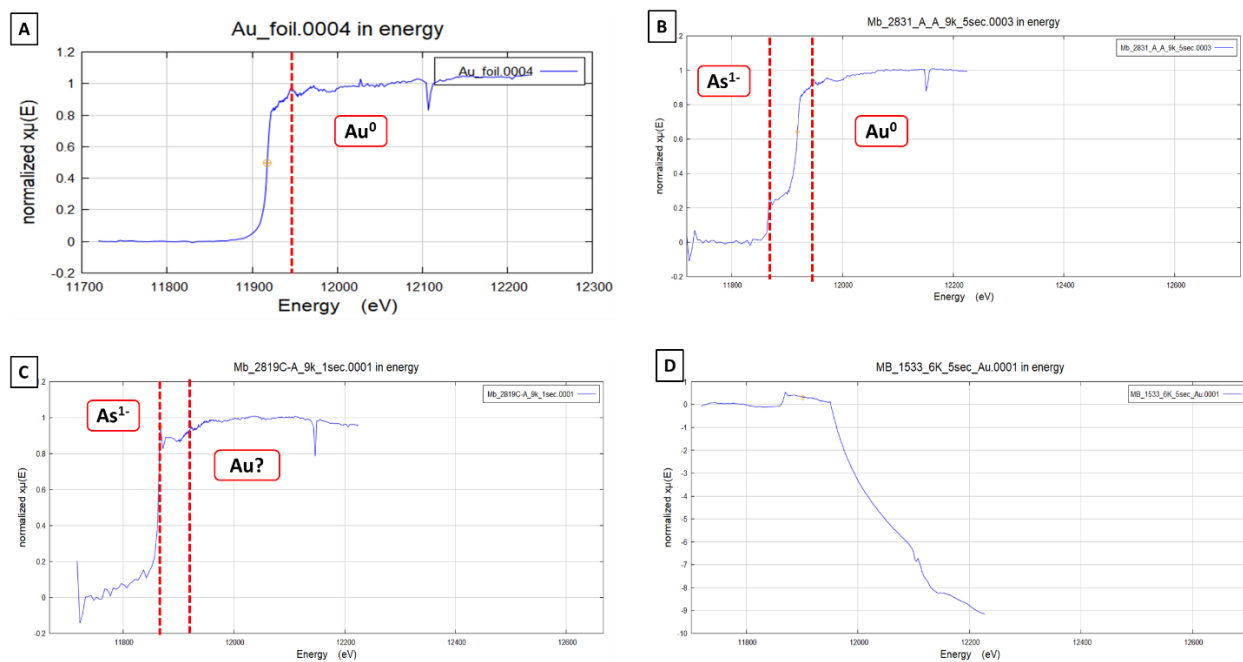


Figure 4-16. A-C. Au L₃-edge micro-XANES spectrum collected directly on gold foil as a standard and 2831 and 2819 half drill core samples examined at APS 20ID Beamline in July 2019. B. As K-edge bulk-XANES spectrum collected directly on 1533 rock powder sample collected at APS 20BM Beamline in July 2019.

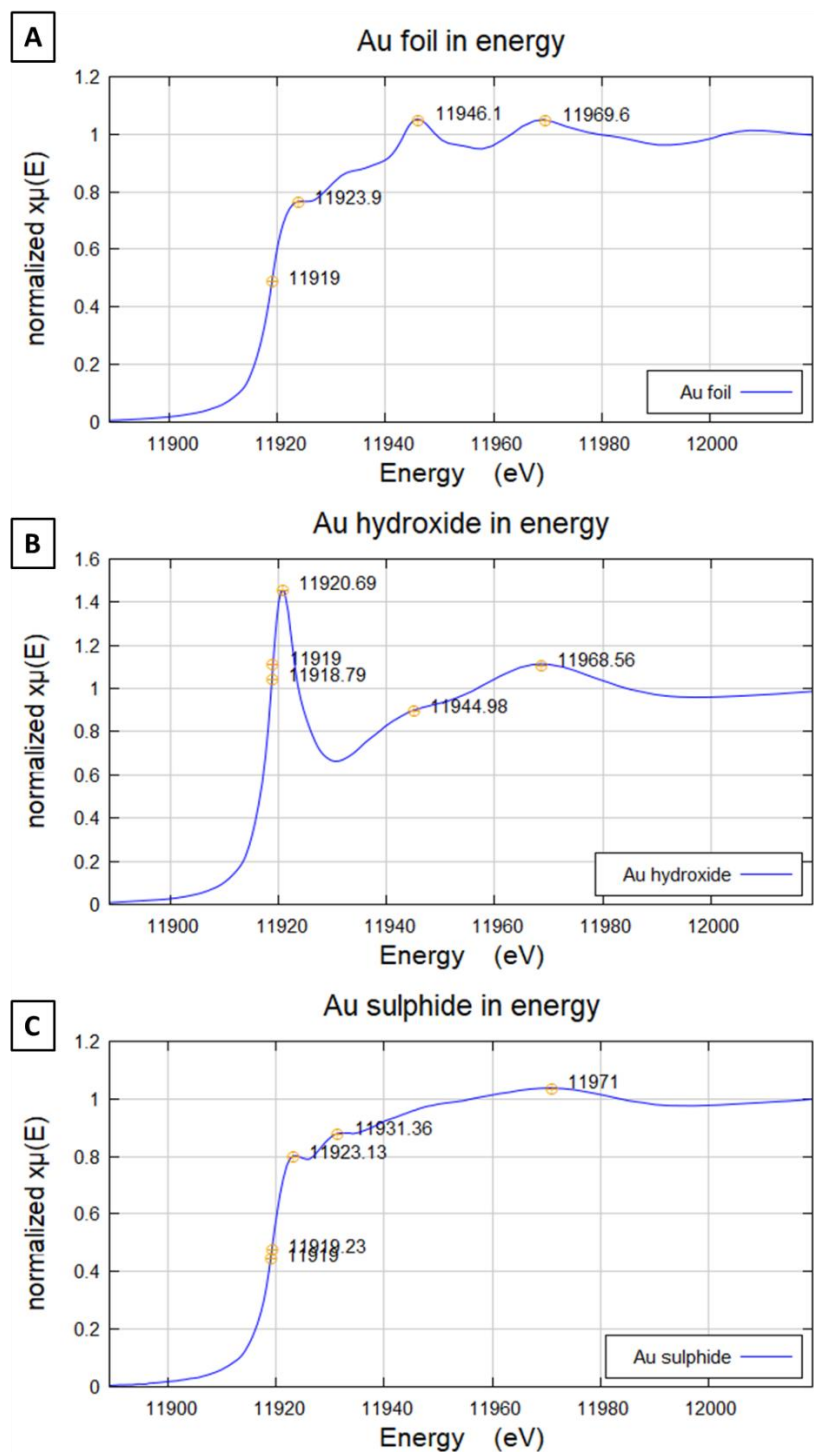


Figure 4-17. A-C. Standard Au L_3 -edge XANES spectrum of gold foil (represents metallic gold, Au^0), gold hydroxide powder (represents refractory gold, Au^{1+}), and gold sulphide powder (represents Au^{3+}) accessed from Hephaestus software (Ravel & Newville, 2005).

4.5 Electron Probe Micro-Analysis (EPMA)

After carbon-coating, 13 thin sections have been analyzed using EPMA, including 9 porphyritic dacite samples, 2 intermediate metavolcanics, 1 felsic metavolcanics, and 1 metasediment (Table 4-3).

Table 4-3. EPMA Dataset of the Monument Bay Project

Hole ID	Western Sample ID	Lithology (by Yamana)	Au Grade (ppm)	Target	10/1/2019	10/4/2019	2/3/2020-2/5/2020
TL-12-481	E5551533 A	Intermediate-Felsic Intrusives: Quartz-Feldspar Porphyry	13.22	TL	EDS Point Analysis (9)		
TL-12-481	E5551533 B	Intermediate-Felsic Intrusives: Quartz-Feldspar Porphyry	13.22	TL		EDS Point Analysis (5)	
TL-11-419	E5551539 B	Intermediate-Felsic Intrusives: Quartz-Feldspar Porphyry	0.91	TLW		EDS Point Analysis (4)	EDS Point Analysis (1)
TL-13-509	E5552845	Intermediate-Felsic Intrusives: Quartz-Feldspar Porphyry	1.13	TLW		EDS Point Analysis (9); EDS element maps on arsenopyrite (1)	
TL-15-564	E5552827	Intermediate-Felsic Intrusives: Quartz-Feldspar Porphyry	close to 9 - ~0.6	TLW			EDS/WDS element maps (4)
TL-16-575	E5552819	Intermediate-Felsic Intrusives: Feldspar Porphyry	7.21	TL			EDS Point Analysis (2)
TL-16-607	E5552857	Intermediate-Felsic Intrusives: Feldspar Porphyry	2.16	TL			EDS Point Analysis (3)
TL-15-568	E5552824	Intermediate-Felsic Intrusives: Feldspar Porphyry	1.91-~8.25	TLW			EDS/WDS element maps (6)
TL-13-504	E5552841	Intermediate-Felsic Intrusives: Feldspar Porphyry	25.2	TLW			EDS/WDS element maps (5)
TL-13-500	E5552834	Intermediate Metavolcanics: Lapilli Tuff	5.21	ME		EDS Point Analysis (10); EDS element maps on pyrite (1)	
TL-16-607	E5552858	Intermediate Metavolcanics: Lapilli Tuff	2.45	TL			EDS/WDS element maps (5)
TL-16-604A	E5552854	Felsic Metavolcanics: Undifferentiated Tuff	10.49	TL			EDS Point Analysis (6)
TL-15-551	E5552831	Clastic Metasediments: Sandstone	2.26	SLS	EDS Point Analysis (10)		

* “Intermediate-Felsic Intrusives: Feldspar Porphyry” samples are labeled in blue, “Intermediate-Felsic Intrusives: Quartz-Feldspar Porphyry” samples are labeled in yellow, “Intermediate Metavolcanics” are labeled in green, “Felsic Metavolcanics” are labeled in pink, and “Clastic Metasediments” are labeled in purple.

4.5.1 Energy-dispersive X-ray spectroscopy (EDS) point analysis

According to EDS point analysis, the matrix is generally albite + potassium feldspar + muscovite ± chlorite. Major sulphides are pyrite, arsenopyrite, chalcopyrite, sphalerite, and galena. Stibnite was observed in a few thin sections. Based on the morphologies, sulphides can be classified as euhedral, subhedral, disseminated, needle-shaped, corroded, fractured, and multiple sulphides phases as a combination. Sulphide may appear in quartz and/or carbonate (calcite ± ankerite) vein, in/near fractures, and/or in the matrix. Pyrite grains are euhedral-subhedral and/or needle-shaped, and most of them are corroded with numerous inclusions inside (Figure 4-18A). A few pyrite grains are anhedral and combined with scheelite. Arsenopyrite grains have three types: 1) fine-grained, euhedral, and disseminated ones in the quartz veins; 2) medium-coarse grained, euhedral-subhedral, or needle-shaped, corroded and fractured ones in the matrix; 3) fine-grained inclusions arsenopyrite in corroded pyrite (Figure 4-18B&C). The typical sulphide combinations are arsenopyrite + pyrite, pyrite + sphalerite, pyrite + chalcopyrite, arsenopyrite + sphalerite, chalcopyrite + galena, sphalerite + chalcopyrite, sphalerite + stibnite and/or arsenopyrite + galena (e.g. Figure 4-18D, E, &F). The corroded and fracture pyrite and arsenopyrite have numerous inclusions inside and/or near the grains. Zircon, ilmenite, scheelite, garnet, hematite, monazite and/or apatite are the general inclusions observed via EPMA.

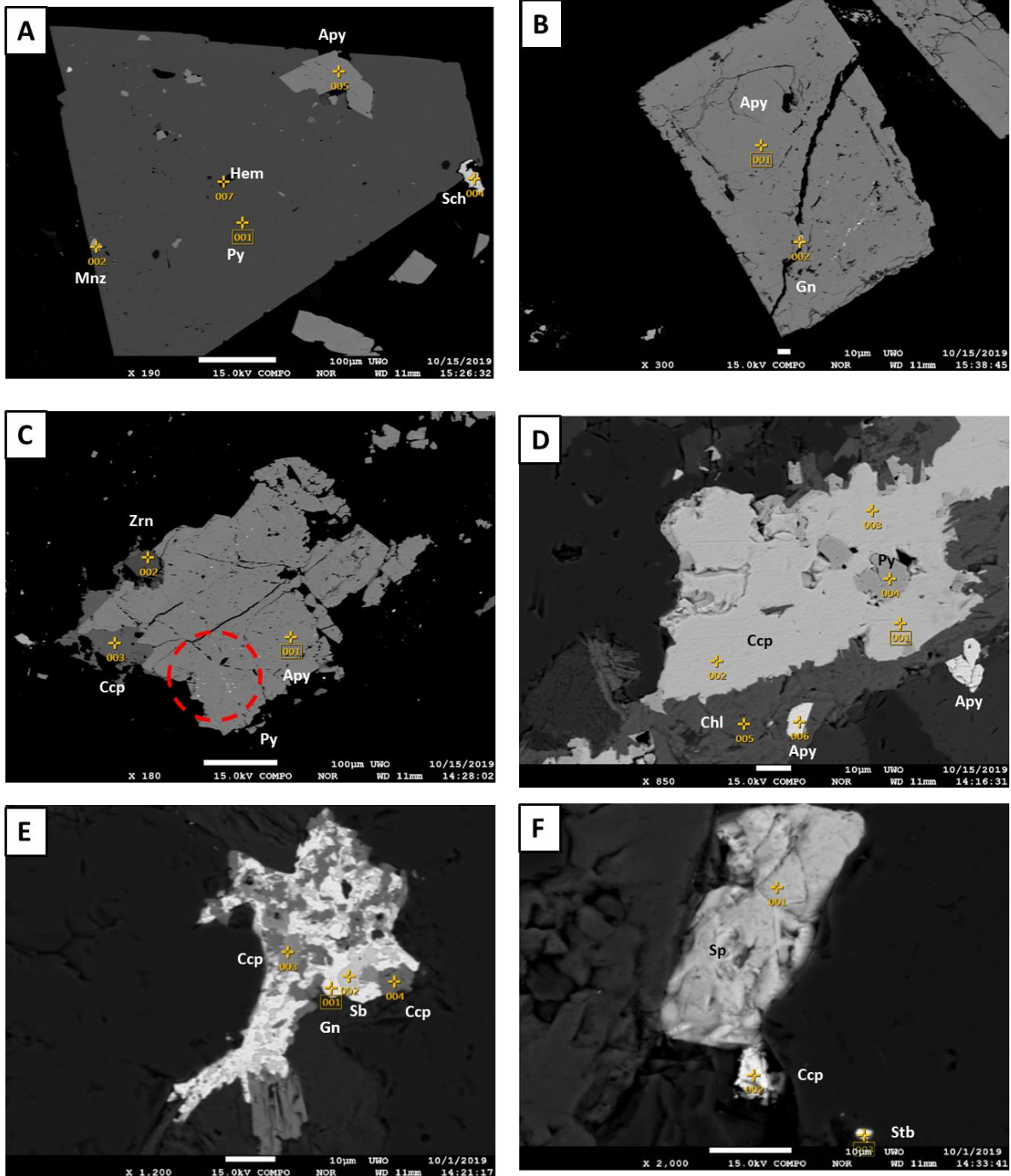


Figure 4-18. Back-scattered images of sulphide morphologies in the Monument Bay Project: A. Anhedra scheelite, subhedra arsenopyrite, hematite, and monazite inclusions in a needle-shaped corroded pyrite grain. B. Fractured euhedral arsenopyrite with galena filled in fractures and as inclusions. C. Fractured subhedra arsenopyrite with zircon and chalcopyrite on the edge and fine-grained pyrite inside. D. Corroded anhedra chalcopyrite grain with pyrite inside, and fine-grained subhedra arsenopyrite grains in chlorite matrix. E. Combination of chalcopyrite + galena + antimony in the matrix. F. Combination of sphalerite + chalcopyrite and stibnite in matrix.

EDS point analysis show two types of gold grains in thin sections: inclusion gold and free gold. Most gold grains are Au + Ag with an average Au/Ag ratio of 14.16 (Figure 4-19). However, a few are pure gold (2831, metasediment and 2834, intermediate metavolcanics) and a few are Au + Sb with an average Au/Sb ratio of 1.46.

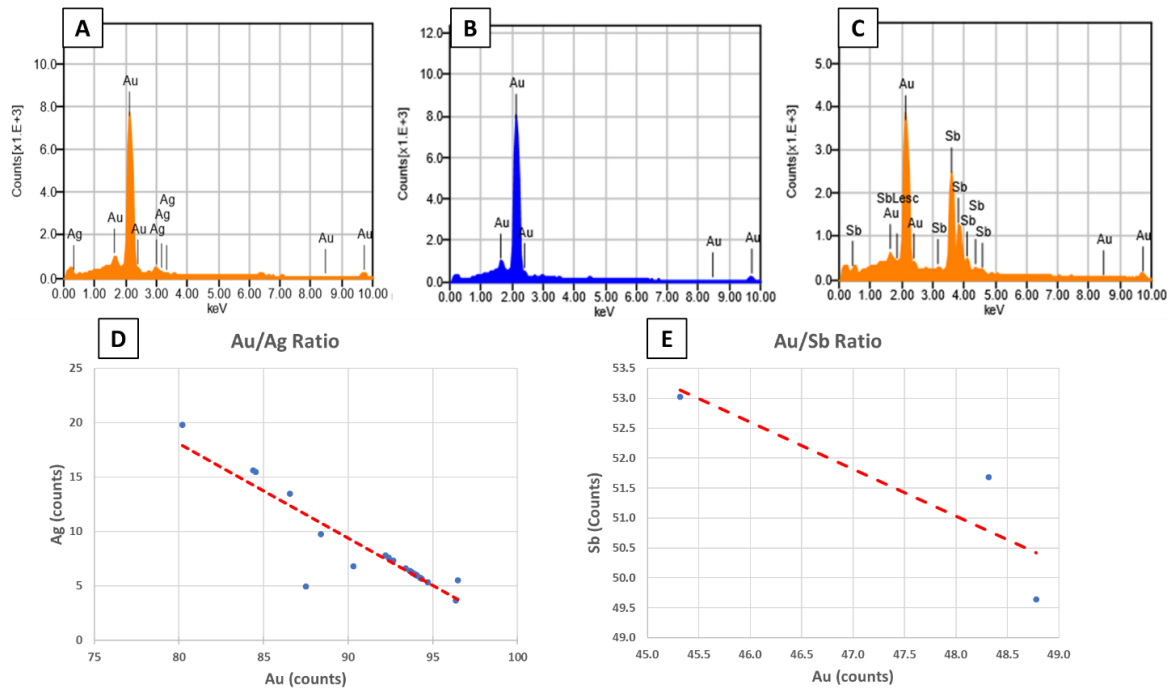


Figure 4-19. A-C. Spectra collected by EDS point analysis on microscopic gold represent: Au + Ag, pure gold, and Au + Sb. D&E. Au/Ag ratio and Au/Sb ratio of microscopic gold.

Gold grains in sulphides grains as inclusions are referred to as inclusion gold (Figure 4-20). There are three compositions of inclusion gold: Au + Ag, Au + Sb, and pure gold. Au + Ag inclusion gold may occur on the edges of subhedral pyrite grains, inside corroded euhedral-subhedral pyrite, inside subhedral arsenopyrite grains, inside the combine of arsenopyrite + pyrite, and anhedral galena (Figure 4-20A, B, &D). 1533A shows a unique combination of inclusion gold and chalcopyrite near corroded anhedral pyrite and fine-grained scheelite and arsenopyrite (Figure 4-20A). Pure gold (100% Au) with rutile is inside combinations of pyrite + Arsenopyrite and sphalerite (Figure 4-20C&F).

Most of free gold grains are all Au + Ag and a few are pure gold (Figure 4-21). Some free gold are near corroded euhedral pyrite (Figure 4-21A); some are near disseminated arsenopyrite (Figure

4-21B); some are in the matrix, not related to sulphides (Figure 4-21C); some are near corroded anhedral pyrite, fine-grained chalcopyrite, fine-grained scheelite and arsenopyrite (Figure 4-21D).

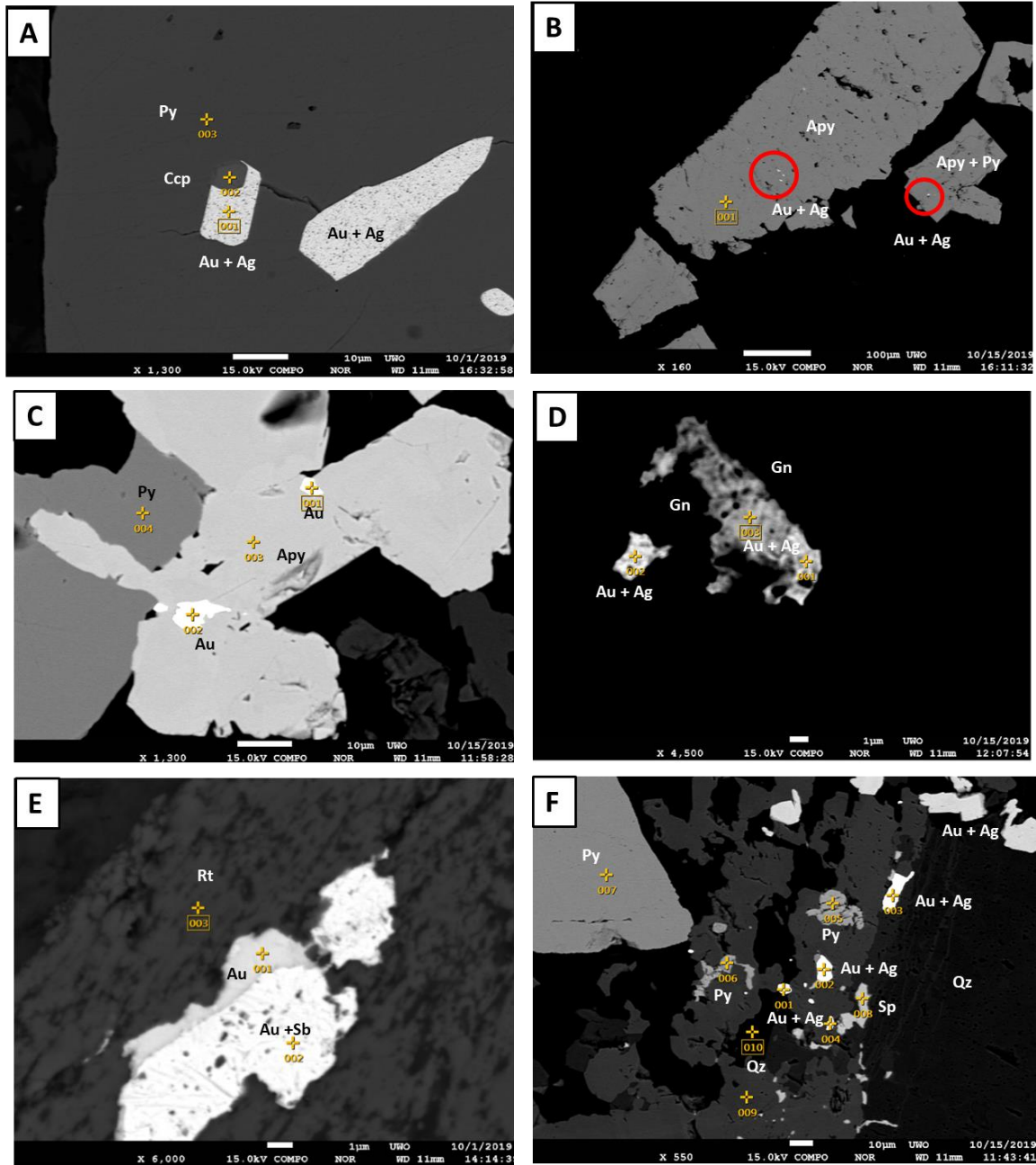


Figure 4-20. Back-scattered images of inclusion gold within sulphides: A. Inclusion gold (Au +Ag) and chalcopyrite in fractured pyrite; B. Inclusion gold (Au +Ag) in corroded subhedral arsenopyrite and arsenopyrite + Pyrite grains; C. Inclusion gold (pure gold) in the combination of pyrite + Arsenopyrite. D. Inclusion gold (Au +Ag) in galena grain, E. Pure gold and Au + Sb in rutile grain; F. Inclusion gold with sphalerite and pyrite in quartz vein.

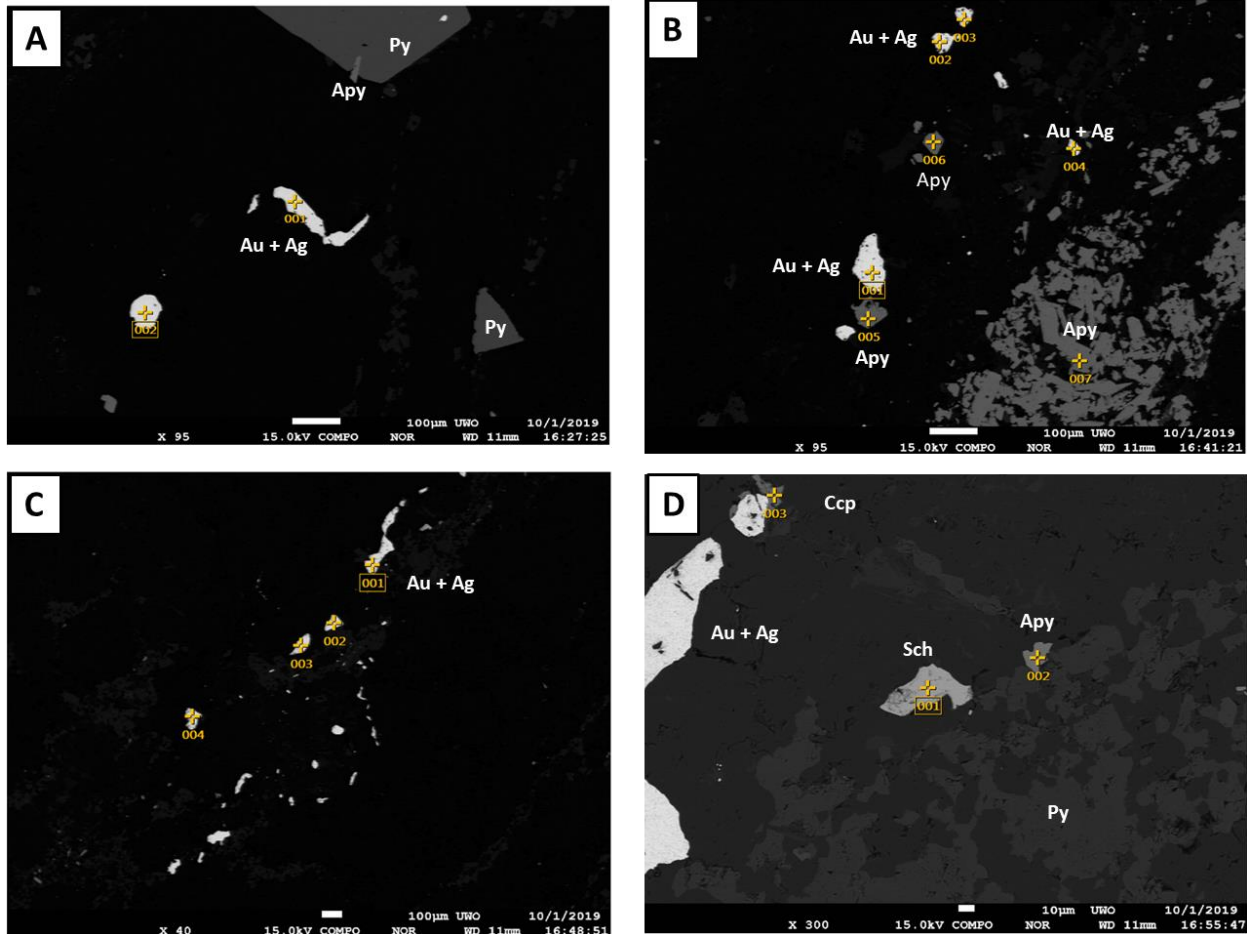


Figure 4-21. Back-scattered images of different types of free gold: A. Free gold near corroded euhedral pyrite; B. Free gold near disseminated arsenopyrite; C. Free gold in the matrix; D. Free gold near corroded anhedronal pyrite, fine-grained chalcopyrite, fine-grained scheelite and arsenopyrite.

4.5.2 EDS/WDS Element Mapping

From the EDS/WDS element maps of 2834 (intermediate metavolcanics), corroded needle-shaped pyrite grain in the quartz vein is strongly fractured and inclusion-rich. Inclusions are mainly arsenopyrite pyrite (As, Fe, and S EDS map) and quartz (Si EDS map). Arsenopyrite are euhedral and fine-grained located in the center and margins of the corroded needle-shaped pyrite. In the Au-EDS map, the high-intensity gold spots are not inside arsenopyrite, but along with fractures in needle pyrite (Figure 4-22A). A few corroded euhedral to subhedral pyrite grains without fractures show zoning texture in As WDS element map and Mg EDS element maps (Figure 4-22 B&C), but there is no high-intensity gold spot.

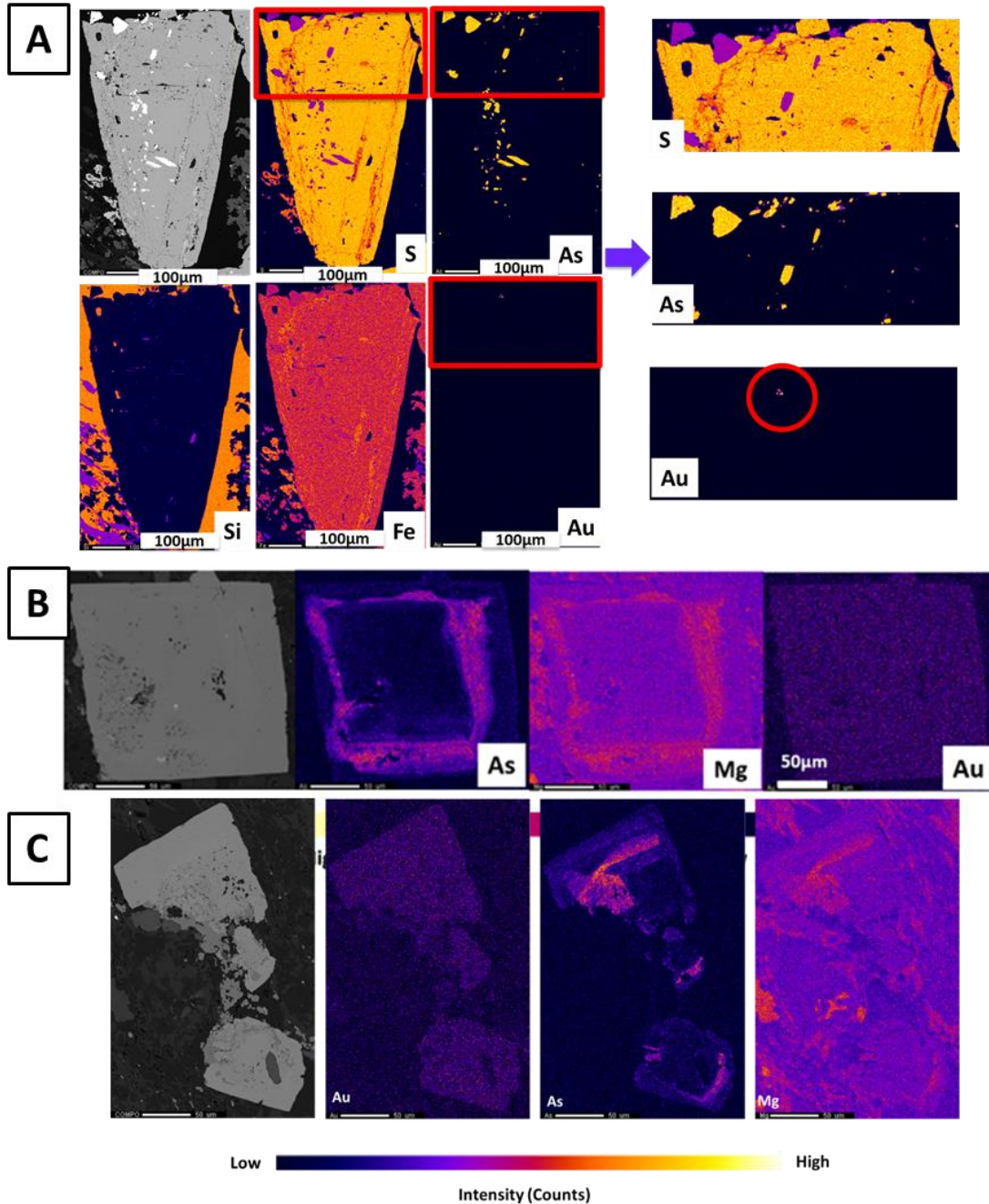


Figure 4-22. A. Back-scattered images and EDS/WDS-EPMA 2D element maps show euhedral arsenopyrite grains and quartz inclusions inside corroded needle-shaped pyrite grains and gold along with the fractures; B&C. Back-scattered images and EDS/WDS-EPMA 2D element maps show zoning texture in corroded euhedral to subhedral pyrite grains without fractures. No high-intensity gold spots in pyrite.

Chapter 5

5 Discussion

The main goal of this project is to determine the gold mineralization and geometallurgy at the Monument Bay Project. Traditional microscopy was used combining with geochemical and mineralogical analytical techniques (Synchrotron X-ray Diffraction (SR-XRD), X-ray Absorption Near-edge Structure (XANES) Spectroscopy, and Electron Probe Microanalysis (EPMA)) and geochemical mapping techniques (Synchrotron Micro X-Ray Fluorescence (SR- μ XRF) mapping). Each technique has its own advantages and disadvantages. The integration of different methods gives supports for each other and make up the limitation of a single method. Mineral distribution and element distribution, the spatial relationship between sulphide morphology and gold distribution, gold and arsenic speciation have been identified to comprehensively understand the gold mineralization system and geometallurgy at the Monument Bay Project. In addition, the deductions of timing relationships, deleterious element characterization, and fluid events of ore-forming processes can guide further exploration, mine planning, and production.

5.1 Element Distribution and Mineral Distribution

Traditional microscopy is a common method for petrology and mineralogy study. Hand sample description and photomicrographs can provide the basic knowledge of the texture, mineral assemblages, alteration, and veining of different rock types. However, owing to the moderate to strong alteration in the samples, the estimation of modal percentages of the host rock matrix can be wrong. Apart from that, thin section cutting might be not representative enough for the host rock lithology of a ~25-cm-long drill core sample. As for SR-XRD, it is an effective method for quickly identifying the modal mineralogy on pulp and powdered rock samples. Because the concentration of minerals varies considerably from one side to the other side of drill core samples, the average mode and mineral assemblages providing by bulk SR-XRD are more representative and detailed than traditional microscopy, even the trace amounts of sulphide minerals can be identified. But the SR-XRD interpretation and peak fitting of diffractograms need strong background knowledge for mineralogy and rock genesis. For instance, during the peak fitting, some samples showed a good fit with pyroxene and spinel. However, considering the samples are

intermediate to felsic, it is impossible to have more than 50% mafic minerals which normally exist in mafic rocks. As a result, the peaks cannot be interpreted as pyroxene or spinel.

Traditional microscopy and SR-XRD illustrates the same results of mineral assemblages in similar host rock lithologies. The major minerals of porphyritic dacite are albite + quartz + muscovite + microcline with minor arsenopyrite + ankerite + calcite + pyrite + sphalerite and trace chalcopyrite ± galena (Figure 5-1). Dolomite, orthoclase, anorthite, and andesine are minor to trace minerals in a few porphyritic dacite samples. Intermediate and felsic metatuff show similar mineral assemblages and the only difference is the modal percentages of feldspar and quartz. The major phase of minerals in metatuff samples is albite + muscovite + quartz + microcline with minor arsenopyrite + ankerite + calcite + pyrite + sphalerite + chalcopyrite ± galena (Figure 5-2). Chlorite and dolomite are minor mineral phases in a few metatuff samples. The major minerals of metasedimentary samples are quartz + albite + muscovite + calcite + chlorite ± orthoclase ± kaolinite with minor pyrite + arsenopyrite + ankerite + chalcopyrite + sphalerite (Figure 5-3).

Large-scale SR- μ XRF mapping provides high-resolution trace elemental variation maps on the flat surface of drill core samples and offcut samples. The SR- μ XRF element maps are used to characterize the mineralizing system by understanding the spatial relationships between key elements in different rock types. The mineralogical analysis using SR-XRD and microscopy prove the similarity of element distribution and mineral distribution. From the SR- μ XRF element maps, Au is associated with K, Ca, Fe, Mg, and Mn in most samples, which corresponds to sericite and carbonate alteration observed in the petrographic analysis. Some Au is associated with As, Cu, and Pb, as inclusions appearing within arsenopyrite, chalcopyrite, and galena grains, respectively. Vein cross-cutting relationships and foliation structures observed in SR- μ XRF element maps can be used to infer the spatial and timing relationship of fluid events associated with gold mineralization. In addition, the petrological research improves the accuracy of peak fitting in MCA full spectrum. For example, Ar is a normal peak in every spectrum, but Ar is a normal element in air, not belongs to rock samples. Thus, normalizing Ar using a normalization filter has made the spectrum more represented and actual (Figure 3-15).

In conclusion, the combination of SR-XRD, SR-XRF, and microscopy improves the accuracy of the conclusions in modal mineralogy, alteration intensity, elemental and mineral distribution.

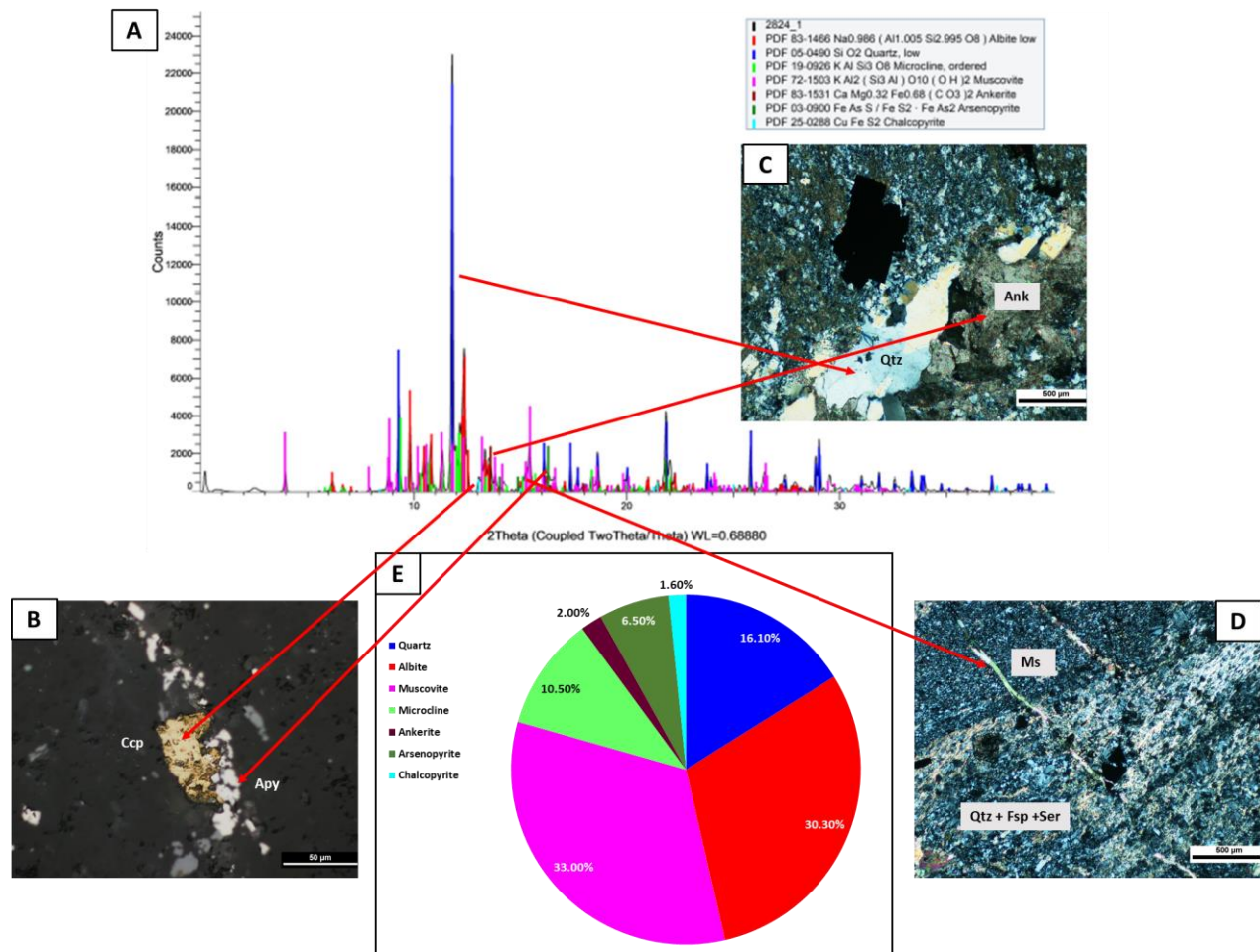


Figure 5-1. A. The SR-XRD diffractogram of a typical porphyritic dacite sample (2824). B. Fine-grained chalcopyrite and arsenopyrite disseminated in the groundmass (RL, X20) C. Carbonate (ankerite) grains and albite phenocrysts and subhedral arsenopyrite inside feldspar + quartz + sericite/muscovite groundmass (XPL, X5). D. Needle arsenopyrite in the quartz vein and the discontinuous very fine muscovite vein crosscut the quartz veins (XPL, X5). E. The pie chart shows the modal percentages of minerals.

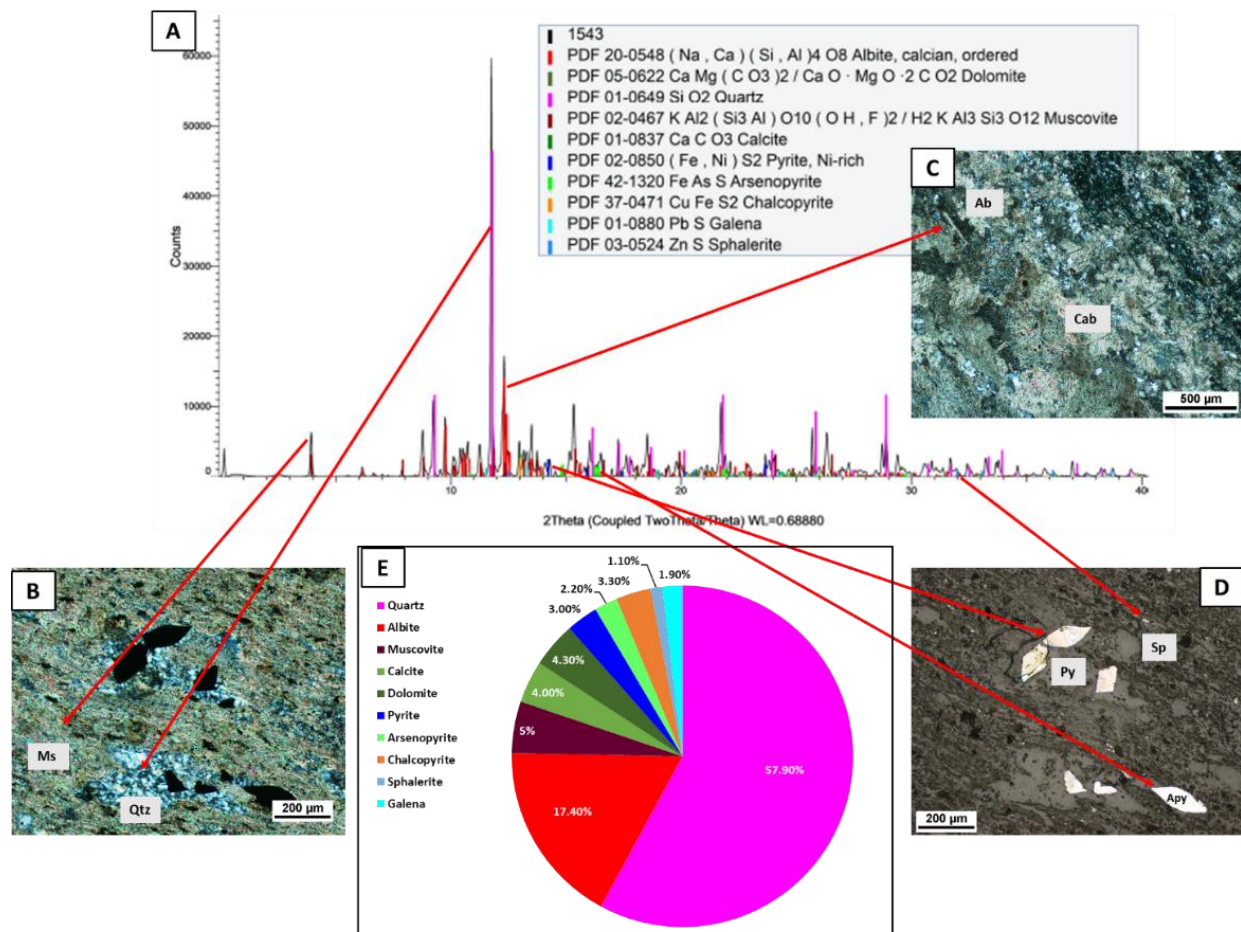


Figure 5-2. A. The SR-XRD diffractogram of a typical metatuff sample (1543). B. Pyrite grain exhibiting quartz pressure shadows on both sides within muscovite-rich groundmass (XPL, X10). C. Carbonate and albite phenocrysts and subhedral arsenopyrite inside feldspar + quartz + sericite/muscovite groundmass (XPL, X5). D. Euhedral pyrite, euhedral arsenopyrite, and fine-grain anhedral sphalerite in the matrix (XPL, X5). E. The pie chart shows the modal percentages of minerals.

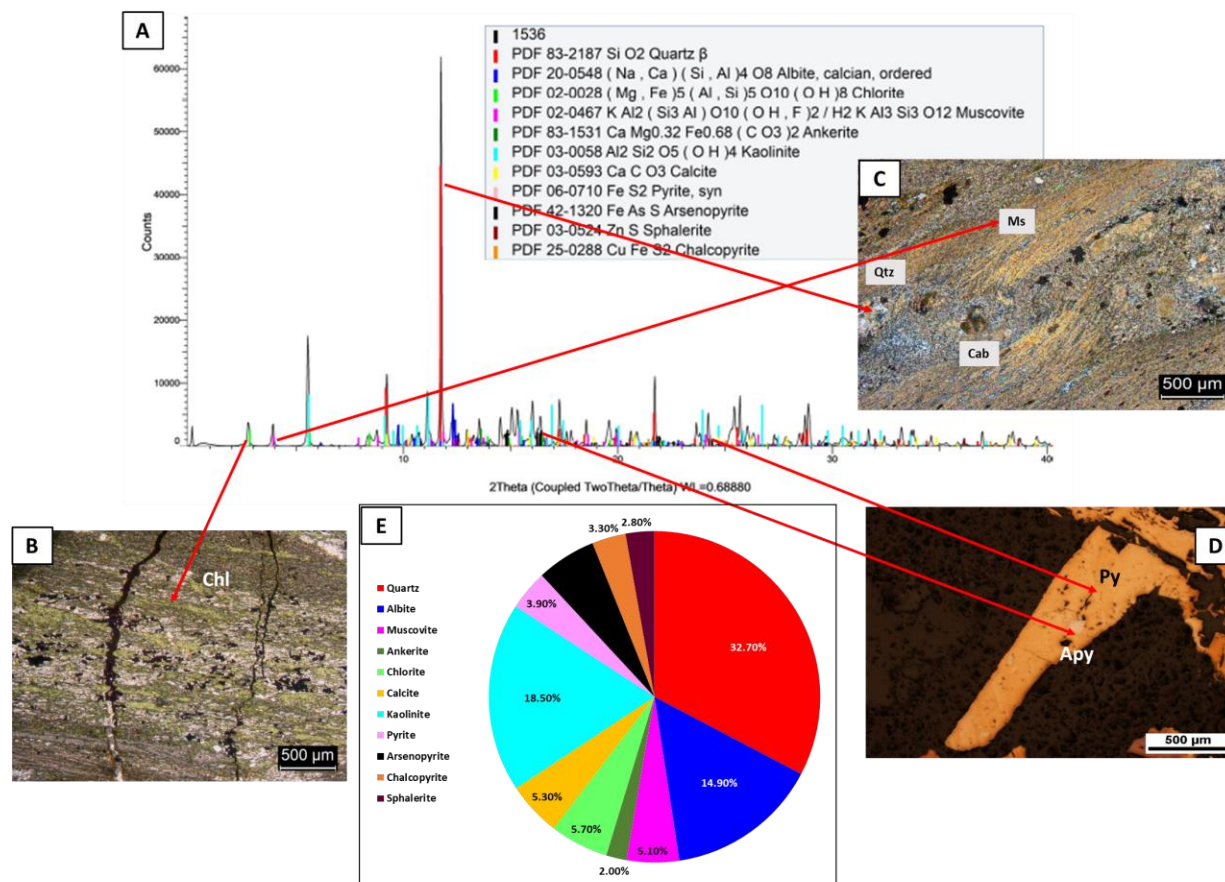


Figure 5-3. A. The SR-XRD diffractogram of a typical metasiltstone sample (1536). B. Chlorite occurring within fine-grained sericite, and crosscutting quartz-carbonate-pyrite veinlet (XPL, X10). C. Recrystallized muscovite crosscut by quartz-carbonate vein, and exhibiting kinematic indicators in the bent muscovite (XPL, X5). D. Coarse to fine-grained euhedral pyrite and fine-grained disseminated in the matrix (XPL, X5). E. The pie chart shows the modal percentages of minerals.

5.2 Sulphide Morphology and Gold Distribution

Optical microscope observation demonstrates that sulphides can be classified by the morphologies and locations within samples. Sulphides can be classified as euhedral, subhedral, and disseminated and appear in veins or in foliated textures. Multiple sulphides phases may occur in combinations (e.g., arsenopyrite + pyrite, pyrite + sphalerite, arsenopyrite + sphalerite, and/or arsenopyrite + galena). Microscopic gold has been observed in eighteen thin sections. Most thin sections with microscopic gold (eight samples) are porphyritic dacite samples. Gold occurring as inclusions in sulphides appears more commonly than free gold. Free gold grains are generally found in the quartz-feldspar-sericite groundmass and not associated with sulphides. Only a few free gold grains are proximal to disseminated fine to medium-grained arsenopyrite and pyrite. Inclusion gold has

been observed on the edges of subhedral pyrite grains, inside subhedral sulphides, in corroded arsenopyrite, or inside chalcopyrite or galena grains (Hao et al., 2020a). EDS point analysis shows most microscopic gold is a mixture of Au + Ag. Pure gold (100% Au) occurs in the foliated matrix of metasandstone and intermediate lapilli metatuff, while a mixture of Au + Sb occurs as inclusion gold within corroded sulphides grains in metasandstone and felsic ash metatuff.

The combination of detailed microscopy with EDS point analysis and EDS/WDS element maps indicate the relationship between sulphide paragenesis and gold mineralization. The different sulphide morphology, microscopic gold type, and their locations reflect different fluid compositions during multiple mineralizing events. There is evidence for four sulphide generations observed in the EDS point analysis and EDS/WDS element maps. Table 5-1 summarizes the key characteristics of each sulphide generation and gold mineralization.

Table 5-1. Summary of the sulphide morphology, microscopic gold, and locations at the Monument Bay Project

Sulphide Type and Morphology	Microscopic Gold	Locations
Apy₁ (fine grained, needle-shaped and euhedral, no inclusion)	No microscopic gold	Quartz vein margins and groundmass
Py₁ & Apy₂ (medium-coarse grained, euhedral to anhedral or needle-shaped, strongly fractured and corroded, sieve-textured, inclusion-rich, some with zoning textured)	Inclusion Gold I (Au + Ag, within Apy ₁ & Apy ₂), Free Gold I (Au + Ag, approximal sulphides)	Quartz veins, quartz-carbonate veins
Ccp, Gn, Sp (fine-grained, anhedral, a few inclusions)	Inclusion Gold II (Au + Ag, with Ccp as inclusions and filled in fractures of Py ₁), Inclusion Gold III (Au + Sb, within Gn, Ccp, Sp), Inclusion Gold IV (pure Au, within Gn, Ccp, Sp)	Quartz-feldspar vein, with scheelite, and within rutile in the groundmass
Py₂ & Apy₃ (fine-grained, anhedral, filled in fractures of Gn, Ccp ₂ , and fractures in groundmass)	Free gold II (pure Au, not associated with sulphides)	Veinlets, fractures in groundmass, in the banded layers of metasandstone

1. Arsenopyrite 1 (Apy₁)

Apy₁ is the earliest sulphide generation, which is characterized by fine-grained needle-shaped and euhedral to subhedral arsenopyrite (Figure 5-4A). Apy₁ grains are ubiquitous in the quartz veins, especially on the margins of the thicker quartz veins (>2 mm). They are also disseminated in the groundmass. Inclusions are rare in this type of arsenopyrite. The Apy₁ grains with quartz, apatite, plagioclase inclusions inside show a progressive zonation of As, Mg, and Ni element maps (Figure 4-22B&C). The inclusions are concentrated in the core of the grains with relatively low-intensity of As, Mg, and Ni, while no inclusion has been observed in the As, Mg, and Ni-rich rims. Some Apy₁ grains occur as inclusions inside later generations of sulphides (Figure 4-22A). No microscopic gold has been found in Apy₁, but Au WDS element maps show some relatively high-intensity spots.

2. Pyrite 1 (Py₁) and Arsenopyrite 2 (Apy₂)

Py₁ and Apy₂ is the second stage of sulphide growth, dominating in the center area of quartz veins and quartz-carbonate veins (Figure 5-4A&B). The combination of Py₁ and Apy₂ has been observed together in quartz veins, which indicates they are the same sulphide generation. Py₁ and Apy₂ grains are generally medium-coarse grained, euhedral to anhedral or needle-shaped, strongly fractured and corroded, sieve-textured. Py₁ is commonly finer, more corroded and fractured than Apy₂. Py₁ grains commonly overgrew on the earlier Apy₁. Both Py₁ and Apy₂ grains are generally inclusion-rich and the inclusion types are various including microscopic gold, albite, apatite, zircon, scheelite, monazite, galena, ankerite, and chalcopyrite. Inclusion Gold I and Free Gold I are associated with this sulphide generation. Inclusion Gold I is Au + Ag inside Apy₂ with an average Au/Ag ratio of 5.77 (Figure 5-5A&B). Free Gold I is also Au + Ag which is close to pyrite and arsenopyrite (Figure 5-5C). The average Au/Ag ratio of Free Gold I is 16.05. Free Gold I which is closer to the sulphide grains has lower Au/Ag ratios.

3. Chalcopyrite (Ccp), Galena (Gn), and Sphalerite (Sp)

Ccp, Gn, and Sp are the third sulphide generation, which exhibits in quartz veins and within rutile grains in the groundmass. Ccp is fine-grained anhedral sieve-textured chalcopyrite with a few inclusions (Figure 5-4C-F). Gn is fine-grained anhedral galena which always filled in the fractures and between Py₁ and Apy₂ grains (Figure 5-4D). Sp is fine-grained anhedral sphalerite disseminated in the groundmass (Figure 5-4C). Ccp, Gn, and Sp commonly occur as a combination

with inclusions including microscopic gold and antimony. According the composition of microscopic gold, there are three types of inclusion gold associated with this sulphide generation: 1) Inclusion Gold II is Au + Ag (average Au/Ag ratio is 14.50, as inclusions with Ccp in Py₁ and filled in fractures of Py₁ (Figure 5-4D and Figure 5-5D); 2) Inclusion Gold III is Au + Sb with an average Au/Sb ratio of 1.46, inside the combination of Gn, Ccp, Sp (Figure 5-4E and Figure 5-5E); 3) Inclusion Gold IV is pure gold inside the combination of Gn, Ccp, Sp (Figure 5-4E and Figure 5-4E).

4. Pyrite 2 (Py₂) and Arsenopyrite 3 (Apy₃)

Py₂ and Apy₃ are the youngest generation of sulphide growth, which are fine-grained anhedral pyrite and arsenopyrite in veinlets, in the groundmass, and filled in fractures of Gn and Ccp as inclusions (Figure 5-4B&F). Py₂ and Apy₃ are inclusion-free. Free Gold II is pure Au, which is not associated with sulphides (Figure 5-4F). Free Gold II deposited simultaneously or after the formation of Py₂ and Apy₃ (Figure 5-5F).

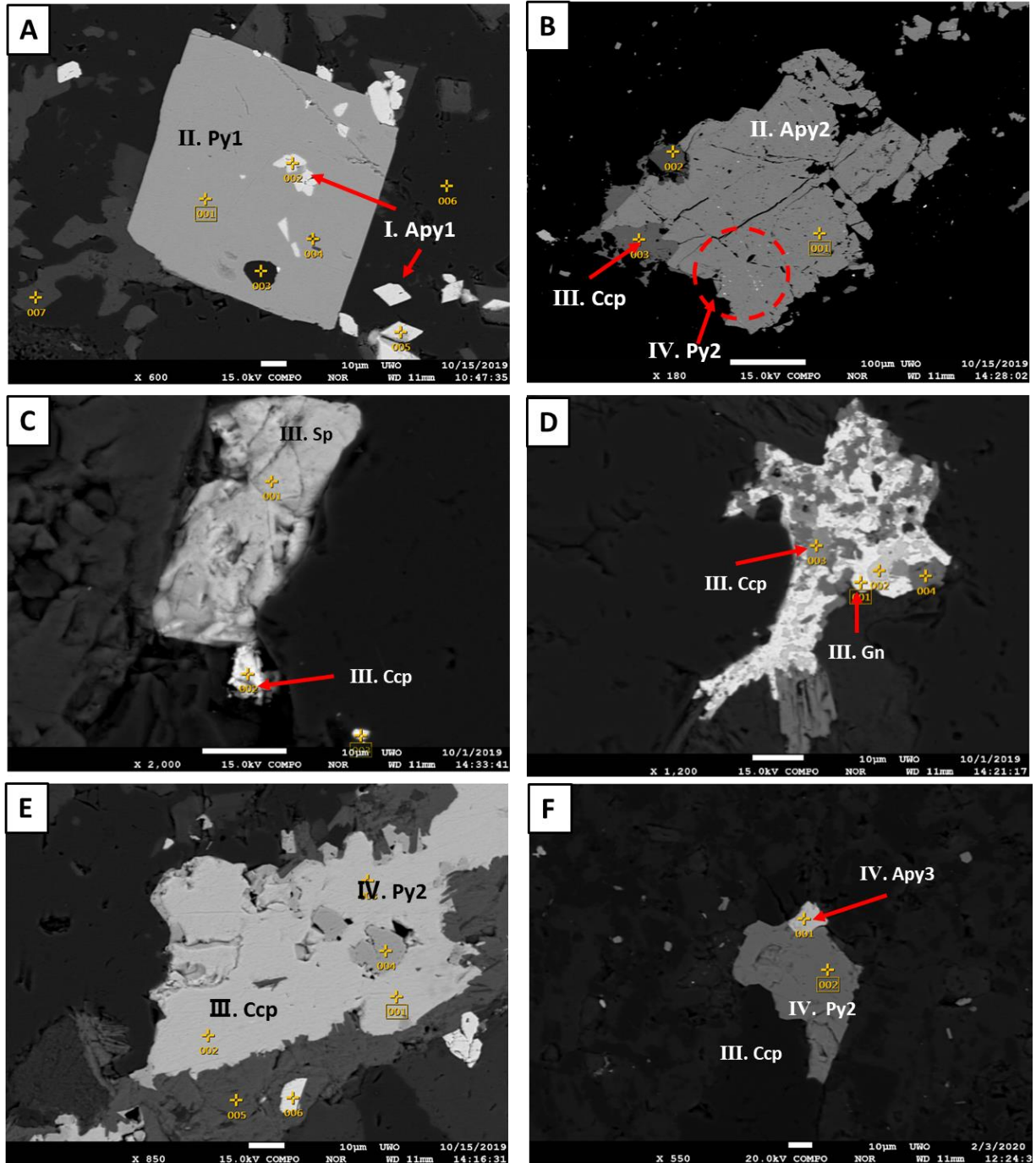


Figure 5-4 A. Arsenopyrite (Apy₁), apatite, plagioclase inside a euhedral pyrite grain (Py₁) and euhedral arsenopyrite (Apy₁) in quartz veins and ankerite matrix; B. Fractured subhedral arsenopyrite (Apy₂) with zircon and chalcopyrite (Ccp) on the edge and fine-grained pyrite (Py₂) inside fractures; C. Combination of sphalerite (Sp) + chalcopyrite (Ccp) in matrix; D. Combination of chalcopyrite (Ccp) + galena (Gn) + antimony in the matrix; E. Corroded anhedral chalcopyrite (Ccp) grain with pyrite (Py₂) inside, and fine-grained subhedral arsenopyrite grains in chlorite matrix; F. Scheelite with anhedral pyrite (Py₂) inside chalcopyrite (Ccp).

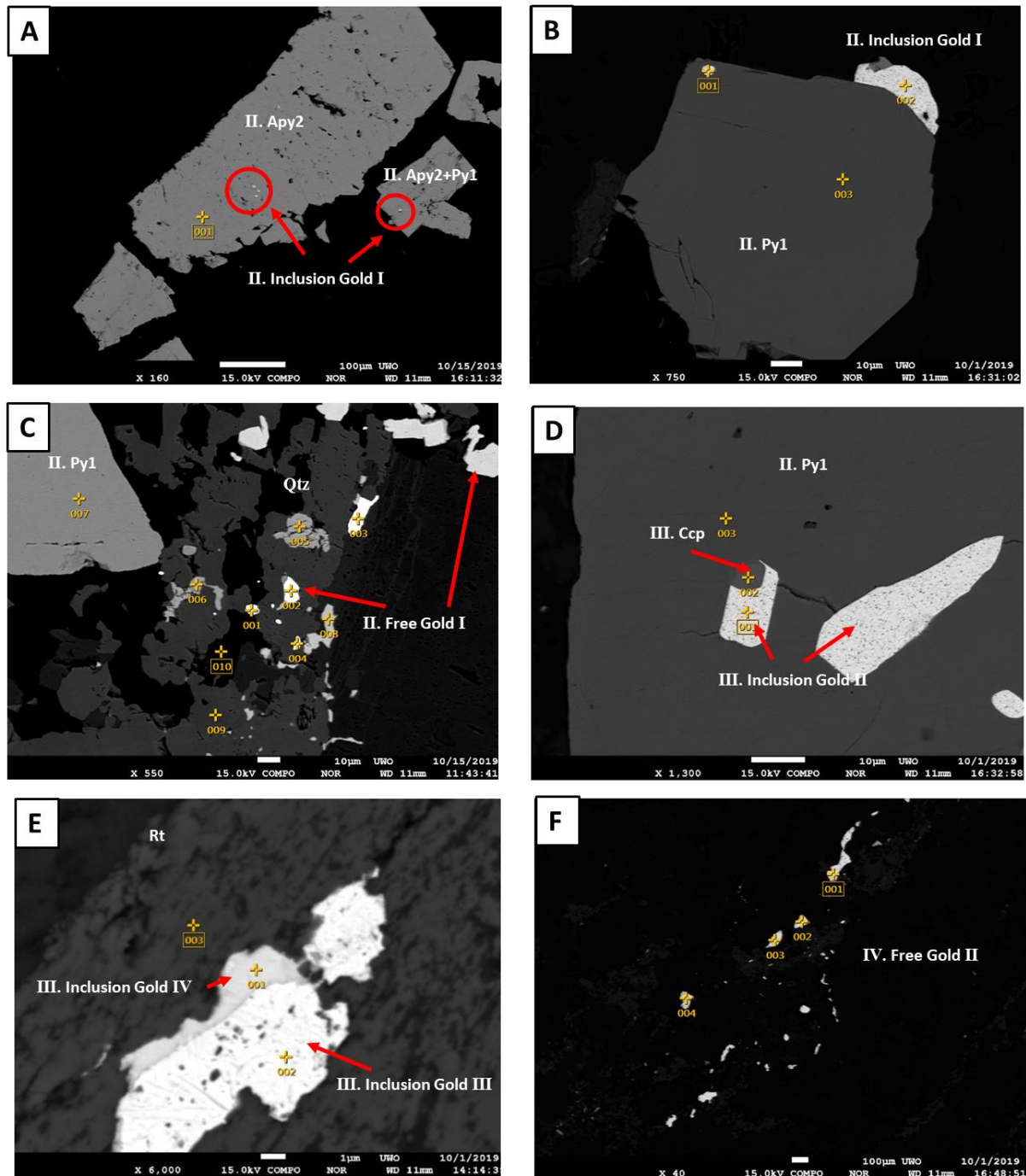


Figure 5-5. A. Inclusion gold I (Au + Ag) in corroded subhedral arsenopyrite (Apy₂) and arsenopyrite + Pyrite grains (Apy₂+Py₁); B. Inclusion gold I (Au + Ag) on the edge of subhedral pyrite (Py₁); C. Free gold I (Au + Ag) near pyrite (Py₁) in quartz vein; D. Inclusion gold II (Au + Ag) and chalcopyrite (Ccp) in fractured pyrite (Py₁); E. Inclusion gold III (Au + Sb) and Inclusion gold IV (Pure gold) with rutile; F. Free gold II (Pure gold) in the matrix.

These four sulphide generations and gold formation suggest at least four ore-forming fluid events at the Monument Bay Project. The morphology of Apy₁ indicates that the earliest hydrothermal fluid was likely Au-barren and As-rich. Considering Apy₁ occurred more commonly on the quartz vein margins than the center, the arsenopyrite was thought to be formed during the fluid interaction with the Fe-rich wall rocks, which brought Fe into the system (e.g., Stromberg, et al., 2019). According to the host rock petrology, mineralogy, and veining in the thin section observation, the following three sulphide generations represent the main auriferous fluid events. However, the correlation between schistosity and regional foliation directions need to be proved in the future work. Py₁ and Apy₂ are the main sulphide generations carrying metallic gold, which are the pathfinder of metallic gold. These sulphide generations correspond to the quartz-tourmaline ± pyrite-arsenopyrite-pyrrhotite veining event (McCracken & Thibault, 2016). Inclusion Gold I and Free Gold I are all Au + Ag with lower Au/Ag ratio (Figure 5-6). In the third sulphide formation event, the trace elements, including Zn, Cu, Pb, Sb, and Au, incorporated into the fractures and the concentrations of them were enhanced at a lower temperature (e.g., Deditius et al., 2014; Stromberg, et al., 2019). It is consistent with quartz-albite-ankerite-scheelite±pyrite-arsenopyrite-sphalerite-chalcopyrite-galena-stibnite veining event (McCracken and Thibault, 2016). The youngest sulphide generation, Py₂ and Apy₃, is inclusion-free and simultaneous with pure free gold. This suggests the remobilization of gold in the auriferous fluid, which is simultaneous with smoky quartz ± pyrite-pyrrhotite-arsenopyrite-chalcopyrite veins within the shear veins in the wall rocks of hanging walls and footwall of the shear zones (McCracken & Thibault, 2016). The wide range of Au/Ag ratio and Au/Sb in metallic gold examples in Figure 5-6 illustrate the complicated fluid compositional changes. The metallic gold grains with the higher Au/Ag ratios are associated with later mineralization (e.g., Stromberg, et al., 2019). Apart from that, the highest Au/Ag ratios in orogenic gold deposits generally show a strong relationship with the presence of Au-bearing micro- to nano-sized inclusions as refractory gold (e.g., Deditius et al., 2014). Thus, Py₂ and Apy₃ will be the potential refractory gold pathfinder and the high-intensity spots in Au WDS map are needed to be analyzed to identify the gold speciation using Micro-XANES in the future.

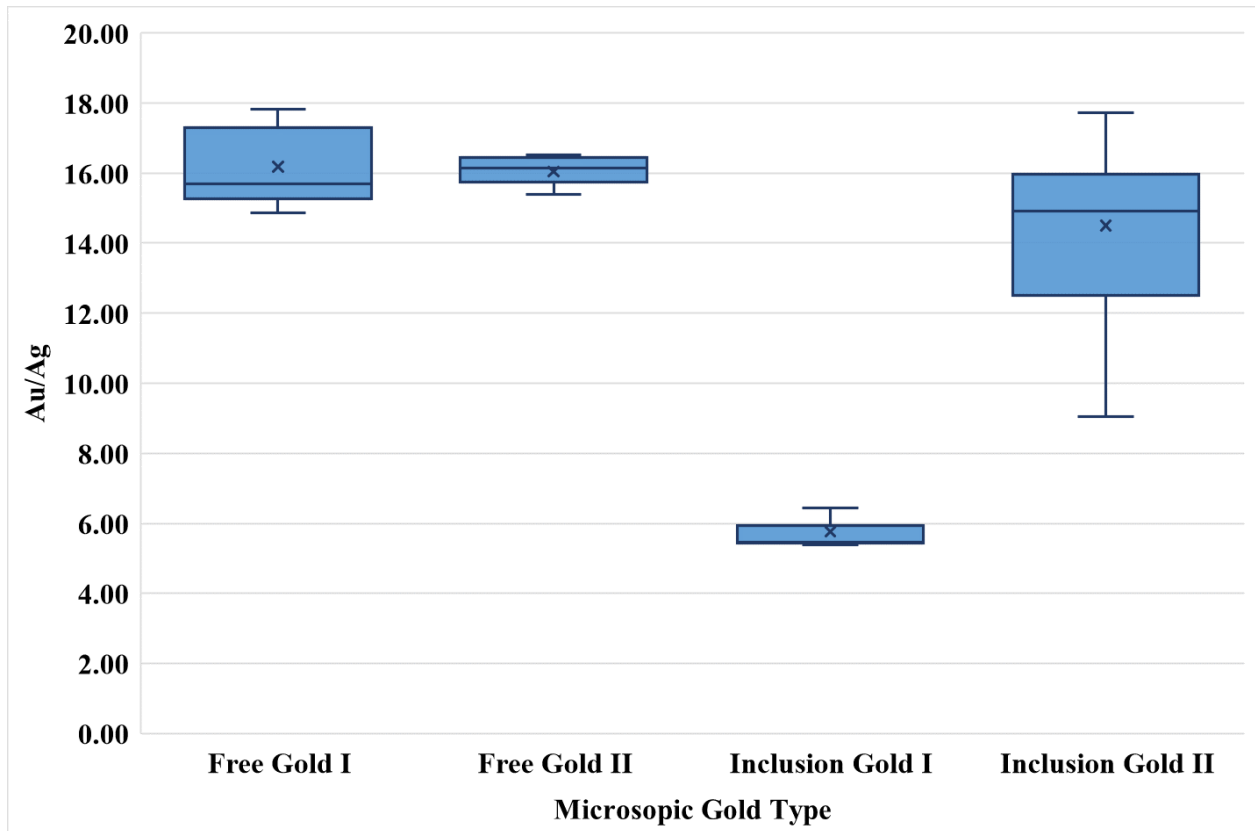


Figure 5-6. Boxplot illustrating the Au/Ag ratio of different types of microscopic gold using EDS point analysis at Western University (Free Gold I (n=4), Free Gold II (n=6), Inclusion Gold I (n=3), Inclusion Gold II (n=16)).

5.3 Arsenic and Gold Speciation

As K-edge micro-XANES spectroscopy identified only As⁻¹ in the samples, which corresponds to arsenopyrite grains observed in the thin sections, and the common association of As and Fe in the SR- μ XRF maps. The toxic form As⁺³ has not been observed, which could mean less environmental contamination in production in the future. Au L₃-edge micro-XANES spectroscopy identified only metallic gold (Au⁰) in the samples, meaning that gold at the Monument Bay Project is not commonly bound in sulphide lattice structures. Thus, the gold in the Monument Bay Project should be relatively easy to process (Hao et al., 2020b).

One of the limitations of the design of micro-XANES spectroscopy experiments was the selection of regions of interest. micro-XANES spectroscopy is the most time-consuming method in this research. Large-scale SR-XRF mapping was done first before micro-XANES spectroscopy experiments (Figure 5-7). As for Au L₃-edge micro-XANES spectroscopy, the red pixels with the relatively high intensity in Au SR-XRF element maps have been chosen as potential test points. There are five main challenges in Au L₃-edge micro-XANES spectroscopy. Firstly, considering the gold nugget effect of the nature of gold mineralization, it is challenging and time-consuming to select a gold spot on one surface of a drill core sample. Secondly, the gold grades of most samples are close to the cut-off grade (1 g/t), which lowers the chance of detecting gold. Thirdly, it is possible that the relatively lower intensity Au pixels (i.e. orange and yellow pixels) represent refractory gold or metallic gold. However, because of the detection limits, there was no good XANES spectra for them. Fourthly, from the MCA full spectrum, the energy of Au-L₃ is pretty close to As K, Zn K, and W L peak, which may cause wrong signal on SR-XRF Au maps. Based on the relative positions of the element peaks, the author classified Au peaks into four types (Figure 4-8): (1) Au peak on the As shoulder on the MCA spectrum, but higher than the shoulder; (2) real Au peak, much higher than As shoulder; (3) Au peak and W peak are overlapped, but Au peak is much higher than As shoulder and W peak; (4) False Au signal caused by overlapped high-intensity W peak. Last but not least, the binding energy of Au-L₃-edge and As K-edge is close (Au L₃-edge: 11919 eV and As K-edge: 11867 eV) and the As concentration is >1000 times of the Au concentration even in the highest gold grade sample. As a result, the post-edge of As K-edge commonly overlaps the Au L₃-edge so that the gold speciation is hard to identify.

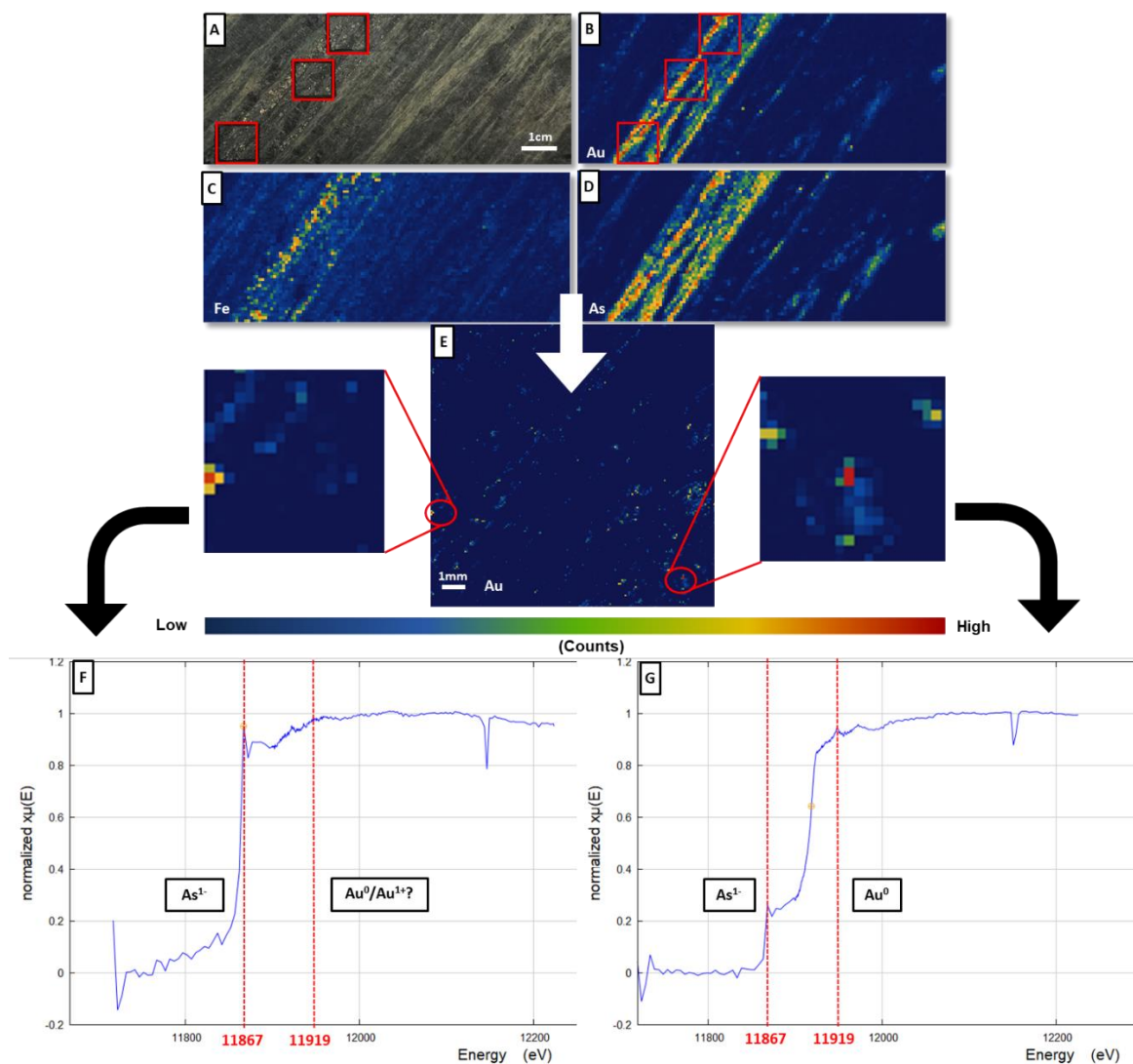


Figure 5-7. A. Photo of 2831 Metasandstone B-D. SR- μ XRF elemental maps collected in Advanced Photon Source (APS) 20ID Beamline with the resolution of 800 μ m. The red squares are the regions of interests with high Au intensity for higher resolution SR- μ XRF mapping. E. A representative SR- μ XRF Au map (the top square in Figure X-5A & B) was collected in APS 20ID Beamline with the resolution of 60 μ m. The red circles are the regions of interests with high Au intensity for XANES spectroscopy. F & G. Au L_3 -edge micro-XANES spectrum collected on the spots in Figure X-5E examined at APS 20ID Beamline in July 2019.

Bulk XANES spectroscopy was used once to identify the gold speciation in pulps and powder samples. In general, pulps and powder samples can provide more representative information than a few single hotspots on the surface of drill core samples. However, because of the detect limits, no good Au- L_3 -edge spectra has been observed in the experiment.

High Energy Resolution Fluorescence Detected (HERFD) XANES spectroscopy and micro-XANES spectroscopy on Au L₂-edge will be better solutions to identify gold speciation. HERFD XANES spectroscopy is an advanced technique to overcome the difficulty of conventional XANES by using a narrow energy band from the emission line of the sample. It will be useful to narrow down the energy range much accurate to the Au L₃-edge and avoid overlaying of the post-edge of As K-edge. In addition, the binding energy of Au L₂-edge is 13734 eV, which is not close to As K-edge any more and can be another solution to solve overlaying problem. The feasibility of these two solutions and further experiment design need to be discussed with the technicians in the beamline in the future.

In addition, some high-intensity gold spots in corroded needle pyrite have been observed in EDS/WDS element maps but could not be found in back-scattered images or under reflected light of the optical microscopy. This type of gold spots is probably a result of the presence of refractory gold bounded in pyrite lattice or just a nano to micron-scale metallic gold. Thus, this will be a perfect spot to test gold speciation in the next XANES spectroscopy experiment.

Chapter 6

6 Conclusion

The Monument Bay Project is located in the Archean Stull Lake Greenstone Belt, in Northern Manitoba, Canada. The Monument Bay Project is composed of three individual deposits: Twin Lakes Deposit, Mid-East Deposit, and AZ Deposit, which are all located in steeply north-dipping shear zones within the Stull-Wunnummin Shear Zone (SWSZ). These three deposits are defined as Archean greenstone belt shear-hosted mesothermal gold-tungsten deposits (Richard J. Goldfarb & Groves, 2015). This thesis focuses on the geometallurgy and gold mineralization of the Monument Bay Deposit in order to better understand the multiple gold mineralizing events and provide a pathfinder to gold mineralization. Microscopy and EPMA are providing insights into sulphide formation and gold distribution on a micro-scale. The combination of traditional petrography, SR- μ XRF, and XANES analyses provides insight into gold mineralization, geometallurgy, and deleterious element characterization.

There is evidence for four sulphide generations identified from microscopy and EDS/WDS element maps: I. Arsenopyrite 1 (Apy₁); II. Pyrite 1 (Py₁) and Arsenopyrite 2 (Apy₂); III. Chalcopyrite (Ccp), Galena (Gn), and Sphalerite (Sp); IV. Pyrite 2 (Py₂) and Arsenopyrite 3 (Apy₃). Microscopic gold at the Monument Bay Project can be divided into inclusion gold and free gold, which are strongly associated with sulphides, especially corroded arsenopyrite and pyrite (Py₁ and Apy₂). Apy₁ is the only sulphide generation that is Au-barren. Free Gold which is closer to the sulphide grains has lower Au concentration. Inclusion gold within arsenopyrite grains has lower Au concentration than that within pyrite grains. No microscopic gold has been found in zoned pyrite without fractures or zoned arsenopyrite. The various Au/Ag and Au/Sb ratios identified using EDS point analysis suggests an episode of Au remobilization during sulphide formation because of changes of temperature and pressure. The spatial distribution of different types of sulphides in different veining events suggests there were three main gold mineralizing events (McCracken & Thibault, 2016). The metallic gold grains with higher Au/Ag ratios are associated with later mineralization (e.g., Stromberg, et al., 2019). Additionally, highest Au/Ag ratios in orogenic gold deposits generally show a strong relationship with the presence of Au-

bearing micro- to nano-sized inclusions as refractory gold (e.g., Deditius et al., 2014). The majority of the gold was deposited as metallic gold in episode II. Py₁ and Apy₂ (episode II) will be the potential metallic gold pathfinder. Apart from that, vein cross-cutting relationships and foliation structures observed in SR- μ XRF element maps can be used to infer the spatial and timing relationship of fluid events associated with gold mineralization. As K-edge XANES spectroscopy identified only As⁻¹ in the samples, which corresponds to arsenopyrite grains observed in the thin sections and the common association of As and Fe in the SR- μ XRF maps. Au L₃-edge XANES spectroscopy identified only metallic gold (Au⁰) in the samples, meaning that gold at the Monument Bay deposit is not bound in sulphide lattice structures. This information is being applied by Yamana to understand the multi-episodic fluid history and environmental characterization of the Monument Bay project and will lead to a better understanding of the mineralogical expression of gold mineralization and geometallurgy at the Monument Bay deposit.

Some high-intensity gold spots in corroded needle pyrite (Py₂) have been observed in EDS/WDS element maps but could not be found in back-scattered images or under reflected light of the optical microscopy. This type of gold spots is probably a result of the presence of refractory gold bounded in pyrite lattice or just a nano to micron-scale metallic gold. Thus, Py₂ and Apy₃ (episode IV) will be the potential refractory gold pathfinder and this type of high-intensity spots in Au WDS map will be a perfect spot to test gold speciation in the next XANES spectroscopy experiment. Furthermore, high energy resolution fluorescence detected (HERFD) XANES spectroscopy and micro-XANES spectroscopy on Au L₂-edge will be better solutions to overcome the overlaying problem of conventional XANES in identifying gold speciation in the future.

References

- Advanced Photon Source. (2020). *Advanced Photon Source (APS)*. <http://www.anl.gov/>
- Aquilanti, G., Vaccari, L., Plaisier, J. R., & Goldoni, A. (2015). Chapter 3: Instrumentation at synchrotron radiation beamlines. In *Synchrotron Radiation: Basics, Methods, and Applications* (pp. 65–104).
- Arehart, G. B., Chryssoulis, S. L., & Kesler, S. E. (1993). Gold and arsenic in iron sulfides from sediment-hosted disseminated gold deposits: implications for depositional processes. *Economic Geology*, 88(1), 171–185.
- Balerna, A., & Mobilio, S. (2015). Chapter 1: Introduction to synchrotron radiation. In *Synchrotron Radiation: Basics, Methods, and Applications* (pp. 3–28).
- Banerjee, N. R., Van Loon, L. L., Botor, R. J., & Flynn, T. J. (2018). Automated Geochemical and Mineralogical Synchrotron Characterization of Bulk Geological Materials: an Innovation for the Minerals Industry. *Microscopy and Microanalysis*, 24(S2), 518–519. <https://doi.org/10.1017/s1431927618014812>
- Brugger, J., Pring, A., Reith, F., Ryan, C., Etschmann, B., Liu, W., O'Neill, B., & Ngothai, Y. (2010). Probing ore deposits formation: New insights and challenges from synchrotron and neutron studies. *Radiation Physics and Chemistry*, 79(2), 151–161. <https://doi.org/10.1016/j.radphyschem.2009.03.071>
- Bruker. (2018). *XRD Software: Diffrac.Suite EVA*. Web.
- Buchan, K. L., & Ernst, R. E. (2004). *Diabase dyke swarms and related units in Canada and adjacent regions*. <https://doi.org/10.4095/214883>
- Buffiere, J., & Baruchel, J. (2015). Chapter 13: Hard X-Ray Synchrotron Imaging Techniques and Applications. In *Synchrotron Radiation: Basics, Methods, and Applications* (pp. 389–407).
- Cabri, L. J., Newville, M., Gordon, R. A., Crozier, E. D., Sutton, S. R., McMahon, G., & Jiang, D. T. (2000). Chemical speciation of gold in arsenopyrite. *Canadian Mineralogist*, 38(5), 1265–

1281. <https://doi.org/10.2113/gscanmin.38.5.1265>

Canadian Light Source. (2020). *Canadian Light Source*.
<https://www.lightsource.ca/beamlines.html>

Card, K. D. (1986). Geology and tectonics of the Archean Superior Province, Canadian Shield. *Lunar and Planetary Inst. Workshop on Early Crustal Genesis: The World's Oldest Rocks*, 27–29.

Card, K. D., & Ciesielski, A. (1986). Subdivisions of the Superior Province of the Canadian Shield. *Geoscience Canada*, 13, 5–13.

Card, K. D., Poulsen, K. H., & Robert, F. (1989). *The Archean Superior Province of the Canadian Shield and Its Lode Gold Deposits*.

Cavallin, Hannah E., Banerjee, N. R., & Van Loon, L. L. (2019). Application of Synchrotron Spectroscopy to Understanding Gold Mineralization at the Monument Bay Project, Stull Lake Greenstone Belt, Manitoba, Canada. *Microscopy and Microanalysis*, 25(S2), 802–803.
<https://doi.org/10.1017/s1431927619004744>

Cavallin, Hannah E. (2017). *Gold Mineralization at the Monument Bay Deposit, Stull Lake Greenstone Belt, Manitoba, Canada*.

Chouinard, A., Paquette, J., & Williams-Jones, A. E. (2005). Crystallographic controls on trace-element incorporation in Auriferous pyrite from the Pascua epithermal high-sulfidation deposit, Chile-Argentina. *Canadian Mineralogist*, 43(3), 951–963.
<https://doi.org/10.2113/gscanmin.43.3.951>

Cook, N. ., Ciobaniu, C. L., Meria, D., Silcock, D., & Wade, B. (2013). Arsenopyrite-Pyrite Association in an Orogenic Gold Ore : Tracing Mineralization History from Textures and Trace Elements. *Economic Geology*, 108, 1273–1283.

Corfu, F., & Lin, S. (2000). Geology and U-Pb geochronology of the Island Lake greenstone belt, northwestern Superior Province, Manitoba. *Canadian Journal of Earth Sciences*, 37(9), 1275–1286. <https://doi.org/10.1139/e00-043>

- Corkery, M. T., Cameron, H. D. M., Lin, S., Skulski, T., Whalen, J. B., & Stern, R. A. (2000). Geological investigations in the Knee Lake belt. *Manitoba Industry, Trades, and Mines, 1977*, 129–136.
- Corkery, M. T., & Skulski, T. (1998). Geology of the Little Stull Lake area. *Manitoba Energy and Mines, Geological Services, March*, 111–118.
- Deditius, A. P., Utsunomiya, S., Ewing, R. C., & Kesler, S. E. (2009). Nanoscale “liquid” inclusions of As-Fe-S in arsenian pyrite. *American Mineralogist*, *94*(2–3), 391–394.
- Deditius, Artur P., Reich, M., Kesler, S. E., Utsunomiya, S., Chryssoulis, S. L., Walshe, J., & Ewing, R. C. (2014). The coupled geochemistry of Au and As in pyrite from hydrothermal ore deposits. *Geochimica et Cosmochimica Acta*, *140*, 644–670. <https://doi.org/10.1016/j.gca.2014.05.045>
- Deditius, Artur P., Utsunomiya, S., Renock, D., Ewing, R. C., Ramana, V. C., Becker, U., & Kesler, S. E. (2008). A proposed new type of arsenian pyrite: Composition, nanostructure and geological significance. *Geochimica et Cosmochimica Acta*, *72*(12), 2919–2933.
- Del Real, I., Smieska, L., Thompson, J. F. H., Martinez, C., Thomas, J., & Layton-Matthews, D. (2019). Using multiple micro-analytical techniques for evaluating quantitative synchrotron-XRF elemental mapping of hydrothermal pyrite. *Journal of Analytical Atomic Spectrometry*, *34*(8), 1724–1738. <https://doi.org/10.1039/c9ja00083f>
- Dubé, B., & Gosselin, P. (2007). Greenstone-hosted quartz-carbonate vein deposits. *Goodfellow, W.D., Ed., Mineral Deposits of Canada: A Synthesis of Major Deposit-Types, District Metallogeny, the Evolution of Geological Provinces, and Exploration Methods: Geological Association of Canada, Mineral Deposits Division, Special Pu(No.5)*, 49–73.
- Eichert, D. (2015). Chapter 14: X-Ray Microscopy. Synchrotron Radiation: Basics, Methods, and Applications. In *Synchrotron Radiation: Basics, Methods, and Applications* (pp. 409–432).
- Fleet, M. E., & Mumin, A. H. (1997). Gold-bearing arsenian pyrite and marcasite and arsenopyrite from Carlin Trend gold deposits and laboratory synthesis. *American Mineralogist*, *82*(1–2), 182–193. <https://doi.org/10.2138/am-1997-1-220>

- Fodje, M., Mundboth, K., Labiuk, S., Janzen, K., Gorin, J., Spasyuk, D., Colville, S., & Grochulski, P. (2020). Macromolecular crystallography beamlines at the Canadian Light Source: Building on success. *Acta Crystallographica Section D: Structural Biology*, 76, 630–635. <https://doi.org/10.1107/S2059798320007603>
- Gebre-Mariam, M., Hagemann, S. G., & Groves, D. I. (1995). A classification scheme for epigenetic Archaean lode-gold deposits. *Mineralium Deposita*, 30(5), 408–410. <https://doi.org/10.1007/BF00202283>
- Goldfarb, R. J., Groves, D. I., & Gardoll, S. (2001). Orogenic gold and geologic time: A global synthesis. *Ore Geology Reviews*, 18(1–2), 1–75. [https://doi.org/10.1016/S0169-1368\(01\)00016-6](https://doi.org/10.1016/S0169-1368(01)00016-6)
- Goldfarb, R.J., Baker, T., Dubé, B., Groves, D. I., Hart, C. J. R., Robert, F., & Gosselin, P. (2005). World distribution, productivity, character, and genesis of gold deposits in metamorphic terranes. In *Economic Geology: Vol. 100th Anni*.
- Goldfarb, Richard J., & Groves, D. I. (2015). Orogenic gold: Common or evolving fluid and metal sources through time. *Lithos*, 233, 2–26. <https://doi.org/10.1016/j.lithos.2015.07.011>
- Goldfarb, Richard J., Leach, D. L., Pickthorn, W. J., & Paterson, C. J. (1988). Origin of lode-gold deposits of the Juneau gold belt, southeastern Alaska. *Geology*, 16(5), 440–443. [https://doi.org/10.1130/0091-7613\(1988\)016<0440:OOLGDO>2.3.CO;2](https://doi.org/10.1130/0091-7613(1988)016<0440:OOLGDO>2.3.CO;2)
- Groves, D. I. (2003). Gold Deposits in Metamorphic Belts: Overview of Current Understanding, Outstanding Problems, Future Research, and Exploration Significance. *Economic Geology*, 98(1), 1–29. <https://doi.org/10.2113/98.1.1>
- Groves, D. I., Goldfarb, R. J., Gebre-Mariam, M., Hagemann, S. G., & Robert, F. (1998). Orogenic gold deposits: a proposed classification in the context of their crustal distribution and relationship to other gold deposit types. *Ore Geology Reviews*, 13(1–5), 7–27. [https://doi.org/10.1016/S0169-1368\(97\)00012-7](https://doi.org/10.1016/S0169-1368(97)00012-7)
- Hao, C., Casali, J., Ghorbani, Z., Cavallin, H., Van Loon, L., & Banerjee, N. (2020a). EPMA Characterization of Gold Associated with Different Sulfide Textures at the Monument Bay

- Deposit, Manitoba, Canada. *Microscopy and Microanalysis*, 1–4. <https://doi.org/10.1017/s1431927620020723>
- Hao, C., Casali, J., Ghorbani, Z., Cavallin, H., Van Loon, L., & Banerjee, N. (2020b). Multi-scale SR- μ XRF Imaging and Characterization of Gold Mineralization at the Monument Bay Deposit, Stull Lake Greenstone Belt, Manitoba, Canada. *Microscopy and Microanalysis*, 8–11. <https://doi.org/10.1017/S1431927620017493>
- Heald, S. M., Cross, J. O., Brewster, D. L., & Gordon, R. A. (2007). The PNC/XOR X-ray microprobe station at APS sector 20. *Nuclear Instruments and Methods in Physics Research, Section A: Accelerators, Spectrometers, Detectors and Associated Equipment*, 582(1), 215–217. <https://doi.org/10.1016/j.nima.2007.08.109>
- Jiang, D., & Corkery, M. . (1998). *A preliminary structural analysis of the Edmund Lake– Little Stull Lake area, northwestern Superior Province, Manitoba.*
- Johan, Z., Marcoux, E., & Bonnemaïson, M. (1989). Arsénopyrite aurifère: mode de substitution de Au dans la structure de FeAsS. In *Geography*.
- Kerrick, R., Goldfarb, R., Groves, D., Garwin, S., & Jia, Y. (2000). The characteristics, origins, and geodynamic settings of supergiant gold metallogenic provinces. *Science in China, Series D: Earth Sciences*, 43(December), 1–68. <https://doi.org/10.1007/BF02911933>
- Kerrick, Robert, & Cassidy, K. F. (1994). Temporal relationships of lode gold mineralization to accretion, magmatism, metamorphism and deformation - Archean to present: A review. *Ore Geology Reviews*, 9(4), 263–310. [https://doi.org/10.1016/0169-1368\(94\)90001-9](https://doi.org/10.1016/0169-1368(94)90001-9)
- Ketchum, J., & Davis, D. W. (2001). U-Pb geochronological results from the Abitibi greenstone belt, Sachigo Subprovince and Onaman-Tashota greenstone belt, Superior Province, Ontario. In *unpublished report of the Jack Satterly Geochronology Laboratory, Royal Ontario Museum,*.
- Lavina, B., Dera, P., & Downs, R. T. (2014). Modern X-ray diffraction methods in mineralogy and geosciences. *Reviews in Mineralogy and Geochemistry*, 78, 1–31. <https://doi.org/10.2138/rmg.2014.78.1>

- Lin, S. (2005). Synchronous vertical and horizontal tectonism in the Neoproterozoic: Kinematic evidence from a synclinal keel in the northwestern Superior craton, Canada. *Precambrian Research*, 139(3–4), 181–194. <https://doi.org/10.1016/j.precamres.2005.07.001>
- Lin, S., Davis, D. W., Rotenberg, E., Corkery, M. T., & Bailes, A. H. (2006). Geological evolution of the northwestern Superior Province: Clues from geology, kinematics, and geochronology in the Gods Lake Narrows area, Oxford-Stull terrane, Manitoba. *Canadian Journal of Earth Sciences*, 43(7), 749–765. <https://doi.org/10.1139/E06-068>
- Lydon, J. W. (2007). An overview of the economic and geological contexts of Canada's major mineral deposit types. *Goodfellow, W.D., Ed., Mineral Deposits of Canada: Synthesis of Major Deposit Types, District Metallogeny, the Evolution of Geological Provinces, and Exploration Methods: Geological Association of Canada, Mineral Deposits Division, Special Publication (No. 5)*, 3–48.
- Maddox, L. M., Bancroft, G. M., Scaini, M. J., & Lorimer, J. W. (1998). Invisible gold: Comparison of Au deposition on pyrite and arsenopyrite. *American Mineralogist*, 83(11-12 PART 1), 1240–1245. <https://doi.org/10.2138/am-1998-11-1212>
- Margaritondo, G. (2015). Chapter 2: Characteristics and properties of synchrotron radiation. In *Synchrotron Radiation: Basics, Methods, and Applications* (pp. 29–63).
- McCracken, T., & Thibault, D. (2016). *Technical Report and Updated Resource Estimate on the Monument Bay Project, Northern Manitoba*.
- Mints, M. V. (2017). The composite North American Craton, Superior Province: Deep crustal structure and mantle-plume model of Neoproterozoic evolution. *Precambrian Research*, 302, 94–121. <https://doi.org/10.1016/j.precamres.2017.08.025>
- Parks, J., Lin, S., Davis, D., & Corkery, T. (2006). New high-precision U-Pb ages for the Island Lake greenstone belt, northern Superior Province: implications for regional stratigraphy and the extent of the North Caribou terrane. *Canadian Journal of Earth Sciences*, 43(7), 789.
- Pecharesky, V. K., & Zavalij, P. Y. (2005). *Fundamentals of Powder Diffraction and Structural Characterization of Materials* (Issue January 2005).

- Percival, J. A., Bleeker, W., Cook, F. A., Rivers, T., Ross, G., & Staal, C. van. (2004). PanLITHOPROBE Workshop IV: Intra-Orogen Correlations and Comparative Orogenic Anatomy. *Geoscience Canada*, 31(1).
- Percival, J. A., Sanborn-Barrie, M., Skulski, T., Stott, G. M., Helmstaedt, H., & White, D. J. (2006). Tectonic evolution of the western Superior Province from NATMAP and Lithoprobe studies. *Canadian Journal of Earth Sciences*, 43(7), 1085–1117. <https://doi.org/10.1139/E06-062>
- Percival, J.A. (2007). Geology and Metallogeny of the Superior Province, Canada. *Mineral Deposits of Canada: A Synthesis of Major Deposit-Types, District Metallogeny, the Evolution of Geological Provinces, and Exploration Methods Special Publication No. 5, X*, 903–928.
- Percival, John A, Skulski, T., Sanborn-Barrie, M., Stott, G. M., Leclair, A. D., Corkery, M. T., & Boily, M. (2012). Geology and Tectonic Evolution of the Superior Province, Canada. The Lithoprobe Perspective. *Tectonic Styles in Canada: The LITHOPROBE Perspective, December 2015*, 321–378.
- Phillips, G. N., & Powell, R. (2010). Formation of gold deposits: A metamorphic devolatilization model. *Journal of Metamorphic Geology*, 28(6), 689–718. <https://doi.org/10.1111/j.1525-1314.2010.00887.x>
- Poulsen, K. H., Robert, F., & Dubé, B. (2000). *Geological Survey of Canada Geological Classification of Canadian Gold Deposits*.
- Powell, R., Will, T. M., & Phillips, G. N. (1991). Metamorphism in Archaean greenstone belts: Calculated fluid compositions and implications for gold mineralization. *Journal of Metamorphic Geology*, 9, 141–150.
- Qian, G., Brugger, J., Testemale, D., Skinner, W., & Pring, A. (2013). Formation of As(II)-pyrite during experimental replacement of magnetite under hydrothermal conditions. *Geochimica et Cosmochimica Acta*, 100, 1–10.
- Quartieri, S. (2015). Chapter 24: Synchrotron Radiation in the Earth Sciences. In *Synchrotron Radiation: Basics, Methods, and Applications* (pp. 641–656).

- Ravel, B., & Newville, M. (2005). ATHENA, ARTEMIS, HEPHAESTUS: Data analysis for X-ray absorption spectroscopy using IFEFFIT. *Journal of Synchrotron Radiation*, 12(4), 537–541. <https://doi.org/10.1107/S0909049505012719>
- Reich, M., Kesler, S. E., Utsunomiya, S., Palenik, C. S., Chryssoulis, S. L., & Ewing, R. C. (2005). Solubility of gold in arsenian pyrite. *Geochimica et Cosmochimica Acta*, 69(11), 2781–2796. <https://doi.org/10.1016/j.gca.2005.01.011>
- Robert, F., & Poulsen, K. H. (1997). World-class Archaean gold deposits in Canada: An overview. *Australian Journal of Earth Sciences*, 44(3), 329–351. <https://doi.org/10.1080/08120099708728316>
- Ross-Lindeman, J., & Kirste, D. (2019). Characterization study of As and Se in pyrites from two historic mines in British Columbia. *E3S Web of Conferences*, 98, 10–14. <https://doi.org/10.1051/e3sconf/20199809026>
- Skulski, T., Corkery, M. T., Stone, D., Whalen, J. B., & Stern, R. A. (2000). *Geological and Geochronological Investigations in the Stull Lake-Edmund Lake Greenstone Belt and Granitoid Rocks of the Northwestern Superior Province*.
- Stone, D. (2005). Geology of the Northern Superior Area, Ontario. In *Ontario Geological Survey, Open File Report 6140*,.
- Stott, G. M., Corkery, M. T., Percival, J. A., Simard, M., & Goutier, J. (2010). *A revised terrane subdivision of the Superior Province. In Summary of Field Work and Other Activities 2010*.
- Stromberg, J. M., Barr, E., Van Loon, L. L., Gordon, R. A., & Banerjee, N. R. (2019). Fingerprinting multiple gold mineralization events at the Dome mine in Timmins, Ontario, Canada: Trace element and gold content of pyrite. *Ore Geology Reviews*, 104(April 2018), 603–619. <https://doi.org/10.1016/j.oregeorev.2018.11.020>
- Stromberg, J. M., Van Loon, L. L., Gordon, R., Woll, A., Feng, R., Schumann, D., & Banerjee, N. R. (2019). Applications of synchrotron X-ray techniques to orogenic gold studies; examples from the Timmins gold camp. *Ore Geology Reviews*, 104(November 2018), 589–602. <https://doi.org/10.1016/j.oregeorev.2018.11.015>

- Sung, Y. H., Brugger, J., Ciobanu, C. L., Pring, A., Skinner, W., & Nugus, M. (2009). Invisible gold in arsenian pyrite and arsenopyrite from a multistage Archaean gold deposit: Sunrise Dam, Eastern Goldfields Province, Western Australia. *Mineralium Deposita*, *44*(7), 765–791. <https://doi.org/10.1007/s00126-009-0244-4>
- Toby, B. H., & Von Dreele, R. B. (2013). GSAS-II : the genesis of a modern open-source all purpose crystallography software package. *Journal of Applied Crystallography*, *46*(2), 544–549. <https://doi.org/10.1107/S0021889813003531>
- Trigub, A. L., Tagirov, B. R., Kvashnina, K. O., Chareev, D. A., Nickolsky, M. S., Shiryaev, A. A., Baranova, N. N., Kovalchuk, E. V., & Mokhov, A. V. (2017). X-ray spectroscopy study of the chemical state of “invisible” Au in synthetic minerals in the Fe-As-S system. *American Mineralogist*, *102*(5), 1057–1065. <https://doi.org/10.2138/am-2017-5832>
- Van Den, Berghe, M. D., Jamieson, H. E., & Palmer, M. J. (2018). Arsenic mobility and characterization in lakes impacted by gold ore roasting, Yellowknife, NWT, Canada. *Environmental Pollution*, *234*, 630–641. <https://doi.org/10.1016/j.envpol.2017.11.062>
- van der Lee, S., & Frederiksen, A. (2005). *Surface wave tomography applied to the North American upper mantle* (pp. 67–80). <https://doi.org/10.1029/157GM05>
- Van Loon, L. L., McIntyre, N. S., Bauer, M., Sherry, N. S. A., & Banerjee, N. R. (2019). Peakaboo: Advanced software for the interpretation of X-ray fluorescence spectra from synchrotrons and other intense X-ray sources. *Software Impacts*, *2*(September), 100010. <https://doi.org/10.1016/j.simpa.2019.100010>
- Wang, Y., Jiao, J. J., Zhu, S., & Li, Y. (2013). Arsenic K-edge X-ray absorption near-edge spectroscopy to determine oxidation states of arsenic of a coastal aquifer-aquitard system. *Environmental Pollution*, *179*, 160–166. <https://doi.org/10.1016/j.envpol.2013.04.005>
- Yamana Gold Inc. (2018). *Q2 financial Report 2018*.
- Yang, J., Liu, J., Dynes, J. J., Peak, D., Regier, T., Wang, J., Zhu, S., Shi, J., & Tse, J. S. (2014). Speciation and distribution of copper in a mining soil using multiple synchrotron-based bulk and microscopic techniques. *Environmental Science and Pollution Research*, *21*(4), 2943–

2954. <https://doi.org/10.1007/s11356-013-2214-8>

Yang, L. Q., Deng, J., Wang, Z. L., Guo, L. N., Li, R. H., Groves, D. I., Danyushevsky, L. V., Zhang, C., Zheng, X. L., & Zhao, H. (2016). Relationships between gold and pyrite at the Xincheng gold deposit, Jiaodong Peninsula, China: Implications for gold source and deposition in a brittle epizonal environment. *Economic Geology*, *111*(1), 105–126. <https://doi.org/10.2113/econgeo.111.1.105>

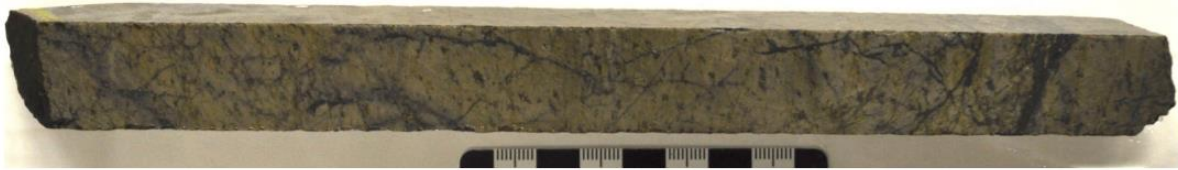
Appendices

Appendix A: Petrographic Description

The sample number with “*” are from Cavallin’s previous sample suite, part of photos and descriptions are referred to Appendix A and B of her master thesis.

Sample Number	1519*	Drill Hole	TL-16-573	Depth	58.18-58.73 m
Lithology from Mining Log	Lapilli Tuff	Target	TL	Gold Grade	1.79 ppm

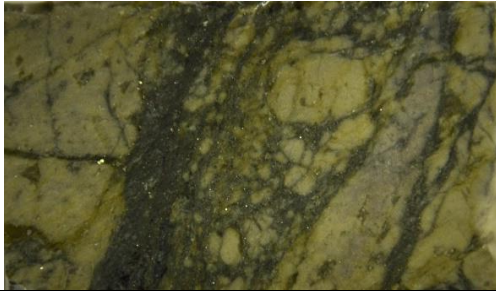
Drill Core Sample:



Sample Description:

Mauve-grey and yellowish green fine-grained lapilli meta-tuff with intense veinlets. The yellowish green area is much more than mauve grey area. Lapilli (>50%, 5-10mm) show as green fragments with sharp edges in the light yellowish green matrix. Lapilli consists of felsic minerals (quartz + feldspar>80%) and sericite (~20%). The veinlets are dark green filled with fine-grained arsenopyrite grains. Subhedral medium-grained pyrite grains are disseminated. And a few fine-grained sphalerite grains are observed.

Offcut & Thin Section:



Thin Section Description:

- Minerals and Modal Percentage: Quartz 40%, Muscovite/sericite 30%, K-feldspar 20%, Plagioclase 5%, Arsenopyrite 2%, Pyrite 2%, carbonate 1%.
- Texture: Feldspar crystal fragments and lapilli within decussate texture quartz-dominant matrix. Crystal fragments are mainly skeletal-textured feldspar (~0.5 mm) which partly altered into sericite. The matrix is composed of disordered fine grained, lath-shaped quartz grains. Quartz pressure shadows are observed around some sulphide grains in the fine-grained recrystallized quartz veins, which indicates ductile deformation. Some recrystallized quartz has subgrain boundaries. Lapilli consists of felsic minerals (quartz + feldspar>80%) and sericite (~20%).
- Veining: Quartz veinlets have been strongly altered and reworked, and consequently infilled with sericite, pyrite, arsenopyrite and a few carbonate minerals. Veinlets filled with sericite and arsenopyrite are throughout the majority of the thin section.
- Alteration: Intense pervasive sericitization throughout the entire sample between the quartz grains in the matrix and in veins. The arsenopyrite fracture-fill veins generally has stronger sericitization. Some sections have carbonate alteration.
- Ore Mineralogy: Arsenopyrite and pyrite are the two main types of sulphides. Arsenopyrite is fine- to medium-grained (0.1-1mm), corroded and fractured, euhedral to subhedral mainly within strongly altered, reworked, and sericitized relict quartz veinlets. Pyrite grains are less than arsenopyrite grains, medium-grained (~2mm), corroded and fractured, euhedral-subhedral. Pyrite gains commonly occurs as lone grains near veins infilled by arsenopyrite. A combination of pyrite + arsenopyrite and pyrite + sphalerite was observed locally. A few microscopic free gold is near arsenopyrite-quartz vein.

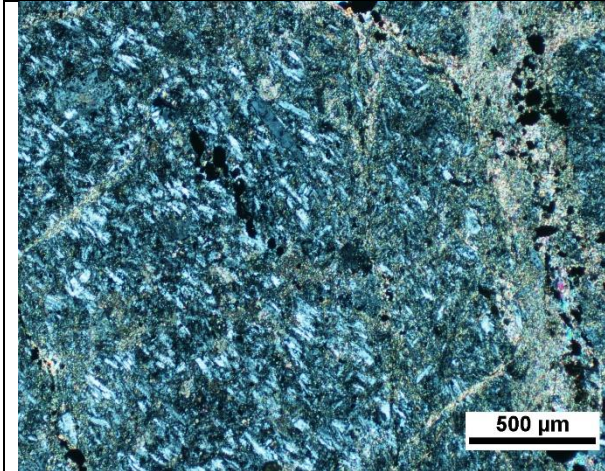


Figure 1. Decussate texture quartz-dominant matrix and sericite veinlets throughout. Some veins are filled with arsenopyrite and pyrite. (XPL, 5X)

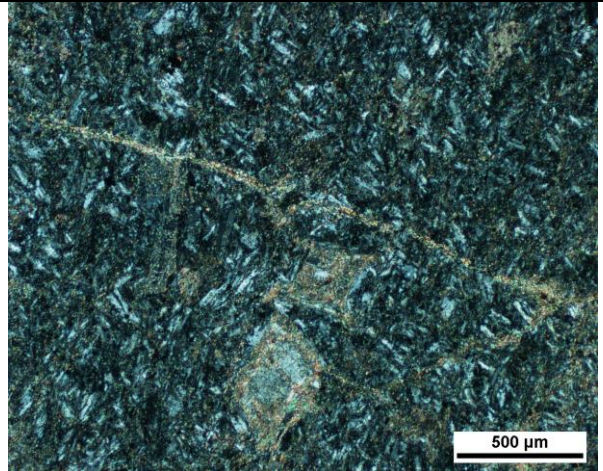


Figure 2. K-feldspar crystal fragments in the decussate texture quartz-dominant matrix, feldspar grains are strongly altered into sericite (XPL, 5X)

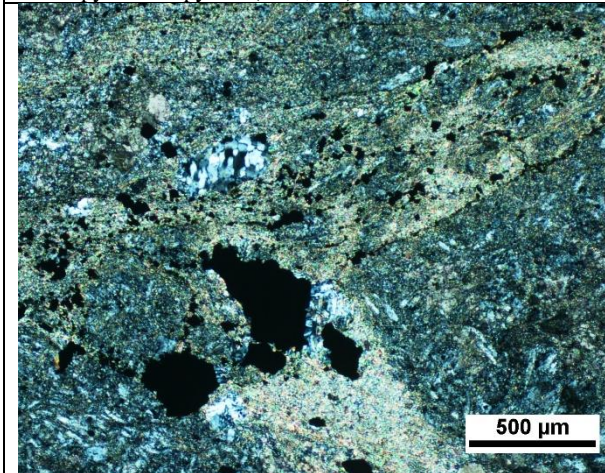


Figure 3. Relict quartz vein which has been intensely altered into sericite and quartz has recrystallization texture and subgrain boundaries. The vein is filled with arsenopyrite and pyrite. Quartz pressure shadows are around pyrite grains (XPL, 5X)

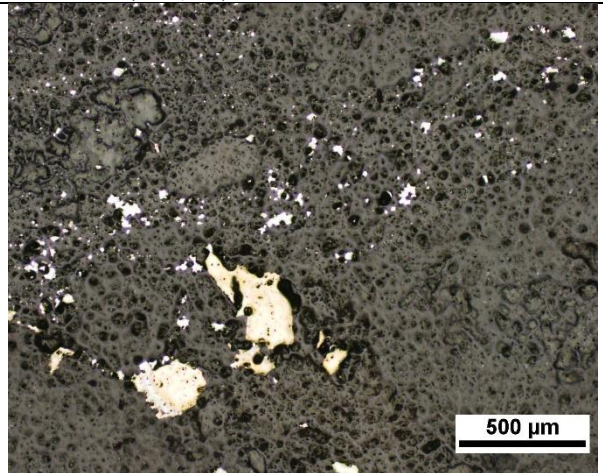


Figure 4. Medium to coarse-grained anhedral strongly fractured pyrite and fine-grained arsenopyrite in sericite-altered quartz veins. (RL, 5X)

Sample Number	2834	Drill Hole	TL-13-500	Depth	195.76-196 m
Lithology from Mining Log	Lapilli Tuff	Target	ME	Gold Grade	5.22 ppm

Drill Core Sample:



Sample Description:

Yellow and light-green foliated lapilli metatuff (schist) with intense folded veinlets. Yellow area is almost as large as the light green area. Lapilli (~50%, 1-5mm) exhibits as dark green fragments along with the foliation. There are two groups of veins cutting the foliated layers: black veins and red veins. Black veins are commonly thicker and less folded than red ones. Red veins are cut by black veins which means black veins are younger than red veins younger than foliation formation. Black veins are formed of smoky quartz with coarse-grained subhedral pyrite and fine-grained arsenopyrite disseminated. Some fine-grained arsenopyrite grains are disseminated in the finer red veins and only a few are in the bedded layers. (Red veins are carbonate veins according to thin section observation)

Offcut & Thin Section:



Thin Section Description:

- Minerals and Modal Percentage: Muscovite/sericite 40%, quartz 20%, plagioclase 15%, carbonate 15%, K-feldspar 5%, pyrite 3%, arsenopyrite 2%, trace gold.
- Texture: Feldspar-dominant lapilli within foliated quartz + feldspar and sericite ± muscovite interbedded matrix. The foliation in the matrix and is wiggly oriented. Veining is throughout the thin section. Lapilli consists of K-feldspar, plagioclase, and quartz. Coarse-grained feldspar fragments are strongly fractured with skeletal texture, which indicates brittle deformation. Coarse-grained plagioclase fragments have polysynthetic twinning and micro-boudinage texture.
- Veining: There are two types of veining system. 1) Relict quartz veinlets have been strongly altered and reworked, and consequently infilled with sericite and muscovite. Some quartz in the veins exhibits recrystallization and subgrain boundaries, but most quartz are fine-grained. 2) Carbonate veinlets is composed of coarse-grained calcite (with twinning planes) and recrystallized fine-grained quartz and a little sericite filled between the calcite grains. This type of veins is infilled with subhedral-euhedral fine-grained arsenopyrite and corroded subhedral medium-to coarse-grained pyrite. Quartz + sericite veins was cut by carbonate + quartz + sericite veins.
- Alteration: Sericitization is more common than carbonate alteration area. Intense pervasive sericitization throughout the entire sample along with the foliation in the matrix and in relict quartz veins. Carbonate alteration is mainly in carbonate veins. Carbonate alteration happen with sericitization, but sericitization does not always happen with carbonate alteration.
- Ore Mineralogy: Arsenopyrite and pyrite are the two main types of sulphides and only occur in carbonate veins. Arsenopyrite is fine-grained (0.1-0.5mm), euhedral to subhedral and occurs on the edge of carbonate veins. Pyrite grains are more than arsenopyrite grains, medium- to coarse-grained (~2mm), corroded and fractured, euhedral-subhedral. Pyrite gains commonly occurs in the middle of carbonate veins. A few microscopic free gold grains are near disseminated fine-grained arsenopyrite.

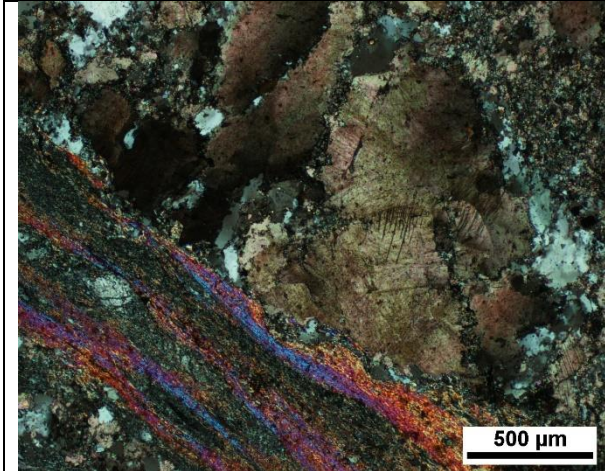


Figure 1. Quartz recrystallized in the fractures of calcite grains in the carbonate vein. The carbonate vein has the direction of the quartz + feldspar and sericite ± muscovite interbedded foliation (XPL, 5X).

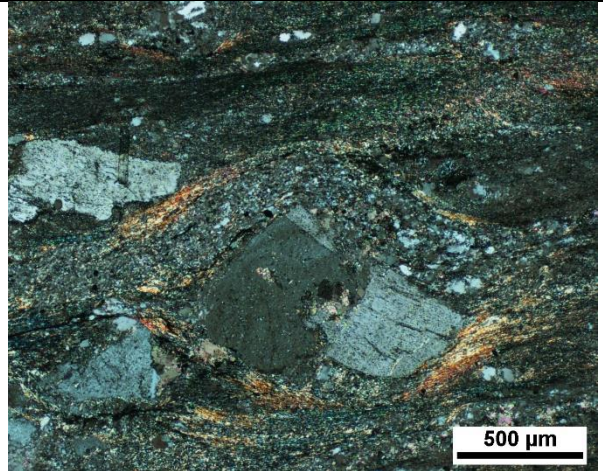


Figure 2. Pressure shadow texture around plagioclase fragments in foliation (XPL, 5X).



Figure 3. Corroded subhedral-euhedral coarse-grained pyrite grains and disseminated euhedral fine-grained arsenopyrite in carbonate vein (RL, 5X).

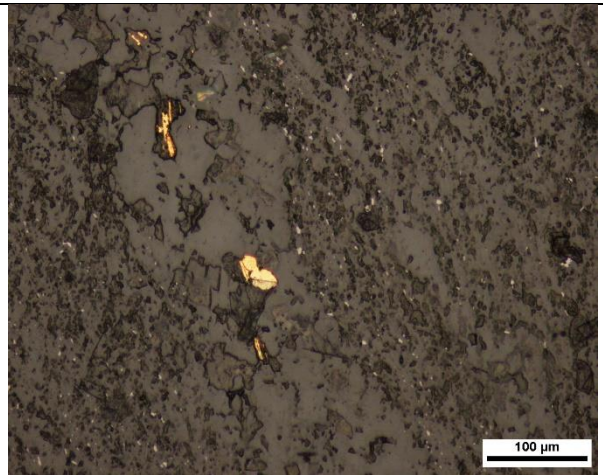


Figure 4. Microscopic free gold grains are near disseminated fine-grained arsenopyrite (RL, 20X)

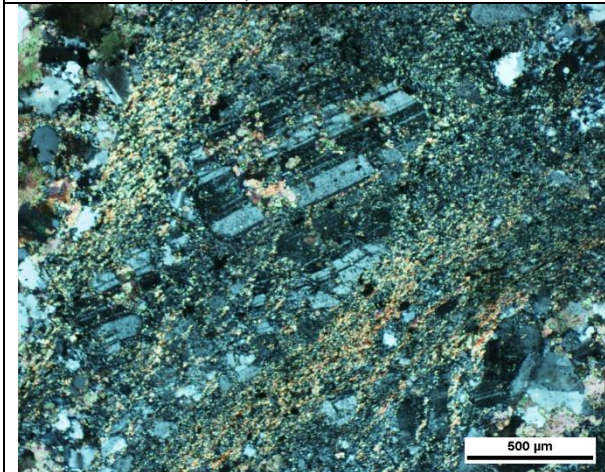


Figure 5. Fractured plagioclase grains with polysynthetic twinning with the same direction of the foliation (XPL, 5X)

Sample Number	2858	Drill Hole	TL-16-607	Depth	817.4-817.6 m
Lithology from Mining Log	Lapilli Tuff	Target	TL	Gold Grade	2.45 ppm

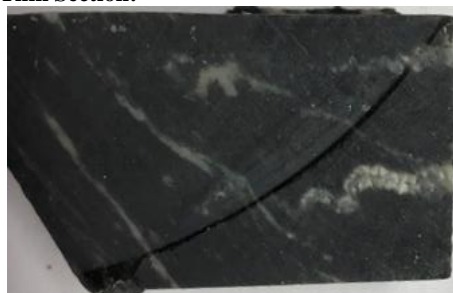
Drill Core Sample:



Sample Description:

Dark grey foliated fine-grained lapilli meta-tuff. Several crosscut quartz veins are folded varying from a few mm to smaller than 1 mm. Sericitization exhibits on the edge of folded quartz veins and faults/fractures. Sulphides (euhedral to subhedral pyrite grains and a few arsenopyrite) are all disseminated following the rims of the quartz veins.

Offcut & Thin Section:



Thin Section Description:

- Minerals and Modal Percentage: Muscovite/sericite 40%, quartz 20%, plagioclase 15%, carbonate 15%, K-feldspar 5%, pyrite 3%, arsenopyrite 2%, trace gold. The majority of this thin section is volcanic ash.
- Texture: Feldspar-dominate volcanic ash and lapilli within foliated quartz + feldspar + sericite matrix. The matrix is dominated by volcanic ash. The foliation in the matrix is oriented. Quartz pressure shadows around pyrite and arsenopyrite grains indicates ductile deformation. K-feldspar in the matrix altered into sericite, while plagioclase altered into carbonate. Recrystallized quartz indicates dynamic recrystallization.
- Veining: Carbonate-quartz veining system (>1000 µm). Carbonate veins also cut through the sericite mass deforming the foliation.
- Alteration: 90% of the rock is altered. Sericitization is more common than carbonate alteration area. Significant pervasive sericitization, being cut by the carbonate veins. Carbonate alteration mainly occurs in carbonate-quartz veins, and a few is in the matrix with the sericitization. Carbonate alteration happens with sericitization, but sericitization does not always happen with carbonate alteration. The layers with the volcanic clasts have more carbonate alteration. Darker lenses with fine grained minerals have more sericitization.
- Ore Mineralogy: Pyrite, arsenopyrite, and sphalerite are the three types of sulphides in this thin section. Most of the sulphides are present in the matrix and present as elongated grains. Pyrite is the most abundant, euhedral to subhedral, fine-coarse grained, usually with sphalerite inclusions inside. Arsenopyrite is smaller and less corroded than arsenopyrite (~100µm), euhedral, disseminated. Sphalerite occurs disseminated, anhedral, boudinaged shape in the matrix (<20µm). A few microscopic free gold grains are in the matrix.

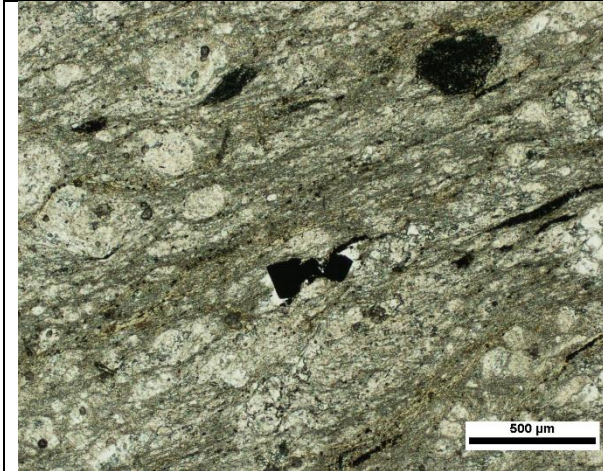


Figure 1. Volcanic lapilli and elongated volcanic ash in foliated matrix. Euhedral pyrite grains and fine-grained arsenopyrite are disseminated. (PPL, 5X)



Figure 2. Fractured coarse-grained needle pyrite along with the foliation in the matrix. Recrystallized quartz formed pressure shadow texture around pyrite grains (XPL, 5X).

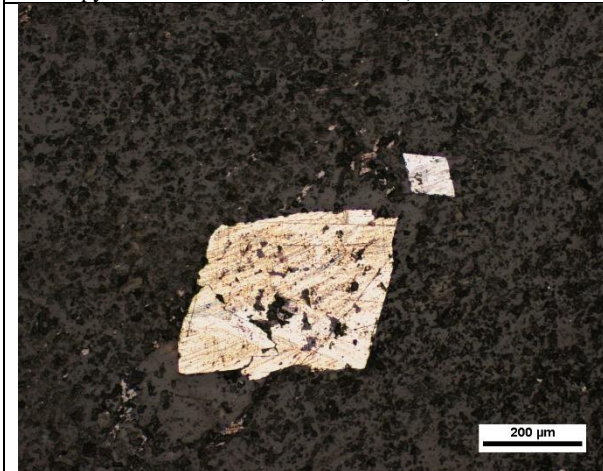


Figure 3. Euhedral arsenopyrite, corroded euhedral pyrite and disseminated anhedral boudinaged sphalerite in the matrix (RL, 20X)

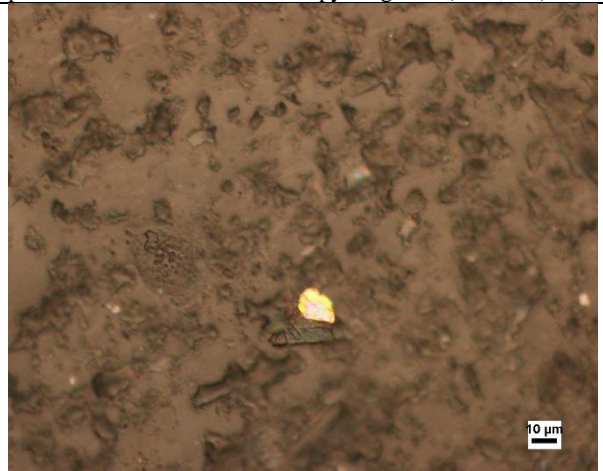


Figure 4. Microscopic free gold grains are in the matrix (RL, 50X).

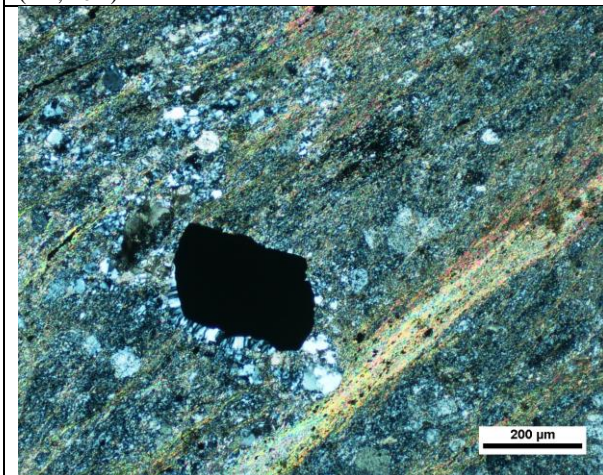


Figure 5. Quartz recrystallized around a corroded euhedral pyrite in the muscovite-rich matrix (XPL, 20X)



Figure 6. Corroded subhedral pyrite in quartz vein (RL, 20X)

Sample Number	1513A*	Drill Hole	TL-16-575	Depth	101-102.05
Lithology from Mining Log	Undifferentiated Intermediate Metavolcanics	Target	TL	Gold Grade	7.568 ppm
Drill Core Sample:					
					
Sample Description: Light yellowish green foliated metatuff (schist) with intense folded veinlets. The matrix is very fine-grained. The 1-2 cm quartz-carbonate veins are along with the foliation and are crosscut by finer quartz-carbonate veins (1-3 mm). There is obvious yellow alteration halo on the edge of the thicker veins. The thicker veins are barren, while the finer veins are filled with smoky quartz and disseminated fine-grained arsenopyrite and pyrite.					
Offcut & Thin Section:					
					
Thin Section Description: <ul style="list-style-type: none"> Minerals and Modal Percentage: Muscovite/sericite 40%, quartz 30%, plagioclase 15%, arsenopyrite 10%, K-feldspar 5%, pyrite 3%, carbonate 2%, trace sphalerite, trace gold. Texture: The high intensity of foliation is visible in aligned arsenopyrite grains and banded muscovite/sericite. Quartz pressure shadows are surrounding arsenopyrite grains (quartz strain fringes). The matrix is foliated, massive, oriented, very fine-grained muscovite/sericite with recrystallized elongate quartz fragments inside. Veining: There are two generations of veins: 1) 2 mm quartz-carbonate vein with medium-fine grained and fractured quartz, carbonate, and plagioclase; 2) <1 mm quartz fine vein is folded with sericite/muscovite halo. The quartz fine vein crosscuts the thicker quartz-carbonate vein. Alteration: Pervasive, extremely strong sericitization along with foliation. Ore Mineralogy: Mainly medium to fine grained, euhedral to subhedral, corroded arsenopyrite. Some fractured arsenopyrite grains are partially replaced by pyrite with very minor sphalerite. Free gold next to fine-grained euhedral prismatic apy and medium-grained subhedral pitted pyrite in the matrix. 					

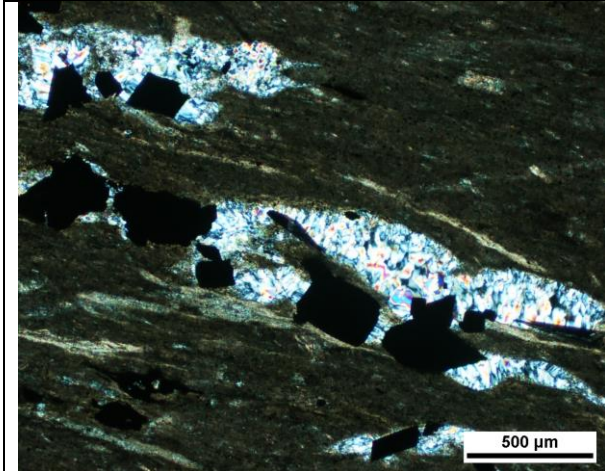


Figure 1. Quartz pressure shadows around euhedral to subhedral aligned arsenopyrite grains along with the foliated sericite in the matrix (XPL, X5).

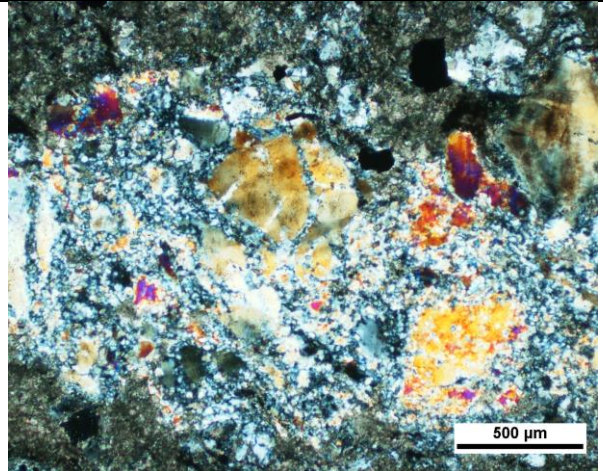


Figure 2. Quartz-carbonate vein has the same orientation as the foliation and partly altered into sericite (XPL, X5).

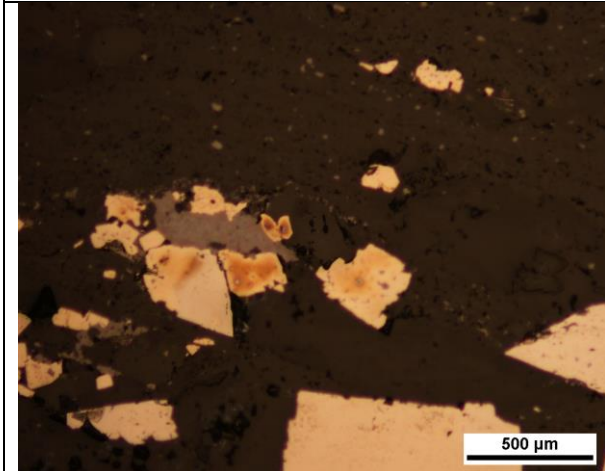


Figure 3. Disseminated arsenopyrite, pyrite, and sphalerite and combinations in the matrix (RL, X20)

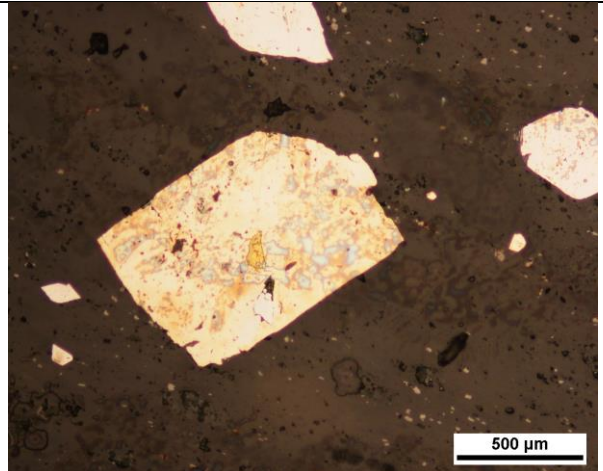


Figure 4. Inclusion gold inside euhedral pyrite (RL, 20X).

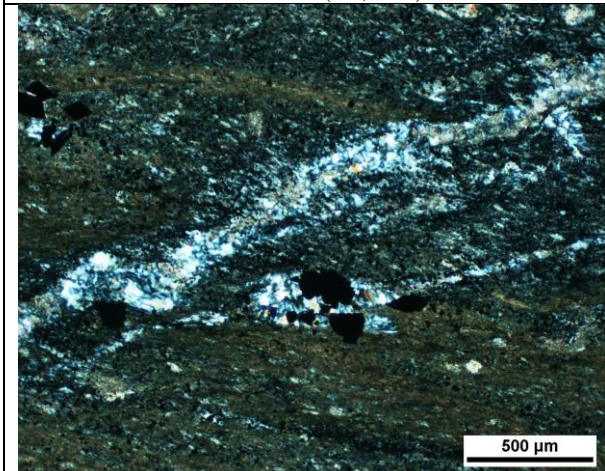


Figure 5. Folded quartz vein crosscut the foliation (XPL, X5)

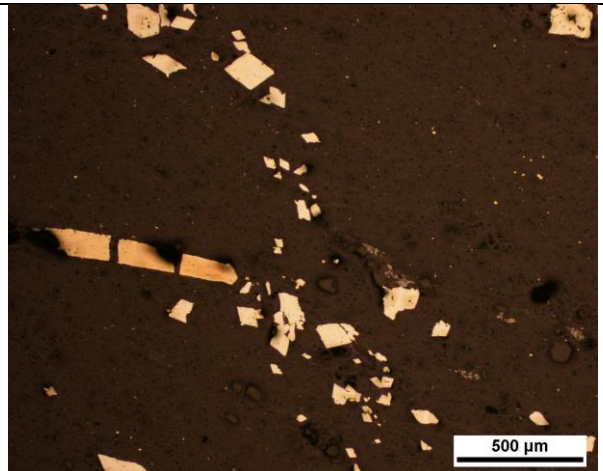


Figure 6. Disseminated euhedral arsenopyrite and pyrite, in the matrix (RL, X5)

Sample Number	1513B*	Drill Hole	TL-16-575	Depth	101-102.05
Lithology from Mining Log	Undifferentiated Intermediate Metavolcanics	Target	TL	Gold Grade	7.568 ppm

Offcut & Thin Section:



Thin Section Description:

- Minerals and Modal Percentage: Muscovite/sericite 30%, quartz 20%, carbonate 20%, K-feldspar 10%, plagioclase 10%, arsenopyrite 5%, pyrite 3%, sphalerite 2% trace epidote, trace gold.
- Texture: High intensity foliation (the same as 1513A) with elongate sericite-replaced lapilli. Quartz pressure shadow around arsenopyrite grains. Medium-grained recrystallized quartz fragments are in the matrix of massive, very fine-grained sericite/muscovite.
- Veining: Quartz-carbonate vein in the middle of the thin section: carbonate (possible calcite) with twinning planes are concentrate on the edge of vein. Quartz recrystallized between the carbonate and feldspar grains. Pyroxene grains show light pink pleochroism under plane-polarized light and high interference colors under cross-polarized light near the vein.
- Alteration: Pervasive, massive, oriented sericitization in the matrix. Carbonate alteration on the edge of the vein.
- Ore Mineralogy: Sulphides are mainly in the matrix, and a few in the folded quartz fine veins. Mainly medium to fine grained, euhedral to subhedral, corroded arsenopyrite. Some fractured arsenopyrite grains are partially replaced by pyrite and sphalerite. Pyrite are very fine-grained and disseminated in the matrix. Possible free gold next to fine-grained euhedral prismatic apy and medium-grained subhedral pitted pyrite in the matrix (Same distribution as 1513A).

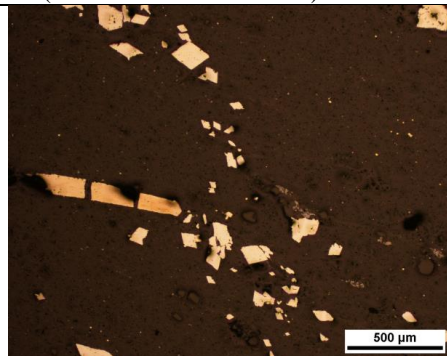
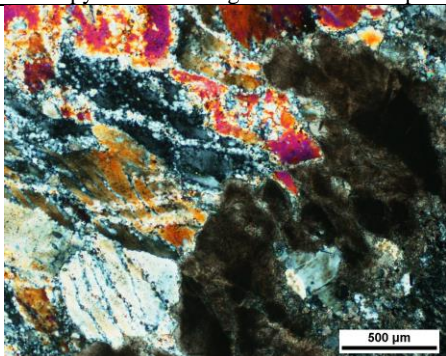


Figure 1. Quartz-carbonate vein in the middle of the thin section: carbonate (possible calcite) with twinning planes are concentrate on the edge of vein. Quartz recrystallized between the carbonate and feldspar grains. Pyroxene grains show light pink pleochroism under plane-polarized light and high interference colors under cross-polarized light. (XPL, X5).

Figure 2. Medium to fine grained arsenopyrite, disseminated very fine-grained pyrite and sphalerite in the matrix. Some fractured arsenopyrite grains are partially replaced by pyrite and sphalerite (RL, X5).

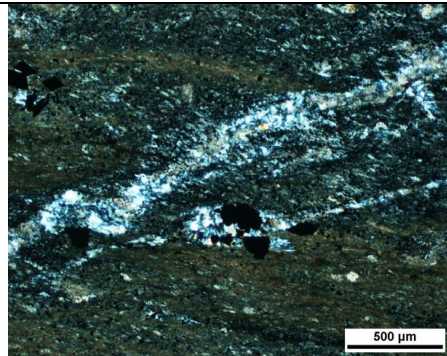
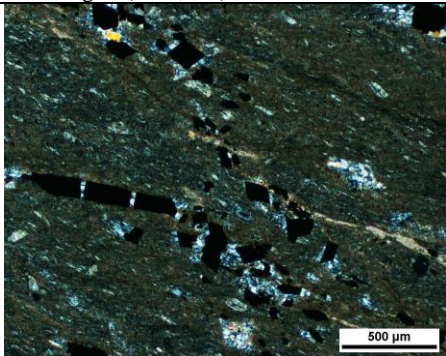


Figure 3. Fractured elongate prismatic arsenopyrite with quartz stain fringes between the gains (XPL, X5).

Figure 4. Fine-grained euhedral arsenopyrite in the folded quartz fine veins (XPL, X5).

Sample Number	1542A*	Drill Hole	TL-11-419	Depth	90-91 m
Lithology from Mining Log	Lapilli Tuff	Target	TLW	Gold Grade	3.541 ppm

Drill Core Sample:



Sample Description:

Dark-light-grey interbedded lapilli meta-tuff (schist). The light grey beds have grey lapilli (>50%, 5-10mm) and strong sericitization. There are two types of veins: 1) white carbonate-quartz veins with weathered surface showing significant oxidation (carbonate with iron) and chlorite alteration; 2) thicker white-smoky quartz veins. Some veins are folded with local faults. Most sulphides (fine-grained arsenopyrite and pyrite) occur within beds, and a few occur associated with carbonate veins. Some medium-grained, euhedral to subhedral pyrite occur throughout sample within dark beds.

Offcut & Thin Section:



Thin Section Description:

- Minerals and Modal Percentage: Muscovite/sericite 30%, quartz 25%, plagioclase 15%, carbonate 10%, chlorite 10%, K-feldspar 5%, pyrite 3%, arsenopyrite 2%, trace epidote, trace gold.
- Texture: Moderate foliated quartz-feldspar-sericite-chlorite matrix which is strongly overprinted. Chlorite occurs surrounding strong fractured, anhedral, coarse-grained pyrite. Sericite in the matrix are very fine-grained with recrystallized muscovite, while carbonate is coarse-grained with twinning planes. Plagioclase in the relict clasts are coarse-grained with polysynthetic twinning.
- Veining: A few discontinuous and folded quartz-feldspar vein in the matrix. Quartz are very fine in the veins.
- Alteration: Sericitization is throughout the whole thin section. Chlorite alteration is surrounding strongly fractured, anhedral, coarse-grained pyrite.
- Ore Mineralogy: There are three types of sulphides: pyrite, arsenopyrite, and sphalerite. Pyrite has two morphology types: 1) strongly fractured, anhedral, coarse-grained pyrite surrounded by chlorite; 2) euhedral, fine-grained pyrite disseminated in the matrix. Arsenopyrite are generally fine-grained, euhedral to subhedral. Sphalerite shows as a combination with arsenopyrite. Inclusion gold are within pyrite, arsenopyrite, sphalerite. Free gold is near euhedral pyrite and arsenopyrite in matrix.

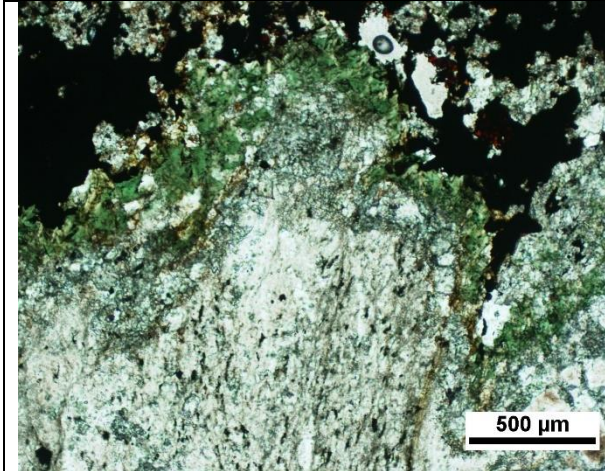


Figure 1. Chlorite alteration is surrounding strongly fractured, anhedral, coarse-grained pyrite.

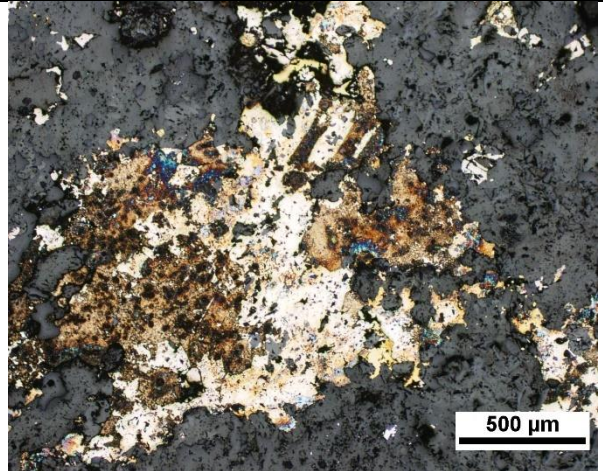


Figure 2. Strongly fractured, anhedral, coarse-grained pyrite.

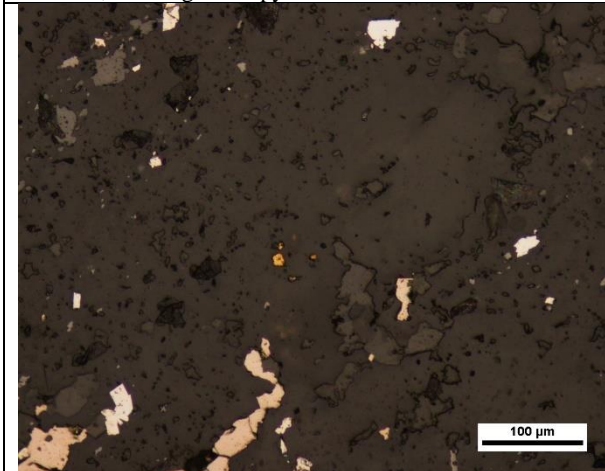


Figure 3. Free gold near euhedral pyrite and arsenopyrite in matrix (RL, X20)

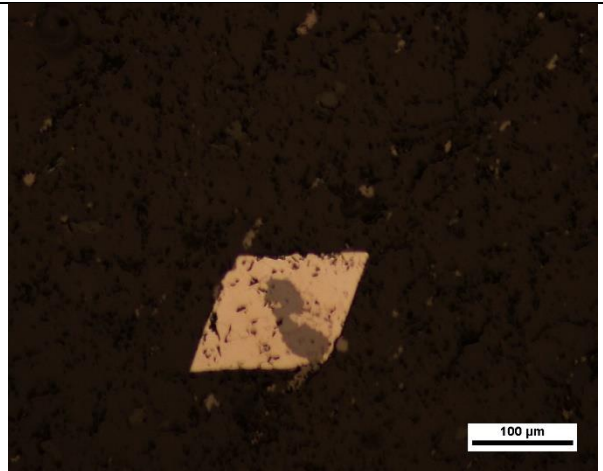


Figure 4. The combination of arsenopyrite and spharite in the matrix (RL, X20)

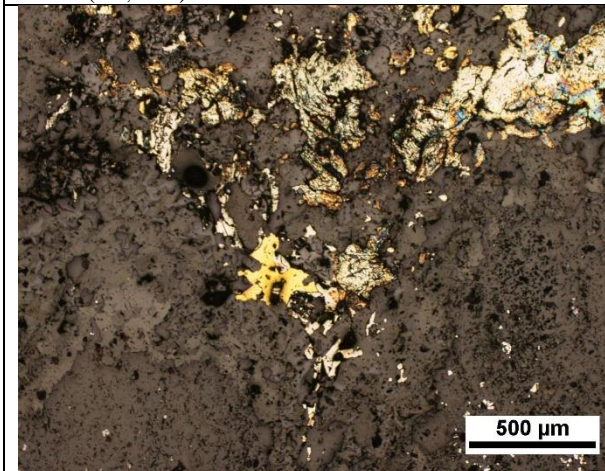


Figure 5. Inclusion gold with strongly fractured, anhedral, coarse-grained pyrite and disseminated pyrite. (RL, X5)



Figure 6. Inclusion gold on the edge of anhedral pyrite (RL, X20)

Sample Number	1543A*	Drill Hole	TL-11-419	Depth	91-92 m
Lithology from Mining Log	Lapilli Tuff	Target	TLW	Gold Grade	4.135 ppm

Drill Core Sample:



Sample Description:

Dark grey lapilli meta-tuff with light grey-to-white clasts. A severely strained and mylonitized BIF unit that is then further stretched (?). Strong sericitization and very few sulphides. Fine-grained pyrite and arsenopyrite near fractures and deformation. And there is a ~1.5 cm quartz vein with sulphides inside.

Offcut & Thin Section:



Thin Section Description:

- Minerals and Modal Percentage: Muscovite/sericite 60%, quartz 20%, plagioclase 15%, carbonate 15%, K-feldspar 5%, pyrite 3%, arsenopyrite 2%, trace chlorite, trace gold.
- Texture: Moderate foliated, very fine-grained quartz-feldspar-sericite matrix. Sample contains several discontinuous, anastomosing and folded quartz-feldspar veins crosscutting the thin section. Several thin, wispy quartz stringer veins also occur within foliation. Clasts are filled with recrystallized quartz and feldspar.
- Veining: Several discontinuous, anastomosing and folded quartz-feldspar veins that crosscut sample within the clast and sericite-chlorite matrix region. Several thin, wispy quartz stringer veins also occur proximal to large band of sericite and recrystallized muscovite within foliation.
- Alteration: Strong sericitization and locally chlorite alteration.
- Ore Mineralogy: Arsenopyrite is dominant, and occurs as coarse euhedral grains within sericite muscovite, or as fractured masses in sericite and proximal to porphyritic quartz-feldspar material, while fine-grained ones are disseminated in the matrix. Inclusion gold is on the edge of subhedral pyrite. Free gold is inside quartz-feldspar-sericite matrix.

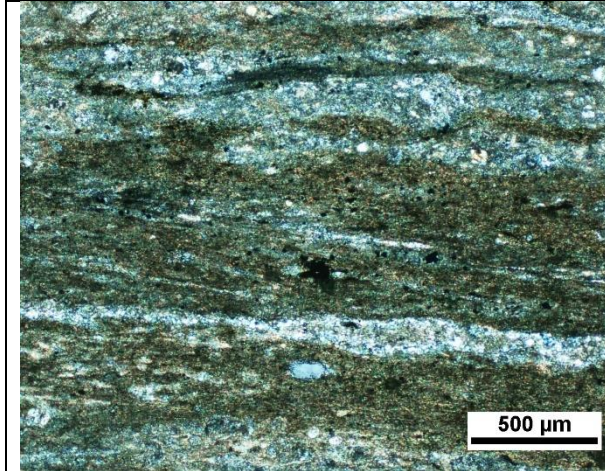


Figure 1. The foliation in the matrix is wiggly oriented (XPL, X5).

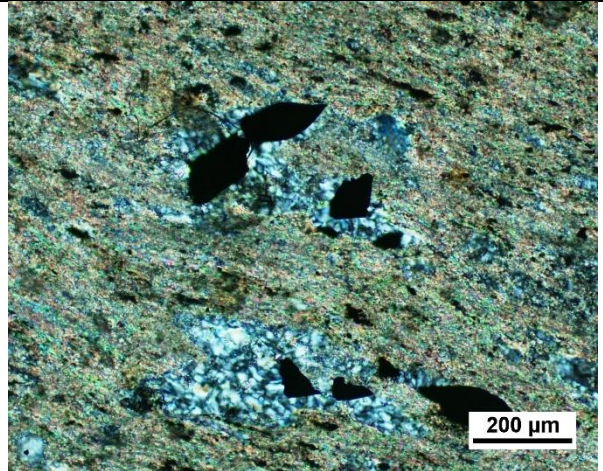


Figure 2. Pyrite grain exhibiting quartz pressure shadows on both sides (XPL, X10).

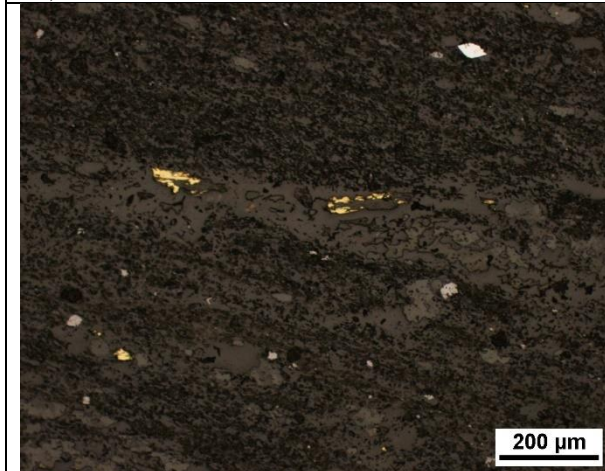


Figure 3. Free gold inside quartz-feldspar-sericite matrix (RL, X10).

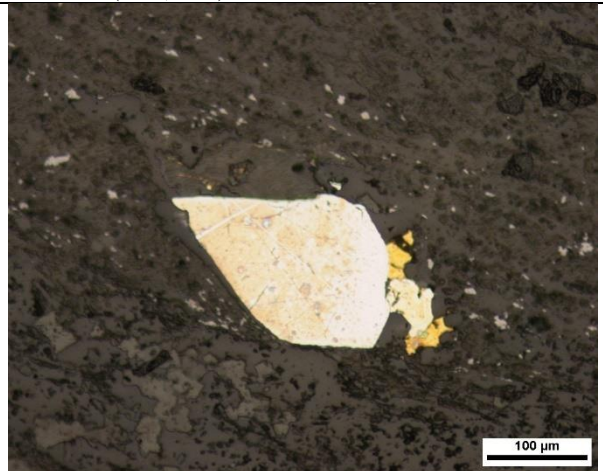


Figure 4. Inclusion gold on the edge of subhedral pyrite and near euhedral disseminated arsenopyrite (RL, X50).

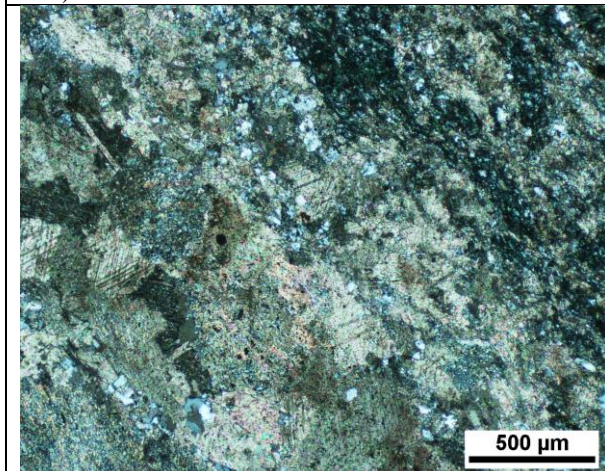


Figure 5. Carbonate + Quartz vein (XPL, X5)

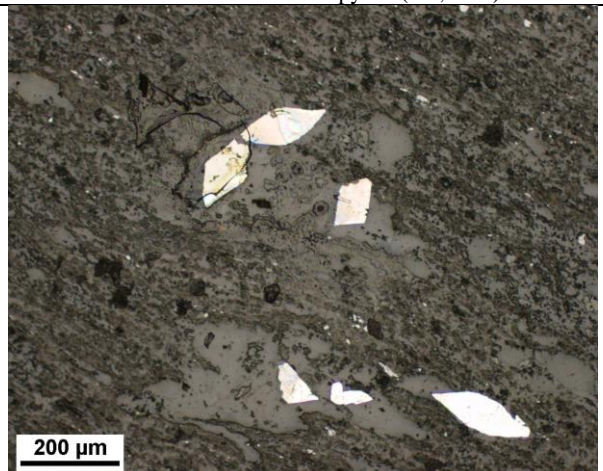


Figure 6. Euhedral arsenopyrite in quartz vein (RL, X10)

Sample Number	1530*	Drill Hole	TL-03-160	Depth	183.78-184.06 m
Lithology from Mining Log	Heterolithic Tuff	Target	ME	Gold Grade	3.28

Drill Core Sample:



Sample Description:

Light yellowish green foliated heterolithic metatuff (schist) with intense foliation and significant shear. The sample is fine-grained with mildly sericitization and carbonate alteration. The fragments in the sample is 1-5 mm. The surface shows maroon-brown oxidation (due to Fe-carbonate). Arsenopyrite is more than pyrite. Arsenopyrite and pyrite mainly exhibit in the carbonate and/or quartz layers. The foliation is cut by a fine quartz vein.

Offcut & Thin Section:



Thin Section Description:

- Minerals and Modal Percentage: quartz 45%, K-feldspar 15%, muscovite/sericite 15%, chlorite 15%, plagioclase 5%, arsenopyrite 3%, pyrite 1%, trace carbonate.
- Texture: Intense foliated and mildly mylonitic texture. The matrix is interbedded by fine to coarse-grained quartz-feldspar layers and sericite-chlorite layers. Quartz was recrystallized surrounding coarse-grained feldspar grains.
- Veining: A few very fine quartz veins cross cut the foliation. The veins are strongly altered into sericite.
- Alteration: All layers within the foliation exhibit some degree of sericitization or overprint. Sericite is also present as banded layers within foliation. Where finest grained materials exist, there is also pervasive, fine grained chlorite alteration.
- Ore Mineralogy: There are two types of sulphides within the foliation: arsenopyrite and pyrite. Pyrite are medium to coarse-grained, strongly fractured, euhedral to anhedral. Arsenopyrite is finer-grained but massive than pyrite, generally euhedral to subhedral, needle or elongate prismatic shape. The combination of pyrite and arsenopyrite shows in the matrix. Quartz stain fringes and pressure shadow exhibit surrounding sulphides. No microscopic gold has been observed.

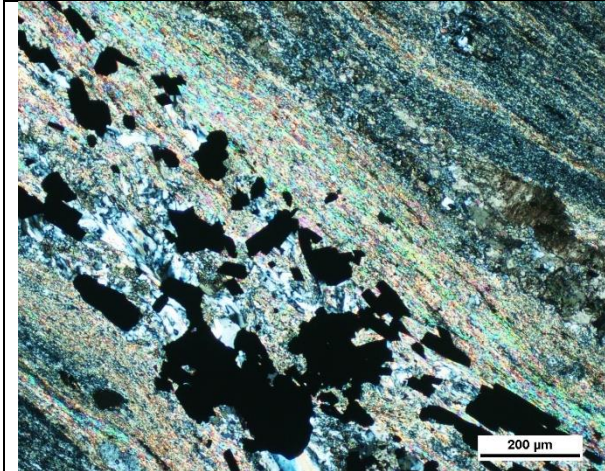


Figure 1. Quartz stain fringes and pressure shadow exhibit surrounding sulphides within intense sericite foliation (XPL, X10).

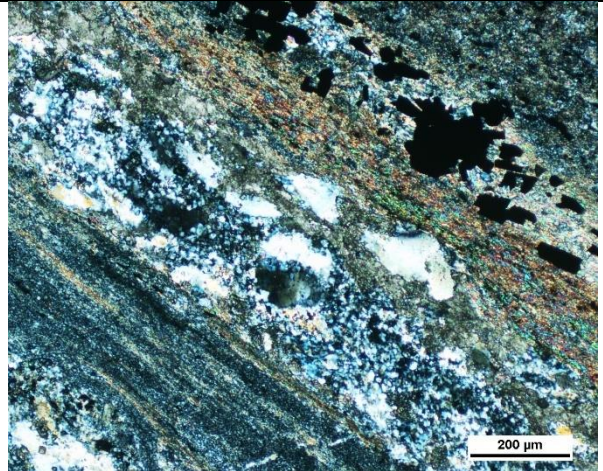


Figure 2. Quartz was recrystallized surrounding coarse-grained feldspar grains (XPL, X10).

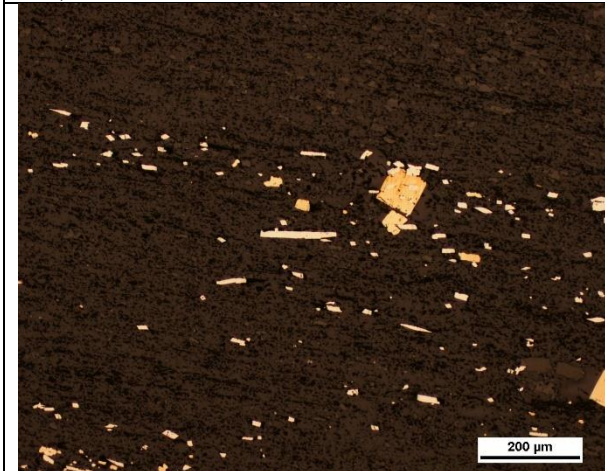


Figure 3. Medium to coarse-grained, euhedral pyrite and needle and elongate prismatic shaped, euhedral fine-grained but massive arsenopyrite in the foliated matrix. (RL, X10)



Figure 4. The combination of pyrite and arsenopyrite in the matrix (RL, X10).

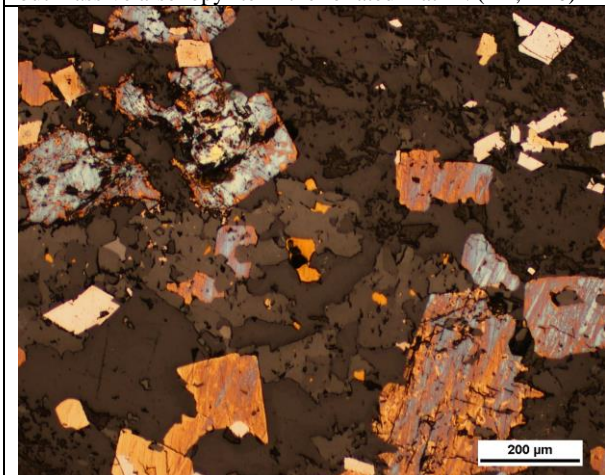
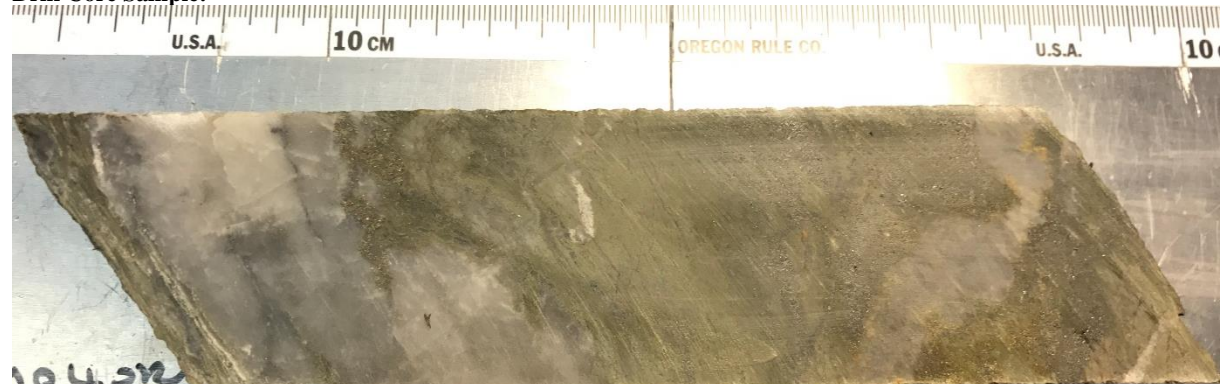


Figure 5. corroded pyrite and euhedral arsenopyrite with free gold in the matrix (RL, X10).

Sample Number	2854	Drill Hole	TL-16-604A	Depth	183.78-184.06 m
Lithology from Mining Log	Undifferentiated Felsic Metavolcanics	Target	TL	Gold Grade	10.49 ppm

Drill Core Sample:



Sample Description:

Light yellowish green felsic meta-tuff with strong smoky quartz veins. There is obvious yellow alteration halo on the edge of the quartz veins. Fine-grained arsenopyrite and medium-grained euhedral-subhedral pyrite are along with the fractures in the veins and the edge of the veins. A few fine-grained pyrite and arsenopyrite are disseminated in the host rock (tuff). The host rock has slightly foliation. Arsenopyrite is far more than pyrite.

Offcut & Thin Section:



Thin Section Description:

- Minerals and Modal Percentage: quartz 35%, muscovite/sericite 25%, arsenopyrite 15%, pyrite 10%, plagioclase 5%, K-feldspar 5%, sphalerite 3%, carbonate 2%.
- Texture: This thin section is the cross section of the main quartz vein without foliation. The thin section has slight sericitization. Muscovite/sericite grows surrounding sulphides grains. Quartz shows strong recrystallization. Carbonate alteration exhibits between the quartz vein and the host rock.
- Veining: Quartz vein with strong recrystallization and carbonate alteration on the edge.
- Alteration: The thin section has slight sericitization and carbonate alteration. Muscovite/sericite grows surrounding sulphides grains and mostly cryptocrystalline. Carbonate alteration exhibits between the quartz vein and the host rock.
- Ore Mineralogy: There are three types of sulphides: arsenopyrite, pyrite, and sphalerite. Sulphides are present in the host rock and in the quartz veins. In the host rock, arsenopyrite and pyrite are fine-grained, euhedral to subhedral, without fractures. In the quartz vein, the arsenopyrite are coarse to medium-grained, intensely fractured and corroded. Sometimes arsenopyrite exhibits as a chunk with anhedral pyrite and inclusion sphalerite inside. No microscopic gold has been found in the thin section.

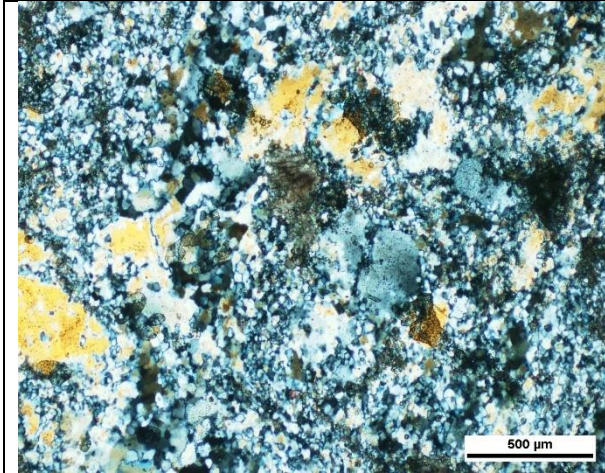


Figure 1. Quartz recrystallized in the quartz vein with feldspar, sericite, and a few carbonate grains (XPL, X5).

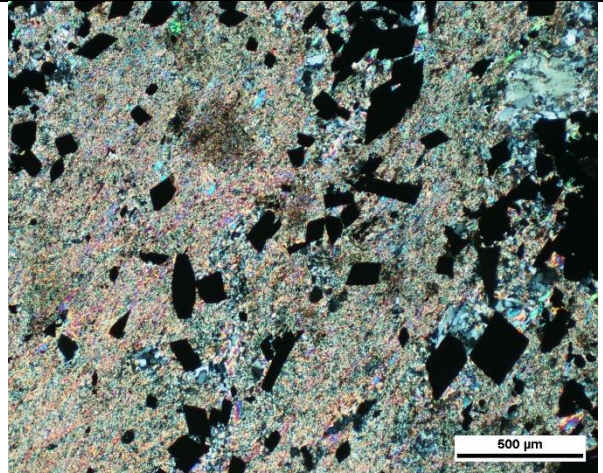


Figure 2. Cryptocrystalline sericite in the host rock with disseminated fine-grained euhedral-subhedral arsenopyrite. Quartz recrystallized surrounding arsenopyrite grains (XPL, X5).

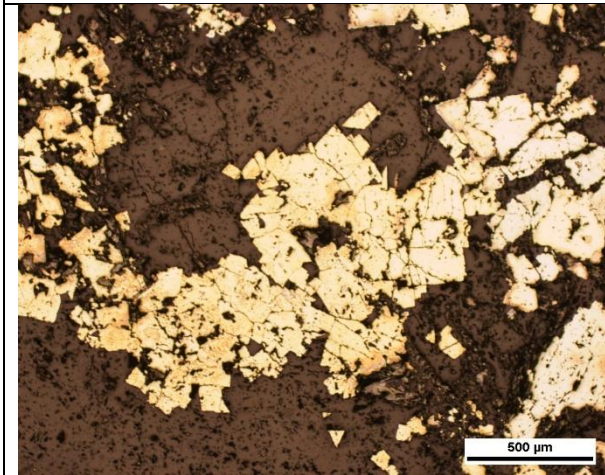


Figure 3. Euhedral to subhedral pyrite and arsenopyrite combination in the quartz vein (RL, X5).

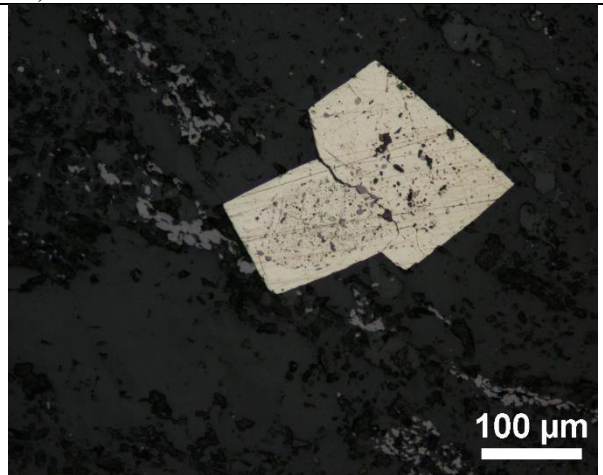


Figure 4. Medium grained corroded euhedral arsenopyrite grains with spahalerite (RL, X20)

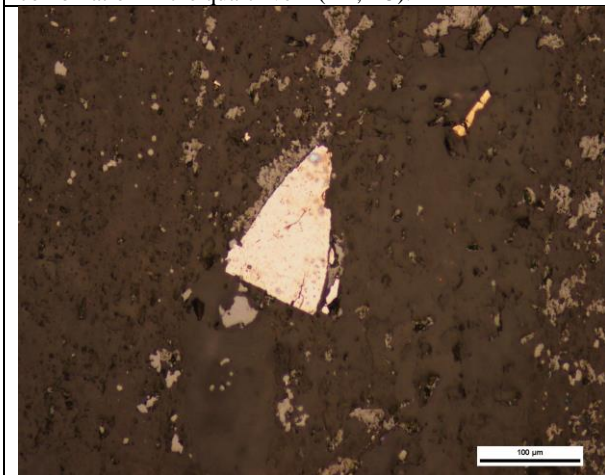


Figure 5. Needle arsenopyrite grains with fine-grained spahalerite and pyrite (RL, X20)

Sample Number	2831	Drill Hole	TL-16-575	Depth	96.8-98 m
Lithology from Mining Log	Metasandstone	Target	SLS	Gold Grade	2.26 ppm

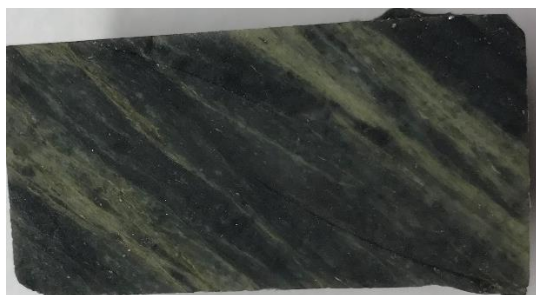
Drill Core Sample:



Sample Description:

Light-dark yellowish green fine-grained layered bedded metasandstone. The sample shows strong sericitic (light green) and chlorite (dark green) alteration. Pyrite and arsenopyrite are in the middle of the sample along the layers. Arsenopyrite > Pyrite.

Offcut & Thin Section:



Thin Section Description:

- Minerals and Modal Percentage: 35% Muscovite/Sericite, 20% Quartz, 15% K-Feldspar, 5% Plagioclase, 4% Arsenopyrite, 1% Pyrite, Trace Gold.
- Texture: Intense foliation with moderate sericitization. The matrix is mainly very fine to fine-grained dirty quartz. Sulphides exhibit quartz pressure shadows. All primary textures have been completely obliterated by intense shearing and alteration. Feldspar clasts are partially altered into sericite.
- Veining: A few quartz-carbonate veins.
- Alteration: carbonate alteration and sericitization.
- Ore Mineralogy: Sulphides are disseminated in the matrix (Arsenopyrite, Sphalerite, Pyrite). Sphalerite grains are anhedral (~100um), corroded and disseminated in the groundmass. Pyrite is euhedral to subhedral with inclusions (~200um). Arsenopyrite grains are subhedral (<100 um) without inclusions. Free gold grains are close to disseminated arsenopyrite grains.
-

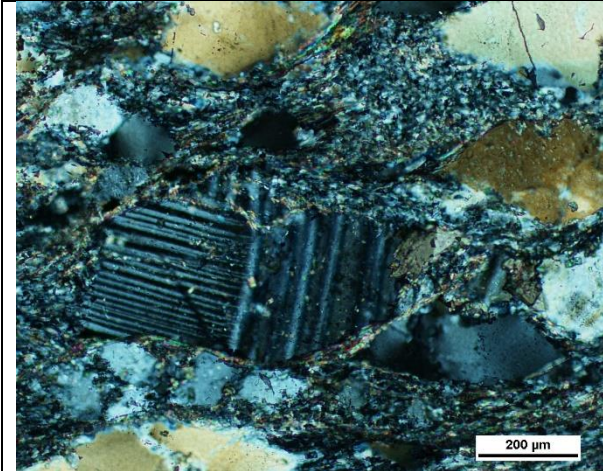


Figure 1. Feldspar clasts and sericite filled within the fractures (XPL, X10)

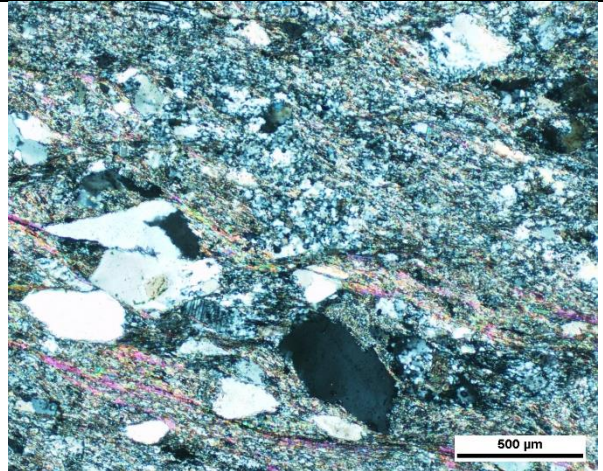


Figure 2. Feldspar clasts with muscovite foliated layers in quartz-dominated matrix (XPL, X5)

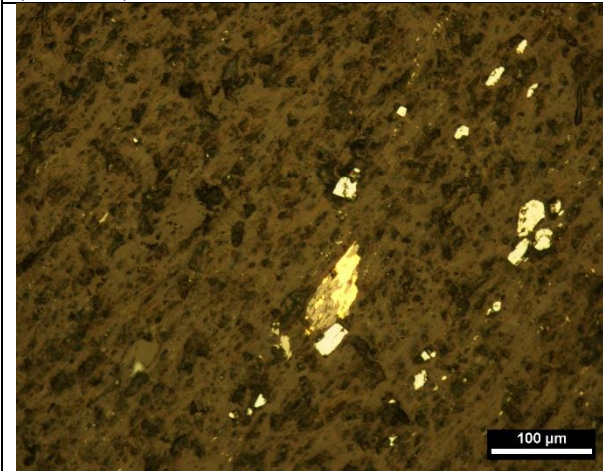


Figure 3. Subhedral fine-grained arsenopyrite and free gold within quartz-dominated matrix (RL, X20)

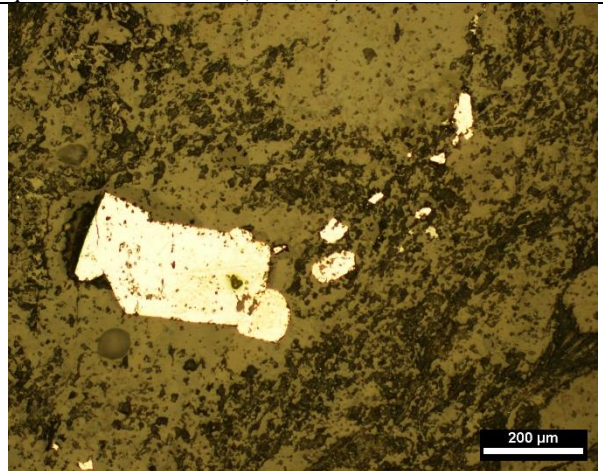


Figure 4. euhedral pyrite in quartz-dominated matrix (RL, X10)

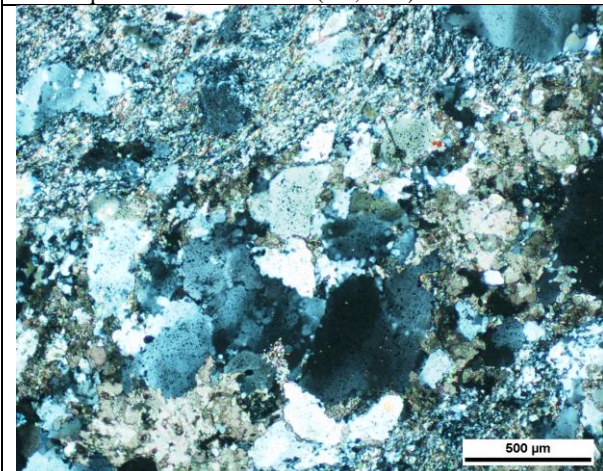


Figure 5. Quartz recrystallized in carbonate-quartz vein (XPL, X5)

Sample Number	1516A*	Drill Hole	TL-13-506	Depth	164.70-165.70 m
Lithology from Mining Log	Metasiltstone	Target	TLW	Gold Grade	4.960 ppm

Drill Core Sample:



Sample Description:

Dark grey to dark green thinly bedded metasiltstone. On the flat surface of the hand sample, dark green, dark grey, and brown layers interbedded. White and orange carbonate veins along with the bedding layers (calcite and ankerite, the orange color is because of the oxidation of Fe in ankerite). Fine to coarse-grained subhedral to euhedral pyrite are aligned on bedding layers.

Offcut & Thin Section:



Thin Section Description:

- Minerals and Modal Percentage: Muscovite/sericite 30%, quartz 25%, plagioclase 15%, carbonate 15% (scheelite and calcite), K-feldspar 5%, chlorite 5%, pyrite 3%, arsenopyrite 2%, trace sphalerite, trace gold.
- Texture: The thin section shows a strong foliation: the matrix is chlorite and sericite interbedded. The feldspar fragments are partly altered into sericite. Quartz are recrystallized showing pressure shadow surrounding sulphide grains.
- Veining: There are two types of possible veining system: 1) relict quartz vein with euhedral to subhedral pyrite and arsenopyrite filled inside; 2) carbonate fine veins along with the bedding layers.
- Alteration: Pervasive sericite and chlorite alteration, and moderate carbonate alteration in veins
- Ore Mineralogy: There are two main types of sulphides: pyrite and arsenopyrite. Pyrite grains are generally medium to coarse-grained, euhedral to subhedral, slightly fractured and corroded. Arsenopyrite grains are mainly medium-grained, subhedral to needle-shaped, more corroded and fractured, and inclusion-rich. Fine to very fine-grained arsenopyrite and pyrite are disseminated in the matrix. Inclusion gold exhibits in subhedral corroded arsenopyrite.

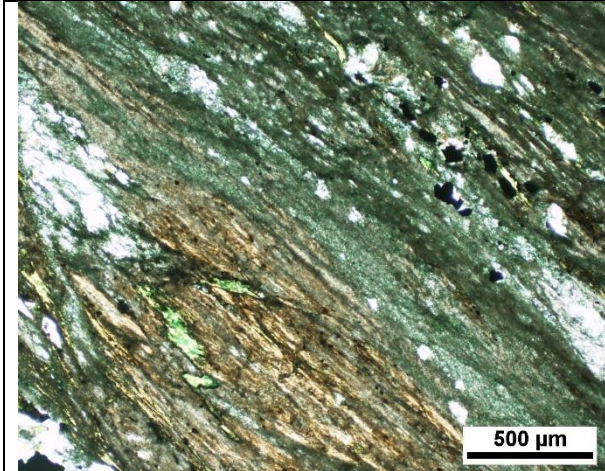


Figure 1. chlorite and sericite interbedded matrix (PPL, X5)

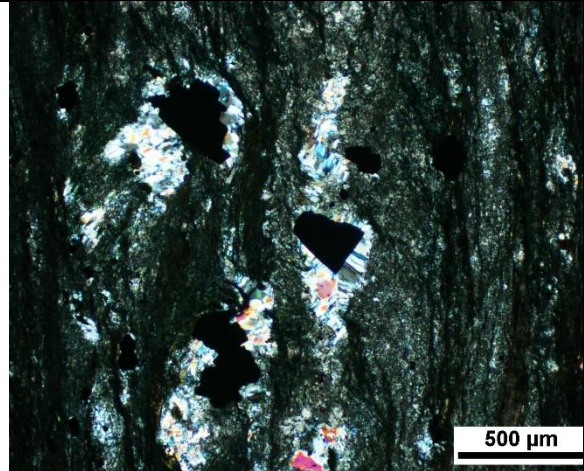


Figure 2. quartz pressure shadow surrounding subhedral and needle pyrite grains along with the foliation (XPL, X5)

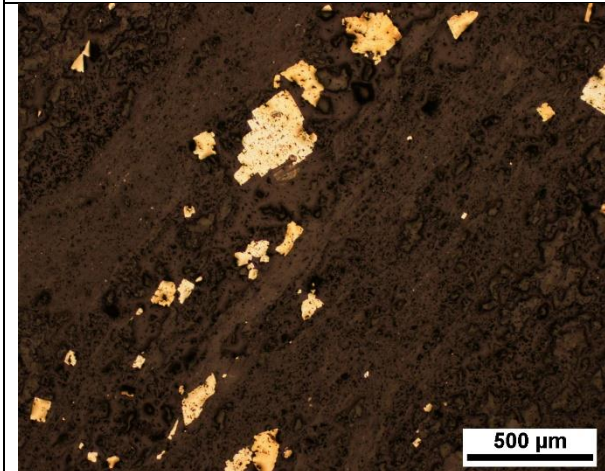


Figure 3. Fine-grained corroded pyrite along with foliation (RL, X5)

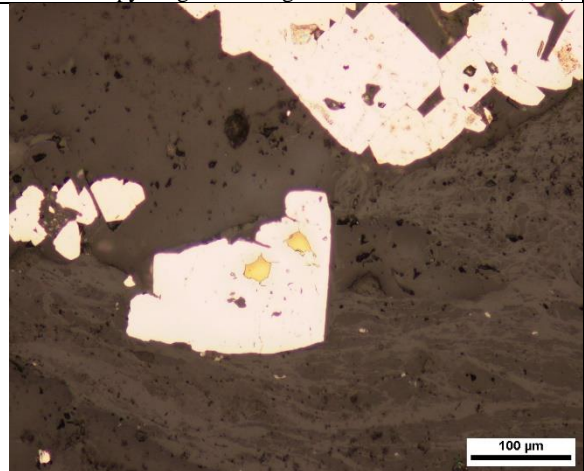


Figure 4. Inclusion gold in subhedral corroded arsenopyrite (RL, X20)

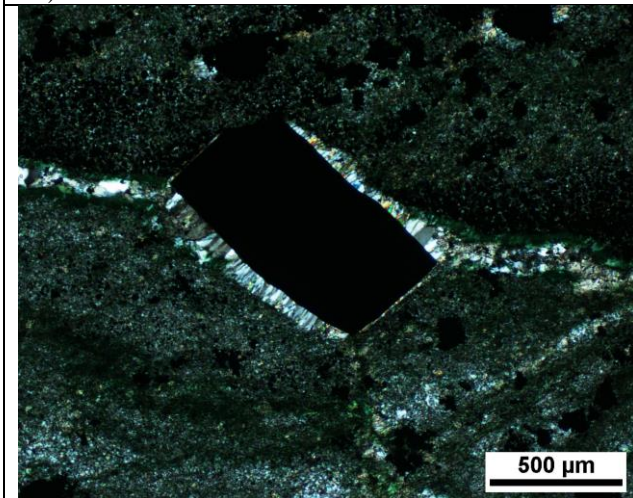


Figure 5. Quartz recrystallized surround euhedral pyrite grain (XPL, X5)

Sample Number	1535B*	Drill Hole	TL-11-419	Depth	83-84 m
Lithology from Mining Log	Metasiltstone	Target	TLW	Gold Grade	4.969 ppm

Drill Core Sample:



Sample Description:

Dark brownish grey bedded metasiltstone with massive veins. There are two types of veins observed on the hand sample which are all along with the bedding layers: 1) severely folded carbonate veins with orange halo (oxidation of Fe in dolomite) on the contacting zone of the vein and host rock. 2) smoky quartz veins. Z-folding has been observed on the hand sample. Fine to medium pyrite and arsenopyrite are disseminated in veins and host rock.

Offcut & Thin Section:



Thin Section Description:

- Minerals and Modal Percentage: quartz 25%, carbonate 20%, plagioclase 15%, chlorite 20%, muscovite/sericite 10%, K-feldspar 5%, pyrite 3%, arsenopyrite 2%, trace sphalerite, trace gold.
- Texture: Intense foliation and schistosity with moderate sericitization. The matrix is mainly very fine to fine-grained dirty quartz and sericite. Sulphides exhibit quartz pressure shadows. All primary textures have been completely obliterated by intense shearing and alteration. Feldspar fragments are partially altered into sericite.
- Veining: quartz-carbonate veins: quartz is fine-grained and recrystallized; carbonate is coarse-grained in the center of the veins. Fine to medium-grained, euhedral to subhedral sulphides always distribute at the outer selvage of quartz veins.
- Alteration: intensely sericitization and moderately chlorite alteration throughout the thin section. Carbonate alteration is common in the relict veins.
- Ore Mineralogy: Pyrite and arsenopyrite occur both together and segregated in different zones or bands/veins in sheared area. Pyrite occurs as medium to coarse grained, subhedral or needle-shaped, strongly corroded and fractured. Arsenopyrite always distributes at the outer selvage of quartz veins as fine to medium-grained, euhedral to subhedral grains. Fine to very fine-grained arsenopyrite and pyrite are disseminated in the matrix. Inclusion gold in coarse-grained subhedral corroded pyrite.

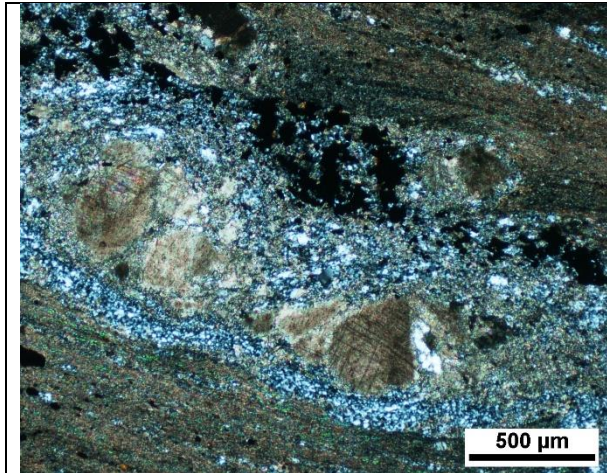


Figure 1. calcite within quartz vein and arsenopyrite distributes at the outer selvage of the vein (XPL, X5)

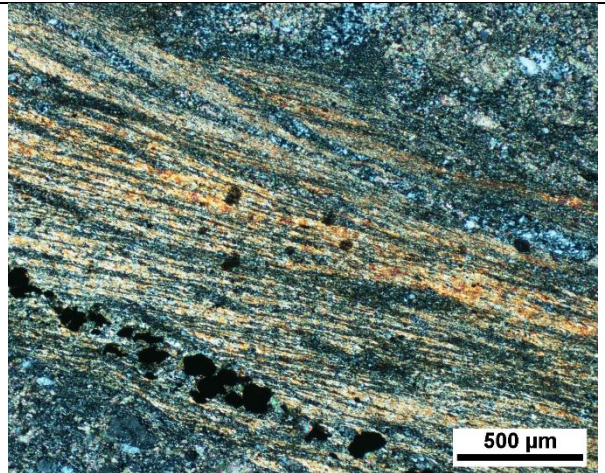


Figure 2. oriented sercite layers and a quartz fine vein filled with arsenopyrite grains (XPL, X5)

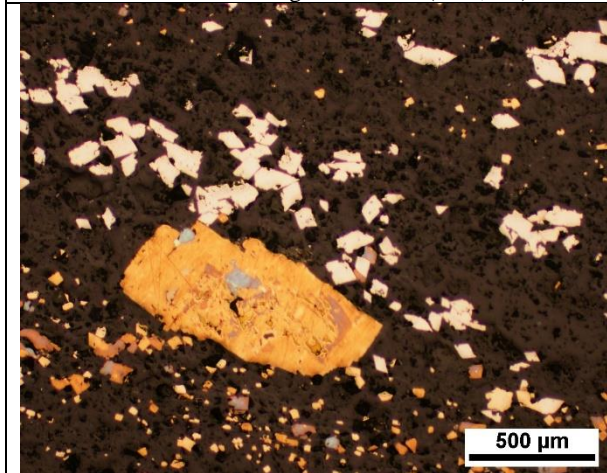


Figure 3. Inclusion gold in coarse-grained subhedral corroded pyrite (RL, X5)

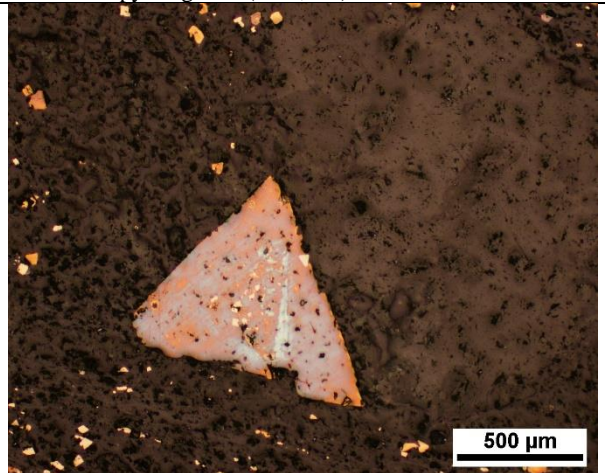


Figure 4. needle-shaped pyrite with fine-grained arsenopyrite filled as inclusions (RL, X5)

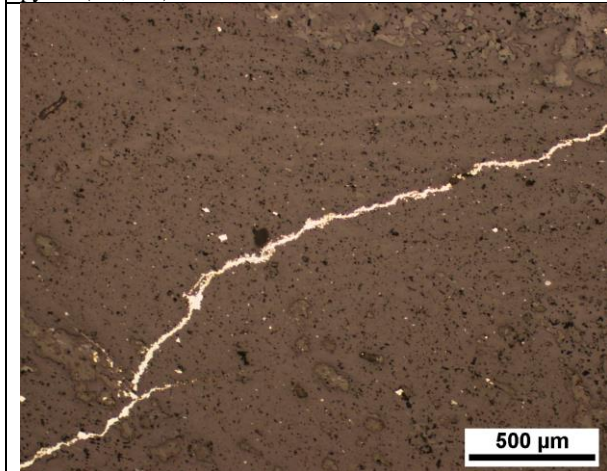


Figure 5. Fine arsenopyrite vein and disseminated arsenopyrite (RL, X5)

Sample Number	1536A*	Drill Hole	TL-11-419	Depth	84-85 m
Lithology from Mining Log	Metasiltstone	Target	TLW	Gold Grade	3.435 ppm
Drill Core Sample:					
					
Sample Description:					
Dark grey and yellowish green bedded metasiltstone. It looks similar to 1535 but with more sulphides throughout the hand sample. Severely folded carbonate veins with orange halo (oxidation of Fe in dolomite) on the contacting zone of the vein and host rock. Z-folding has been observed on the hand sample. Fine to medium pyrite and arsenopyrite are disseminated in veins and host rock.					
Offcut & Thin Section:					
					
Thin Section Description:					
<ul style="list-style-type: none"> • Minerals and Modal Percentage: quartz 30%, muscovite/sericite 20%, plagioclase 15%, carbonate 10%, chlorite 15%, K-feldspar 5%, pyrite 4%, arsenopyrite 1%, trace sphalerite, trace chalcopyrite, trace gold. • Texture: Intense foliation and schistosity with moderate sericitization. The matrix is mainly very fine to fine-grained dirty quartz and sericite. Quartz are all recrystallized. Sulphides appear within chlorite foliated layers. All primary textures have been completely obliterated by intense shearing and alteration. Rare fragments are partially altered into sericite. • Veining: very fine microcrystalline quartz-carbonate along with the foliation and pyrite-fill veinlets and muscovite veinlets crosscut the foliation. Euhedral arsenopyrite has been observed within pyrite-fill veinlets. • Alteration: intensely sericitization and moderately chlorite alteration throughout the thin section. All primary textures have been completely obliterated by intense shearing and alteration. • Ore Mineralogy: Pyrite is the major sulphides, appearing as anhedral fractured grains in the matrix and filled within veinlets. Euhedral arsenopyrite has been observed within pyrite-fill veinlets. Fine to very fine-grained arsenopyrite and pyrite are disseminated in the matrix. No microscopic gold has been found in the thin section. 					

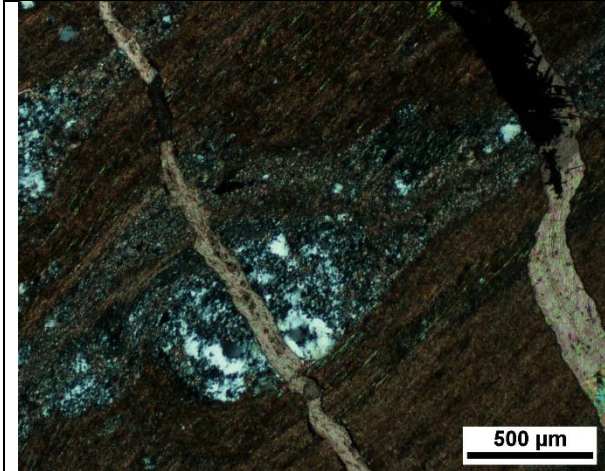


Figure 1. pressure shadow surrounding a recrystallized quartz clast and muscovite veinlets crosscut the foliation (XPL, X5)

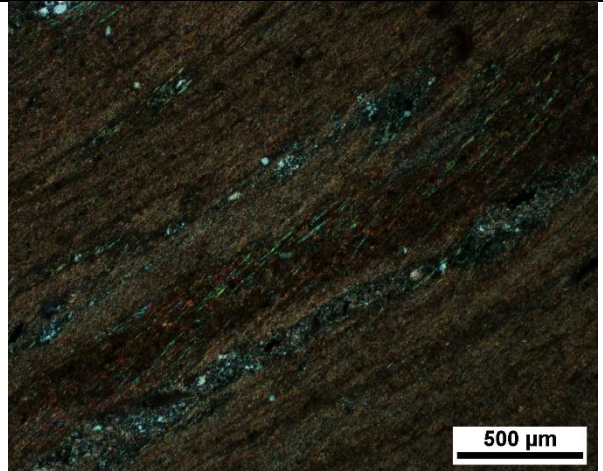


Figure 2. fine microcrystalline quartz-carbonate along with the foliation (XPL, X5)

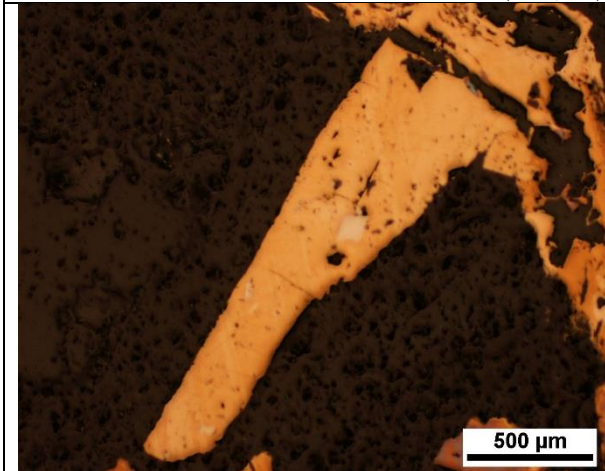


Figure 3. Euhedral arsenopyrite within pyrite-fill veinlets (RL, X5)

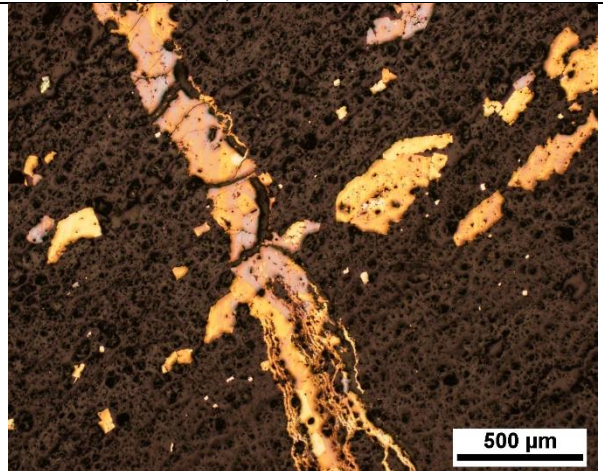


Figure 4. pyrite-fill veinlets crosscut the foliation (RL, X5)

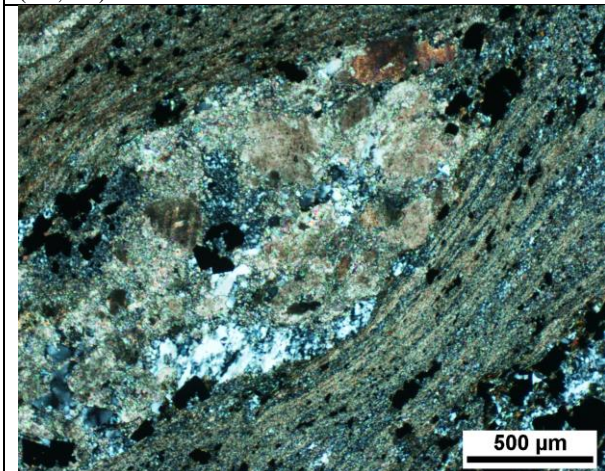
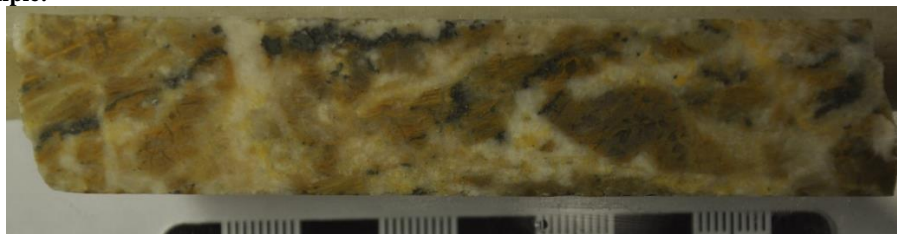


Figure 5. pressure shadow surrounding a carbonate + quartz + feldspar clast (XPL, X5)

Sample Number	1544A*	Drill Hole	TL-06-315	Depth	125.7-126.39 m
Lithology from Mining Log	Metaconglomerate	Target	AZ	Gold Grade	2.86 ppm

Drill Core Sample:



Sample Description:

Light brown brecciated metaconglomerate. There are a lot of white quartz/albite breccias (doesn't effervesce using HCl) filled within the fractures and mauve clasts (carbonate?) in veins. Sulphides occur in veins, fractures, and inside mauve clasts. Sulphides are mainly arsenopyrite and a few pyrite grains.

Offcut & Thin Section:



Thin Section Description:

- Minerals and Modal Percentage: Muscovite/sericite 40%, quartz 20%, carbonate 15%, plagioclase 10%, pyroxene 5%, K-feldspar 5%, arsenopyrite 4%, pyrite 1%, trace gold.
- Texture: Intense foliated texture with massive veins. The primary host rock matrix is typical porphyritic texture formed by very fine to ultra fine-grained feldspar + quartz + sericite/muscovite. There is a thick muscovite-dominate vein along with the foliation in the middle of the thin section. In this thick vein, pyroxene grains show light pink pleochroism under plane-polarized light and high interference colors under cross-polarized light. And muscovite exhibits pressure shadow surrounding the coarse-grained euhedral arsenopyrite grains. There are also some recrystallized quartz fine veins and carbonate veins in this thin section.
- Veining: There are three types of veins along with the foliation: 1) a thick muscovite-dominate vein along with the foliation in the middle of the thin section with coarse-grained euhedral arsenopyrite grains inside. 2) recrystallized quartz fine veins without sulphides; 3) folded and boudinaged carbonate veins with very corroded and fractured arsenopyrite.
- Alteration: pervasive sericitization in the primary host rock matrix and recrystallized muscovite in the thick vein. Carbonate alteration in the veins.
- Ore Mineralogy: coarse-grained, euhedral to subhedral or needle-shaped, fractured arsenopyrite occurs within the thick sericite vein. Pyrite are finer and less common than arsenopyrite. Free gold occurs between coarse-grained euhedral arsenopyrite grains. No inclusion gold has been found in the thin section.

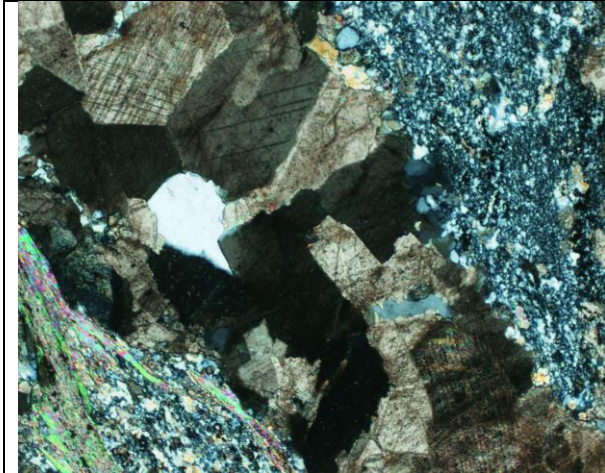


Figure 1. Carbonate vein and muscovite along with the vein (XPL, X5)

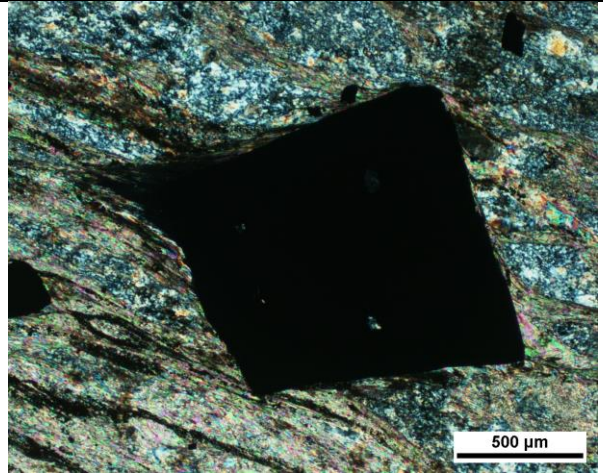


Figure 2. Muscovite foliation around a coarse-grained euhedral arsenopyrite grain (XPL, X5)

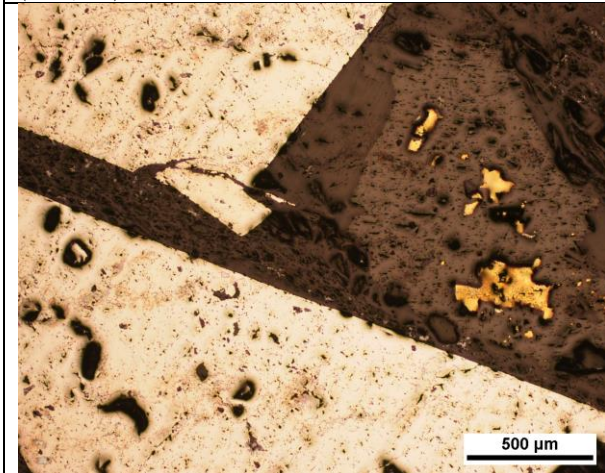


Figure 3. Free gold between coarse-grained needle-shaped arsenopyrite grains (RL, X5)

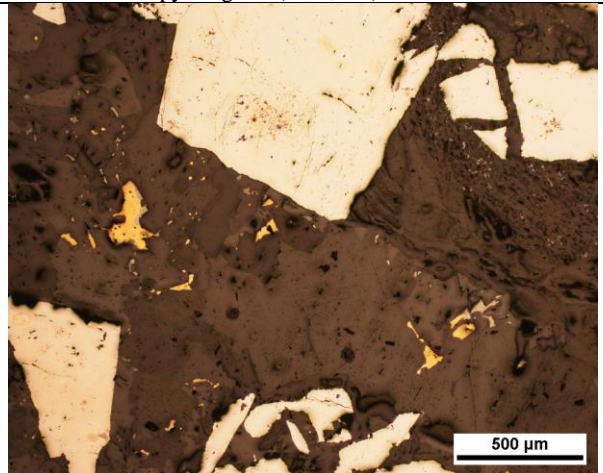


Figure 4. Free gold between coarse-grained euhedral arsenopyrite grains (RL, X5)

Sample Number	2827	Drill Hole	TL-15-564	Depth	183-183.23 m
Lithology from Mining Log	QFP	Target	TLW	Gold Grade	close to 9 - ~0.6

Drill Core Sample:



Sample Description:

Yellowish green porphyritic dacite (called intermediate-felsic intrusive: Quartz-Feldspar Porphyry in mining log). There are two parallel sulphide (mainly arsenopyrite) + quartz veins. Arsenopyrite are medium to coarse-grained and euhedral to subhedral.

Offcut & Thin Section:



Thin Section Description:

- Minerals and Modal Percentage: plagioclase/albite 30%, quartz 30%, muscovite/sericite 20%, K-feldspar 15%, arsenopyrite 4%, pyrite 1%, trace sphalerite, trace gold.
- Texture: Typical porphyritic texture. The groundmass is very fine to ultra fine-grained feldspar + quartz + sericite/muscovite. The phenocrysts are albite (~0.5 mm) with albite twinning, plagioclase (0.5-1 mm) with polysynthetic twinning, and K-feldspar with Carlsbad twinning. All phenocrysts are strongly fractured and partly altered into sericite.
- Veining: There is a 1 mm quartz-sulphide vein crosscut the thin section and a few quartz fine veins. Quartz are all recrystallized into very fine-grained. Sulphides are disseminated on the edge of the vein and a few chucks are filled in the veins as well.
- Alteration: Sericitization is massive in the groundmass and filled in the fractures of phenocrysts and sulphides. Carbonate alteration is less common than sericitization, occurring surrounding the vein.
- Ore Mineralogy: Arsenopyrite is the major sulphide. In the thick quartz vein, arsenopyrite is coarse-grained and fractured chucks in the middle and fine-grained on the edge. There are some sphalerite inclusions inside arsenopyrite. Euhedral fine-grained pyrite and anhedral sphalerite are in the fine quartz veins. No microscopic gold has been found in the thin section.

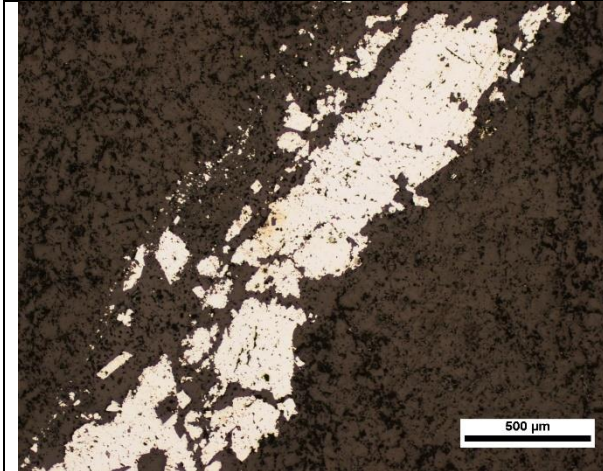


Figure 1. Coarse-grained fractured arsenopyrite in the middle of the quartz vein and fine-grained arsenopyrite on the edge of the vein (RL, X5).

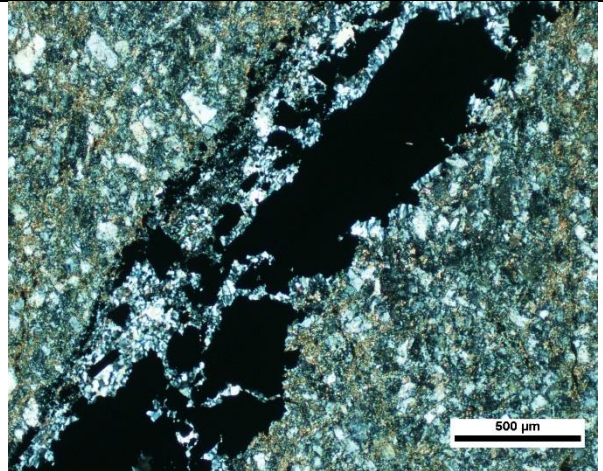


Figure 2. The groundmass is porphyritic textured with feldspar phenocrysts. Quartz is recrystallized and filled between the sulphides grains (XPL, X5)

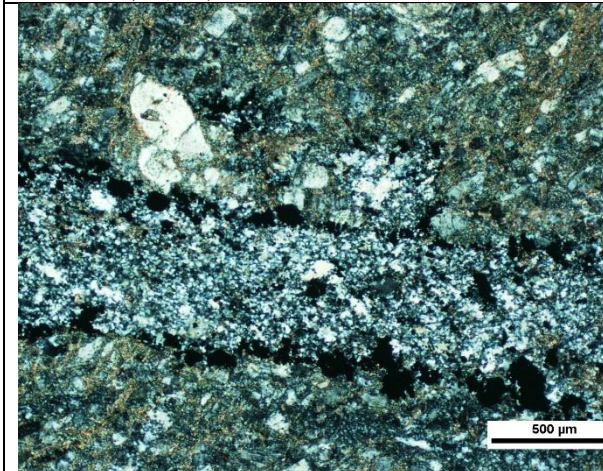


Figure 3. The groundmass is porphyritic textured with feldspar phenocrysts. Quartz is recrystallized in the vein and the fine-grained arsenopyrite grains on the edge (XPL, X5).

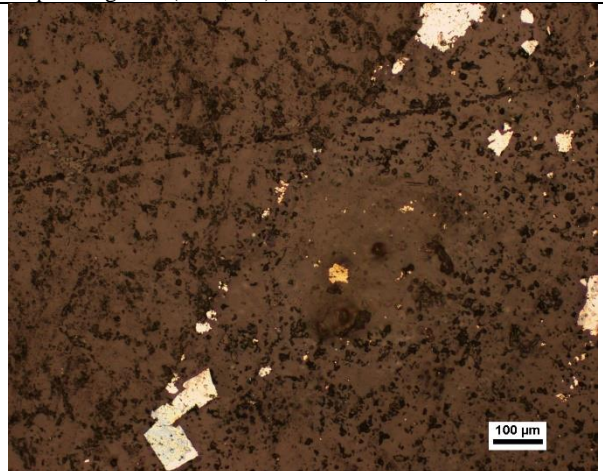


Figure 4. Disseminated euhedral pyrite and arsenopyrite in the groundmass (RL, X10)

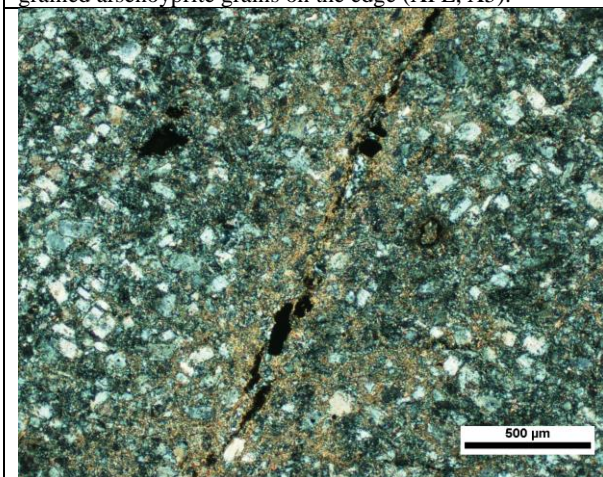


Figure 5. arsenopyrite vein crosscut the quartz + feldspar groundmass, the area next to te vein is strongly altered into sercite (XPL, X5).

Sample Number	2845	Drill Hole	TL-13-509	Depth	235.6-235.86 m
Lithology from Mining Log	QFP	Target	TLW	Gold Grade	1.13 ppm

Drill Core Sample:



Sample Description:

Light yellowish green-light pink porphyritic dacite with massive veinlets (called intermediate-felsic intrusive: Quartz-Feldspar Porphyry in mining log). In the fractures, the sericitization is more intense showing yellowish green. The other part of host rock is light pink. There are two types of fine veins (0.1-0.5 mm): carbonate veins and quartz veins. Subhedral-euhedral medium to fine-grained sulphides (pyrite and arsenopyrite) are filled in the quartz veins. Sericitization seems younger than veining.

Offcut & Thin Section:



Thin Section Description:

- Minerals and Modal Percentage: plagioclase 35%, muscovite/sericite 30%, quartz 15%, K-feldspar 10%, carbonate 3%, pyrite 3%, arsenopyrite 2%, chalcopyrite 2%, trace gold.
- Texture: Typical porphyritic texture. The groundmass is very fine to ultra fine-grained feldspar + quartz + sericite/muscovite. The phenocrysts are plagioclase (0.5-1 mm) with polysynthetic twinning, recrystallized quartz (~0.5 mm), and K-feldspar (0.5-1 mm) with Carlsbad twinning. All phenocrysts are strongly fractured and partly altered into sericite.
- Veining: There are several quartz + carbonate fine veins with disseminated sulphides inside and sericite is filled in the veins.
- Alteration: The groundmass is 45% altered into sericite and the veins is 10% altered into carbonate and 20% altered into sericite.
- Ore Mineralogy: There are three types of sulphides: arsenopyrite, pyrite, and sphalerite. Arsenopyrite in the groundmass is euhedral to subhedral, medium to fine-grained; while in the quartz-carbonate veins, arsenopyrite is coarser, more corroded and with more fractures. Pyrite and sphalerite are very fine-grained and disseminated in the thin section.

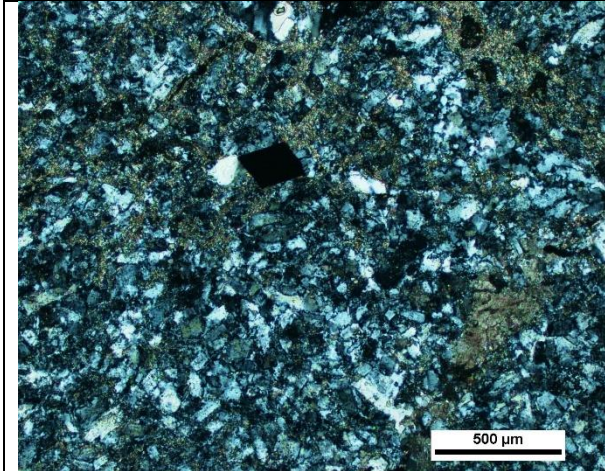


Figure 1. The groundmass is porphyritic textured with quartz and feldspar phenocrysts with sericite (XPL, X5).

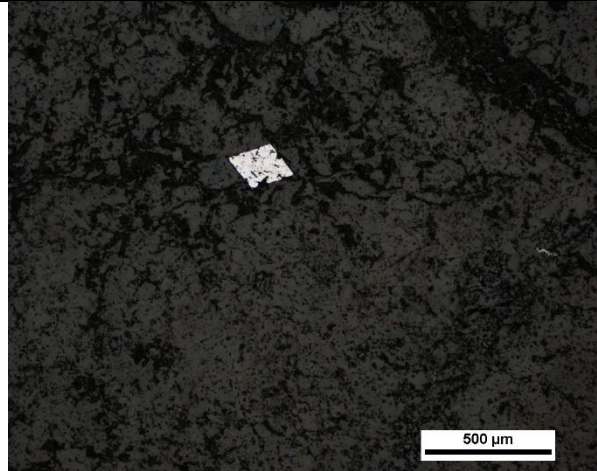


Figure 2. Fine-grained euhedral arsenopyrite in the groundmass (RL, X5).

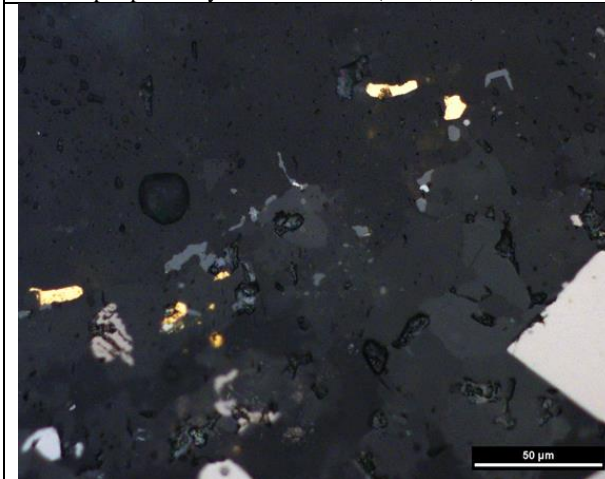


Figure 3. Free gold next to euhedral arsenopyrite and anhedral sphalerite in the groundmass (RL, X20)

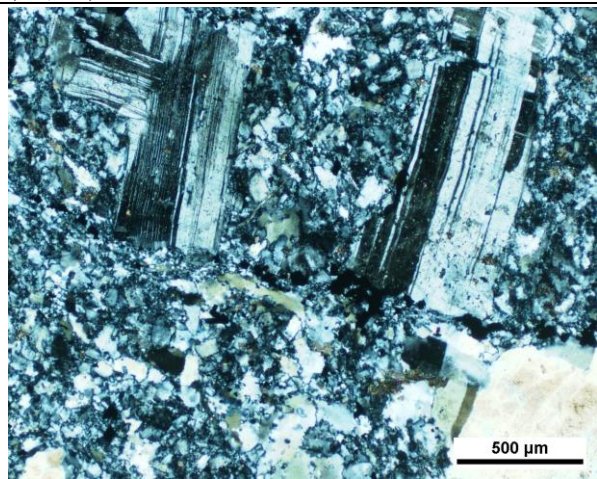


Figure 4. Coarse euhedral plagioclase phenocryst in the groundmass (XPL, X5)

Sample Number	2819	Drill Hole	TL-16-575	Depth	154.1-154.32 m
Lithology from Mining Log	FP	Target	TL	Gold Grade	7.21 ppm

Drill Core Sample:



Sample Description:

Dark grey dacite with massive veinlets (called intermediate-felsic intrusive: Feldspar Porphyry in mining log). The sample is intensely silicified and slightly fractured. Fine-grained sulphides (arsenopyrite and pyrite) are disseminated evenly in the drill core sample. The veins are very fine with the dark grey color (smoky quartz). The sample has little sericitization.

Offcut & Thin Section:



Thin Section Description:

- Minerals and Modal Percentage: K-feldspar 40%, quartz 20%, muscovite/sericite 15%, plagioclase 10%, carbonate 5%, arsenopyrite 5%, pyrite 3%, sphalerite 2%, chalcopyrite trace, no gold.
- Texture: porphyritic texture with fine quartz veins. The groundmass is very fine to ultra fine-grained feldspar + quartz + sericite/muscovite. K-feldspar is fine grained, 20-50um in groundmass. Some parts altered into sericite, have decussate texture within feldspar-dominant groundmass with sericitization throughout. Quartz is fine grained (20-100um) in quartz veins, anhedral, clear white under PPL, and undulatory extinction under XPL. Plagioclase is fine-medium grained, 50-100um, anhedral in groundmass, has polysynthetic twin under XPL. Carbonate (calcite), ~200um, fine-medium grained, dark brown under PPL, dark yellow interference color under XPL.
- Veining: fine quartz-carbonate veinlets (<0.5 mm) with disseminated sulphides grains. Quartz in the veins are recrystallized into very fine grains.
- Alteration: Sericite recrystallized in the fractures of quartz veins; and some K-feldspar in groundmass altered into sericite.
- Ore Mineralogy: Several kinds of sulphides have been found in this thin section: arsenopyrite, sphalerite, pyrite and chalcopyrite. Arsenopyrite is the major type of sulphide has 3 types: 1) Euhedral-subhedral, fine-medium grained, 20-100um in groundmass, square, diamond, triangle and needle, the surface is flat and uncorroded; 2) Subhedral, ~50um, corroded on the edge and still kept the previous shape (needle and triangle), a few are with sieve-textured; 3) Fine-grained, euhedral-subhedral, 20-50 um disseminated arsenopyrite in matrix and in the fractures. Pyrite is fine-medium grained, 10-100um, subhedral- anhedral, disseminated in groundmass. Sphalerite is anhedral, fine grained, 10-50um, boudinaged and disseminated in groundmass. Chalcopyrite is fine grained, 50um, anhedral, sieve texture, appeared with arsenopyrite. There are a couple of sulphide combinations: arsenopyrite + sphalerite, arsenopyrite + pyrite, arsenopyrite + chalcopyrite, and arsenopyrite + pyrite + sphalerite. No microscopic gold has been found in this section.

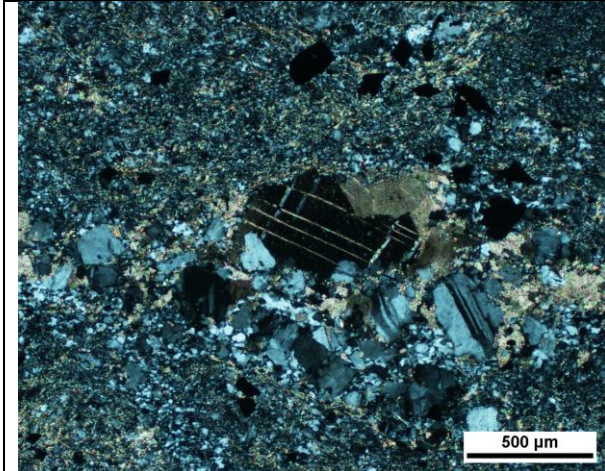


Figure 1. The groundmass is porphyritic textured with plagioclase and carbonate phenocrysts (XPL, X5).

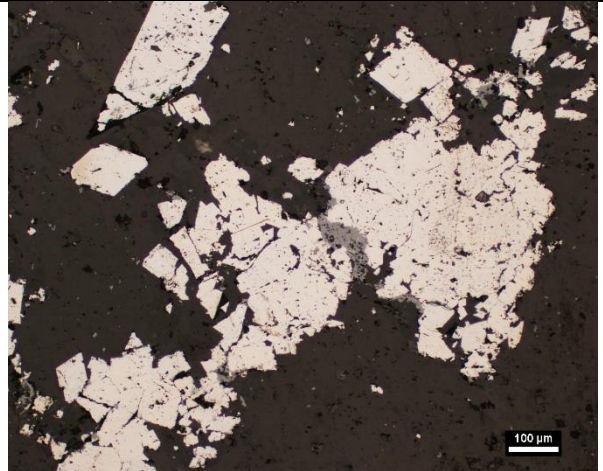


Figure 2. Coarse-grained fractured and corroded arsenopyrite grains with sphalerite filled (RL, X10)

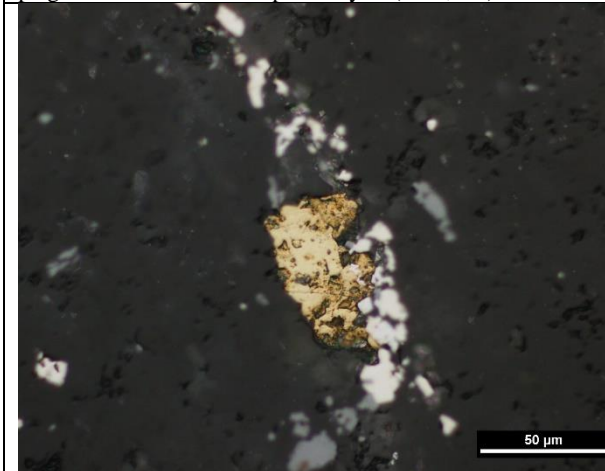


Figure 3. Fine-grained chalcopyrite and arsenopyrite disseminated in the groundmass (RL, X20)

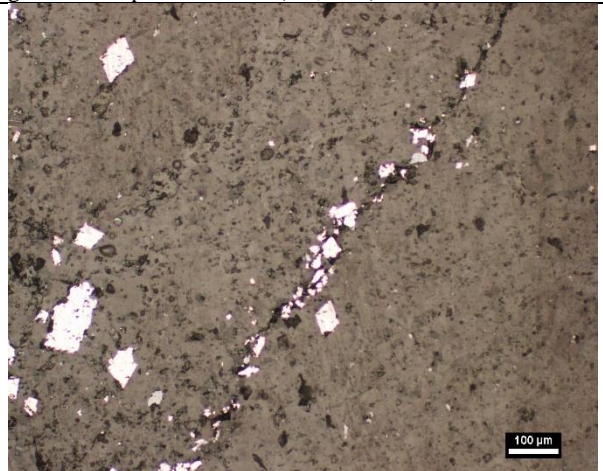


Figure 4. Fine-grained arsenopyrite filled in the fracture and disseminated in the groundmass (RL, X10)

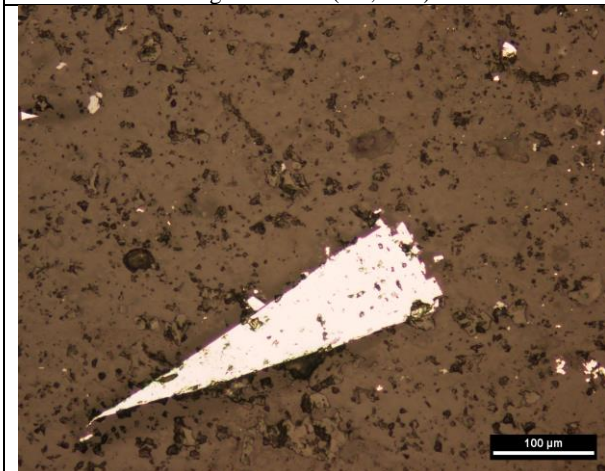


Figure 5. Needle arsenopyrite in the groundmass (RL, X10)

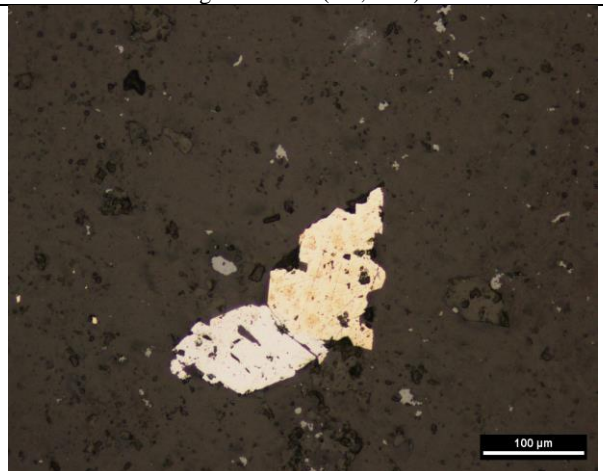
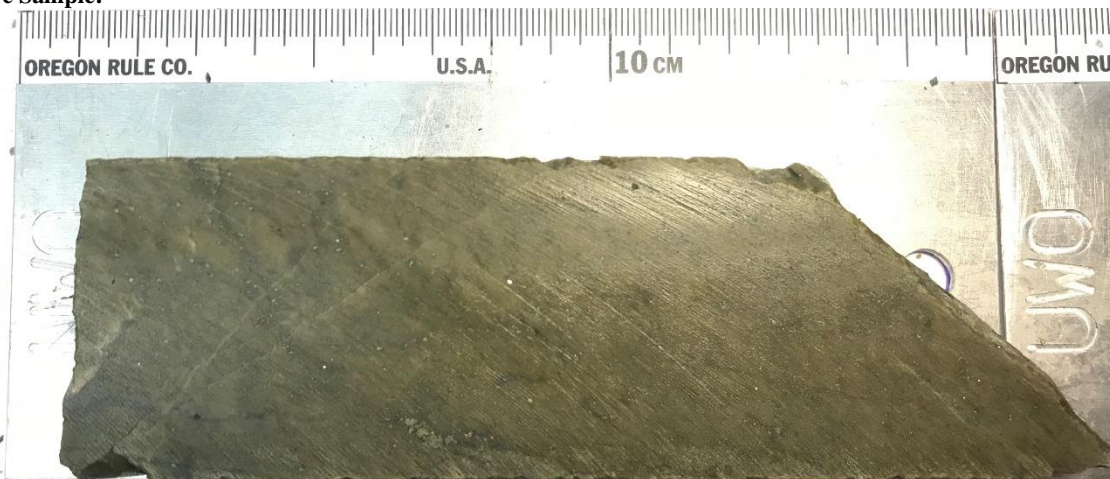


Figure 6. A combination of pyrite +arsenopyrite in the groundmass (RL, X10)

Sample Number	2824	Drill Hole	TL-15-568	Depth	200.62-200.82 m
Lithology from Mining Log	FP	Target	TLW	Gold Grade	1.91- ~8.25 ppm

Drill Core Sample:



Sample Description:

Light yellowish green dacite (called intermediate-felsic intrusive: Feldspar Porphyry in mining log). The sample has an intense sericitization. Sample has fractures and some quartz veining. From the inside to the outside of veins, the color changed from dark grey (sulphides)-light grey (smoky quartz)-yellowish green (sericitization). Ore minerals occurs within veins and also disseminated all smaller than 1 mm. Pyrite is euhedral to subhedral medium-grained. Subhedral arsenopyrite is fine-grained and disseminated. Subhedral chalcopyrite were also observed but were less common. The discontinuity of veining system shows a brittle system.

Offcut & Thin Section:



Thin Section Description:

- Minerals and Modal Percentage: plagioclase 30%, K-feldspar 20%, quartz 15%, carbonate 15%, muscovite/sericite 15%, arsenopyrite 3%, pyrite 2%, trace sphalerite, trace chalcopyrite.
- Texture: Typical porphyritic texture. The groundmass is very fine to ultra fine-grained feldspar + quartz + sericite/muscovite. The phenocrysts are plagioclase (0.5-1 mm) with polysynthetic twinning, recrystallized quartz (~0.5 mm), and K-feldspar (0.5-1 mm) with Carlsbad twinning. All phenocrysts are strongly fractured and partly altered into sericite.
- Veining: there are two types of veins: quartz + albite + carbonate veins and sericite veins. In the quartz + albite + carbonate veins, euhedral sulphide grains (mostly arsenopyrite) are disseminated inside and quartz recrystallized surrounding sulphides as very fine grains. The sericite veins are much finer than the quartz + albite + carbonate vein and discontinuous, which illustrates a brittle system. The sericite vein crosscut the quartz + albite + carbonate vein, thus, sericitization is younger.
- Alteration: The quartz vein is 30% altered into carbonate as coarse to medium grains. Sericitization is pervasive and slightly foliated in the groundmass.
- Ore Mineralogy: There are three types of sulphides: arsenopyrite, pyrite, and sphalerite. Arsenopyrite is the major type of sulphides: 1) Euhedral-subhedral, medium grained, corroded, some with needle and sieve texture; 2) fine-grained, subhedral to anhedral, disseminated in the quartz veins and groundmass. Pyrite is generally medium-grained, more corroded and more sieve-textured than arsenopyrite. A few medium-grained pyrite has some sphalerite inclusions inside. The combination of arsenopyrite and pyrite occurs locally. No microscopic gold has been found in this section.

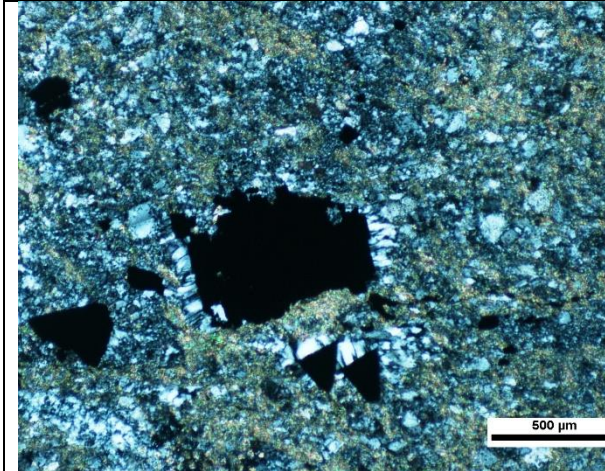


Figure 1. Medium-grained subhedral sieved textured arsenopyrite and quartz strain fringes recrystallized surrounding arsenopyrite grains (XPL, X5).

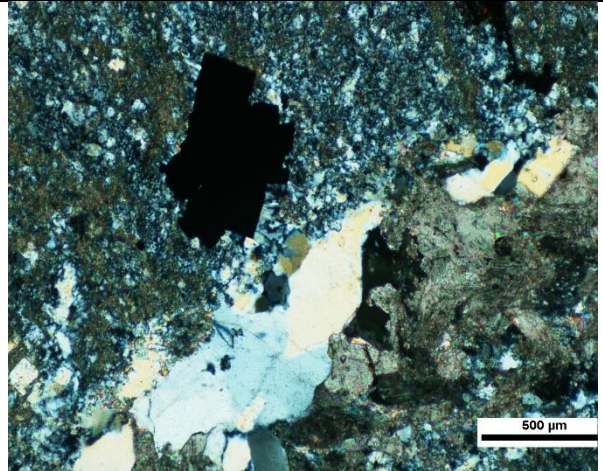


Figure 2. Carbonate (calcite) and albite phenocrysts and subhedral arsenopyrite inside Feldspar + quartz + sericite/muscovite groundmass (XPL, X5).



Figure 3. Corroded subhedral arsenopyrite with sphalerite inclusions in the pit sand fractures (RL, X10).

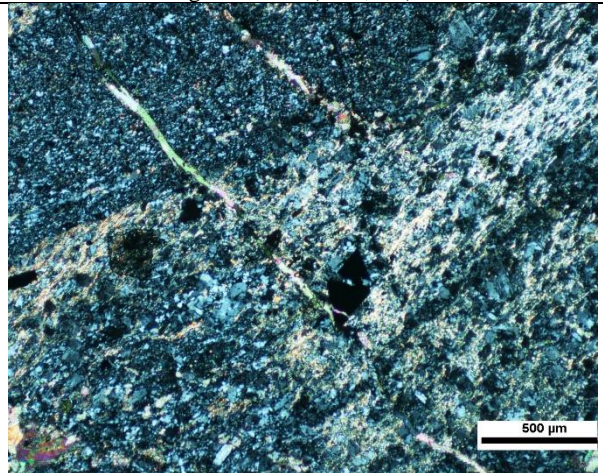


Figure 4. Needle arsenopyrite in the quartz vein and the discontinuous very fine sericite vein crosscut the quartz veins (XPL, X5)



Figure 5. Fractured subhedral arsenopyrite in the groundmass (RL, X10).

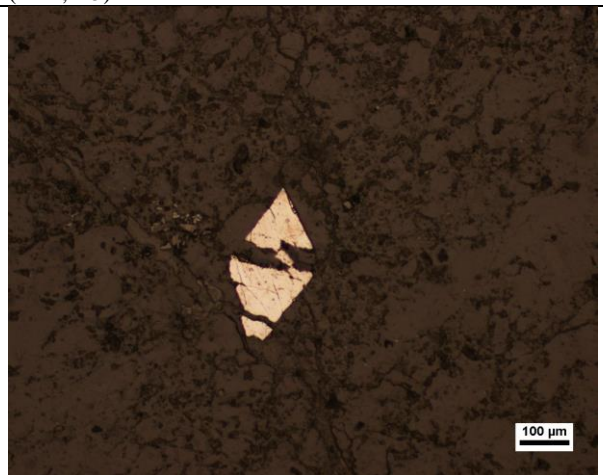


Figure 6. Needle arsenopyrite in the quartz vein (XPL, X10)

Sample Number	2841	Drill Hole	TL-13-504	Depth	190.5-190.78 m
Lithology from Mining Log	FP	Target	TLW	Gold Grade	25.2 ppm

Drill Core Sample:



Sample Description:

Mauve green dacite (called intermediate-felsic intrusive: Feldspar Porphyry in mining log). There are pervasive veinlets throughout the sample. Most of veins are folded and affected by fractures and faults which shows a brittle system. Sericitization is not strong. Pyrite and arsenopyrite are filled in veins and fractures.

Offcut & Thin Section:



Thin Section Description:

- Minerals and Modal Percentage: plagioclase 35%, K-feldspar 20%, quartz 15%, carbonate 10%, muscovite/sericite 10%, chlorite 5%, arsenopyrite 3%, pyrite 2%, trace sphalerite, trace chalcopyrite.
- Texture: Typical porphyritic texture with pervasive veinlets. The groundmass is very fine to ultra fine-grained feldspar + quartz + sericite/muscovite. The phenocrysts are plagioclase (0.5-1 mm) with polysynthetic twinning, recrystallized quartz (~0.5 mm), calcite with twinning planes, and K-feldspar (0.5-1 mm) with Carlsbad twinning. All phenocrysts are strongly fractured and partly altered into sericite.
- Veining: There are massive fine veinlets in this thin section. Most veins are recrystallized quartz veins. A few veins are strongly folded sulphide fine veins and crosscut the quartz veins. Recrystallized quartz and sericite are filled between the sulphide grained.
- Alteration: The sericitization (30%) is mainly in the groundmass and in the veins. Chlorite alteration (10%) is in the groundmass. And carbonate is as phenocrysts (10%).
- Ore Mineralogy: There are three types of sulphide distribution: 1) fine-grained euhedral to subhedral arsenopyrite filled in folded veins; 2) medium to fine-grained anhedral to euhedral corroded arsenopyrite filled with the fractures and surrounding the coarse grained plagioclase phenocrysts; 3) disseminated fine to medium grained subehedral to anhedral pyrite, arsenopyrite, and sphalerite in the groundmass. No microscopic gold has been found in this section.

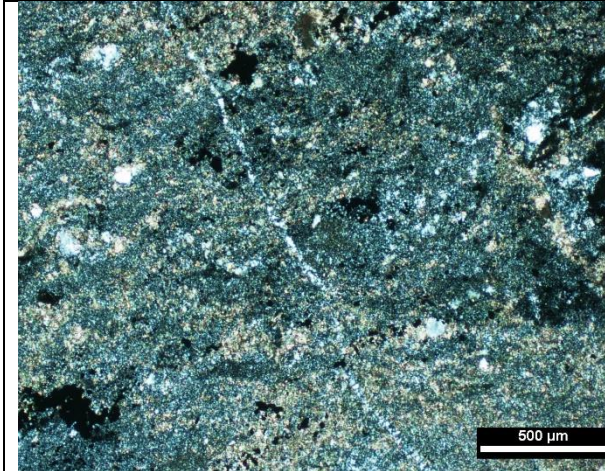


Figure 1. Fine recrystallized quartz vein with micro fault in the feldspar + quartz + sericite/muscovite groundmass (XPL, X5)

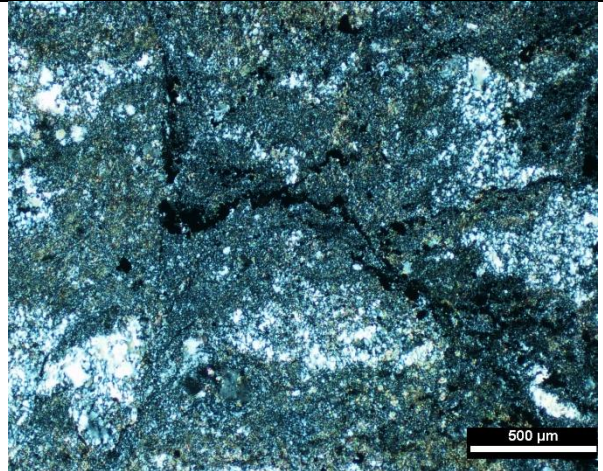


Figure 2. Folded arsenopyrite vein within the feldspar + quartz + sericite/muscovite groundmass and with the recrystallized quartz+ feldspar phenocrysts (XPL, X5)

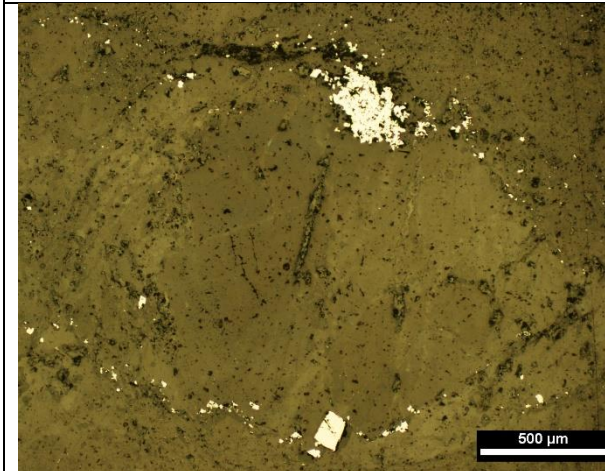


Figure 3. Corroded medium-grained and euhedral medium to fine-grained arsenopyrite surrounding the plagioclase phenocrysts (RL, 5X).

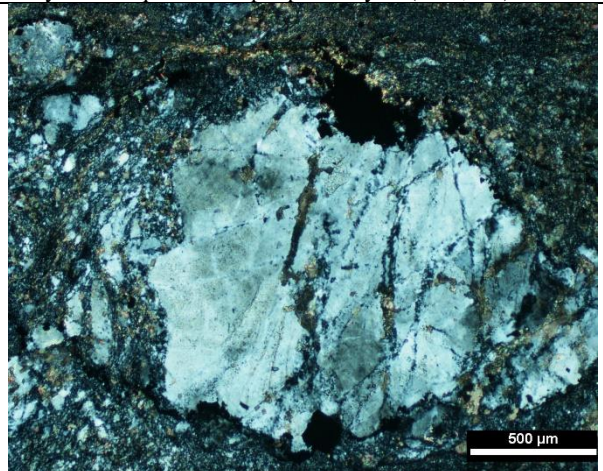


Figure 4. A strongly fractures coarse-grained plagioclase phenocrysts with sericite and feldspar filled in the fractures and arsenopyrite surrounded.

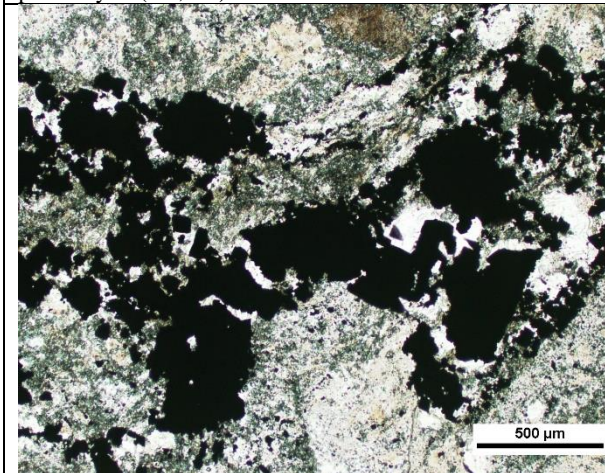


Figure 5. Fractured subhedral coarse-grained arsenopyrite in the quartz vein with chlorite and carbonate alteration in the groundmass. Quartz recrystallized surrounding the sulphides grains (PPL, X5).

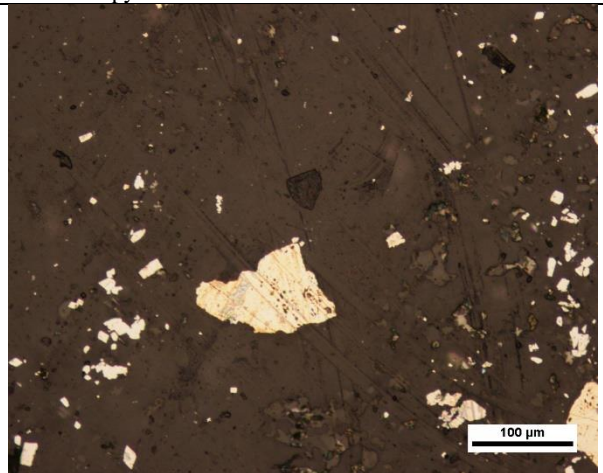


Figure 6. Anhedral medium-grained pyrite and euhedral to subhedral fine-grained arsenopyrite in the groundmass (RL, X10).

Sample Number	2853	Drill Hole	TL-16-604A	Depth	643.96-644.24 m
Lithology from Mining Log	PF	Target	TL	Gold Grade	7.73 ppm

Drill Core Sample:



Sample Description:

Dark grey dacite (called intermediate-felsic intrusive: Feldspar Porphyry in mining log). There are two types of veins in this core sample: smoky quartz vein and orange carbonate (ankerite + scheelite) vein. The carbonate vein reflects orange under UV light. Euhedral arsenopyrite crystals occur with the pyrite crystals close to the smoky quartz intrusions. Euhedral pyrite crystals occur disseminated on the sample. Euhedral arsenopyrite crystals occur with the pyrite crystals close to the smoky quartz intrusions.

Offcut & Thin Section:



Thin Section Description:

- Minerals and Modal Percentage: plagioclase 30%, K-feldspar 20%, quartz 15%, carbonate 15%, muscovite/sericite 15%, arsenopyrite 3%, pyrite 2%, trace sphalerite, trace chalcopyrite.
- Texture: Typical porphyritic texture. The groundmass is very fine to ultra fine-grained feldspar + quartz + sericite/muscovite. The phenocrysts are plagioclase (0.5-2 mm) with polysynthetic twinning, recrystallized quartz (~0.5 mm), and K-feldspar (0.5-1 mm) with Carlsbad twinning. All phenocrysts are strongly fractured and partly altered into sericite.
- Veining: There are two types of veins: carbonate veins and quartz veins. Carbonate veins are more and thicker than quartz veins and host sulphides. These two types of veins are strong recrystallized and partly altered into sericite.
- Alteration: The alteration is composed of 60% sericitization and 40% carbonate alteration. Carbonate alteration is mainly in the veins and as pervasive alteration. Sericite is very fine grained in the plagioclase fractures and groundmass.
- Ore Mineralogy: Arsenopyrite (0.1-0.2mm) euhedral is not corroded, some have needle shapes. Pyrite (0.05-0.5 mm) is corroded and anhedral with variable sizes. Sphalerite (0.1-0.3 mm) is anhedral, corroded, strongly altered usually related with the pyrite grains. No microscopic gold has been found in this section.

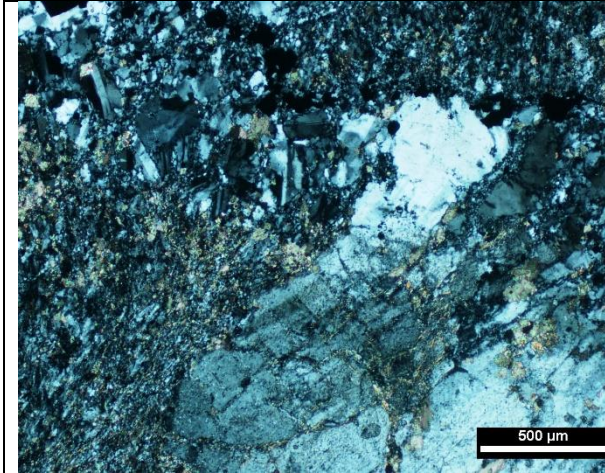


Figure 1. Strongly fractures coarse-grained plagioclase phenocrysts with sericite and feldspar filled in the fractures and arsenopyrite surrounded (XPL, X5).

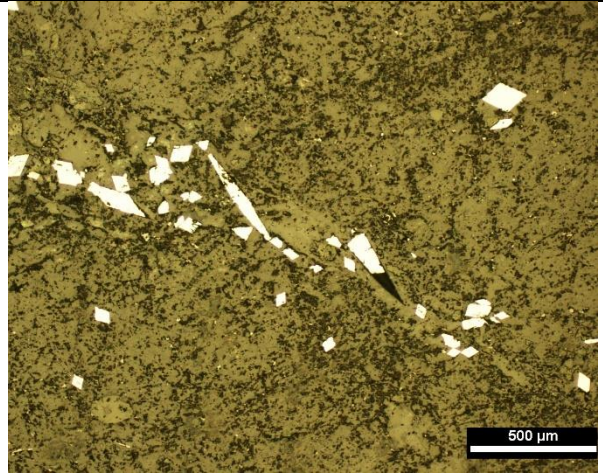


Figure 2. Euhedral to subhedral fine-grained arsenopyrite in the quartz vein with chlorite and carbonate alteration in the groundmass. Quartz recrystallized surrounding the sulphides grains (RL, X5).

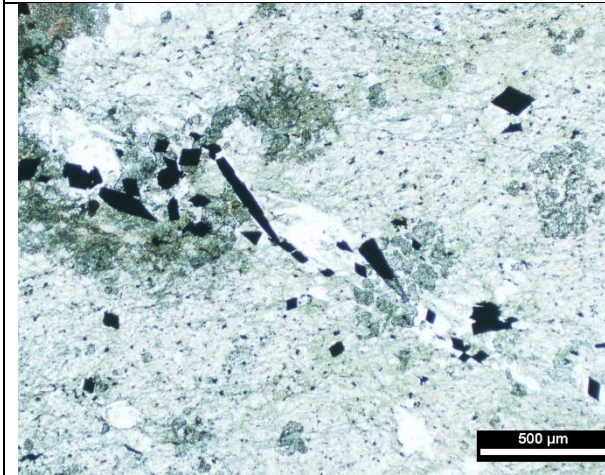


Figure 3. Euhedral to subhedral fine-grained arsenopyrite in the quartz vein with chlorite and carbonate alteration in the groundmass. Quartz recrystallized surrounding the sulphides grains (PPL, X5).

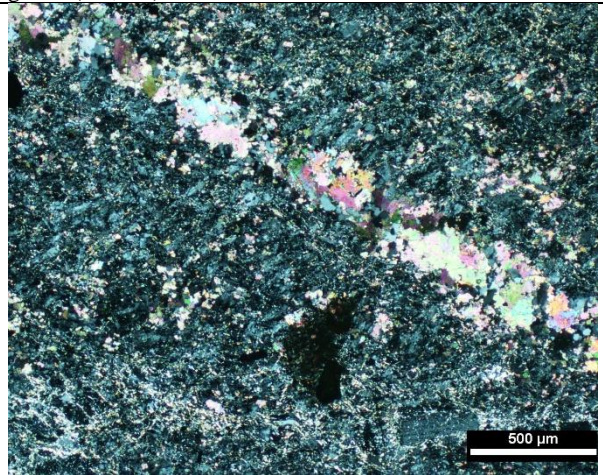


Figure 4. Recrystallized carbonate vein in the fine-grained feldspar + quartz + sericite/muscovite groundmass (XPL, X5).

Sample Number	2857	Drill Hole	TL-16-575	Depth	718.4-716.66 m
Lithology from Mining Log	PF	Target	TL	Gold Grade	2.16 ppm

Drill Core Sample:



Sample Description:

Foliated dark gray dacite with intense light gray quartz veins (called intermediate-felsic intrusive: Feldspar Porphyry in mining log). The quartz veins are varied in size, shape and direction. Calcite is included in the center of the some of the thicker veins. The sulphide specs disseminated throughout sample. Not much sericitization can be seen in the hand sample.

Offcut & Thin Section:



Thin Section Description:

- Minerals and Modal Percentage: plagioclase 30%, K-feldspar 15%, quartz 15%, carbonate 15%, muscovite/sericite 10%, arsenopyrite 3%, pyrite 2%.
- Texture: Typical porphyritic texture. The groundmass is very fine to ultra fine-grained feldspar + quartz + sericite/muscovite. The phenocrysts are plagioclase (mainly albite, 0.5-1 mm) with polysynthetic twinning, recrystallized quartz (~0.5 mm), and K-feldspar (0.5-1 mm) with Carlsbad twinning. All phenocrysts are strongly fractured and partly altered into sericite.
- Veining: Veins are crosscutting each other. Most veins are quartz veins, and a few are carbonate veins. The thickest vein (~0.4mm) in the thin section is also the youngest vein with the recrystallization of quartz. The primary vein is <500 µm and partly altered into sericite.
- Alteration: The sample is strongly altered (~50%). Very fine to fine grained sericite has been observed in groundmass, in the fracture of feldspar phenocrysts, and fine quartz veins. The sericitization is a little oriented and along with the foliation. The carbonate alteration occurs in carbonate veins.
- Ore Mineralogy: There are two types of sulphides in this thin section, arsenopyrite and pyrite. Arsenopyrite > pyrite. Arsenopyrite is mostly fine-grained, euhedral to subhedral, needle/cube shaped, and disseminated in the groundmass and also in the fine quartz veins. Pyrite is coarser, more corroded and fracture than arsenopyrite. No microscopic gold has been found in this section.

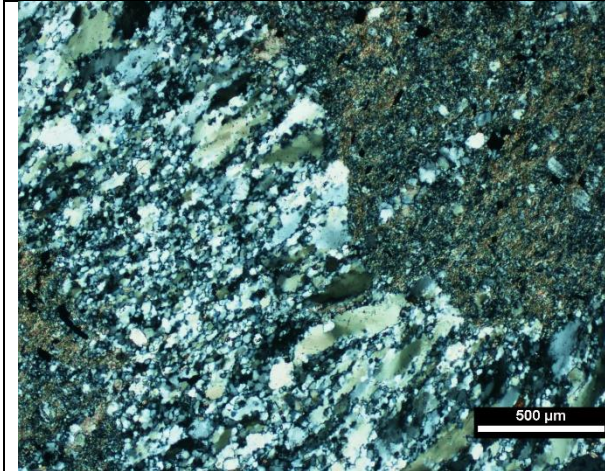


Figure 1. Quartz and feldspar recrystallized in the quartz vein (XPL, X5)

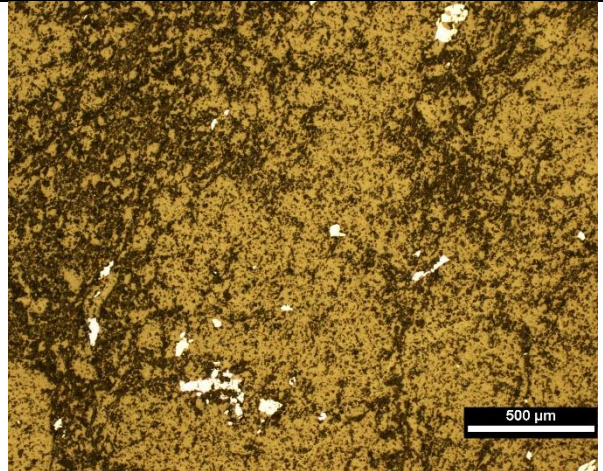


Figure 2. Disseminated fine-grained arsenopyrite in the groundmass (RL, X5)

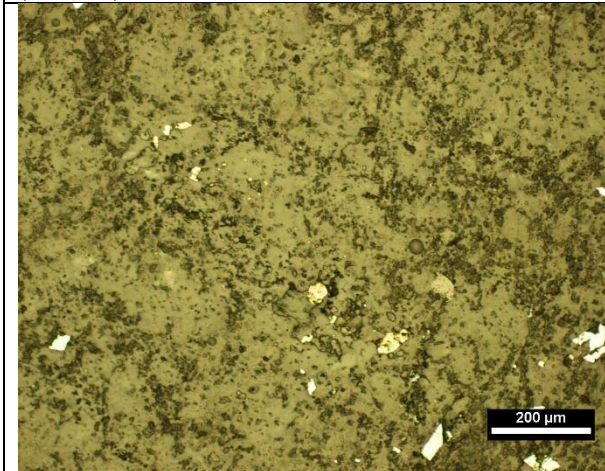


Figure 3. Disseminated fine-grained arsenopyrite and pyrite in the groundmass (RL, X5)

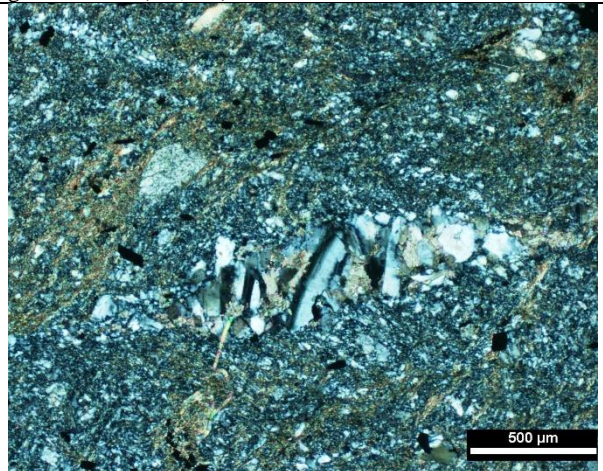


Figure 4. Plagioclase phenocrysts in the feldspar + quartz + sericite/muscovite groundmass (XPL, X5)

Sample Number	1511*	Drill Hole	TL-16-587	Depth	252.6-253.4 m
Lithology from Mining Log	PF	Target	TL	Gold Grade	2.289 ppm

Drill Core Sample:



Sample Description:

Foliated dark grey dacite with intense silicification (light-grey colored) and yellowish-green sericitization (called intermediate-felsic intrusive: Feldspar Porphyry in mining log). Yellowish-green sericitization occurs in the shear band between silicification. Fine-grained pyrite and arsenopyrite are throughout the thin section, especially in the fine quartz veins.

Offcut & Thin Section:



Thin Section Description:

- Minerals and Modal Percentage: plagioclase 20%, K-feldspar 20%, quartz 15%, carbonate 15%, muscovite/sericite 15%, chlorite 10%, arsenopyrite 3%, pyrite 2%, trace sphalerite, trace chalcopyrite.
- Texture: Typical porphyritic texture. The groundmass is very fine to ultra fine-grained feldspar + quartz + sericite/muscovite. The phenocrysts are plagioclase (0.5-1 mm) with polysynthetic twinning, recrystallized quartz (~0.5 mm), and K-feldspar (0.5-1 mm) with Carlsbad twinning. Feldspar phenocrysts are strongly fractured with sericite filled in the fractures.
- Veining: There are three types of veins: 1) feldspar + carbonate vein is the thickest vein in the middle of the in section. Fine-grained quartz recrystallized in the fractures of this vein. 2) Sericite fine veins is along with the foliation. 3) quartz veins with pyrite and arsenopyrite filled inside. Muscovite are recrystallized on the outside of this type of veins.
- Alteration: Carbonate alteration are in the feldspar + carbonate vein and also in the groundmass. Chlorite alteration can be seen as green-colored cryptocrystalline under plan-polarized light. Sericitization is the major type of alteration, occurring in veins, fractures, and along with the foliation. Muscovite are recrystallized on the outside of quartz veins and surrounding feldspar phenocrysts.
- Ore Mineralogy: Fine-grained euhedral to anhedral pyrite and arsenopyrite are disseminated in the groundmass and in quartz veins. Free gold grain near pcorroded anhedral pyrite and arsenopyrite grains within feldspar + quartz + sericite/muscovite groundmass.

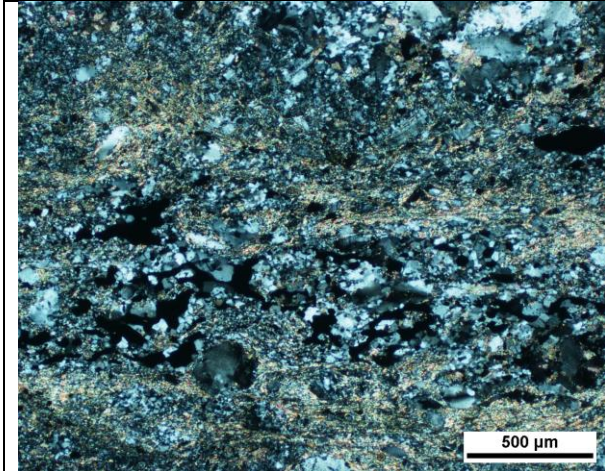


Figure 1. quartz veins with pyrite and arsenopyrite filled inside. Muscovite are recrystallized on the outside of the vein.

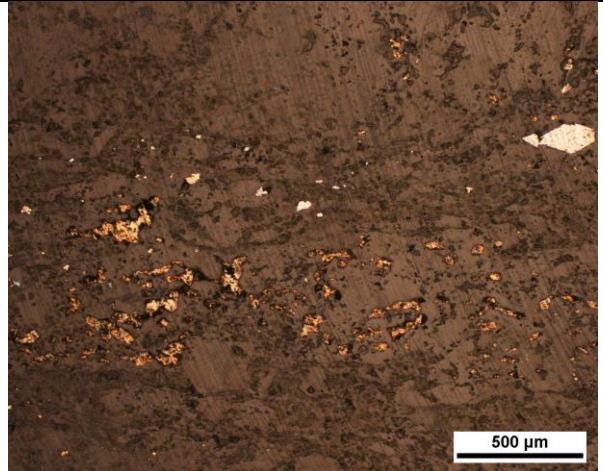


Figure 2. pyrite and arsenopyrite filled in the quartz veins (RL, X5)

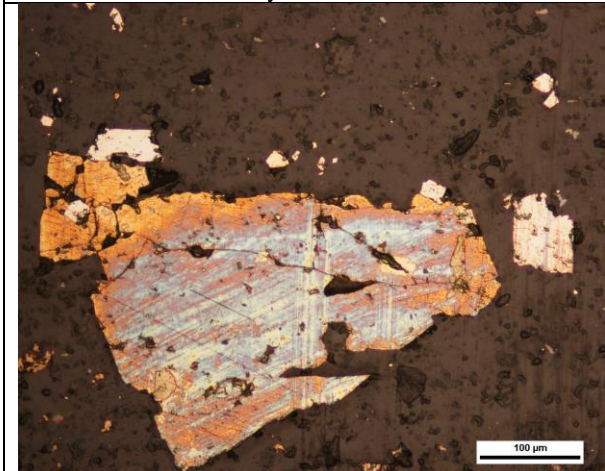


Figure 3. Inclusion gold and euhedral arsenopyrite inside needle-shaped corroded pyrite (RL, X5)

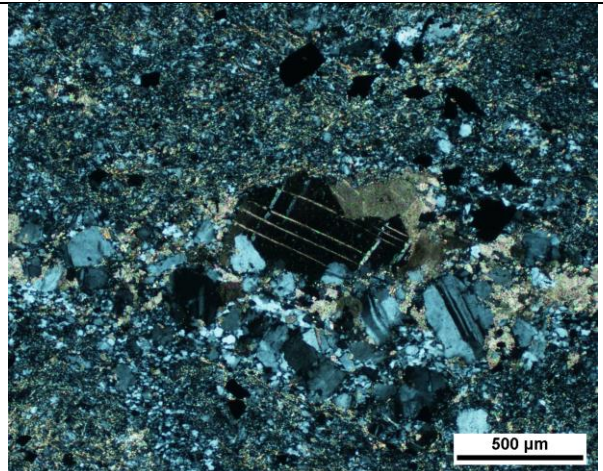


Figure 4. quartz recrystallized in the carbonate +quartz vein (XPL, X5)

Sample Number	1514B*	Drill Hole	TL-14-523	Depth	105.42-106 m
Lithology from Mining Log	PF	Target	TL	Gold Grade	5.702 ppm

Drill Core Sample:



Sample Description:

Dark grey to yellowish green dacite with massive breccias and foliation (called intermediate-felsic intrusive: Feldspar Porphyry in mining log). The area with intense sericitization is light yellowish green. Breccias are mainly altered, but there are also some non-altered ones and the center of large breccias. There is a large smoky quartz vein in the middle of the hand sample. The contact zone of the large smoky quartz vein with the host rock is white (feldspar and quartz?). A lot of dark quartz veinlets are throughout the sample. The dark grey area has fine-grained arsenopyrite and pyrite inside, while no sulphide grains has been observed in the light yellowish green area.

Offcut & Thin Section:



Thin Section Description:

- Minerals and Modal Percentage: quartz 30%, plagioclase 20%, K-feldspar 15%, carbonate 15%, muscovite/sericite 15%, arsenopyrite 3%, pyrite 2%, trace sphalerite, trace chalcopyrite.
- Texture: Typical porphyritic texture with intense foliation. Aligned arsenopyrite grains and banded quartz-muscovite consist of the foliation. The groundmass is very fine to ultra fine-grained feldspar + quartz + sericite/muscovite. The phenocrysts are plagioclase (0.5-1 mm) with polysynthetic twinning, recrystallized quartz (~0.5 mm), and K-feldspar (0.5-1 mm) with Carlsbad twinning. All phenocrysts are strongly fractured and partly altered into sericite. Quartz pressure shadows are commonly observed around boudinaged arsenopyrite grains.
- Veining: albite + sericite + quartz vein along with the foliation.
- Alteration: Pervasive sericitization and carbonate alteration.
- Ore Mineralogy: Arsenopyrite are mainly medium-grained, euhedral, corroded and fractured, disseminated and/or boudinaged in the groundmass. Pyrite are fine to coarse-grained, anhedral, more corroded and fractured. No microscopic gold has been found in this section.

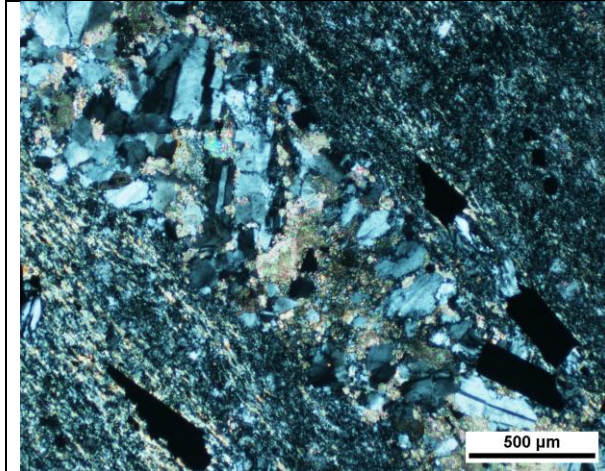


Figure 1. carbonate + quartz +feldpar vein along with the foliation (XPL, X5).

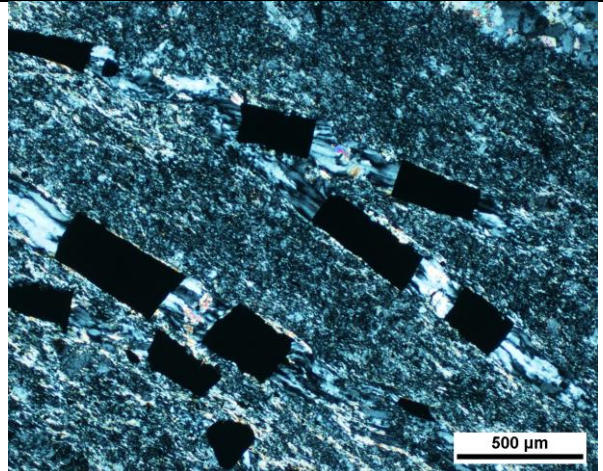


Figure 2. Quartz pressure shadows around boudinaged arsenopyrite grains (XPL, X5).

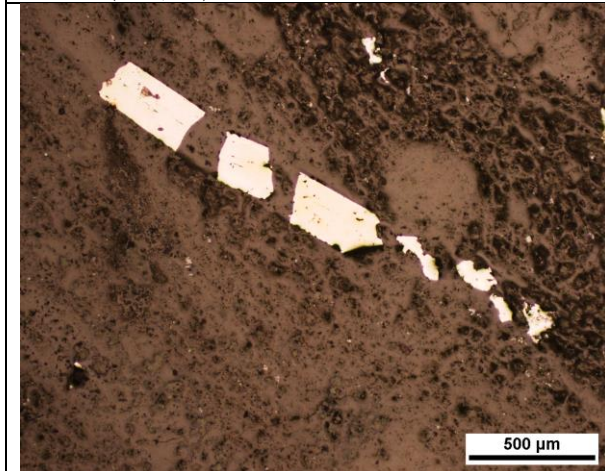


Figure 3. boudinaged arsenopyrite grains near albite + sericite + quartz vein (RL, X5).

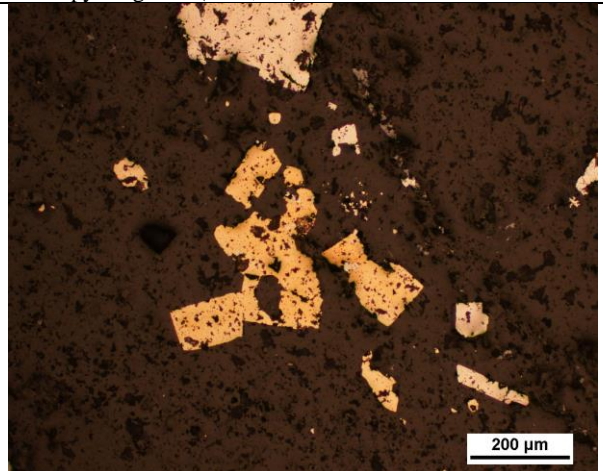
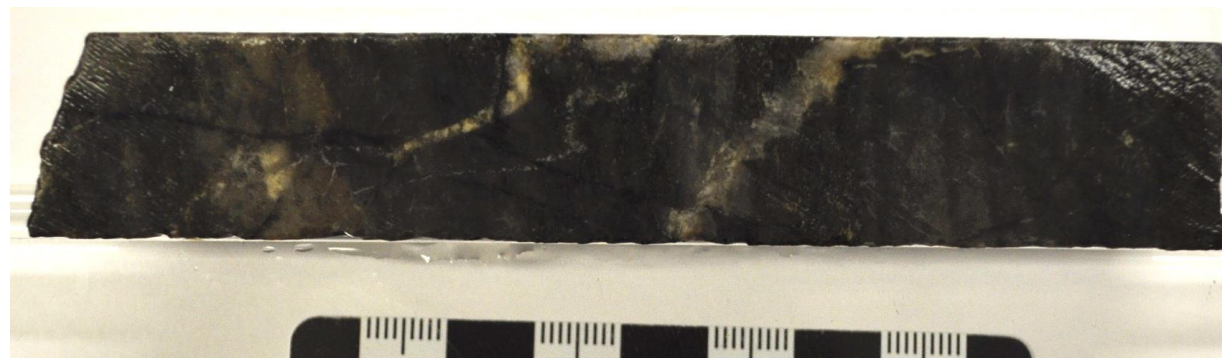


Figure 4. Medium-grained corroded pyrite, arsenopyrite, and sphalerite in the groundmass (RL, X10).

Sample Number	1515*	Drill Hole	TL-13-506	Depth	164-164.7 m
Lithology from Mining Log	PF	Target	TLW	Gold Grade	1.533

Drill Core Sample:



Sample Description:

Dark grey dacite (called intermediate-felsic intrusive: Feldspar Porphyry in mining log). Quartz vein and carbonate veins can be observed in the hand sample. Multiple stages of veining can be identified by the cross-cutting relationships: thin dark quartz veinlets are younger than white carbonate veins younger than smoky quartz veins. Fine-grained arsenopyrite grains are disseminated throughout the sample and a few veins are filled with arsenopyrite. The arsenopyrite grains are coarser in the strongly sericite altered area.

Offcut & Thin Section:



Thin Section Description:

- Minerals and Modal Percentage: plagioclase 30%, quartz 20%, K-feldspar 15%, chlorite 15%, muscovite/sericite 15%, arsenopyrite 3%, pyrite 2%, trace sphalerite, trace chalcopyrite, trace gold.
- Texture: Typical porphyritic texture with intense foliation. The groundmass is very fine to ultra fine-grained feldspar + quartz + sericite/muscovite and moderate oriented. The phenocrysts are plagioclase (0.5-1 mm) with polysynthetic twinning, recrystallized quartz (~0.5 mm), and K-feldspar (0.5-1 mm) with Carlsbad twinning. All phenocrysts are strongly fractured and partly altered into sericite. Quartz pressure shadows are observed around arsenopyrite grains.
- Veining: There is three types of veins: 1) feldspar vein with arsenopyrite and sericite filled in the fractures and quartz recrystallized on the edge of vein; 2) chlorite fine veins; 3) fine quartz veins.
- Alteration: Pervasive sericitization throughout the groundmass and veinlets. Chlorite alteration locally occurs in chlorite veins.
- Ore Mineralogy: Sulphides are mainly fine to medium grained arsenopyrite. Free gold has been found in the groundmass, but not associated with sulphides.

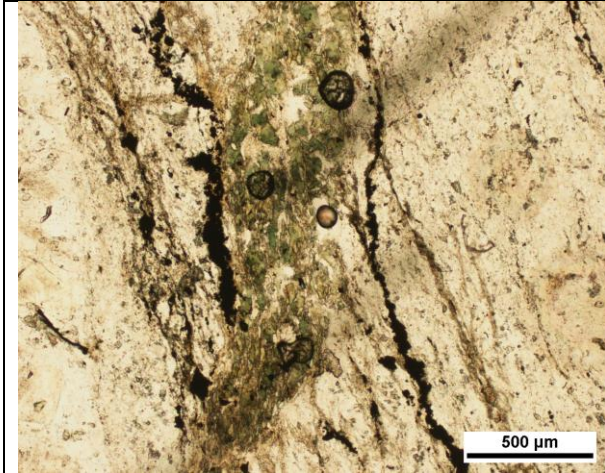


Figure 1. Chlorite vein crosscut the foliation (PPL, X5)

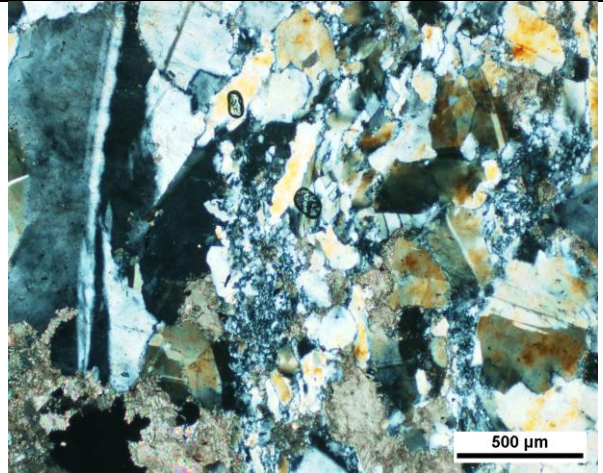


Figure 2. feldspar vein with arsenopyrite and sericite filled in the fractures and quartz recrystallized on the edge of vein (XPL, X5)

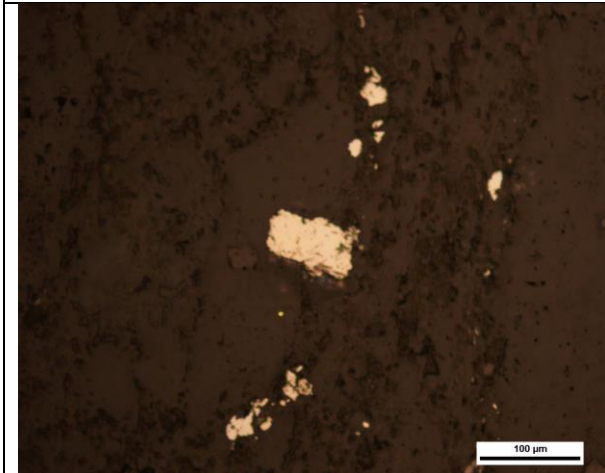


Figure 3. Free gold grains near euhedral arsenopyrite grains within quartz + plagioclase + sericite groundmass (RL, X20)

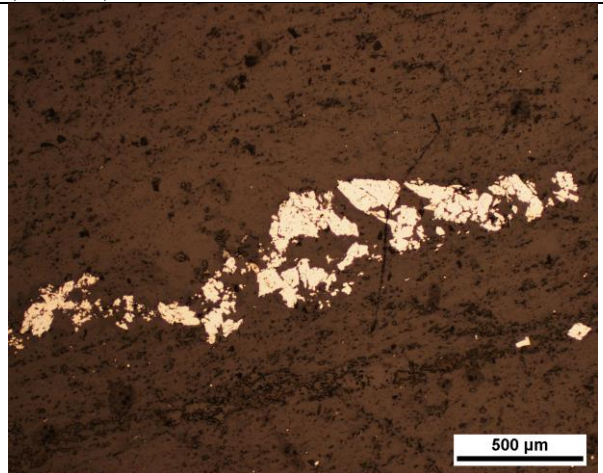


Figure 4. Corroded coarse grained arsenopyrite within feldspar vein (RL, X5)

Sample Number	1517A*	Drill Hole	TL-16-573	Depth	49-50 m
Lithology from Mining Log	PF	Target	TL	Gold Grade	8.457 ppm
Drill Core Sample:					
					
Sample Description:					
<p>Light grey and yellowish green dacite with intense veinlets (called intermediate-felsic intrusive: Feldspar Porphyry in mining log). Arsenopyrite grains are disseminated throughout the hand sample and filled in veins. The veins crosscut each other. The veins are mainly quartz veins, and a few are carbonate veins. The yellowish green part is strongly sericite altered and is smaller than the light grey area.</p>					
Offcut & Thin Section:					
					
Thin Section Description:					
<ul style="list-style-type: none"> Minerals and Modal Percentage: quartz 30%, plagioclase 20%, K-feldspar 20%, muscovite/sericite 15%, carbonate 10%, arsenopyrite 3%, pyrite 2%, trace sphalerite, trace chalcopyrite. Texture: Typical porphyritic texture. The groundmass is decussate texture formed by fine-grained lath-shaped quartz grains. The phenocrysts are plagioclase (0.5-1 mm) with polysynthetic twinning, and K-feldspar (0.5-1 mm) with Carlsbad twinning. All phenocrysts are strongly fractured and partly altered into sericite. Veining: There are four generations of veining: 1) ~1 mm quartz vein with minor feldspar and carbonate, with quartz recrystallization and fine-grained needle-shaped arsenopyrite on the edge; 2) Very thin, cross-cutting recrystallized quartz veinlets without sulphides; 3) Fine grained, fracture-fill, acicular arsenopyrite veinlets; 4) very thin sericite veins with minor feldspar. Alteration: Sericitization is moderate in the groundmass and filled within the fractures of plagioclase phenocryst. Carbonate alteration in the thick quartz vein. Ore Mineralogy: The sulphides are mainly fine-grained occurring on the edge of quartz veins. Arsenopyrite is fine to very fine-grained, needle-shaped in the fine veins and medium-grained in the groundmass. Pyrite is medium-grained, euhedral to subhedral, corroded and fractured in the groundmass. Inclusion gold has been found on the edge of euhedral pyrite and free gold is approximal to pyrite grains. 					

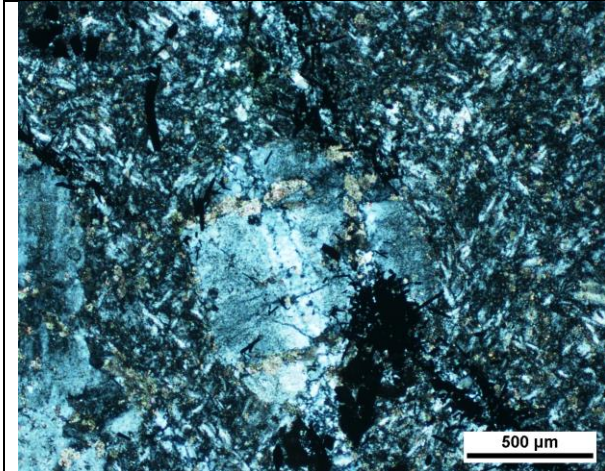


Figure 1. Decussate texture formed by fine-grained lath-shaped quartz grains and plagioclase phenocryst (XPL, X5).

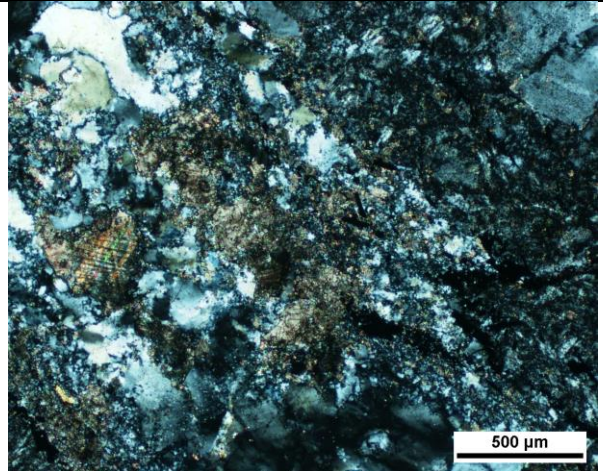


Figure 2. Thick feldspar + carbonate vein with sercite and recrystallized quartz filled in the fractures (XPL, X5).

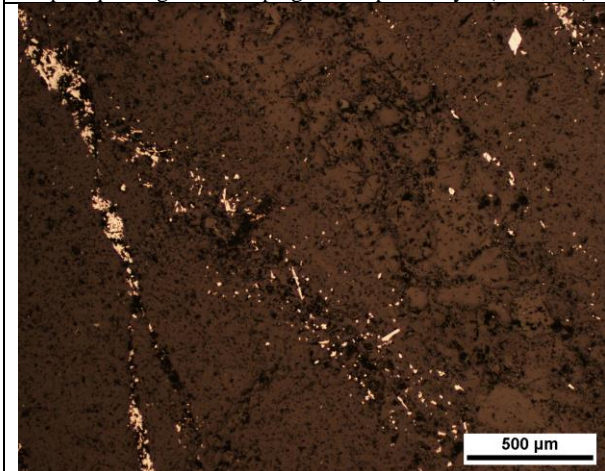


Figure 3. Fine to very fine-grained arsenopyrite on the edge of the thick quartz-feldspar vein (XPL, X5).

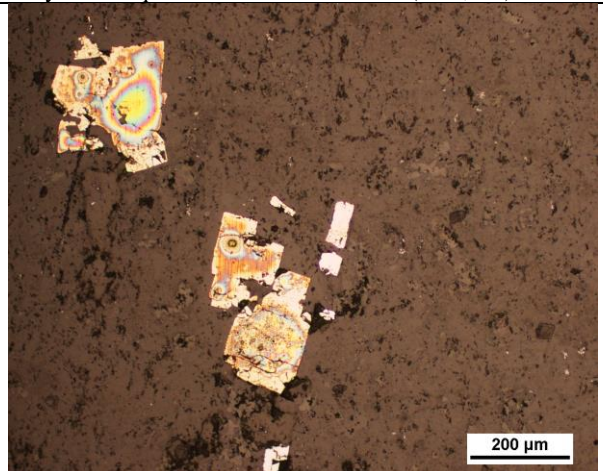


Figure 4. Subhedral corroded pyrite grains with probable inclusion gold inside (RL, X10).

Sample Number	1518*	Drill Hole	TL-16-573	Depth	56-57 m
Lithology from Mining Log	PF	Target	TL	Gold Grade	5.372 ppm

Drill Core Sample:



Sample Description:

Light grey and yellowish green dacite with intense veinlets (called intermediate-felsic intrusive: Feldspar Porphyry in mining log). The appearance of 1518 is similar to 1517, but less veins. Arsenopyrite grains are disseminated throughout the hand sample and filled in veins. Pyrite is filled in some fine veins. The veins crosscut each other, and some are folded. The veins are mainly quartz veins, and a few are carbonate veins. The yellowish green part is strongly sericite altered and is smaller than the light grey area.

Offcut & Thin Section:



Thin Section Description:

- Minerals and Modal Percentage: muscovite/sericite 25%, quartz 25%, K-feldspar 15%, carbonate 15%, plagioclase 15%, arsenopyrite 3%, pyrite 2%, trace sphalerite, trace chalcopyrite.
- Texture: Typical porphyritic texture. The groundmass is decussate texture formed by fine-grained lath-shaped quartz grains and sericite. The phenocrysts are plagioclase (0.5-3 mm) with polysynthetic twinning, and K-feldspar (0.5-1 mm) with Carlsbad twinning. All phenocrysts are strongly fractured and partly altered into sericite. This thin section is similar to 1517, but more altered.
- Veining: One large (1-4 mm) quartz-carbonate folded vein crosscuts the sample. Vein contains dominantly recrystallized quartz and intense sericitization. There are some very thin sericite veinlets.
- Alteration: Pervasive strong sericitization throughout the groundmass. Carbonate alteration occurs in the large folded vein.
- Ore Mineralogy: Sulphides are coarse-grained, euhedral to subhedral, corroded, and often fractured pyrite grains and fine-grained arsenopyrite within fractures and veins. Anhedral medium-grained corroded sphalerite grains were observed with pyrite grains. No microscopic gold has been found in this section.

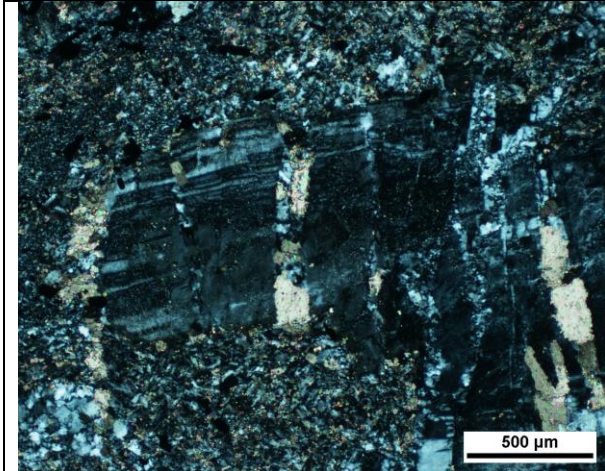


Figure 1. Large, fractured feldspar phenocryst within fine grained quartz groundmass. Phenocryst is actively undergoing sericitization, visible within fractures and at grain boundaries (XPL, 5X).

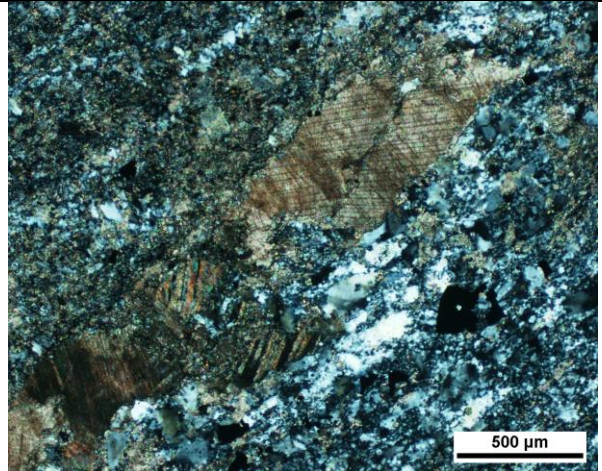


Figure 2. One large (1-4mm) quartz-carbonate folded vein crosscuts the sample (XPL, 5X).

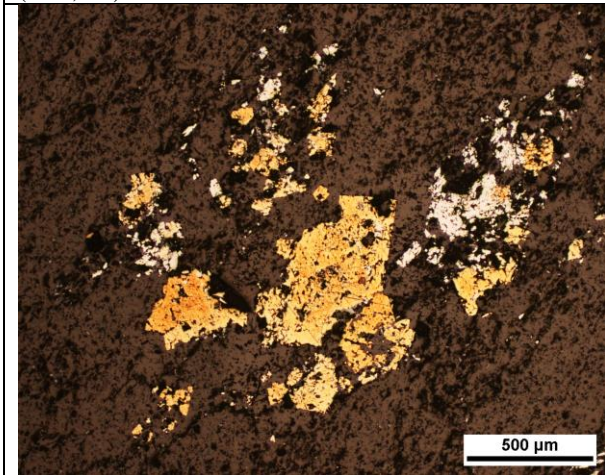


Figure 3. subhedral, corroded, and fractured pyrite grains with sphalerite (RL, X5)

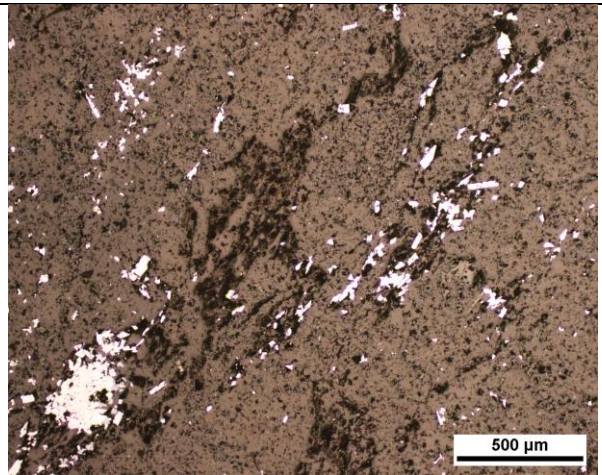


Figure 4. Fine-grained arsenoprite in quartz veins (RL, X5)

Sample Number	1521A*	Drill Hole	TL-14-520	Depth	59-60 m
Lithology from Mining Log	PF	Target	TLW	Gold Grade	6.597 ppm

Drill Core Sample:



Sample Description:

Dark grey-green rock with intense silicification and sericitization. Black minerals visible in relict foliation. Fine white quartz-carbonate vein with fine smoky quartz veinlets at margins. Carbonate veins were observed on fracture surfaces. Very fine-grained arsenopyrite grains are disseminated in the hand sample, some pyrite and arsenopyrite are filled in veins and veinlets. Some red brown sphalerite grains are in carbonate veinlets.

Offcut & Thin Section:



Thin Section Description:

- Minerals and Modal Percentage: quartz 30%, muscovite/sericite 20%, plagioclase 20%, K-feldspar 15%, carbonate 10%, pyrite 3%, arsenopyrite 2%, trace sphalerite, trace chalcopyrite.
- Texture: Typical porphyritic texture. The groundmass is decussate texture formed by disordered fine-grained lath-shaped quartz grains and intense pervasive sericite. The thin section can be divided into two parts by the fault in the middle. The grains of the left bottom corner are coarser and more altered than the right top corner. Sericite/muscovite is filled in the boundary of two parts. The phenocrysts are plagioclase (0.5-1 mm) with polysynthetic twinning, recrystallized quartz (~0.8 mm), and K-feldspar (0.5-1 mm) with Carlsbad twinning. All feldspar phenocrysts are strongly fractured and partly altered into sericite.
- Veining: Fine cross-cutting quartz veins occur within the fine-grained quartz groundmass. A few of the quartz veins have arsenopyrite filled inside.
- Alteration: Pervasive moderate sericitization throughout the thin section, filled in the fractures of phenocrysts, and the boundary of two parts groundmass. The intensity of the sericitization in the coarser-grained groundmass part is higher than the finer-grained groundmass part.
- Ore Mineralogy: Fine to very fine-grained, euhedral to subhedral arsenopyrite, pyrite, and sphalerite are disseminated in the decussate-textured groundmass. Corroded coarse-grained pyrite and subhedral medium-grained arsenopyrite has been observed in the finer-grained groundmass. Arsenopyrite is also filled in the fine quartz veins. No microscopic gold has been found in this section.

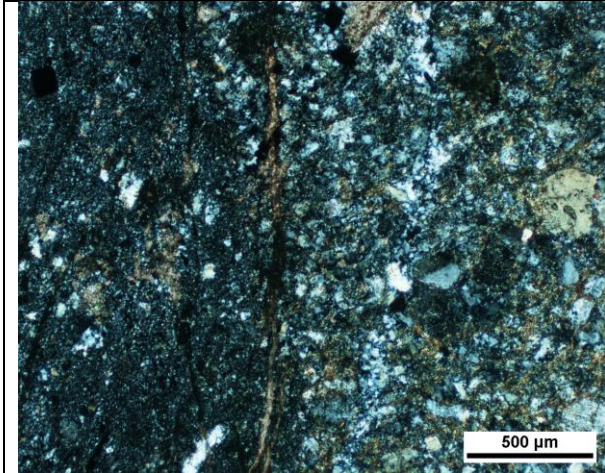


Figure 1. Decussate texture groundmass formed by disordered fine-grained lath-shaped quartz grains and intense pervasive sericite. The grains in the right are coarser and more altered than the left. Sericite/muscovite is filled in the boundary of two parts (XPL, X5).

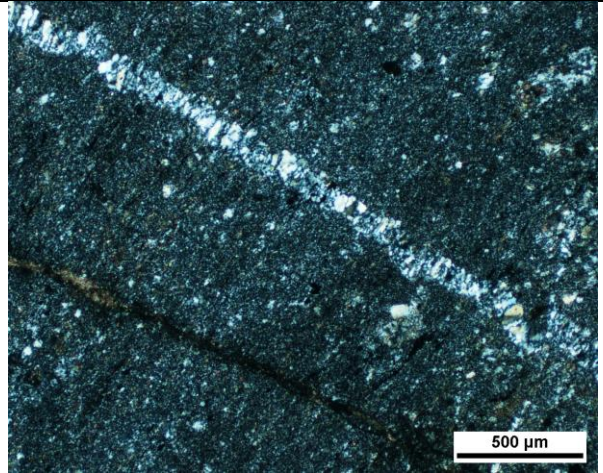


Figure 2. Sericite/muscovite filled in the fractures and a recrystallized quartz vein (XPL, X5).

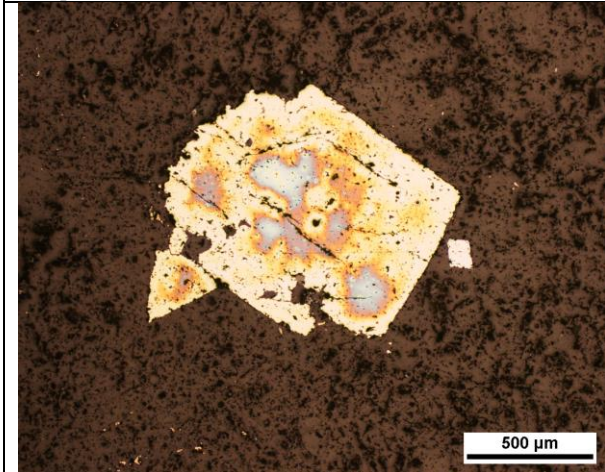


Figure 3. Corroded coarse-grained pyrite and subhedral fine-grained arsenopyrite in the finer-grained groundmass (RL, X5).

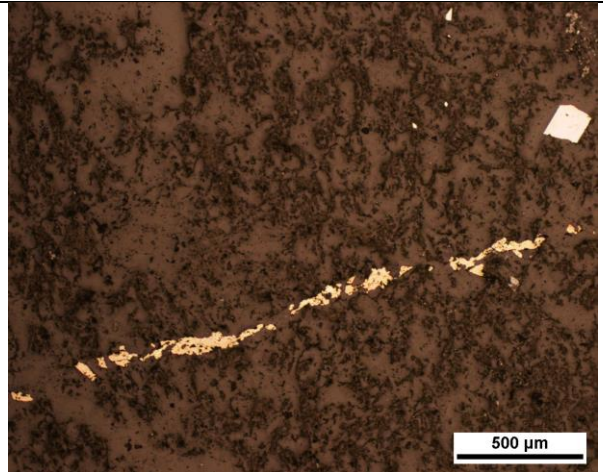


Figure 4. Arsenopyrite filled in the fine quartz vein (RL, X5).

Sample Number	1523*	Drill Hole	TL-15-559	Depth	114.4-115.1 m
Lithology from Mining Log	PF	Target	TLW	Gold Grade	1.6 ppm

Drill Core Sample:



Sample Description:

Light grey and yellowish green dacite with intense silicification, veining sericitization (called intermediate-felsic intrusive: Feldspar Porphyry in mining log). There are three types of veins observed in the hand sample: 1) ~1 mm quartz veins, most of them are filled with arsenopyrite; 2) <1 mm arsenopyrite veins; 3) carbonate veins are varied from 0.5-2 mm, the finer ones crosscut the quartz veins. Pyrite and arsenopyrite grains are disseminated in the groundmass.

Offcut & Thin Section:



Thin Section Description:

- Minerals and Modal Percentage: plagioclase 40%, quartz 20%, carbonate 10%, chlorite 10%, K-feldspar 10%, muscovite/sericite 3%, arsenopyrite 3%, pyroxene 3%, trace pyrite, trace sphalerite.
- Texture: The primary texture has been overprinted by intense alteration. The groundmass is very fine to ultra fine-grained feldspar + quartz + sericite/muscovite. The phenocrysts are plagioclase (0.5-1 mm) with polysynthetic twinning, recrystallized quartz (~0.5 mm), and K-feldspar (0.5-1 mm) with Carlsbad twinning. Pyroxene grains show light pink pleochroism under plane-polarized light and high interference colors under cross-polarized light. All phenocrysts are strongly fractured, partly altered into sericite, and quartz recrystallized in fractures (the alteration is stronger than other dacite samples).
- Veining: There are three types of veins: 1)
- Alteration: Locally chlorite alteration near veins. Carbonate alteration inside veins. Carbonate grains are coarse with twinning planes. Pervasive intense sericitization throughout the thin section. Feldspar phenocrysts are partly or completely altered into sericite.
- Ore Mineralogy: There are less sulphide than other dacite samples. Arsenopyrite are fine to medium-grained, subhedral to anhedral, filled in the recrystallized quartz veins. Fine-grained, needle pyrite grains are disseminated in the groundmass. No microscopic gold has been found in this section.

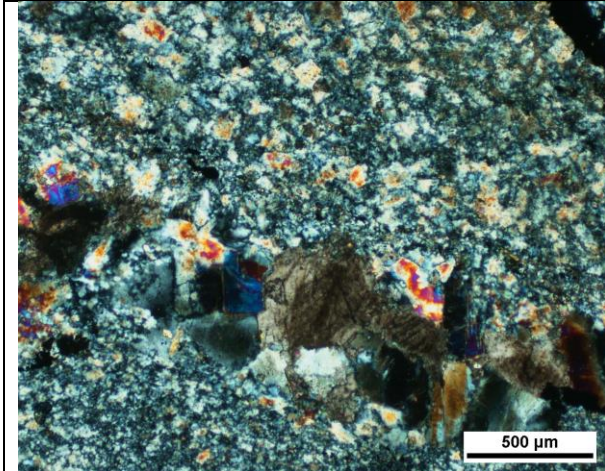


Figure 1. Carbonate grains are coarse with twinning planes. Pyroxene grains shows light pink pleochroism under plane-polarized light and high interference colors under cross-polarized light (XPL, X5).

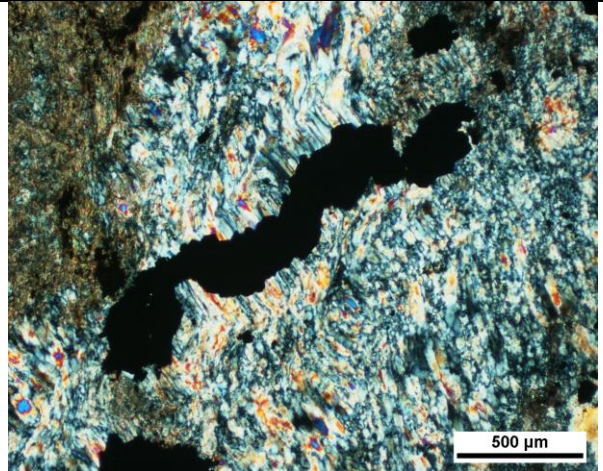


Figure 2. Fine to medium-grained, subhedral to anhedral arsenopyrite filled in the recrystallized quartz veins (XPL, X5).

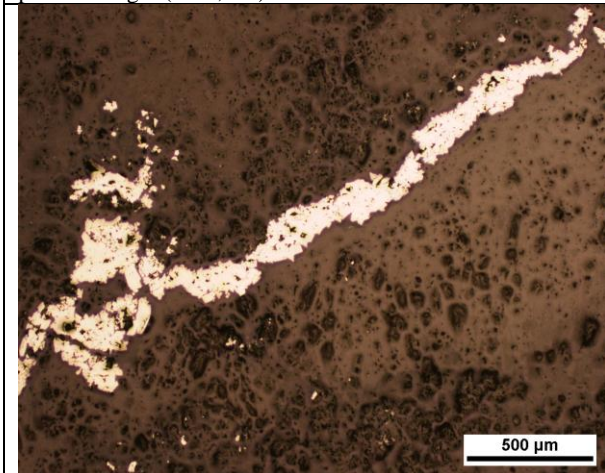


Figure 3. Fine to medium-grained, subhedral to anhedral arsenopyrite filled in the recrystallized quartz veins (RL, X5)

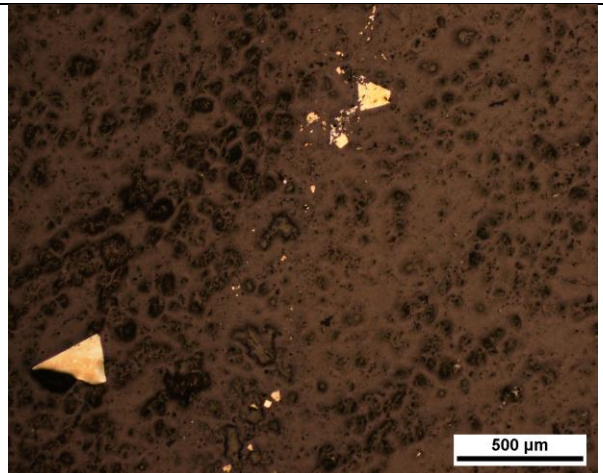


Figure 4. Fine-grained, needle pyrite grains are disseminated in the groundmass (RL, X5).

Sample Number	1532A*	Drill Hole	TL-12-481	Depth	183.78-184.06 m
Lithology from Mining Log	PF	Target	TL	Gold Grade	3.463 ppm

Drill Core Sample:



Sample Description:

Light grey-light yellowish green-dark grey dacite with significant veining and brecciation (called intermediate-felsic intrusive: Feldspar Porphyry in mining log). The light yellowish green is with intense sericitization. The veinlets in the hand sample are orange, showing oxidation of Fe-rich carbonate. The thicker veins are folded. Fine-grained pyrite and arsenopyrite are disseminated near/inside the veins. The veins glowed a bright sky-blue under the UV light, showing the presence of scheelite.

Offcut & Thin Section:



Thin Section Description:

- Minerals and Modal Percentage: quartz 65%, muscovite/sericite 10%, pyrite 10%, plagioclase 5%, K-feldspar 5%, arsenopyrite 3%, carbonate 2%, trace sphalerite, trace gold.
- Texture: This thin section mainly shows the texture of a thick quartz vein. The quartz vein consists of anhedral coarse-grained fractured quartz with undulose extinction. Quartz are recrystallized in the fractures and between the coarse quartz grains. Sericite, carbonate, and feldspar occurs locally. The host rock texture cannot be observed clearly. The host groundmass is typical porphyritic texture formed by very fine to ultra fine-grained feldspar + quartz + sericite/muscovite. The phenocrysts are dominantly plagioclase.
- Veining: The whole thin section is vein material.
- Alteration: Locally slight sericitization and carbonate alteration.
- Ore Mineralogy: The main type of sulphide is pyrite, which are mainly coarse-grained, fractured, corroded, subhedral to euhedral. Arsenopyrite are finer, and less corroded than pyrite. A few needle-shaped arsenopyrite are inside corroded coarse pyrite. There is a fine pyrite vein in the top right. Inclusion gold has been observed inside pyrite.

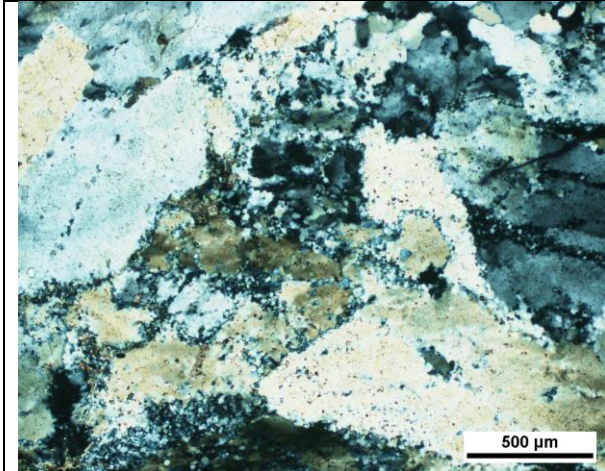


Figure 1. Quartz recrystallized in the fractures and between the coarse quartz grains (XPL, X5).

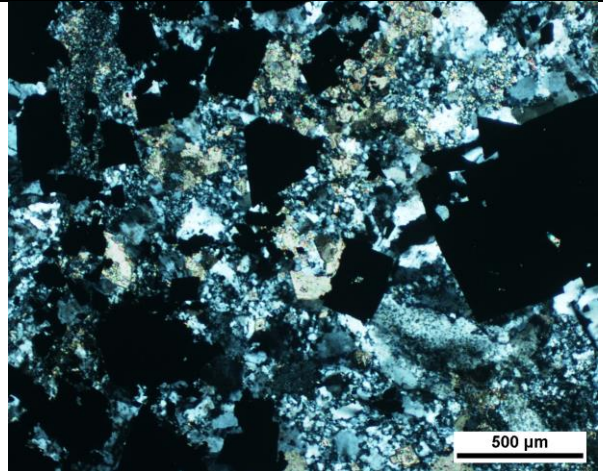


Figure 2. Quartz pressure shadow recrystallized between the euhedral corroded pyrite grains (XPL, X5).

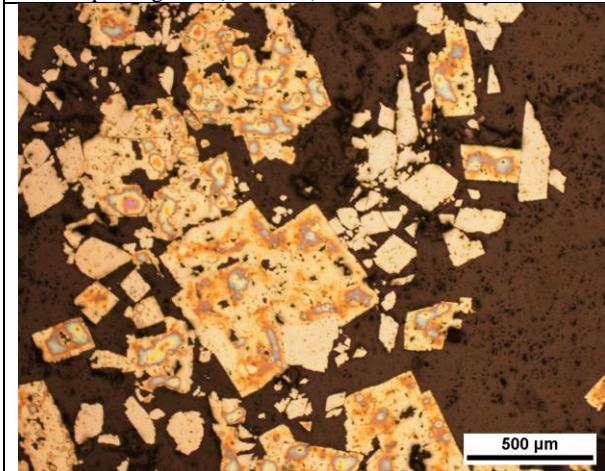


Figure 3. A coarse-grained, fractured, corroded, subhedral pyrite with a needle-shaped arsenopyrite inside (RL, X5).

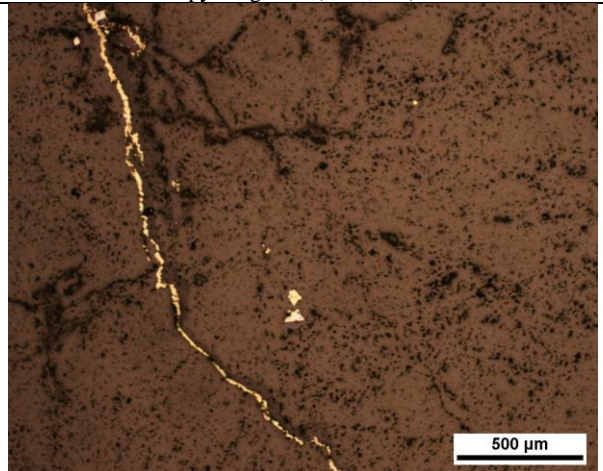
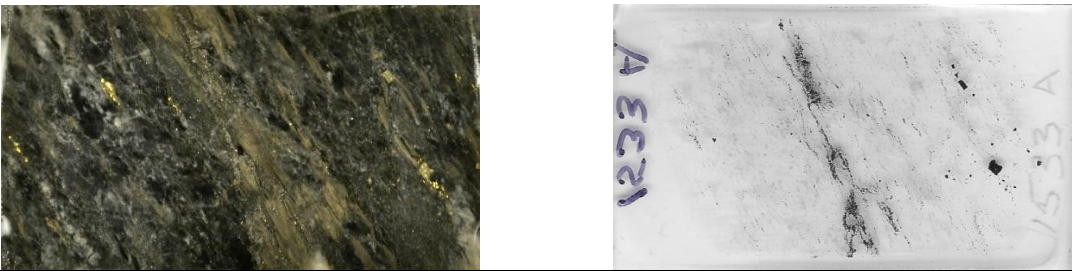


Figure 4. A fine pyrite vein and disseminated fine-grained arsenopyrite (RL, X5).

Sample Number	1533A*	Drill Hole	TL-12-481	Depth	99-100.1 m
Lithology from Mining Log	PF	Target	TL	Gold Grade	13.22 ppm
Drill Core Sample:					
					
Sample Description:					
<p>Light grey dacite with intense veining and moderate veining (called intermediate-felsic intrusive: Feldspar Porphyry in mining log). There are three types of veins in the hand sample: 1) orange-colored Fe-rich oxidized carbonate veins; 2) white-colored carbonate veins; 3) smoky quartz veins. Smoky quartz veins are generally parallel to white carbonate veins and crosscut by orange Fe-rich oxidized carbonate veins. The white veins glowed a bright sky-blue under the UV light, showing the presence of scheelite. Pyrite, arsenopyrite, and some gold grains are disseminated in the hand sample.</p>					
Offcut & Thin Section:					
					
Thin Section Description:					
<ul style="list-style-type: none"> • Minerals and Modal Percentage: quartz 65%, muscovite/sericite 10%, pyrite 10%, plagioclase 5%, K-feldspar 5%, arsenopyrite 2%, carbonate 2%, gold 1%, trace sphalerite. • Texture: Typical porphyritic texture with intense foliation. The primary texture has been obliterated by pervasive alteration overprint. The groundmass is very fine to ultra fine-grained feldspar + quartz + sericite/muscovite. The phenocrysts are not a lot: plagioclase with polysynthetic twinning and recrystallized quartz. All phenocrysts are strongly fractured and partly altered into sericite. Very fine to fine-grained quartz has recrystallized between feldspar and quartz phenocrysts and fractures. • Veining: The whole thin section is vein material. • Alteration: Pervasive sericitization: sericite has infilled the fractures of feldspar phenocrysts and sulphide grains. • Ore Mineralogy: Coarse to fine-grained, euhedral to subhedral corroded, fractured pyrite and arsenopyrite grains are disseminated throughout the sample, especially within fractures. There are several types of microscopy gold: 1) free gold near medium-grained euhedral disseminated arsenopyrite; 2) free gold near corroded euhedral pyrite; 3) inclusion gold within corroded euhedral pyrite. 					

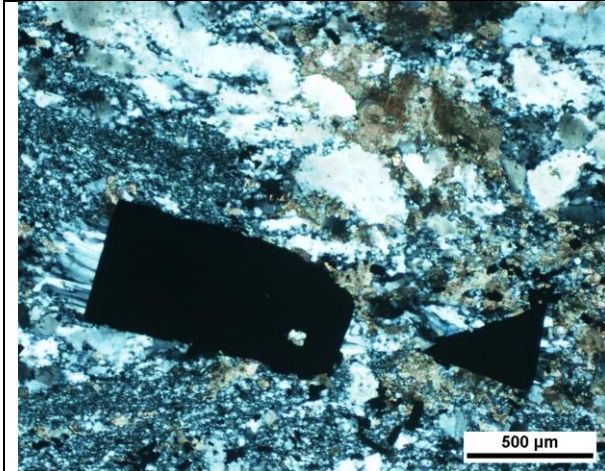


Figure 1. Quartz strain fringes surrounding euhedral and needle pyrite grains (XPL, X5).

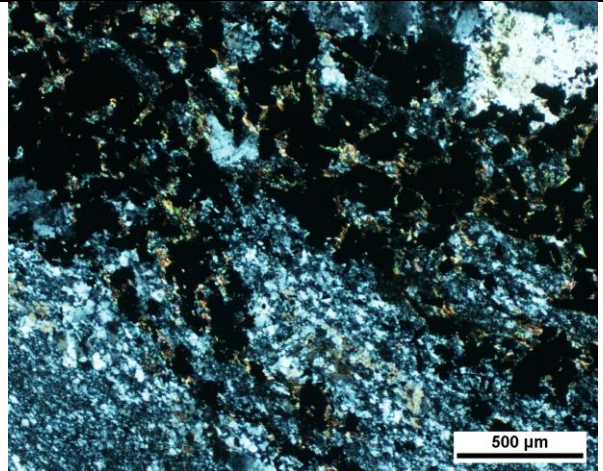


Figure 2. Sericite has infilled the fractures of feldspar phenocrysts and arsenopyrite grains (XPL, X5).

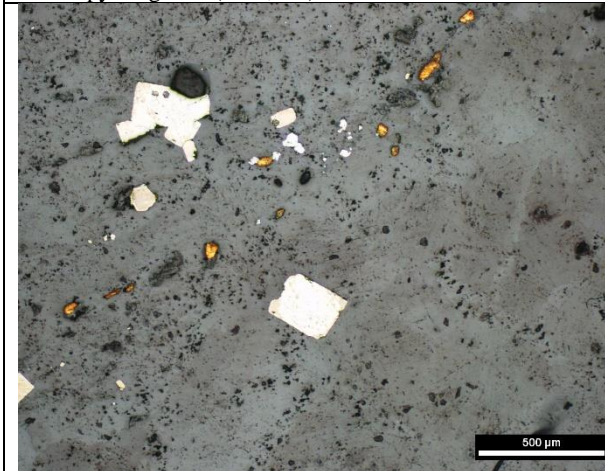


Figure 3. Free gold near medium-grained euhedral disseminated arsenopyrite (RL, X5)

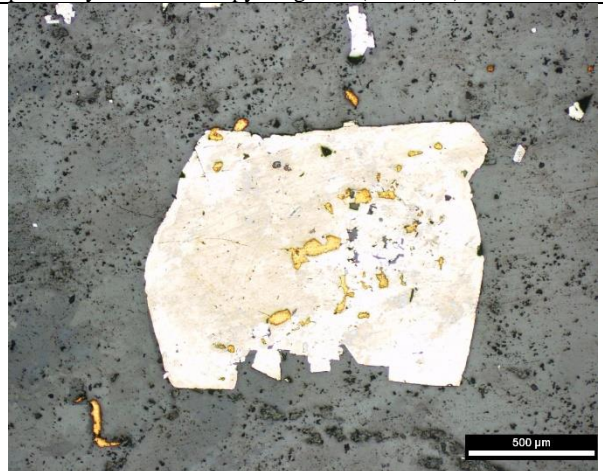


Figure 4. Free gold and inclusion gold with corroded euhedral pyrite (RL, X5)

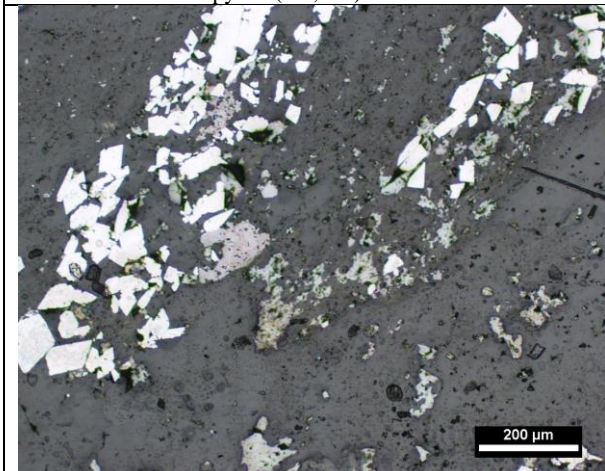


Figure 4. Disseminated arsenopyrite in quartz vein (RL, X10)

Sample Number	1533B*	Drill Hole	TL-12-481	Depth	99-100.1 m
Lithology from Mining Log	PF	Target	TL	Gold Grade	13.22 ppm

Offcut & Thin Section:



Thin Section Description:

- Minerals and Modal Percentage: quartz 65%, muscovite/sericite 10%, pyrite 10%, plagioclase 5%, K-feldspar 5%, arsenopyrite 2%, carbonate 2%, gold 1%, trace sphalerite.
- Texture: Typical porphyritic texture with intense foliation, similar to 1533A. The primary texture has been obliterated by pervasive alteration overprint. The groundmass is very fine to ultra fine-grained feldspar + quartz + sericite/muscovite. The phenocrysts are not a lot: plagioclase with polysynthetic twinning and recrystallized quartz. All phenocrysts are strongly fractured and partly altered into sericite. Very fine to fine-grained quartz has recrystallized between feldspar and quartz phenocrysts and fractures.
- Veining: <1 mm recrystallized quartz veins throughout the thin section.
- Alteration: Pervasive sericitization: sericite has infilled the fractures of feldspar phenocrysts and sulphide grains.
- Ore Mineralogy: Coarse to fine-grained, euhedral to subhedral corroded, fractured pyrite and arsenopyrite grains are disseminated throughout the sample, especially within fractures. No microscopic gold has been found in this section.

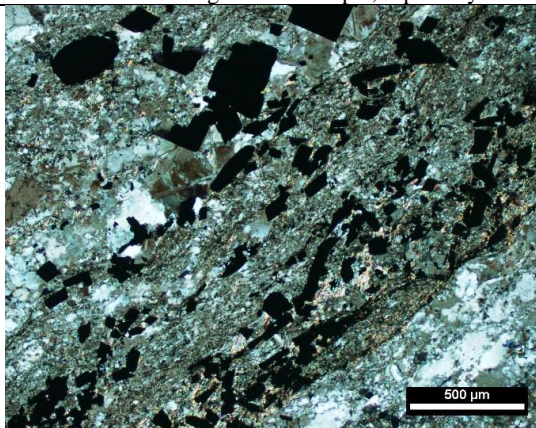


Figure 1. Fine-grained euhedral and needle arsenopyrite grains aligned with strongly altered quartz vein (XPL, X5).

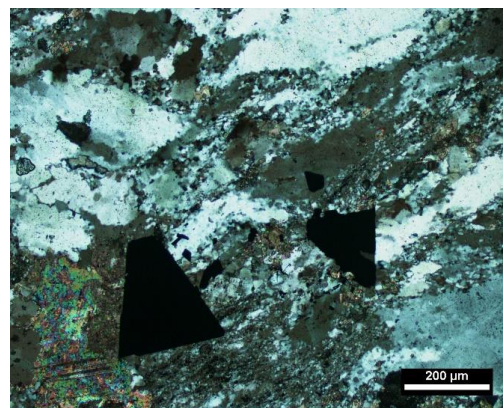


Figure 2. Needle pyrite within recrystallized quartz veins (XPL, X5).

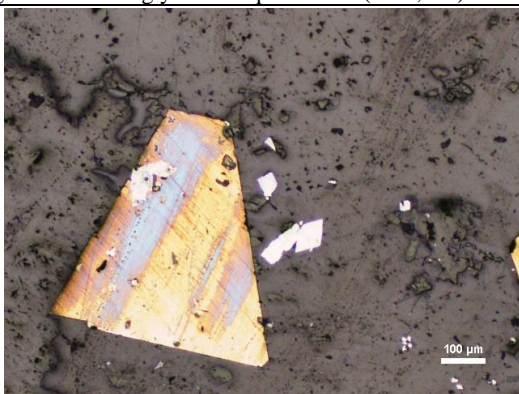


Figure 3. Needle corroded pyrite with euhedral arsenopyrite as inclusion within recrystallized quartz veins (RL, X10).

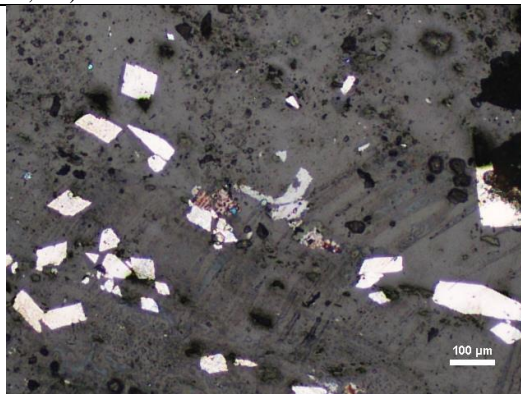


Figure 4. Fine grained, euhedral and needle arsenopyrite and anhedral sphalerite in the quartz vein (RL, X10).

Sample Number	1540A*	Drill Hole	TL-11-419	Depth	88-89 m
Lithology from Mining Log	PF	Target	TLW	Gold Grade	1.556 ppm

Drill Core Sample:



Sample Description:

Orange to dark green dacite (called intermediate-felsic intrusive: Feldspar Porphyry in mining log). The dark green area shows intense sericitization. Very fine-grained disseminated arsenopyrite is throughout the entire sample and fine-grained arsenopyrite is filled in the breccia cracks and fractures. Coarser arsenopyrite grains are associated with sericite. The orange area shows wispy carbonate overprint and weathering.

Offcut & Thin Section:



Thin Section Description:

- Minerals and Modal Percentage: quartz 35%, plagioclase 20%, K-feldspar 15%, muscovite/sericite 15%, carbonate 10%, arsenopyrite 5%, trace pyrite, trace sphalerite, trace chalcopyrite.
- Texture: Typical porphyritic texture with moderate foliation. The groundmass is very fine to ultra fine-grained feldspar + quartz + sericite/muscovite. The phenocrysts are plagioclase (0.5-1 mm) with polysynthetic twinning, recrystallized quartz (~0.5 mm), and K-feldspar (0.5-1 mm) with Carlsbad twinning. All phenocrysts are strongly fractured and partly altered into sericite. Muscovite recrystallized along with the foliation and filled within the fractures of phenocrysts.
- Veining: Folded strong altered relict quartz-carbonate veins with sulphides filled inside.
- Alteration: Pervasive moderate sericitization throughout the thin section. Slight carbonate alteration exhibits in the quartz-carbonate veins.
- Ore Mineralogy: Sulphides are mainly highly fractured and corroded anhedral to subhedral arsenopyrite. No microscopic gold has been found in this section.

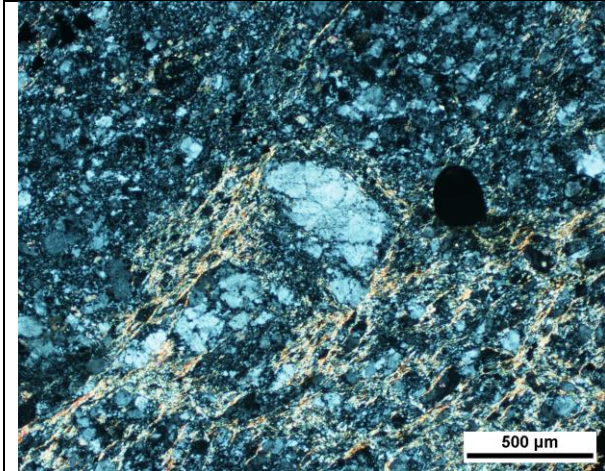


Figure 1. Feldspar phenocryst and muscovite filled within the fractures (XPL, X5)

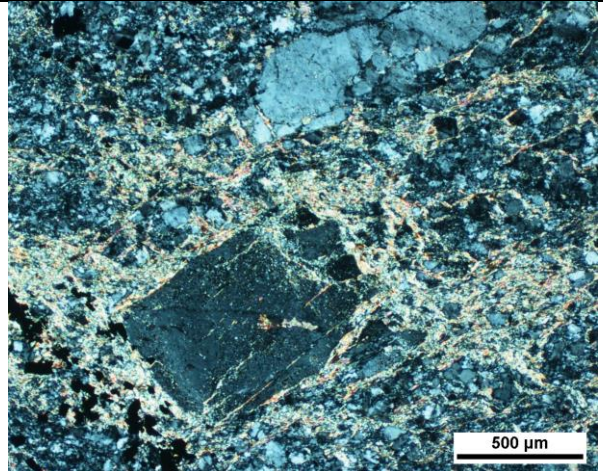


Figure 2. Muscovite pressure shadow around feldspar phenocryst (XPL, X5)

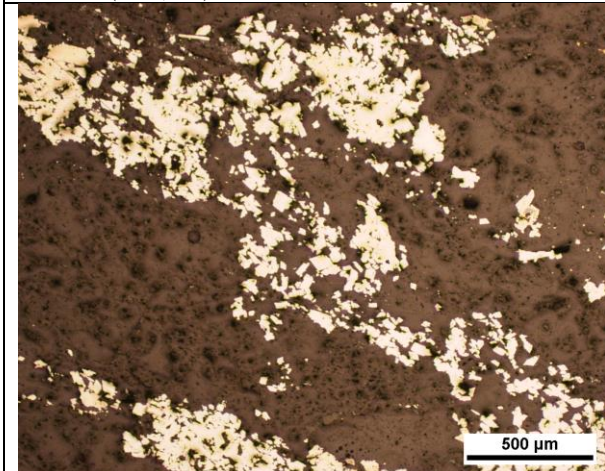


Figure 3. Euhedral prismatic arsenopyrite grains in the relict quartz-carbonate veins (RL, X5)

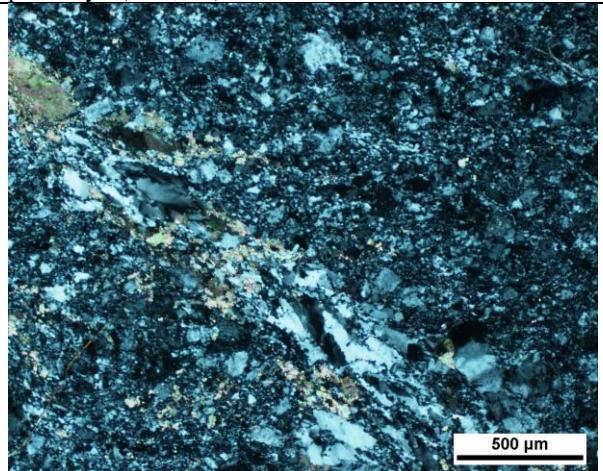


Figure 4. Recrystallized quartz-carbonate vein in the groundmass (XPL, X5)

Sample Number	1541A*	Drill Hole	TL-11-419	Depth	89-90 m
Lithology from Mining Log	PF	Target	TLW	Gold Grade	2.816ppm

Drill Core Sample:



Sample Description:

Dark grey to dark yellowish green dacite (called intermediate-felsic intrusive: Feldspar Porphyry in mining log). Smoky quartz veinlets are throughout the hand sample. The dark yellowish green area shows intense sericitization. Some white minerals distribute locally along with the foliation. The white minerals glowed a bright sky-blue under the UV light, showing the presence of scheelite. Pyrite and arsenopyrite grains are disseminated throughout the sample, especially in the veinlets. Pyrite is coarser, more euhedral, and more common than arsenopyrite.

Offcut & Thin Section:



Thin Section Description:

- Minerals and Modal Percentage: plagioclase 30%, K-feldspar 20%, quartz 15%, carbonate 15% (mainly scheelite), muscovite/sericite 15%, arsenopyrite 3%, pyrite 2%, trace sphalerite, trace chalcopyrite.
- Texture: Typical porphyritic texture with intense foliation. The groundmass is very fine to ultra fine-grained feldspar + quartz + sericite/muscovite. The phenocrysts are plagioclase (0.5-1 mm) with polysynthetic twinning, recrystallized quartz (~0.5 mm), and K-feldspar (0.5-1 mm) with Carlsbad twinning. All phenocrysts are strongly fractured and partly altered into sericite.
- Veining: There are two types of veins: 1) relict quartz-feldspar veins with arsenopyrite filled inside; 2) strongly folded quartz-feldspar-scheelite veins which are reworked, and sericite recrystallized in the fractures.
- Alteration: pervasive moderate sericitization along with the foliation and filled in the fractures of feldspar phenocrysts.
- Ore Mineralogy: The major type of sulphides is arsenopyrite, which is filled within relict quartz-feldspar veins. Arsenopyrite grains in the veins are mainly coarse-grained anhedral, and strongly fractured and corroded. Fine-grained arsenopyrite grains are disseminated in the foliated groundmass. Free gold grains are within the groundmass of muscovite/sericite.

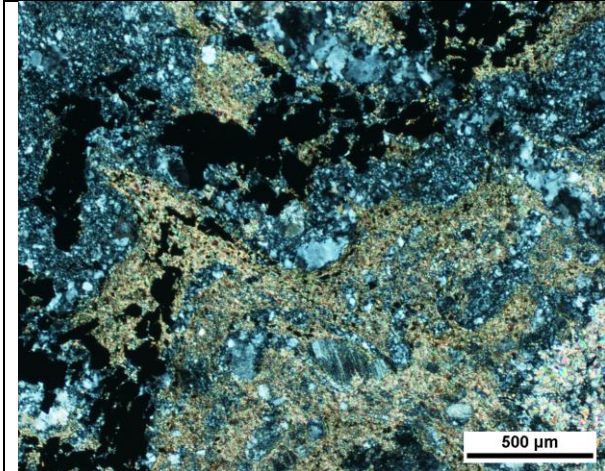


Figure 1. Chevron folds of sericite, sulphides, and scheelite (XPL, X5)

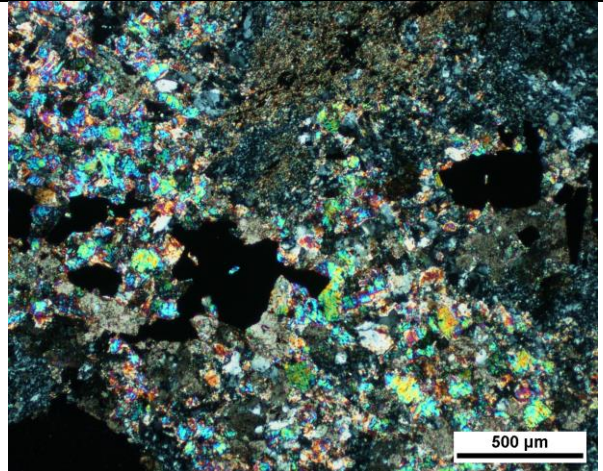


Figure 2. Free gold within the groundmass of muscovite (XPL, X5)

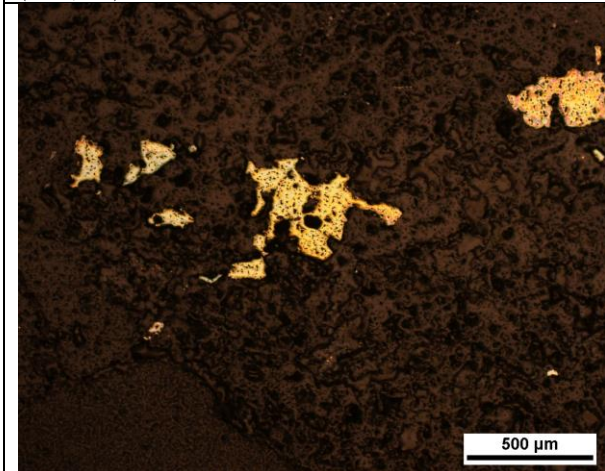


Figure 3. Free gold within the groundmass of muscovite (RL, X5)

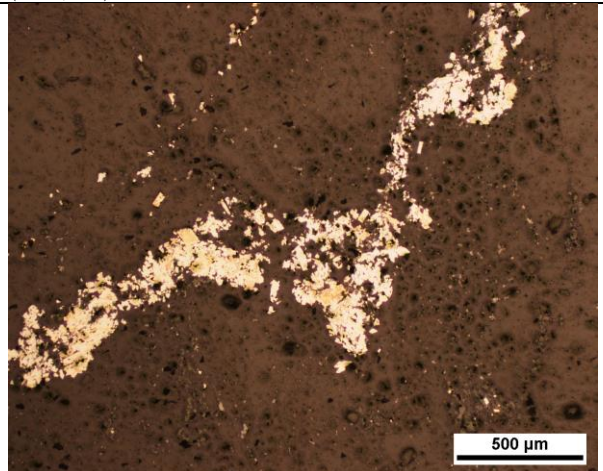


Figure 4. Anhedral corroded arsenopyrite disseminated in the groundmass along with the foliation (RL, X5)

Appendix B: Low Gold Grade Drill Core Samples (<1 ppm) at the Monument Bay Project

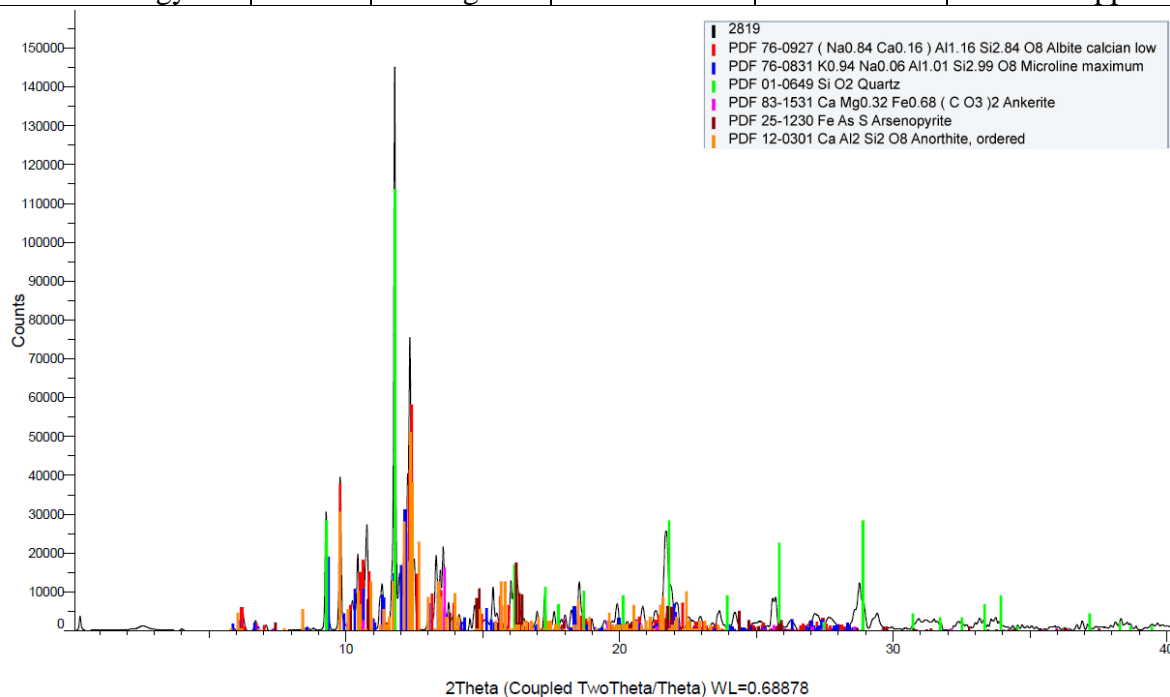
Hole ID	Western Sample ID	Sampled From	Sampled To	Target	Au Grade (ppm)	W Grade (ppm)	Lithology (by Yamana)
TL-02-96	E5552364	45.34	45.57	AZ	0.11	NA	Clastic Metasediments: Conglomerate
TL-03-160	E5551531	195.1	196.1	ME	0.09	50	Intermediate-Felsic Intrusives: Feldspar Porphyry
TL-06-312	E5551528	91.8	92.5	AZ	0.5	NA	Clastic Metasediments: Conglomerate
TL-06-312	E5551529	106.91	107.75	AZ	0.005	NA	Clastic Metasediments: Conglomerate
TL-06-312	E5551547	98	98.9	AZ	0.17	NA	Clastic Metasediments: Conglomerate
TL-06-315	E5552366	89.06	89.34	AZ	0.003	NA	Clastic Metasediments: Conglomerate
TL-06-315	E5552367	148.47	148.65	AZ	0.04	NA	Clastic Metasediments: Conglomerate
TL-11-381	E5551548	318.6	319.6	AZ	0.167	NA	Felsic Metavolcanics: Heterolithic Tuff
TL-11-419	E5551537	85	86	TLW	0.409	NA	Clastic Metasediments: Siltstone
TL-11-419	E5551538	86	87	TLW	0.531	NA	Clastic Metasediments: Siltstone
TL-11-419	E5551539	87	88	TLW	0.914	NA	Intermediate-Felsic Intrusives: Feldspar Porphyry
TL-12-453	E5552848	74.65	74.8	TL	0.003	NA	Felsic Metavolcanics: Undifferentiated Tuff
TL-12-453	E5552849	249.5	249.68	TL	0.007	NA	Clastic Metasediments: Sandstone
TL-12-468	E5551520	157	158	ME	0.283	NA	Intermediate-Felsic Intrusives: Quartz Feldspar Porphyry
TL-12-468	E5551527	241	242	ME	0.033	NA	Intermediate Metavolcanics: Ash Tuff
TL-12-481	E5551534	100.1	101	TL	0.026	NA	Felsic Metavolcanics: Lapilli Tuff
TL-13-486	E5552368	139.59	139.8	TL	0.02	NA	Intermediate Metavolcanics: Feldspar Phyric Flow
TL-13-486	E5552369	288.5	288.77	TL	0.377	50	Intermediate-Felsic Intrusives: Feldspar Porphyry
TL-13-486	E5552370	308.7	308.9	TL	0.5	50	Intermediate Metavolcanics: Undifferentiated
TL-13-500	E5552833	117.29	117.46	ME	0.006	NA	Clastic Metasediments: Siltstone
TL-13-500	E5552835	268.64	268.85	ME	0.025	NA	Clastic Metasediments: Greywacke
TL-13-500	E5552836	361	361.2	ME	0.025	NA	Felsic Metavolcanics: Undifferentiated
TL-13-501	E5552837	157.4	157.6	TL	0.75	NA	Intermediate-Felsic Intrusives: Quartz-Feldspar Porphyry
TL-13-501	E5552838	250.69	250.92	TL	0.361	NA	Clastic Metasediments: Siltstone/Argillite
TL-13-501	E5552839	101.74	102	TL	0.0025	NA	Clastic Metasediments: Siltstone/Argillite
TL-13-504	E5552840	145.1	145.3	TLW	0.06	50	Felsic Metavolcanics: Waterlain Tuff
TL-13-504	E5552842	149.8	150	TLW	0.01	590	Felsic Metavolcanics: Waterlain Tuff
TL-13-504	E5552844	204.85	205	TLW	0.05	50	Intermediate Metavolcanics: Feldspar Phyric Flow
TL-13-504	E5552844	205	205.15	TLW	0.05	50	Intermediate Metavolcanics: Feldspar Phyric Flow
TL-13-506	E5551549	169.5	170	TL	0.848	1320	Intermediate-Felsic Intrusives: Feldspar Porphyry
TL-13-509	E5552846	263.45	263.63	TLW	0.0025	50	Intermediate Metavolcanics: Feldspar Phyric Flow
TL-13-509	E5552847	283.38	283.62	TLW	0.8	50	Clastic Metasediments: Greywacke
TL-14-520	E5551522	53	54	TLW	0.131	NA	Clastic Metasediments: Siltstone
TL-15-551	E5552830	37.13	37.36	SLS	0.008	NA	Clastic Metasediments: Undifferentiated
TL-15-559	E5551524	133	134	TLW	0.915	153	Intermediate-Felsic Intrusives: Feldspar Porphyry
TL-15-559	E5551525	137.3	138.4	TLW	0.332	50	Intermediate Metavolcanics: Feldspar Phyric Flow
TL-15-560	E5551546	63	64	TLW	0.002	204	Intermediate-Felsic Intrusives: Feldspar Porphyry
TL-15-564	E5552826	115.57	115.76	TL	0.014	217	Clastic Metasediments: Undifferentiated

Hole ID	Western Sample ID	Sampled From	Sampled To	Target	Au Grade (ppm)	W Grade (ppm)	Lithology (by Yamana)
TL-15-564	E5552828	148	148.2	TL	0.34	NA	Clastic Metasediments: Undifferentiated
TL-15-564	E5552829	294.4	294.63	TL	0.0025	NA	Intermediate Metavolcanics: Feldspar Phyric Flow
TL-15-568	E5552823	58.6	58.83	TLW	0.014	50	Clastic Metasediments: Undifferentiated
TL-15-568	E5552825	249.15	249.36	TLW	0.0025	NA	Intermediate Metavolcanics: Lapilli Tuff
TL-16-575	E5552820	151.68	151.82	TL	0.75	50	Intermediate-Felsic Intrusives: Feldspar Porphyry
TL-16-575	E5552822	210	210.15	TL	0.17	50	Intermediate-Felsic Intrusives: Feldspar Porphyry
TL-16-578	E5552816	141.65	141.88	TL	0.39	50	Intermediate Metavolcanics: Feldspar Phyric Flow
TL-16-578	E5552817	204.5	204.72	TL	0.45	50	Intermediate-Felsic Intrusives: Feldspar Porphyry
TL-16-578	E5552818	283.6	283.84	TL	0.006	NA	Intermediate Metavolcanics: Feldspar Phyric Flow
TL-16-583	E5552812	156.11	156.31	TL	0.98	50	Intermediate-Felsic Intrusives: Quartz-Feldspar Porphyry
TL-16-583	E5552813	171.63	171.88	TL	0.0025	50	Intermediate Metavolcanics: Feldspar Phyric Flow
TL-16-583	E5552814	237.89	238.19	TL	0.023	50	Intermediate Metavolcanics: Undifferentiated
TL-16-583	E5552815	267.89	268.03	TL	0.06	50	Intermediate Metavolcanics: Massive Flow
TL-16-587	E5551510	255.7	256.7	TL	0.303	50	Intermediate Metavolcanics: Undifferentiated
TL-16-587	E5551512	247	248	TL	0.943	50	Intermediate-Felsic Intrusives: Feldspar Porphyry
TL-16-591	E5551545	274	275	TL	0.192	50	Intermediate-Felsic Intrusives: Feldspar Porphyry
TL-16-604A	E5552851	282.55	282.75	TL	0.003	178	Clastic Metasediments: Undifferentiated
TL-16-604A	E5552855	686.87	687.04	TL	0.005	50	Felsic Metavolcanics: Undifferentiated Tuff
TL-16-607	E5552859	843.5	843.7	TL	0.006	NA	Intermediate Metavolcanics: Feldspar Phyric Flow
TL-17-616	E5552361	314	314.23	SLS	0.008	NA	Intermediate-Felsic Intrusives: Quartz-Feldspar Porphyry
TL-17-616	E5552362	342.5	343.9	SLS	0.011	NA	Clastic Metasediments: Siltstone
TL-17-616	E5552363	344	344.25	SLS	0.009	NA	Intermediate-Felsic Intrusives: Feldspar Porphyry
TL-18-673	E5552371	114.62	114.84	SLS	0.0025	NA	Intermediate Metavolcanics: Ash Tuff
TL-18-673	E5552372	204.65	204.85	SLS	0.0025	NA	Clastic Metasediments: Mudstone
TL-18-673	E5552373	280.23	280.45	SLS	0.0025	NA	Clastic Metasediments: Mudstone
TL-18-673	E5552374	309	309.2	SLS	0.007	NA	Clastic Metasediments: Greywacke
TL-18-675	E5552375	222.28	222.5	SLS	0.0025	NA	Clastic Metasediments: Mudstone
TL-18-675	E5552376	310.23	310.45	SLS	0.009	NA	Intermediate Metavolcanics: Feldspar Phyric Flow
TL-18-675	E5552377	392.19	392.43	SLS	0.036	NA	Felsic Metavolcanics: Undifferentiated Tuff
TL-18-676	E5552378	191.6	191.75	SLS	0.0025	NA	Clastic Metasediments: Siltstone
TL-18-676	E5552379	196.3	196.53	SLS	0.0025	NA	Clastic Metasediments: Conglomerate
TL-18-676	E5552380	245.73	245.87	SLS	0.0025	NA	Clastic Metasediments: Conglomerate
TL-18-676	E5552381	316.14	316.33	SLS	0.0025	NA	Clastic Metasediments: Conglomerate

*Samples in Table 3-1 are listed by the Hole ID. “Intermediate-Felsic Intrusives: Feldspar Porphyry” samples are labeled in blue, “Intermediate-Felsic Intrusives: Quartz-Feldspar Porphyry” samples are labeled in yellow, “Intermediate Metavolcanics” are labeled in green, “Felsic Metavolcanics” are labeled in pink, and “Clastic Metasediments” are labeled in purple. TW=Twin Lakes, TLE=Twin Lakes East, TLW=Twin Lakes West, SLS=South Limb Shear, ME=Mideast.

Appendix C: Synchrotron X-ray Diffraction (SR-XRD)

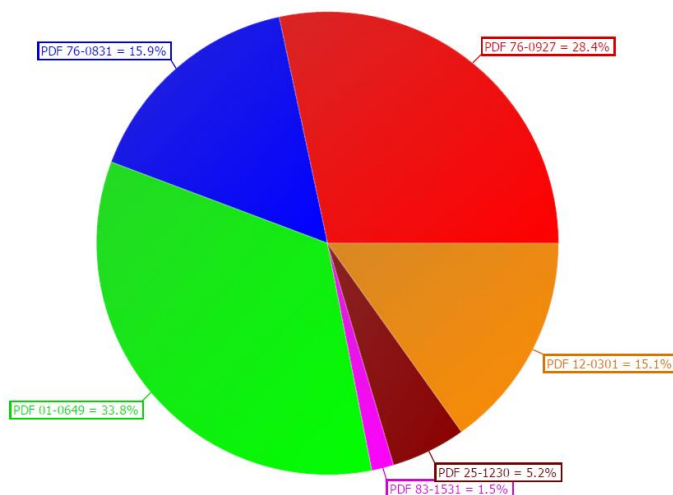
Sample Number	2819	Drill Hole	TL-16-575	Depth	154.1-154.32 m
Lithology	FP	Target	TL	Gold Grade	7.21 ppm



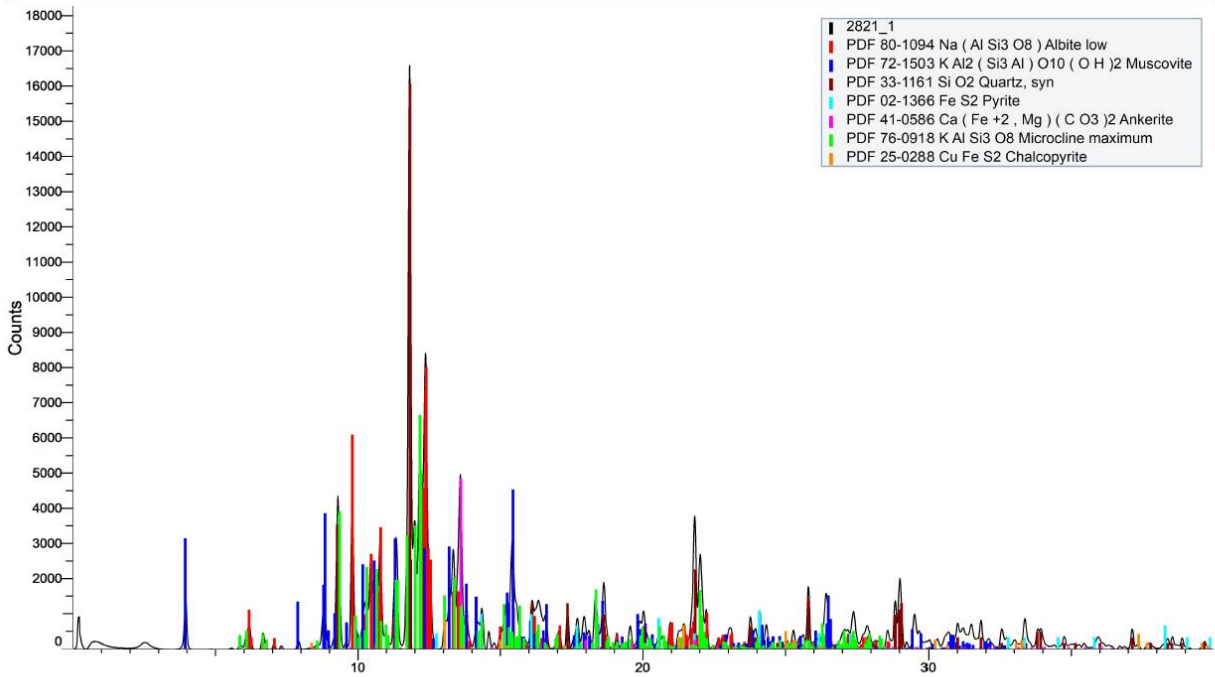
Pattern List #1

Show	Icon	Compound Name	S-Q	Concentration Level	Formula
Yes	■	Quartz	33.8%	Major	Si O ₂
Yes	■	Albite calcian low	28.4%	Major	(Na _{0.84} Ca _{0.16}) Al _{1.16} Si _{2.84} O ₈
Yes	■	Microline maximum	15.9%	Major	K _{0.94} Na _{0.06} Al _{1.01} Si _{2.99} O ₈
Yes	■	Anorthite, ordered	15.1%	Major	Ca Al ₂ Si ₂ O ₈
Yes	■	Arsenopyrite	5.2%	Major	Fe As S
Yes	■	Ankerite	1.5%	Minor	Ca Mg _{0.32} Fe _{0.68} (C O ₃) ₂

S-Q

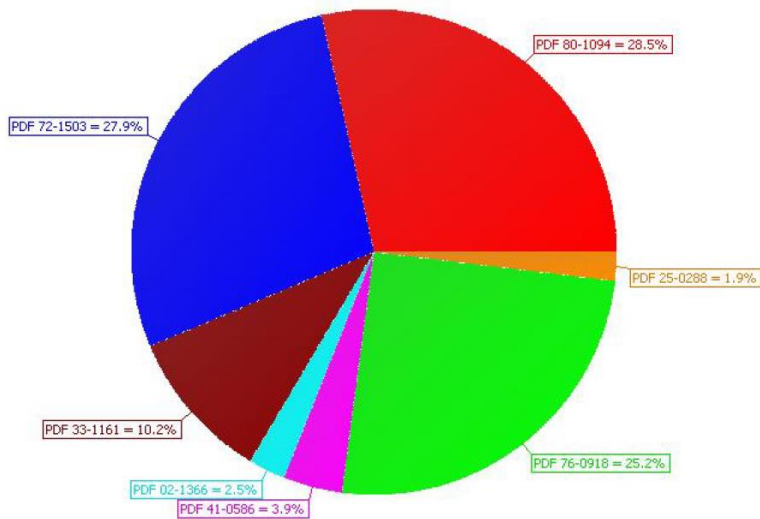


Sample Number	2821	Drill Hole	TL-16-575	Depth	183.78-184.06 m
Lithology	Ash Tuff	Target	TL	Gold Grade	3.38 ppm

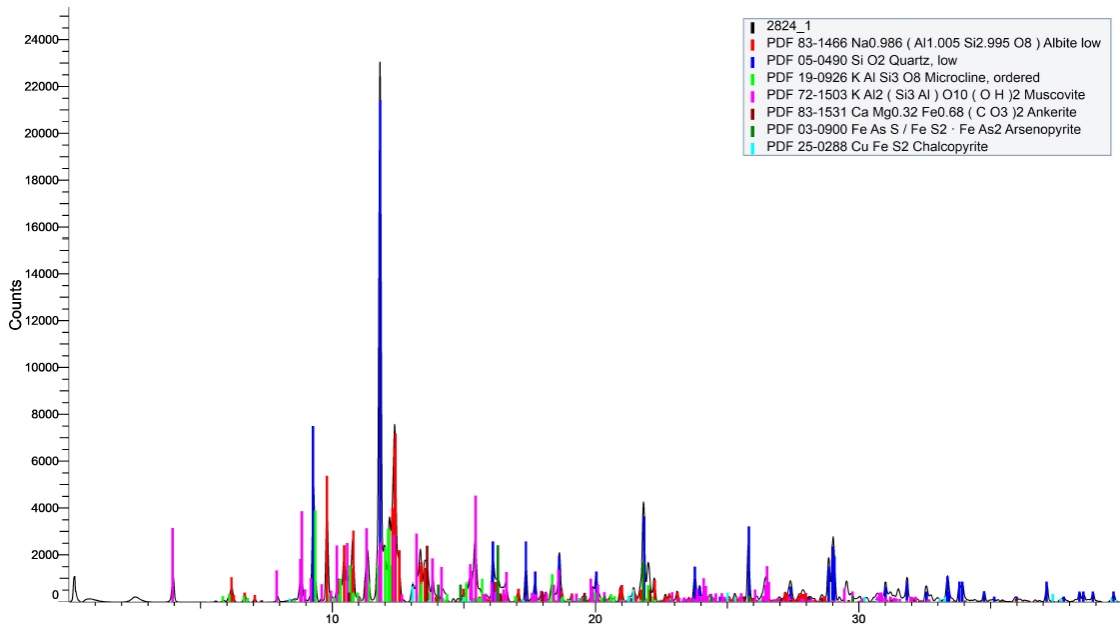


Show	Icon	Compound Name	S-Q	Concentration Level	Formula
Yes		Albite low	28.5%	Major	Na (Al Si3 O8)
Yes		Muscovite	27.9%	Major	K Al2 (Si3 Al) O10 (OH)2
Yes		Microcline maximum	25.2%	Major	K Al Si3 O8
Yes		Quartz, syn	10.2%	Major	Si O2
Yes		Ankerite	3.9%	Minor	Ca (Fe +2 , Mg) (C O3)2
Yes		Pyrite	2.5%	Minor	Fe S2
Yes		Chalcopyrite	1.9%	Minor	Cu Fe S2

S-Q



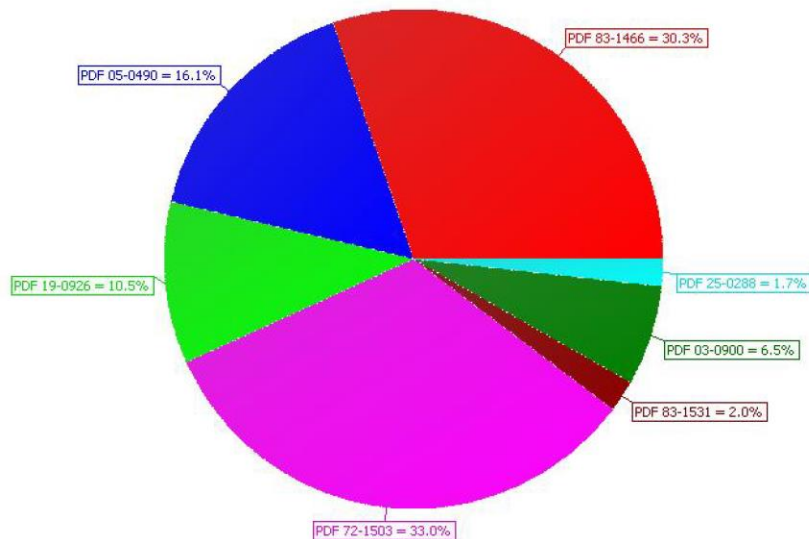
Sample Number	2824	Drill Hole	TL-15-568	Depth	200.62-200.82 m
Lithology	FP	Target	TLW	Gold Grade	1.91- ~8.25 ppm



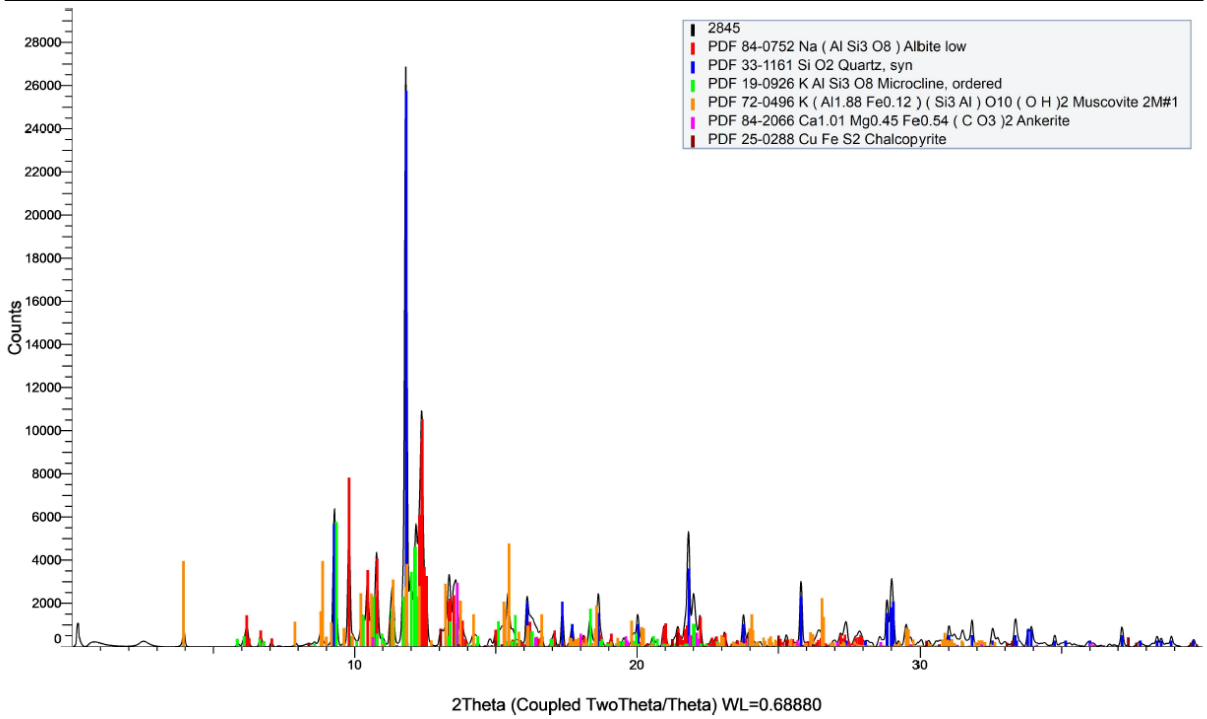
2Theta (Coupled TwoTheta/Theta) WL=0.68880

Show	Icon	Color	Compound Name	Formula	Quality	S-Q	Concentration Level
Yes			Quartz, low	Si O2	Star (*)	16.1%	Major
Yes			Albite low	Na0.986 (Al1.005 Si2.995 O8)	Calculated	30.3%	Major
Yes			Muscovite	K Al2 (Si3 Al) O10 (O H)2	Calculated	33.0%	Major
Yes			Microcline, ordered	K Al Si3 O8	Star (*)	10.5%	Major
Yes			Arsenopyrite	Fe As S / Fe S2 · Fe As2	Blank	6.5%	Major
Yes			Ankerite	Ca Mg0.32 Fe0.68 (C O3)2	Calculated	2.0%	Minor
Yes			Chalcopyrite	Cu Fe S2	Indexed	1.7%	Minor

S-Q

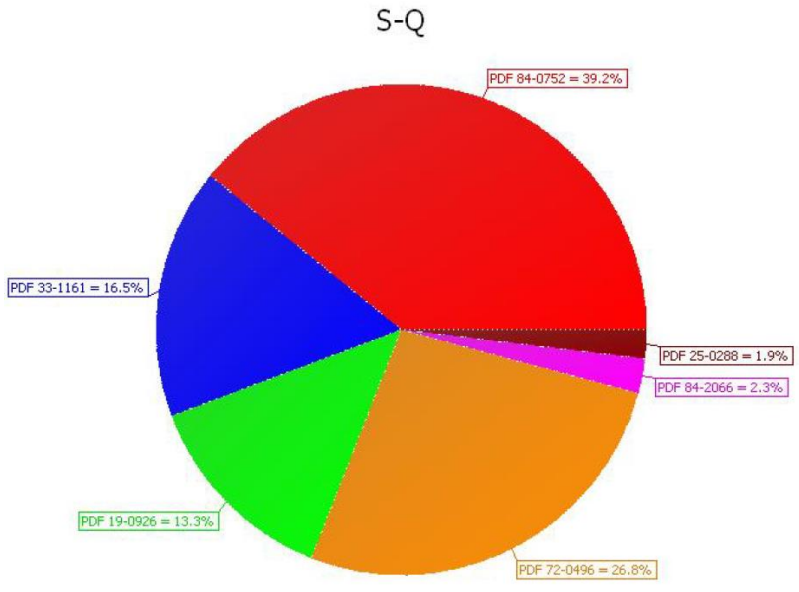


Sample Number	2845	Drill Hole	TL-13-509	Depth	235.6-235.86 m
Lithology	QFP	Target	TLW	Gold Grade	1.13 ppm

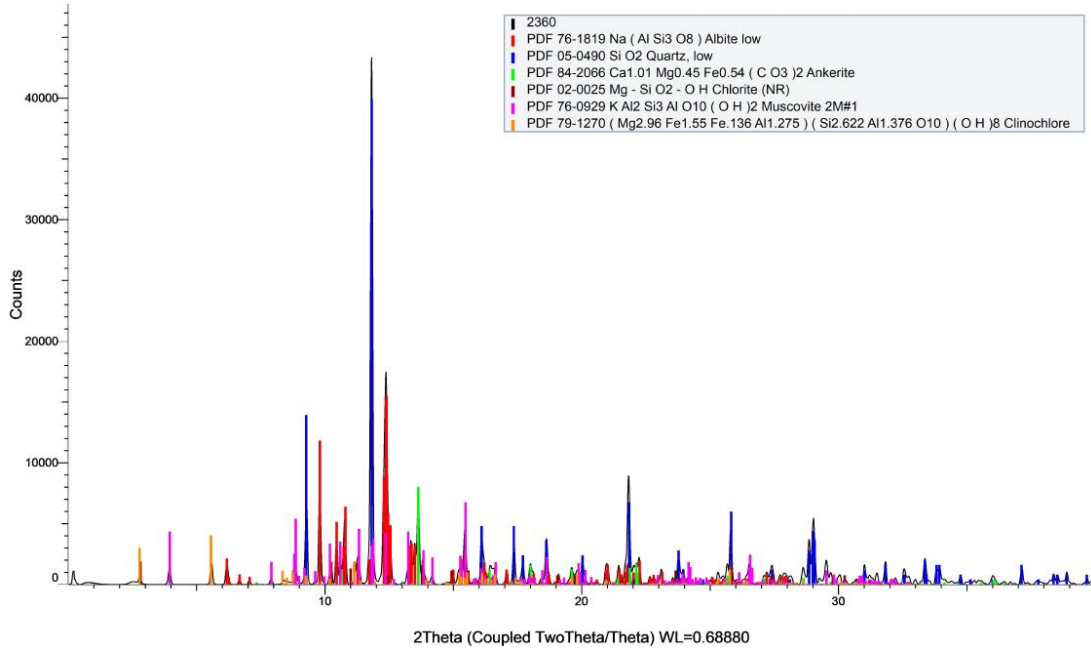


Pattern List #1

Show	Icon	Compound Name	S-Q	Concentration Level	Formula
Yes		Albite low	39.2%	Major	Na (Al Si3 O8)
Yes		Muscovite 2M#1	26.8%	Major	K (Al1.88 Fe0.12) (Si3 Al) O10 (O H)2
Yes		Quartz, syn	16.5%	Major	Si O2
Yes		Microcline, ordered	13.3%	Major	K Al Si3 O8
Yes		Ankerite	2.3%	Minor	Ca1.01 Mg0.45 Fe0.54 (C O3)2
Yes		Chalcopyrite	1.9%	Minor	Cu Fe S2

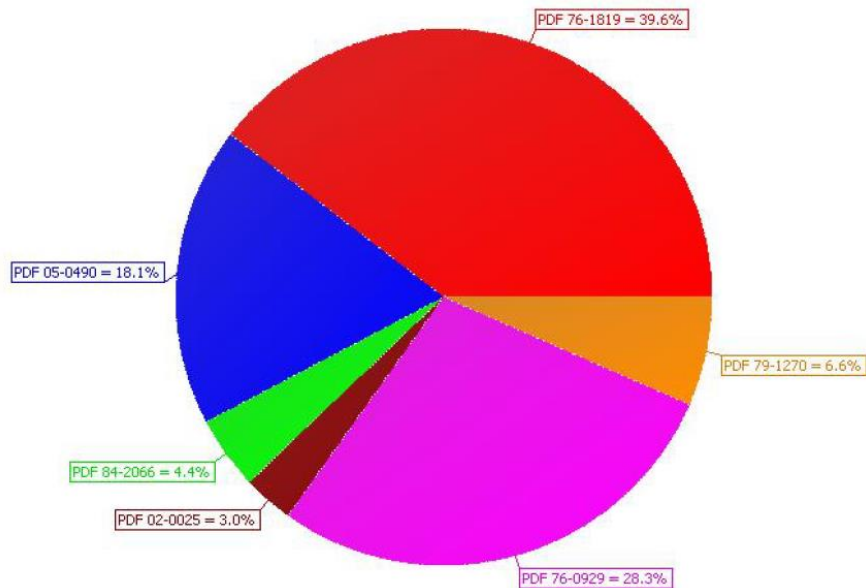


Sample Number	2360	Drill Hole	TL-17-616	Depth	148.6-148.8m
Lithology	Lapilli Tuff	Target	TLE	Gold Grade	1.2-0.01 ppm

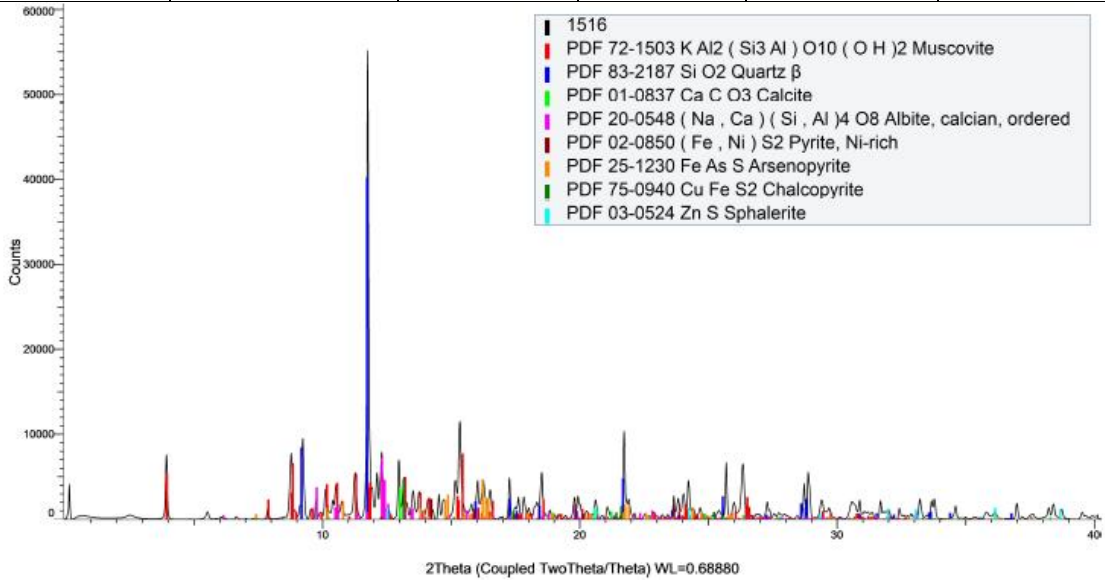


Icon	Compound Name	S-Q	Concentration Level	Formula
	Albite low	39.6%	Major	Na (Al Si3 O8)
	Muscovite 2M#1	28.3%	Major	K Al2 Si3 Al O10 (O H)2
	Quartz, low	18.1%	Major	Si O2
	Clinocllore	6.6%	Major	(Mg2.96 Fe1.55 Fe.136 Al1.275) (Si2.622 Al1.376 O10) (O H)8
	Ankerite	4.4%	Minor	Ca1.01 Mg0.45 Fe0.54 (C O3)2
	Chlorite (NR)	3.0%	Minor	Mg - Si O2 - O H

S-Q

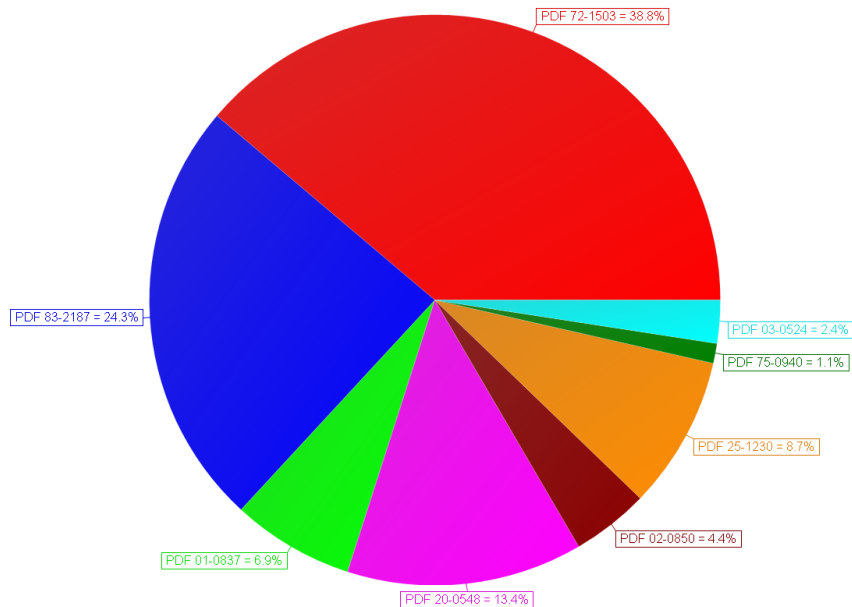


Sample Number	1516*	Drill Hole	TL-13-506	Depth	164.7-165.6 m
Lithology	Chemical Metasediments	Target	TLW	Gold Grade	4.96 ppm

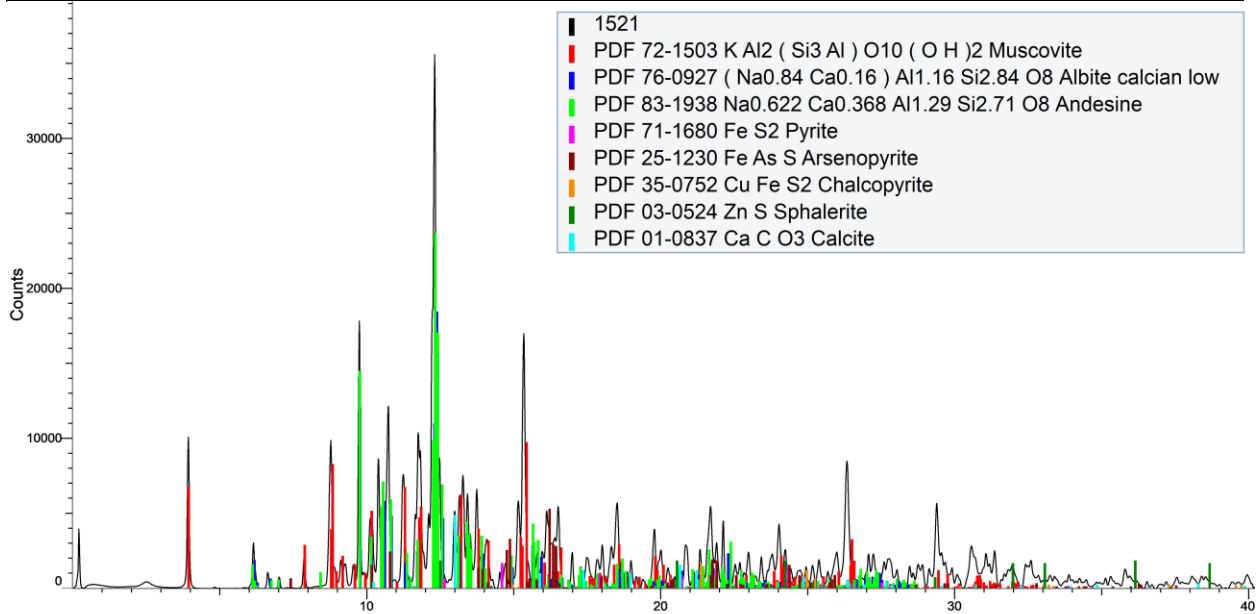


Icon	Color	Compound Name	Formula	Quality	S-Q	Concentration Level
	Red	Muscovite	$K Al_2 (Si_3 Al) O_{10} (OH)_2$	Calculated	38.8%	Major
	Blue	Quartz β	$Si O_2$	Calculated	24.3%	Major
	Green	Calcite	$Ca C O_3$	Blank	6.9%	Major
	Magenta	Albite, calcian, ordered	$(Na , Ca) (Si , Al)_4 O_8$	Calculated	13.4%	Major
	Brown	Pyrite, Ni-rich	$(Fe , Ni) S_2$	Low precision	4.4%	Minor
	Orange	Arsenopyrite	$Fe As S$	Calculated	8.7%	Major
	Dark Green	Chalcopyrite	$Cu Fe S_2$	Calculated	1.1%	Minor
	Cyan	Sphalerite	$Zn S$	Blank	2.4%	Minor

S-Q



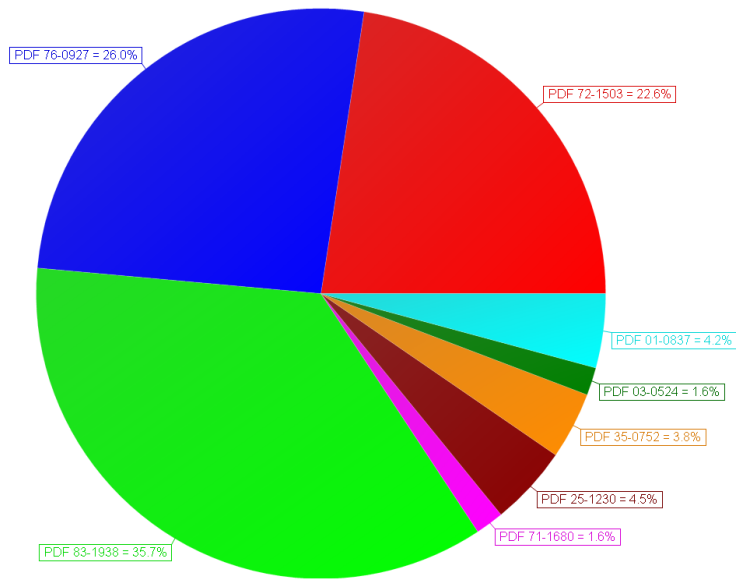
Sample Number	1521*	Drill Hole	TL-14-520	Depth	59-60 m
Lithology from Mining Log	PF	Target	TLW	Gold Grade	6.597 ppm



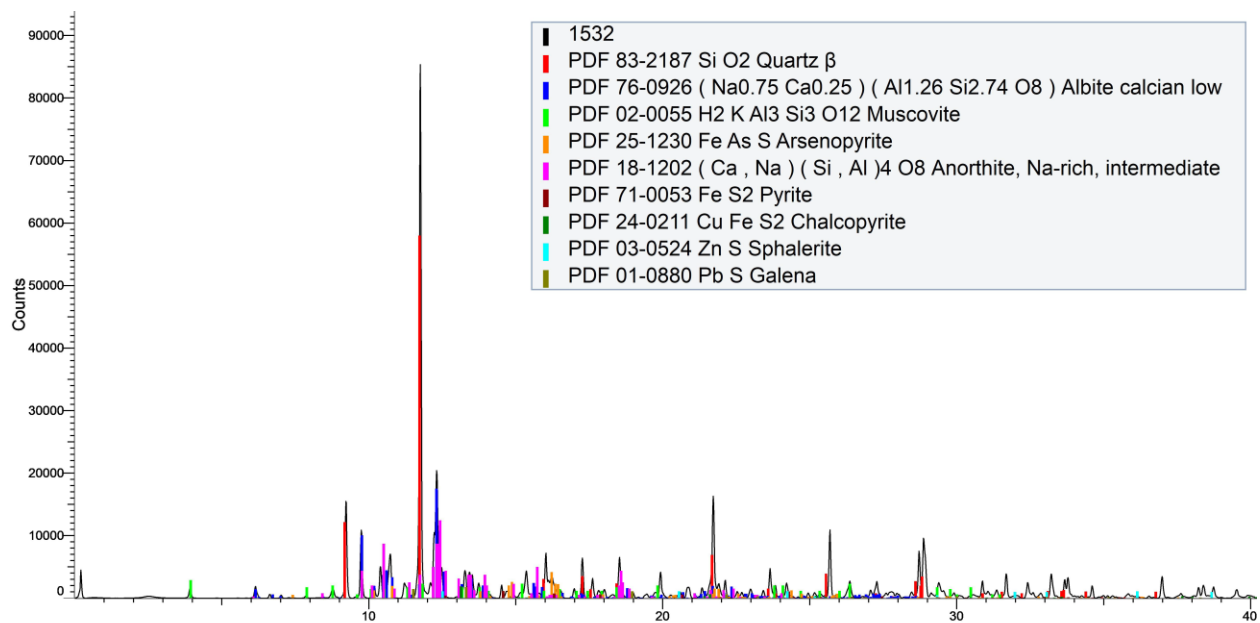
2Theta (Coupled TwoTheta/Theta) WL=0.68880

Icon	Color	Compound Name	Formula	S-Q	Concentration Level
[Red]	Red	Muscovite	$K Al_2 (Si_3 Al) O_{10} (OH)_2$	22.6%	Major
[Blue]	Blue	Albite calcian low	$(Na_{0.84} Ca_{0.16}) Al_{1.16} Si_{2.84} O_8$	26.0%	Major
[Green]	Green	Andesine	$Na_{0.622} Ca_{0.368} Al_{1.29} Si_{2.71} O_8$	35.7%	Major
[Magenta]	Magenta	Pyrite	$Fe S_2$	1.6%	Minor
[Brown]	Brown	Arsenopyrite	$Fe As S$	4.5%	Minor
[Orange]	Orange	Chalcopyrite	$Cu Fe S_2$	3.8%	Minor
[Dark Green]	Dark Green	Sphalerite	$Zn S$	1.6%	Minor
[Cyan]	Cyan	Calcite	$Ca C O_3$	4.2%	Minor

S-Q



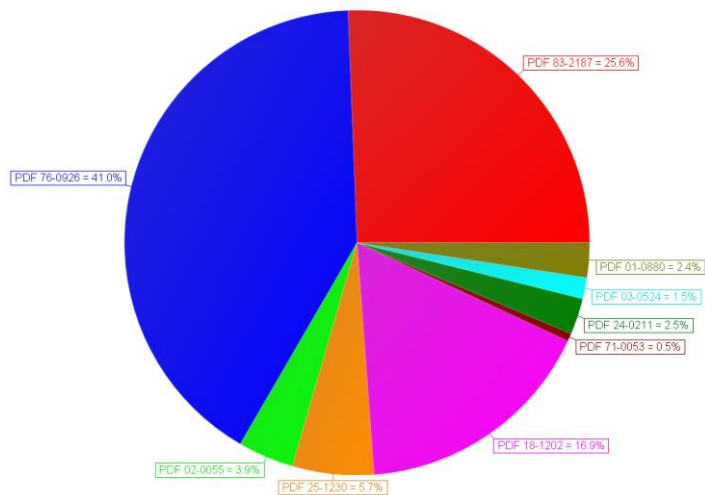
Sample Number	1532*	Drill Hole	TL-12-481	Depth	183.78-184.06 m
Lithology	PF	Target	TL	Gold Grade	3.463 ppm



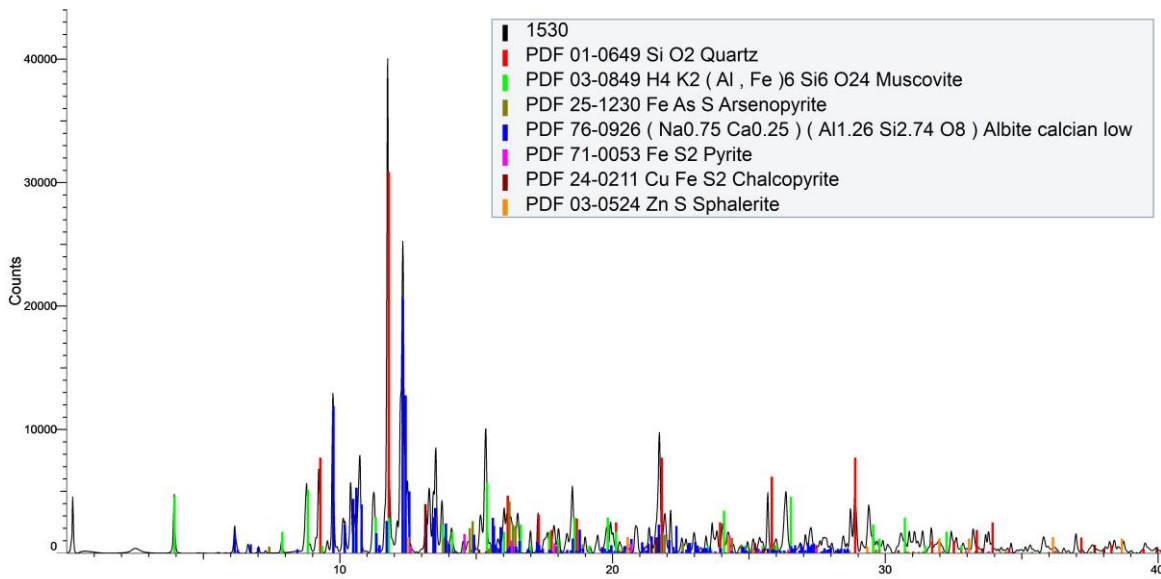
2Theta (Coupled TwoTheta/Theta) WL=0.68880

Icon	Color	Compound Name	Formula	S-Q	Concentration Level
	Red	Quartz β	Si O2	25.6%	Major
	Blue	Albite calcian low	(Na0.75 Ca0.25) (Al1.26 Si2.74 O8)	41.0%	Major
	Green	Muscovite	H2 K Al3 Si3 O12	3.9%	Minor
	Orange	Arsenopyrite	Fe As S	5.7%	Major
	Magenta	Anorthite, Na-rich, intermediate	(Ca . Na) (Si . Al)4 O8	16.9%	Major
	Brown	Pyrite	Fe S2	0.5%	Trace
	Dark Green	Chalcopyrite	Cu Fe S2	2.5%	Minor
	Cyan	Sphalerite	Zn S	1.5%	Minor
	Olive	Galena	Pb S	2.4%	Minor

S-Q

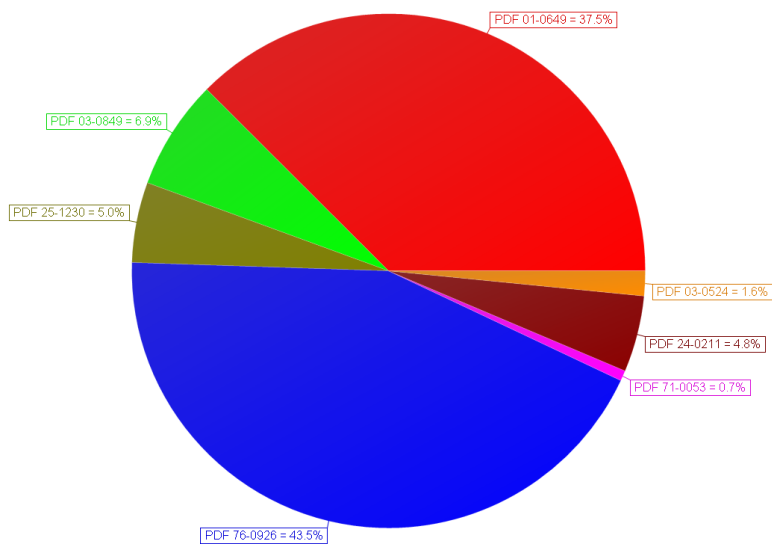


Sample Number	1530*	Drill Hole	TL-03-160	Depth	183.78-184.06 m
Lithology	Heterolithic Tuff	Target	ME	Gold Grade	3.28

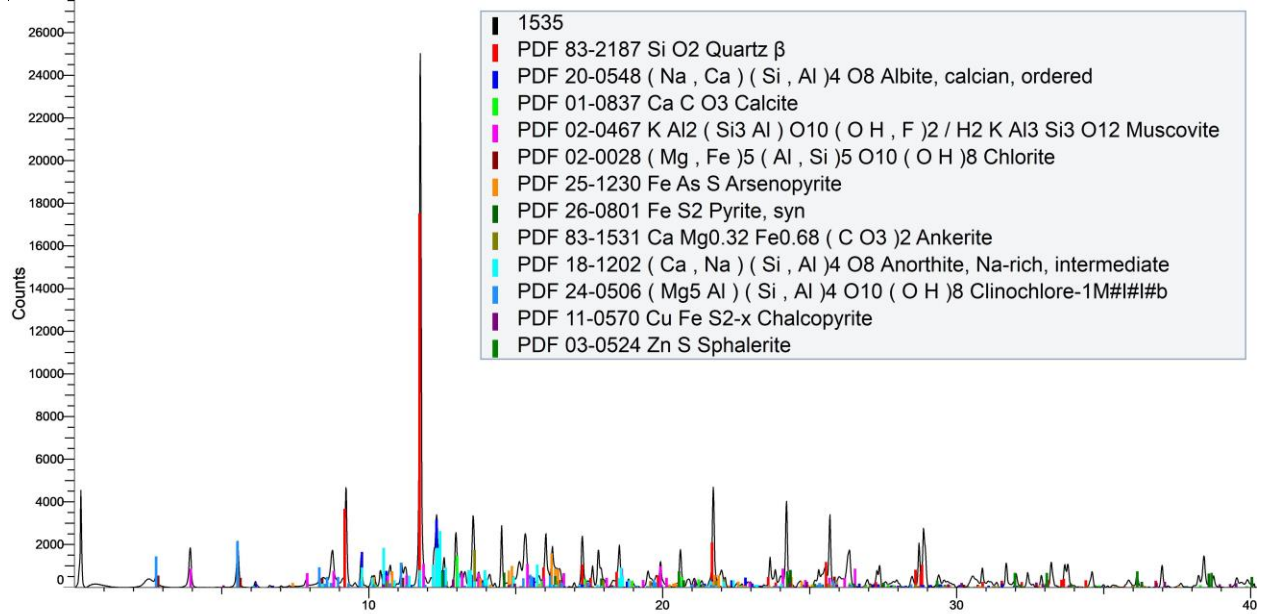


Show	Icon	Color	Compound Name	Formula	S-Q	Concentration Level
Yes			Quartz	Si O2	37.5%	Major
Yes			Muscovite	H4 K2 (Al , Fe)6 Si6 O24	6.9%	Major
Yes			Arsenopyrite	Fe As S	5.0%	Major
Yes			Albite calcian low	(Na0.75 Ca0.25) (Al1.26 Si2.74 O8)	43.5%	Major
Yes			Pyrite	Fe S2	0.7%	Trace
Yes			Chalcopyrite	Cu Fe S2	4.8%	Minor
Yes			Sphalerite	Zn S	1.6%	Minor

S-Q



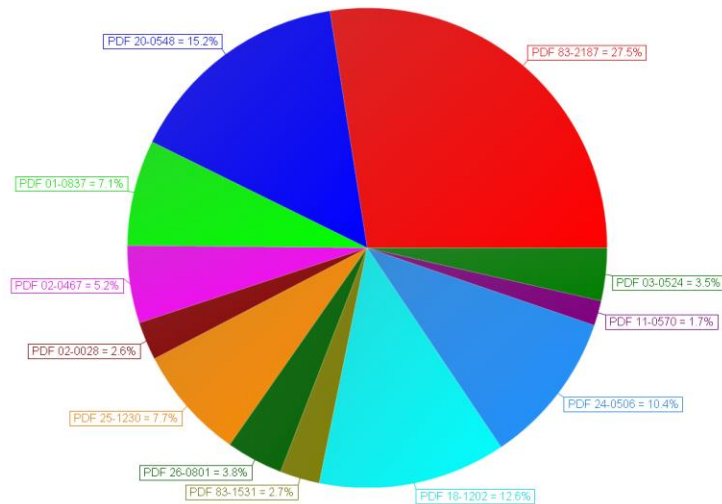
Sample Number	1535*	Drill Hole	TL-11-419	Depth	83-84 m
Lithology	Metasiltstone	Target	TLW	Gold Grade	4.969 ppm



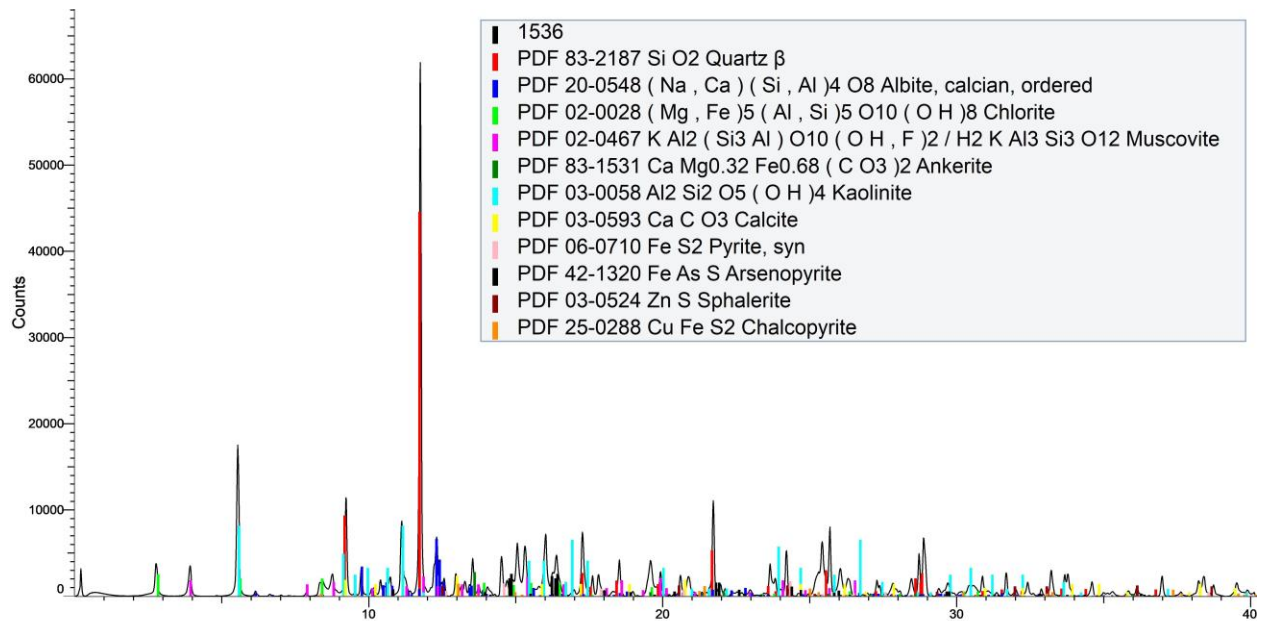
2Theta (Coupled TwoTheta/Theta) WL=0.68880

Show	Icon	Color	Compound Name	Formula	S-Q	Concentration Level
Yes		Red	Quartz β	Si O2	27.5%	Major
Yes		Blue	Albite, calcian, ordered	(Na , Ca) (Si , Al)4 O8	15.2%	Major
Yes		Green	Calcite	Ca C O3	7.1%	Major
Yes		Magenta	Muscovite	K Al2 (Si3 Al) O10 (O H , F)2 / H2 K Al3 Si3 O12	5.2%	Major
Yes		Brown	Chlorite	(Mg , Fe)5 (Al , Si)5 O10 (O H)8	2.6%	Minor
Yes		Orange	Arsenopyrite	Fe As S	7.7%	Major
Yes		Dark Green	Pyrite, syn	Fe S2	3.8%	Minor
Yes		Olive	Ankerite	Ca Mg0.32 Fe0.68 (C O3)2	2.7%	Minor
Yes		Cyan	Anorthite, intermediate Na-rich,	(Ca , Na) (Si , Al)4 O8	12.6%	Major
Yes		Light Blue	Clinocllore-1M#1#b	(Mg5 Al) (Si , Al)4 O10 (O H)8	10.4%	Major
Yes		Purple	Chalcopyrite	Cu Fe S2-x	1.7%	Minor
Yes		Dark Green	Sphalerite	Zn S	3.5%	Minor

S-Q



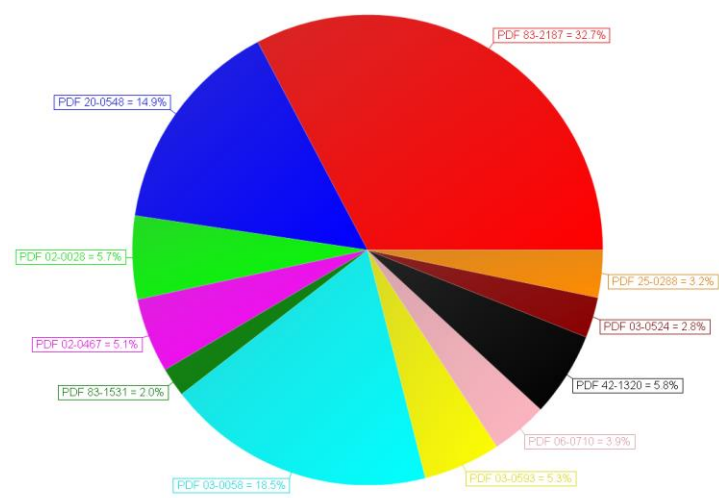
Sample Number	1536*	Drill Hole	TL-11-419	Depth	84-85 m
Lithology	Metasiltstone	Target	TLW	Gold Grade	3.435 ppm



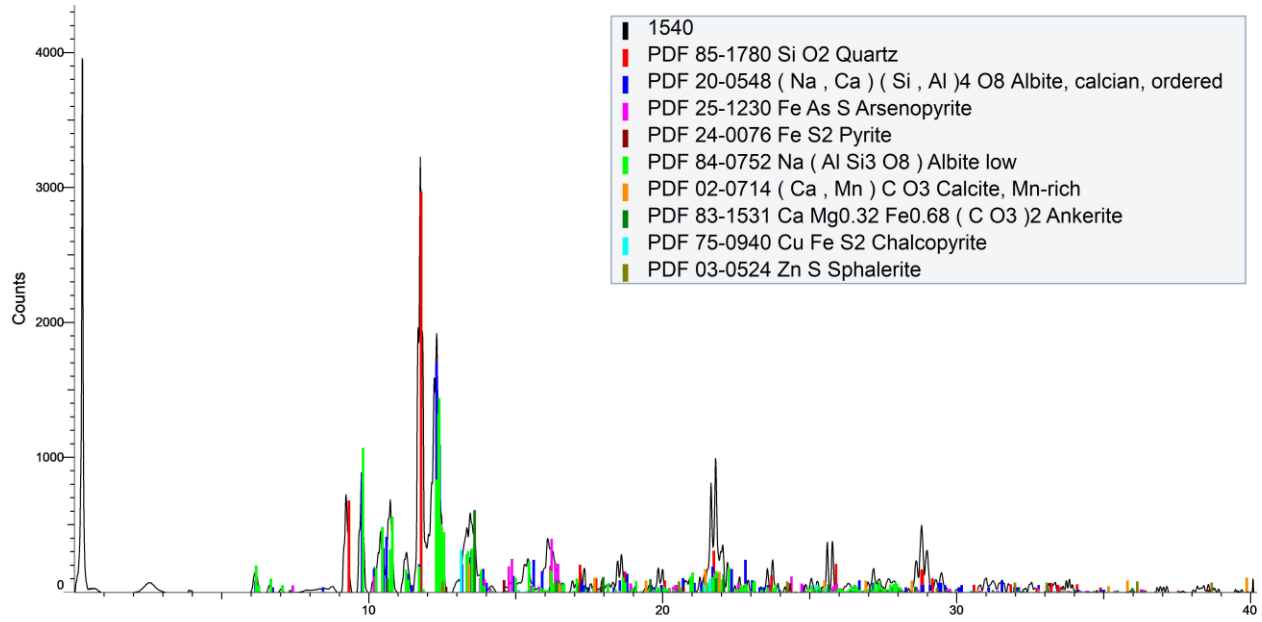
2Theta (Coupled TwoTheta/Theta) WL=0.68880

Show	Icon	Color	Compound Name	Formula	S-Q	Concentration Level
Yes		Red	Quartz β	Si O2	32.7%	Major
Yes		Blue	Albite, calcian, ordered	(Na , Ca) (Si , Al)4 O8	14.9%	Major
Yes		Green	Chlorite	(Mg , Fe)5 (Al , Si)5 O10 (O H)8	5.7%	Major
Yes		Magenta	Muscovite	K Al2 (Si3 Al) O10 (O H , F)2 / H2 K Al3 Si3 O12	5.1%	Major
Yes		Dark Green	Ankerite	Ca Mg0.32 Fe0.68 (C O3)2	2.0%	Minor
Yes		Cyan	Kaolinite	Al2 Si2 O5 (O H)4	18.5%	Major
Yes		Yellow	Calcite	Ca C O3	5.3%	Major
Yes		Pink	Pyrite, syn	Fe S2	3.9%	Minor
Yes		Black	Arsenopyrite	Fe As S	5.8%	Major
Yes		Brown	Sphalerite	Zn S	2.8%	Minor
Yes		Orange	Chalcopyrite	Cu Fe S2	3.2%	Minor

S-Q

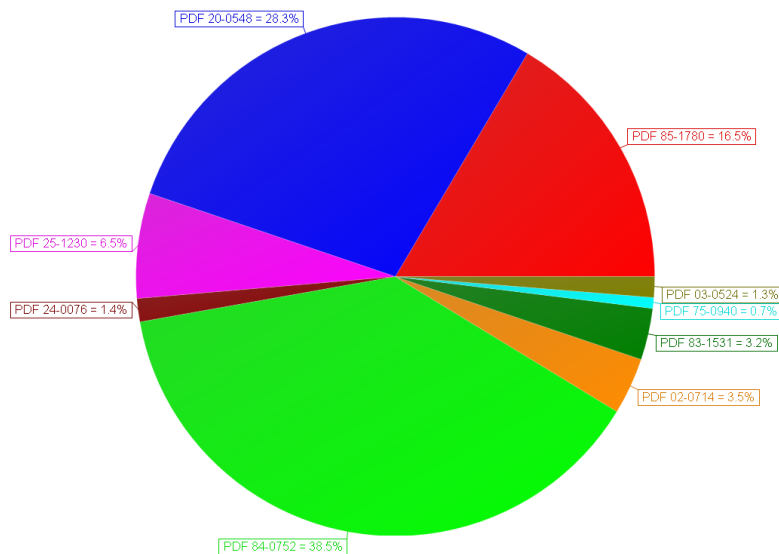


Sample Number	1540*	Drill Hole	TL-11-419	Depth	88-89 m
Lithology	PF	Target	TLW	Gold Grade	1.556 ppm

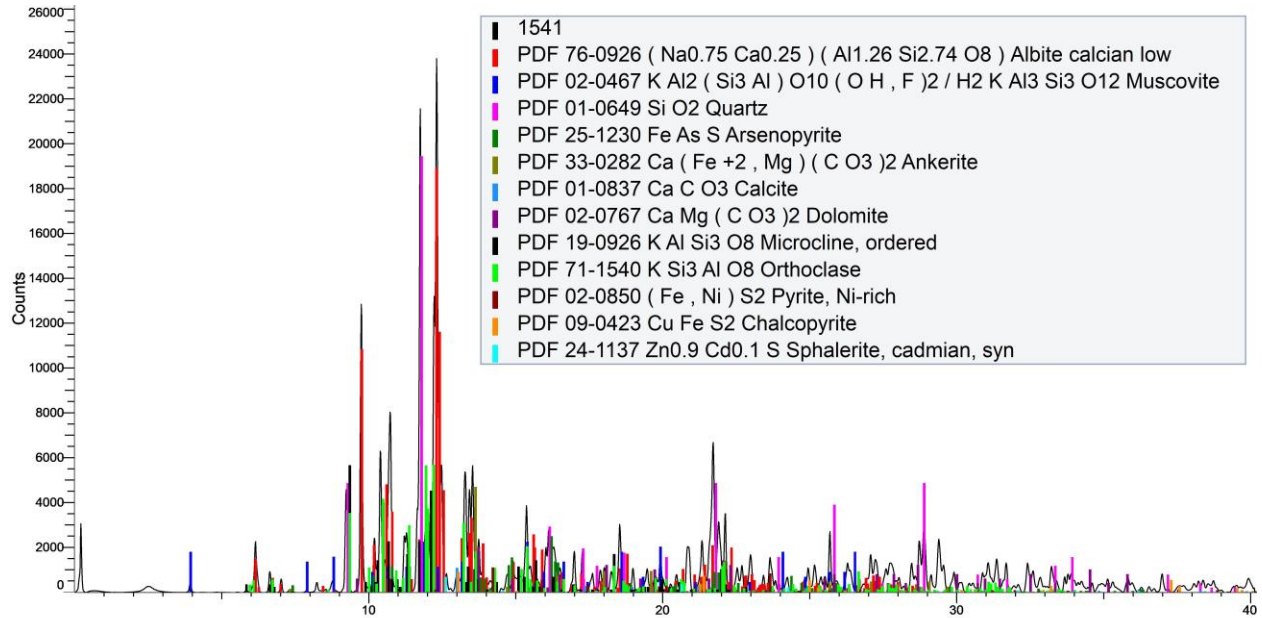


Show	Icon	Color	Compound Name	Formula	S-Q	Concentration Level
Yes		Red	Quartz	Si O2	16.5%	Major
Yes		Blue	Albite, calcian, ordered	(Na , Ca) (Si , Al)4 O8	28.3%	Major
Yes		Magenta	Arsenopyrite	Fe As S	6.5%	Major
Yes		Brown	Pyrite	Fe S2	1.4%	Minor
Yes		Green	Albite low	Na (Al Si3 O8)	38.5%	Major
Yes		Orange	Calcite, Mn-rich	(Ca , Mn) C O3	3.5%	Minor
Yes		Dark Green	Ankerite	Ca Mg0.32 Fe0.68 (C O3)2	3.2%	Minor
Yes		Cyan	Chalcopyrite	Cu Fe S2	0.7%	Trace
Yes		Olive	Sphalerite	Zn S	1.3%	Minor

S-Q

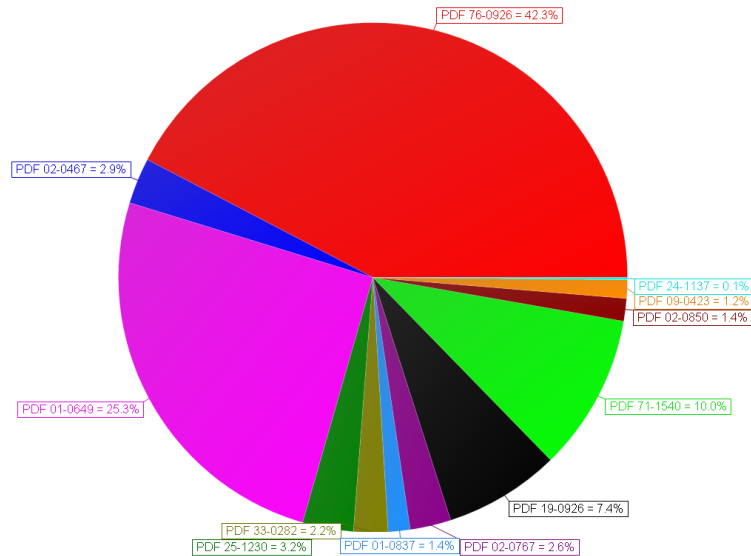


Sample Number	1541*	Drill Hole	TL-11-419	Depth	89-90 m
Lithology	PF	Target	TLW	Gold Grade	2.816ppm

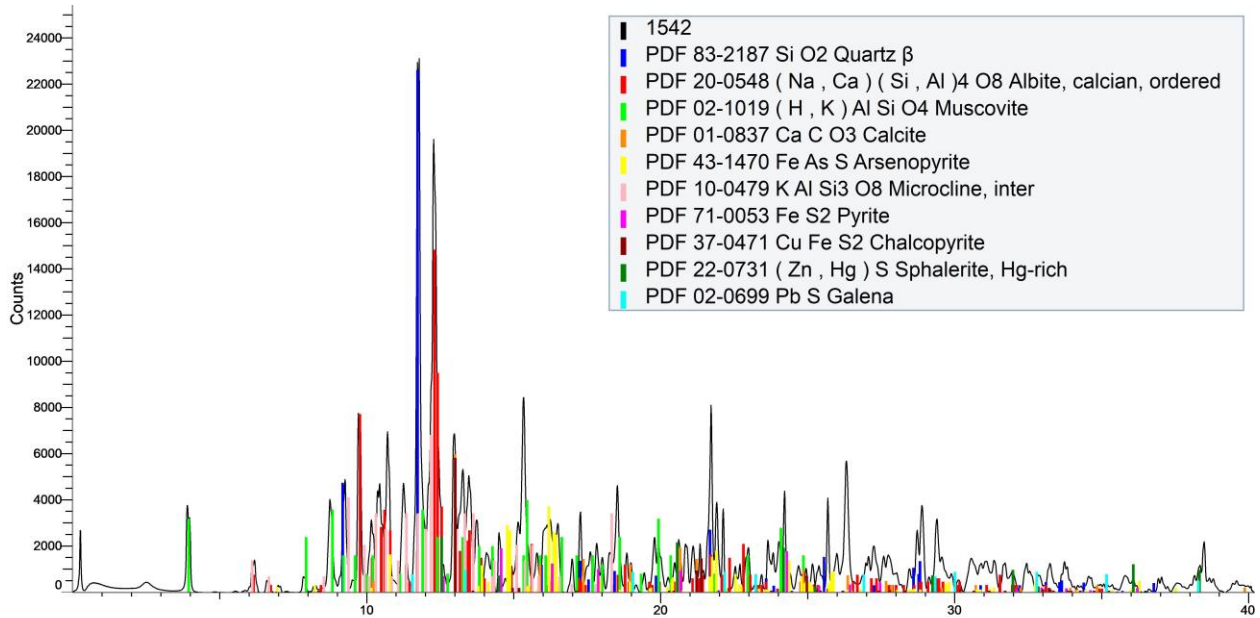


Show	Icon	Color	Compound Name	Formula	S-Q	Concentration Level
Yes		Red	Albite calcian low	(Na0.75 Ca0.25) (Al1.26 Si2.74 O8)	42.3%	Major
Yes		Blue	Muscovite	K Al2 (Si3 Al) O10 (O H , F)2 / H2 K Al3 Si3 O12	2.9%	Minor
Yes		Magenta	Quartz	Si O2	25.3%	Major
Yes		Green	Arsenopyrite	Fe As S	3.2%	Minor
Yes		Olive	Ankerite	Ca (Fe +2 , Mg) (C O3)2	2.2%	Minor
Yes		Light blue	Calcite	Ca C O3	1.4%	Minor
Yes		Purple	Dolomite	Ca Mg (C O3)2	2.6%	Minor
Yes		Black	Microcline, ordered	K Al Si3 O8	7.4%	Major
Yes		Light green	Orthoclase	K Si3 Al O8	10.0%	Major
Yes		Brown	Pyrite, Ni-rich	(Fe , Ni) S2	1.4%	Minor
Yes		Orange	Chalcopyrite	Cu Fe S2	1.2%	Minor
Yes		Cyan	Sphalerite, cadmian, syn	Zn0.9 Cd0.1 S	0.1%	Trace

S-Q

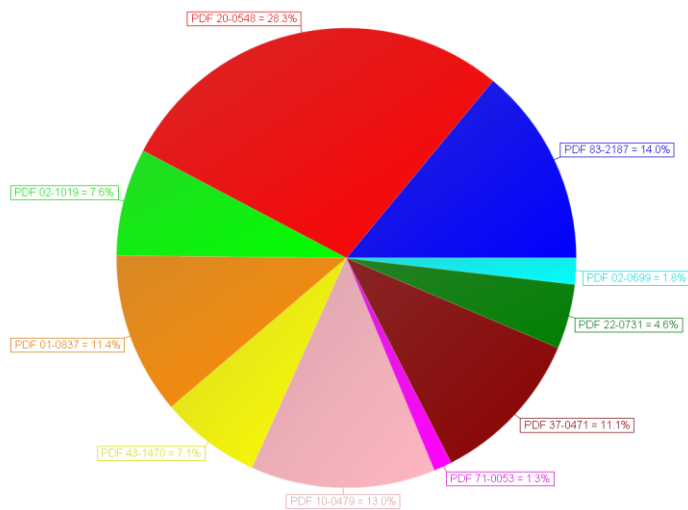


Sample Number	1542*	Drill Hole	TL-11-419	Depth	90-91 m
Lithology	Lapilli Tuff	Target	TLW	Gold Grade	3.541 ppm

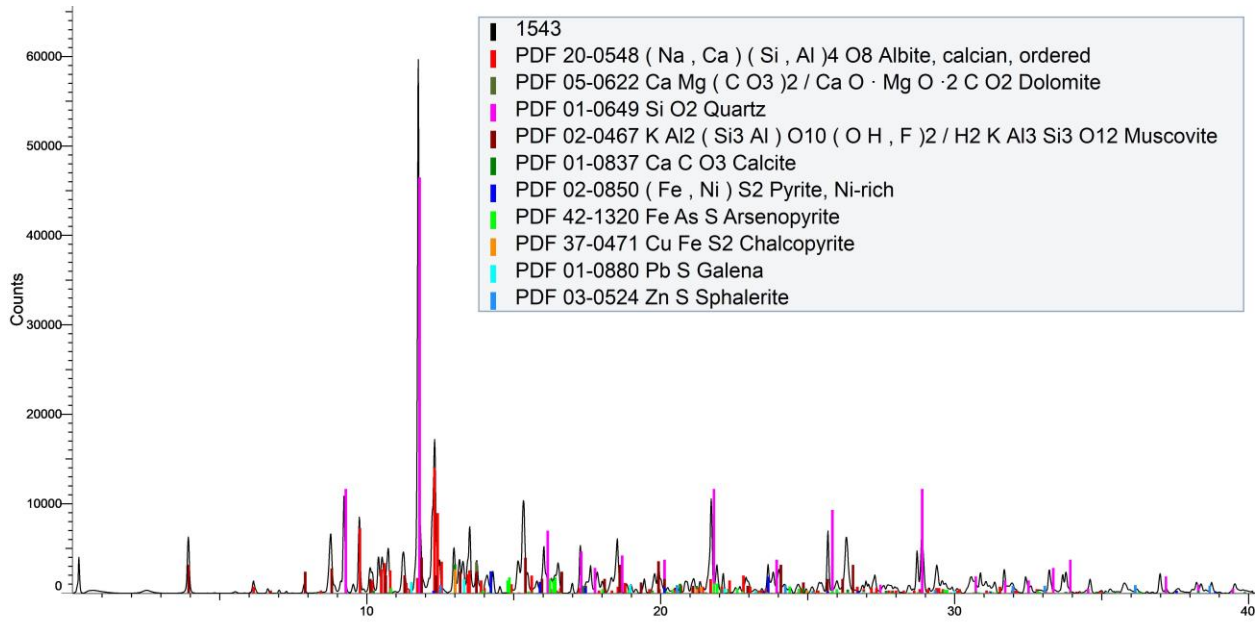


Show	Icon	Color	Compound Name	Formula	S-Q	Concentration Level
Yes		Blue	Quartz β	Si O2	14.0%	Major
Yes		Red	Albite, calcian, ordered	(Na , Ca) (Si , Al)4 O8	28.3%	Major
Yes		Green	Muscovite	(H , K) Al Si O4	7.6%	Major
Yes		Orange	Calcite	Ca C O3	11.4%	Major
Yes		Yellow	Arsenopyrite	Fe As S	7.1%	Major
Yes		Pink	Microcline, inter	K Al Si3 O8	13.0%	Major
Yes		Magenta	Pyrite	Fe S2	1.3%	Minor
Yes		Dark red	Chalcopyrite	Cu Fe S2	11.1%	Major
Yes		Dark green	Sphalerite, Hg-rich	(Zn , Hg) S	4.6%	Minor
Yes		Cyan	Galena	Pb S	1.8%	Minor

S-Q

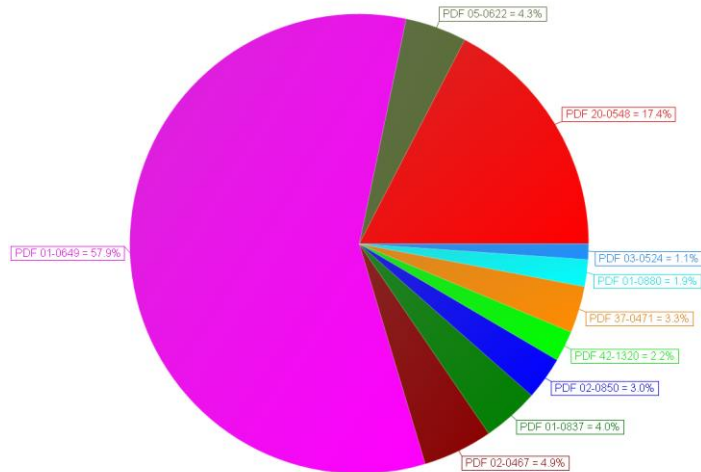


Sample Number	1543*	Drill Hole	TL-11-419	Depth	91-92 m
Lithology	Lapilli Tuff	Target	TLW	Gold Grade	4.135 ppm

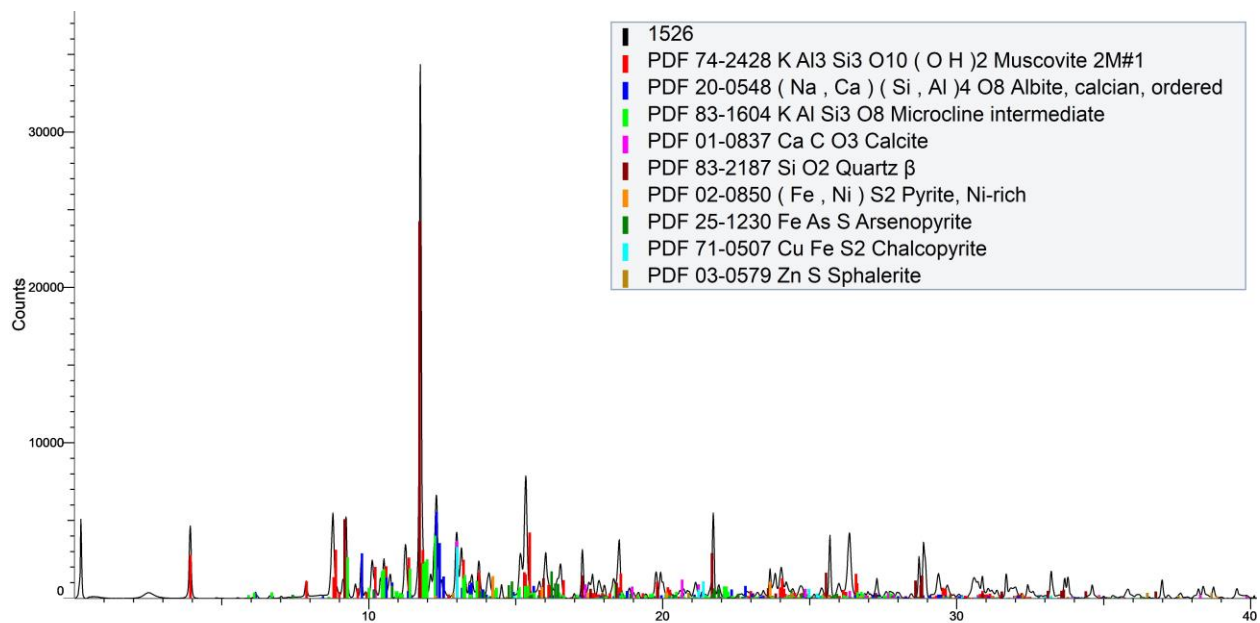


Show	Icon	Color	Compound Name	Formula	S-Q	Concentration Level
Yes		Red	Albite, calcian, ordered	(Na, Ca) (Si, Al)4 O8	17.4%	Major
Yes		Green	Dolomite	Ca Mg (C O3)2 / Ca O · Mg O · 2 C O2	4.3%	Minor
Yes		Magenta	Quartz	Si O2	57.9%	Major
Yes		Brown	Muscovite	K Al2 (Si3 Al) O10 (O H, F)2 / H2 K Al3 Si3 O12	4.9%	Minor
Yes		Dark Green	Calcite	Ca C O3	4.0%	Minor
Yes		Blue	Pyrite, Ni-rich	(Fe, Ni) S2	3.0%	Minor
Yes		Light Green	Arsenopyrite	Fe As S	2.2%	Minor
Yes		Orange	Chalcopyrite	Cu Fe S2	3.3%	Minor
Yes		Cyan	Galena	Pb S	1.9%	Minor
Yes		Light Blue	Sphalerite	Zn S	1.1%	Minor

S-Q



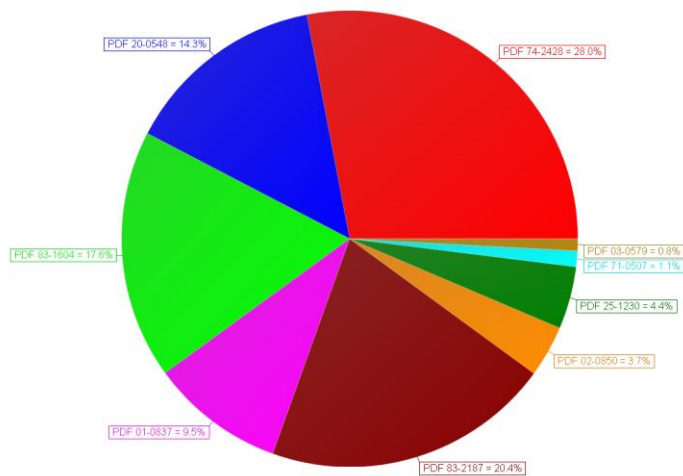
Sample Number	1526*	Drill Hole	TL-12-468	Depth	243-244 m
Lithology	Ash Tuff	Target	ME	Gold Grade	1.112 ppm



2Theta (Coupled TwoTheta/Theta) WL=0.68880

Show	Icon	Color	Compound Name	Formula	S-Q	Concentration Level
Yes			Muscovite 2M#1	K Al ₃ Si ₃ O ₁₀ (OH) ₂	28.0%	Major
Yes			Albite, calcian, ordered	(Na, Ca) (Si, Al) ₄ O ₈	14.3%	Major
Yes			Microcline intermediate	K Al Si ₃ O ₈	17.6%	Major
Yes			Calcite	Ca C O ₃	9.5%	Major
Yes			Quartz beta	Si O ₂	20.4%	Major
Yes			Pyrite, Ni-rich	(Fe, Ni) S ₂	3.7%	Minor
Yes			Arsenopyrite	Fe As S	4.4%	Minor
Yes			Chalcopyrite	Cu Fe S ₂	1.1%	Minor
Yes			Sphalerite	Zn S	0.8%	Trace

S-Q



Appendix D: Synchrotron Micro-X-ray Fluorescence Data Processing and Maps

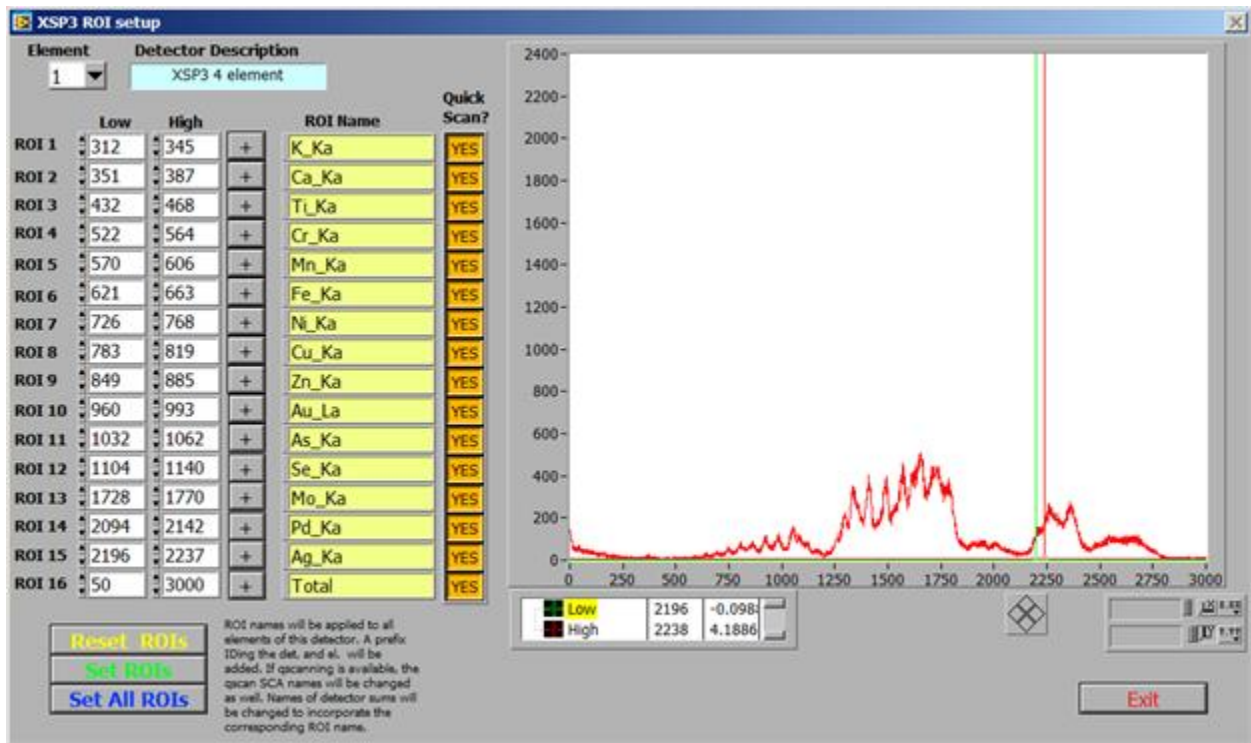
APS 20ID-Feb. 2019

Beamtime and Beamline Details:

Detector: XSP3 4 element detector

Monochromator Crystal Set: Si (311)

ROI Setup applied to all elements of the detector: K $K\alpha$, Ca $K\alpha$, Ti $K\alpha$, Cr $K\alpha$, Mn $K\alpha$, Fe $K\alpha$, Ni $K\alpha$, Cu $K\alpha$, Zn $K\alpha$, Au $L\alpha$, As $K\alpha$, Se $K\alpha$, Mo $K\alpha$, Pd $K\alpha$, Ag $K\alpha$ and total sum



Incident Energy: 27 KeV

Max energy: 41 KeV

Mode: Quick scan

Beam spot size: 800 μm x 800 μm & 300 μm x 300 μm

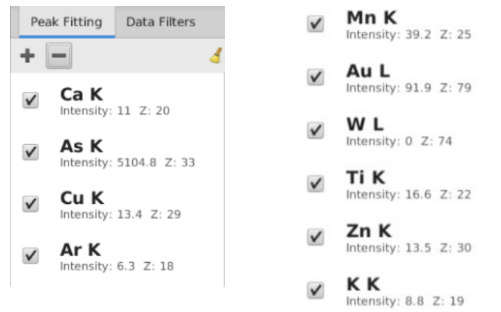
Dwell time: 250 msec

Use standard to calibrate: NIST SRM 610, 612, 614

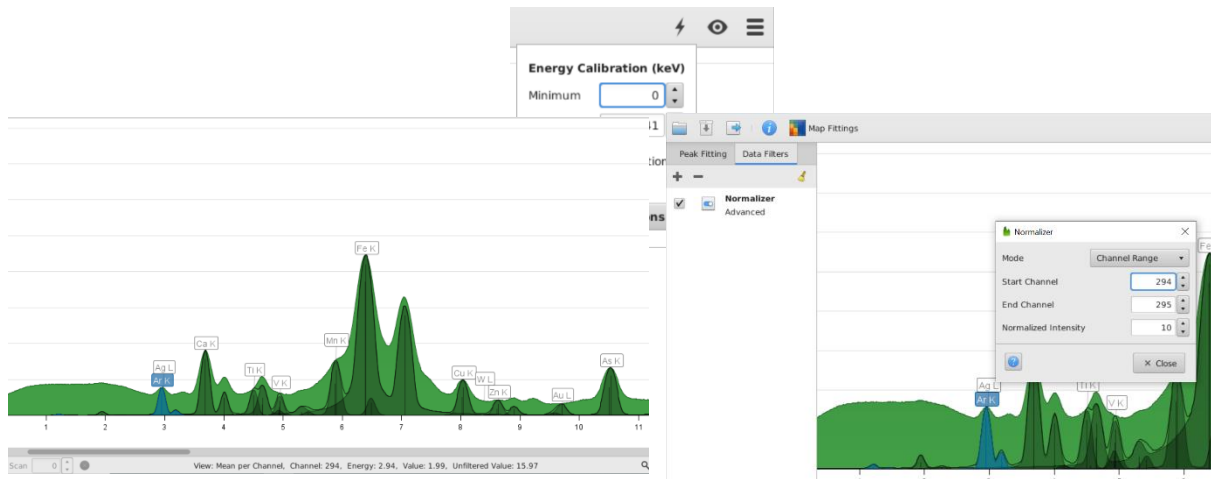
Samples: 11 half-drill core samples and 11 offcuts (offcuts were analyzed twice: once with the beam spot size of 800 μm x 800 μm , once of 300 μm x 300 μm . 300 μm ones has higher resolution, but 800 μm ones are with larger scanning area)

Data Processing:

1. Energy Calibration Maximum: 41 keV, using Fe K peak to adjust the energy.
2. Peak fitting: Fe K, Ca K, As K, Cu K, Ar K, Mn K, Au L, Zn K, Ag L, K K, W L, Ti K, V K. Save these as a session for later use.



3. Ar Normalization: use the cursor to check the Ar channel at the bottom of the window. Different dataset has different Ar channel. For this one, Ar channel is 294. Use Data Filter-Advanced- Normalizer, mode: channel range, start channel:294, end

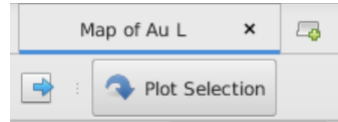


channel: 295, normalized intensity: 10 (the best channel range was checked using Ar XRF map with lowest intensity range).

4. Map fitting: check the visible button.



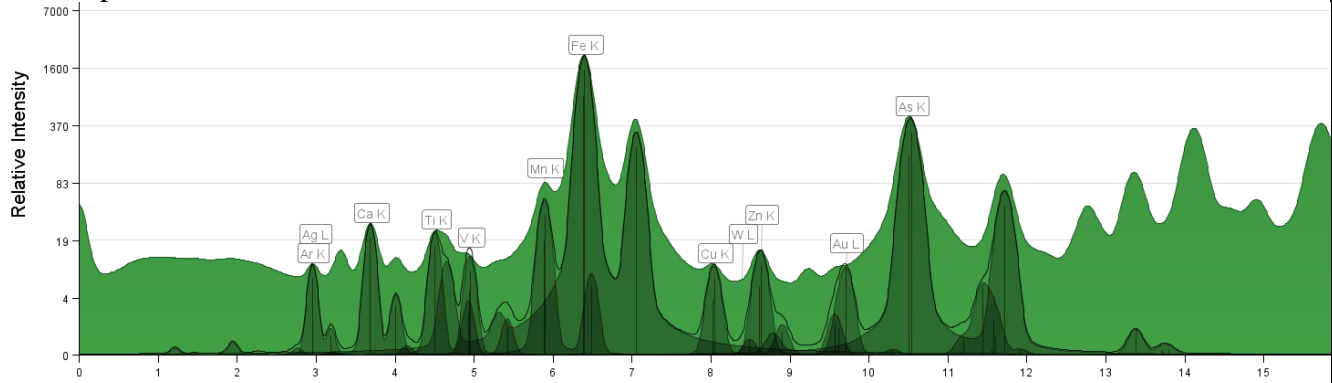
5. Save MCA Spectrum and maps of each sample.
6. Check Au map to make sure if each high-intensity spot is the real gold signal: select the spot and plot selection → take notes of the relationship of Au and other element curves (on the shoulder/ real peak/ overlaid other element peaks/ false signal).



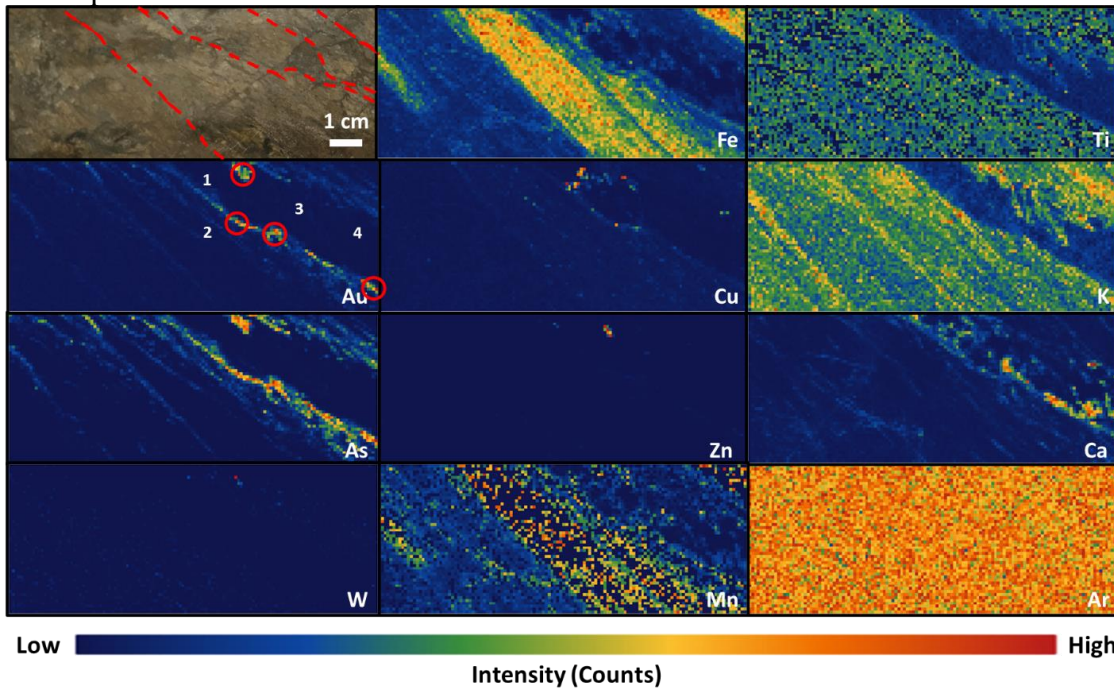
SR- μ XRF Maps:

Sample Number	2841	Drill Hole	TL-13-504	Depth	190.5-190.78 m
Lithology	FP	Map Size	10 cm x 3.5 cm	Gold Grade	25.2 ppm

MCA Spectrum:



SR- μ XRF Maps:

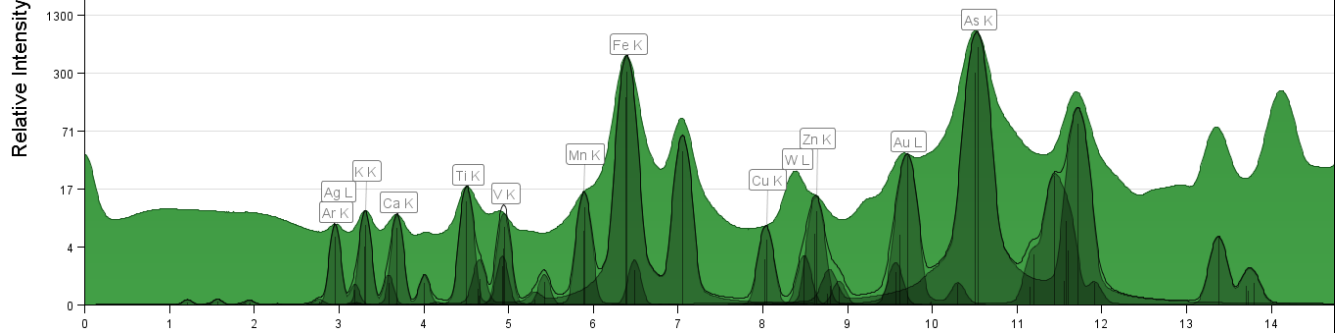


Description:

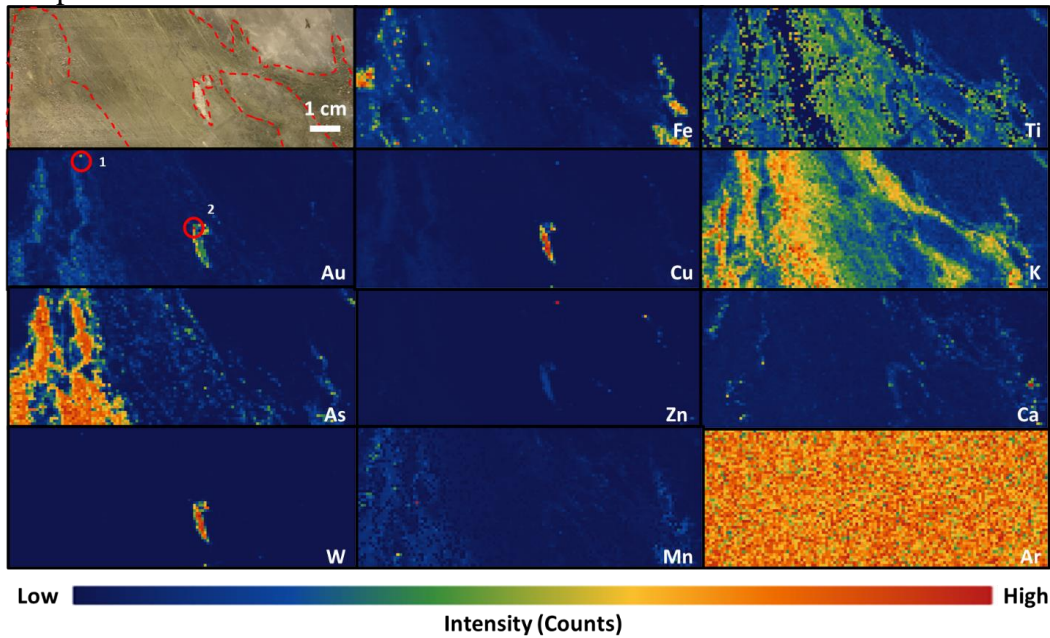
1. Au & As have the same distribution: along with the foliation texture, higher counts on the edge of the foliation layers.
2. Au spots: 1. W, false Au signal; 2-4. Au peak on the As shoulder on the MCA Spectrum, but higher than the shoulder.
3. Cu, Zn, and W: disseminated on the edge of the foliation layers.
4. Mn & Fe have the same distribution in some foliation layers.
5. Ti & K have the same distribution and opposite to Ca.
6. Ar intensity (without filter \rightarrow with filter): 532.4 \rightarrow 159.2

Sample Number	2854	Drill Hole	TL-16-604A	Depth	729.02-729.2m
Lithology	Metavolcanic Tuff	Map Size	10 cm x 3.5 cm	Gold Grade	10.49 ppm

MCA Spectrum:



SR- μ XRF Maps:

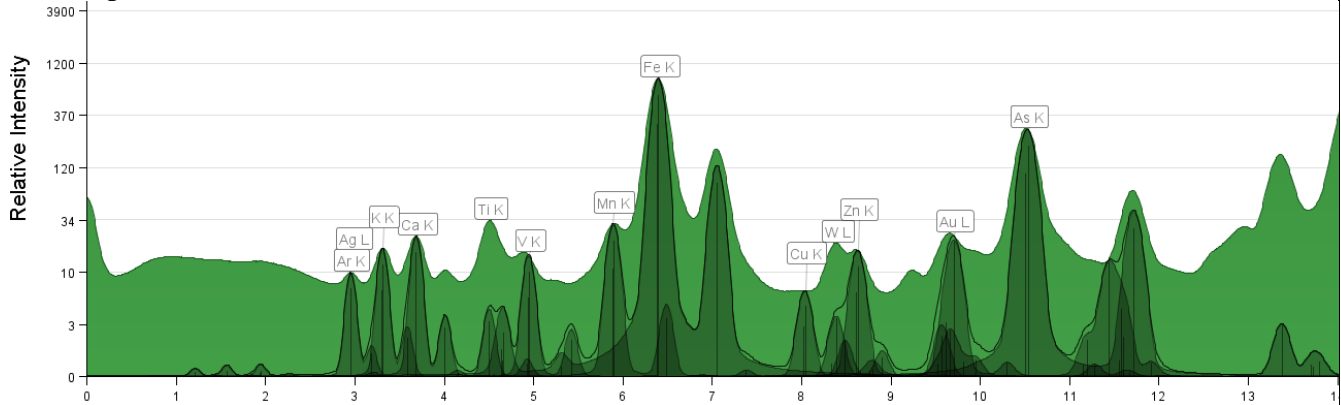


Description:

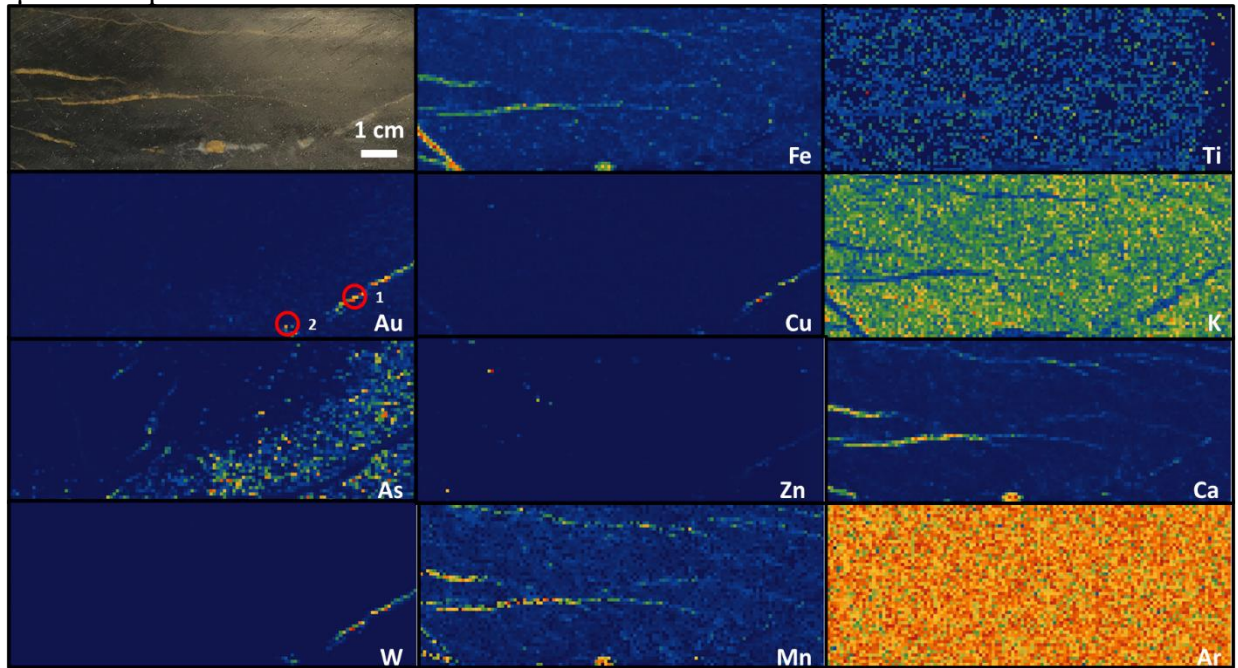
1. Au, W & Cu have the same distribution in grains.
2. As & Fe have the same distribution along with intrusive texture.
3. Ti K Ca Mn have the same distribution along with intrusive texture.
4. Zn is disseminated.
5. Au spots: 1&2. W, false Au signal.
6. Ar intensity (without filter \rightarrow with filter): 722.9 \rightarrow 159.4

Sample Number	2853	Drill Hole	TL-16-604A	Depth	643.96-644.24m
Lithology	QFP	Map Size	10 cm x 3.5 cm	Gold Grade	7.73 ppm

MCA Spectrum:



SR- μ XRF Maps:



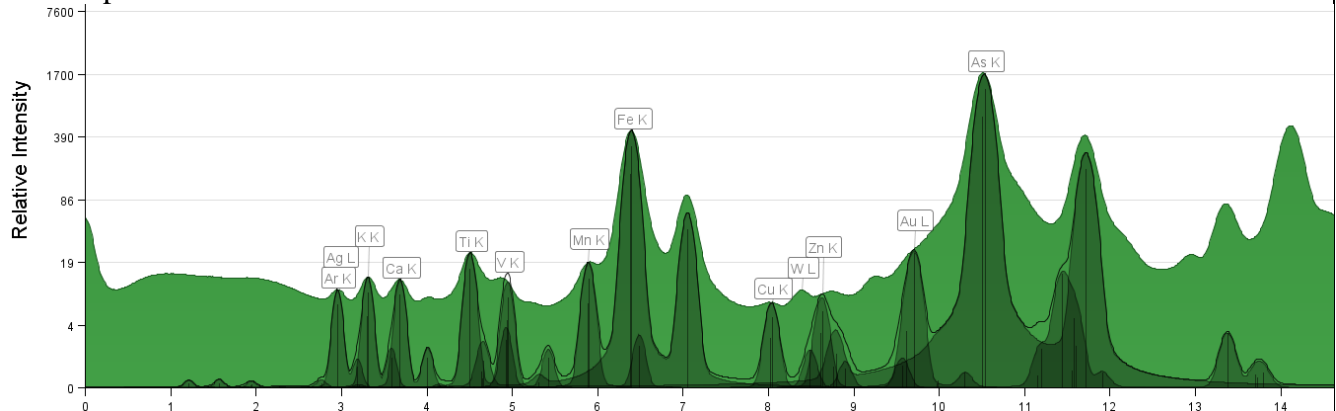
Low High
Intensity (Counts)

Description:

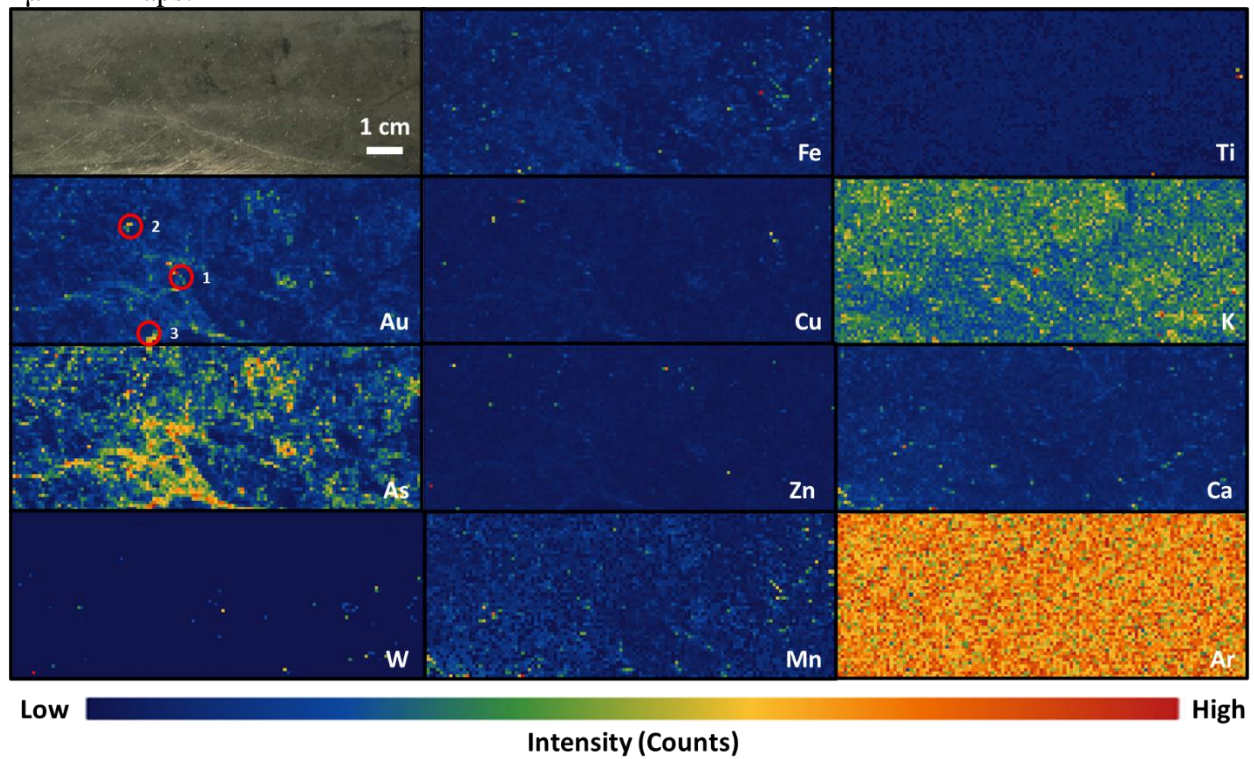
1. Au W Cu have the same distribution along with a white vein.
2. Fe Mn Ca have the same distribution along with orange veins.
3. K Ti have the same distribution opposite to the veins.
4. Zn As are disseminated.
5. Au spots: 1. W, false Au signal, 2. Real Au peak, much higher than As and W shoulder.
6. Ar intensity (without filter \rightarrow with filter): 424.3 \rightarrow 150.9

Sample Number	2819	Drill Hole	TL-16-575	Depth	154.1-154.32 m
Lithology	QFP	Map Size	10 cm x 3.5 cm	Gold Grade	7.21 ppm

MCA Spectrum:



SR- μ XRF Maps:

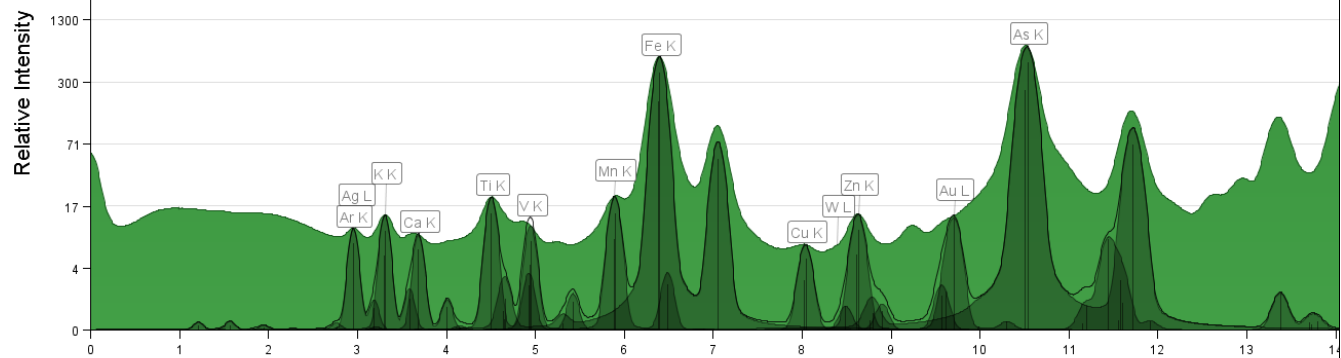


Description:

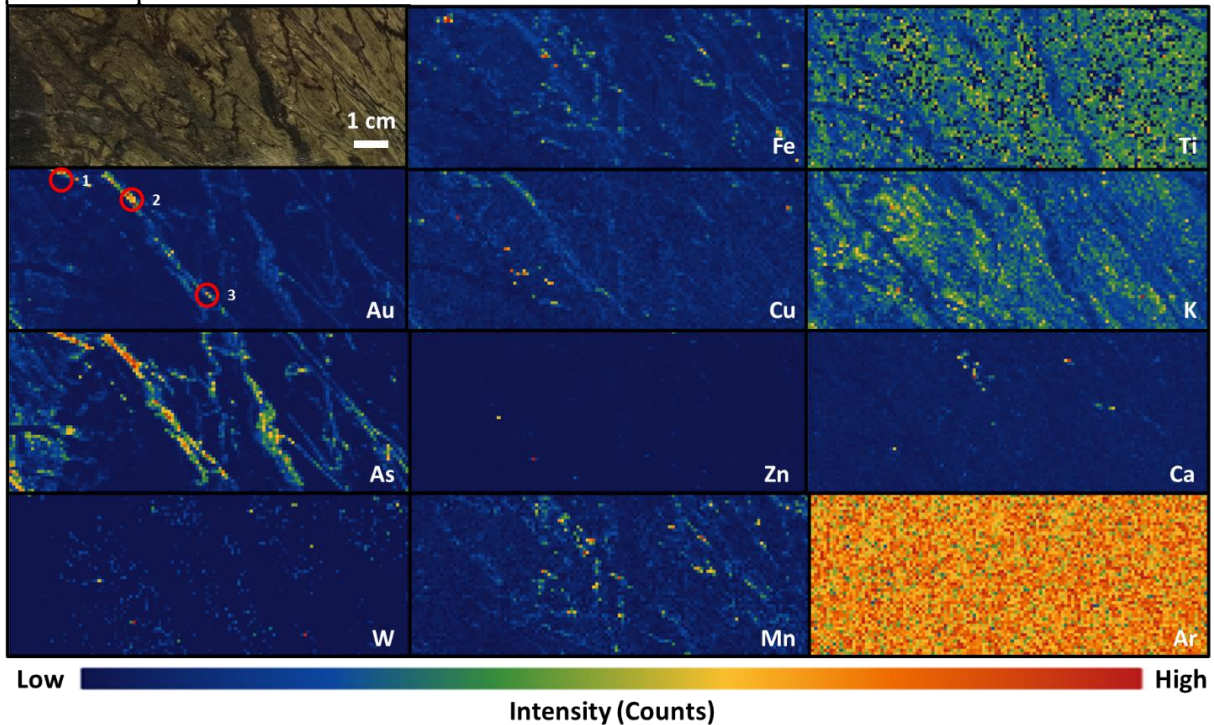
1. Au W Cu Zn Fe Mn Ti Ca are disseminated.
2. As is along with fractures and the distribution is opposite to K.
3. Au spots: 1,2&3. Ar intensity (without filter→ with filter):525.4→151.1

Sample Number	2834	Drill Hole	TL-13-500	Depth	195.76-196 m
Lithology	Lapilli Tuff	Map Size	10 cm x 3.5 cm	Gold Grade	5.21 ppm

MCA Spectrum:



SR- μ XRF Maps:

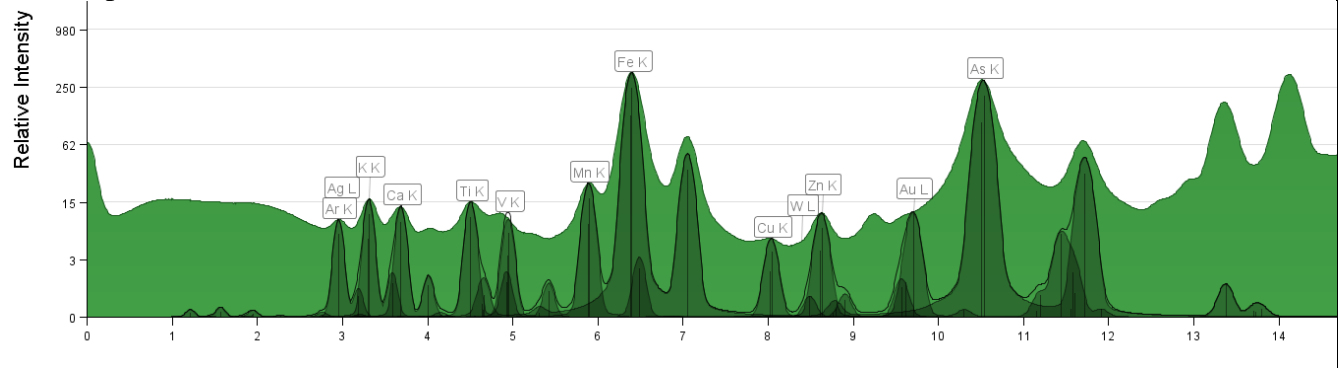


Description:

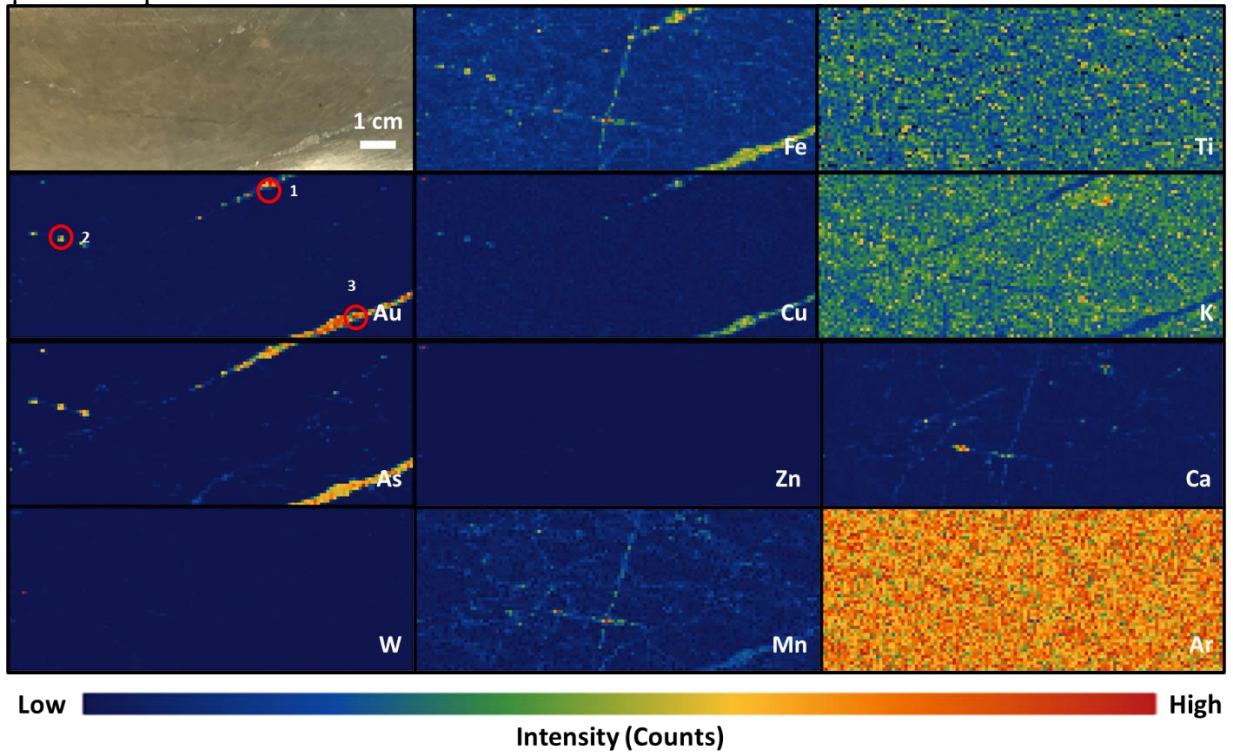
1. Au As Mn Cu Fe have the same distribution along with the red veins.
2. Ti K have the same distribution opposite to the veins.
3. W Zn Mn Cu Ca are disseminated.
4. Au spots: 1-3. Au peak on the As shoulder on the MCA Spectrum, but higher than the shoulder.
5. Ar intensity (without filter \rightarrow with filter): 489.2 \rightarrow 151.1

Sample Number	2827	Drill Hole	TL-15-564	Depth	183-183.23m
Lithology	QFP	Map Size	10 cm x 3.5 cm	Gold Grade	Close to 9 ~0.6 ppm

MCA Spectrum:



SR- μ XRF Maps:

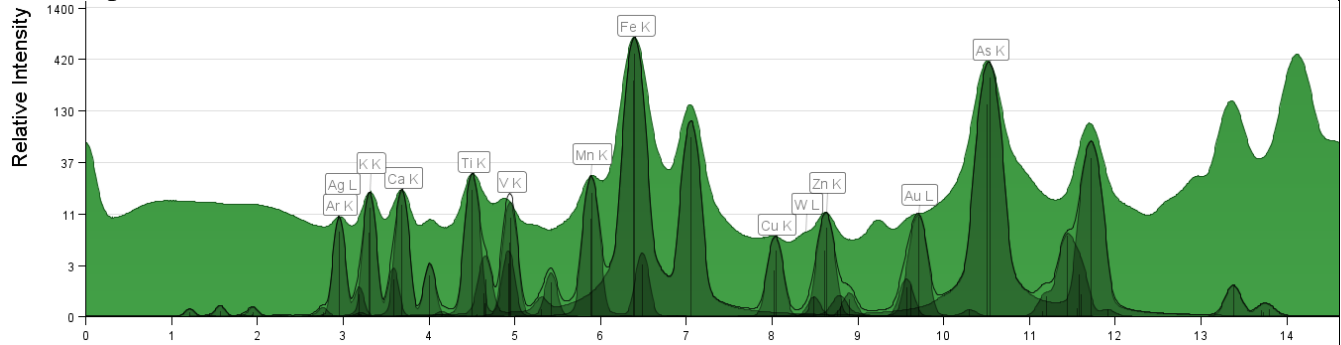


Description:

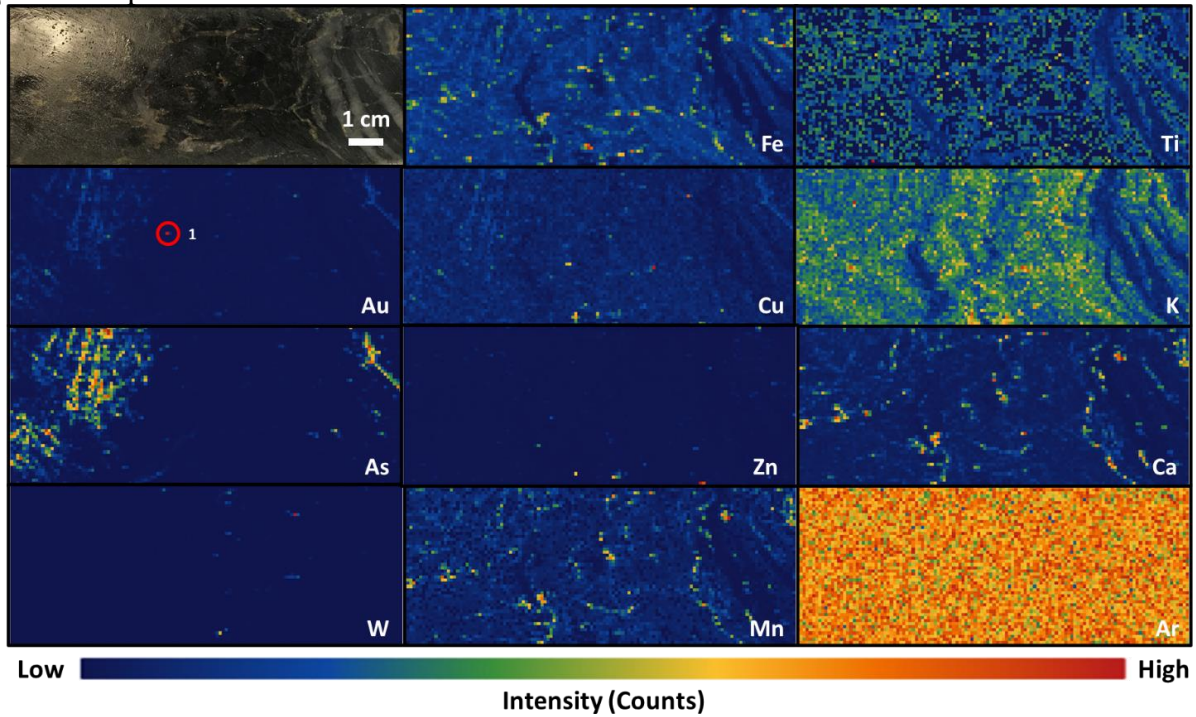
1. Au As Cu Fe (partly) have the same distribution along with sulphide veins.
2. Mn Ca Fe (partly) have the same distribution along with the dark color veins. These two veins are cutting each other.
3. K has the opposite distribution to the veins.
4. W Zn Ca are disseminated.
5. Au spots: 1-3. Au peak on the As shoulder on the MCA Spectrum, but higher than the shoulder.
6. Ar intensity (without filter \rightarrow with filter): 695.3 \rightarrow 151

Sample Number	2821	Drill Hole	TL-16-575	Depth	183.78-184.06 m
Lithology	Ash Tuff	Map Size	10 cm x 3.5 cm	Gold Grade	3.38 ppm

MCA Spectrum:



SR- μ XRF Maps:

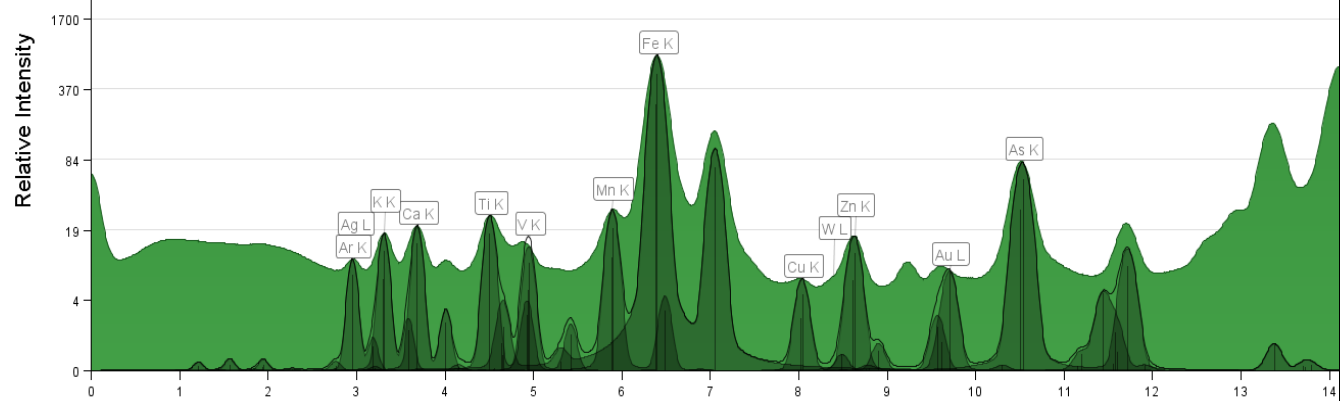


Description:

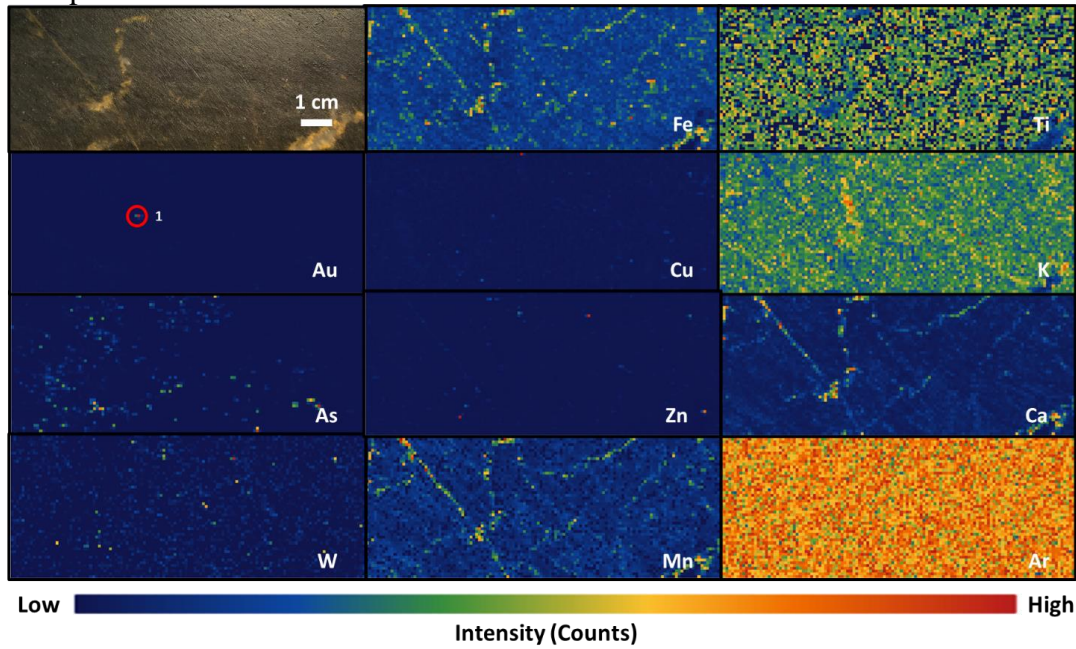
1. Fe Mn Ca have the same distribution along with the fractured texture.
2. Ti K have the same distribution opposite to the white veins.
3. As distributes along with white veins.
4. Au Cu W Zn Cu are disseminated.
5. Au spots: 1. real Au peak, much higher than As shoulder.
6. Ar intensity (without filter→ with filter):490.4→151.2

Sample Number	2858	Drill Hole	TL-16-607	Depth	817.4-817.6m
Lithology	Lapilli Tuff	Map Size	10 cm x 3.5 cm	Gold Grade	2.45 ppm

MCA Spectrum:



SR- μ XRF Maps:

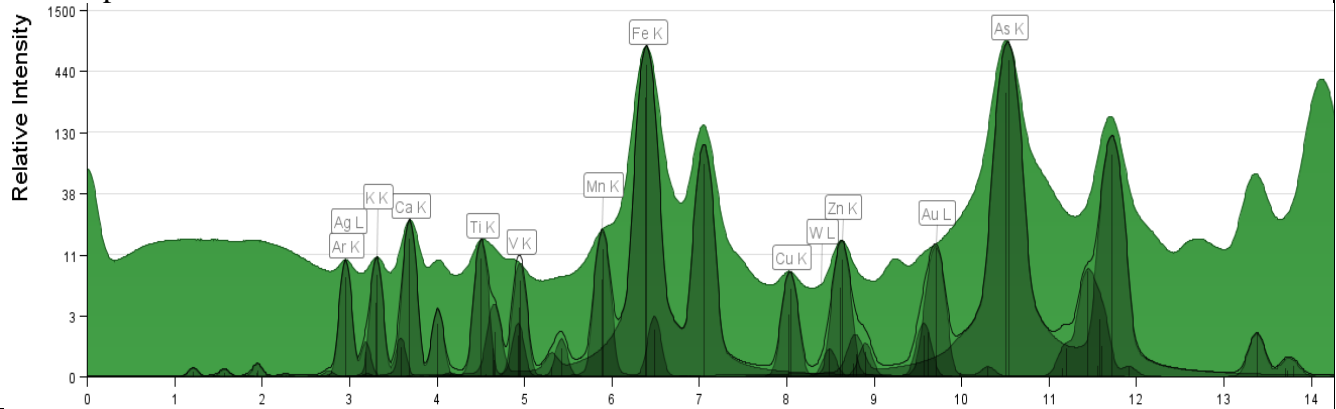


Description:

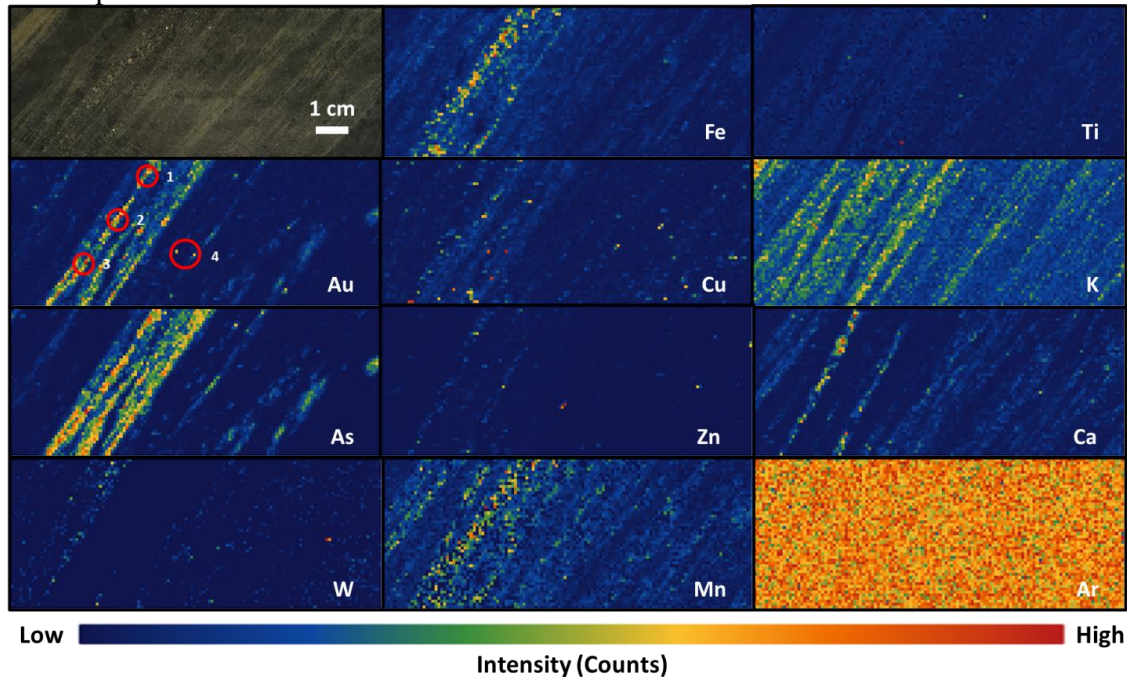
7. Ca Mn Fe have the same distribution along with fractured texture and in the white veins.
8. Ti K have the same distribution opposite to the white veins.
9. Au As W Cu Zn are disseminated.
10. Au spots: 1. real Au peak, much higher than As shoulder.
11. Ar intensity (without filter→ with filter):370.6→150.8

Sample Number	2831	Drill Hole	TL-15-551	Depth	96.8-97m
Lithology	Metasandstone	Map Size	10 cm x 3.5 cm	Gold Grade	2.26 ppm

MCA Spectrum:



SR- μ XRF Maps:

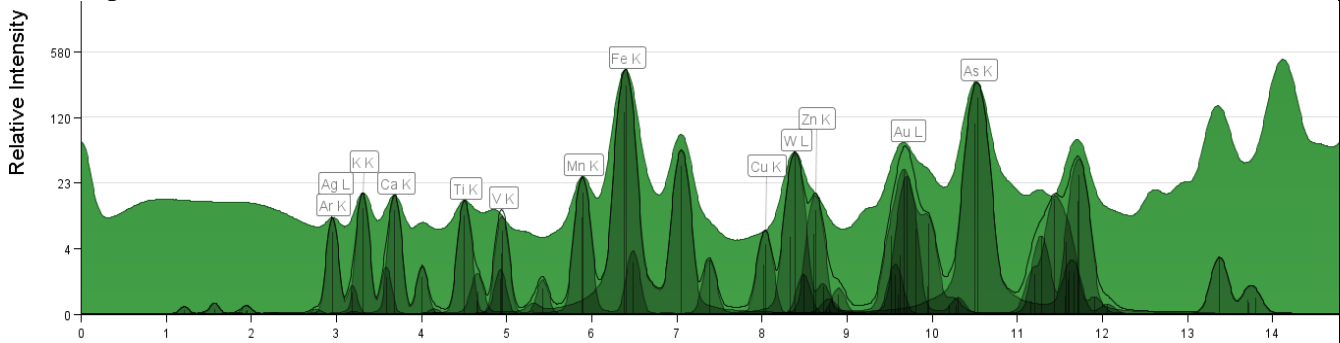


Description:

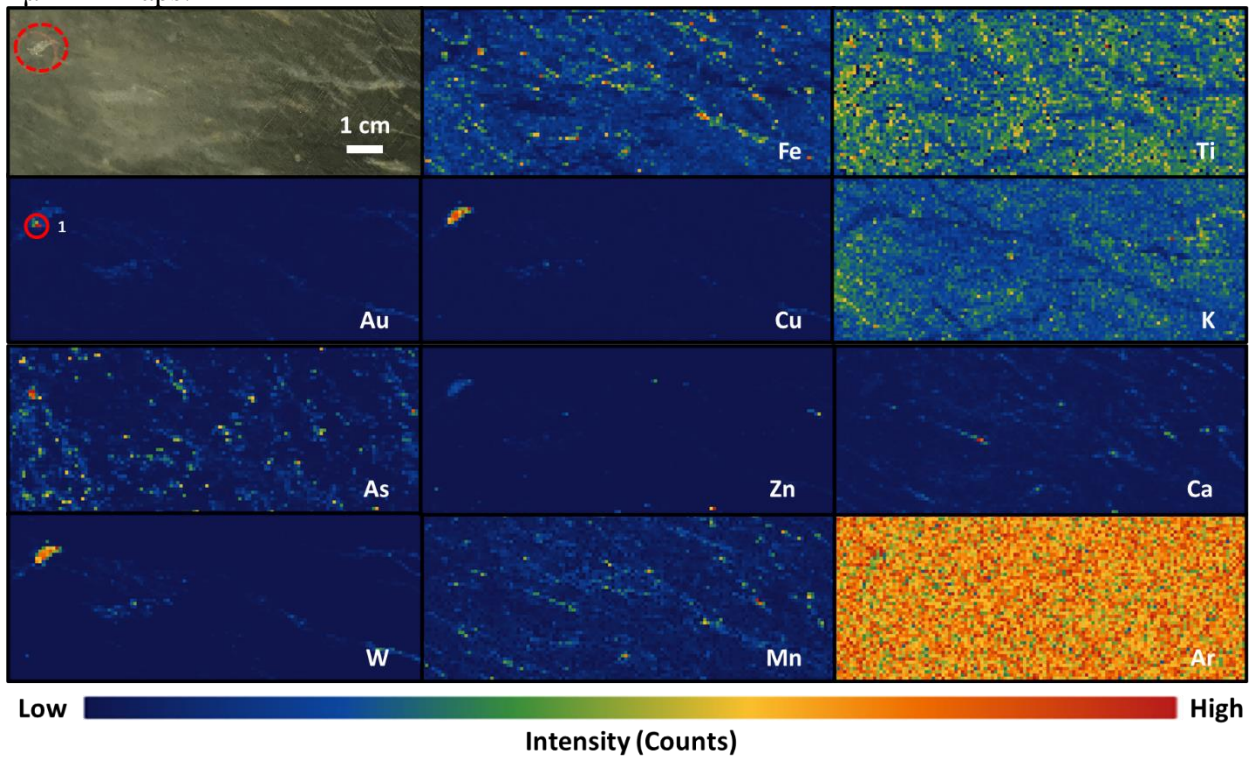
1. Au As Fe have the same distribution along with the sulphide veins.
2. Mn K have the same distribution along with the light green foliation layers.
3. Ca distributes along with the dark green foliation layers, especially the layers besides the sulphide veins.
4. W Cu Zn Ti are disseminated.
5. Au spots: 1-3. Au peak on the As shoulder on the MCA Spectrum, but higher than the shoulder, 4. real Au peak, much higher than As shoulder.
6. Ar intensity (without filter \rightarrow with filter): 485.2 \rightarrow 150.9

Sample Number	2857	Drill Hole	TL-16-607	Depth	718.4-718.66 m
Lithology	QFP	Map Size	10 cm x 3.5 cm	Gold Grade	2.16 ppm

MCA Spectrum:



SR- μ XRF Maps:

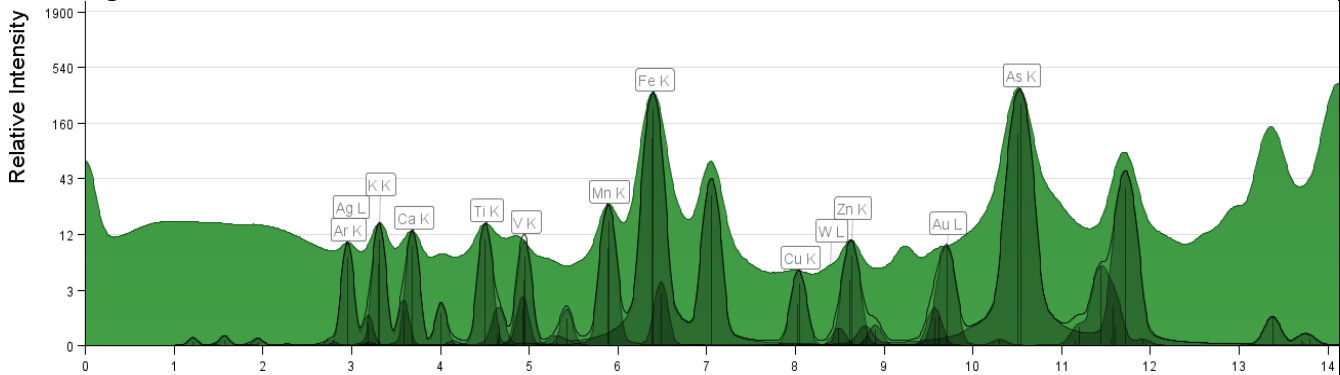


Description:

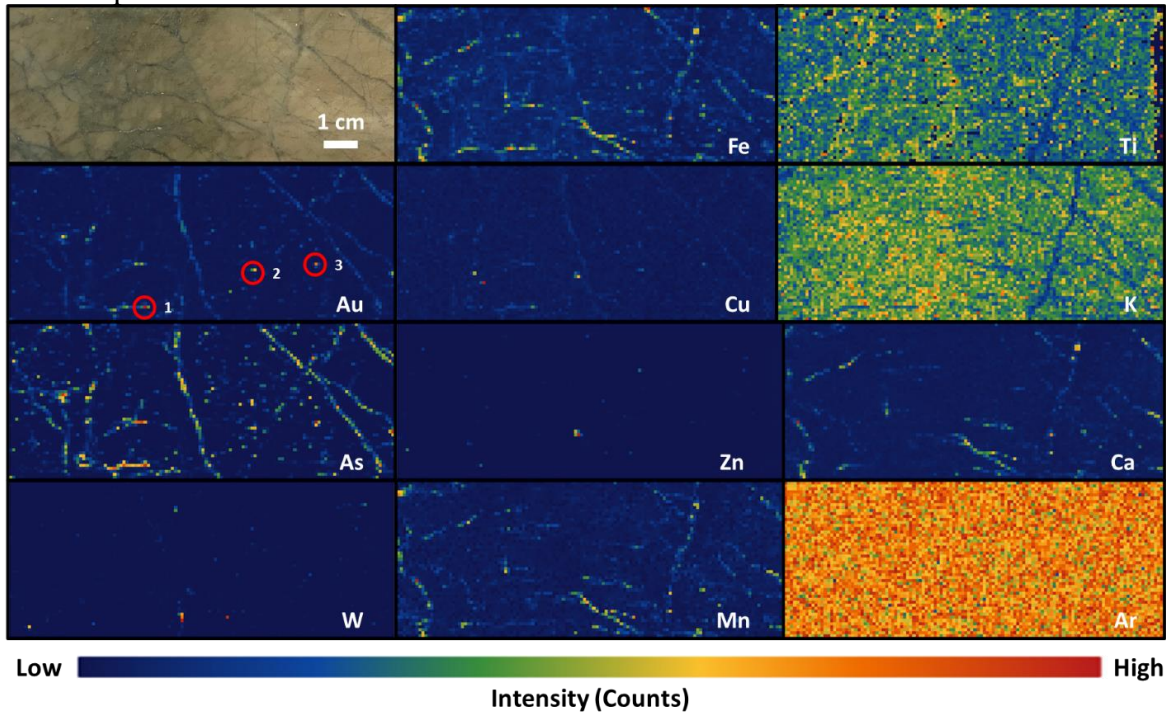
1. Au W Cu have the same distribution in a sulphide grain.
2. Ti K have the same distribution opposite to the white veins.
3. Fe Mn have the same distribution along with the white veins.
4. As Zn Ca are disseminated in the veins.
5. Au spots: 1. real Au peak, much higher than As shoulder.
6. Ar intensity (without filter \rightarrow with filter): 286.2 \rightarrow 151.2

Sample Number	2845	Drill Hole	TL-13-509	Depth	235.6-235.86 m
Lithology	QFP	Map Size	10 cm x 3.5 cm	Gold Grade	1.13 ppm

MCA Spectrum:



SR- μ XRF Maps:

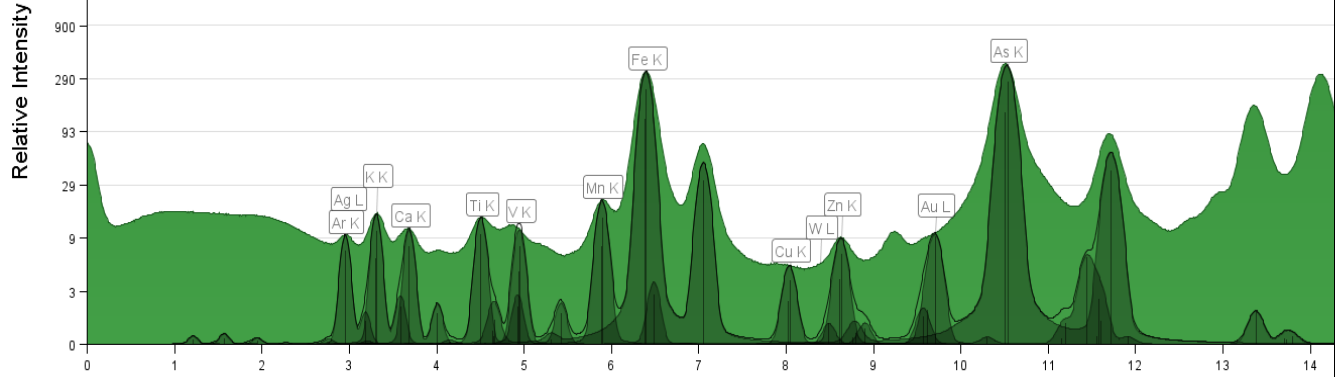


Description:

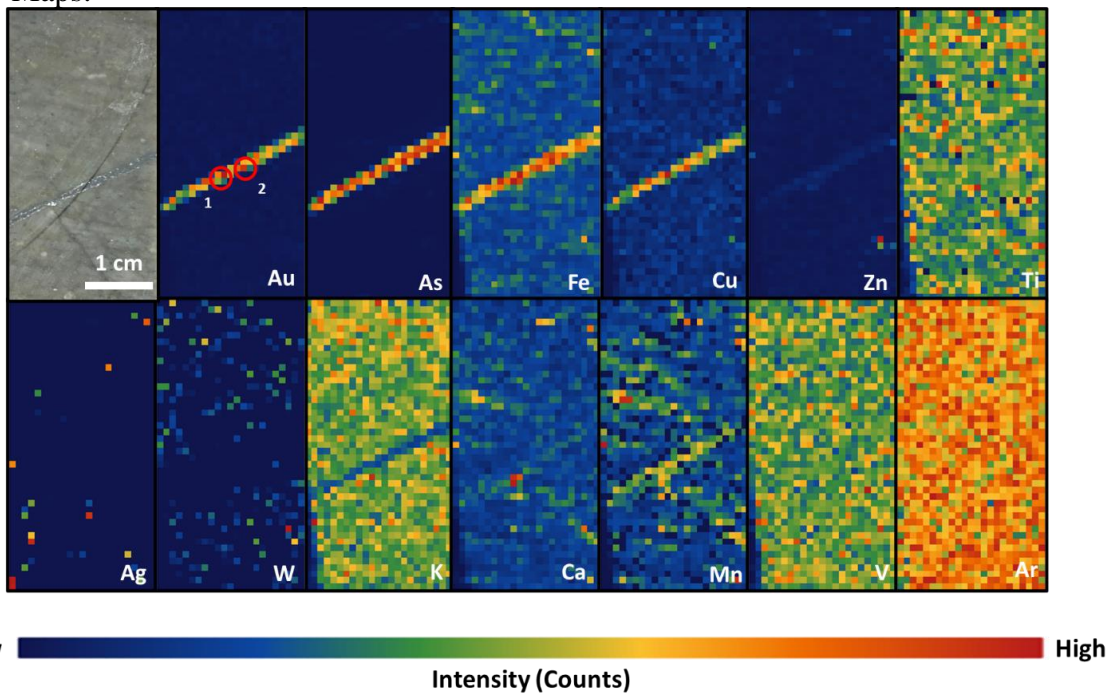
1. Fe As Mn Ca have the same distribution in the dark color veins.
2. Ti K have the same distribution opposite to the dark color veins.
3. Au W Zn Cu are disseminated in the thick dark color veins.
4. Au spots: 1-3. Au peak on the As shoulder on the MCA Spectrum, but higher than the shoulder.
5. Ar intensity (without filter \rightarrow with filter): 567.4 \rightarrow 151

Sample Number	2827 (800 μm)	Drill Hole	TL-15-564	Depth	183-183.23 m
Lithology	QFP	Map Size	2 cm x 3.5 cm	Gold Grade	Close to 9 ~0.6 ppm

MCA Spectrum:



SR-μXRF Maps:

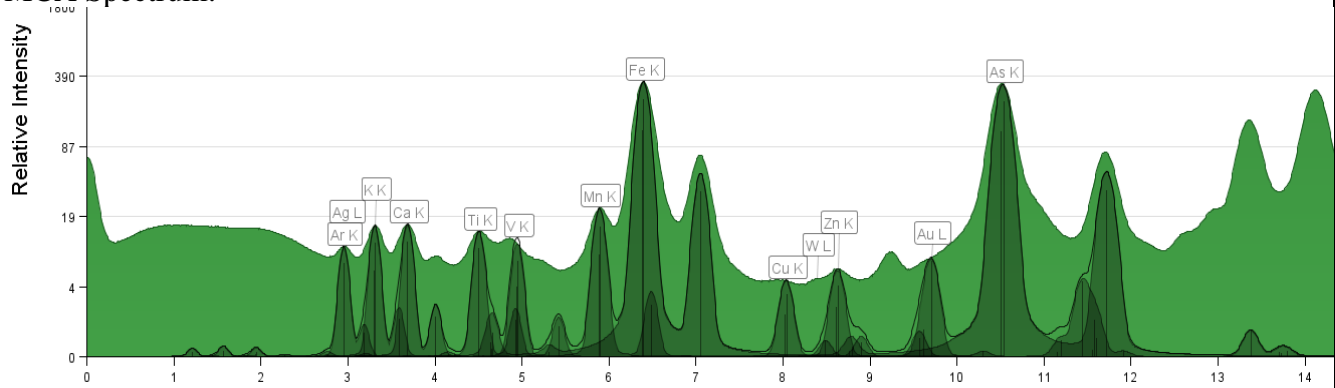


Description:

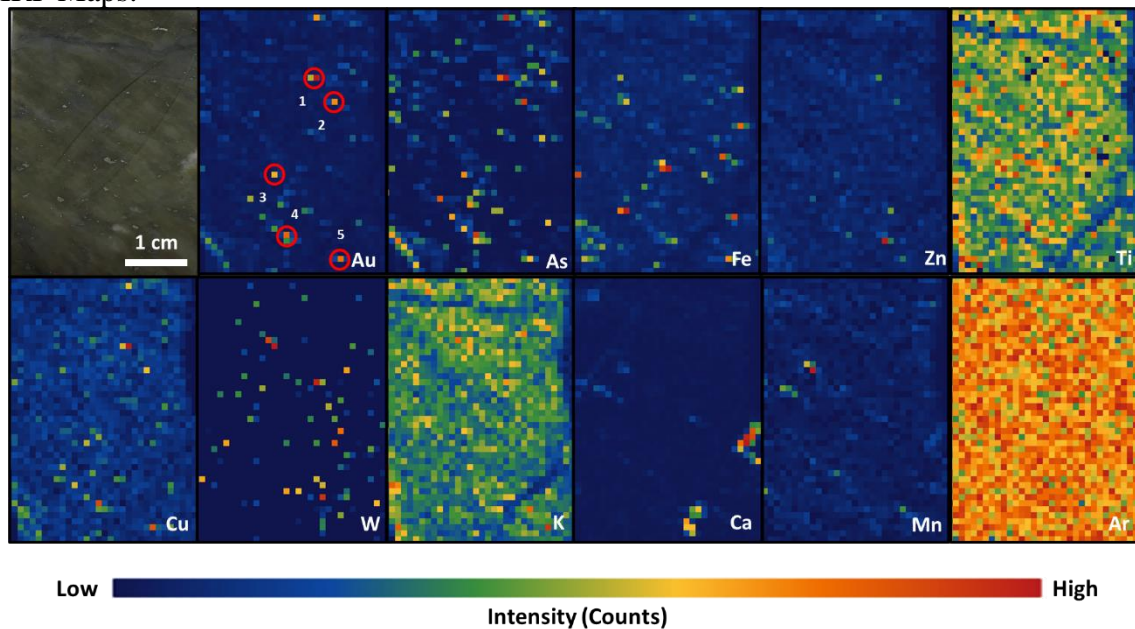
1. Au As Cu Fe have the same distribution along with sulphide veins.
2. Ca Mn have the same distribution.
3. Ti V have the same distribution.
4. W Zn Ag are disseminated.
5. K has the opposite distribution to the vein.
6. Au spots: 1&2 Au peak on the As shoulder on the MCA Spectrum, but higher than the shoulder.
7. Ar intensity (without filter→ with filter): 243.7→151.1

Sample Number	2824 (800 μm)	Drill Hole	TL-15-568	Depth	200.62-200.82 m
Lithology	QFP	Map Size	2 cm x 3.5 cm	Gold Grade	1.91-8.25 ppm

MCA Spectrum:



SR-μXRF Maps:

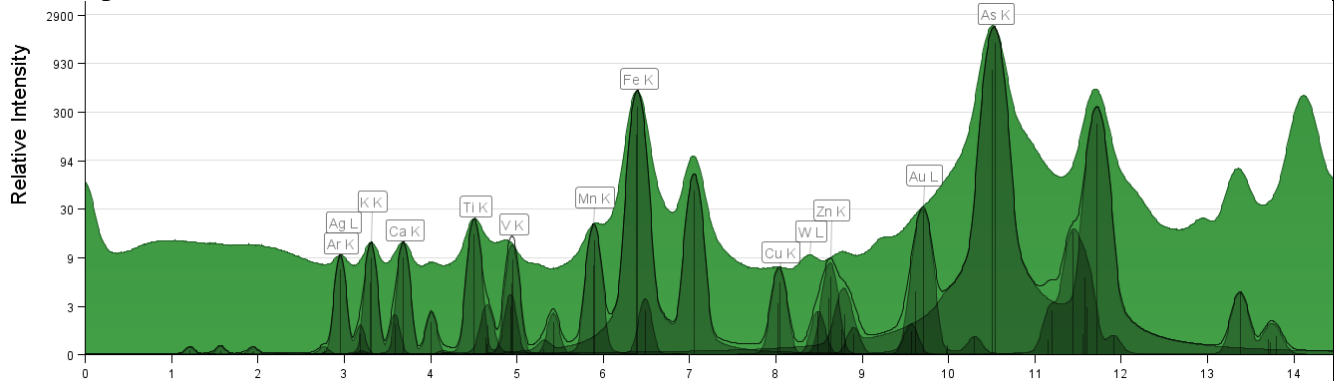


Description:

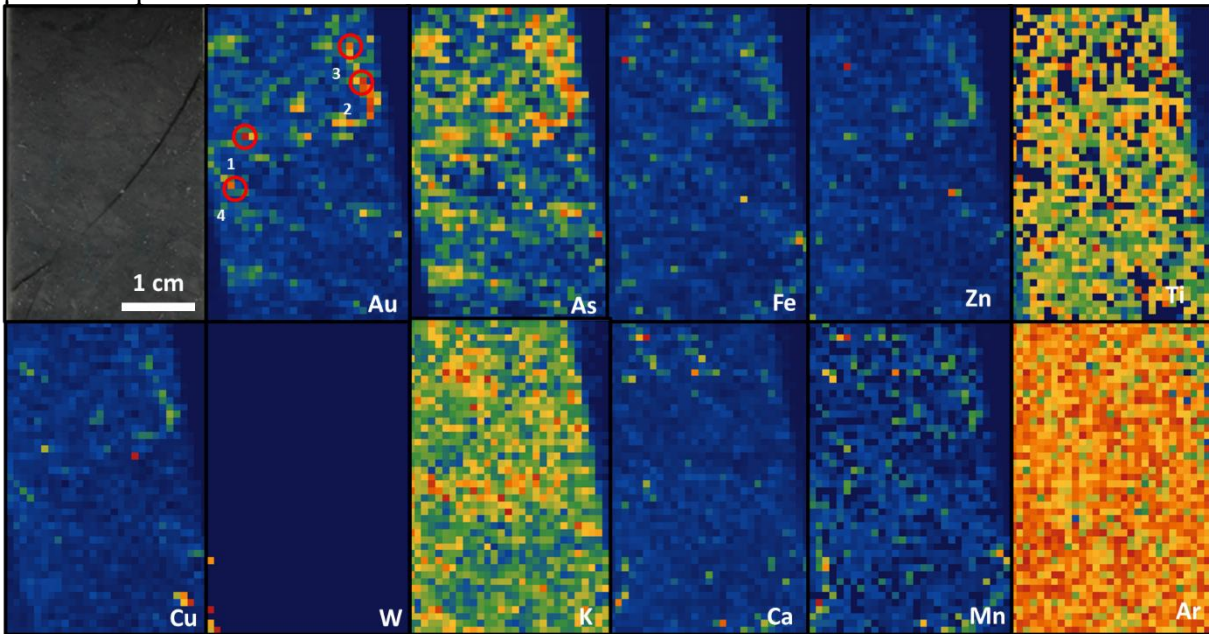
1. Ti & K have the same distribution which is opposite to the fractures.
2. Au & As have the same distribution and these two elements are disseminated on the offcut.
3. Ca distributes in the white intrusion on the offcut.
4. Fe Zn Cu W Mn are disseminated.
5. Au spots: 1-5. Au peak on the As shoulder on the MCA Spectrum, but higher than the shoulder,
6. Ar intensity (without filter→ with filter): 243.7→150.2

Sample Number	2819 (800 μm)	Drill Hole	TL-16-575	Depth	154.1-154.32 m
Lithology	QFP	Map Size	2 cm x 3.5 cm	Gold Grade	7.21 ppm

MCA Spectrum:



SR-μXRF Maps:

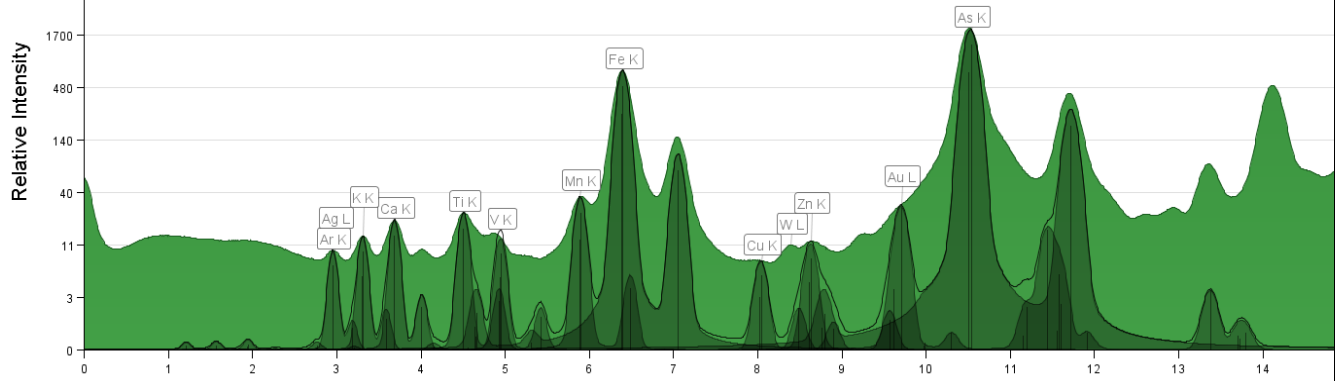


Description:

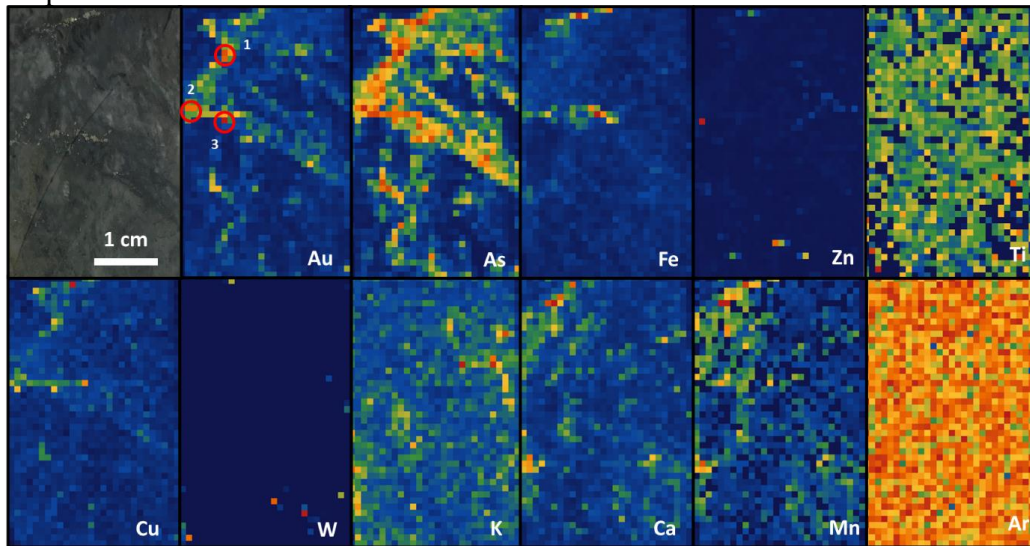
1. Au & As have the same distribution along with the black foliation layers.
2. Fe Zn Cu have the same distribution.
3. No W in this sample.
4. Zn Ca Mn are disseminated.
5. K & Ti are all over the sample.
6. Au spots: 1-4. Au peak on the As shoulder on the MCA Spectrum, but higher than the shoulder.
7. Ar intensity (without filter→ with filter): 243.7→150.2

Sample Number	2841(800 μm)	Drill Hole	TL-13-504	Depth	190.5-190.78 m
Lithology	QFP	Map Size	2 cm x 3.5 cm	Gold Grade	25.2 ppm

MCA Spectrum:



SR-μXRF Maps:



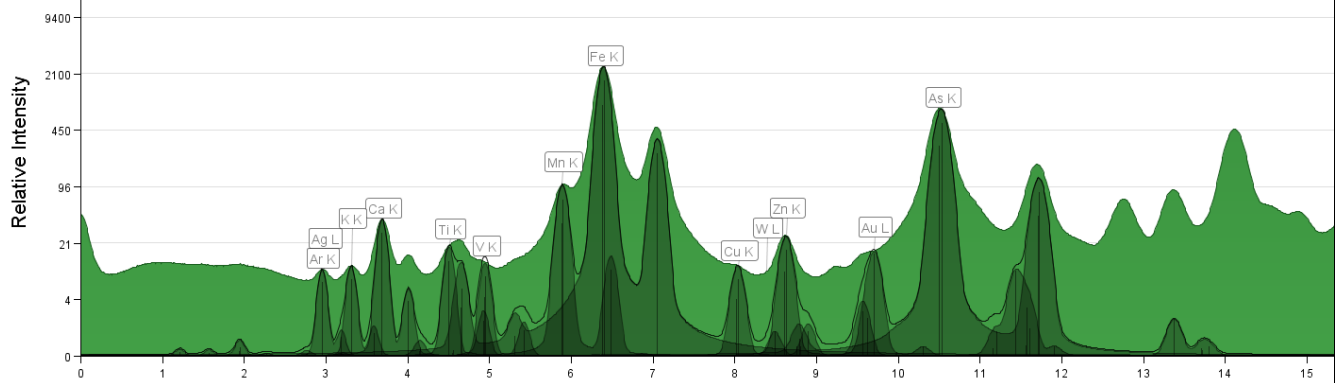
Low  High
Intensity (Counts)

Description:

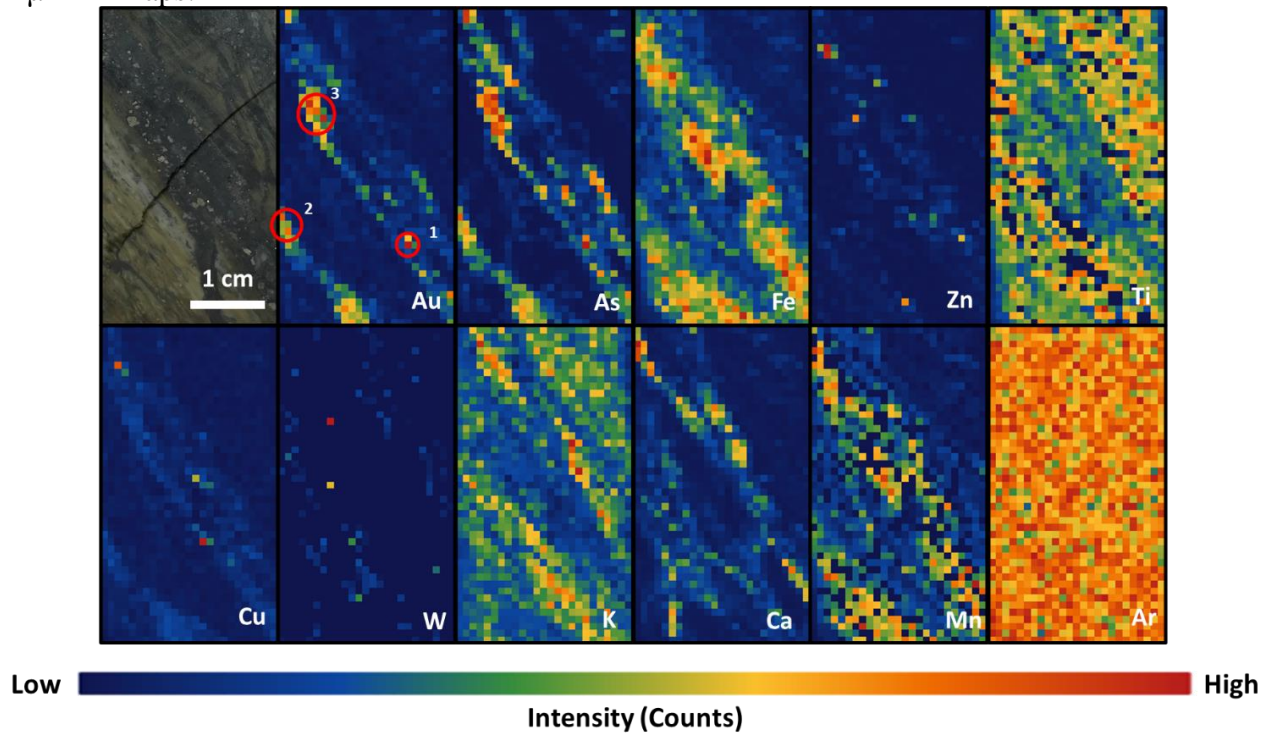
1. Au & As have the same distribution along with the folded sulphide veins.
2. Cu & Fe are disseminated in the folded sulphide veins.
3. Zn & W are disseminated.
4. K distributes on the edge of the darker grey layer and lighter grey layer of the foliation texture; while Ca & Mn distribute in the darker grey layer which next to the folded sulphide veins.
5. Au spots: 1-3. Au peak on the As shoulder on the MCA Spectrum, but higher than the shoulder,
6. Ar intensity (without filter → with filter): 243.7 → 150

Sample Number	2834 (800 μm)	Drill Hole	TL-13-500	Depth	195.76-196 m
Lithology	Lapilli Tuff	Map Size	2 cm x 3.5 cm	Gold Grade	5.21 ppm

MCA Spectrum:



SR-μXRF Maps:

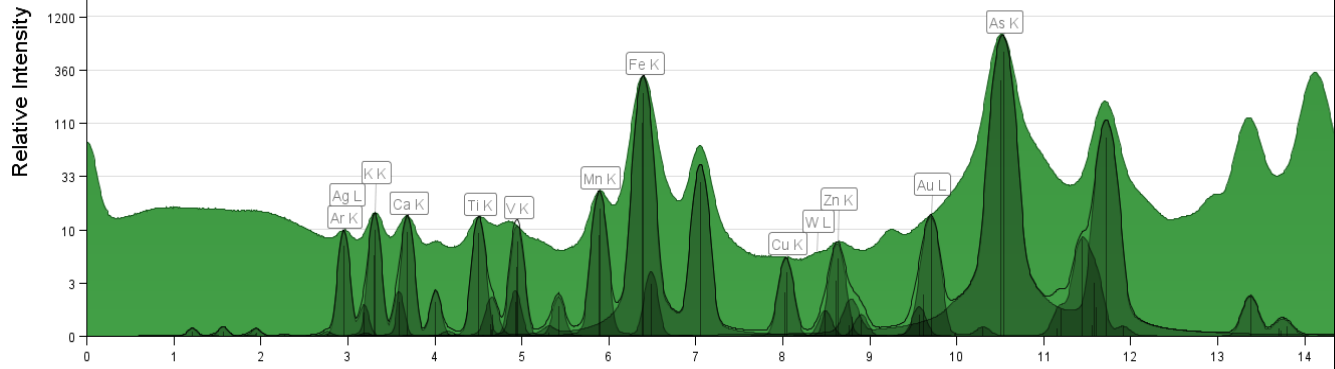


Description:

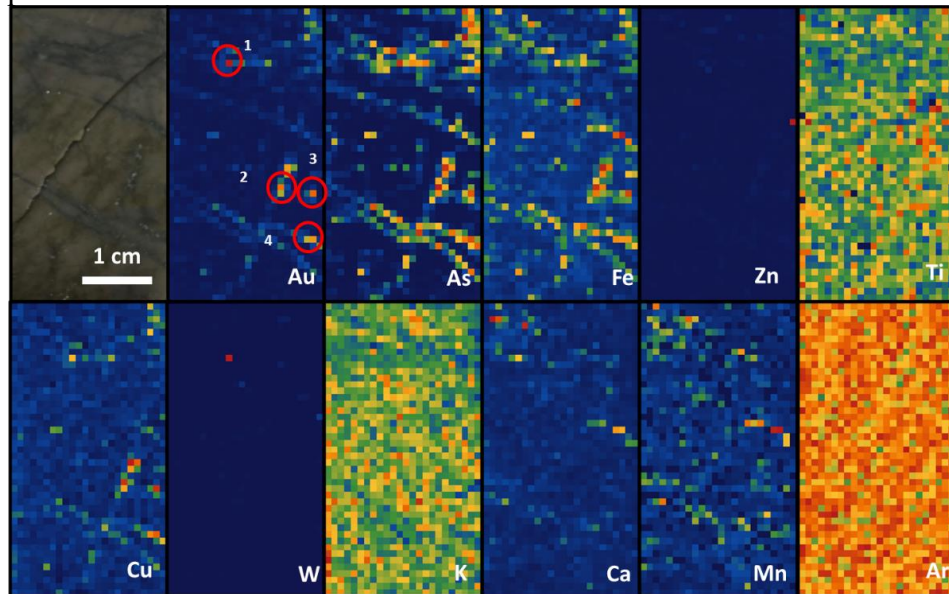
1. Au & As have the same distribution along with the sulphide veins.
2. Fe & Mn distribute in the dark foliated layers next to the sulphide veins.
3. Ca distributes in the dark red veinlets.
4. Ti & K distribute opposite to the dark red veinlets.
5. Cu Zn W are disseminated in the sulphide veins.
6. Au spots: 1&2. Au peak on the As shoulder on the MCA Spectrum, but higher than the shoulder; 3. real Au peak, much higher than As shoulder.
7. Ar intensity (without filter→ with filter): 243.7 →149.4

Sample Number	2845 (800 μm)	Drill Hole	TL-13-509	Depth	235.6-235.86 m
Lithology	QFP	Map Size	2 cm x 3.5 cm	Gold Grade	1.13 ppm

MCA Spectrum:



SR-μXRF Maps:

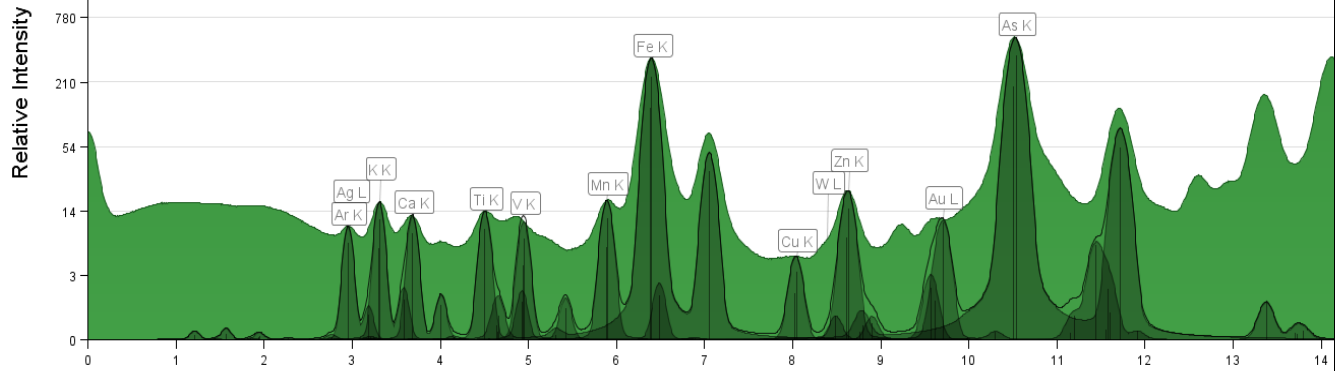


Description:

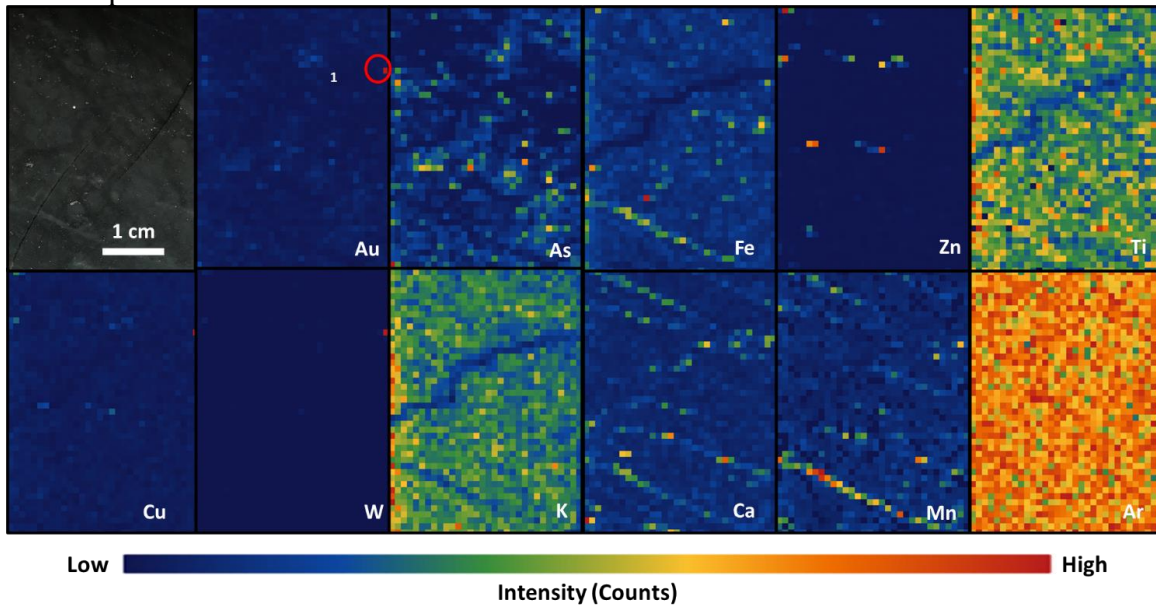
1. Au As Fe Cu have the same distribution along with the dark fine veinlets.
2. W Zn Ca Mn are disseminated.
3. Au spots: 1. Au peak and W peak are overlapped, but Au peak is much higher than As shoulder and W peak; 2-4. Au peak on the As shoulder on the MCA Spectrum, but higher than the shoulder,
4. Ar intensity (without filter→ with filter): 569.9→149.6

Sample Number	2857 (800 μm)	Drill Hole	TL-16-607	Depth	718.4-718.66 m
Lithology	QFP	Map Size	2 cm x 3.5 cm	Gold Grade	2.16 ppm

MCA Spectrum:



SR- μ XRF Maps:

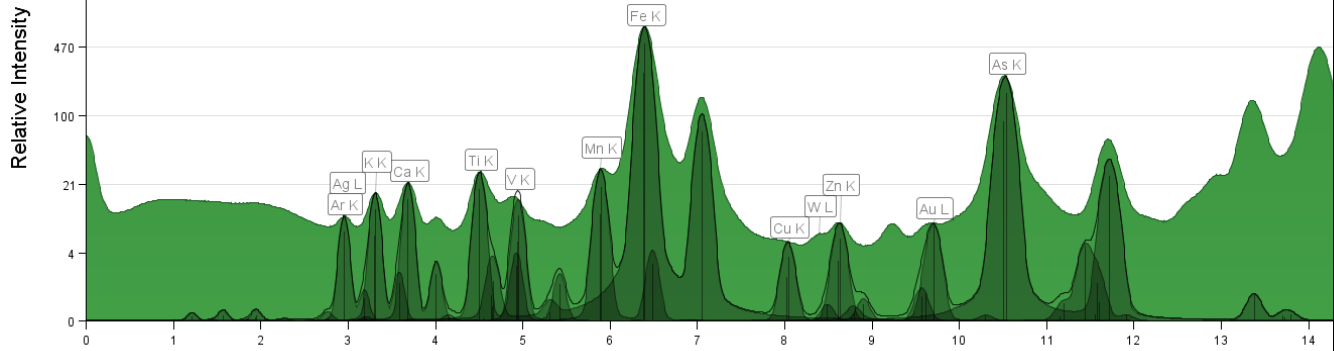


Description:

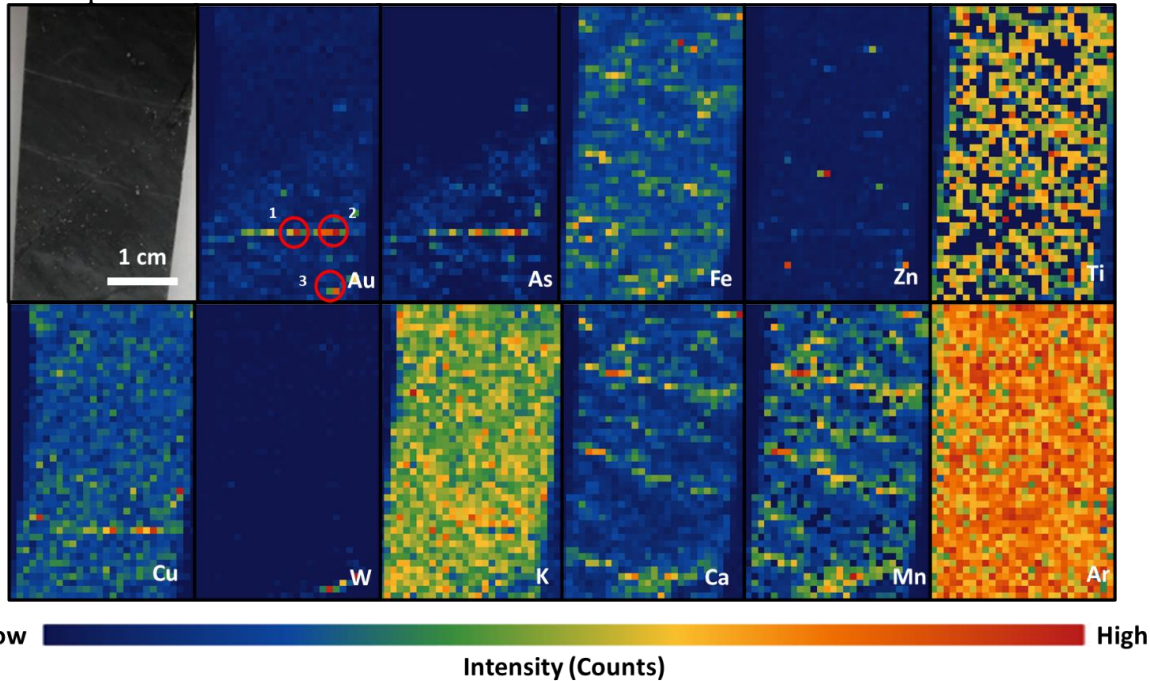
1. Au W Cu have the same distribution which is a high-intensity spot on the right-top corner
2. As Zn are disseminated.
3. Au spots: 1. W peak, false Au signal.
4. Fe Ca Mn have the same distribution along with the sulphide veins.
5. Ti & K have the same distribution opposite to the sulphide veins and fractures.
6. Ar intensity (without filter \rightarrow with filter): 569.9 \rightarrow 150.7

Sample Number	2853 (800 μm)	Drill Hole	TL-16-604A	Depth	643.96-644.24m
Lithology	QFP	Map Size	2 cm x 3.5 cm	Gold Grade	7.73 ppm

MCA Spectrum:



SR-μXRF Maps:

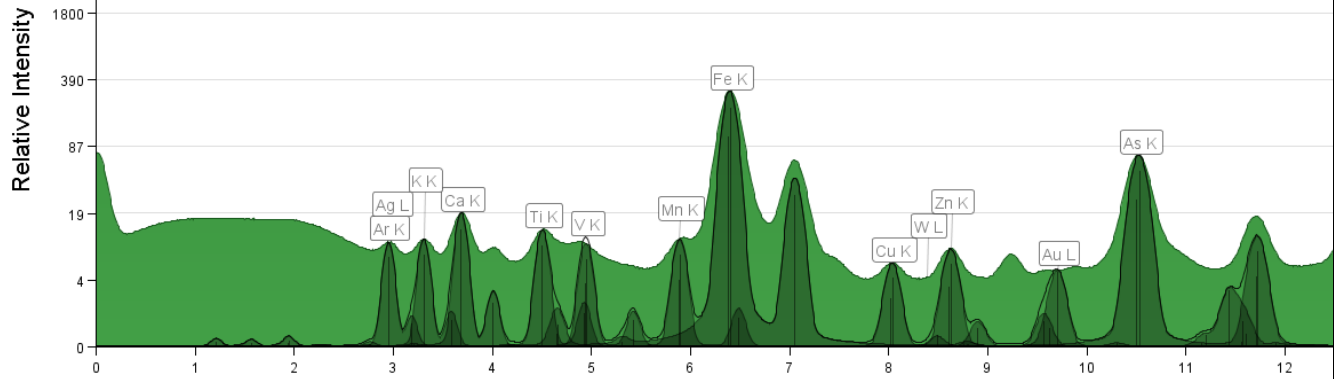


Description:

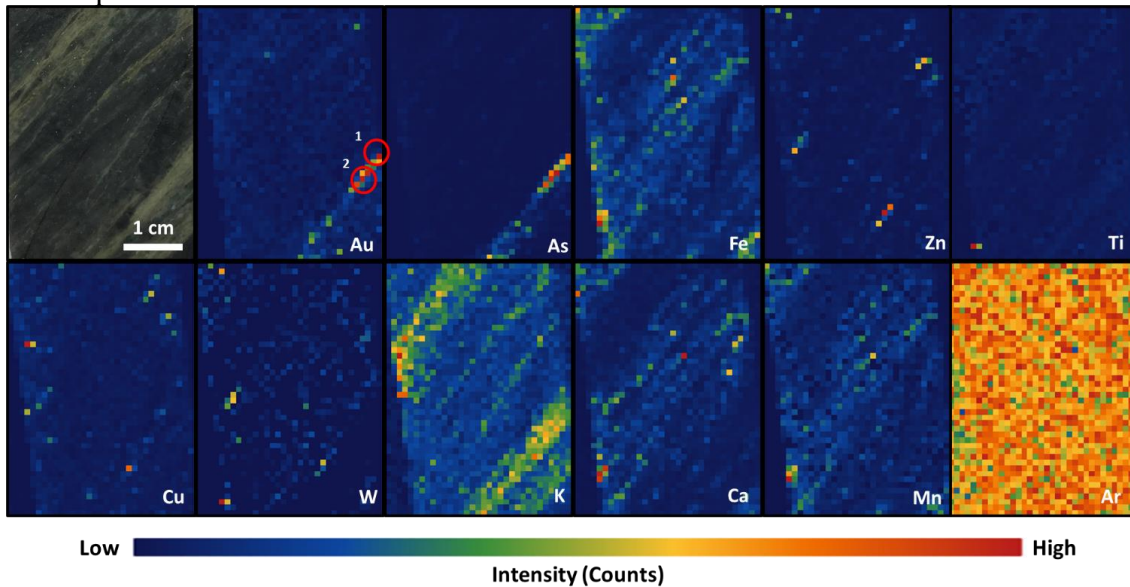
1. Au As Cu have the same distribution in the middle (look like data crash, fake signal).
2. Ca Fe Mn have the same distribution along with the light grey layers of the foliation.
3. Zn & W are disseminated.
4. Au spots: 1 & 2 Au peak on the As shoulder on the MCA Spectrum, but higher than the shoulder; 3. Au peak and W peak are overlapped, but Au peak is much higher than As shoulder and W peak.
5. Ar intensity (without filter→ with filter): 569.9→150.5

Sample Number	2831 (800 μm)	Drill Hole	TL-15-551	Depth	96.8-97 m
Lithology	Metasandstone	Map Size	2 cm x 3.5 cm	Gold Grade	2.26 ppm

MCA Spectrum:



SR-μXRF Maps:

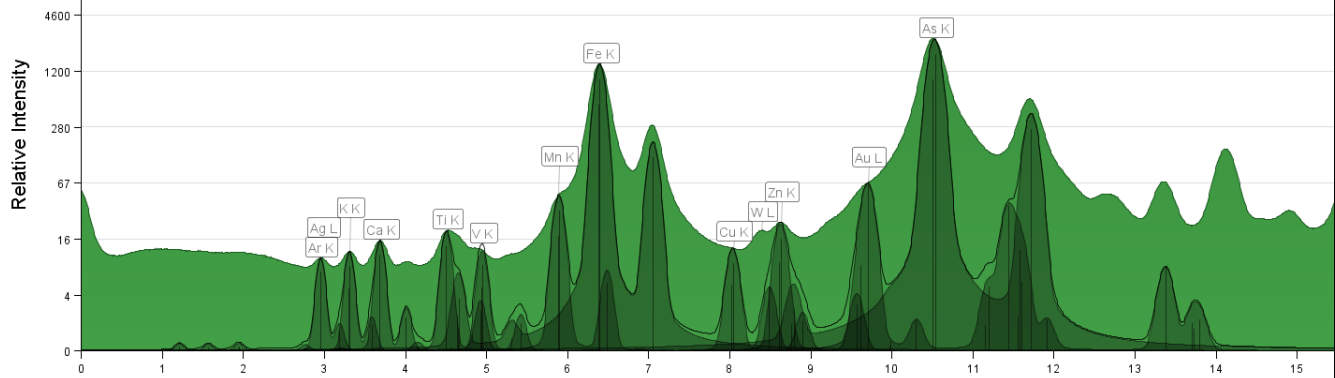


Description:

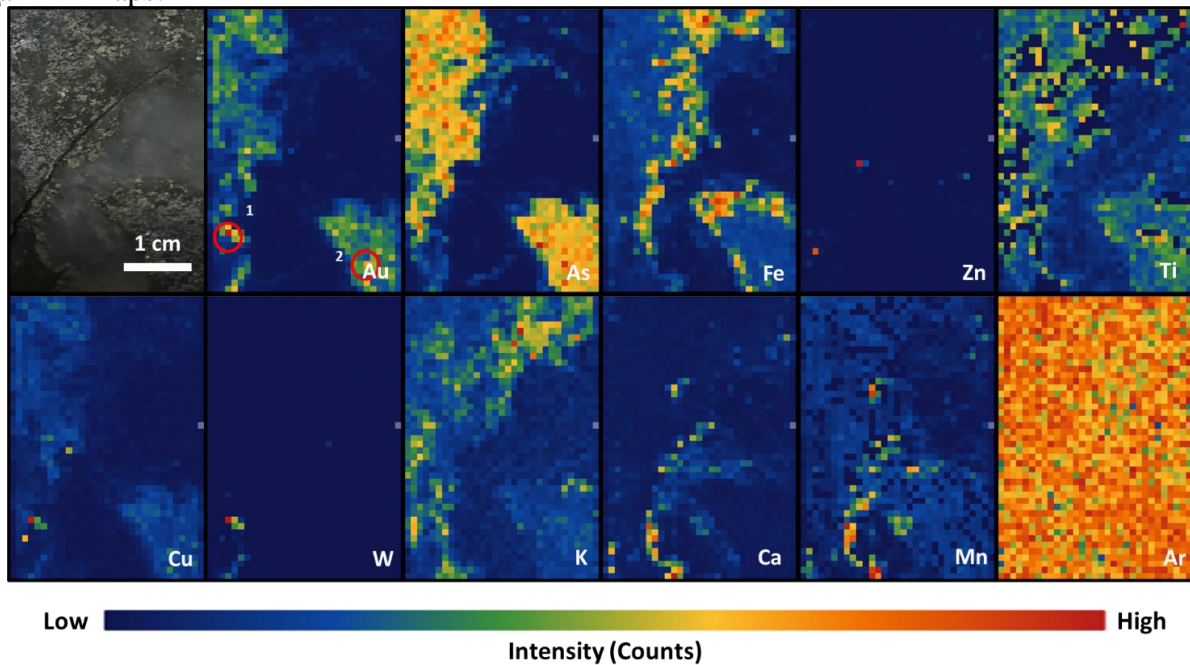
1. Au & As have the same distribution along with the light green layer of foliation.
2. Zn Ti Cu W Ca Mn are disseminated.
3. K distributes in the light green layers of foliation.
4. Au spots: 1&2. Au peak on the As shoulder on the MCA Spectrum, but higher than the shoulder.
5. Ar intensity (without filter→ with filter): 569.9 →151

Sample Number	2854 (800 μm)	Drill Hole	TL-16-604A	Depth	729.02-729.2m
Lithology	Metavolcanic Tuff	Map Size	2 cm x 3.5 cm	Gold Grade	10.49 ppm

MCA Spectrum:



SR- μ XRF Maps:

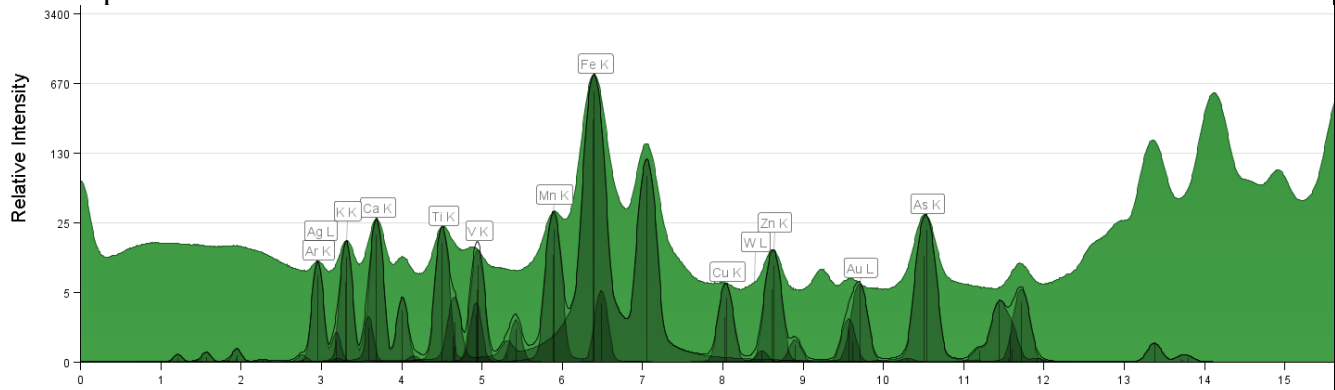


Description:

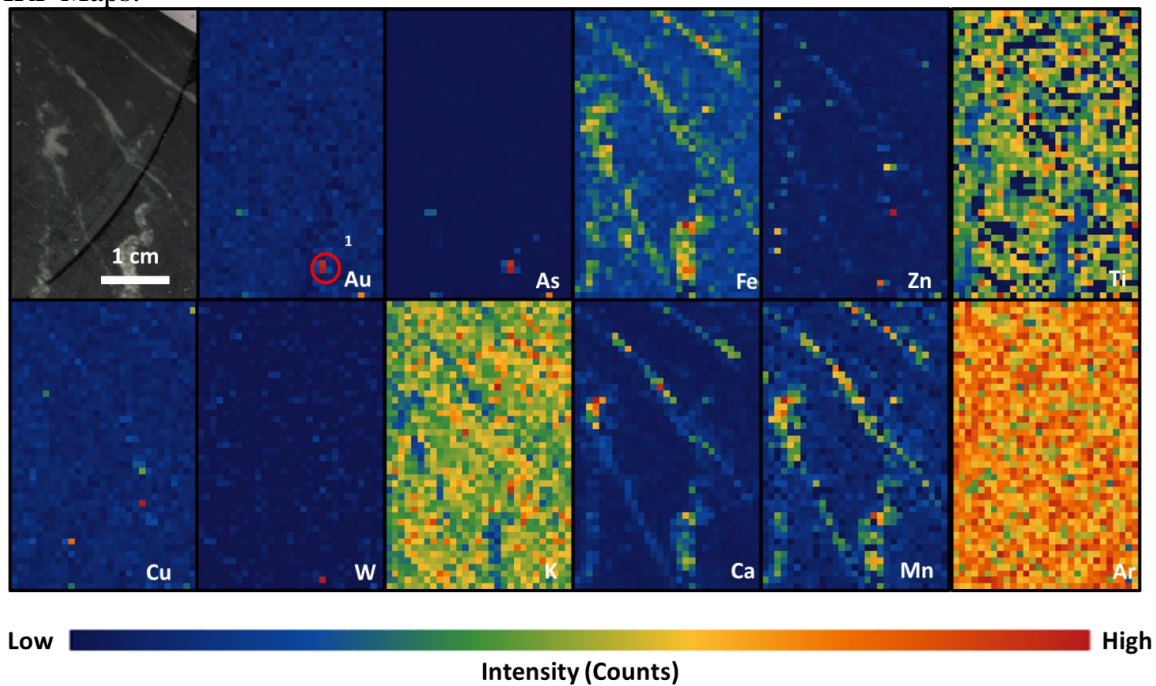
1. Au & As have the same distribution in the sulphide intrusion.
2. Fe & K have the same distribution in the sulphide intrusion, and there is higher intensity on the edge of the intrusion.
3. Ca Ti Mn have the same distribution along with the sulphide intrusion in the white vein, and the side beside the intrusion has higher intensity.
4. Cu W Zn are disseminated.
5. Au spots: 1. W peak, false Au signal; 2. Au peak on the As shoulder on the MCA Spectrum, but higher than the shoulder,
6. Ar intensity (without filter \rightarrow with filter): 628.2 \rightarrow 151.2

Sample Number	2858 (800 μm)	Drill Hole	TL-16-607	Depth	817.4-817.6 m
Lithology	Lapilli Tuff	Map Size	2 cm x 3.5 cm	Gold Grade	2.45 ppm

MCA Spectrum:



SR-μXRF Maps:

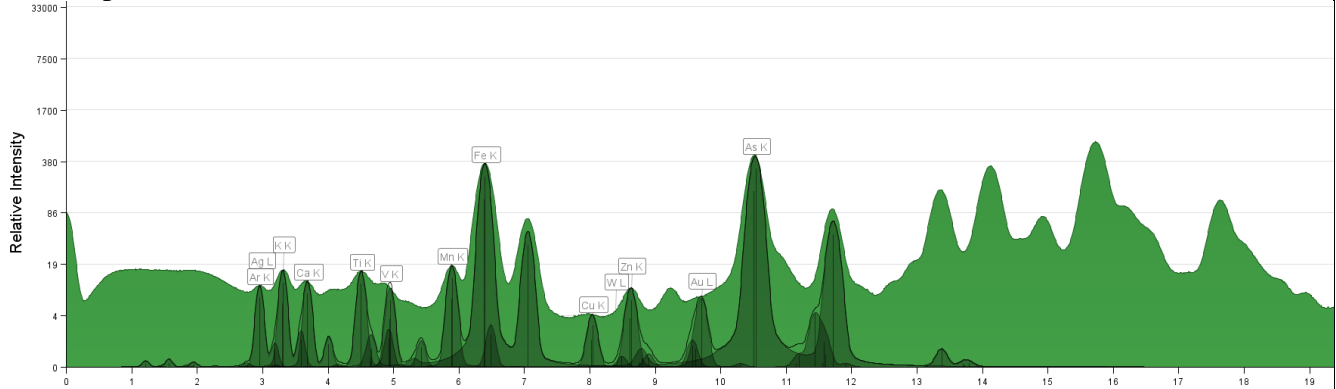


Description:

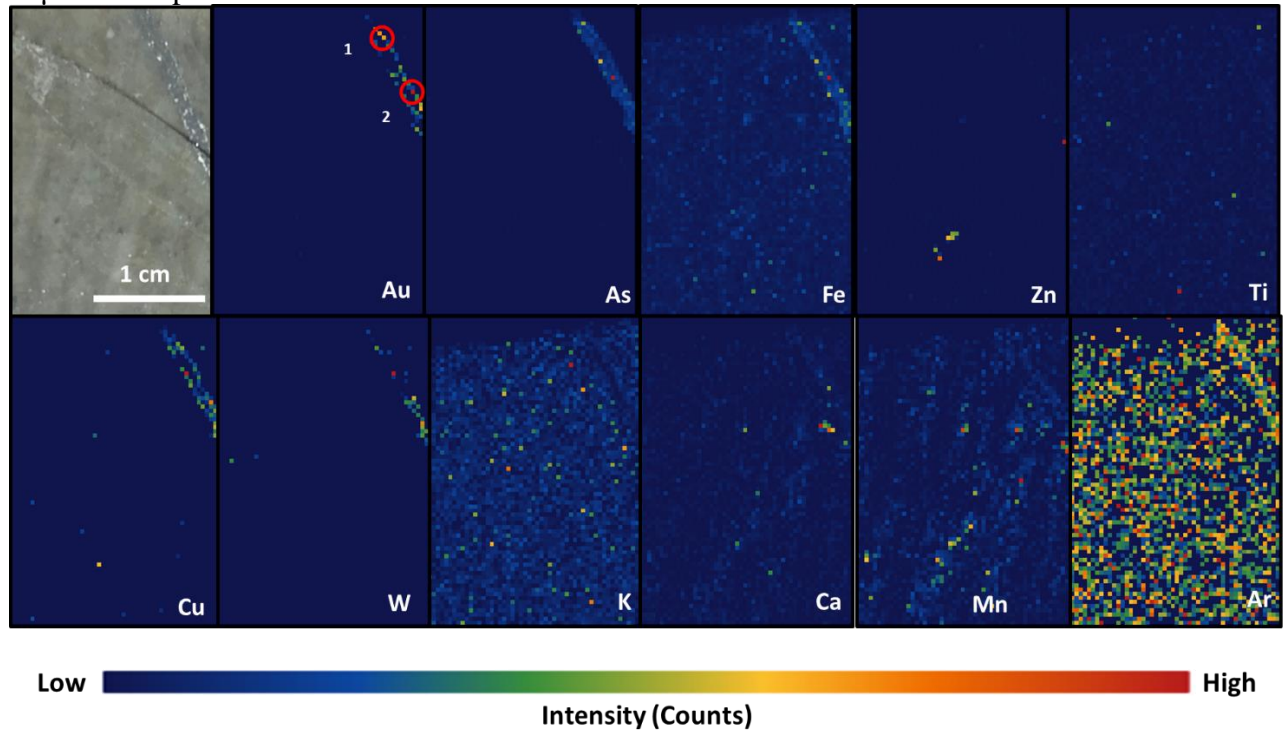
1. Au & As have the same distribution in the sulphide intrusion.
2. Ca Fe Mn have the same distribution along with the white veins and sulphide intrusion.
3. Cu W Zn are disseminated in the white veins.
4. Ti & K have the same distribution opposite to the white veins and sulphide intrusion.
5. Au spots: 1. Au peak on the As shoulder on the MCA Spectrum, but higher than the shoulder.
6. Ar intensity (without filter → with filter): 628.2 → 150.9

Sample Number	2827 (300 μm)	Drill Hole	TL-15-564	Depth	183-183.23m
Lithology	QFP	Map Size	2 cm x 3.5 cm	Gold Grade	Close to 9-0.6 ppm

MCA Spectrum:



SR-μXRF Maps:

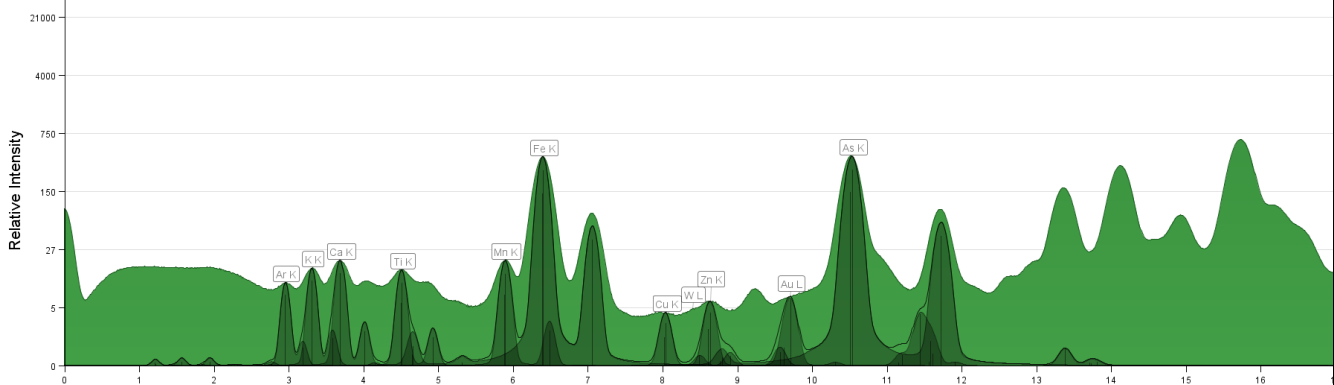


Description:

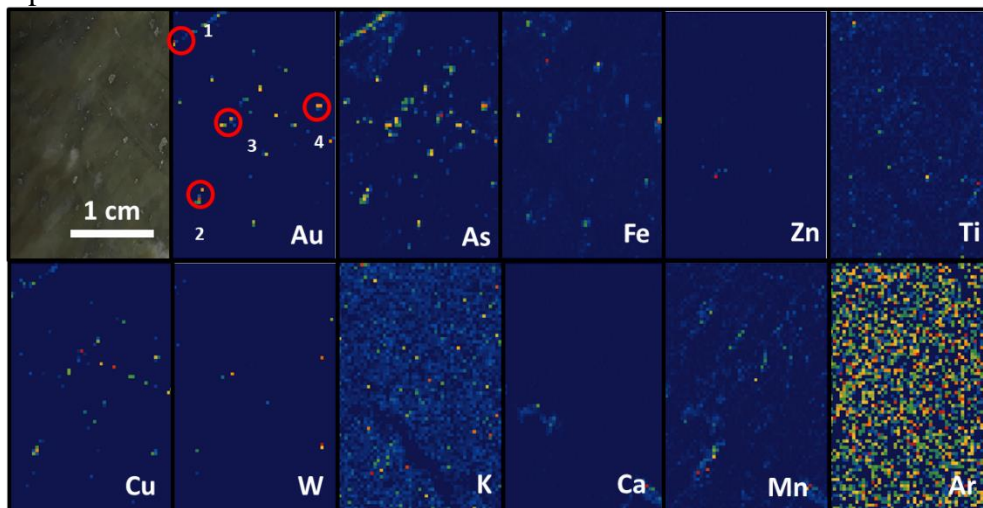
1. Au As Cu Fe have the same distribution along with sulphide veins.
2. Ca Mn have the same distribution.
3. Ti V have the same distribution.
4. W Zn Ag are disseminated.
5. K has the opposite distribution to the vein.
6. Au spots: 1&2 Au peak on the As shoulder on the MCA Spectrum, but higher than the shoulder.
7. Ar intensity (without filter→ with filter): 129.1→145.3

Sample Number	2824 (300 μm)	Drill Hole	TL-15-568	Depth	200.62-200.82 m
Lithology	QFP	Map Size	2 cm x 3.5 cm	Gold Grade	1.91-8.25 ppm

MCA Spectrum:



SR-μXRF Maps:

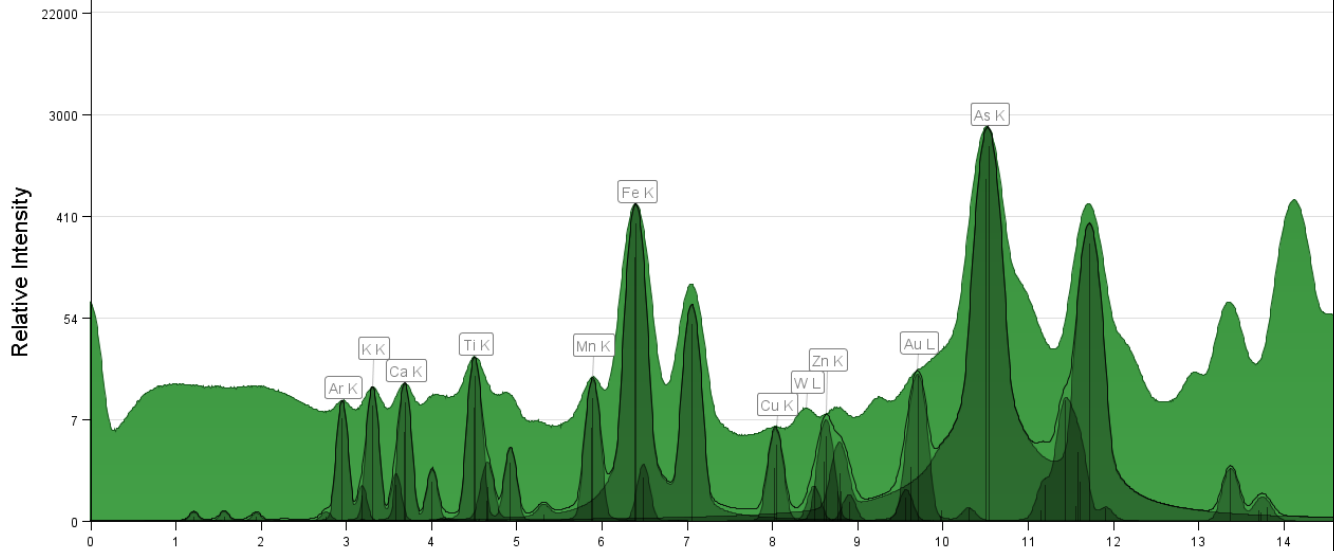


Description:

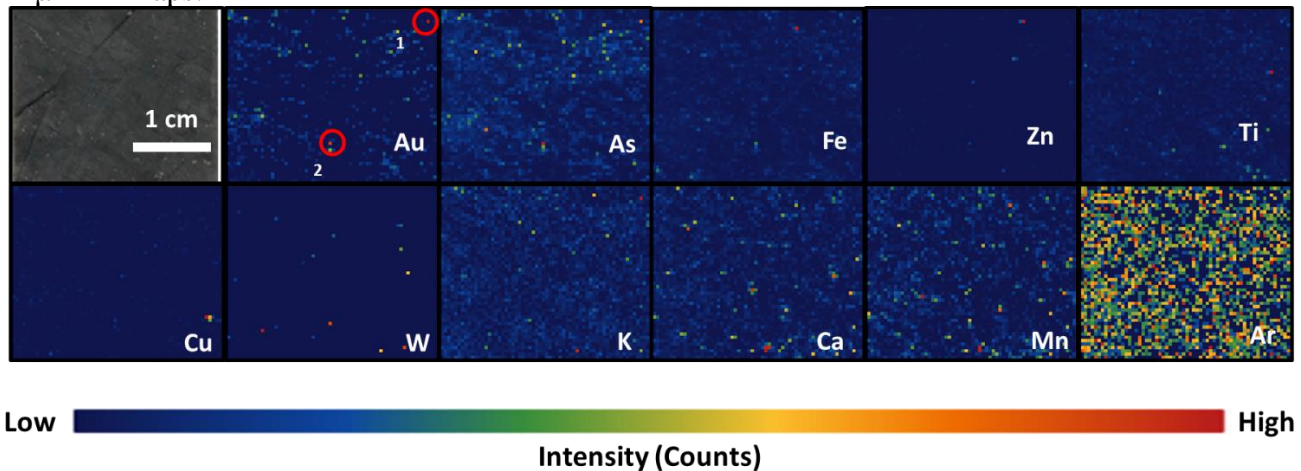
1. Ti & K have the same distribution which is opposite to the fractures.
2. Au & As have the same distribution and these two elements are disseminated on the offcut.
3. Ca distributes in the white intrusion on the offcut.
4. Fe Zn Cu W Mn are disseminated.
5. Au spots: 1-4. Au peak on the As shoulder on the MCA Spectrum, but higher than the shoulder,
6. Ar intensity (without filter→ with filter): 129.1→145.4

Sample Number	2819 (300 μm)	Drill Hole	TL-16-575	Depth	154.1-154.32 m
Lithology	QFP	Map Size	10 cm x 3.5 cm	Gold Grade	7.21 ppm

MCA Spectrum:



SR- μ XRF Maps:

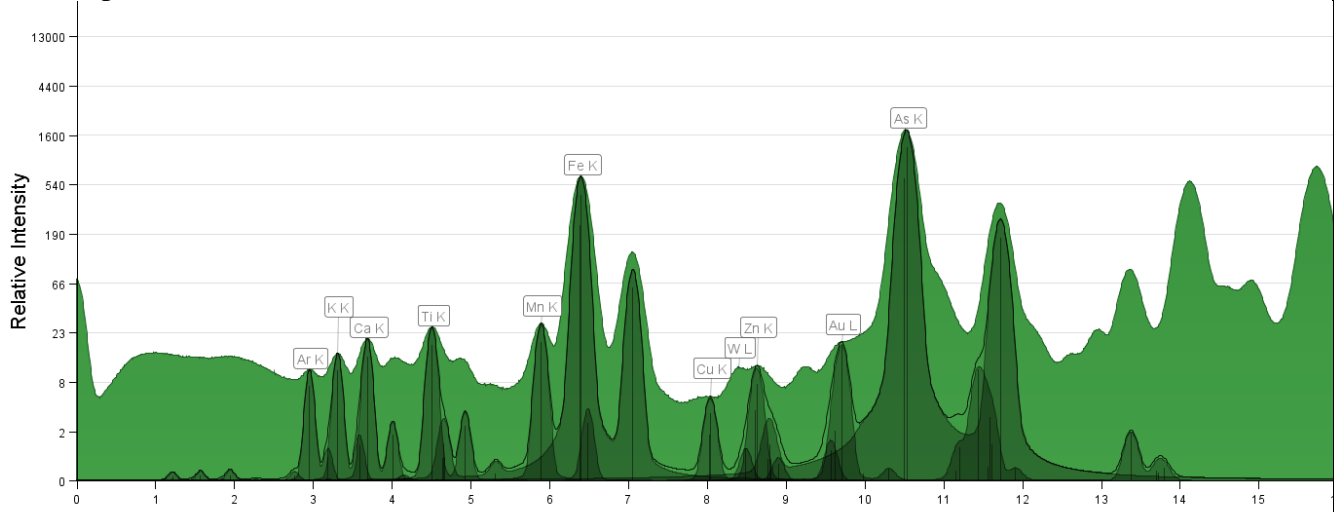


Description:

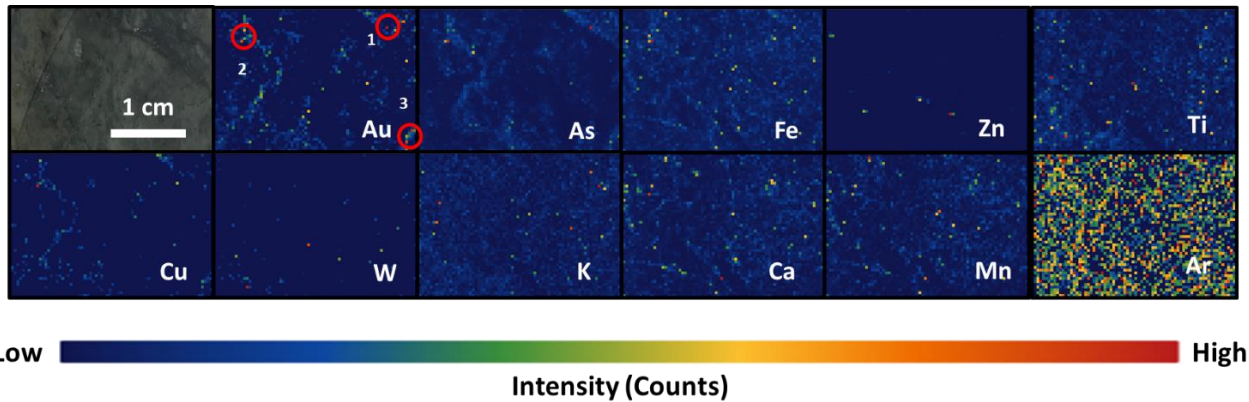
1. Au & As have the same distribution along with the black foliation layers.
2. Fe Zn Cu have the same distribution.
3. No W in this sample.
4. Zn Ca Mn are disseminated.
5. K & Ti are all over the sample.
6. Au spots: 1-2. Au peak on the As shoulder on the MCA Spectrum, but higher than the shoulder,
7. Ar intensity (without filter \rightarrow with filter): 129.1 \rightarrow 145.3

Sample Number	2841(300 μm)	Drill Hole	TL-13-504	Depth	190.5-190.78 m
Lithology	FP	Map Size	2 cm x 3.5 cm	Gold Grade	25.2 ppm

MCA Spectrum:



SR-μXRF Maps:

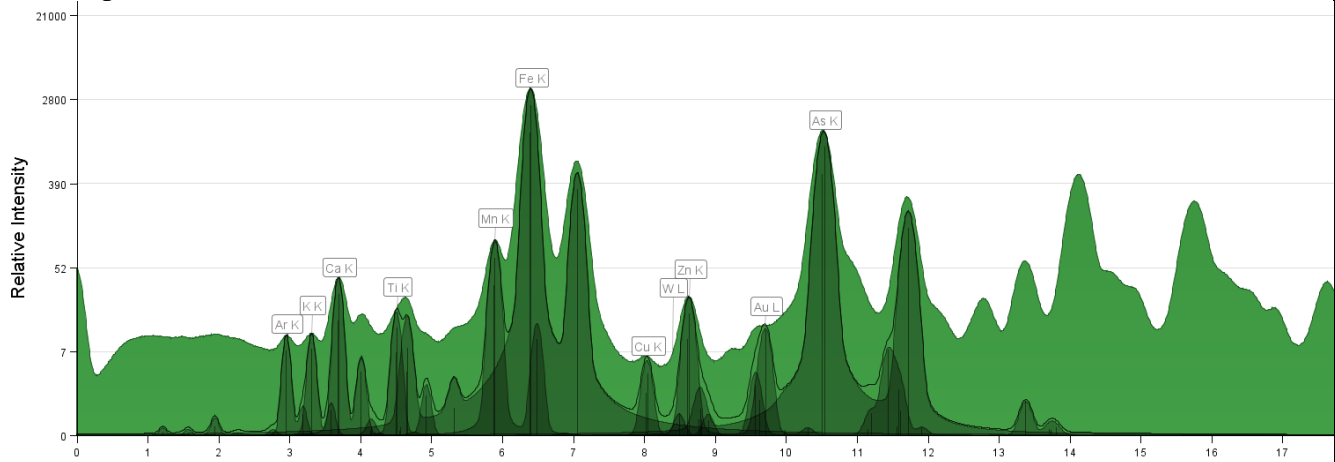


Description:

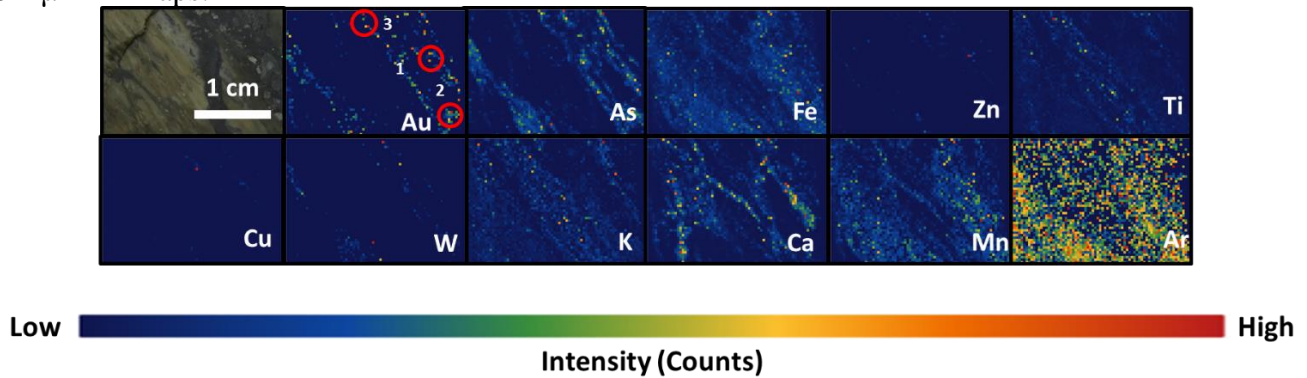
1. Au & As have the same distribution along with the folded sulphide veins.
2. Cu & Fe are disseminated in the folded sulphide veins.
3. Zn & W are disseminated.
4. K distributes on the edge of the darker grey layer and lighter grey layer of the foliation texture; while Ca & Mn distribute in the darker grey layer which next to the folded sulphide veins.
5. Au spots: 1-3. Au peak on the As shoulder on the MCA Spectrum, but higher than the shoulder,
6. Ar intensity (without filter→ with filter): 129.1 →145.2

Sample Number	2834 (300 μ m)	Drill Hole	TL-13-500	Depth	195.76-196 m
Lithology	Lapilli Tuff	Map Size	2 cm x 3.5 cm	Gold Grade	5.21 ppm

MCA Spectrum:



SR- μ XRF Maps:

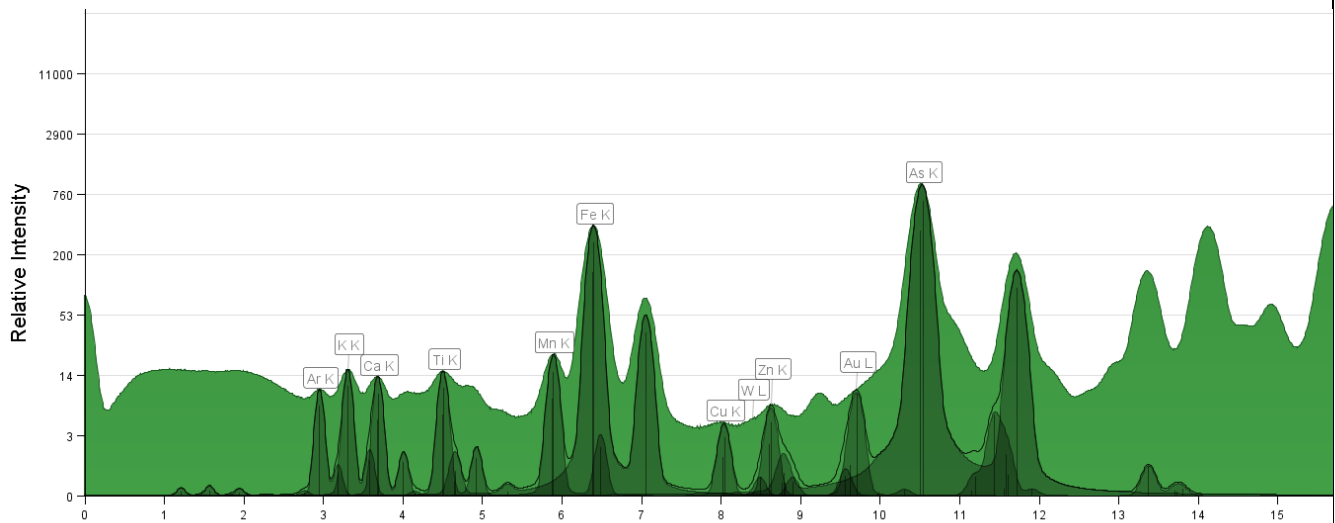


Description:

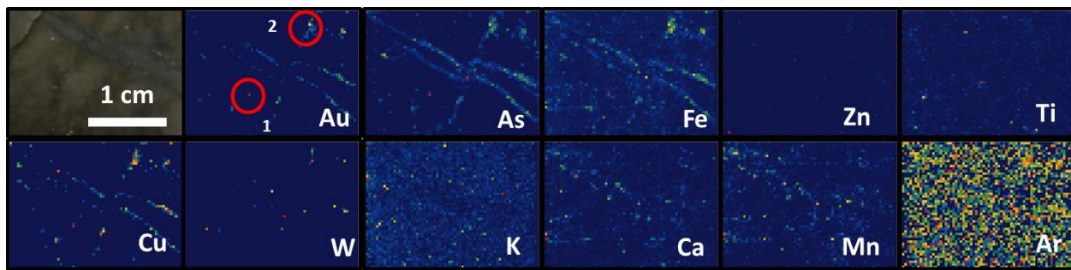
1. Au & As have the same distribution along with the sulphide veins.
2. Fe & Mn distribute in the dark foliated layers next to the sulphide veins.
3. Ca distributes in the dark red veinlets.
4. Ti & K distribute opposite to the dark red veinlets.
5. Cu Zn W are disseminated in the sulphide veins.
6. Au spots: 1. real Au peak, much higher than As shoulder. 2&3. Au peak on the As shoulder on the MCA Spectrum, but higher than the shoulder.
7. Ar intensity (without filter \rightarrow with filter): 129.1 \rightarrow 144.7

Sample Number	2845 (300 μm)	Drill Hole	TL-13-509	Depth	235.6-235.86 m
Lithology	QFP	Map Size	2 cm x 3.5 cm	Gold Grade	1.13 ppm

MCA Spectrum:



SR-μXRF Maps:

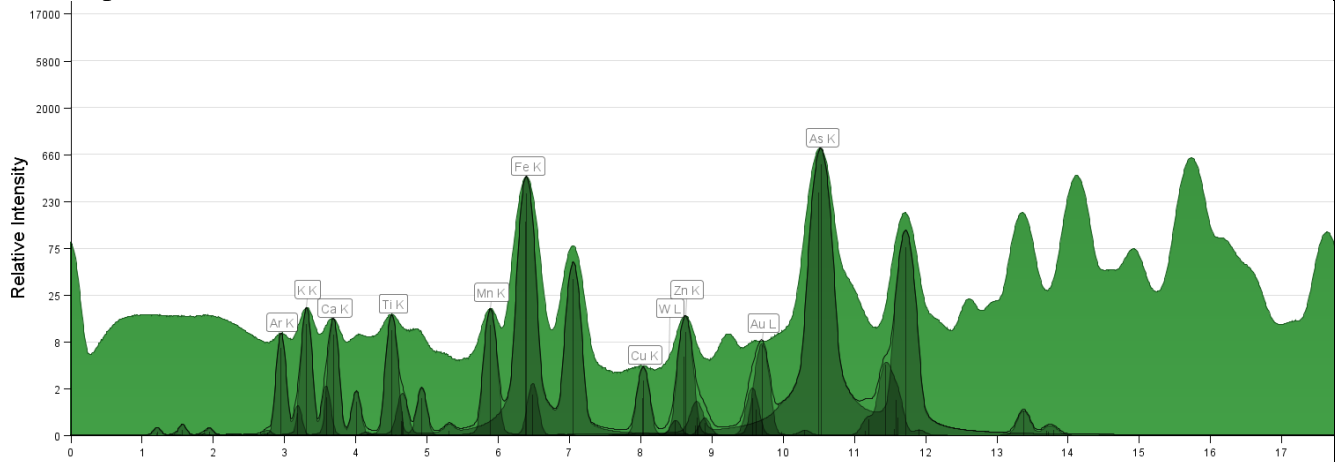


Description:

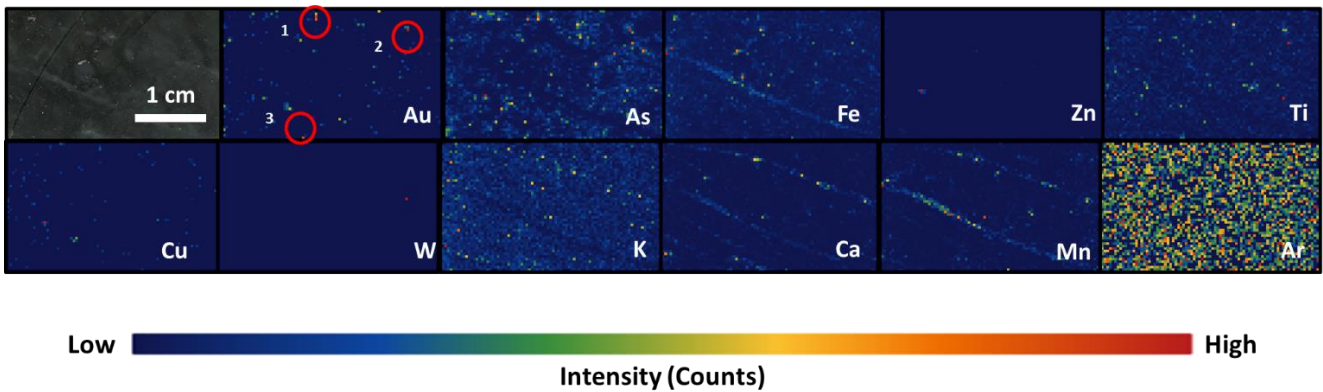
1. Au As Fe Cu have the same distribution along with the dark fine veinlets.
2. W Zn Ca Mn are disseminated.
3. Au spots: 1-2. Au peak on the As shoulder on the MCA Spectrum, but higher than the shoulder.
4. Ar intensity (without filter→ with filter): 140→145.4

Sample Number	2857 (300 μm)	Drill Hole	TL-16-607	Depth	718.4-718.66 m
Lithology	QFP	Map Size	2 cm x 3.5 cm	Gold Grade	2.16 ppm

MCA Spectrum:



SR- μ XRF Maps:

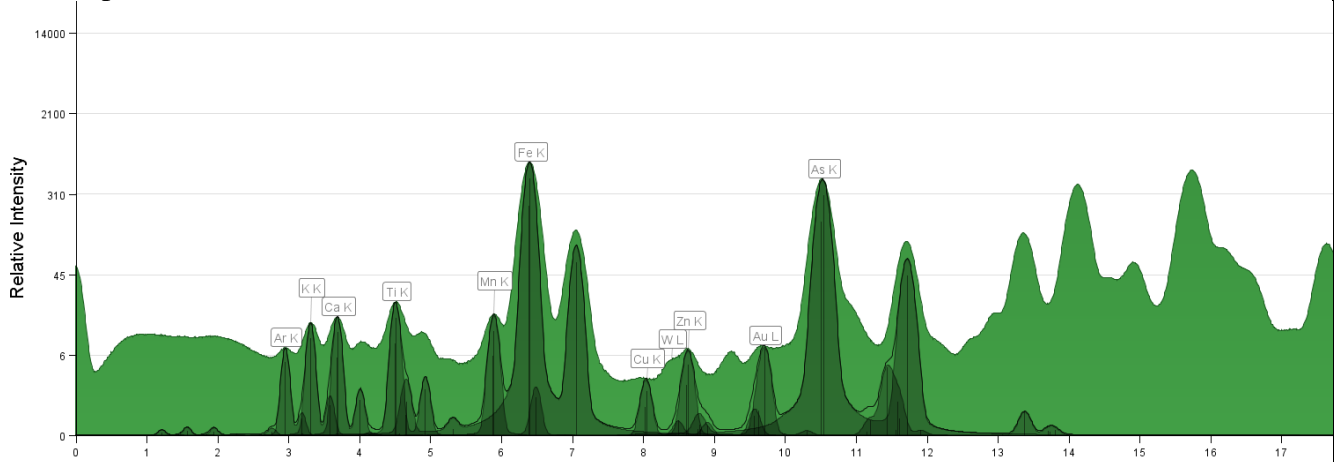


Description:

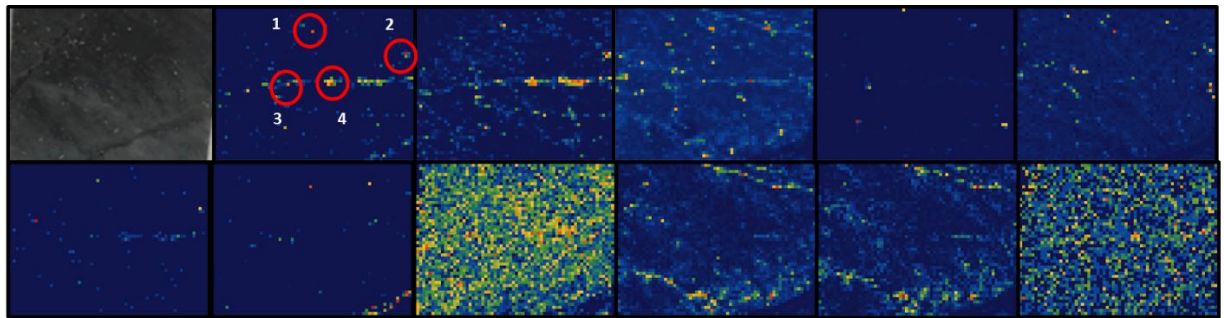
1. Au W Cu have the same distribution which is a high-intensity spot on the right-top corner
2. Zn is disseminated.
3. Au spots: 1-3. Au peak on the As shoulder on the MCA Spectrum, but higher than the shoulder.
4. Fe Ca Mn have the same distribution along with the sulphide veins.
5. Ti & K have the same distribution opposite to the sulphide veins and fractures.
6. Ar intensity (without filter \rightarrow with filter): 140 \rightarrow 145.3

Sample Number	2853 (300 μm)	Drill Hole	TL-16-604A	Depth	643.96-644.24m
Lithology	QFP	Map Size	2 cm x 3.5 cm	Gold Grade	7.73 ppm

MCA Spectrum:



SR-μXRF Maps:

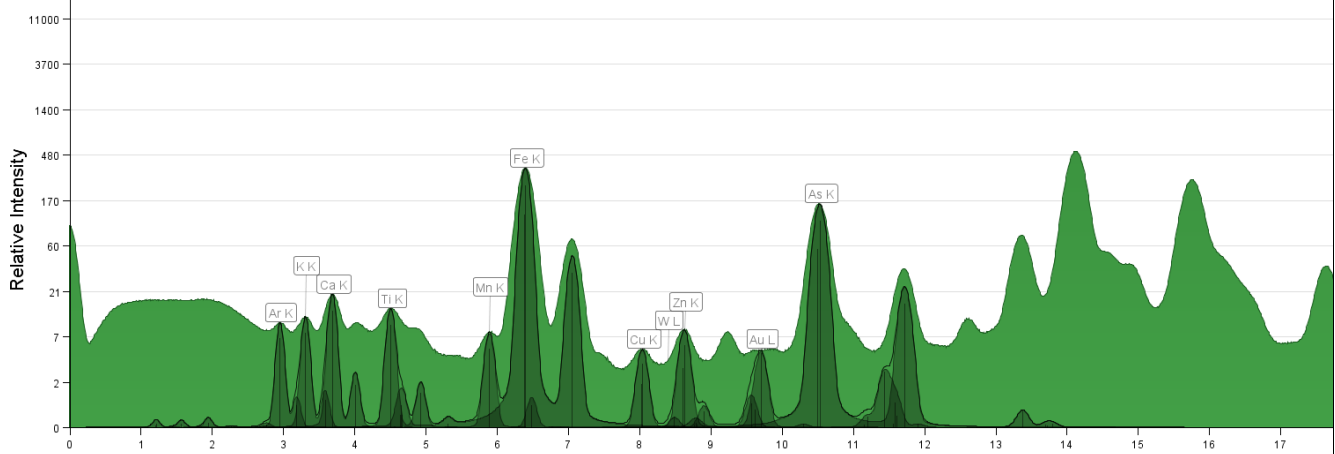


Description:

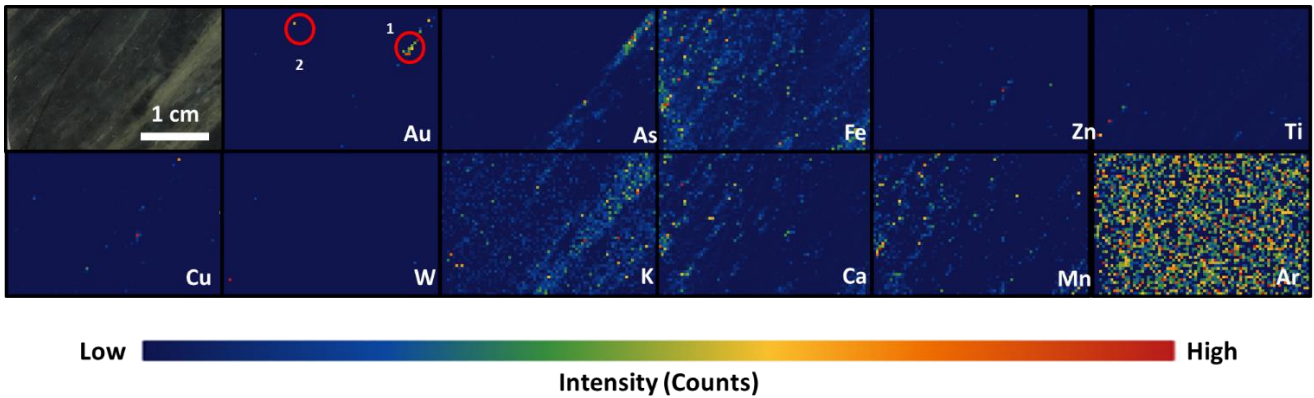
1. Au As Cu have the same distribution in the middle (look like data crash, fake signal).
2. Ca Fe Mn have the same distribution along with the light grey layers of the foliation.
3. Zn & W are disseminated.
4. Au spots: 1. W, false Au signal; 2&4. Au peak on the As shoulder on the MCA Spectrum, but higher than the shoulder; 3. Au peak and W peak are overlapped, but Au peak is much higher than As shoulder and W peak.
5. Ar intensity (without filter→ with filter): 140→135.1

Sample Number	2831 (300 μ m)	Drill Hole	TL-15-551	Depth	96.8-97 m
Lithology	Metasandstone	Map Size	2 cm x 3.5 cm	Gold Grade	2.26 ppm

MCA Spectrum:



SR- μ XRF Maps:



Description:

1. Au & As have the same distribution along with the light green layer of foliation.
2. Zn Ti Cu W Ca Mn are disseminated.
3. K distributes in the light green layers of foliation.
4. Au spots: 1&2. Au peak on the As shoulder on the MCA Spectrum, but higher than the shoulder.
5. Ar intensity (without filter \rightarrow with filter): 140 \rightarrow 145.4

CLS VESPERS-February 2019

Beamtime and Beamline Details:

Detector: Vortex four-element SDD

Max energy: 20.46 KeV

Mode: Pink Beam

Beam spot size: 100 μm x 100 μm , 10 μm x 10 μm

Dwell time: 1 sec

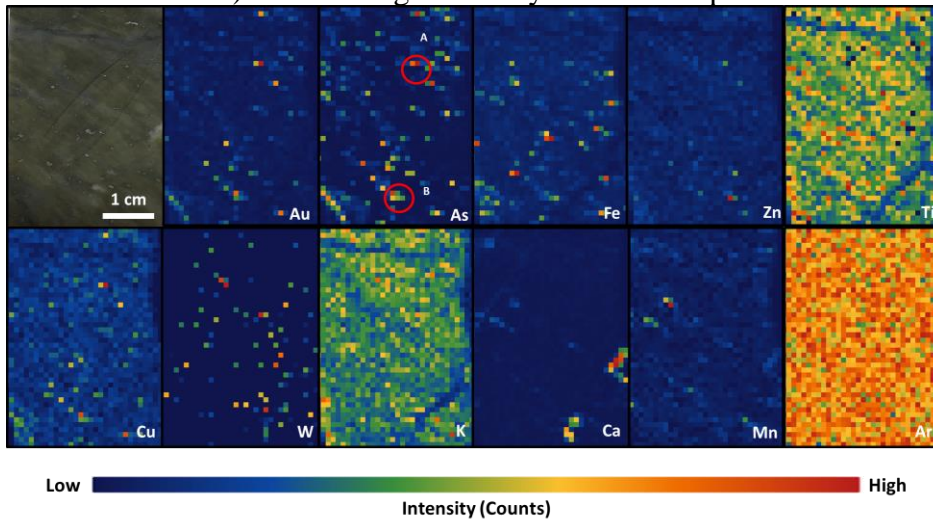
Samples: 7 offcuts

*These maps were for analyzed for select As and Au hotspot for XANES.

Data Processing:

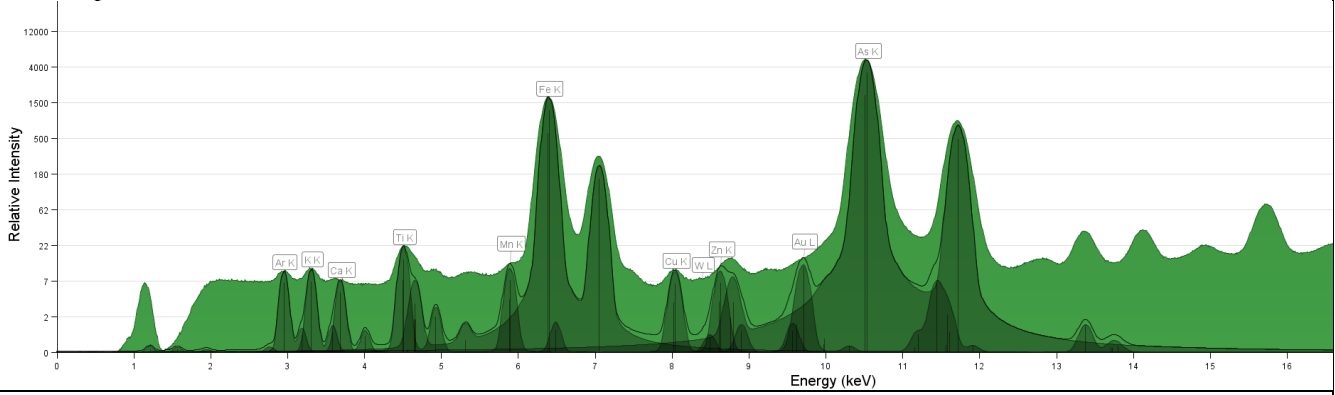
1. Energy Calibration Maximum: 20.46 keV, using Fe K peak to adjust the energy.
2. Peak fitting: Fe K, Ca K, As K, Cu K, Ar K, Mn K, Au L, Zn K, Ag L, K K, W L, Ti K, V K.
3. Ar Normalization: use the cursor to check the Ar channel at the bottom of the window. Different dataset has different Ar channel. For this one, Ar channel is 295.
Use Data Filter-Advanced- Normalizer, mode: channel range, start channel:295, end channel: 297, normalized intensity: 10 (the best channel range was checked using Ar XRF map with lowest intensity range).
Without filter: 553.3
295-296:142.3
294-295: 152.2
295-295: 152.8
293-294: 179.3
293-295: 163
295-297: 138.9
294-296: 143.1
4. Map fitting: check the visible button.
5. Save MCA Spectrum and maps of each sample.
6. Check Au map to make sure if each high-intensity spot is the real gold signal: select the spot and plot selection → take notes of the relationship of Au and other element curves (on the shoulder/ real peak/ overlaid other element peaks/ false signal).

2824 (800µm-20ID APS Feb.): A & B. High intensity Au and As spots.

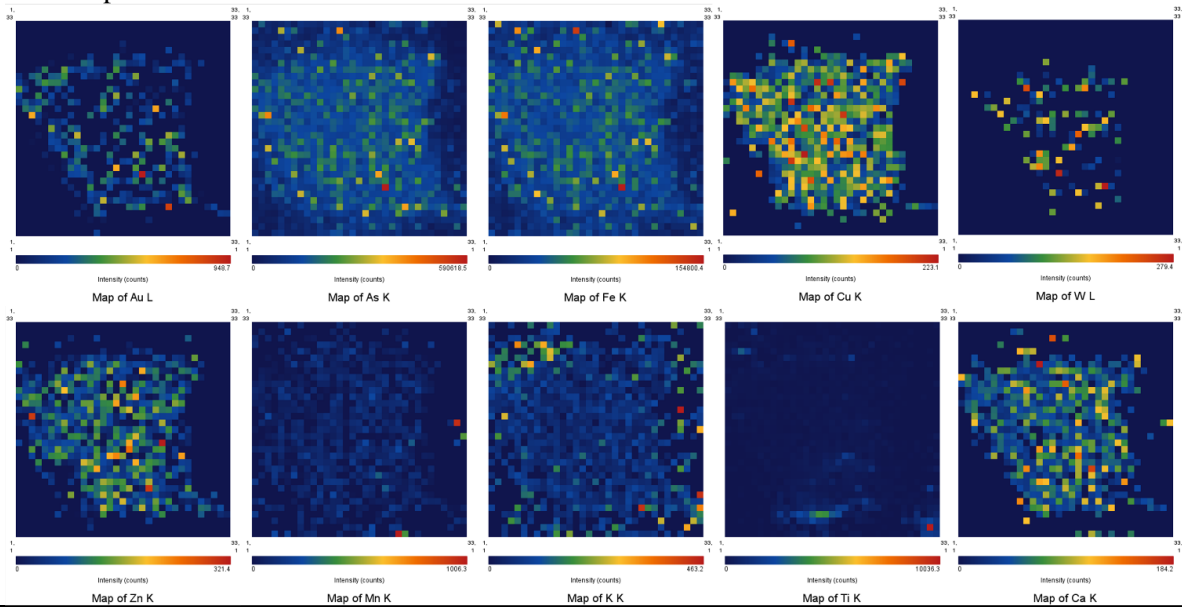


Sample Number	2824A (10 µm)	Drill Hole	TL-15-568	Depth	200.62-200.82 m
Lithology	QFP	Map Size	0.33 mm X 0.33 mm	Gold Grade	1.91-8.25 ppm

MCA Spectrum:

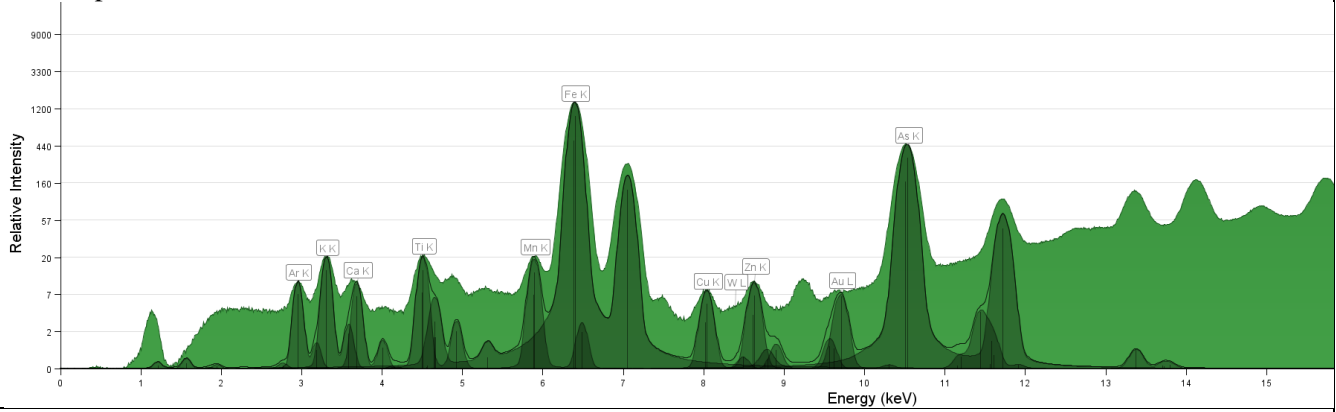


SR-µXRF Maps:

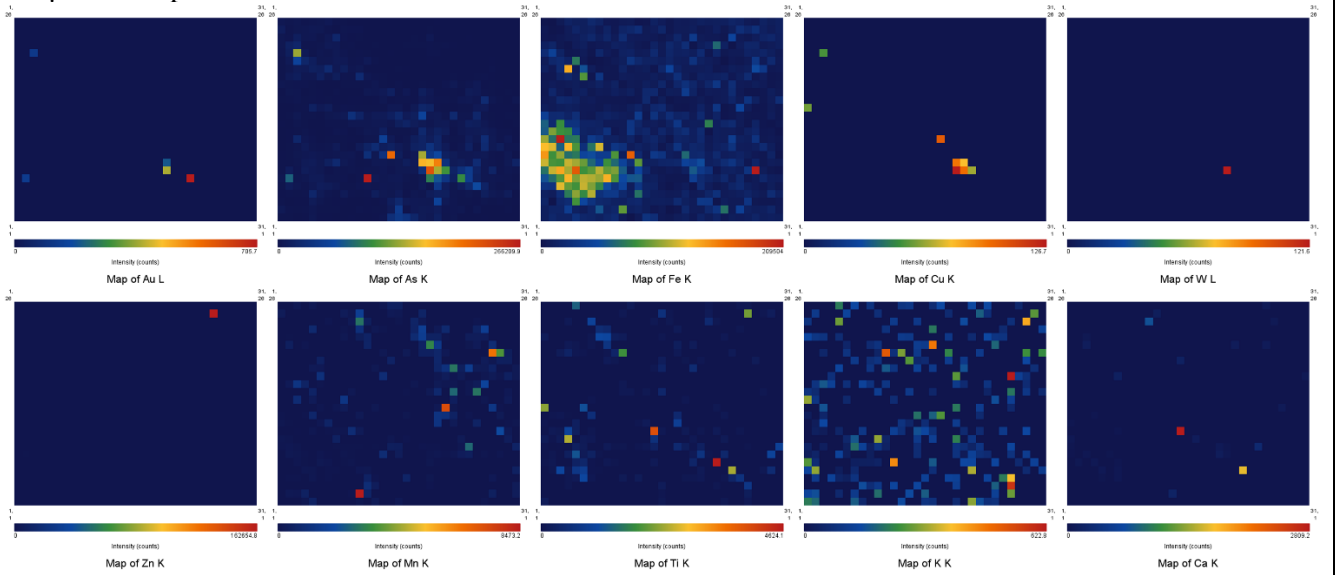


Sample Number	2824A (100 µm)	Drill Hole	TL-15-568	Depth	200.62-200.82 m
Lithology	QFP	Map Size	0.33 mm X 0.33 mm	Gold Grade	1.91-8.25 ppm

MCA Spectrum:

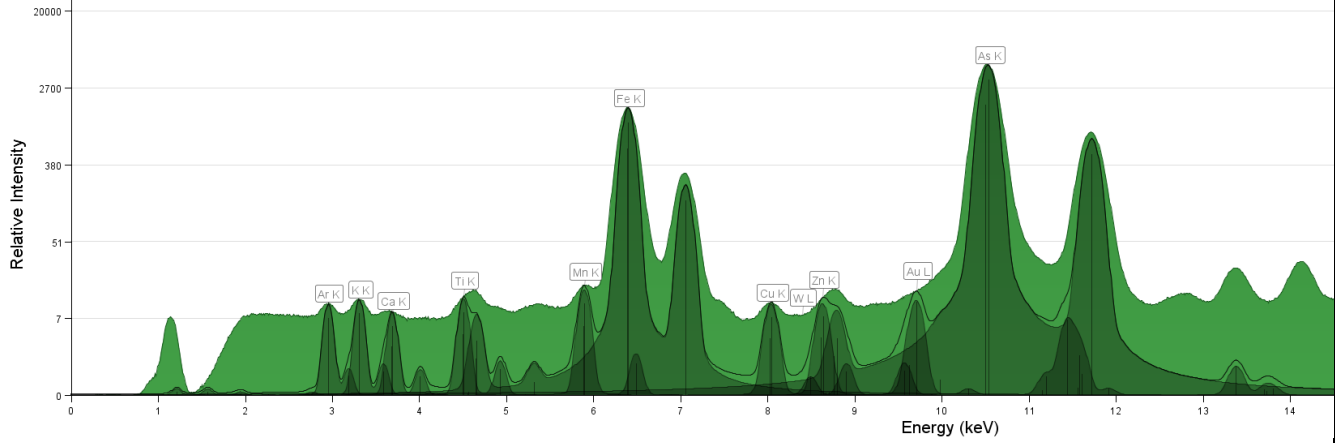


SR-µXRF Maps:

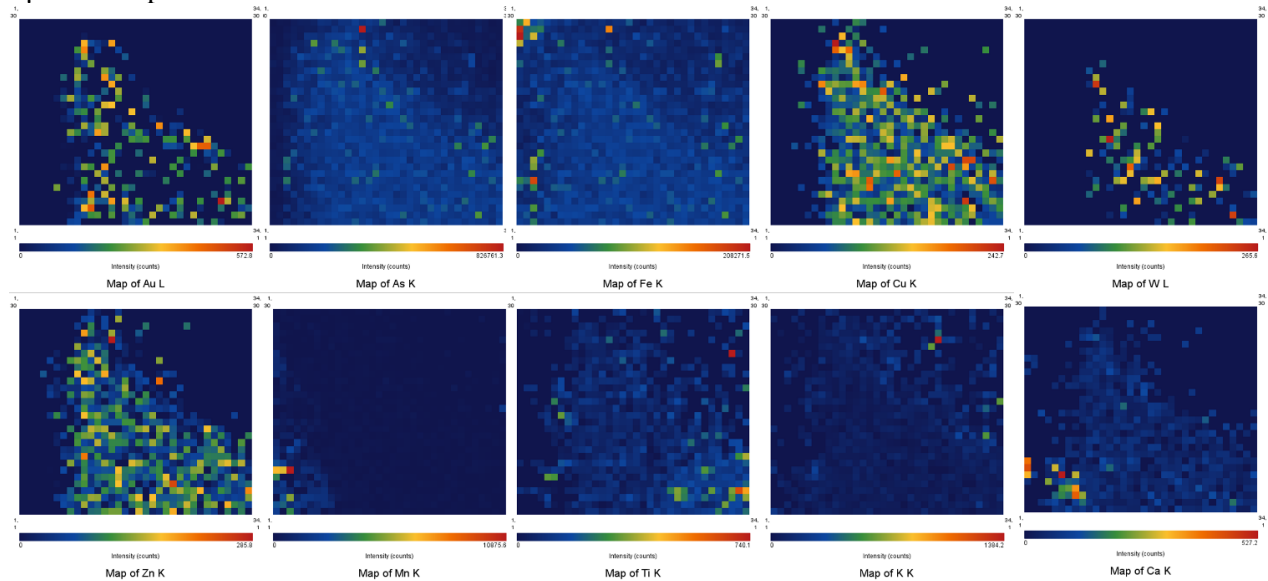


Sample Number	2824B (10 μ m)	Drill Hole	TL-15-568	Depth	200.62-200.82 m
Lithology	QFP	Map Size	0.26 mm X 0.26 mm	Gold Grade	1.91-8.25 ppm

MCA Spectrum:

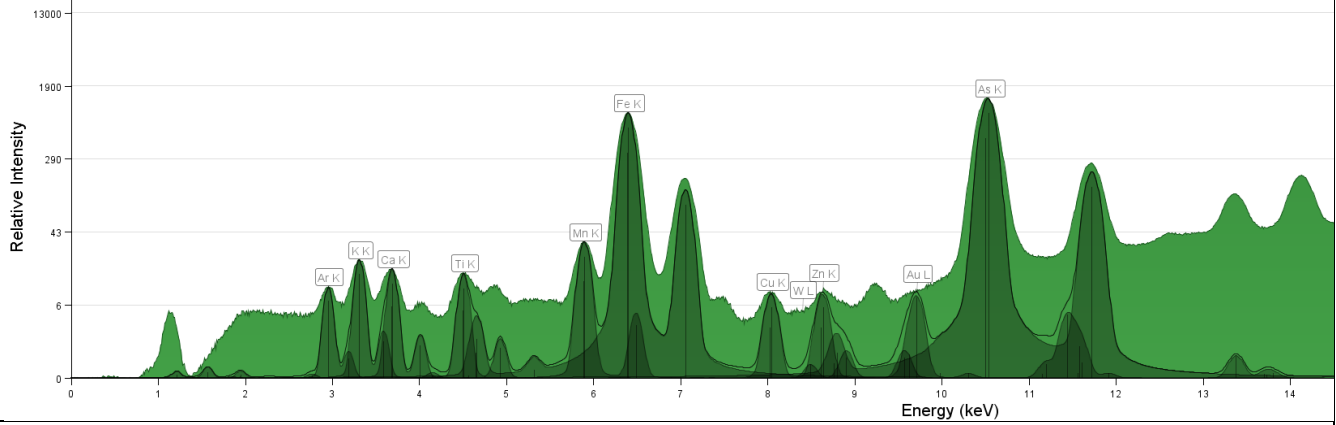


SR- μ XRF Maps:

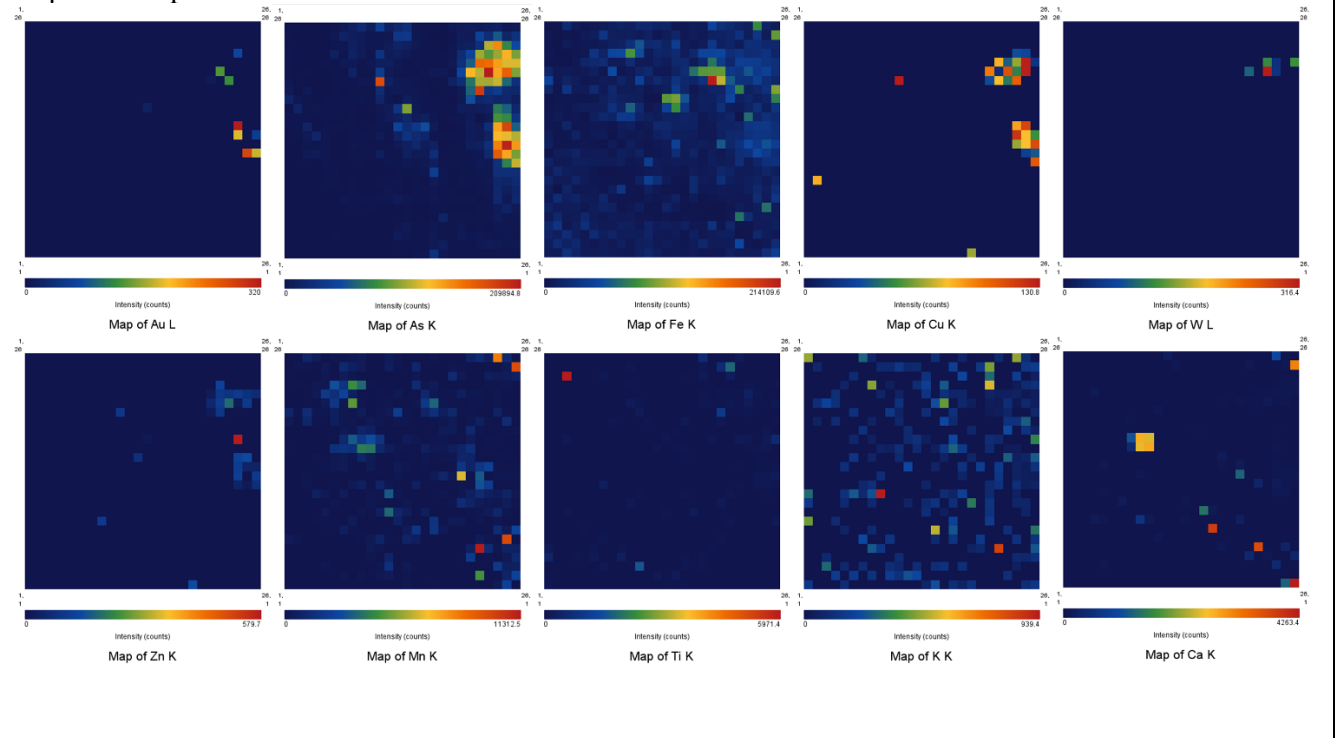


Sample Number	2824B (100 μm)	Drill Hole	TL-15-568	Depth	200.62-200.82 m
Lithology	QFP	Map Size	0.26 mm X 0.26 mm	Gold Grade	1.91-8.25 ppm

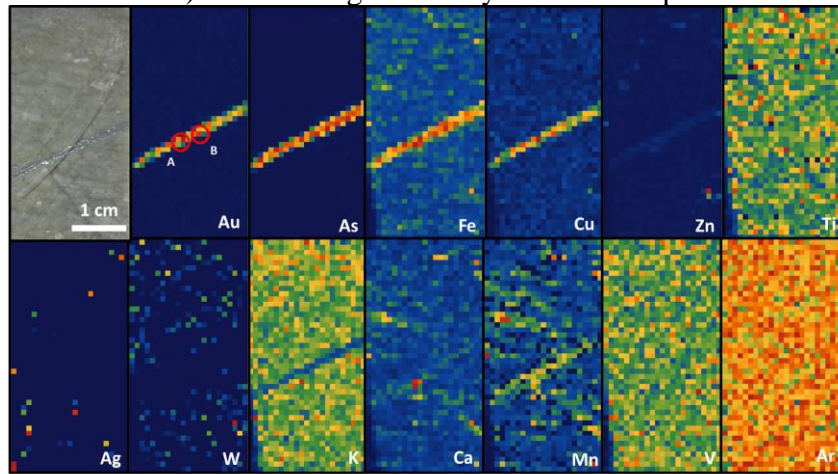
MCA Spectrum:



SR-μXRF Maps:

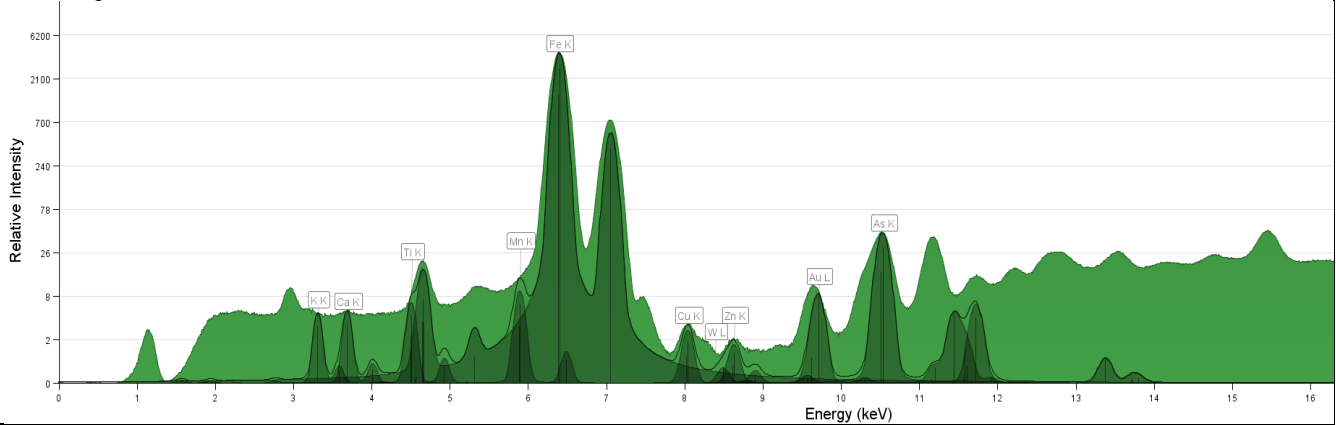


2827 (800µm-20ID APS Feb.): A & B. High intensity Au and As spots.

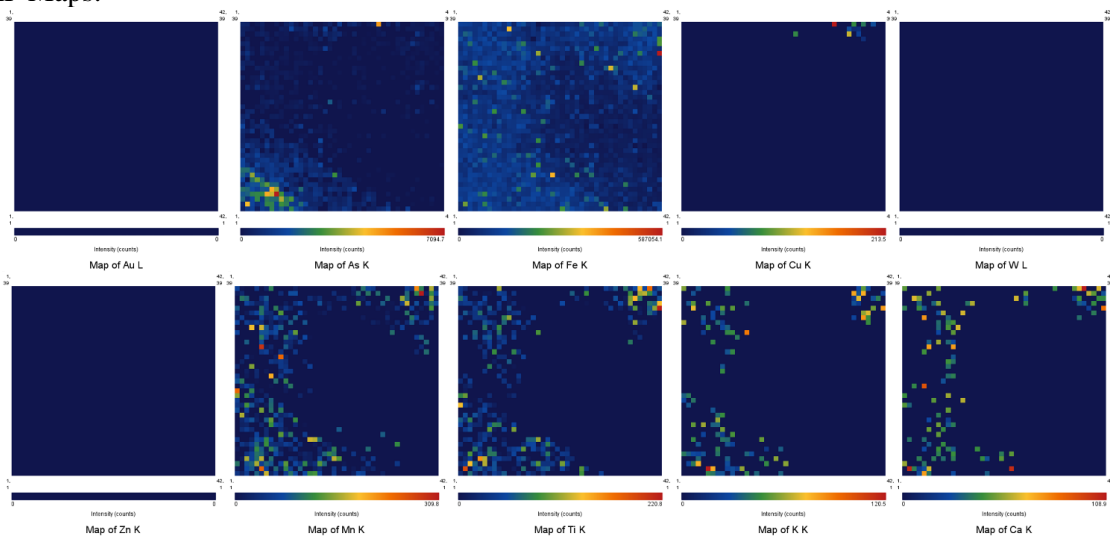


Sample Number	2827B (10 µm)	Drill Hole	TL-15-564	Depth	183-183.23m
Lithology	QFP	Map Size	2 cm x 3.5 cm	Gold Grade	Close to 9 --0.6 ppm

MCA Spectrum:

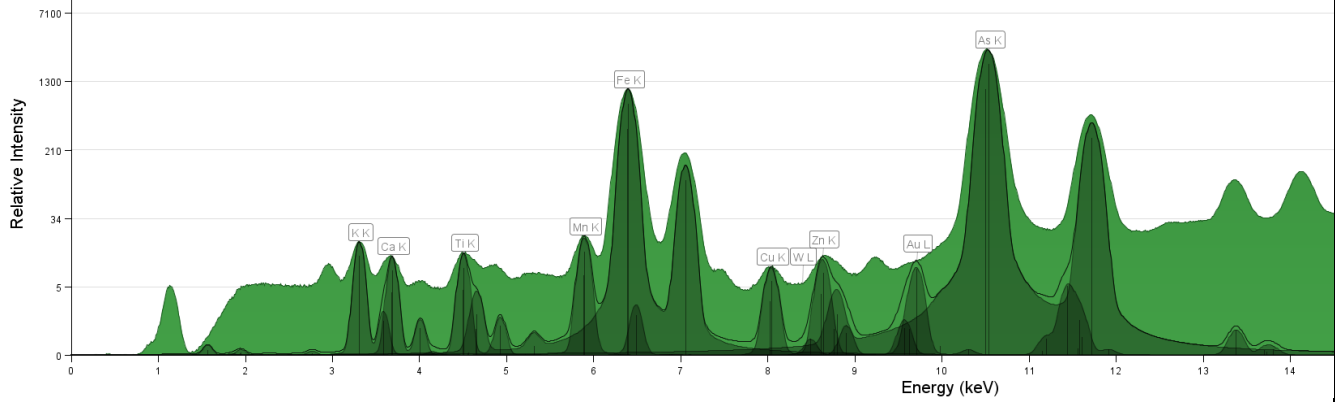


SR-µXRF Maps:

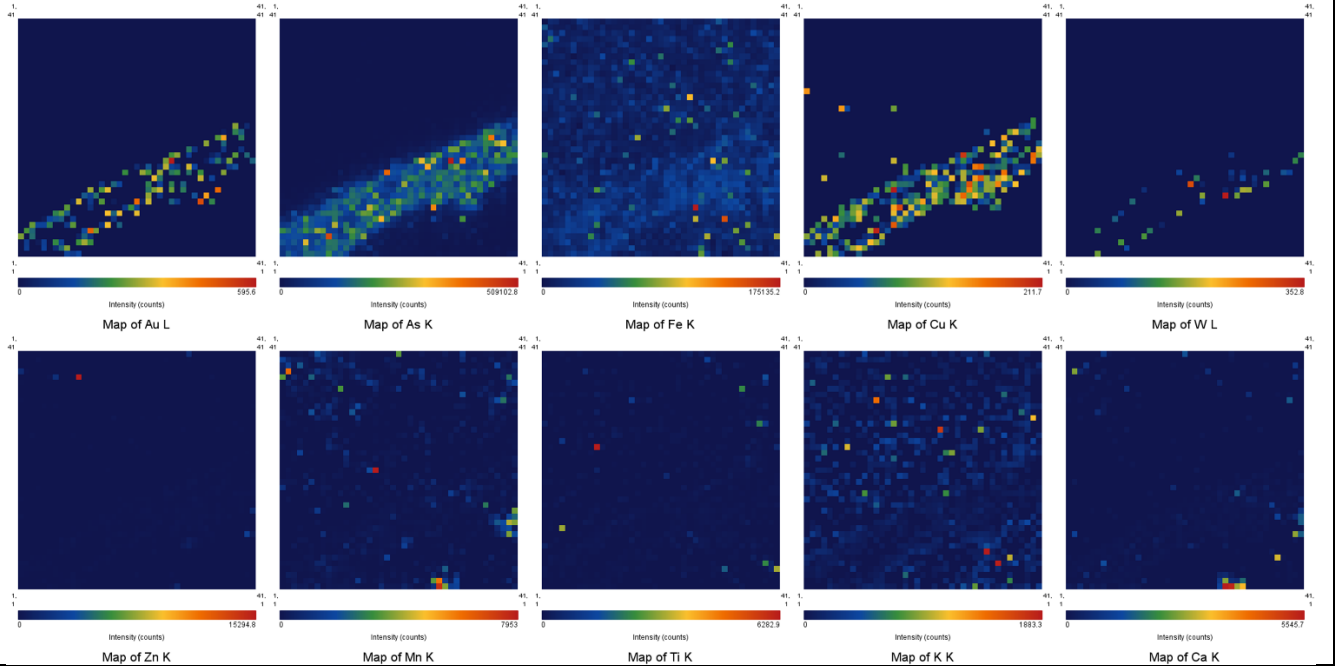


Sample Number	2827B (100 µm)	Drill Hole	TL-15-564	Depth	183-183.23m
Lithology	QFP	Map Size	0.41 mm X 0.41 mm	Gold Grade	Close to 9 ~0.6 ppm

MCA Spectrum:

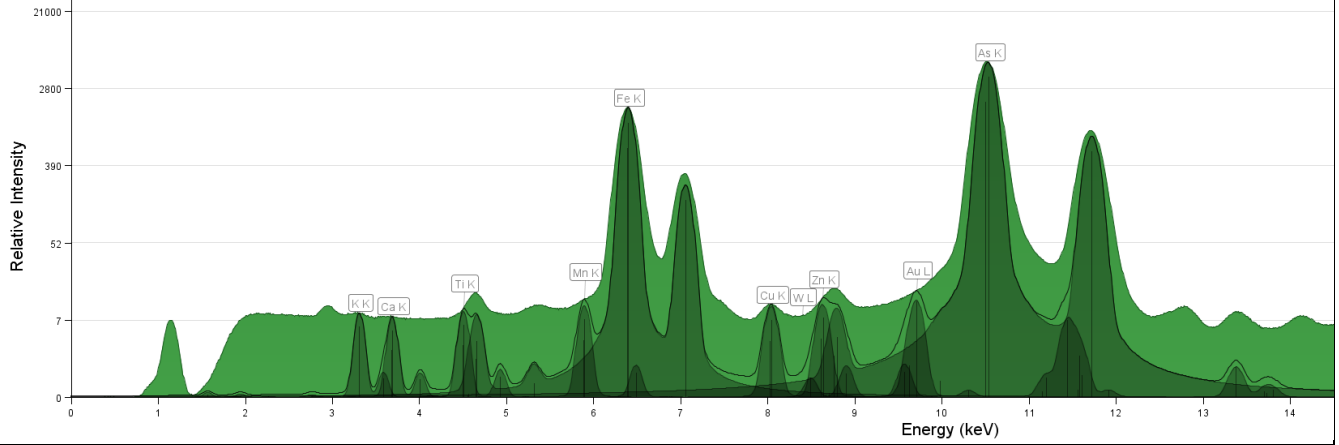


SR-µXRF Maps:

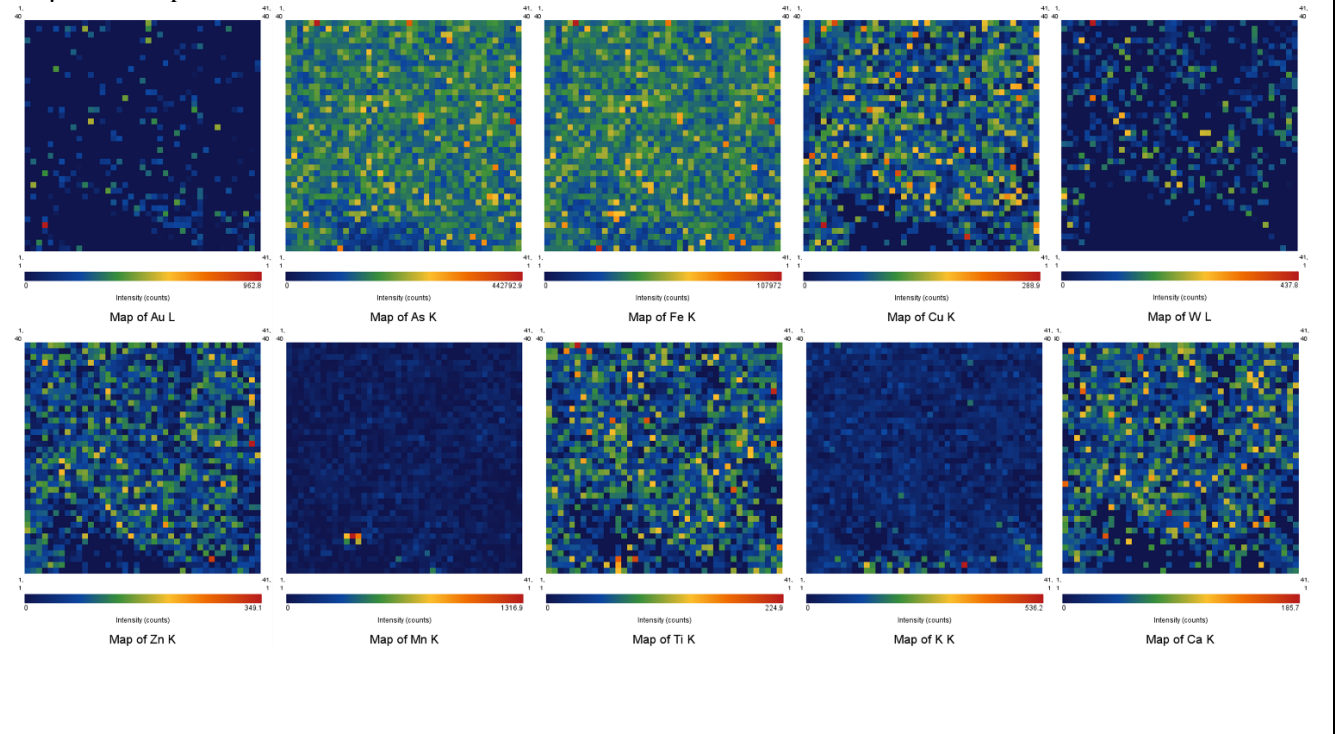


Sample Number	2827A (10 μm)	Drill Hole	TL-15-564	Depth	183-183.23m
Lithology	QFP	Map Size	2 cm x 3.5 cm	Gold Grade	Close to 9 ~0.6 ppm

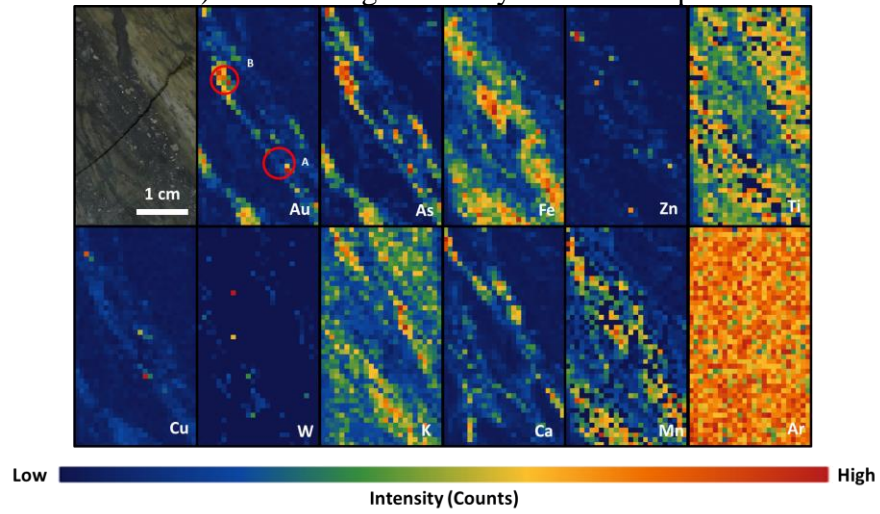
MCA Spectrum:



SR-μXRF Maps:

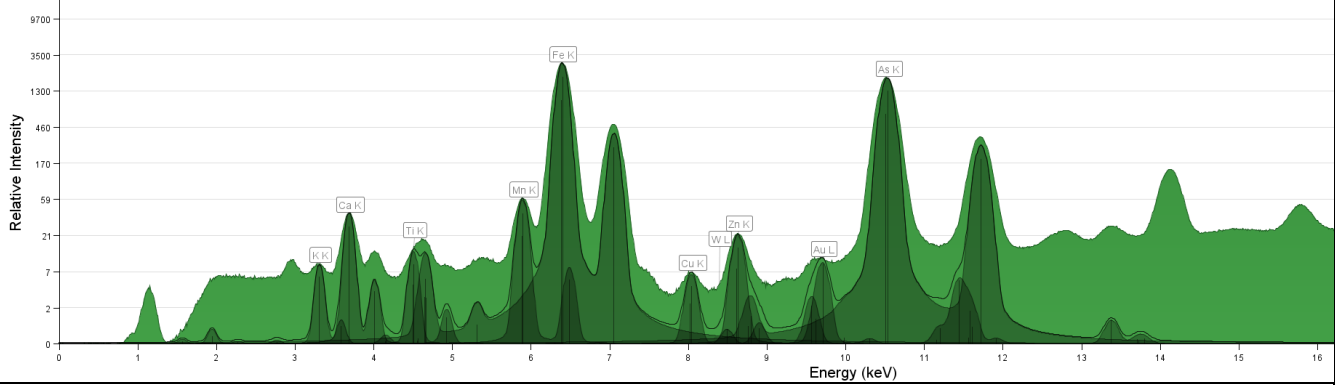


2834 (800µm-20ID APS Feb.): A & B. High intensity Au and As spots.

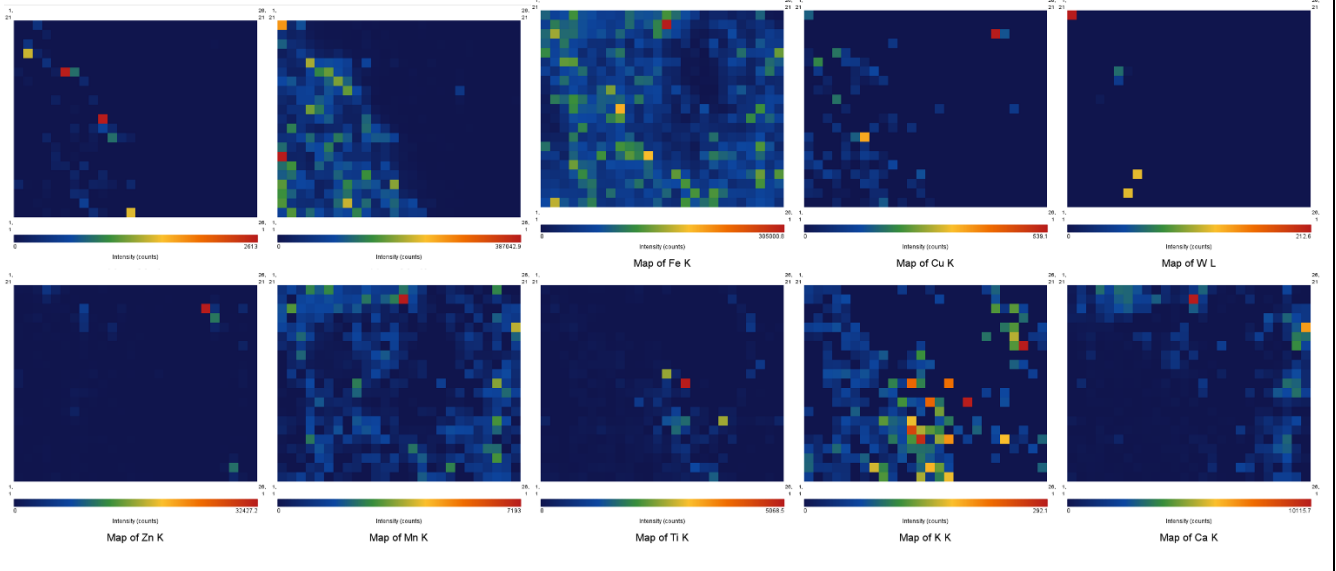


Sample Number	2834A (100 µm)	Drill Hole	TL-13-500	Depth	195.76-196 m
Lithology	Lapilli Tuff	Map Size	0.21 mm X 0.26 cm	Gold Grade	5.21 ppm

MCA Spectrum:

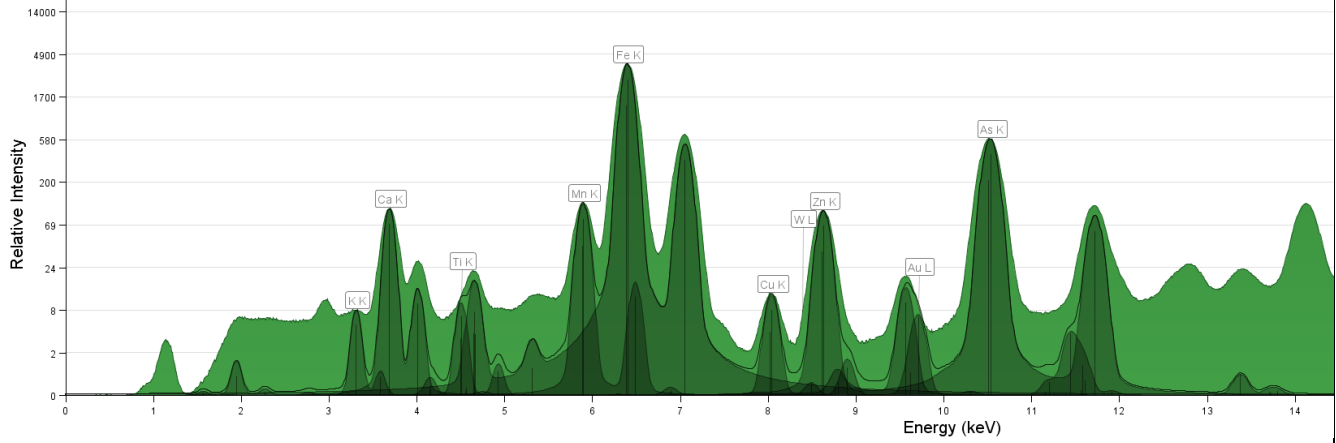


SR-µXRF Maps:

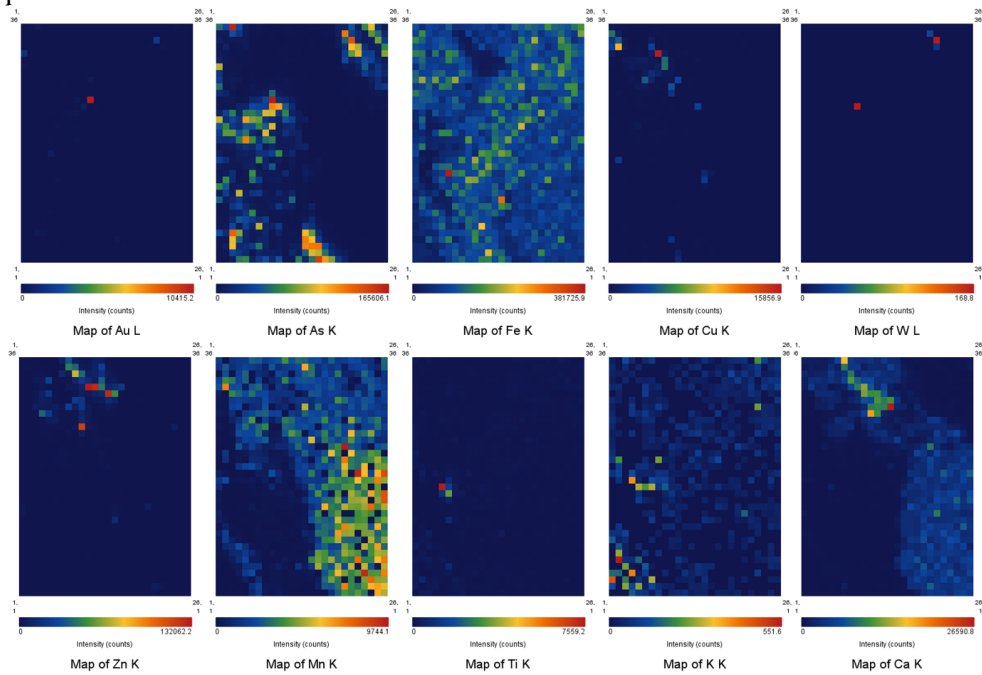


Sample Number	2834B (100 μ m)	Drill Hole	TL-13-500	Depth	195.76-196 m
Lithology	Lapilli Tuff	Map Size	0.36 mm X 0.26 cm	Gold Grade	5.21 ppm

MCA Spectrum:

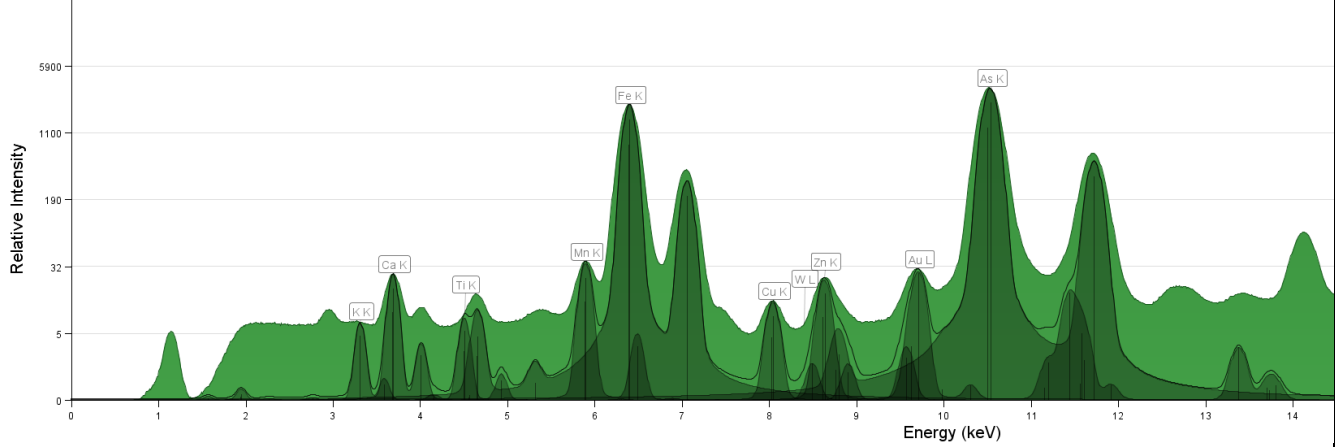


SR- μ XRF Maps:

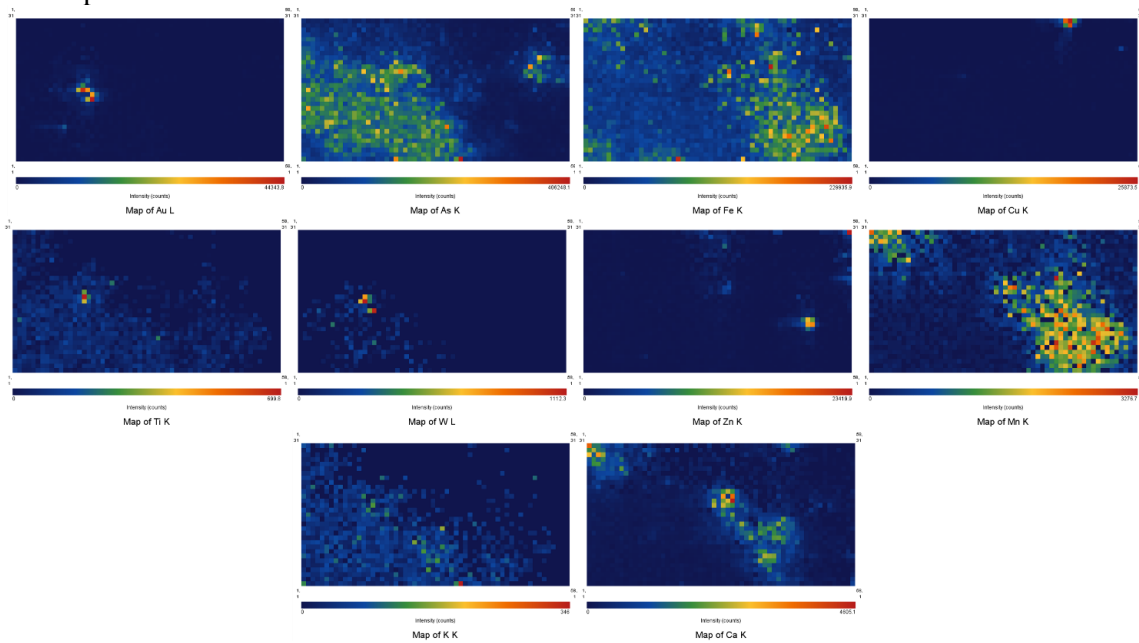


Sample Number	2834A (10 μ m)	Drill Hole	TL-13-500	Depth	195.76-196 m
Lithology	Lapilli Tuff	Map Size	0.21 mm X 0.26 cm	Gold Grade	5.21 ppm

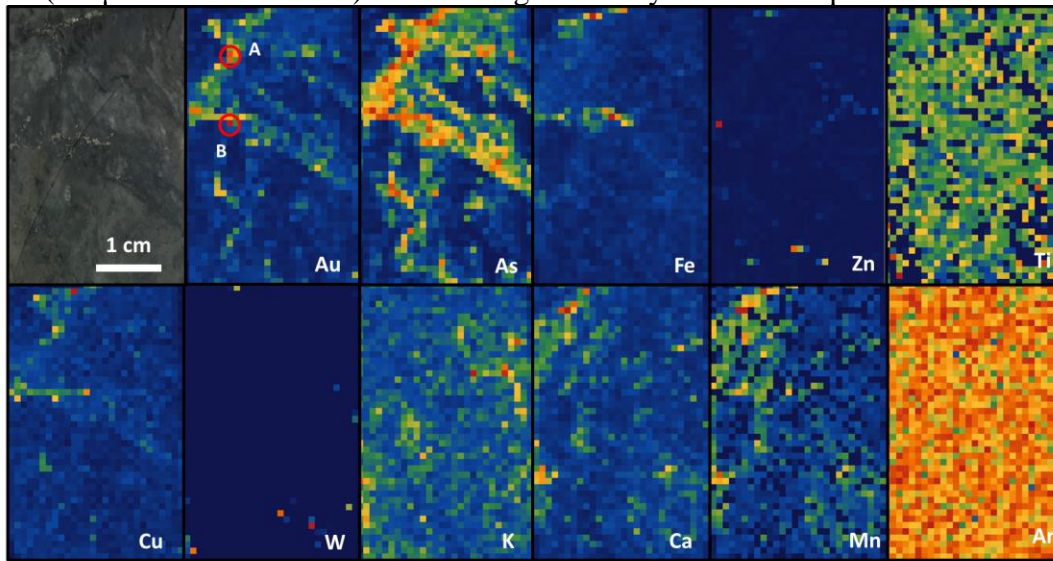
MCA Spectrum:



SR- μ XRF Maps:

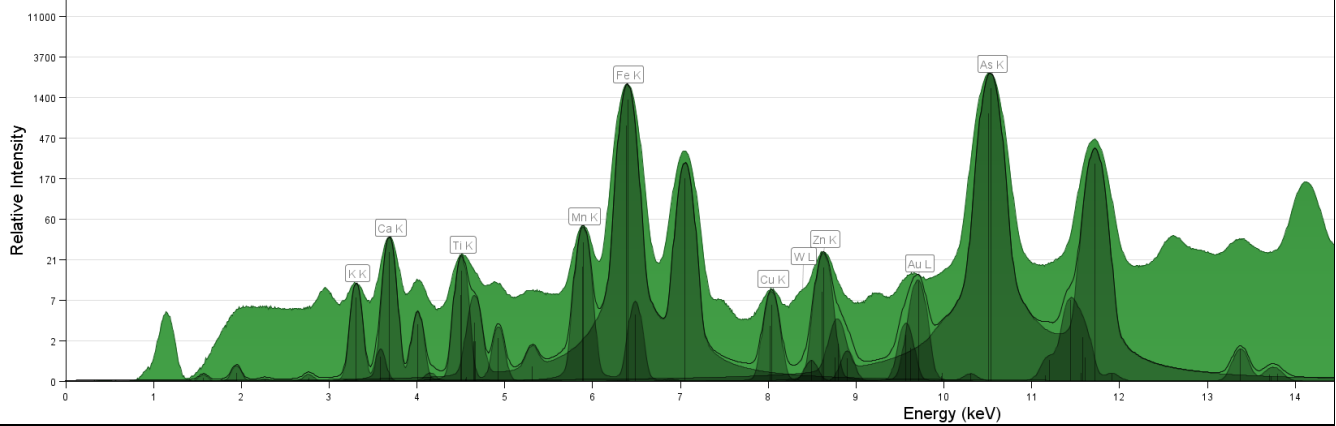


2841 (800µm-20ID APS Feb.): A & B. High intensity Au and As spots.

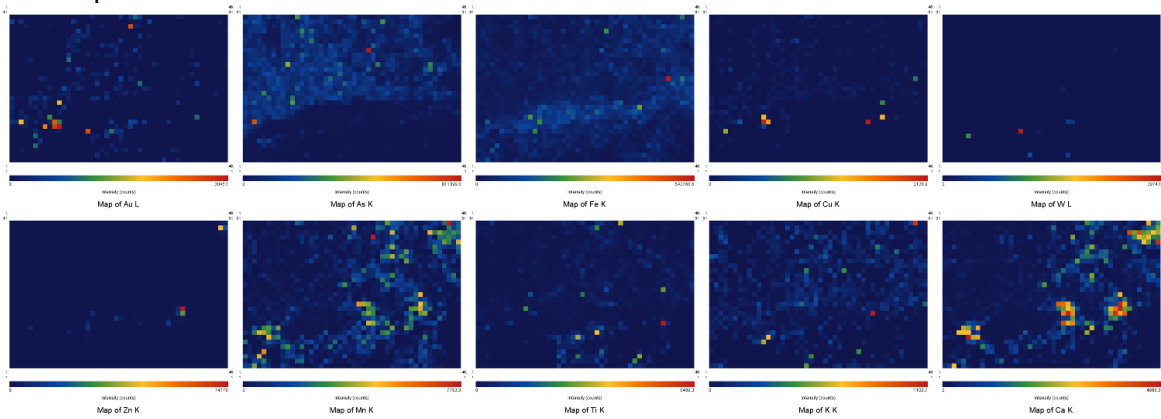


Sample Number	2841A (100 µm)	Drill Hole	TL-13-504	Depth	190.5-190.78 m
Lithology	QFP	Map Size	0.2 mm X 0.68 mm	Gold Grade	25.2 ppm

MCA Spectrum:

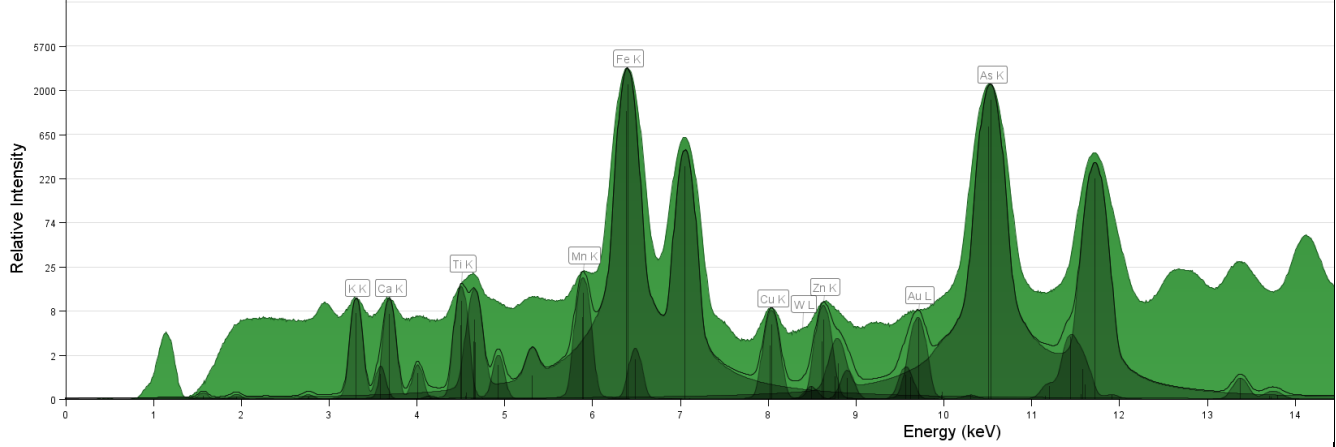


SR-µXRF Maps:

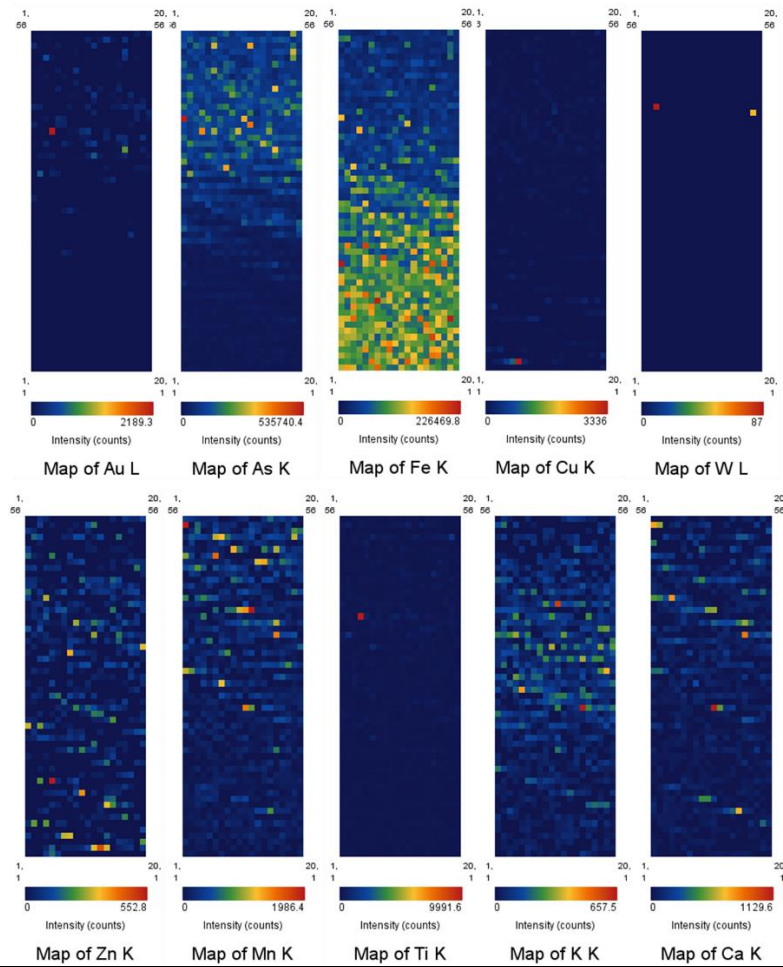


Sample Number	2841A (10 μm)	Drill Hole	TL-13-504	Depth	190.5-190.78 m
Lithology	QFP	Map Size	0.2 mm X 0.68 mm	Gold Grade	25.2 ppm

MCA Spectrum:

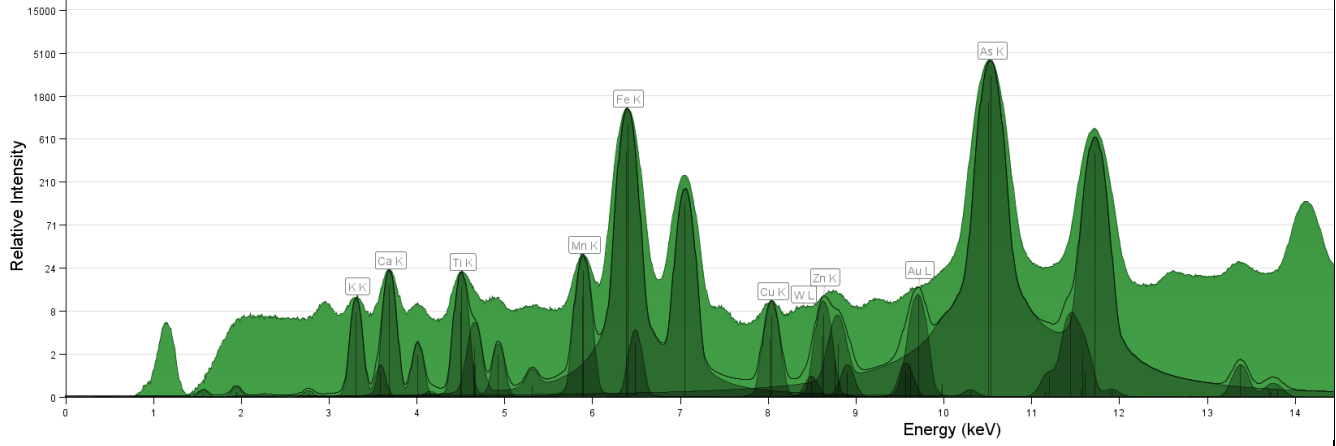


SR-μXRF Maps:

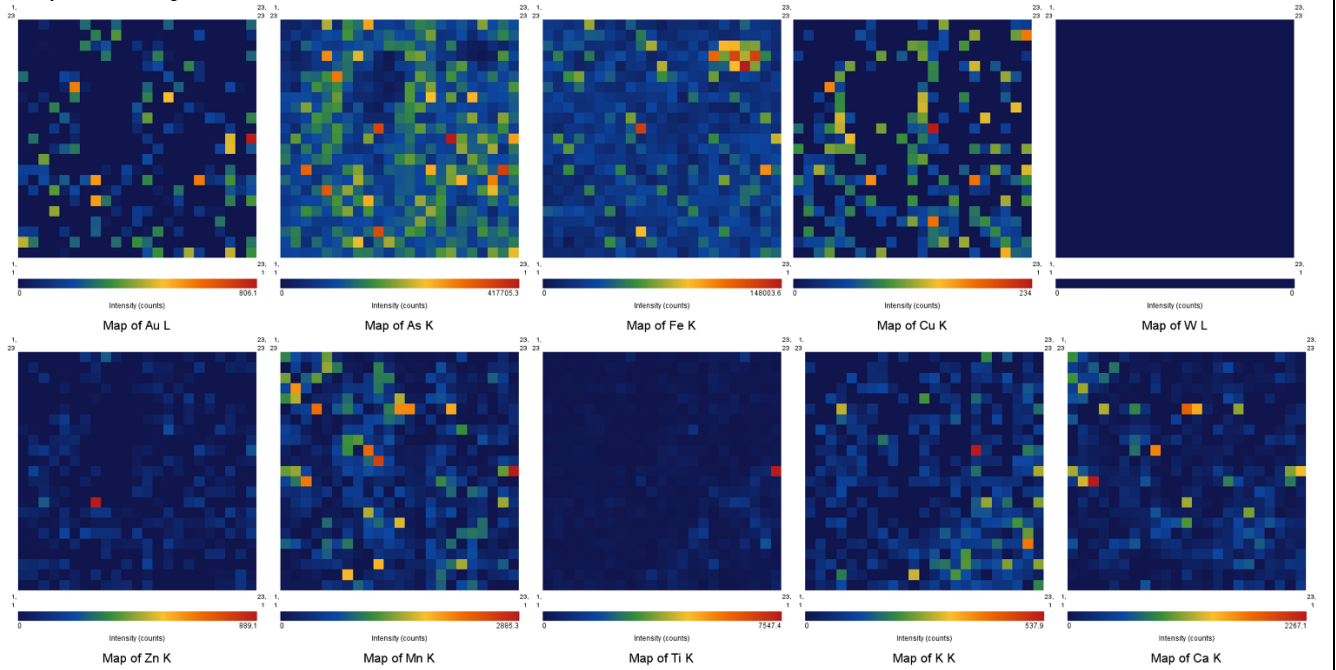


Sample Number	2841B (100 μm)	Drill Hole	TL-13-504	Depth	190.5-190.78 m
Lithology	QFP	Map Size	0.23 mm X 0.23 mm	Gold Grade	25.2 ppm

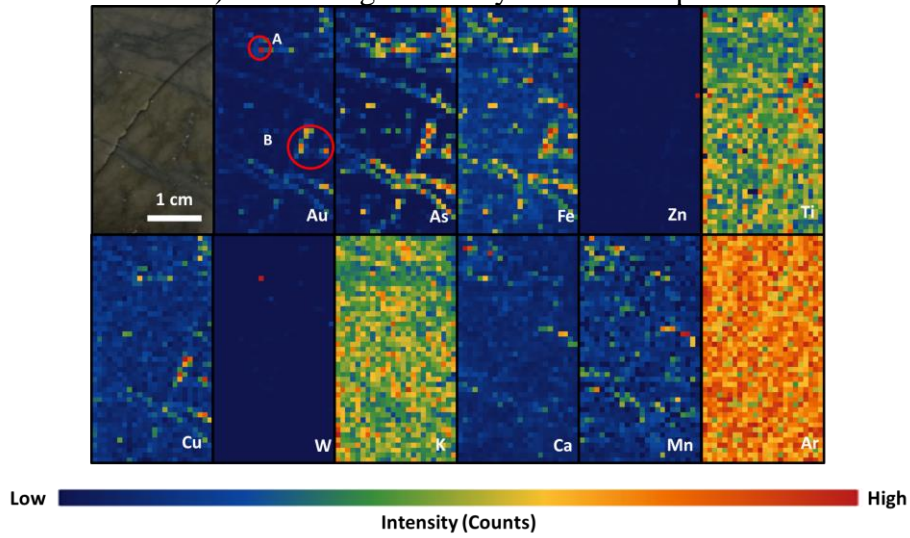
MCA Spectrum:



SR-μXRF Maps:

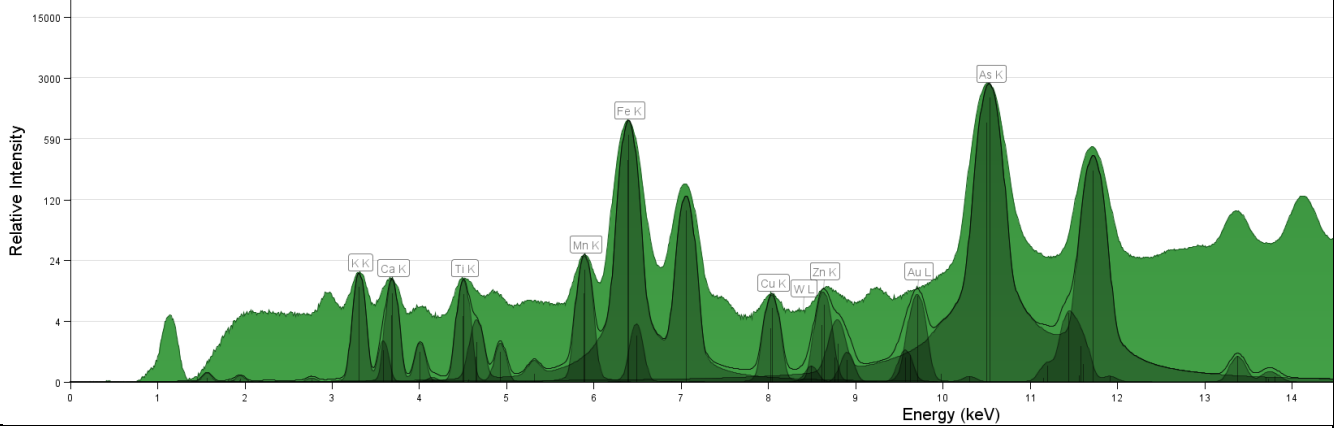


2845 (800µm-20ID APS Feb.): A&B. High intensity Au and As spots.

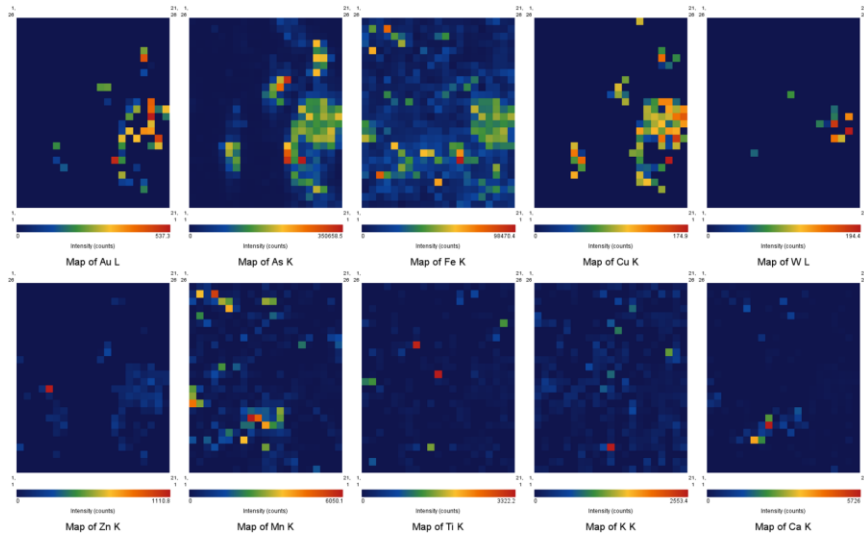


Sample Number	2845A (100 µm)	Drill Hole	TL-13-509	Depth	235.6-235.86 m
Lithology	QFP	Map Size	0.26 mm X 0.21 mm	Gold Grade	1.13 ppm

MCA Spectrum:

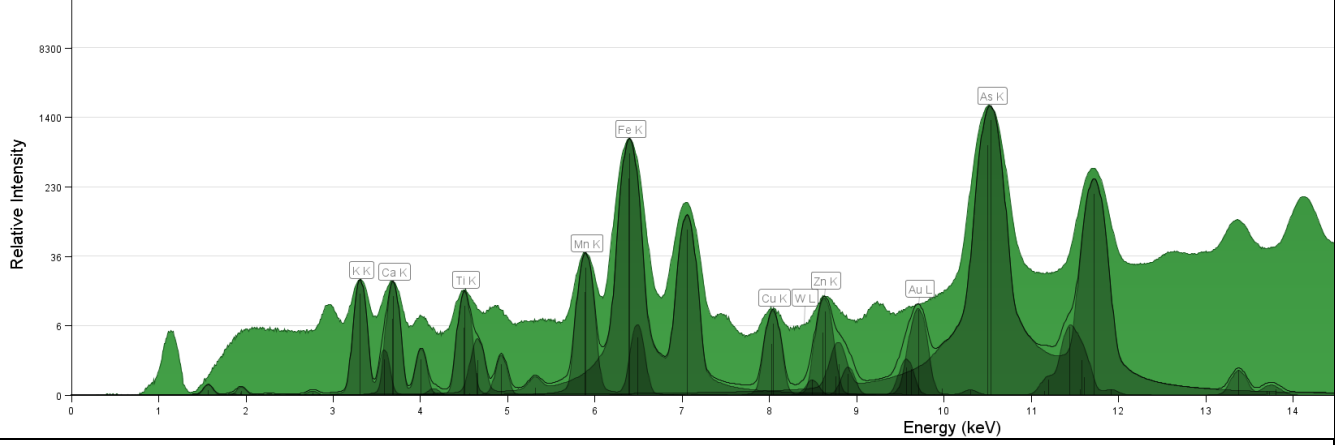


SR-µXRF Maps:

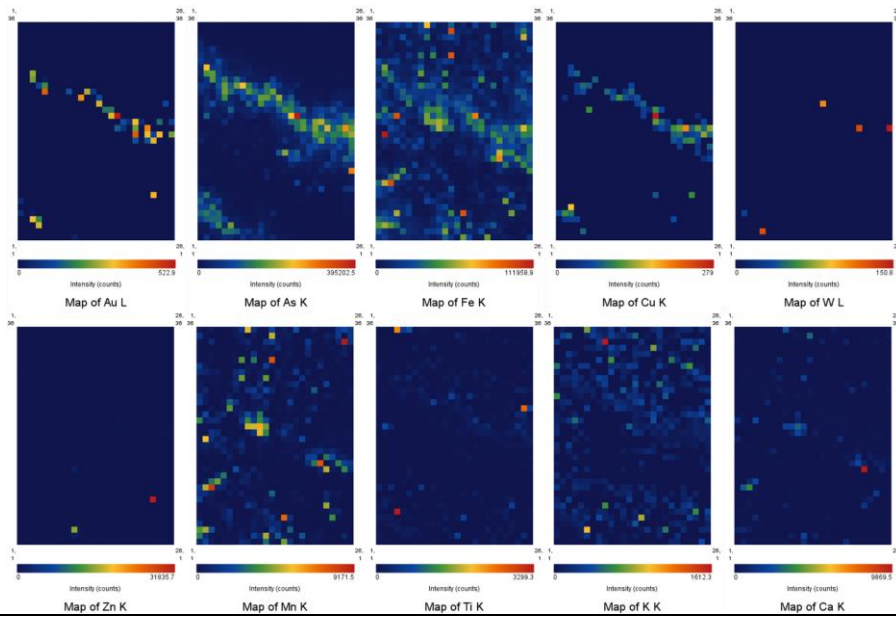


Sample Number	2845A (10 μm)	Drill Hole	TL-13-509	Depth	235.6-235.86 m
Lithology	QFP	Map Size	0.26 mm X 0.21 mm	Gold Grade	1.13 ppm

MCA Spectrum:

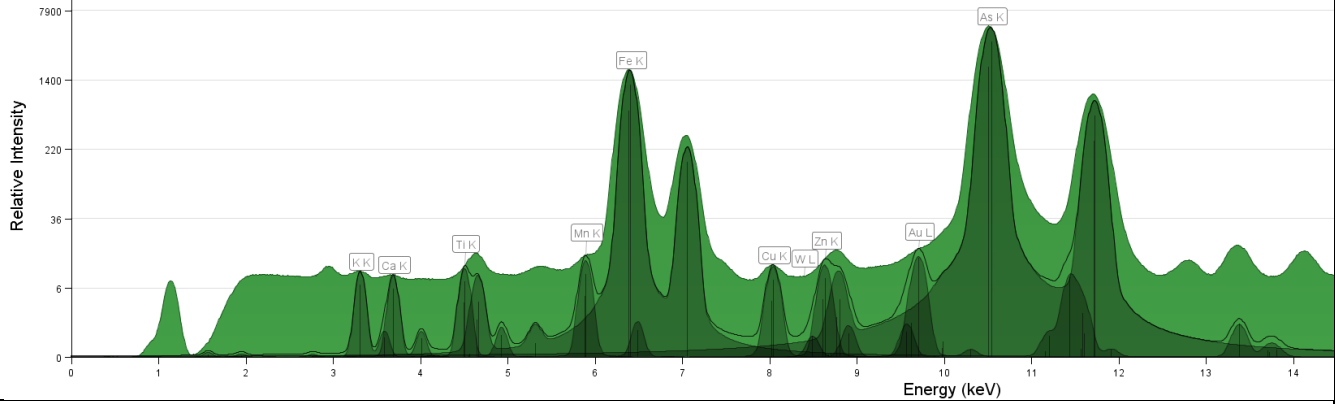


SR-μXRF Maps:

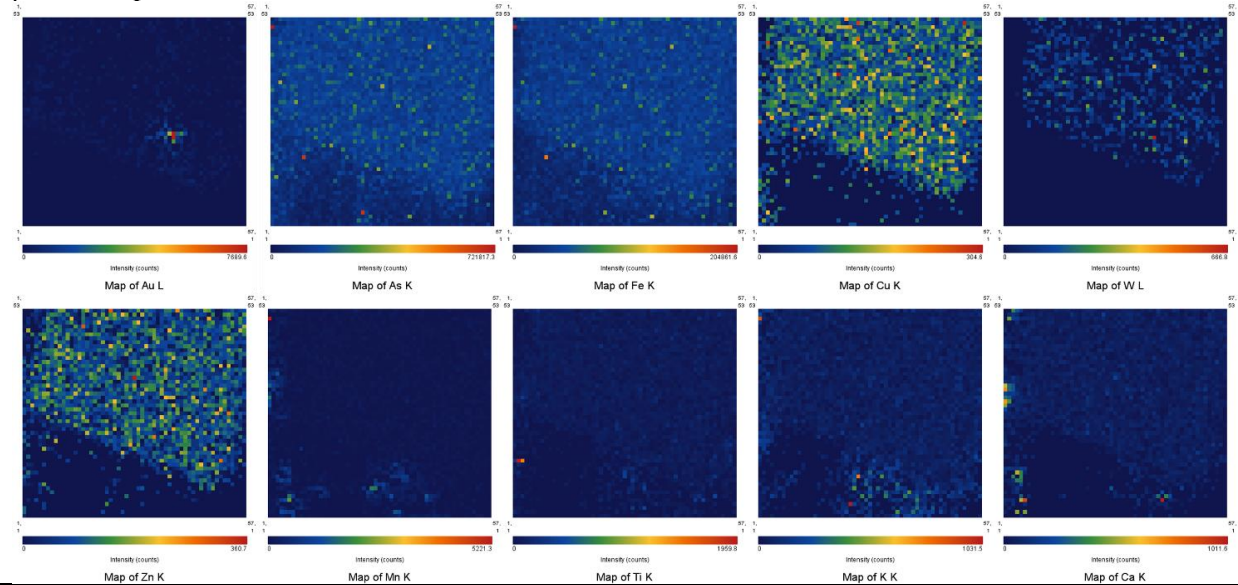


Sample Number	2845B (100 µm)	Drill Hole	TL-13-509	Depth	235.6-235.86 m
Lithology	QFP	Map Size	0.26 mm X 0.21 mm	Gold Grade	1.13 ppm

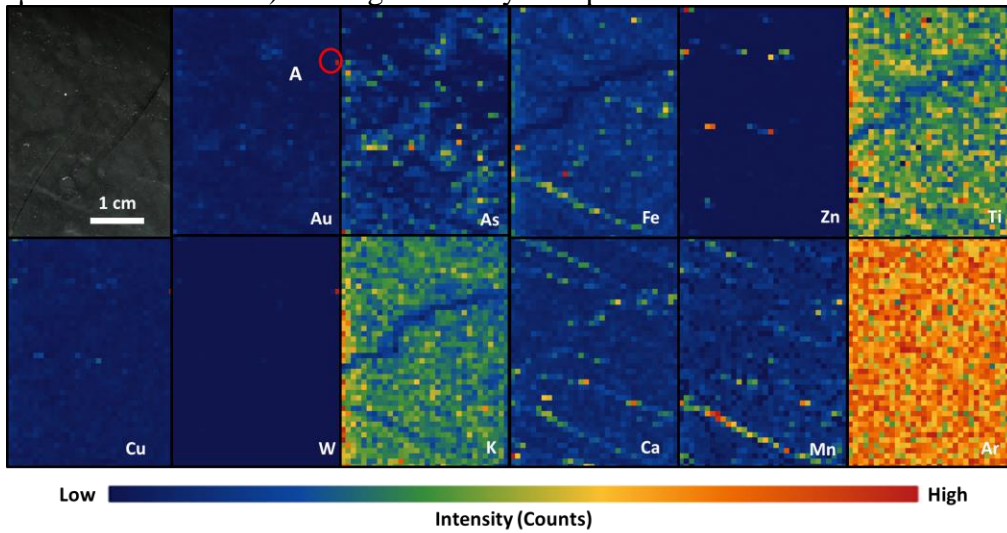
MCA Spectrum:



SR-µXRF Maps:

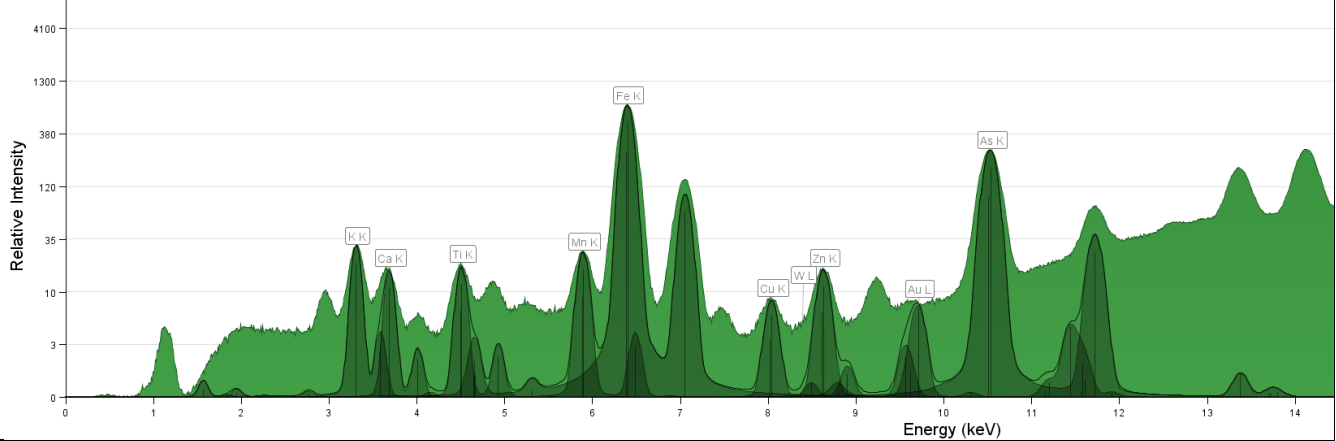


2857 (800 μ m-20ID APS Feb.): A. High intensity Au spot.

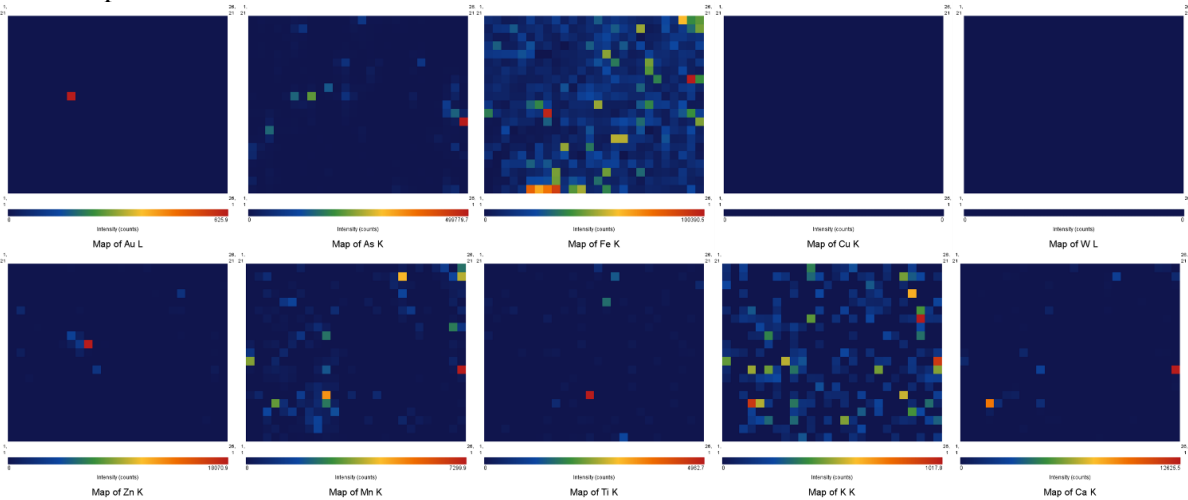


Sample Number	2857A (100 μ m)	Drill Hole	TL-16-607	Depth	718.4-718.66 m
Lithology	QFP	Map Size	0.26 mm X 0.21 mm	Gold Grade	2.16 ppm

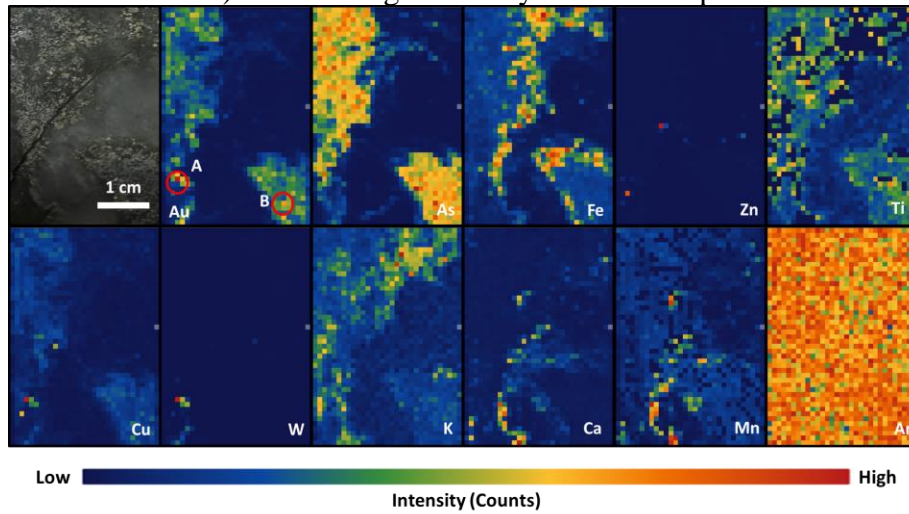
MCA Spectrum:



SR- μ XRF Maps:

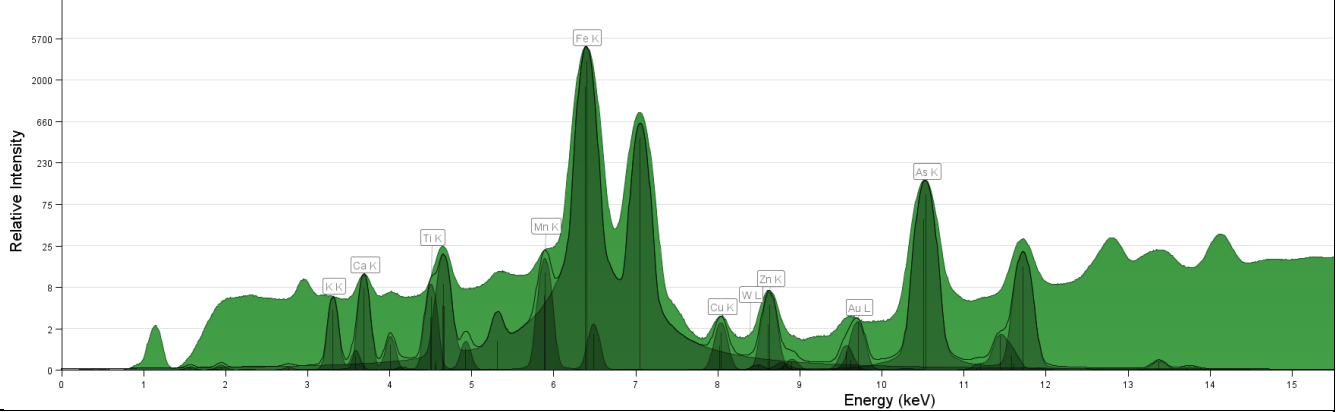


2854 (800µm-20ID APS Feb.): A & B. High intensity Au and As spots.

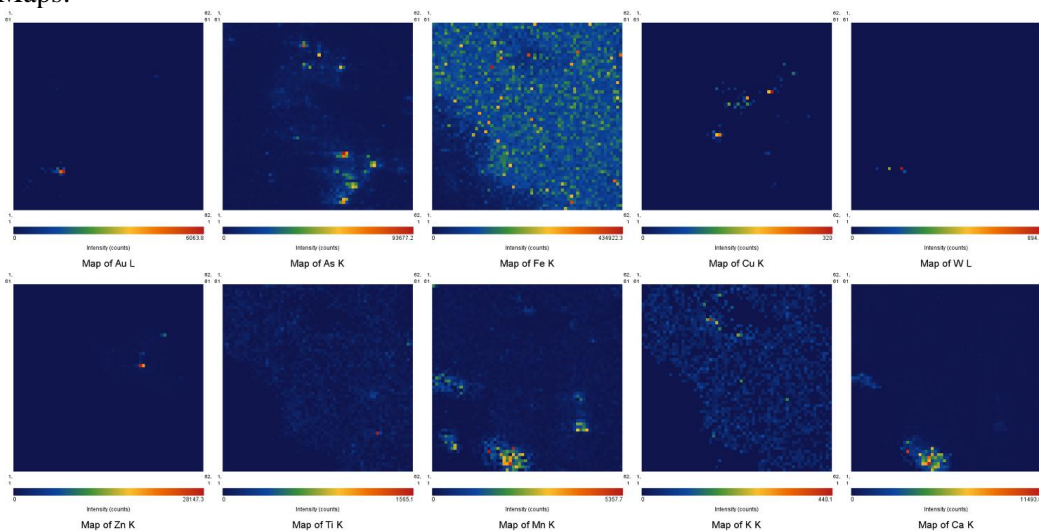


Sample Number	2854A (10 µm)	Drill Hole	TL-16-604A	Depth	729.02-729.2m
Lithology	Metavolcanic Tuff	Map Size	0.26 mm X 0.21 mm	Gold Grade	10.49 ppm

MCA Spectrum:

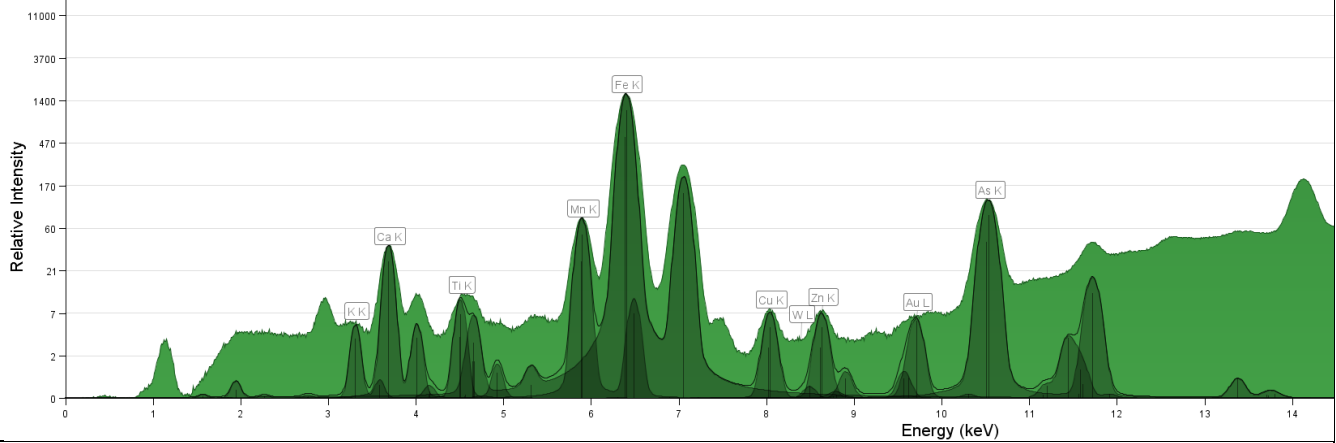


SR-µXRF Maps:

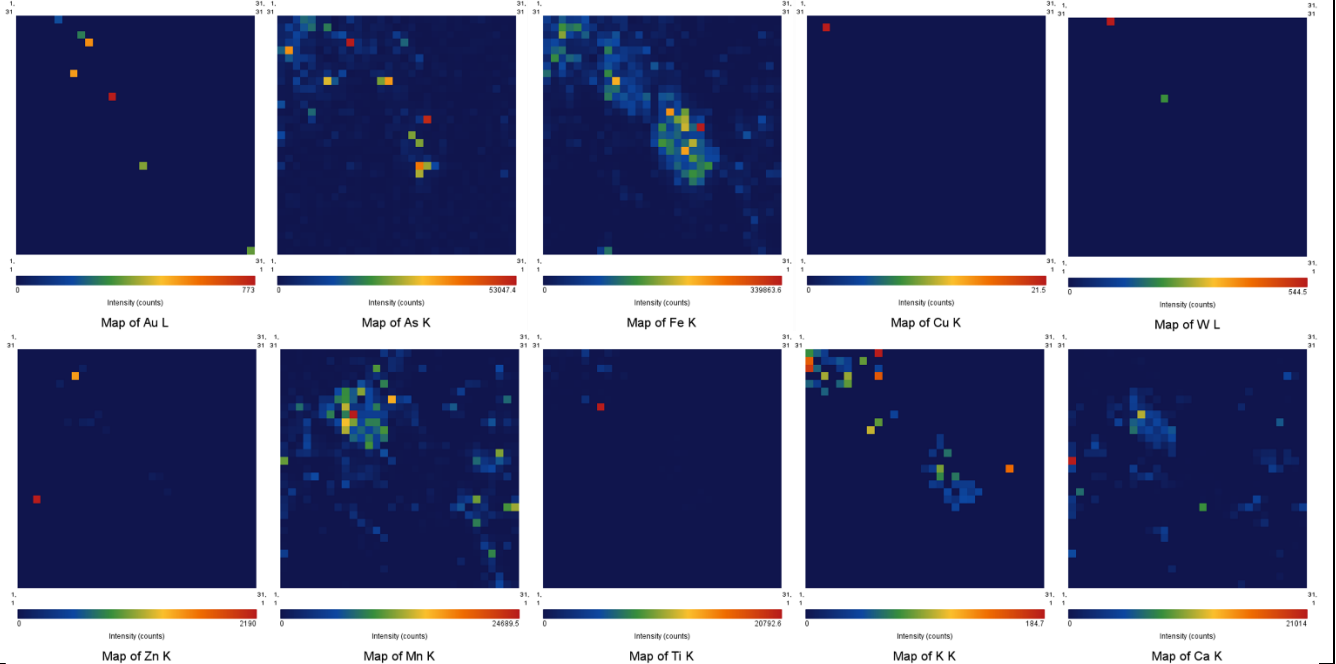


Sample Number	2854A (100 μm)	Drill Hole	TL-16-604A	Depth	729.02-729.2m
Lithology	Metavolcanic Tuff	Map Size	0.26 mm X 0.21 mm	Gold Grade	10.49 ppm

MCA Spectrum:

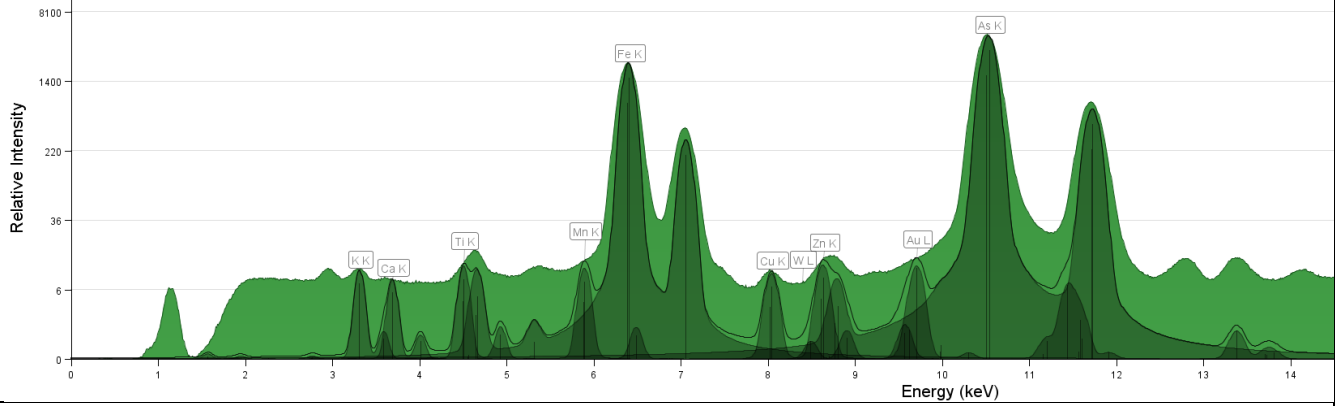


SR-μXRF Maps:

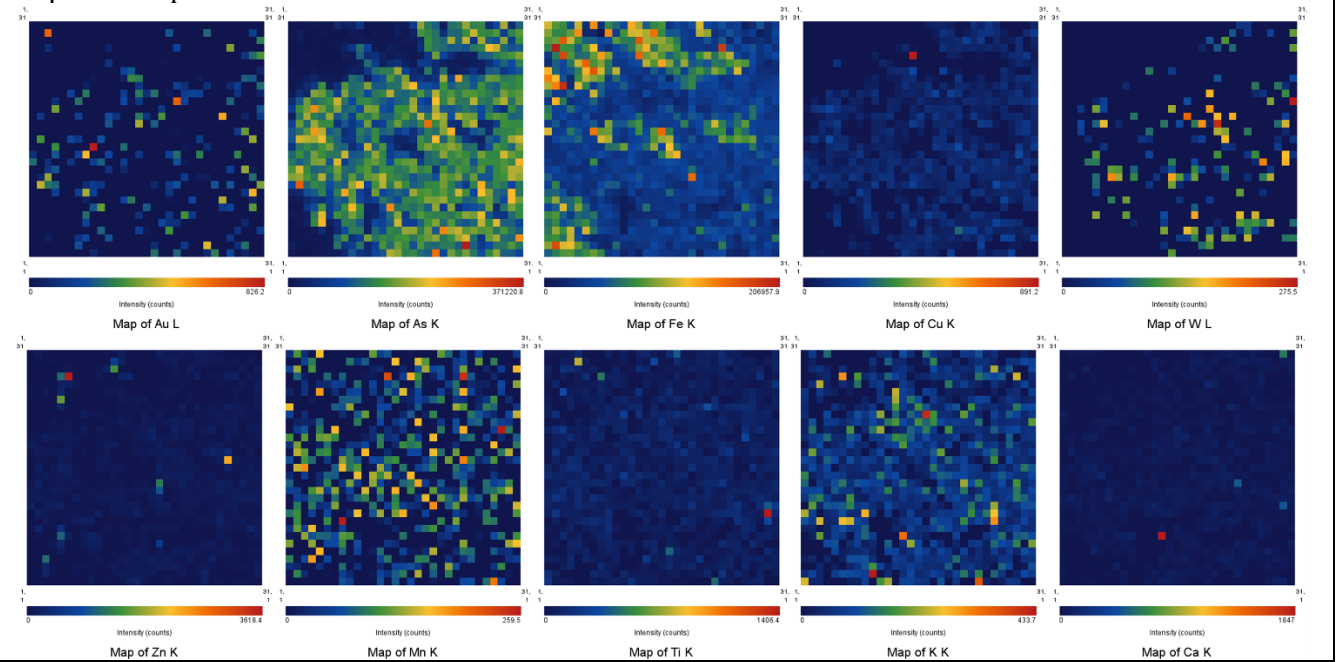


Sample Number	2854B (100 μm)	Drill Hole	TL-16-604A	Depth	729.02-729.2m
Lithology	Metavolcanic Tuff	Map Size	0.26 mm X 0.21 mm	Gold Grade	10.49 ppm

MCA Spectrum:



SR-μXRF Maps:



APS 8BM-B-March 2019

Beamtime and Beamline Details:

Detector: Vortex four-element SDD (SII Nanotechnology)

Incident Energy: 15.36 KeV

Max energy: 23.7 KeV

Mode: Fly scan XRF

Beam spot size: 500 μm x 500 μm

Dwell time: 0.2 sec (some samples ran at 0.2, 0.15, 0.1, 0.25 sec respectively to compare the dwell time)

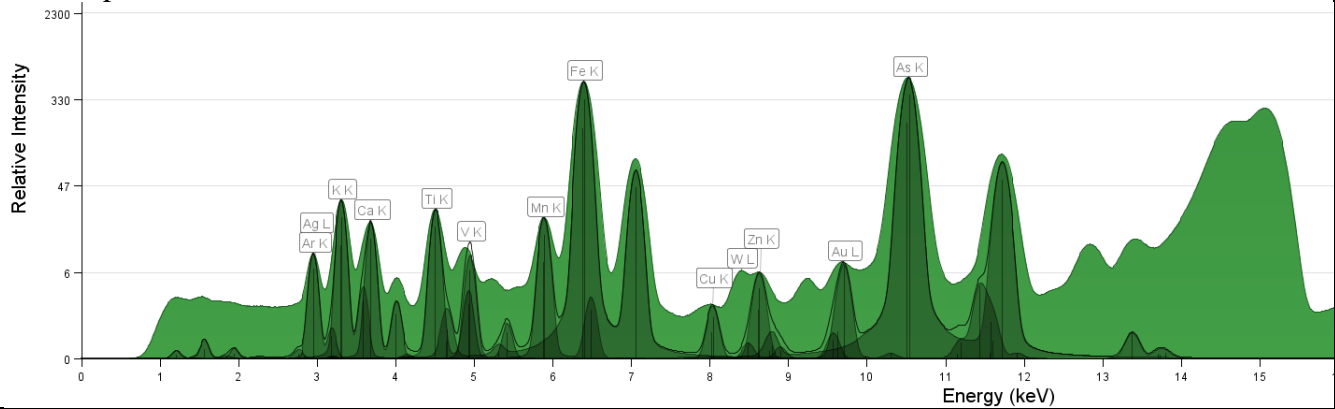
Samples: 8 half-drill core samples and 8 offcuts

Data Processing:

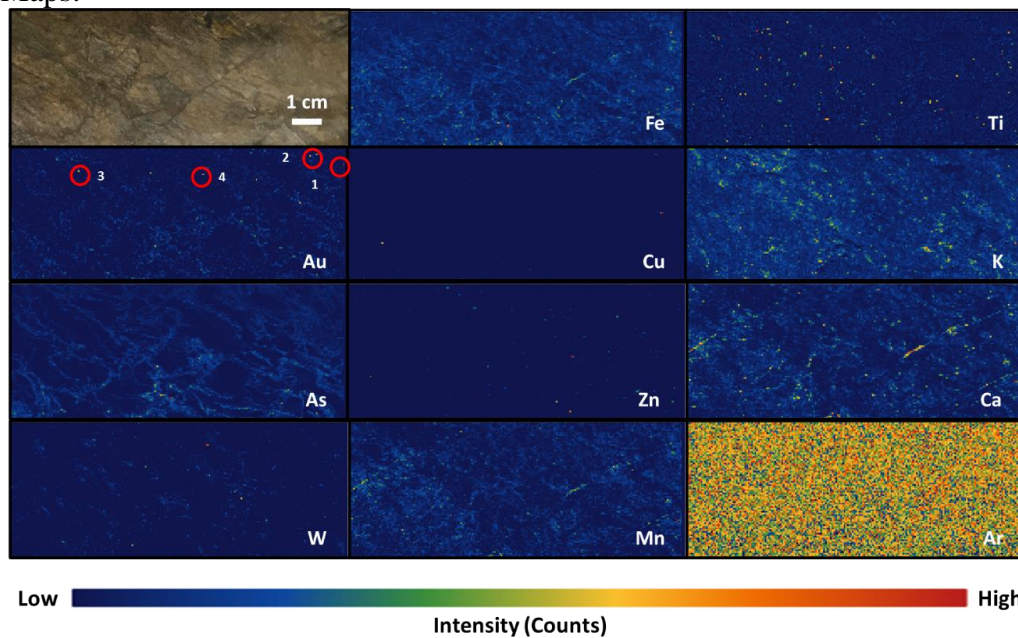
1. Energy Calibration Maximum: 23.7 keV, using Fe K peak to adjust the energy.
2. Peak fitting: Fe K, Ca K, As K, Cu K, Ar K, Mn K, Au L, Zn K, Ag L, K K, W L, Ti K, V K.
3. Ar Normalization: use the cursor to check the Ar channel at the bottom of the window. Different dataset has different Ar channel. For this one, Ar channel is 255. Use Data Filter-Advanced- Normalizer, mode: channel range, start channel:256, end channel: 257, normalized intensity: 10 (the best channel range was checked using Ar XRF map with lowest intensity range).
Without filter: 448.4
254-255:135.7
253-255: 144.3
254-256: 127.5
255-256: 123.3
256-256: 121.6
256-257: 121.6
257-258: 124.1
4. Map fitting: check the visible button.
5. Save MCA Spectrum and maps of each sample.
6. Check Au map to make sure if each high-intensity spot is the real gold signal: select the spot and plot selection \rightarrow take notes of the relationship of Au and other element curves (on the shoulder/ real peak/ overlaid other element peaks/ false signal).

Sample Number	2841	Drill Hole	TL-13-504	Depth	190.5-190.78 m
Lithology	QFP	Map Size	10 cm x 4 cm	Gold Grade	25.2 ppm

MCA Spectrum:



SR- μ XRF Maps:

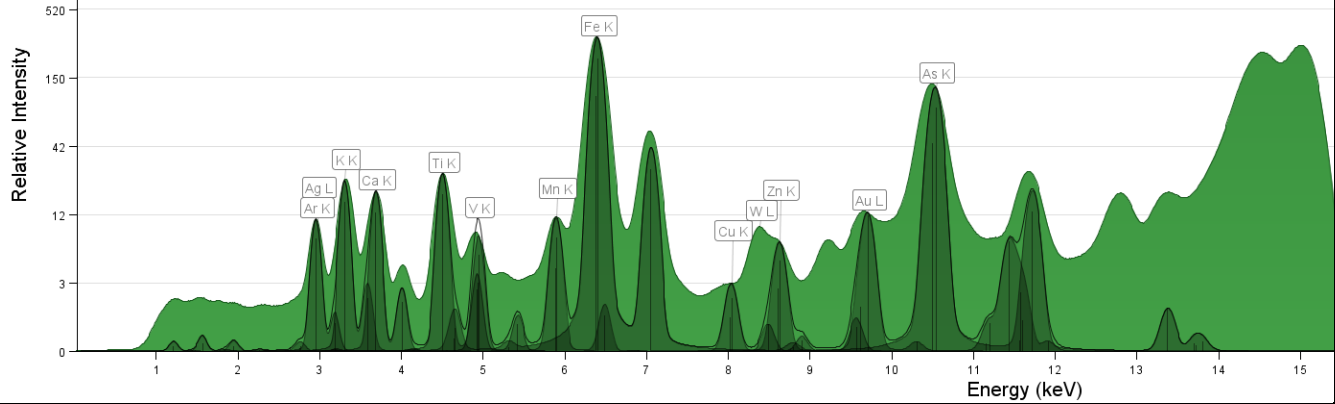


Description:

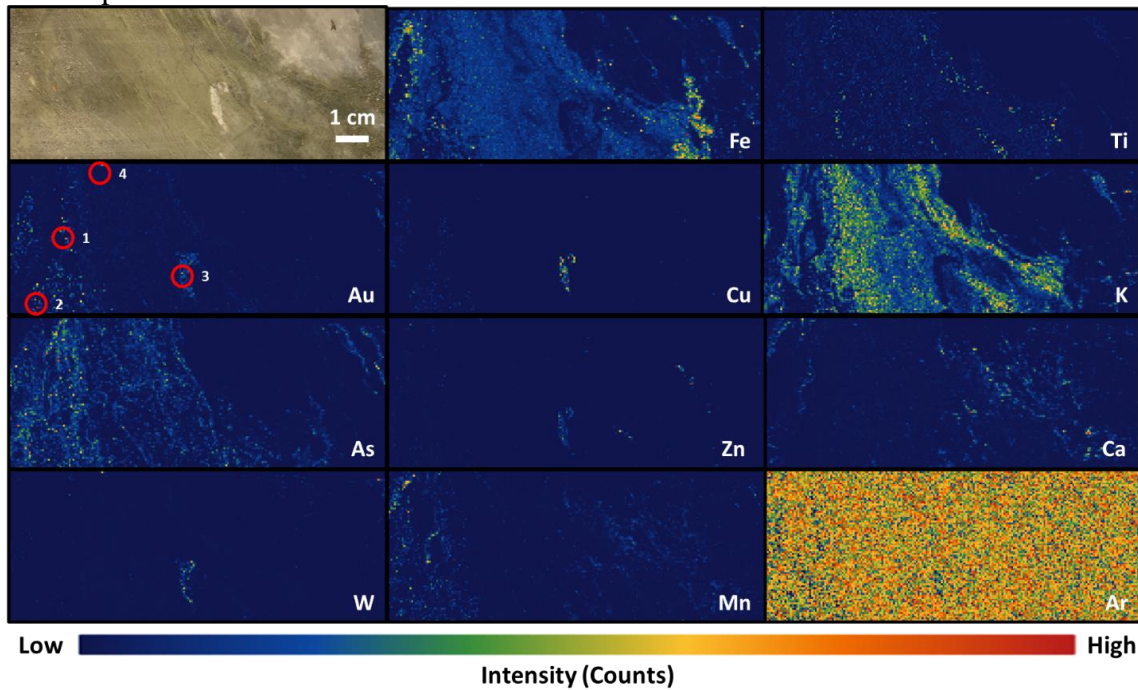
1. Fe Mn Ca have the same distribution along with the foliation texture and higher intensity in the dark green layers.
2. Au & As have the same distribution along with the foliation texture.
3. Ti & K have the same distribution in the light green layers of foliation.
4. Cu, Zn, and W are disseminated.
5. Au spots: 1&2. Au peak on the As shoulder on the MCA Spectrum, but higher than the shoulder; 3&4. real Au peak, much higher than As shoulder. Au 4 is next to W red pixel.
6. Ar intensity (without filter \rightarrow with filter): 448.4 \rightarrow 121.6
7. Comparing to APS 20ID-Feb 2019: shows more micro texture, W and Au are easier to distinguish because of higher resolution. Analyzed area is not exactly the same.

Sample Number	2854	Drill Hole	TL-16-604A	Depth	729.02-729.2m
Lithology	Metavolcanic Tuff	Map Size	10 cm x 4 cm	Gold Grade	10.49 ppm

MCA Spectrum:



SR- μ XRF Maps:

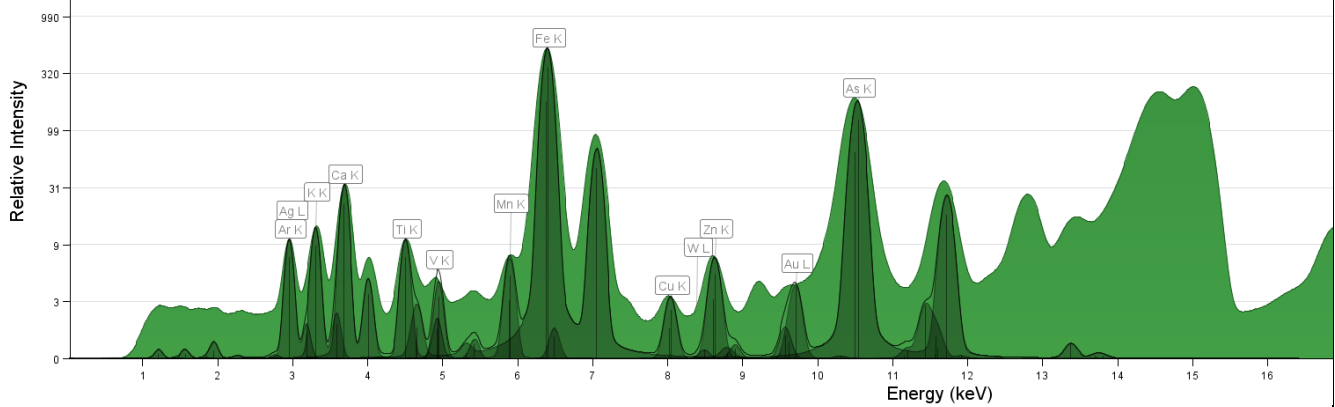


Description:

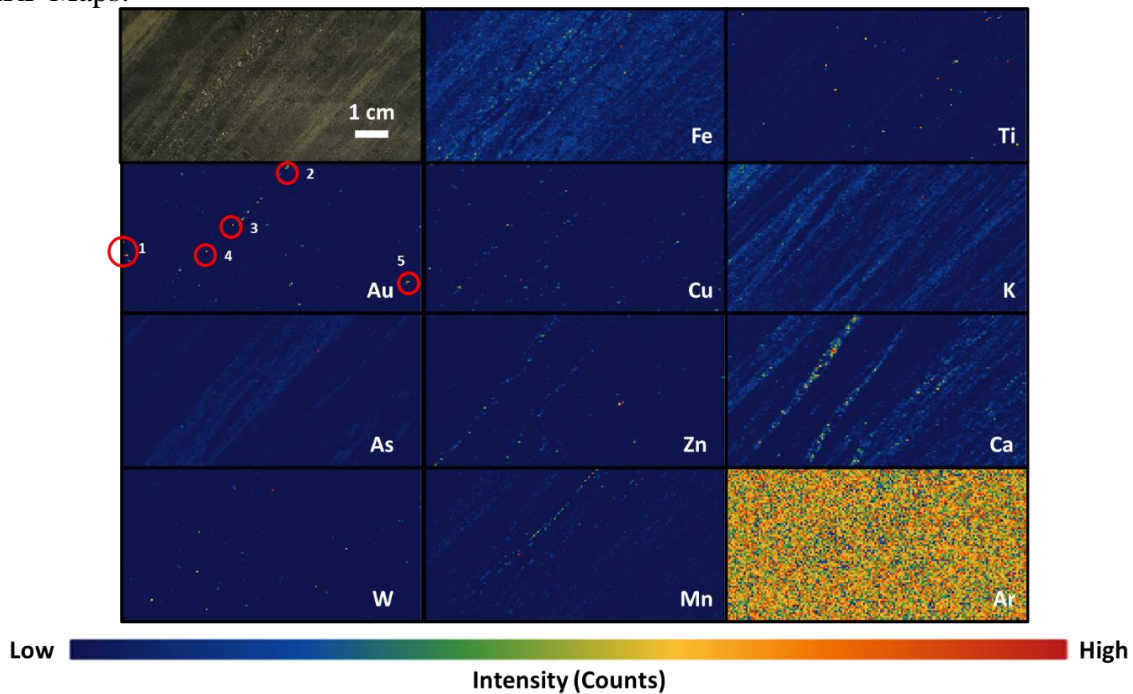
1. Au, W Zn Cu have the same distribution in sulphide grains.
2. As Fe K Ti Ca Mn have the same distribution along with intrusive texture. Higher intensity on the edge.
3. Au spots: 1&2. real Au peak, much higher than As shoulder; 3&4. W, false Au signal.
4. Ar intensity (without filter \rightarrow with filter): 684.6 \rightarrow 121.7
5. Comparing to APS 201D-Feb 2019: Fe & As maps show more detailed texture; real Au peak spots have been detected.

Sample Number	2831	Drill Hole	TL-15-551	Depth	96.8-97 m
Lithology	Metasandstone	Map Size	10 cm x 3.5 cm	Gold Grade	2.26 ppm

MCA Spectrum:



SR- μ XRF Maps:

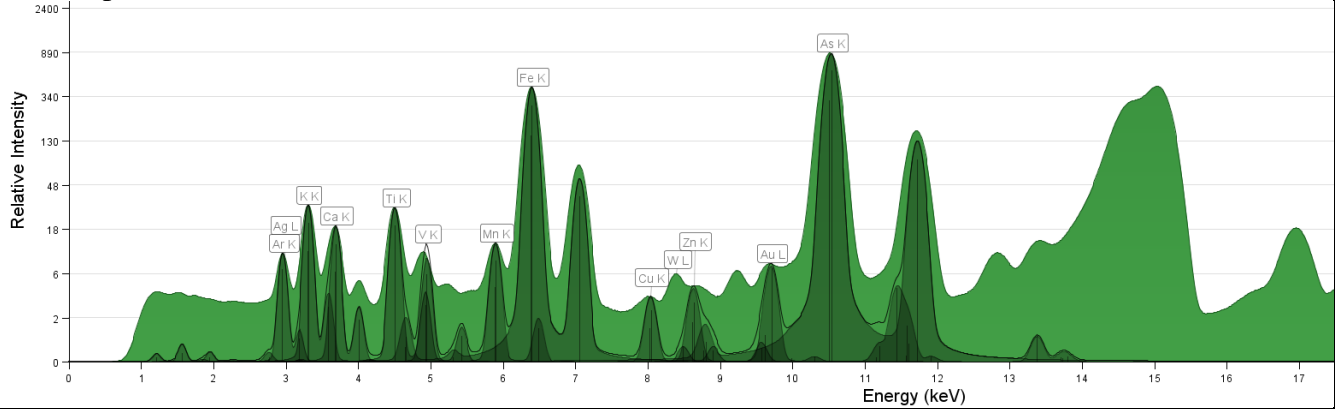


Description:

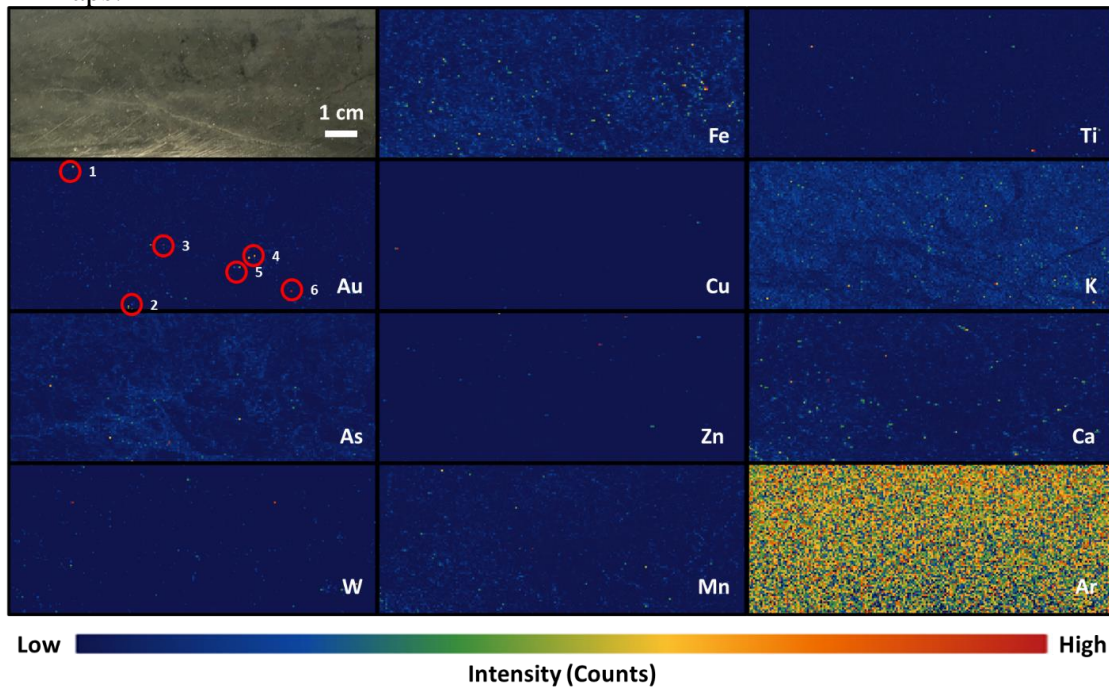
1. have the same distribution
2. Au As W Cu Zn Ti are disseminated in the sulphide veins.
3. K Mn have the same distribution along with the light green foliation layers.
4. Ca distributes along with the dark green foliation layers, especially the layers besides the sulphide veins.
5. Au spots: 1,4&5 real Au peak, much higher than As shoulder; 2&3, Au peak on the As shoulder on the MCA Spectrum, but higher than the shoulder.
6. Ar intensity (without filter→ with filter): 503.9→121.7
7. Comparing to APS 20ID-Feb 2019: Analyzed area is smaller. Background noise is much smaller. More real Au spots has been found.

Sample Number	2819	Drill Hole	TL-16-575	Depth	154.1-154.32 m
Lithology	QFP	Map Size	10 cm x 4cm	Gold Grade	7.21 ppm

MCA Spectrum:



SR- μ XRF Maps:

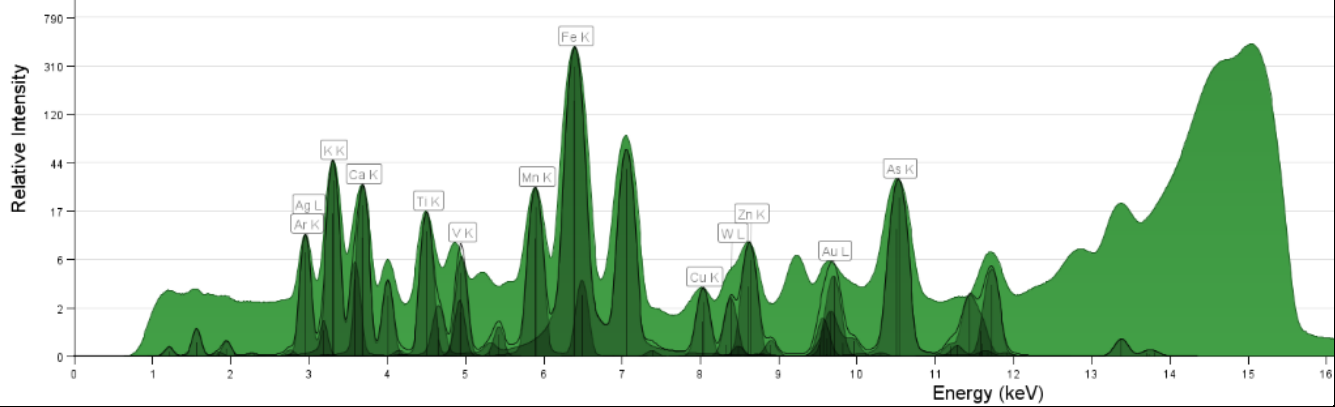


Description:

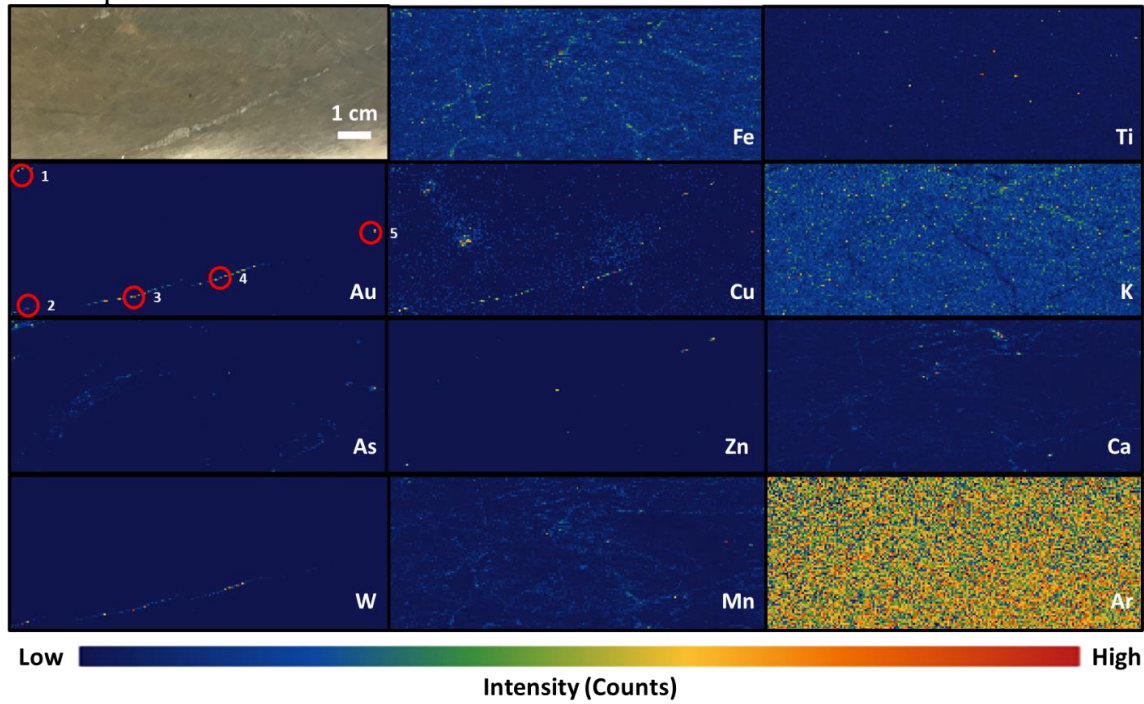
1. All elements are disseminated: As is along with fractures and the distribution is opposite to K.
2. Au spots: 1. Au peak and W peak are overlapped, but Au peak is much higher than As shoulder and W peak; 2&3. Au peak on the As shoulder on the MCA Spectrum, but higher than the shoulder; 4-6. real Au peak, much higher than As shoulder.
3. Ar intensity (without filter \rightarrow with filter): 416.6 \rightarrow 121.5
4. Comparing to APS 20ID-Feb 2019: More Au spots has been found. As map shows less texture.

Sample Number	2827	Drill Hole	TL-15-564	Depth	183-183.23m
Lithology	QFP	Map Size	10 cm x 4 cm	Gold Grade	Close to 9-0.6 ppm

MCA Spectrum:



SR- μ XRF Maps:

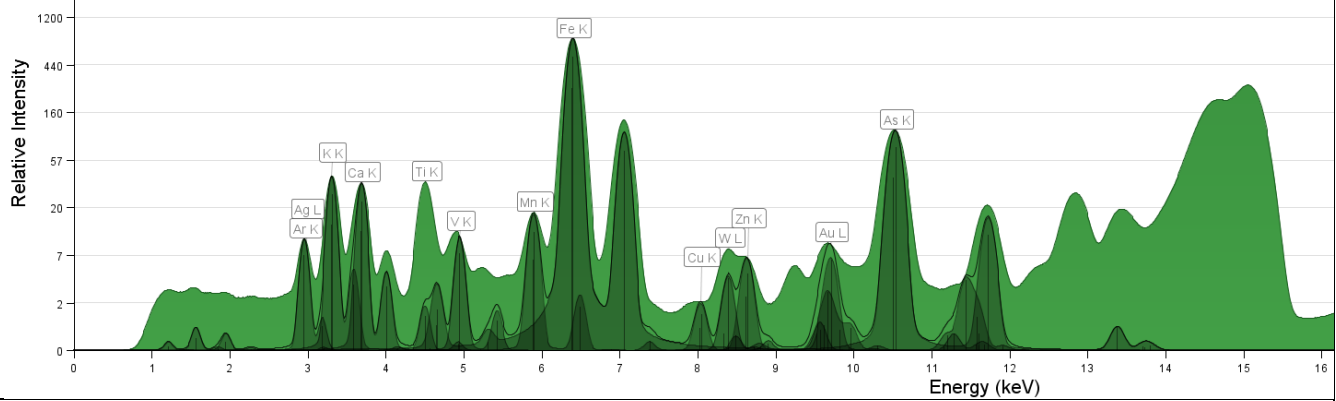


Description:

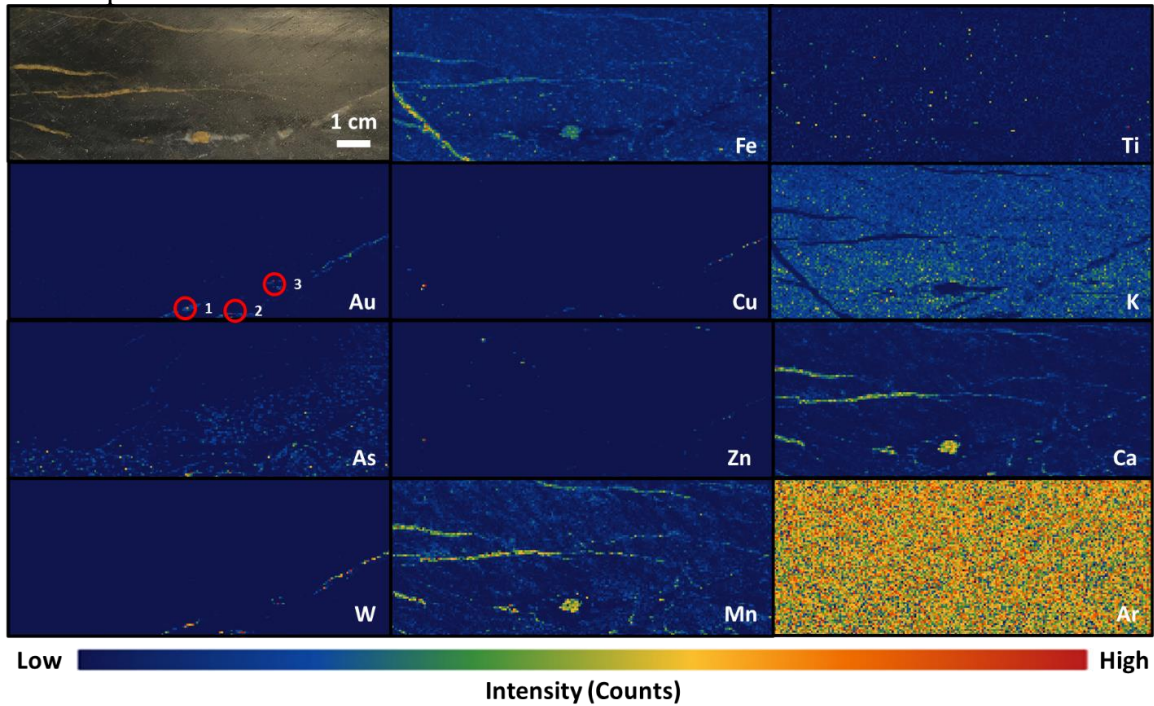
1. W Au Cu (partly) have the same distribution along with the sulphide vein.
2. As Au Cu (partly) Zn Ca Mn Ti are disseminated.
3. K & Fe have the same distribution in the fractures.
4. Au spots: 1&5. Au peak on the As shoulder on the MCA Spectrum, but higher than the shoulder; 2-4. W, false Au signal.
5. Ar intensity (without filter \rightarrow with filter): 455.3 \rightarrow 121.5
6. Comparing to APS 201D-Feb 2019: Analyzed area is not exactly the same. K map is different. More false Au spots have been found.

Sample Number	2853	Drill Hole	TL-16-604A	Depth	643.96-644.24m
Lithology	QFP	Map Size	10 cm x 4 cm	Gold Grade	7.73 ppm

MCA Spectrum:



SR- μ XRF Maps:

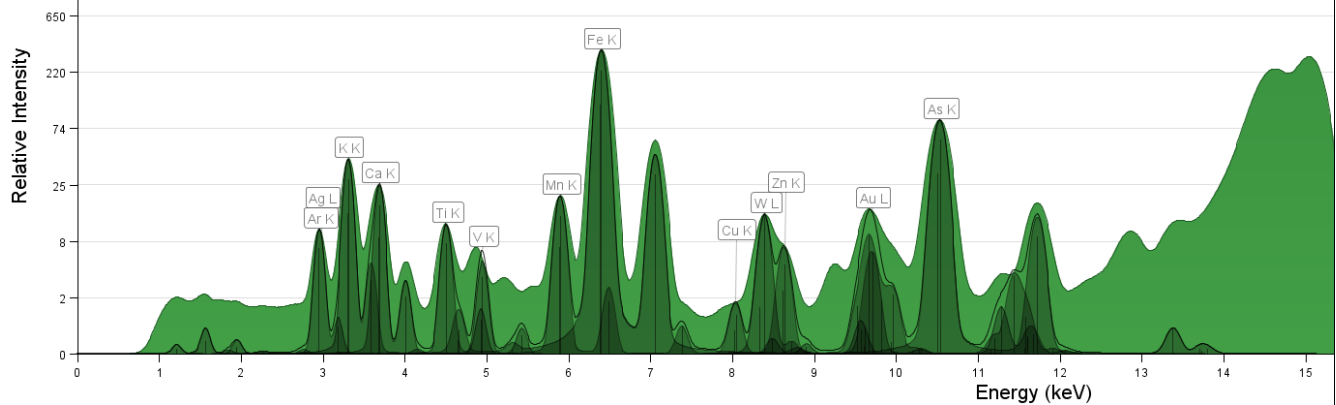


Description:

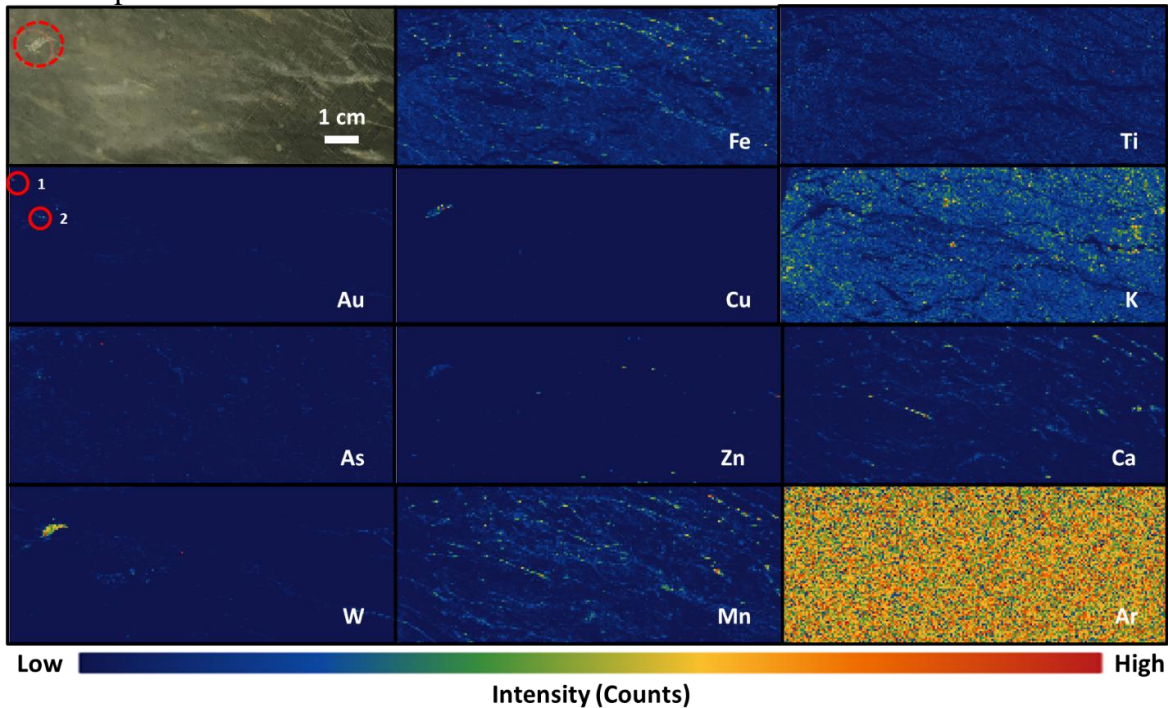
1. Au W Cu have the same distribution along with a white vein.
2. Fe Mn Ca have the same distribution along with orange veins.
3. K Ti have the same distribution opposite to the veins.
4. Zn As are disseminated.
5. Au spots: 1&2. W, false Au signal; 3. real Au peak, much higher than As shoulder.
6. Ar intensity (without filter→ with filter): 605.6→121.5
7. Comparing to APS 201D-Feb 2019: the same results.

Sample Number	2857	Drill Hole	TL-16-607	Depth	718.4-718.66 m
Lithology	QFP	Map Size	10 cm x 4 cm	Gold Grade	2.16 ppm

MCA Spectrum:



SR-μXRF Maps:

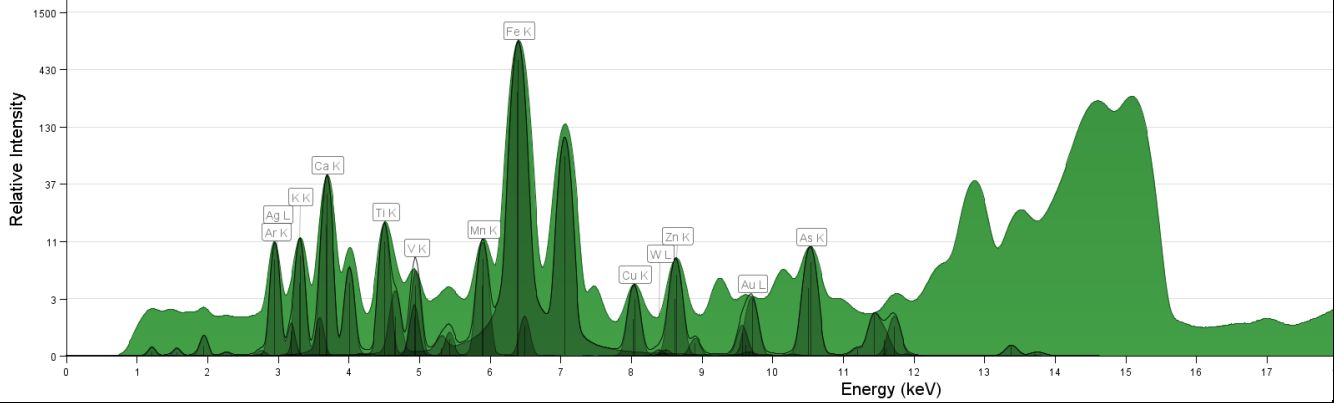


Description:

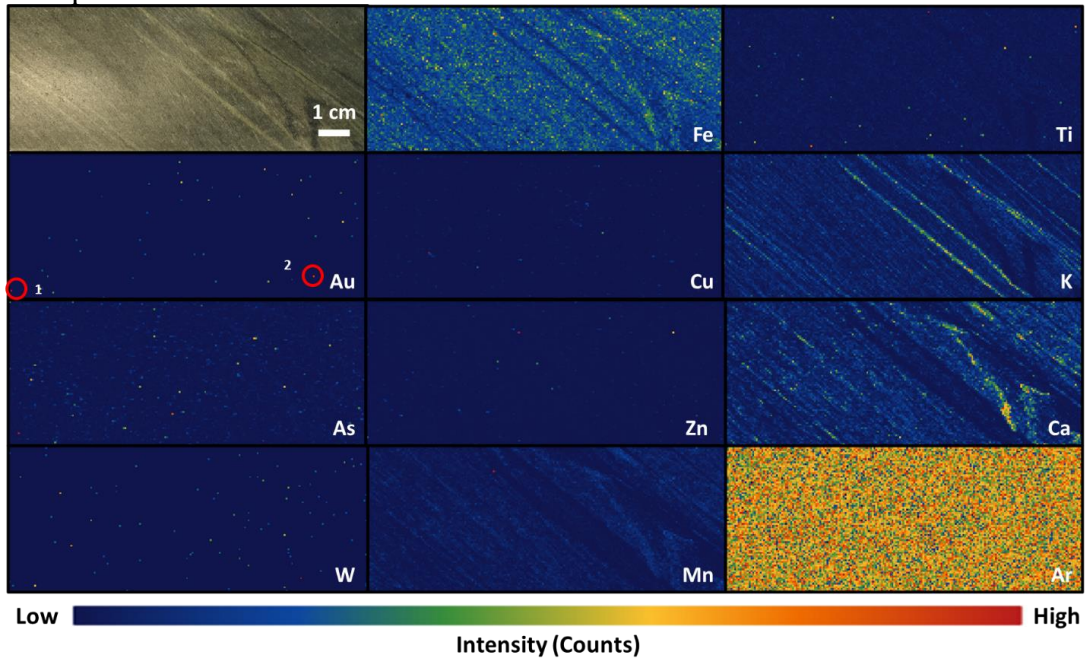
1. Au W Cu have the same distribution in a sulphide grain (red circle).
2. Ti K have the same distribution opposite to the white veins.
3. Fe Mn Ca have the same distribution along with the white veins.
4. As Zn are disseminated in the veins.
5. Au spots: 1. real Au peak, much higher than As peak; 2. W, false Au signal.
6. Ar intensity (without filter→ with filter): 543.1→121.6
7. Comparing to APS 20ID-Feb 2019: easy to distinguish W and Au high-intensity spot. Ca map shows more texture.

Sample Number	2360	Drill Hole	TL-17-616	Depth	148.6-148.8m
Lithology	Lapilli Tuff	Map Size	10 cm x 4 cm	Gold Grade	1.2-0.01 ppm

MCA Spectrum:



SR- μ XRF Maps:

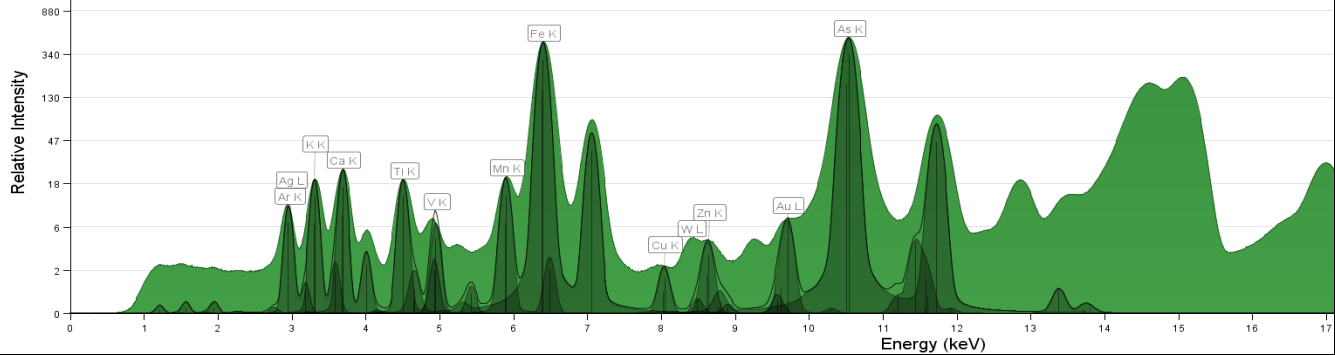


Description:

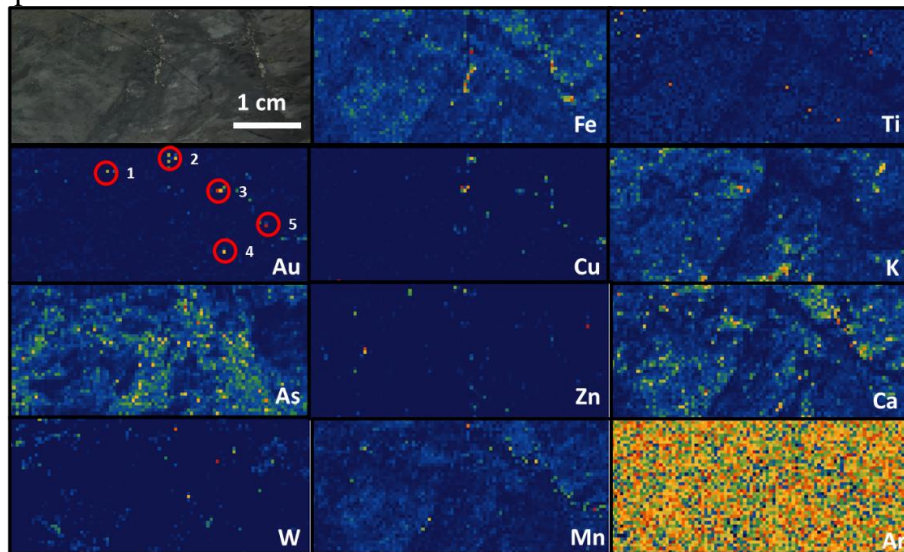
1. Fe & Ca have the same distribution in the dark green layers of foliation; K distributes in the light green layers of foliation.
2. Au As W Zn Mn Cu Ti are disseminated.
3. Au spots: 1&2. Weak Au signal.
4. Ar intensity (without filter \rightarrow with filter): 542.9 \rightarrow 121.4
5. 2360 was not analyzed in APS 20ID-Feb 2019.

Sample Number	2841 (offcut)	Drill Hole	TL-13-504	Depth	190.5-190.78 m
Lithology	QFP	Map Size	10 cm x 4 cm	Gold Grade	25.2 ppm

MCA Spectrum:



SR-μXRF Maps:

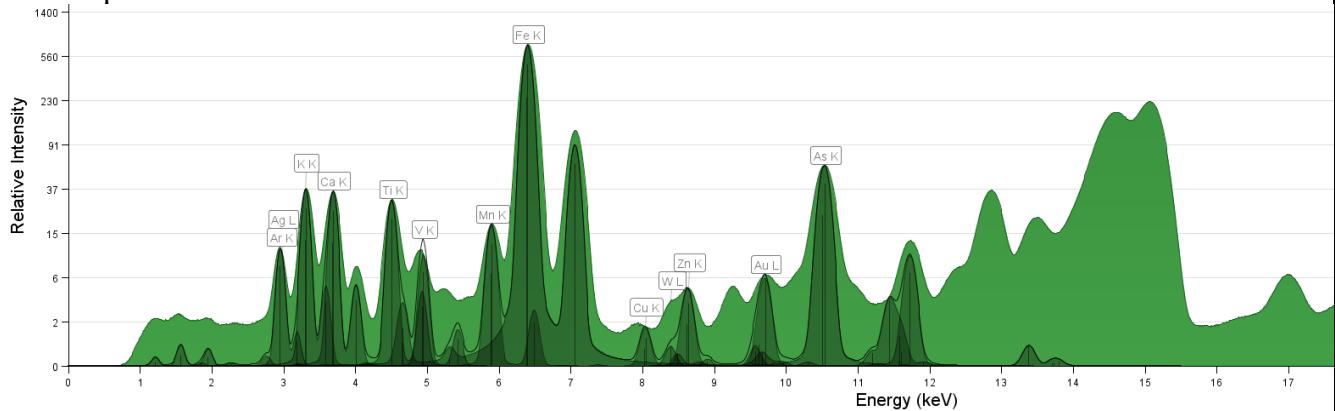


Description:

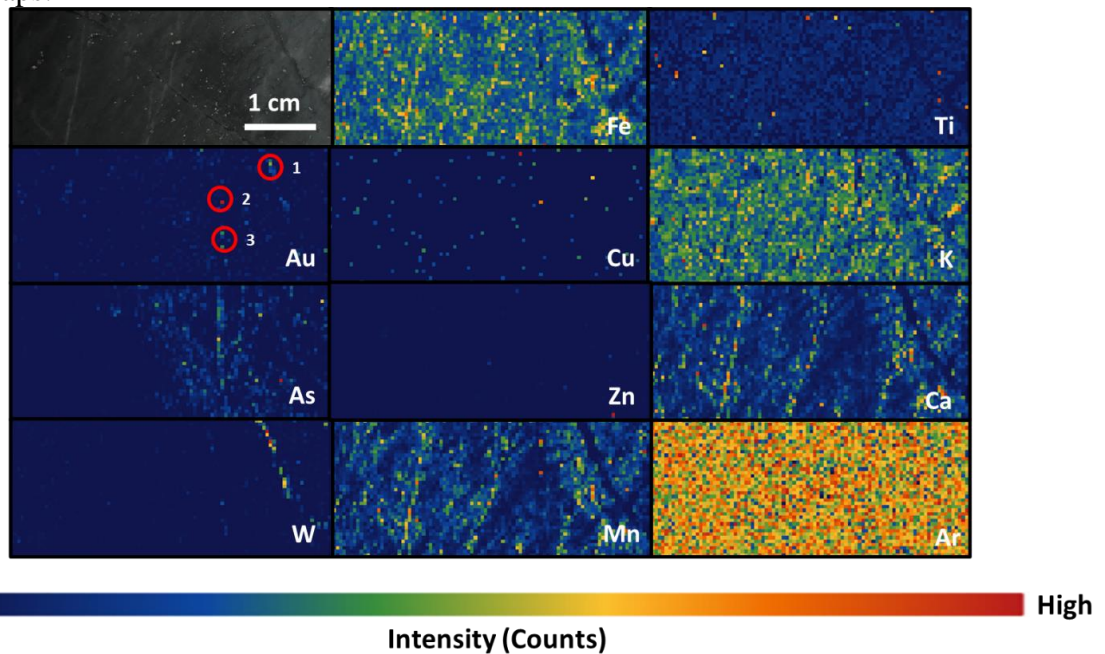
- As distributes along with the folded sulphide veins.
- Cu Au Fe are disseminated in the folded sulphide veins.
- Zn & W are disseminated.
- K distributes on the edge of the darker grey layer and lighter grey layer of the foliation texture, while Ca & Mn distribute in the darker grey layer which next to the folded sulphide veins.
- Au spots: 1. Au peak on the As shoulder on the MCA Spectrum, but higher than the shoulder; 2&3. Au peak and W peak are overlapped, but Au peak is much higher than As shoulder and W peak; 4&5 real Au peak, much higher than As shoulder
- Ar intensity (without filter → with filter): 698.5 → 121.5
- Comparing to APS 201D-Feb 2019: Au map changed. More real gold spots have been found.

Sample Number	2853 (offcut)	Drill Hole	TL-16-604A	Depth	643.96-644.24m
Lithology	QFP	Map Size	2 cm x 3.5 cm	Gold Grade	7.73 ppm

MCA Spectrum:



SR-μXRF Maps:

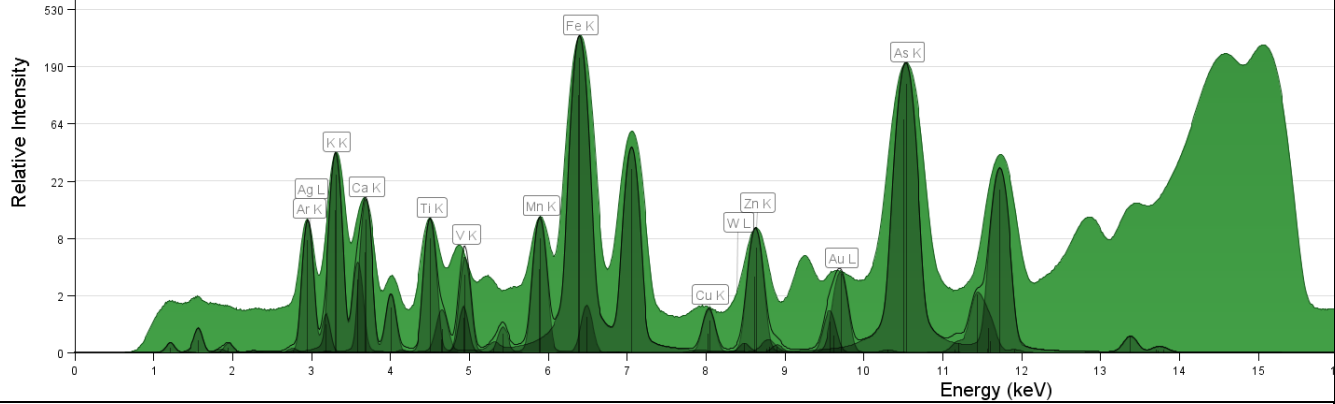


Description:

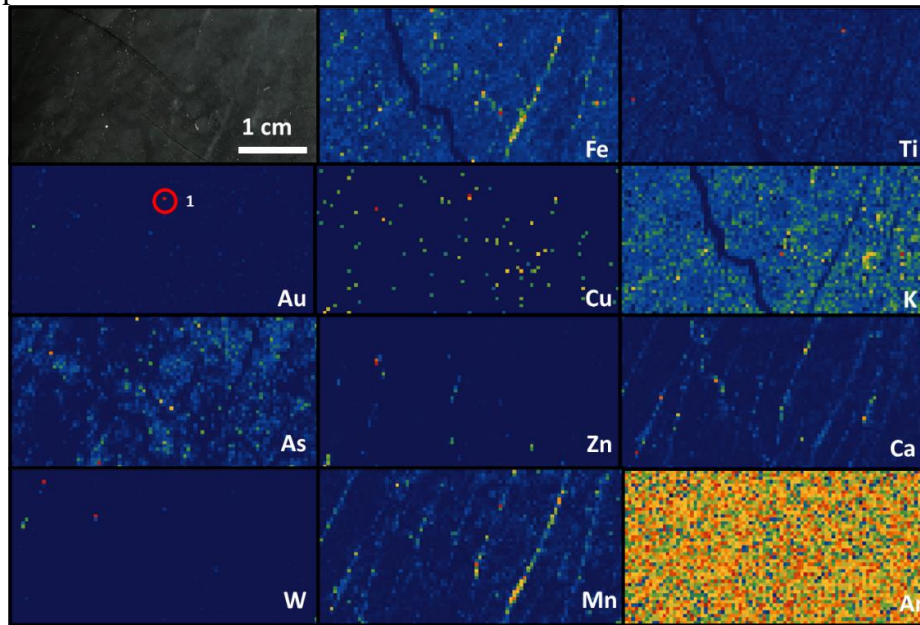
1. Au As have the same distribution in the middle of the sample.
2. Ca Fe Mn K have the same distribution along with the light grey layers of the foliation and fractures.
3. Zn Cu Ti are disseminated.
4. W distributes in a fracture.
5. Au spots: 1. W, false Au signal; 2. Au peak on the As shoulder on the MCA Spectrum, but higher than the shoulder; 3. real Au peak, much higher than As shoulder.
6. Ar intensity (without filter→ with filter): 698.5→121.5
7. Comparing to APS 201D-Feb 2019: Cu Ti maps are different.

Sample Number	2857 (offcut)	Drill Hole	TL-16-607	Depth	718.4-718.66 m
Lithology	QFP	Map Size	2 cm x 3.5 cm	Gold Grade	2.16 ppm

MCA Spectrum:



SR- μ XRF Maps:



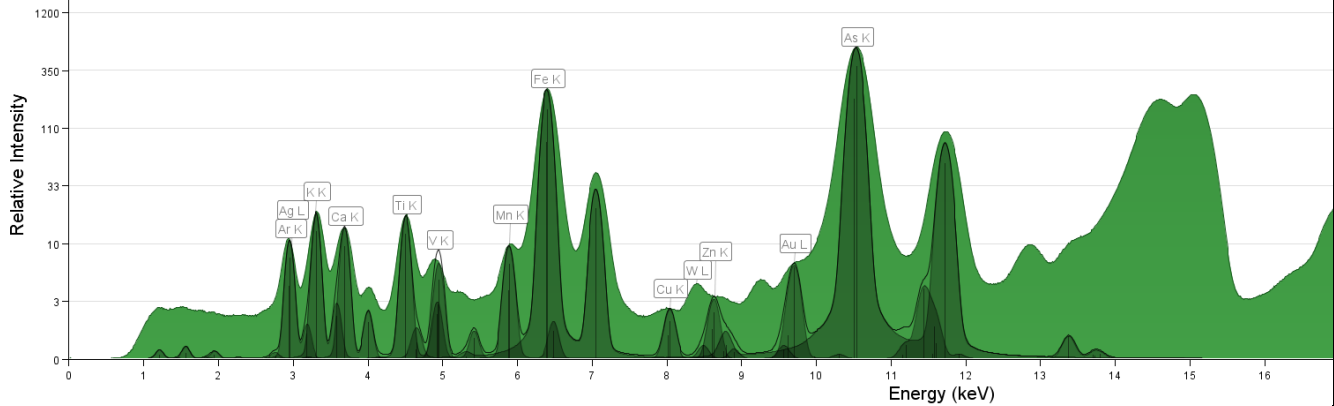
Low  High
Intensity (Counts)

Description:

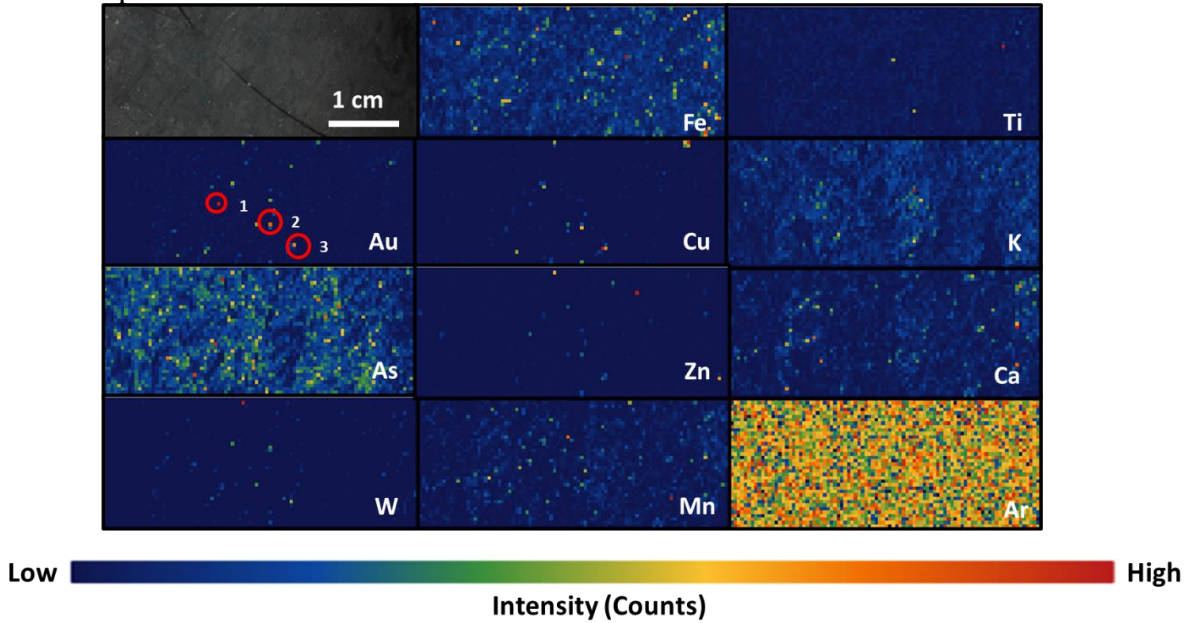
1. Zn W Ti Cu W Au is disseminated.
2. Fe Ca Mn Zn have the same distribution along with the sulphide veins.
3. As K distribute opposite to the sulphide veins and fractures.
4. Au spots: 1. Au peak and W peak are overlapped, but Au peak is much higher than As shoulder and W peak.
5. Ar intensity (without filter→ with filter): 698.5→121.5
6. Comparing to APS 20ID-Feb 2019: Au spot type changes. Cu map changes.

Sample Number	2819 (offcut)	Drill Hole	TL-16-575	Depth	154.1-154.32 m
Lithology	QFP	Map Size	2 cm x 3.5 cm	Gold Grade	7.21 ppm

MCA Spectrum:



SR- μ XRF Maps:

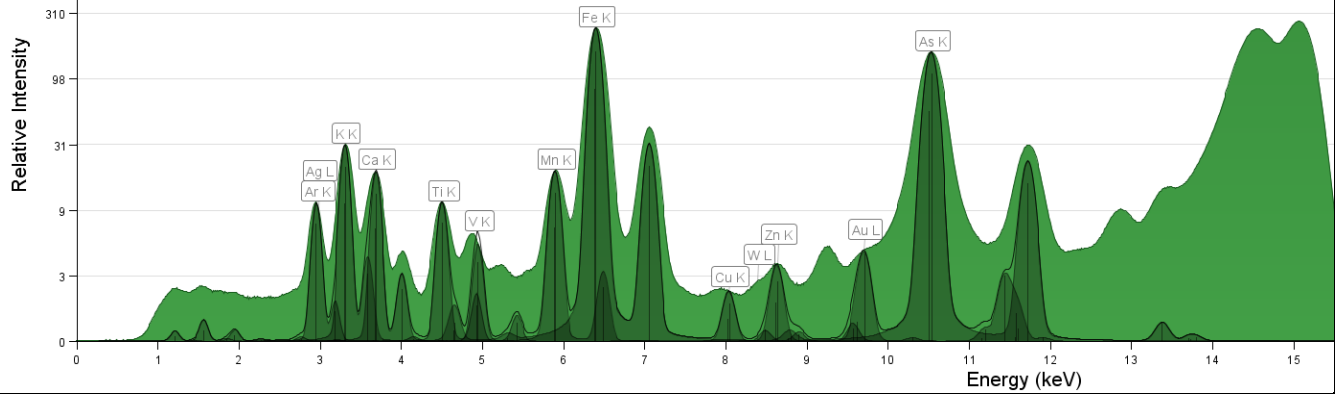


Description:

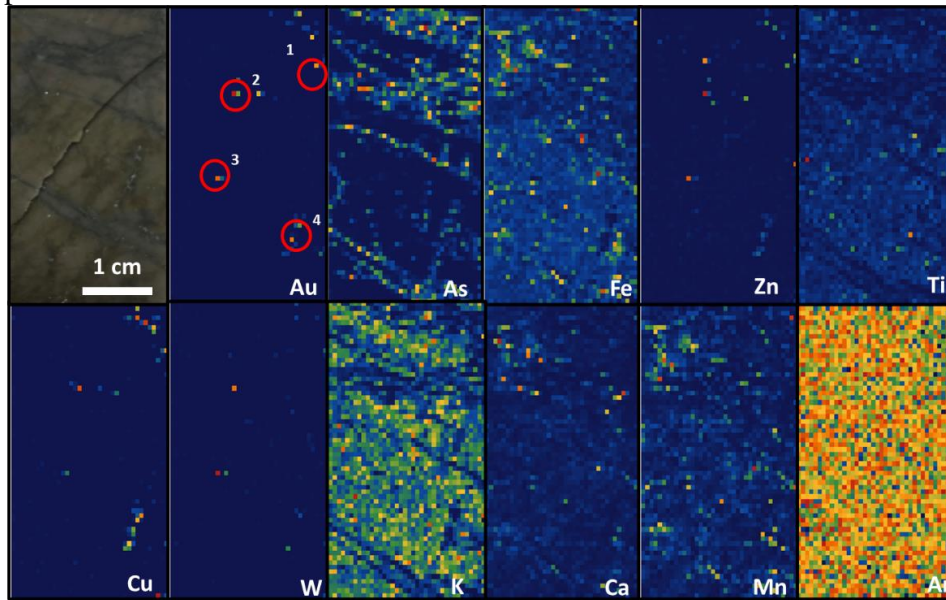
- As distributes along with the black foliation layers.
- Fe Zn Cu have the same distribution.
- Au Zn Ca Mn W Ti K are disseminated.
- Au spots: 1. real Au peak, much higher than As shoulder; 2&3. Au peak on the As shoulder on the MCA Spectrum, but higher than the shoulder.
- Ar intensity (without filter \rightarrow with filter): 698.5 \rightarrow 121.6
- Comparing to APS 201D-Feb 2019: Au W Ti K distribution change. Mapping area is smaller than APS 201D-Feb 2019.

Sample Number	2845 (offcut)	Drill Hole	TL-13-509	Depth	235.6-235.86 m
Lithology	QFP	Map Size	2 cm x 3.5 cm	Gold Grade	1.13 ppm

MCA Spectrum:



SR-μXRF Maps:

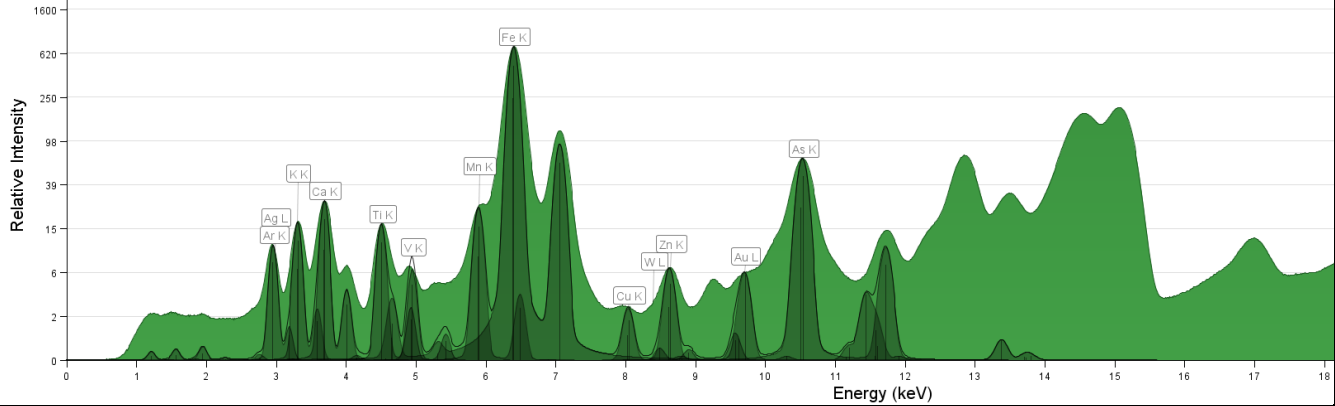


Description:

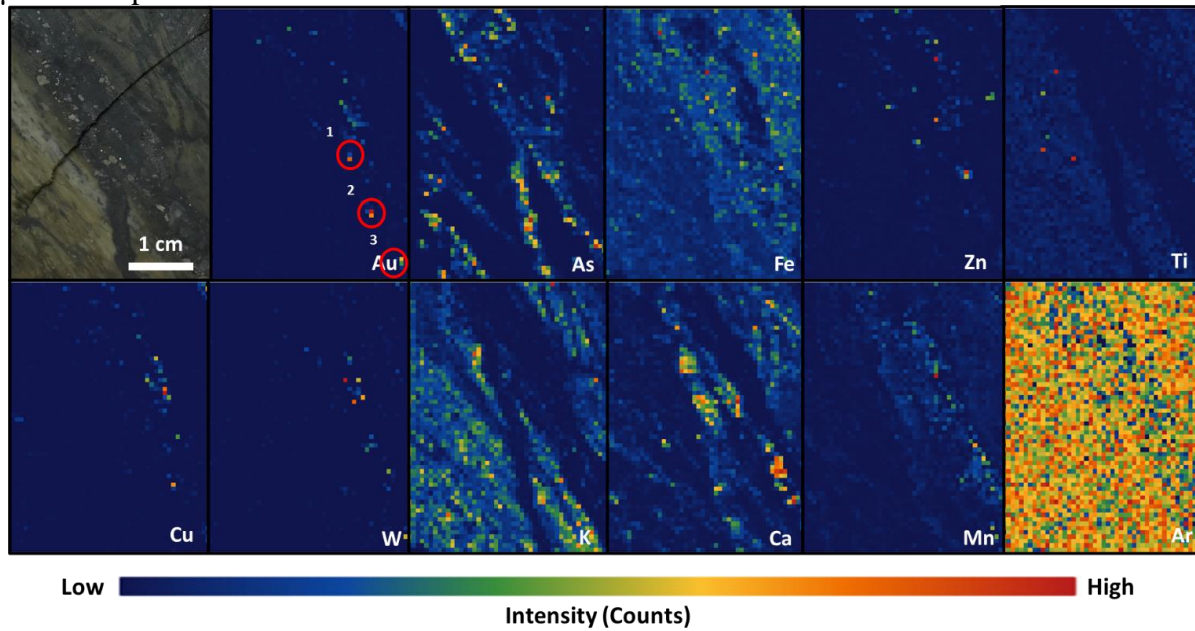
1. As Fe Cu have the same distribution along with the dark fine veinlets.
2. Au W Zn Ca Mn are disseminated in the dark fine veinlets.
3. Ti & K distribute opposite to the dark fine veinlets.
4. Au spots: 1&4 Au peak on the As shoulder on the MCA Spectrum, but higher than the shoulder; 2&3. Au peak and W peak are overlapped, but Au peak is much higher than As shoulder and W peak.
5. Ar intensity (without filter→ with filter): 556.9→121.6
6. Comparing to APS 20ID-Feb 2019: K &Ti maps show more texture. Au spots are more accurate.

Sample Number	2834 (offcut)	Drill Hole	TL-13-500	Depth	195.76-196 m
Lithology	Lapilli Tuff	Map Size	2 cm x 3.5 cm	Gold Grade	5.21 ppm

MCA Spectrum:



SR- μ XRF Maps:

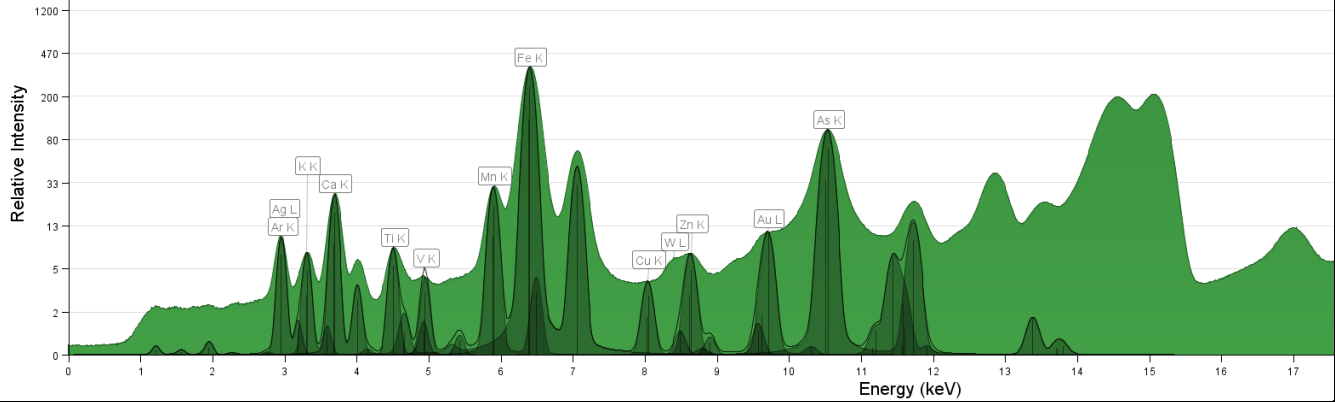


Description:

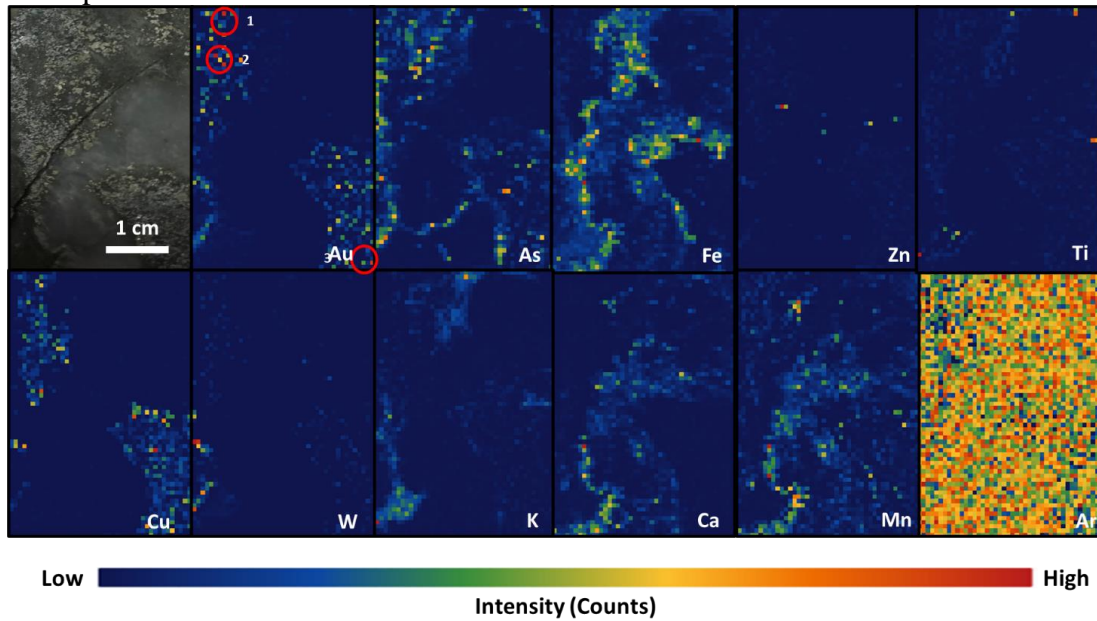
- As distributes along with the sulphide veins.
- Fe & Mn are disseminated in the dark foliated layers next to the sulphide veins.
- Ca distributes in the dark red veinlets.
- K distributes opposite to the dark red veinlets.
- Au Ti Cu Zn W are disseminated in the sulphide veins.
- Au spots: 1. Au peak on the As shoulder on the MCA Spectrum, but higher than the shoulder; 2&3. real Au peak, much higher than As shoulder.
- Ar intensity (without filter \rightarrow with filter): 556.9 \rightarrow 121.5
- Comparing to APS 201D-Feb 2019: Vein cutting is clearer. Au spot is more accurate.

Sample Number	2854 (offcut)	Drill Hole	TL-16-604A	Depth	729.02-729.2m
Lithology	Metavolcanic Tuff	Map Size	2 cm x 3.5 cm	Gold Grade	10.49 ppm

MCA Spectrum:



SR-μXRF Maps:

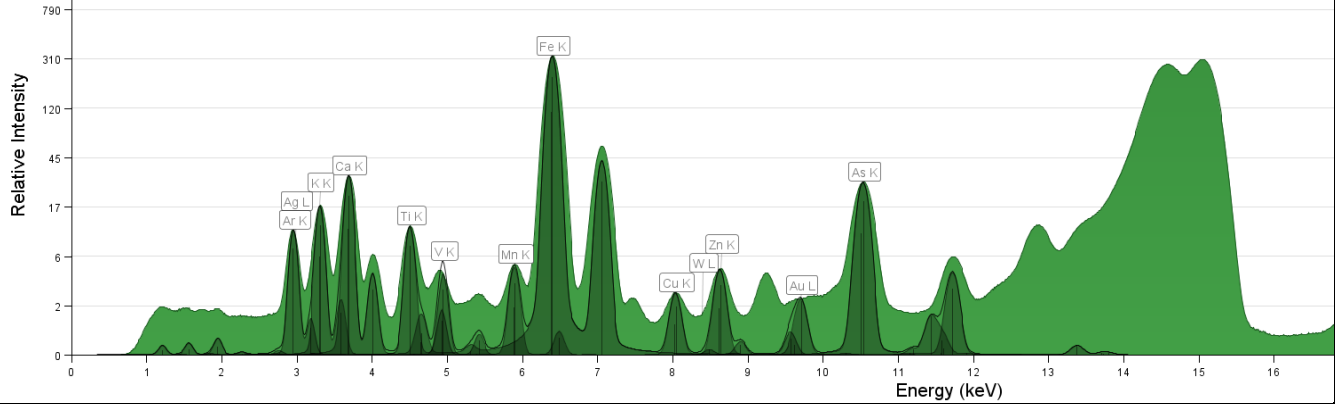


Description:

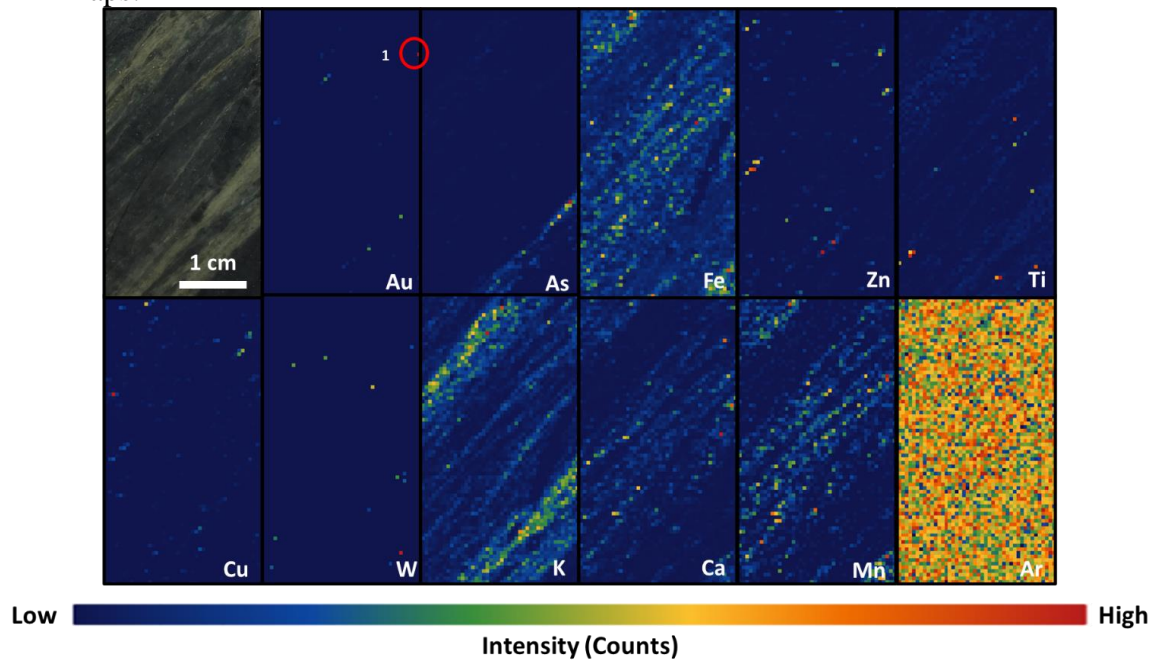
1. Au Cu As have the same distribution in the sulphide intrusion.
2. Fe & K have the same distribution in the sulphide intrusion, and there is higher intensity on the edge of the intrusion.
3. Ca & Mn have the same distribution along with the sulphide intrusion in the white vein, and the side beside the intrusion has higher intensity.
4. W Zn Ti are disseminated in the sulphide intrusion.
5. Au spots: 1-4. Au peak and W peak are overlapped, but Au peak is much higher than As shoulder and W peak.
6. Ar intensity (without filter→ with filter): 556.9→121.6
7. Comparing to APS 201D-Feb 2019: No false Au spot any more.

Sample Number	2831 (offcut)	Drill Hole	TL-15-551	Depth	96.8-97 m
Lithology	Metasandstone	Map Size	2 cm x 3.5 cm	Gold Grade	2.26 ppm

MCA Spectrum:



SR- μ XRF Maps:

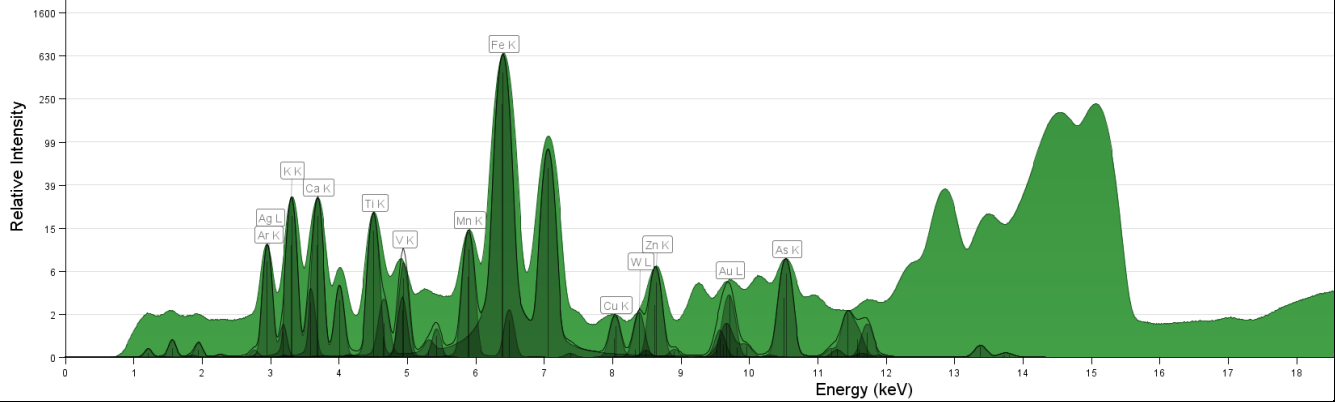


Description:

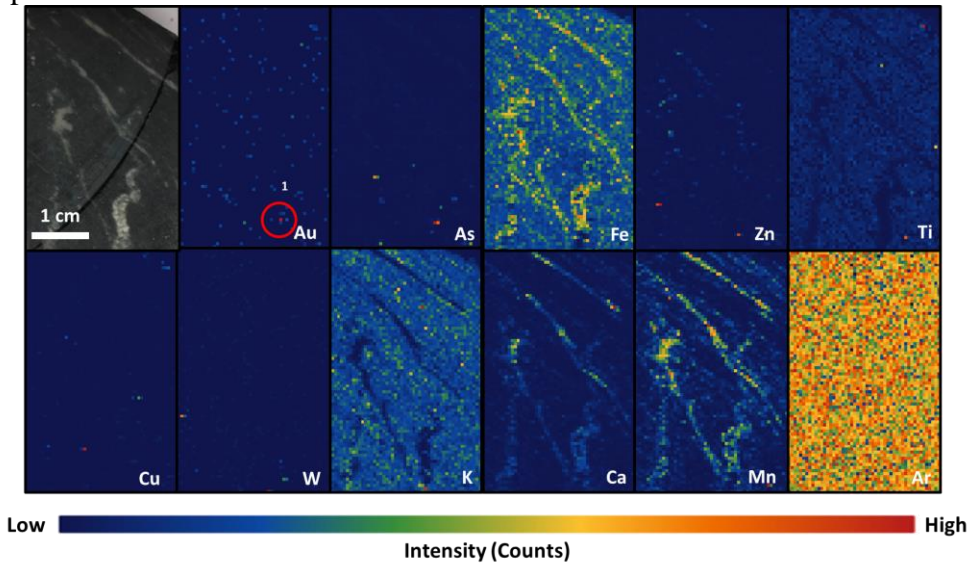
1. Au & As have the same distribution along with the light green layer of foliation.
2. Zn Ti Cu W Ca Mn are disseminated in the dark green layers of foliation.
3. K distributes in the light green layers of foliation.
4. Au spots: 1. W, false Au signal.
5. Ar intensity (without filter \rightarrow with filter): 510.5 \rightarrow 121.6
6. Comparing to APS 201D-Feb 2019: Au spot location is different.

Sample Number	2858 (offcut)	Drill Hole	TL-16-607	Depth	817.4-817.6 m
Lithology	Lapilli Tuff	Map Size	2 cm x 3.5 cm	Gold Grade	2.45 ppm

MCA Spectrum:



SR- μ XRF Maps:



Description:

1. Au & As have the same distribution in the sulphide intrusion.
2. Ca Fe Mn have the same distribution along with the white veins and sulphide intrusion.
3. Cu W Zn are disseminated in the white veins.
4. Ti & K have the same distribution opposite to the white veins and sulphide intrusion.
5. Au spots: 1. Au peak and W peak are overlapped, but Au peak is much higher than As shoulder and W peak.
6. Ar intensity (without filter \rightarrow with filter): 548.5 \rightarrow 121.4
7. Comparing to APS 201D-Feb 2019: Au spot didn't change, but gold type changed.

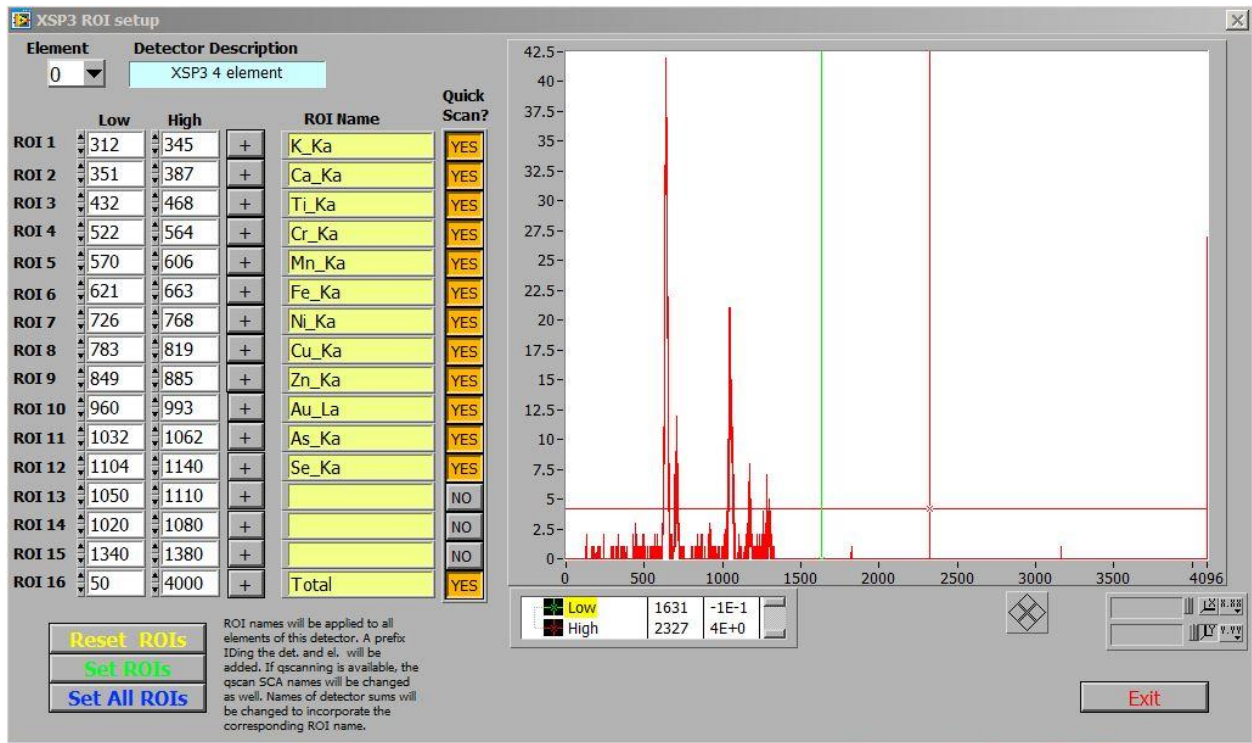
APS 20ID-July 2019

Beamtime and Beamline Details:

Detector: Vortex Si drift (single, 4-element)

Monochromator Crystal Set: Si (311)

ROI Setup applied to all elements of the detector: K $K\alpha$, Ca $K\alpha$, Ti $K\alpha$, Cr $K\alpha$, Mn $K\alpha$, Fe $K\alpha$, Ni $K\alpha$, Cu $K\alpha$, Zn $K\alpha$, Au $L\alpha$, As $K\alpha$, Se $K\alpha$, and total sum



Incident Energy: 13 KeV

Max energy: 41 KeV

Mode: Quick scan

Beam spot size: 60 μm x 60 μm

Step size: 150 μm

Dwell time: 200 msec

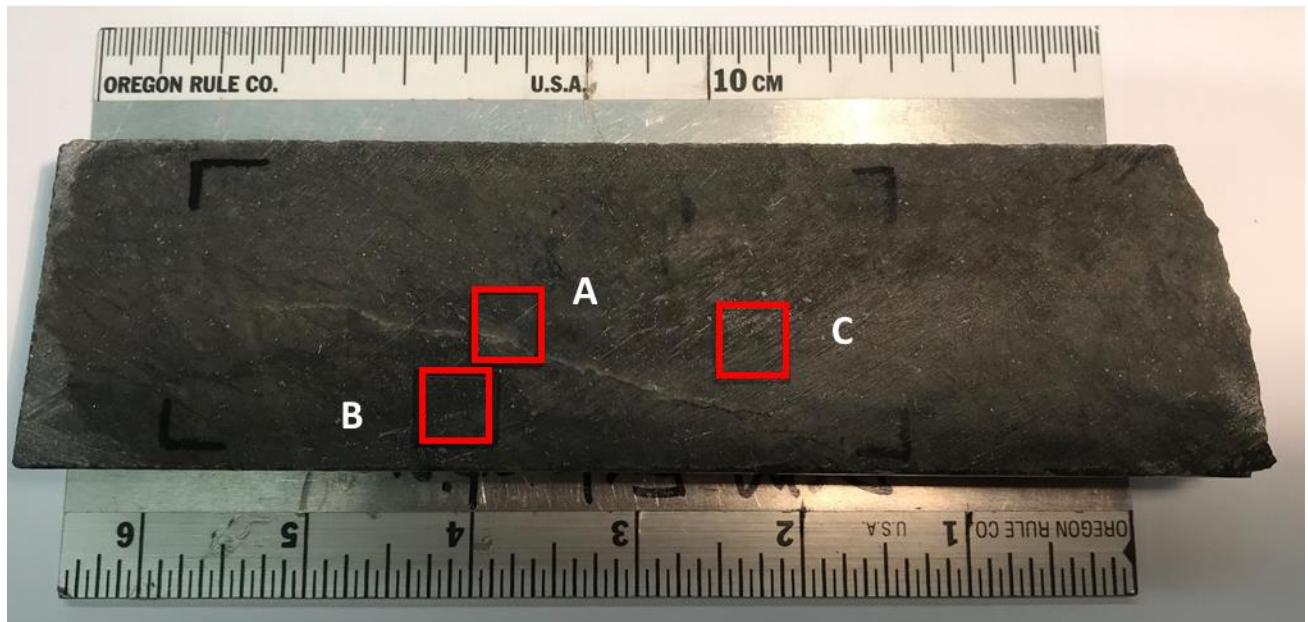
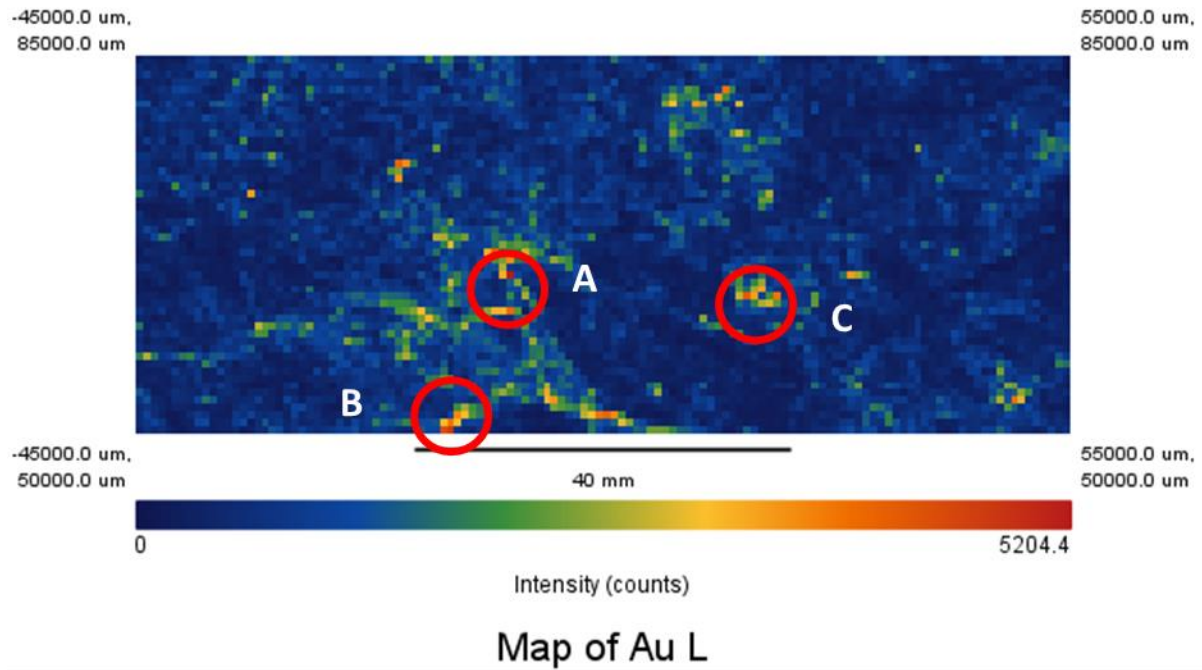
Samples: 1 cm x 1 cm interest regions with high Au intensity which are chosen from 800 μm x 800 μm maps from APS 20ID Feb.

Data Processing:

7. Energy Calibration Maximum: 40.04 keV, using Fe K peak to adjust the energy.
8. Peak fitting: Fe K, Ca K, As K, Cu K, Ar K, Mn K, Au L, Zn K, K K, W L, Ti K. Save these as a session for later use.
9. Ar Normalization: use the cursor to check the Ar channel at the bottom of the window. Different dataset has different Ar channel. For this one, Ar channel is 294.
Use Data Filter-Advanced- Normalizer, mode: channel range, start channel:295, end channel: 296, normalized intensity: 10 (the best channel range was checked using Ar XRF map with lowest intensity range).
No filter: 316.8
294-295: 145.7
294-294: 153.3
295-295: 143.1
295-296: 139.5
296-296: 139.5
296-297: 139.5
297-297: 141.9
10. Map fitting: check the visible button.
11. Save MCA Spectrum and maps of each sample.
12. Check Au map to make sure if each high-intensity spot is the real gold signal: select the spot and plot selection → take notes of the relationship of Au and other element curves (on the shoulder/ real peak/ overlaid other element peaks/ false signal).

SR- μ XRF Maps:

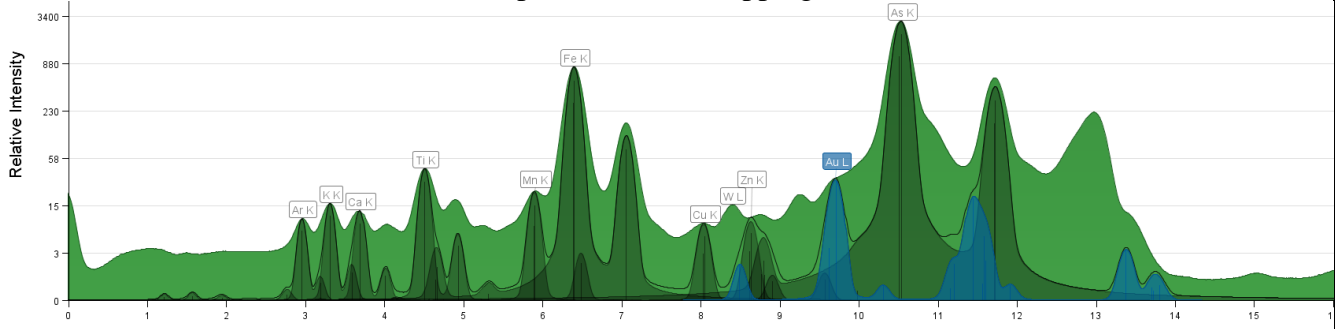
2819:



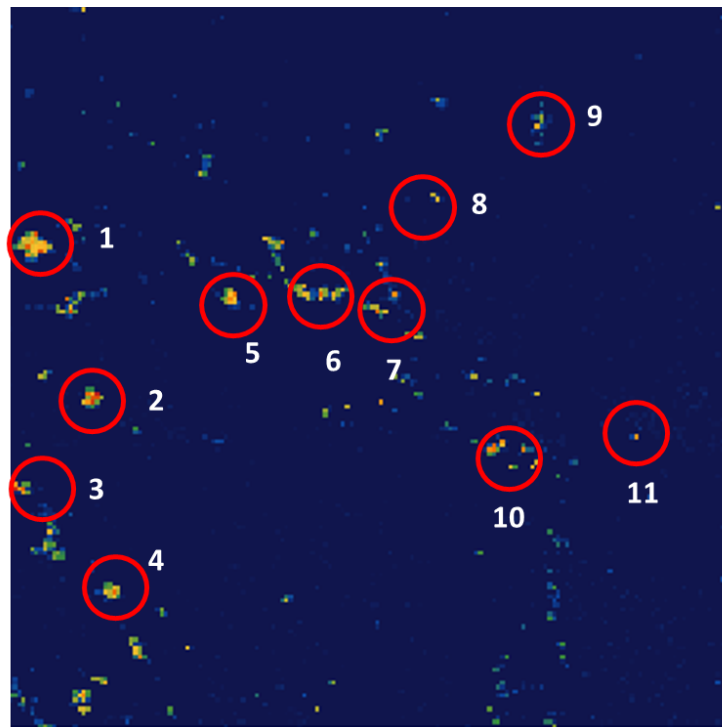
A, B, C: Au peak on the As shoulder on the MCA Spectrum, but higher than the shoulder.

Sample Number	2819A	Drill Hole	TL-16-575	Depth	154.1-154.32 m
Lithology	QFP	Map Size	1 cm x 1 cm	Gold Grade	7.21 ppm

MCA Spectrum (Full Mapping Area):



SR- μ XRF Au Map:



4 mm

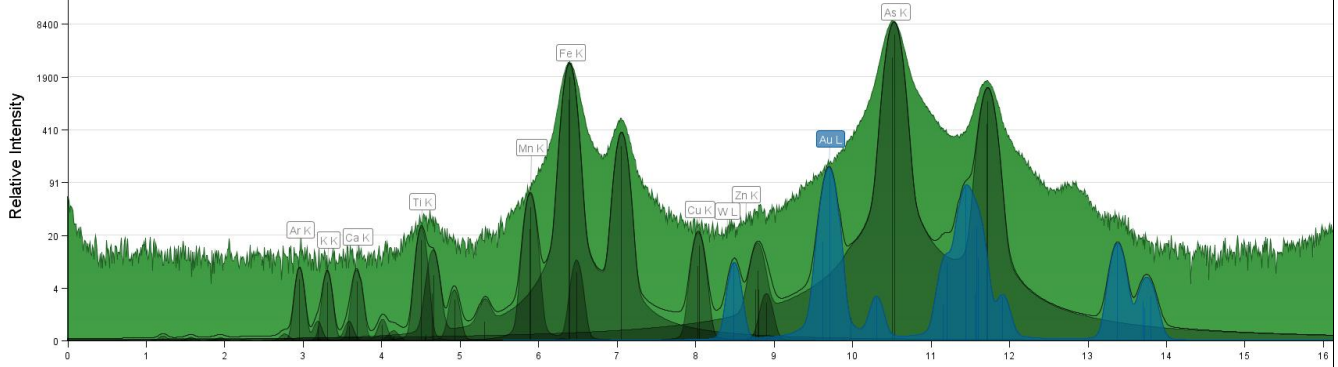
Low High
Intensity (Counts)

Additional Notes:

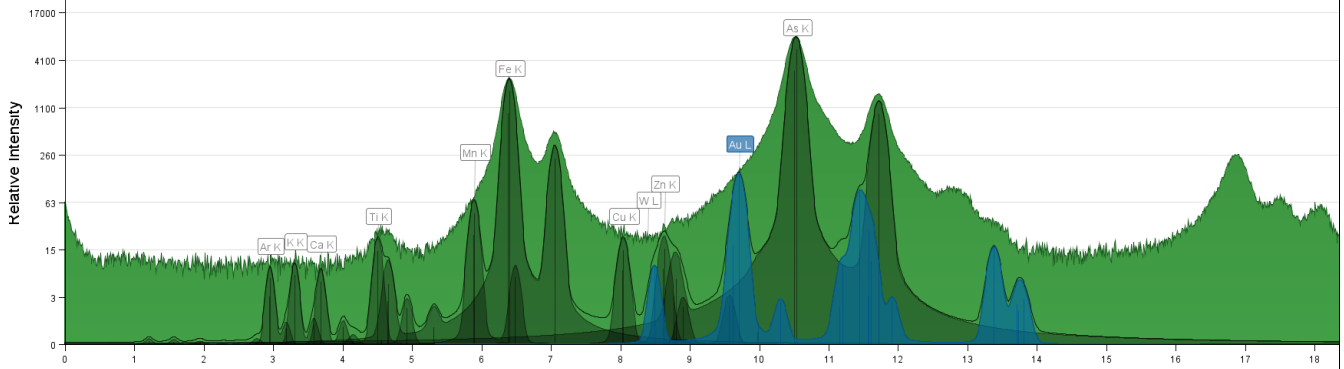
Ar intensity (without filter \rightarrow with filter): 316.8 \rightarrow 139.5

MCA Spectrum (Au spots):

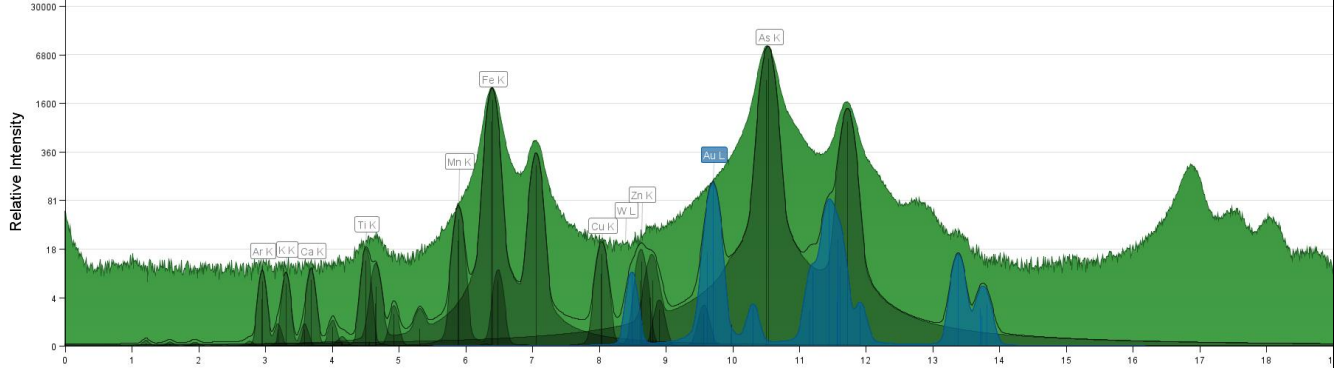
1. Au peak on the As shoulder on the MCA Spectrum, but higher than the shoulder.



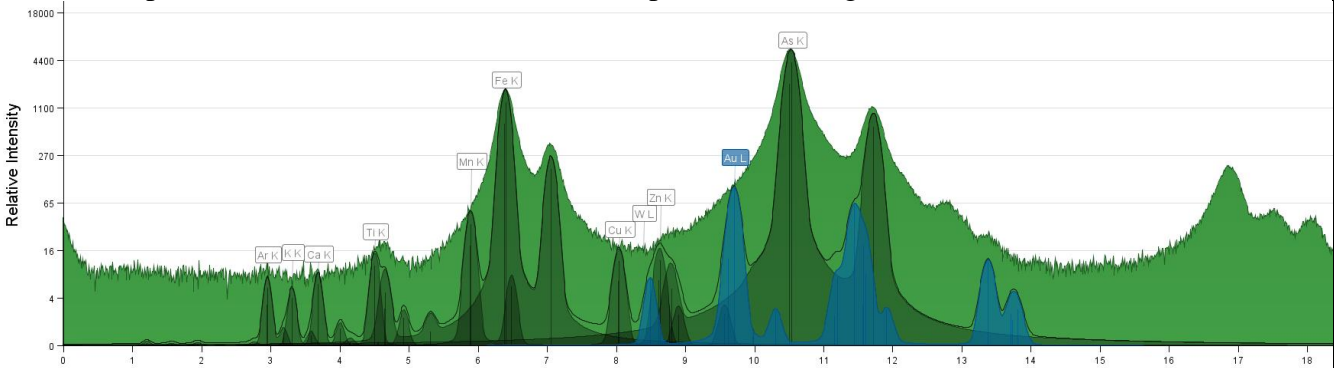
2. Au peak on the As shoulder on the MCA Spectrum, but higher than the shoulder



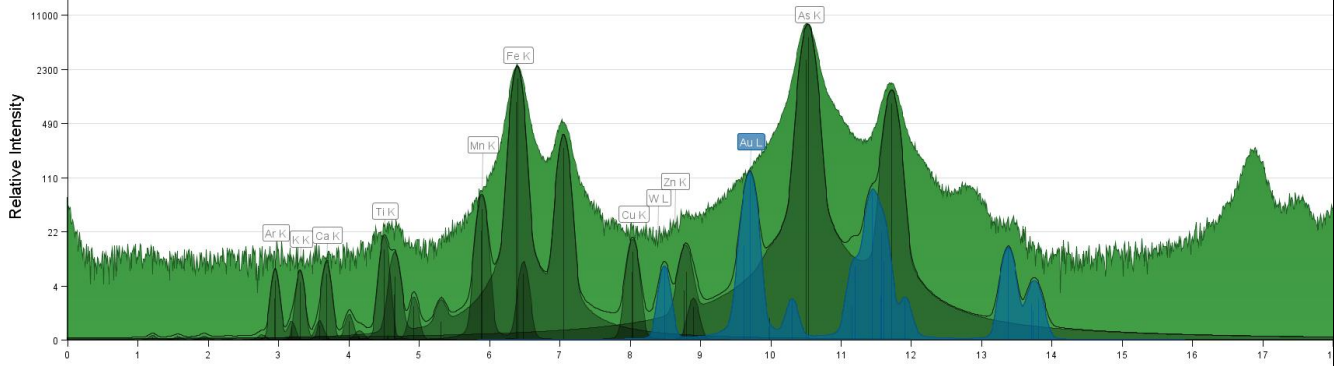
3. Au peak on the As shoulder on the MCA Spectrum, but higher than the shoulder.



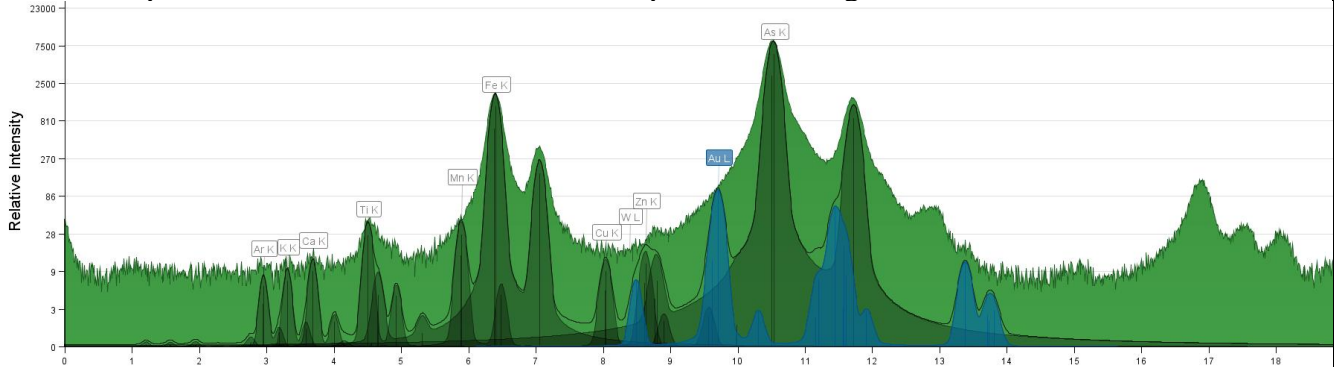
4. Au peak on the As shoulder on the MCA Spectrum, but higher than the shoulder.



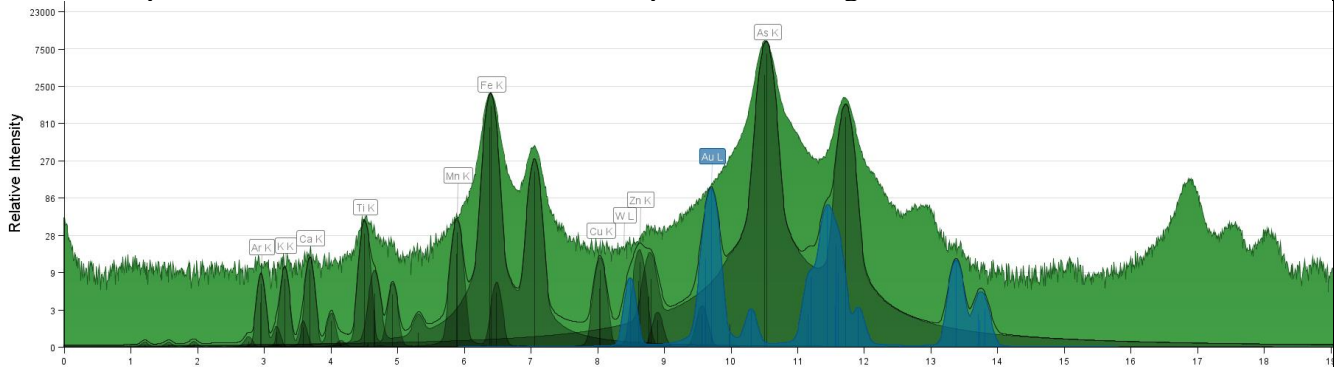
5. Au peak on the As shoulder on the MCA Spectrum, but higher than the shoulder



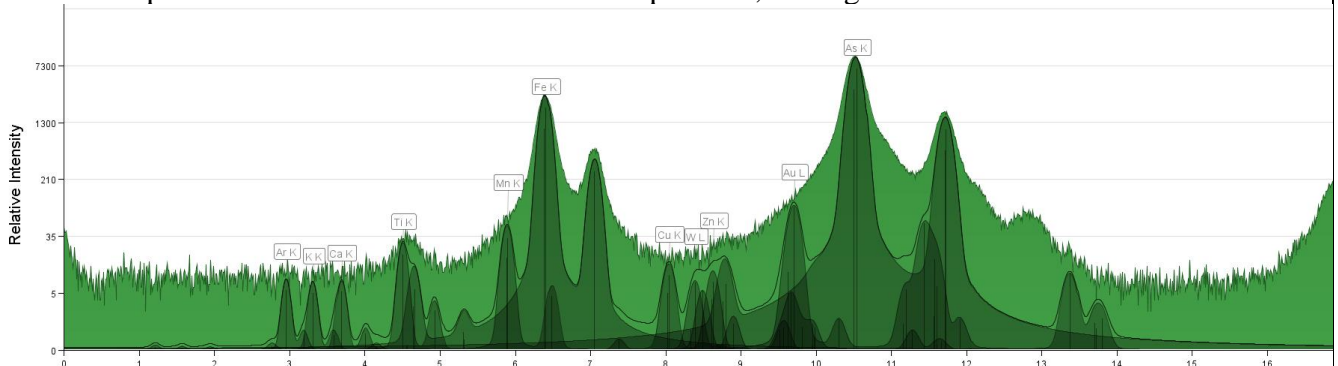
6. Au peak on the As shoulder on the MCA Spectrum, but higher than the shoulder



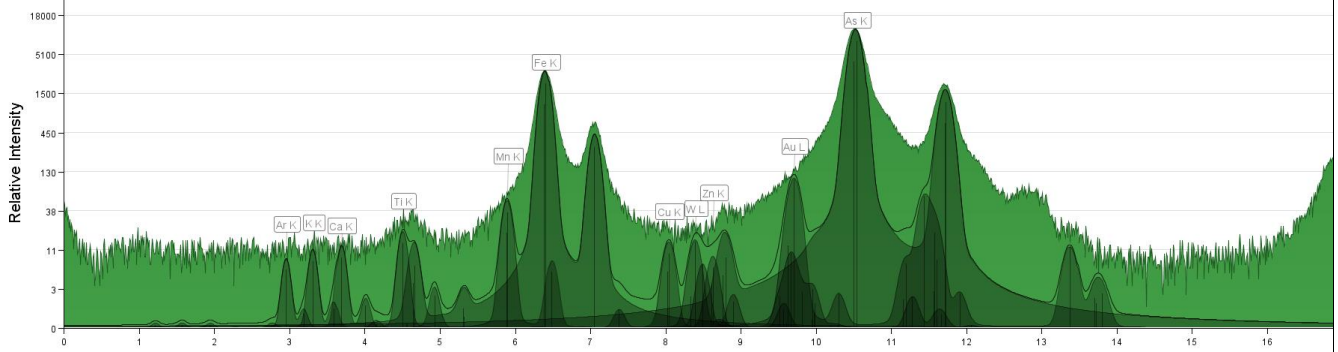
7. Au peak on the As shoulder on the MCA Spectrum, but higher than the shoulder



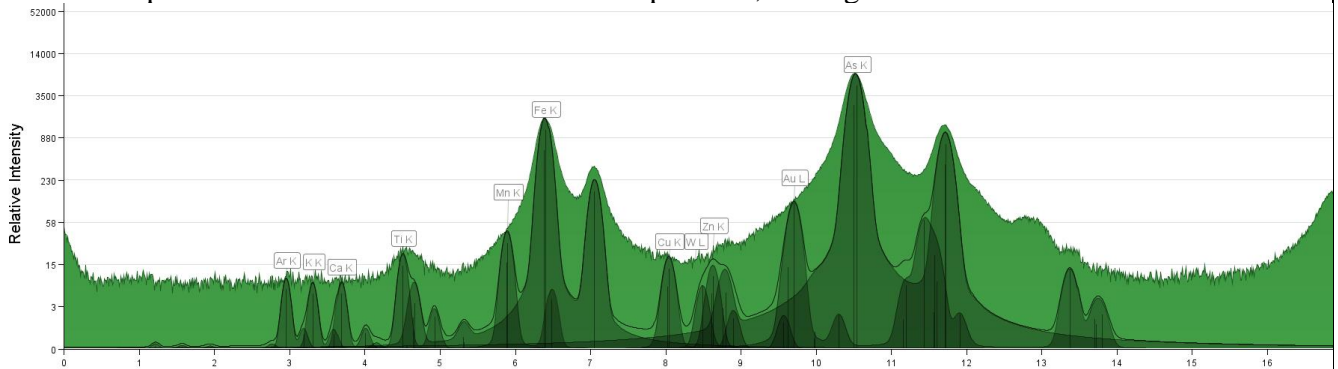
8. Au peak on the As shoulder on the MCA Spectrum, but higher than the shoulder



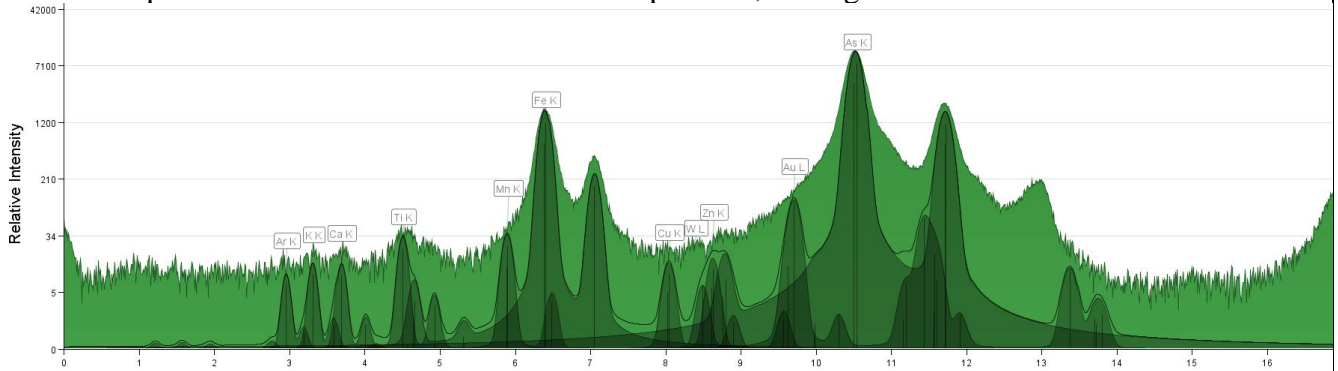
9. Au peak on the As shoulder on the MCA Spectrum, but higher than the shoulder



10. Au peak on the As shoulder on the MCA Spectrum, but higher than the shoulder

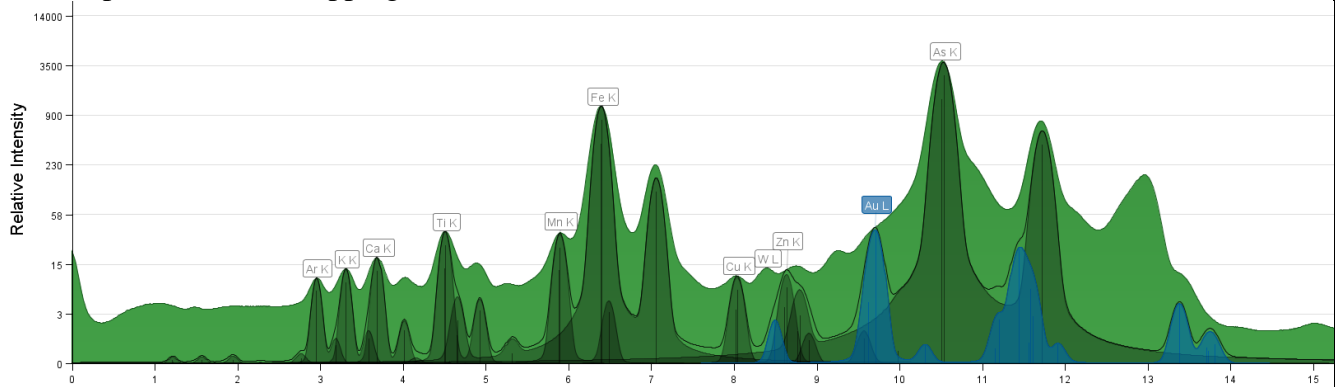


11. Au peak on the As shoulder on the MCA Spectrum, but higher than the shoulder

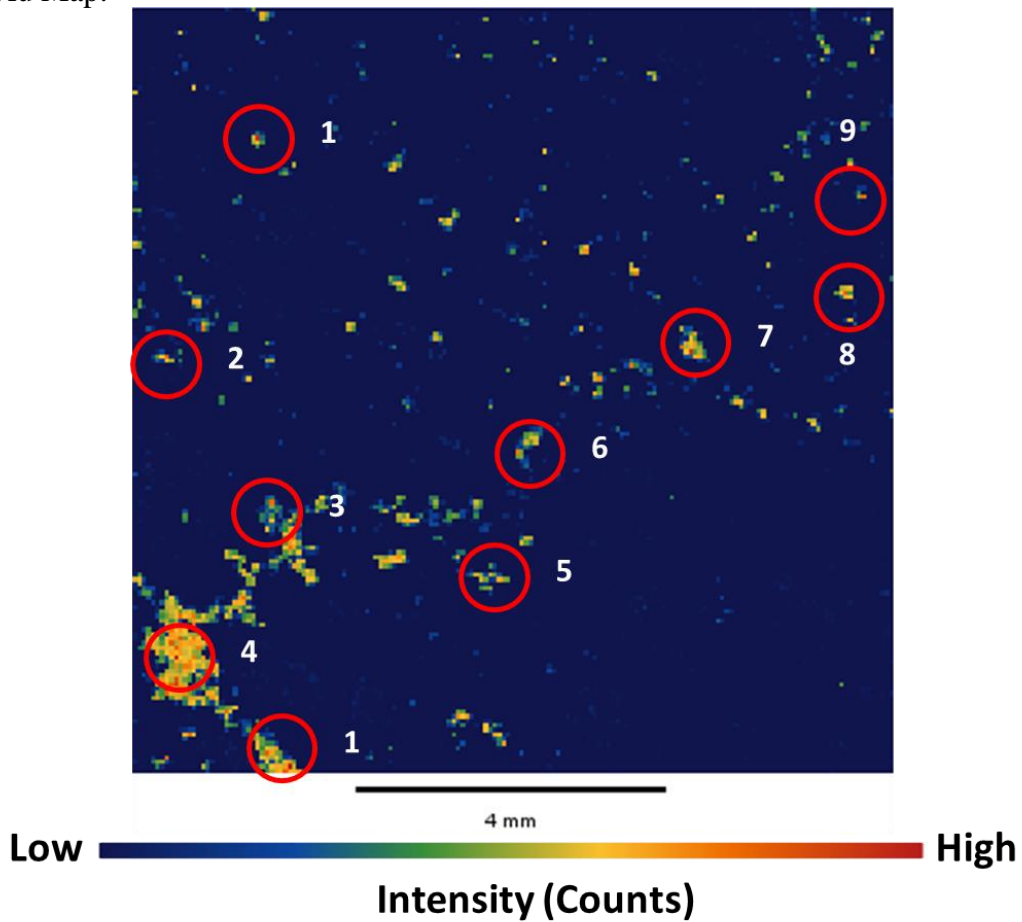


Sample Number	2819 B	Drill Hole	TL-16-575	Depth	154.1-154.32 m
Lithology	QFP	Map Size	1 cm x 1 cm	Gold Grade	7.21 ppm

MCA Spectrum (Full Mapping Area):



SR- μ XRF Au Map:

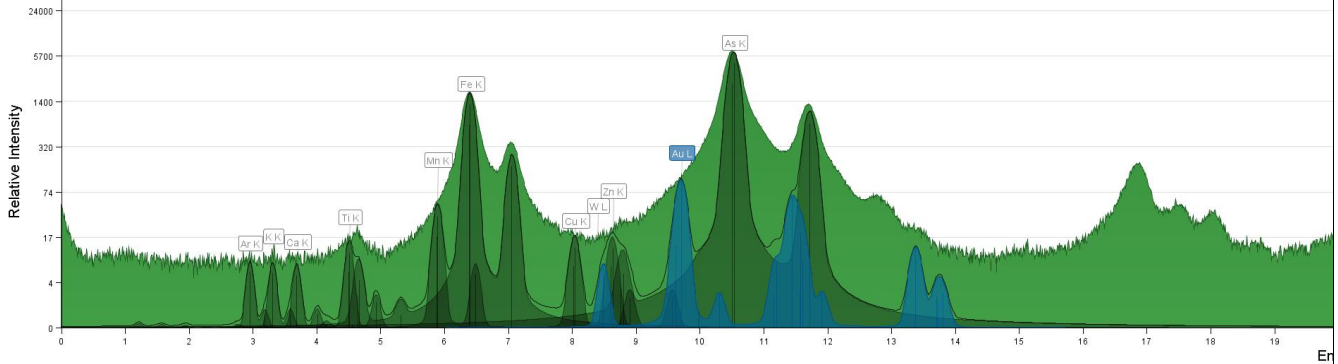


Additional Notes:

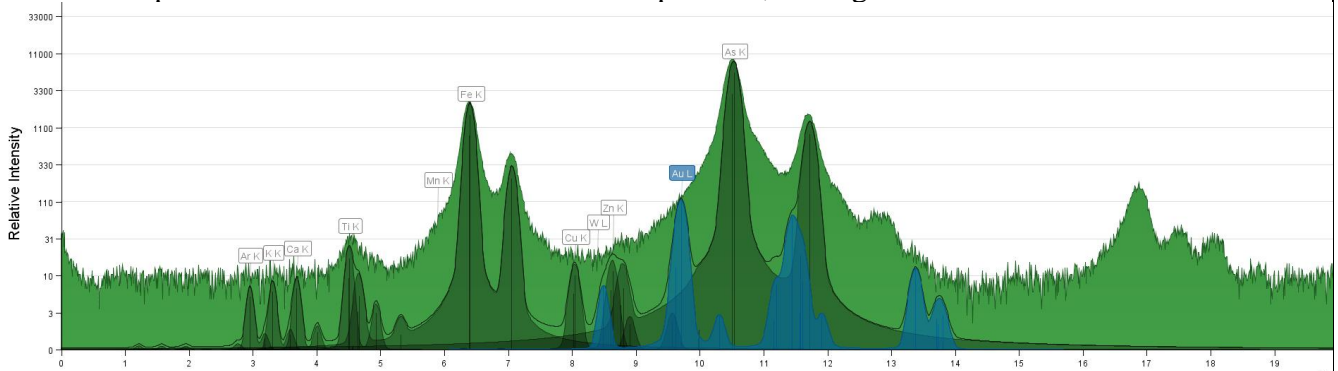
Ar intensity (without filter \rightarrow with filter): 319.9 \rightarrow 140

MCA Spectrum (Au spots):

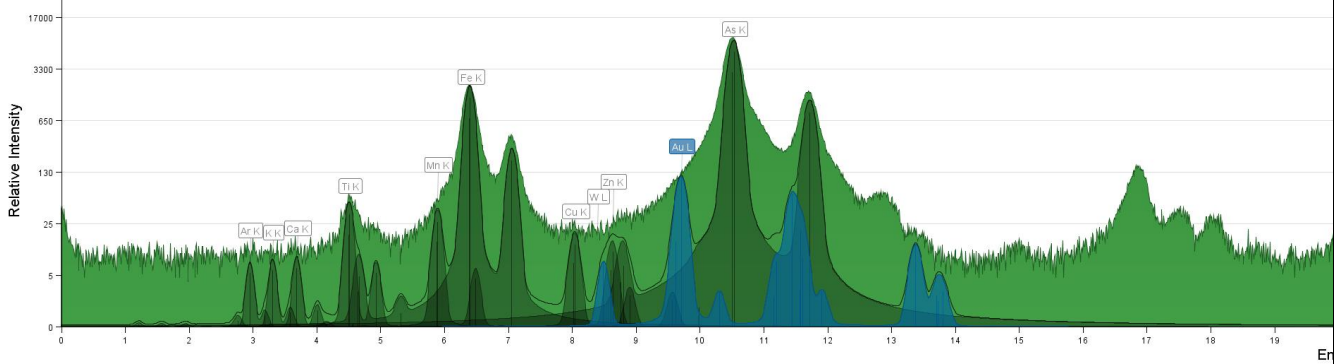
1. Au peak on the As shoulder on the MCA Spectrum, but higher than the shoulder.



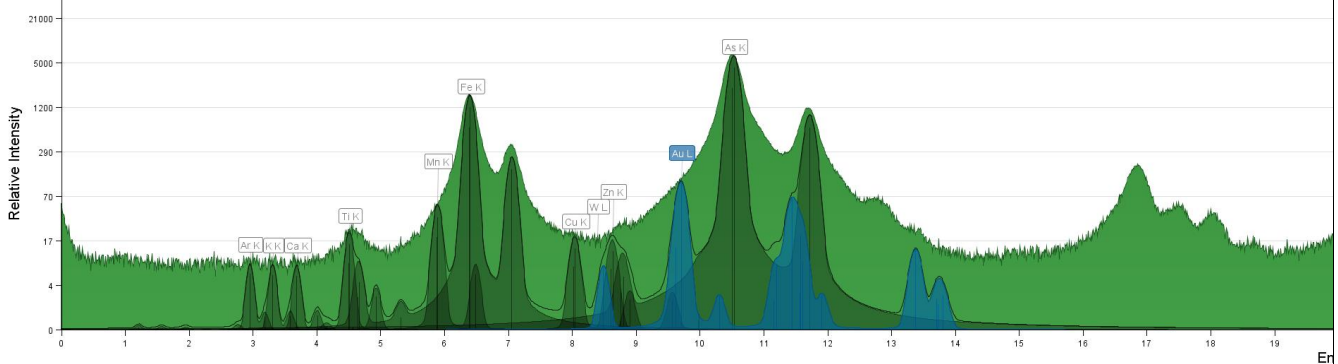
2. Au peak on the As shoulder on the MCA Spectrum, but higher than the shoulder.



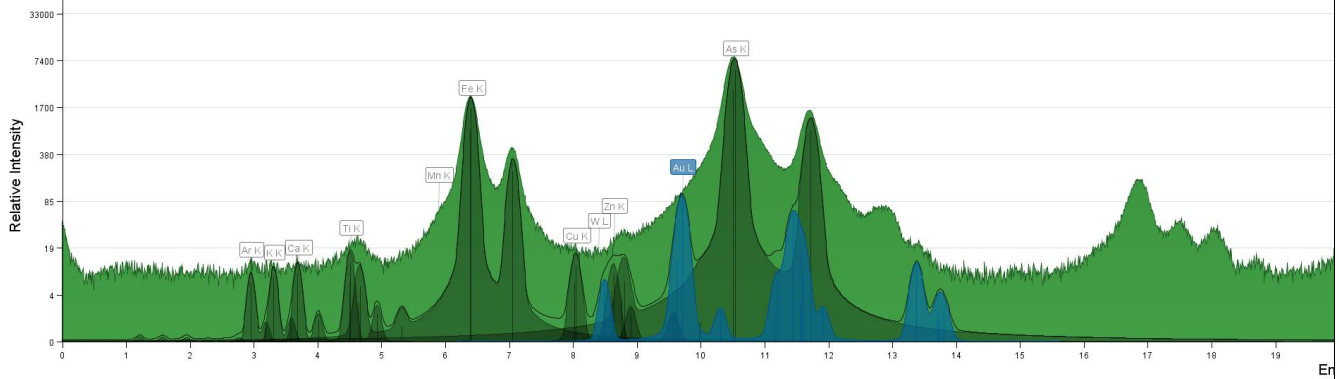
3. Au peak on the As shoulder on the MCA Spectrum, but higher than the shoulder.



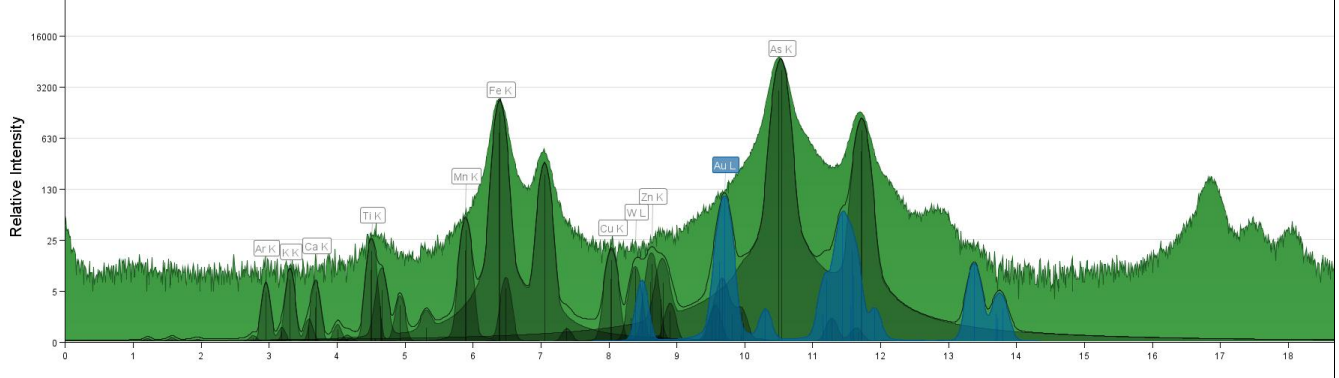
4. Au peak on the As shoulder on the MCA Spectrum, but higher than the shoulder.



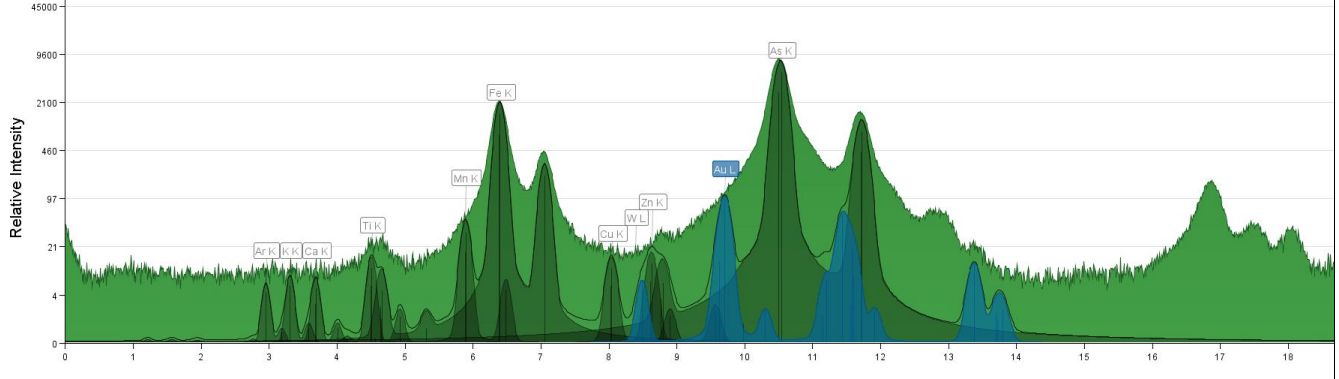
5. Au peak on the As shoulder on the MCA Spectrum, but higher than the shoulder.



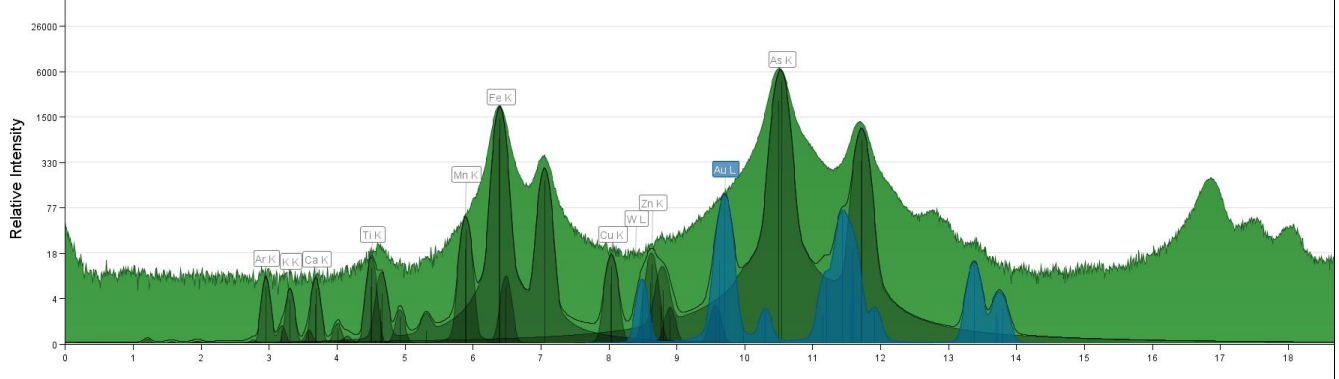
6. Au peak on the As shoulder on the MCA Spectrum, but higher than the shoulder.



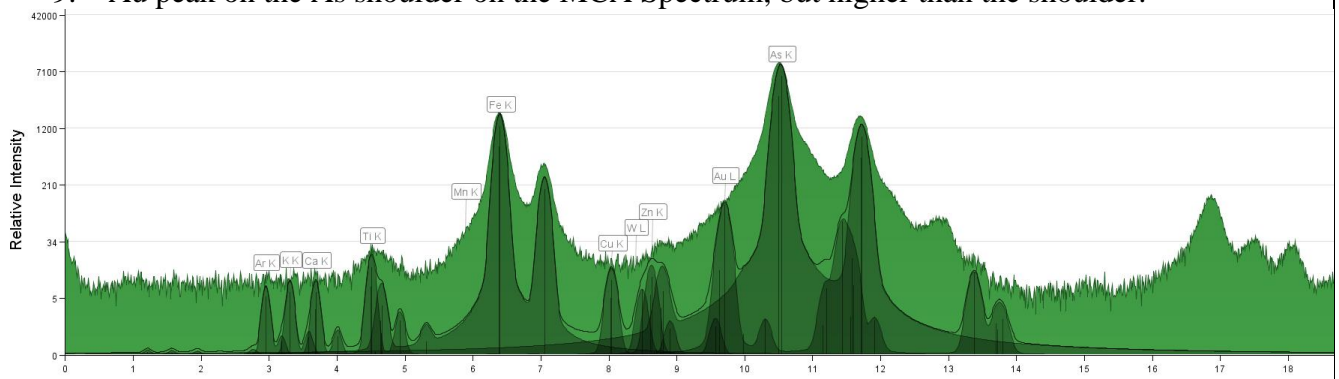
7. Au peak on the As shoulder on the MCA Spectrum, but higher than the shoulder.



8. Au peak on the As shoulder on the MCA Spectrum, but higher than the shoulder.

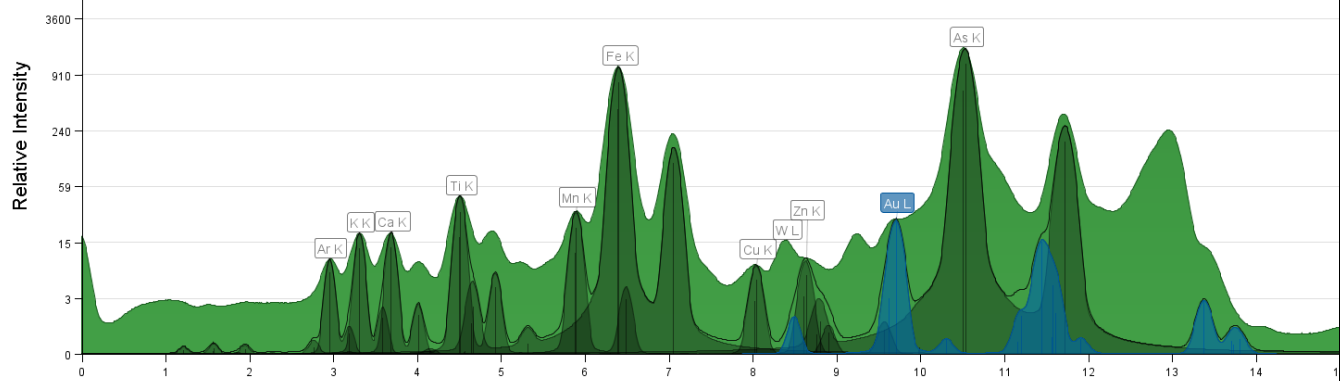


9. Au peak on the As shoulder on the MCA Spectrum, but higher than the shoulder.

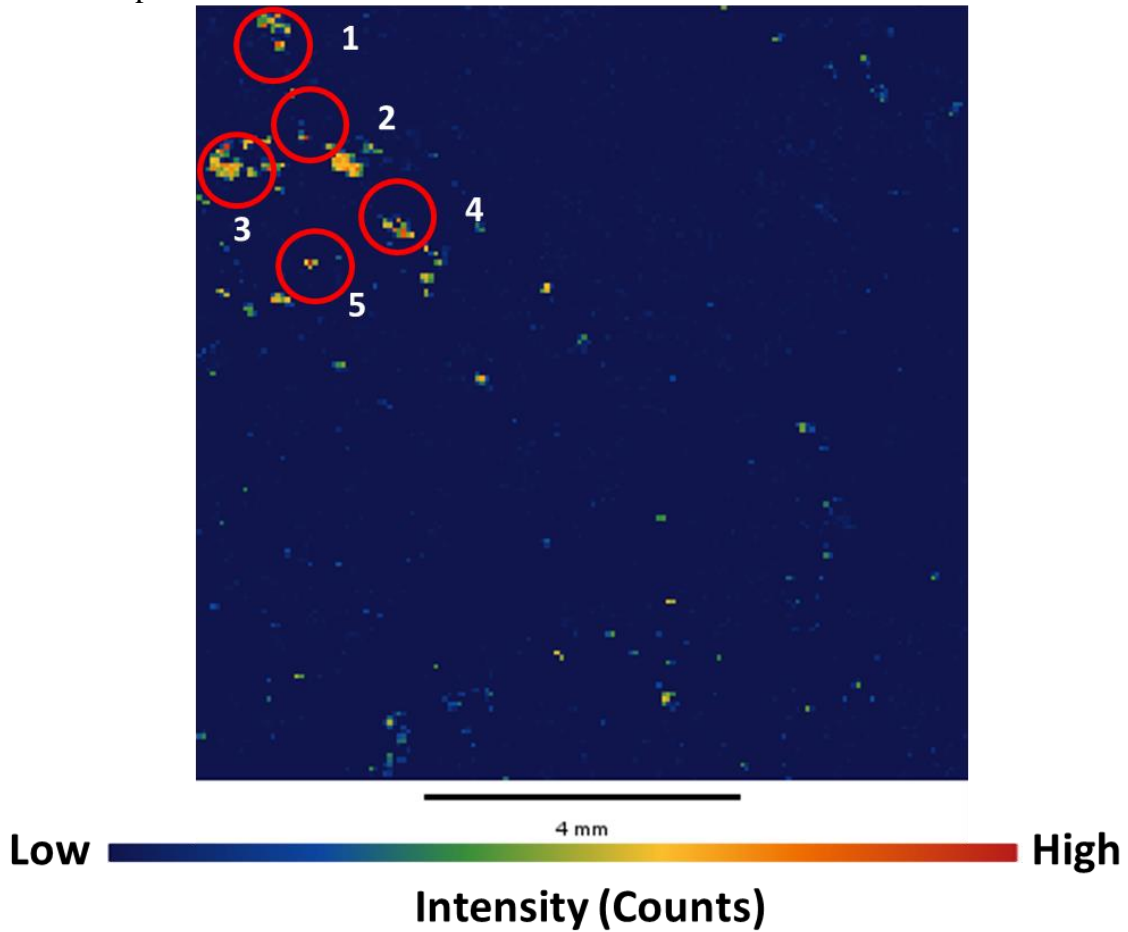


Sample Number	2819 C	Drill Hole	TL-16-575	Depth	154.1-154.32 m
Lithology	QFP	Map Size	1 cm x 1 cm	Gold Grade	7.21 ppm

MCA Spectrum (Full Mapping Area):



SR- μ XRF Au Map:

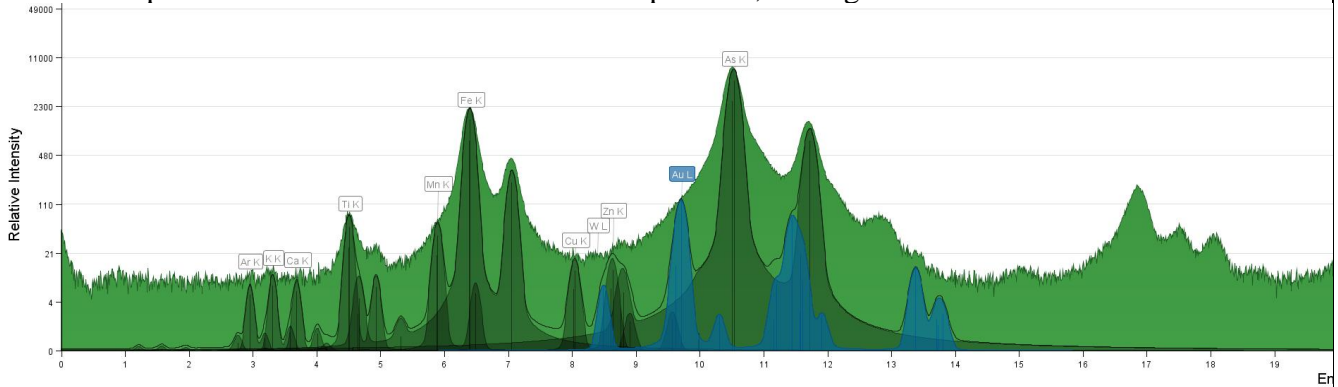


Additional Notes:

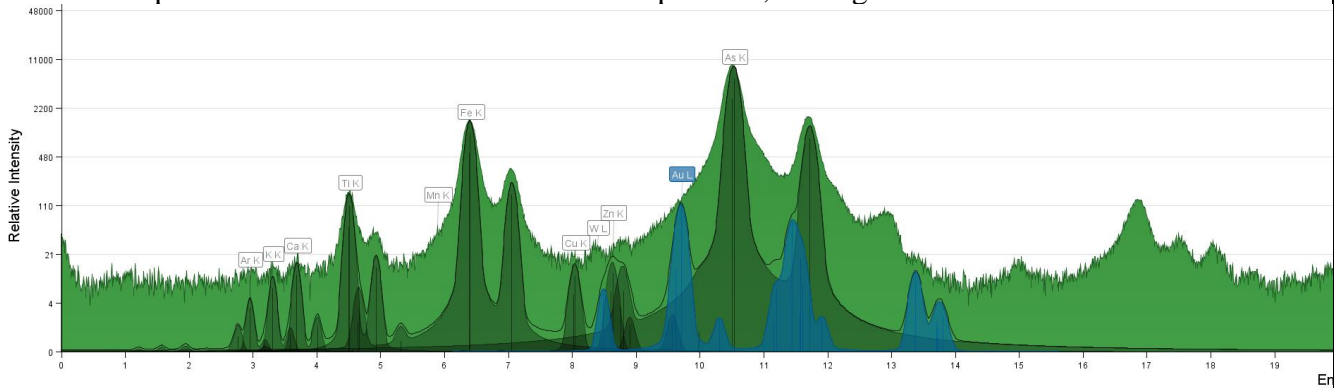
Ar intensity (without filter \rightarrow with filter): 318.3 \rightarrow 140

MCA Spectrum (Au spots):

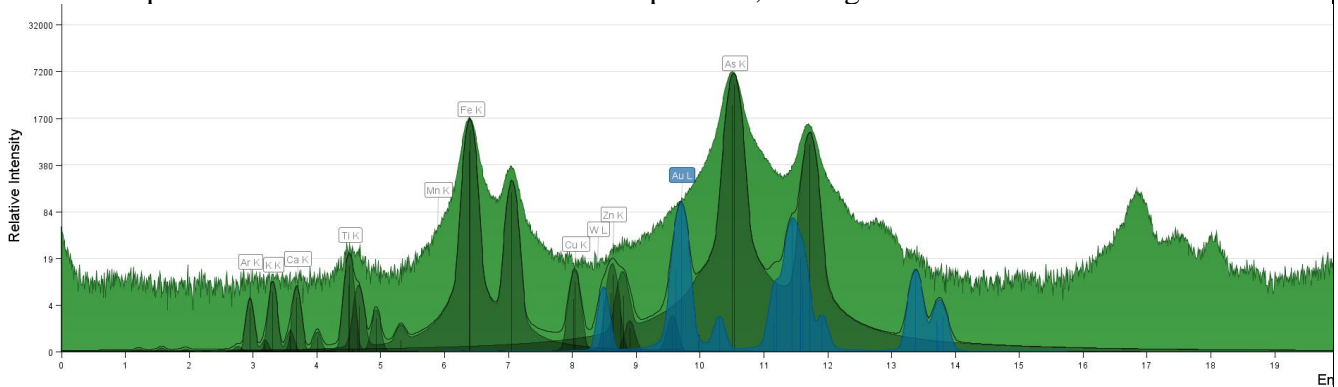
1. Au peak on the As shoulder on the MCA Spectrum, but higher than the shoulder.



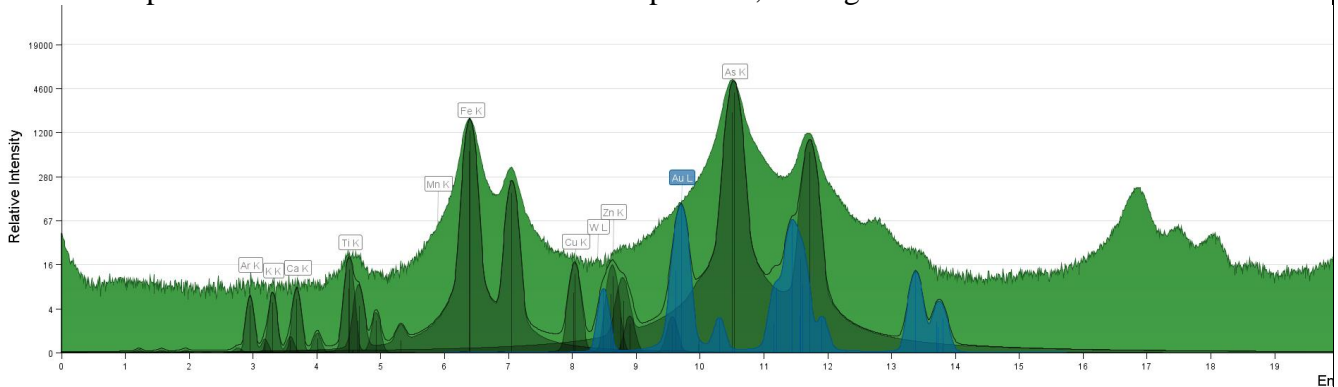
2. Au peak on the As shoulder on the MCA Spectrum, but higher than the shoulder.



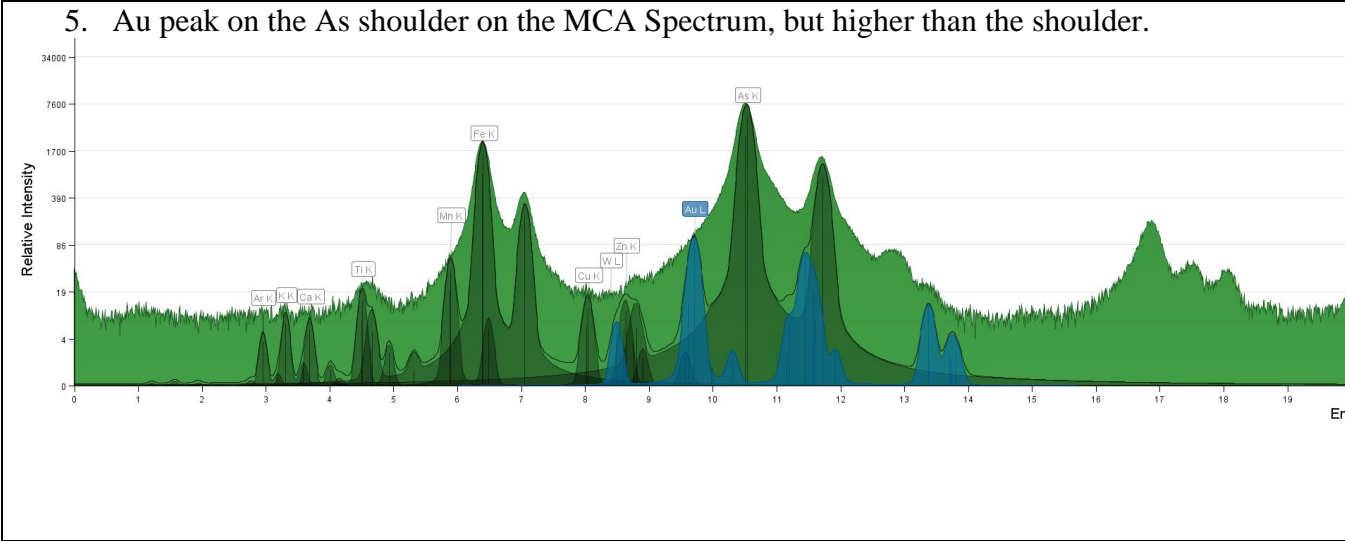
3. Au peak on the As shoulder on the MCA Spectrum, but higher than the shoulder.



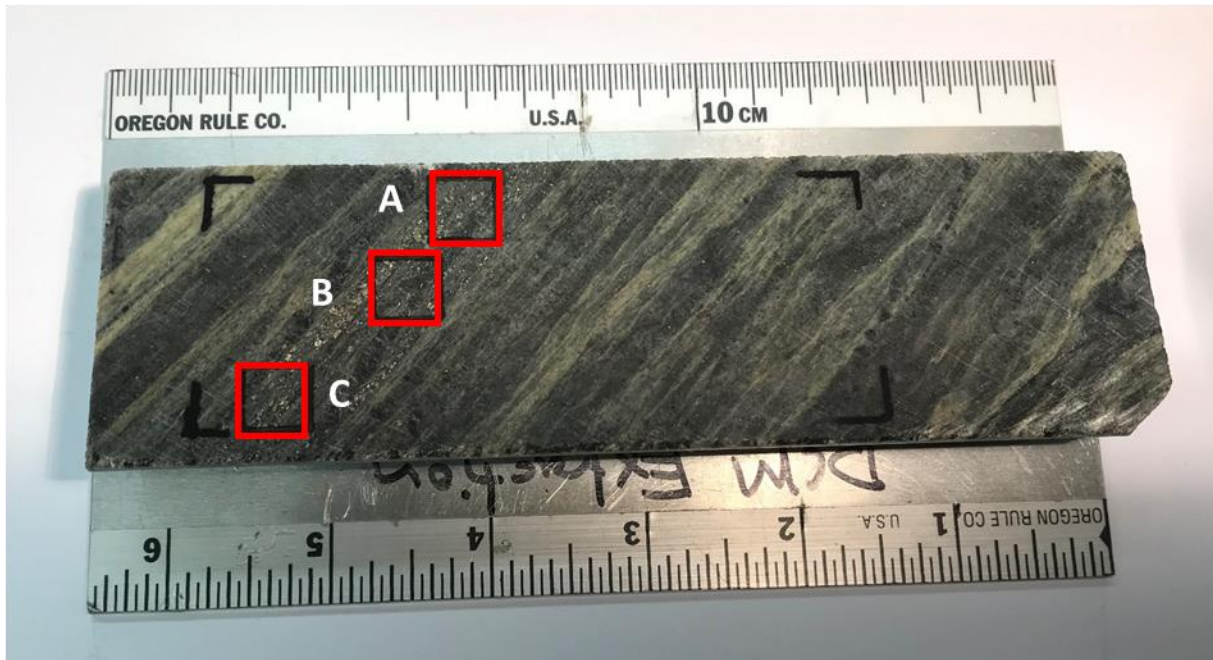
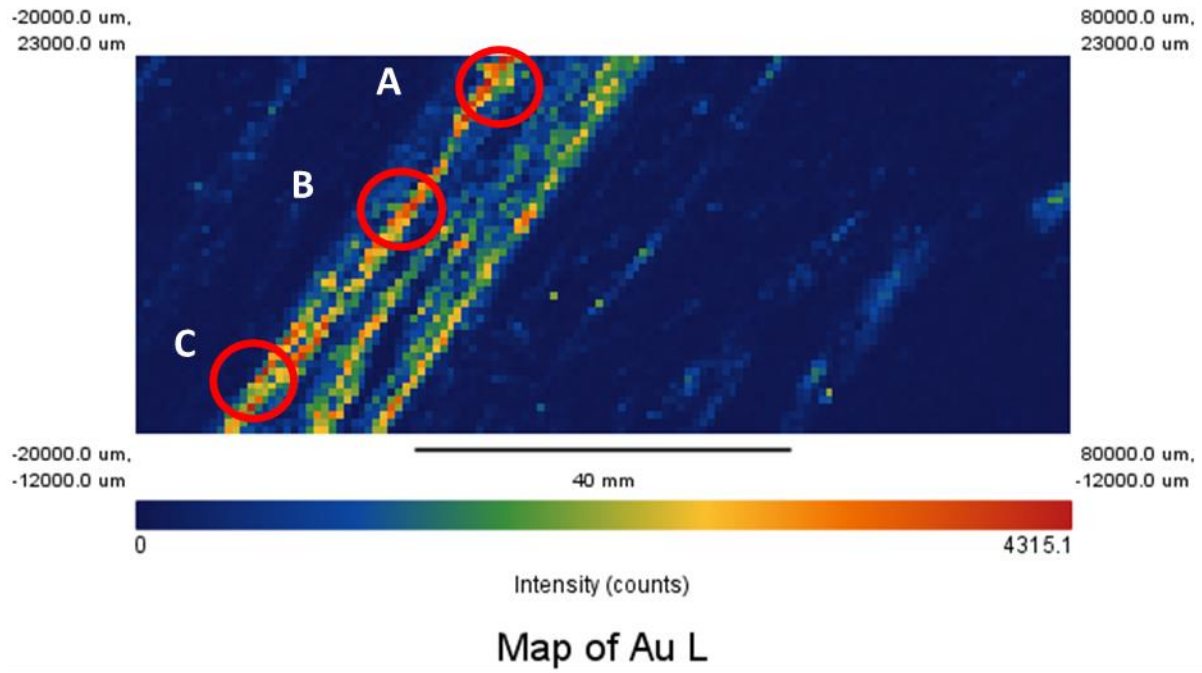
4. Au peak on the As shoulder on the MCA Spectrum, but higher than the shoulder.



5. Au peak on the As shoulder on the MCA Spectrum, but higher than the shoulder.



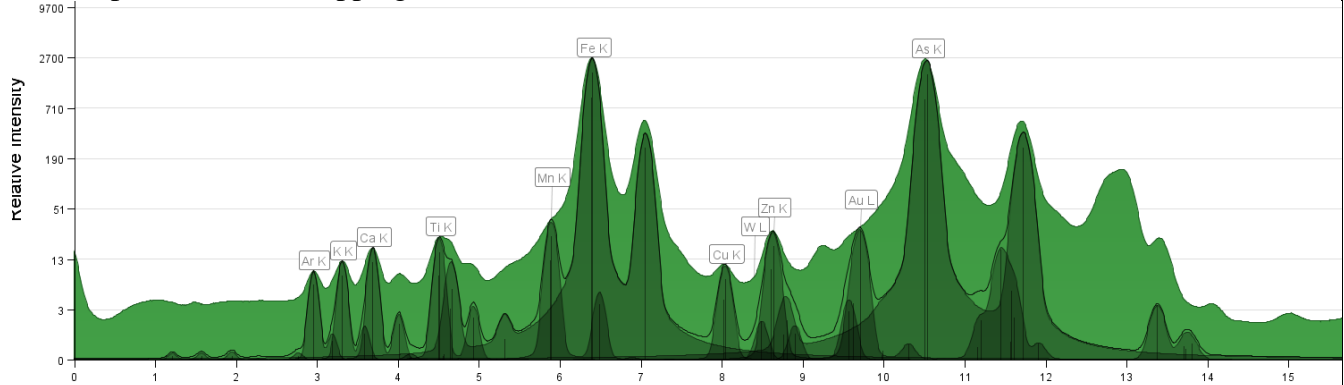
2831:



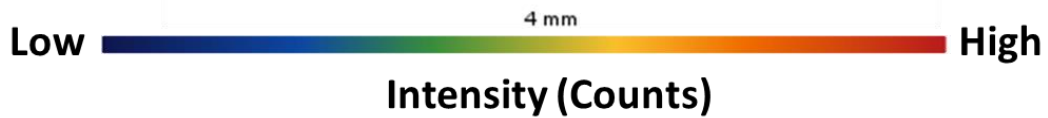
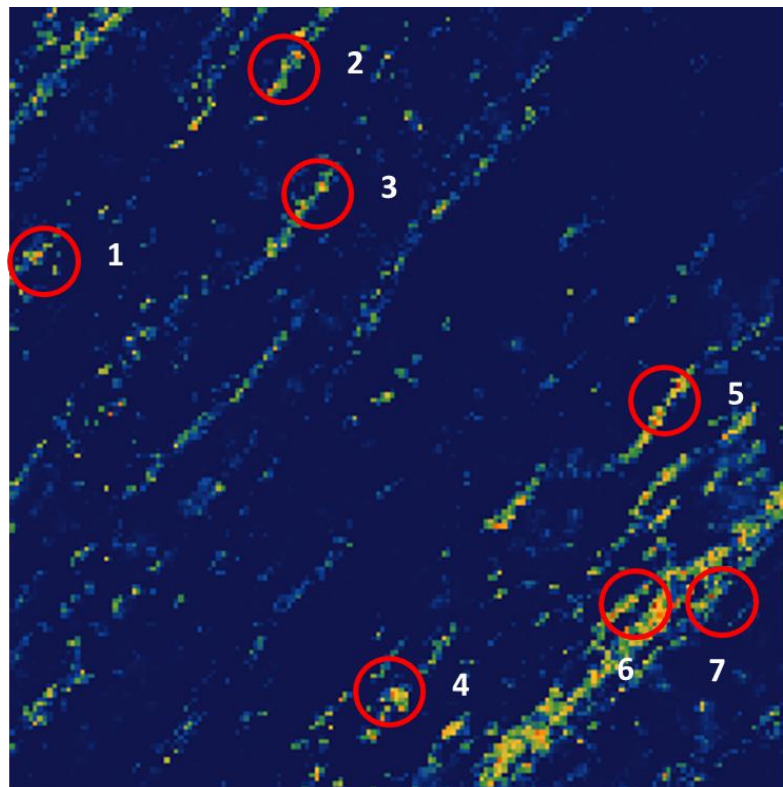
A, B, C: Au peak on the As shoulder on the MCA Spectrum, but higher than the shoulder.

Sample Number	2831 A	Drill Hole	TL-15-551	Depth	96.8-97 m
Lithology	Metasandstone	Map Size	1 cm x 1 cm	Gold Grade	2.26 ppm

MCA Spectrum (Full Mapping Area):



SR- μ XRF Au Map:

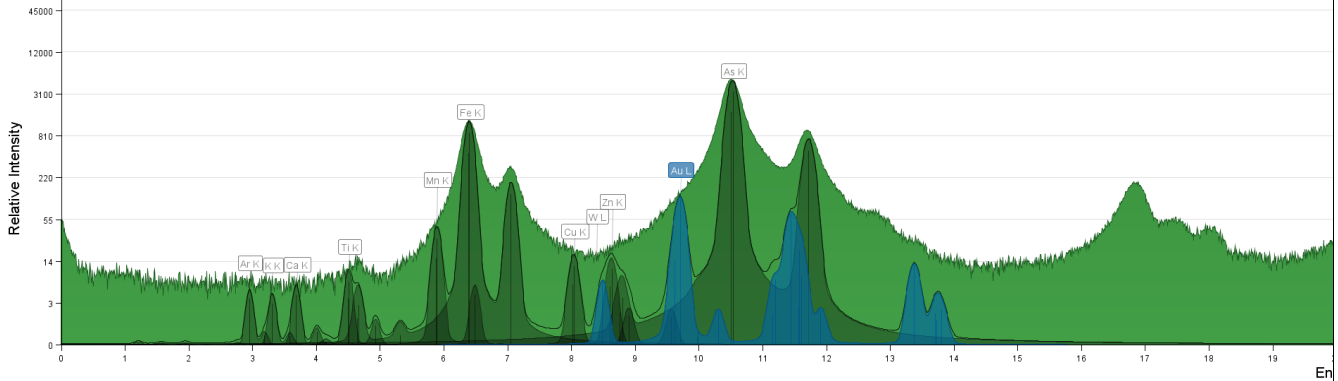


Additional Notes:

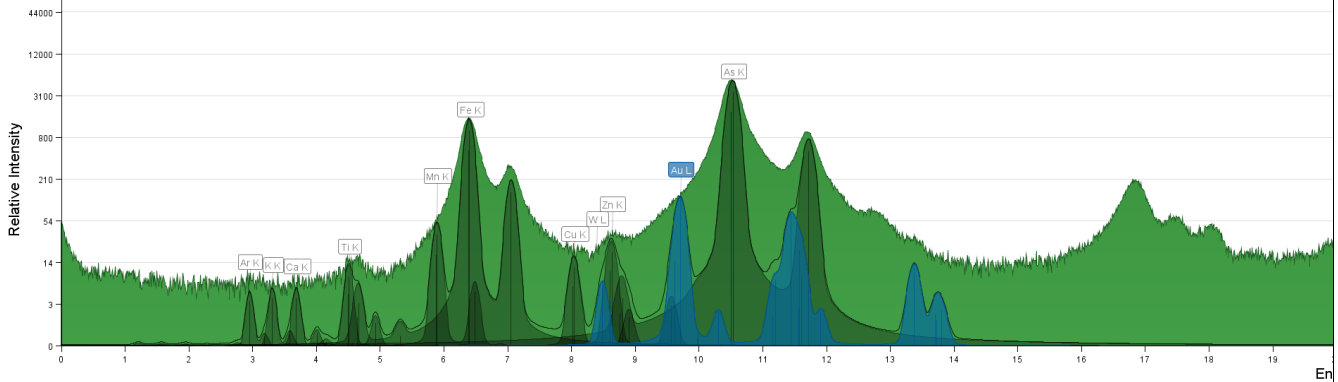
Ar intensity (without filter \rightarrow with filter): 389.8 \rightarrow 139.9

MCA Spectrum (Au spots):

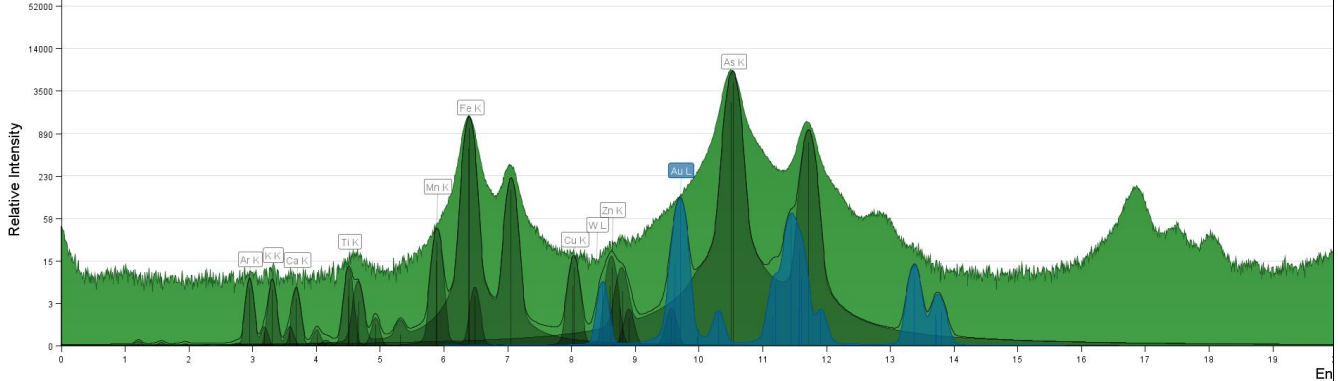
1. Au peak on the As shoulder on the MCA Spectrum, but higher than the shoulder.



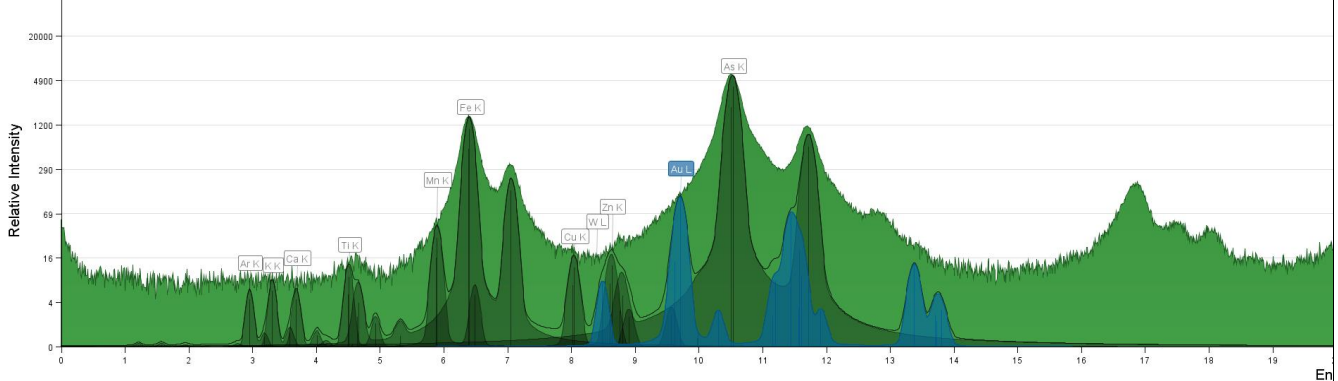
2. Au peak on the As shoulder on the MCA Spectrum, but higher than the shoulder.



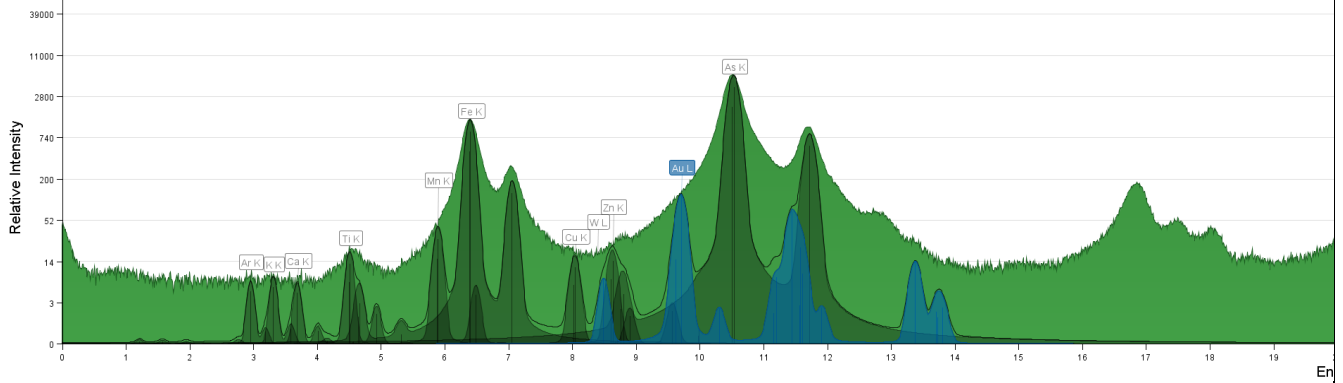
3. Au peak on the As shoulder on the MCA Spectrum, but higher than the shoulder.



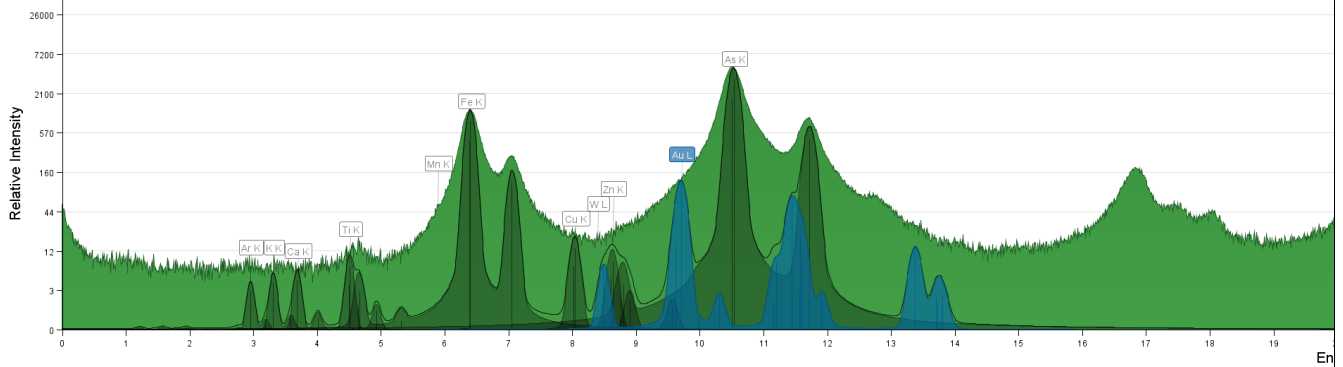
4. Au peak on the As shoulder on the MCA Spectrum, but higher than the shoulder.



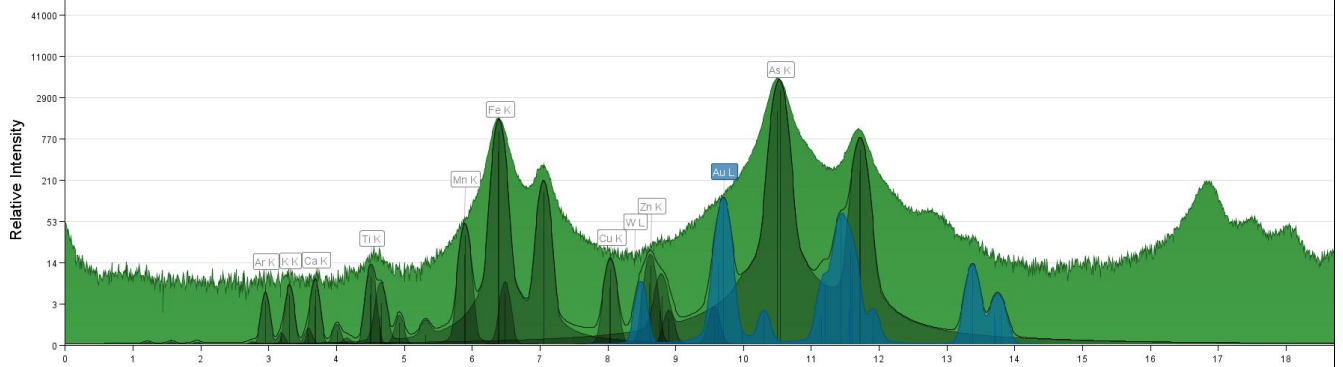
5. Au peak on the As shoulder on the MCA Spectrum, but higher than the shoulder.



6. Au peak on the As shoulder on the MCA Spectrum, but higher than the shoulder.

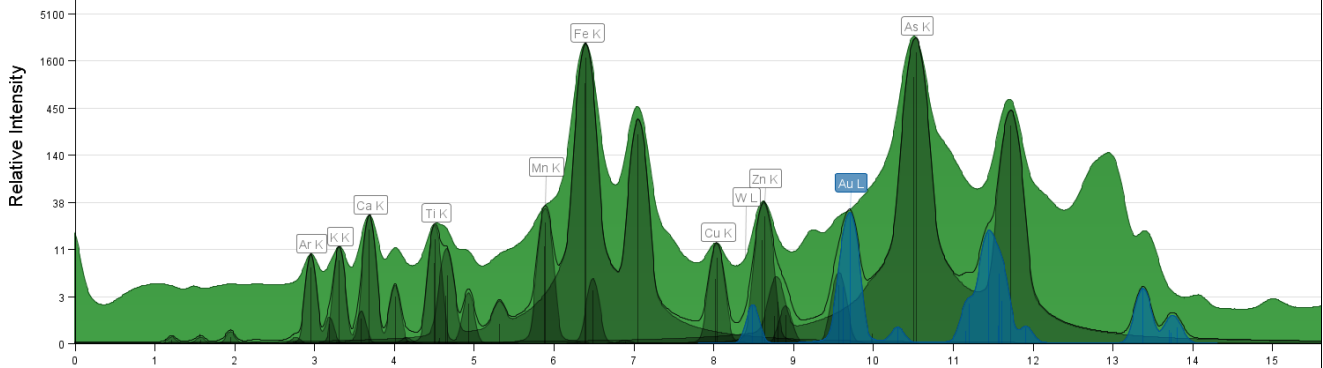


7. Au peak on the As shoulder on the MCA Spectrum, but higher than the shoulder.

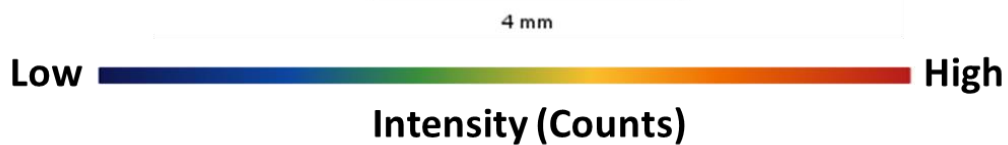
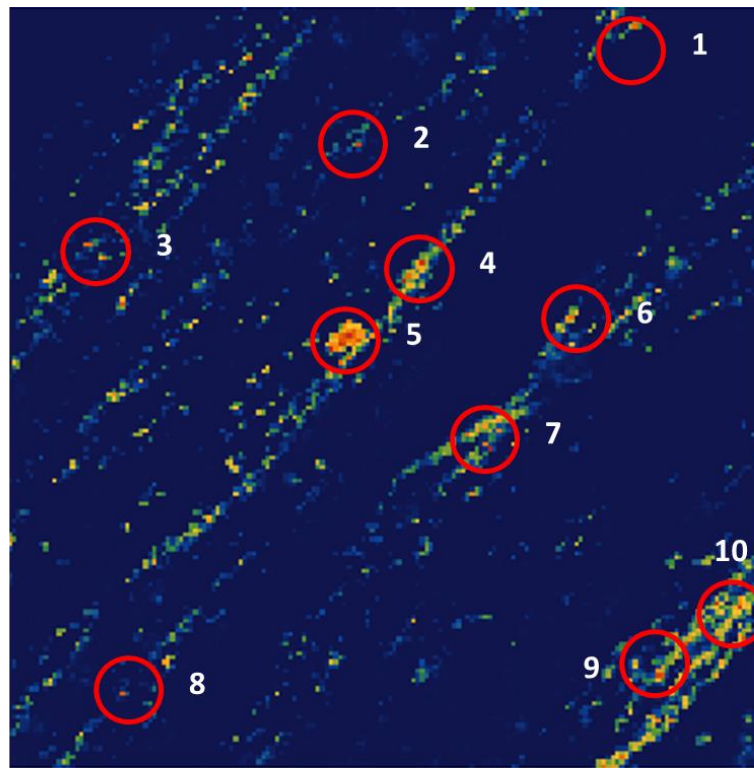


Sample Number	2831 B	Drill Hole	TL-15-551	Depth	96.8-97 m
Lithology	Metasandstone	Map Size	1 cm x 1 cm	Gold Grade	2.26 ppm

MCA Spectrum (Full Mapping Area):



SR- μ XRF Au Map:

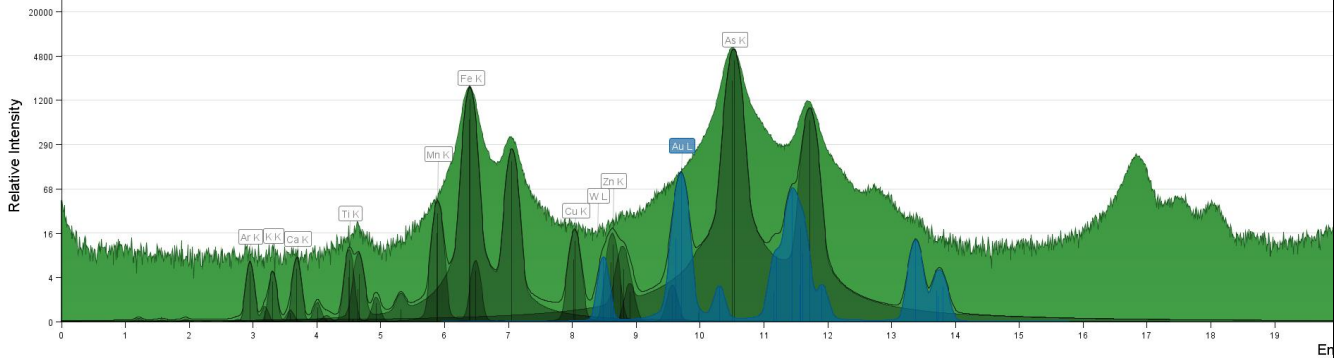


Additional Notes:

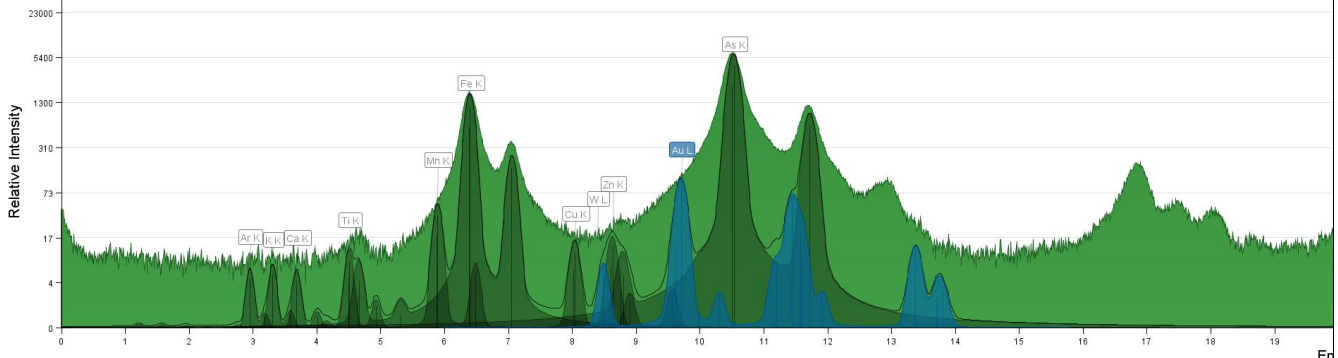
Ar intensity (without filter \rightarrow with filter): 361.9 \rightarrow 140

MCA Spectrum (Au spots):

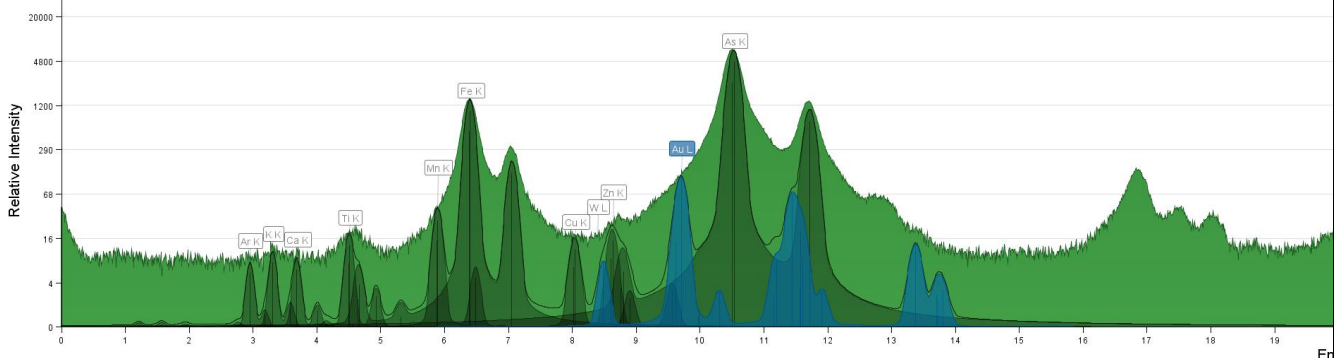
1. Au peak on the As shoulder on the MCA Spectrum, but higher than the shoulder.



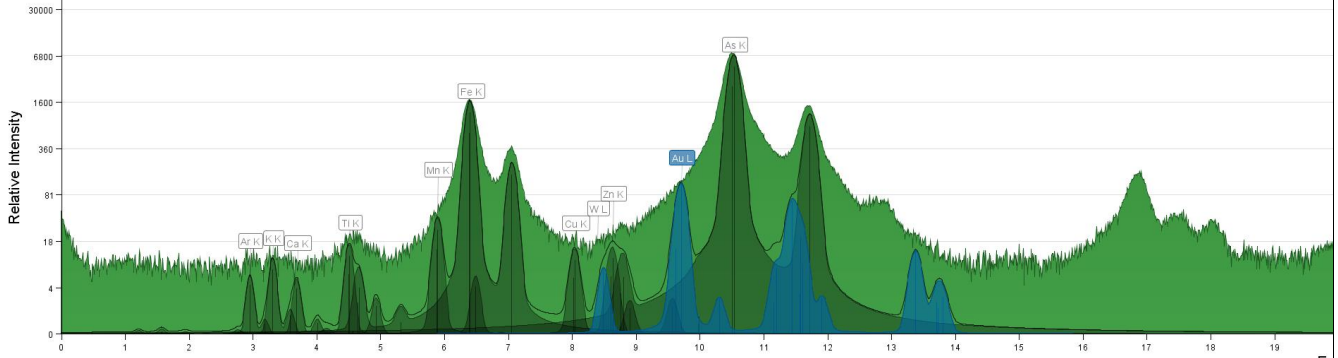
2. Au peak on the As shoulder on the MCA Spectrum, but higher than the shoulder.



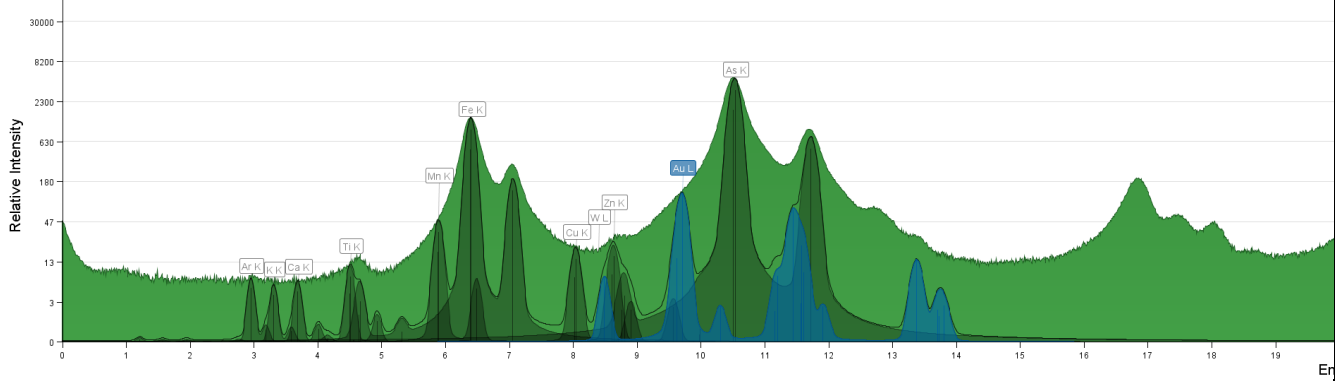
3. Au peak on the As shoulder on the MCA Spectrum, but higher than the shoulder.



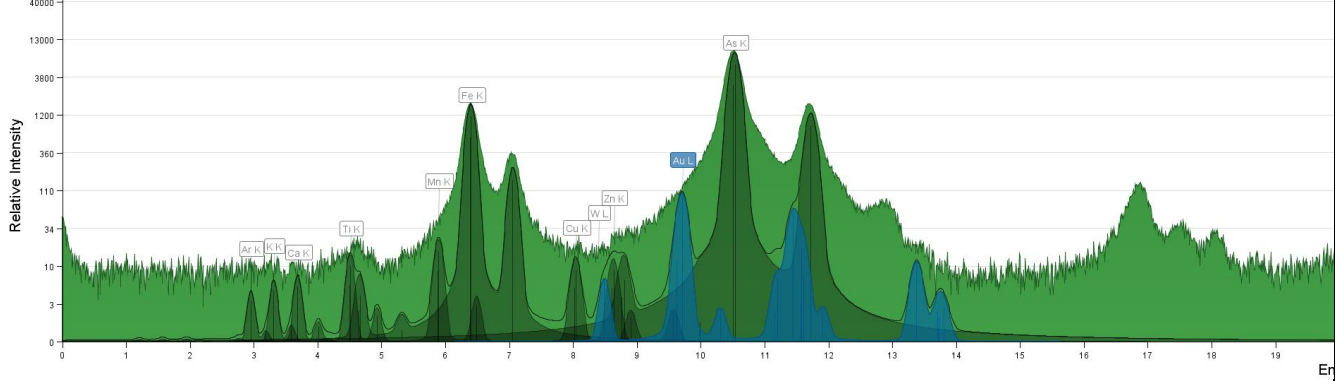
4. Au peak on the As shoulder on the MCA Spectrum, but higher than the shoulder.



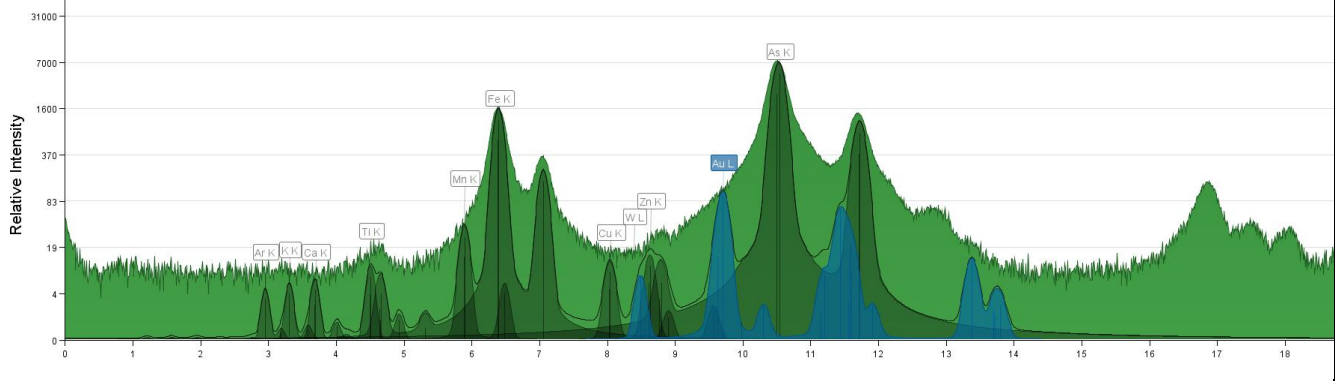
5. Au peak on the As shoulder on the MCA Spectrum, but higher than the shoulder.



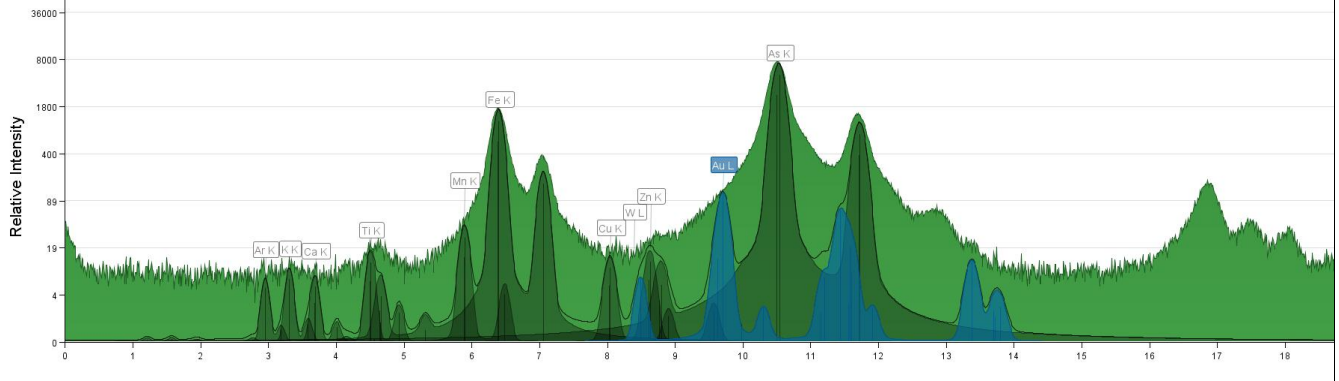
6. Au peak on the As shoulder on the MCA Spectrum, but higher than the shoulder.



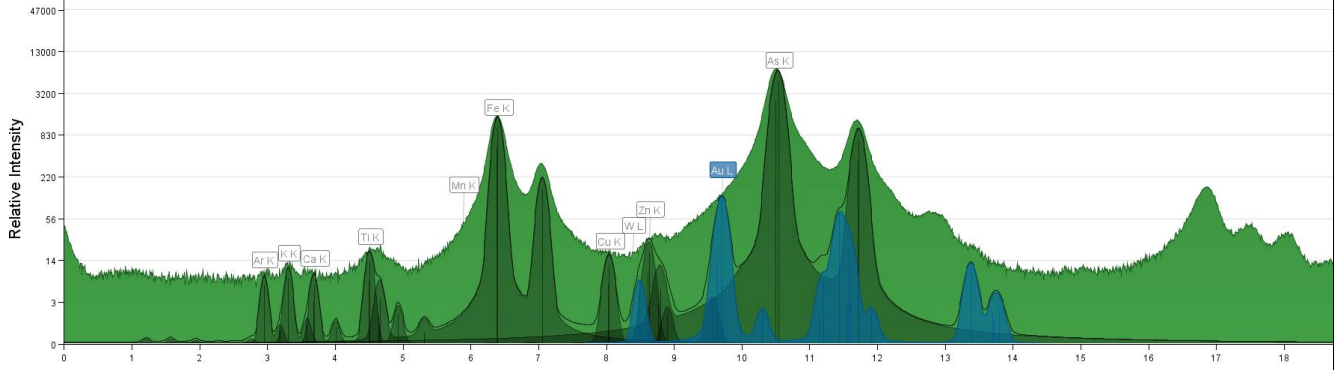
7. Au peak on the As shoulder on the MCA Spectrum, but higher than the shoulder.



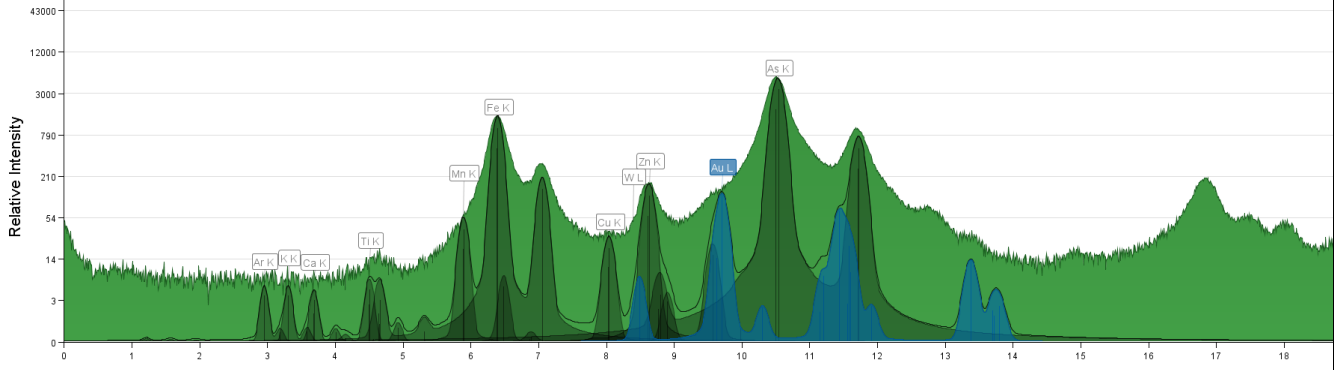
8. Au peak on the As shoulder on the MCA Spectrum, but higher than the shoulder.



9. Au peak on the As shoulder on the MCA Spectrum, but higher than the shoulder.

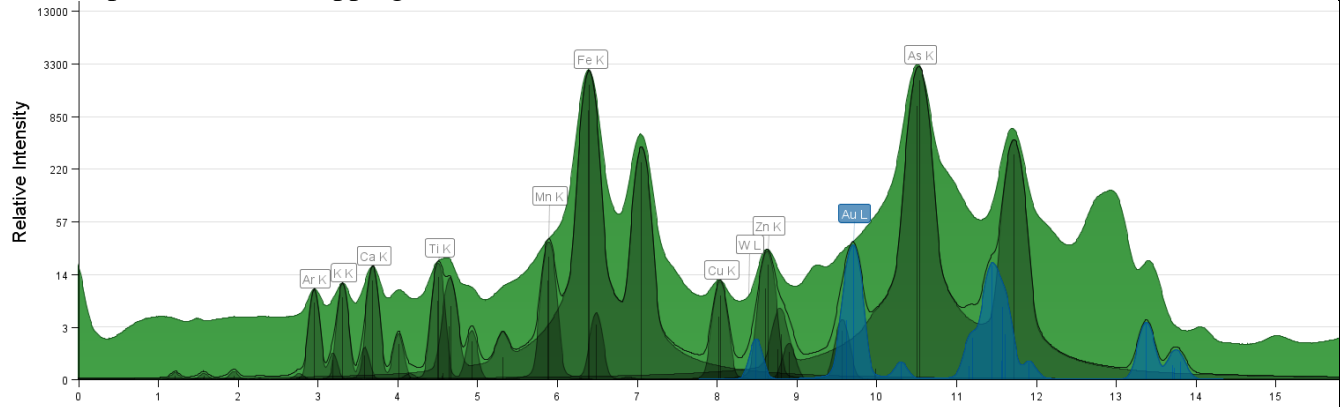


10. Au peak on the As shoulder on the MCA Spectrum, but higher than the shoulder.

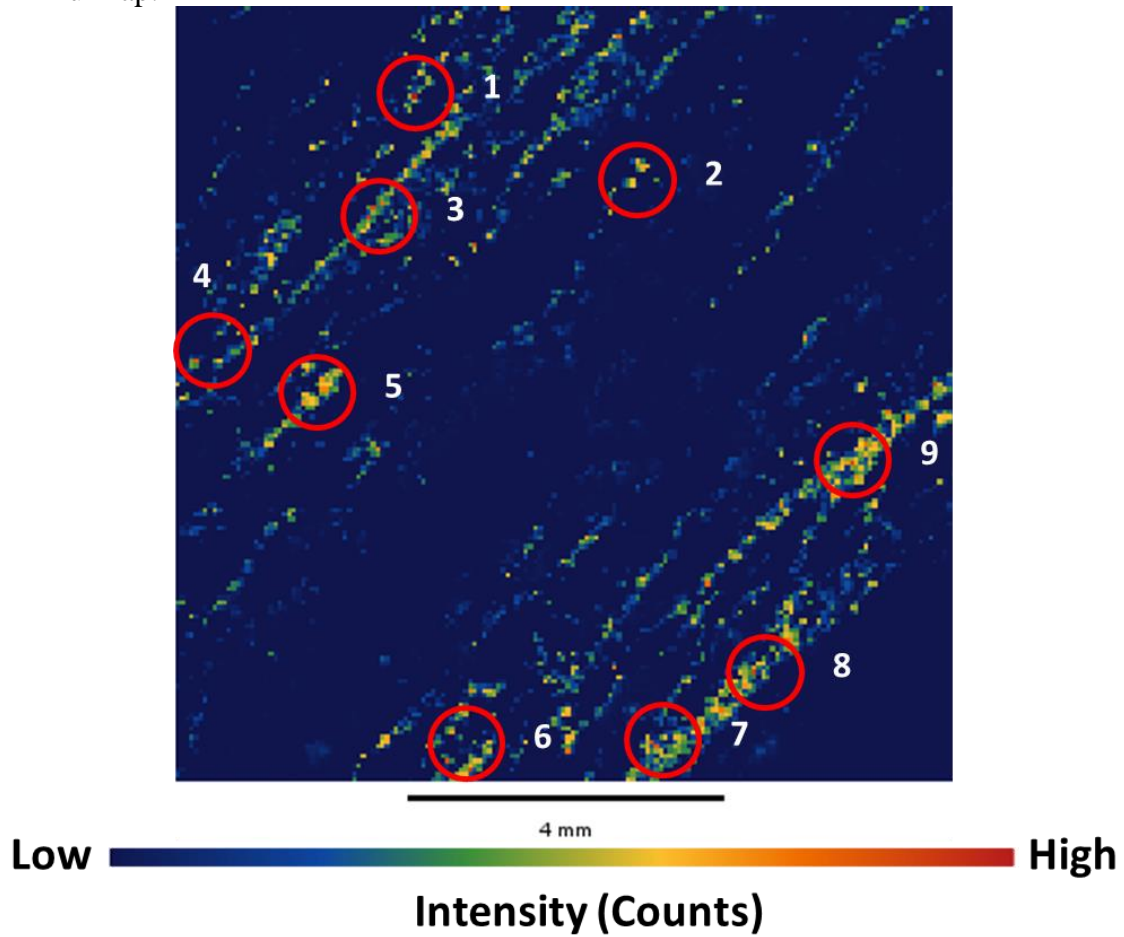


Sample Number	2831 C	Drill Hole	TL-15-551	Depth	96.8-97 m
Lithology	Metasandstone	Map Size	1 cm x 1 cm	Gold Grade	2.26 ppm

MCA Spectrum (Full Mapping Area):



SR- μ XRF Au Map:

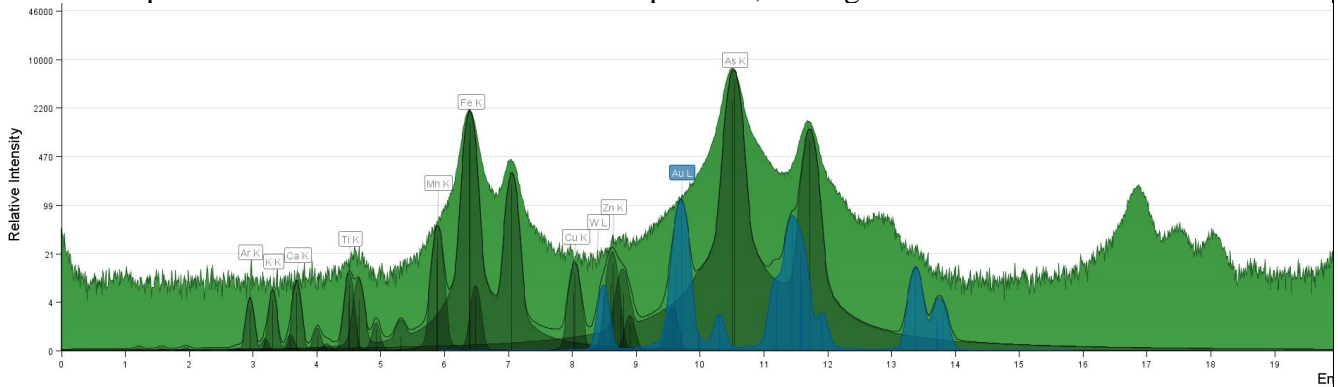


Additional Notes:

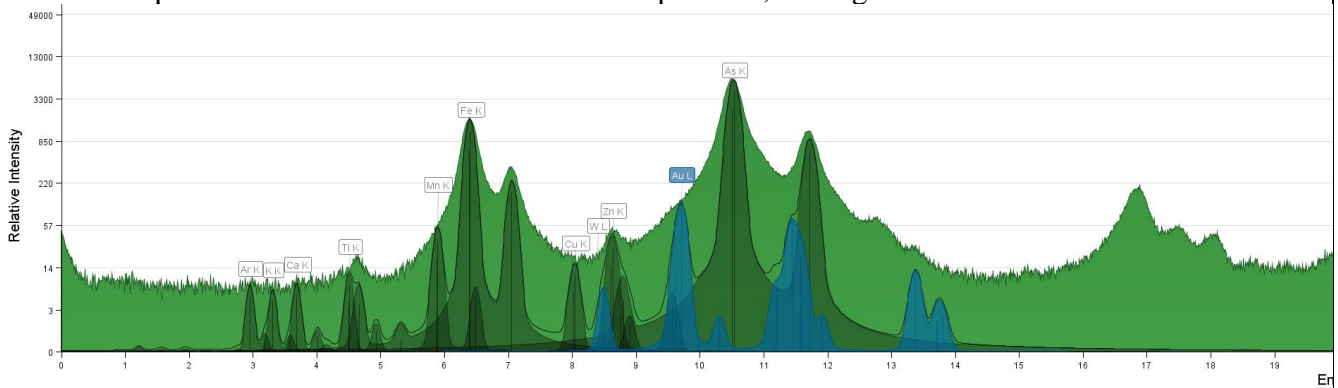
Ar intensity (without filter \rightarrow with filter): 348 \rightarrow 140

MCA Spectrum (Au spots):

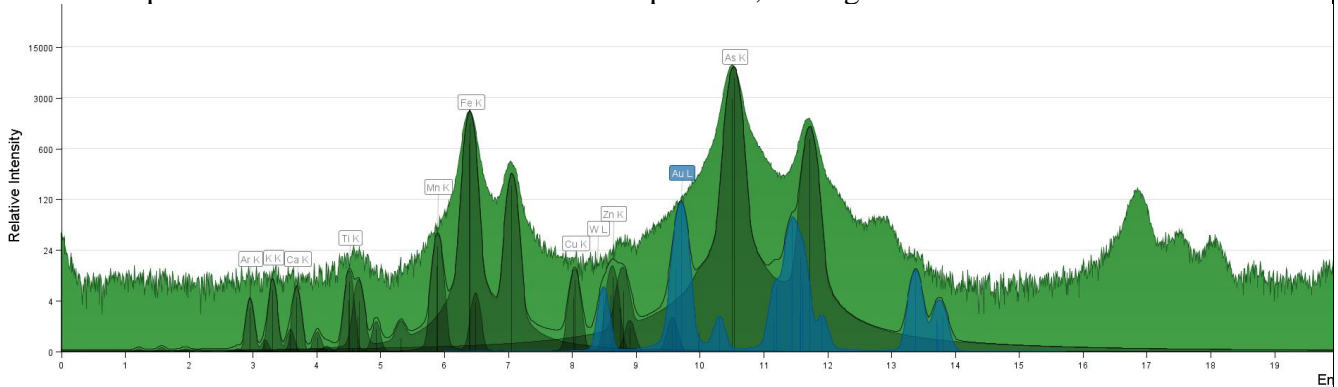
1. Au peak on the As shoulder on the MCA Spectrum, but higher than the shoulder.



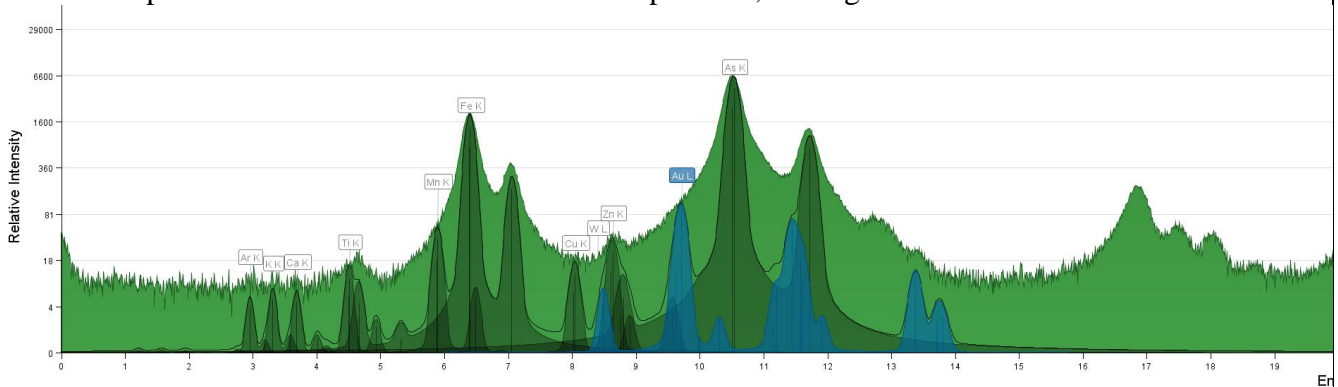
2. Au peak on the As shoulder on the MCA Spectrum, but higher than the shoulder.



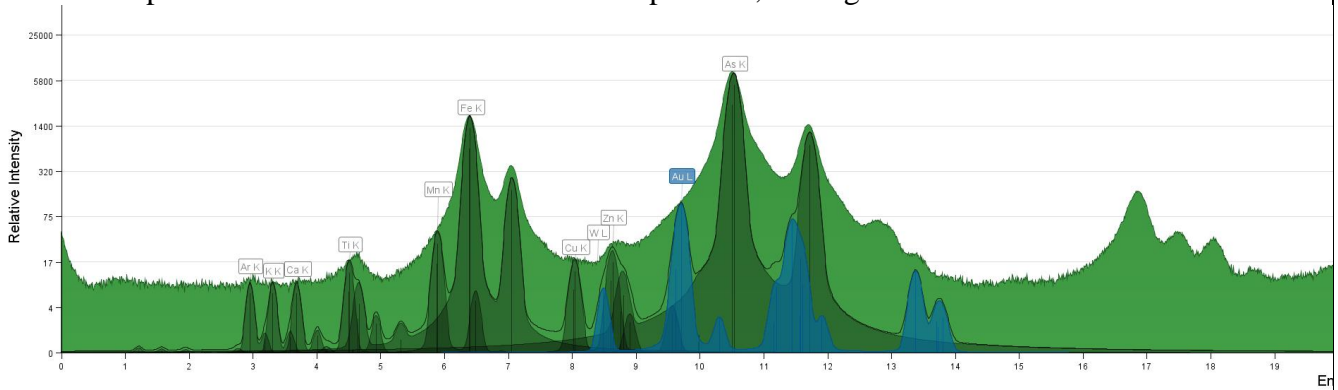
3. Au peak on the As shoulder on the MCA Spectrum, but higher than the shoulder.



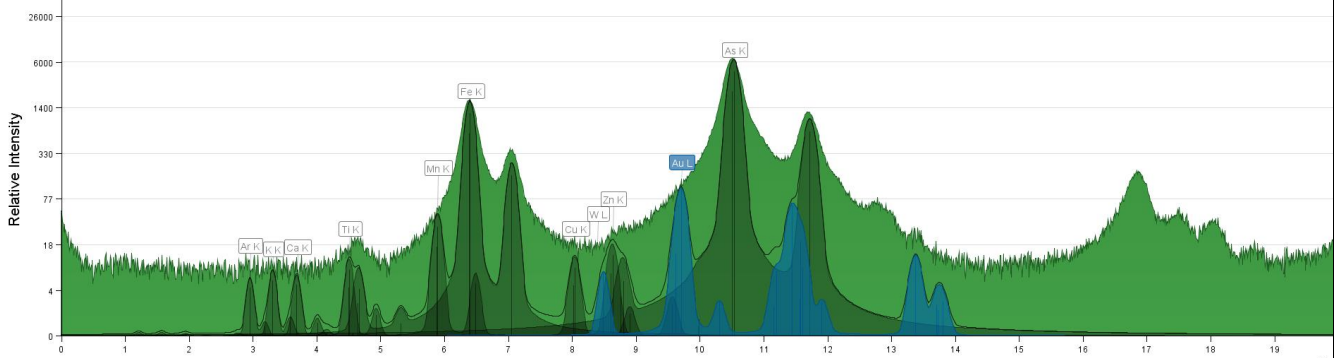
4. Au peak on the As shoulder on the MCA Spectrum, but higher than the shoulder.



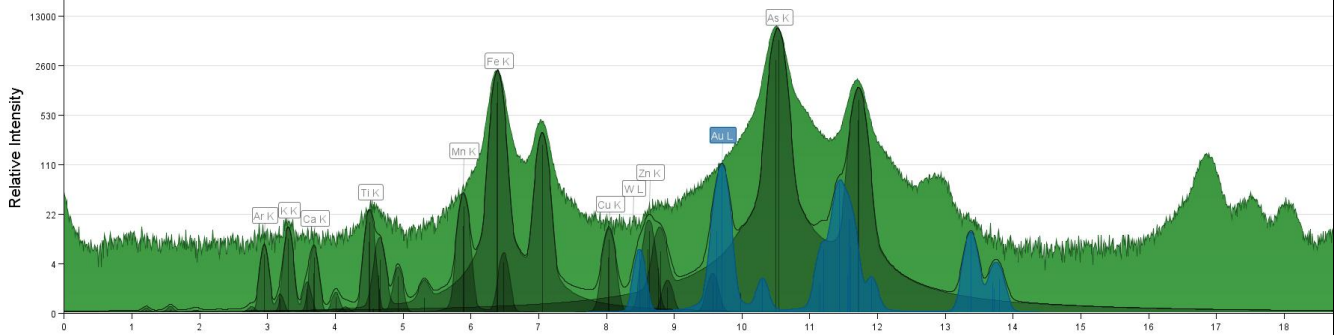
5. Au peak on the As shoulder on the MCA Spectrum, but higher than the shoulder.



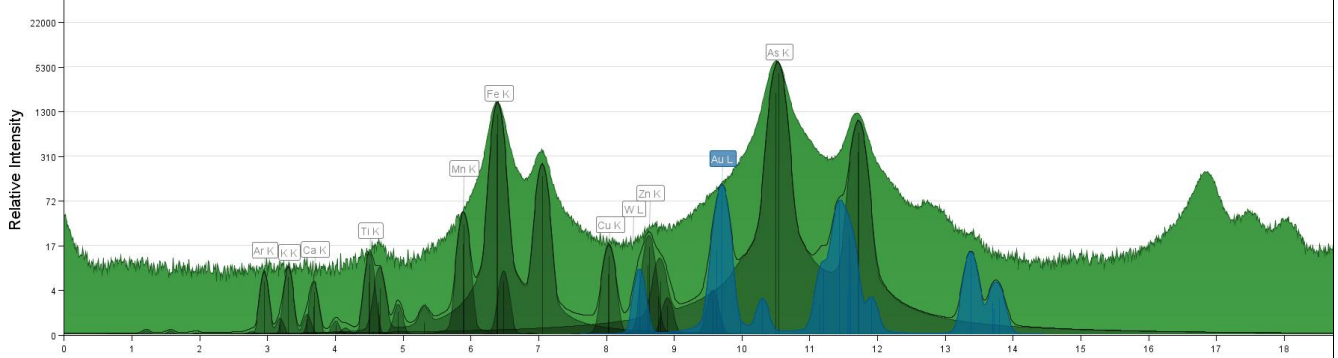
6. Au peak on the As shoulder on the MCA Spectrum, but higher than the shoulder.



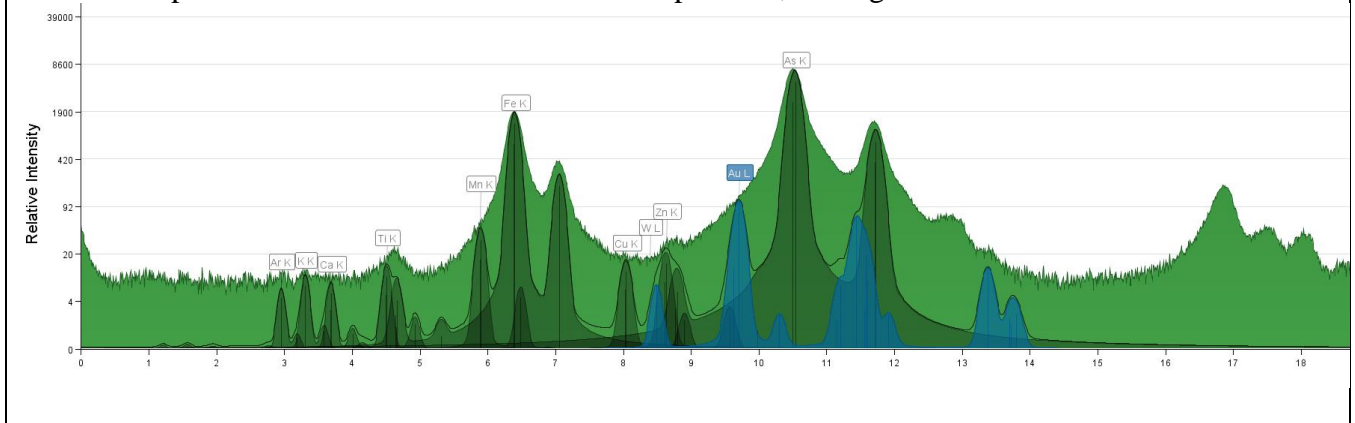
7. Au peak on the As shoulder on the MCA Spectrum, but higher than the shoulder.



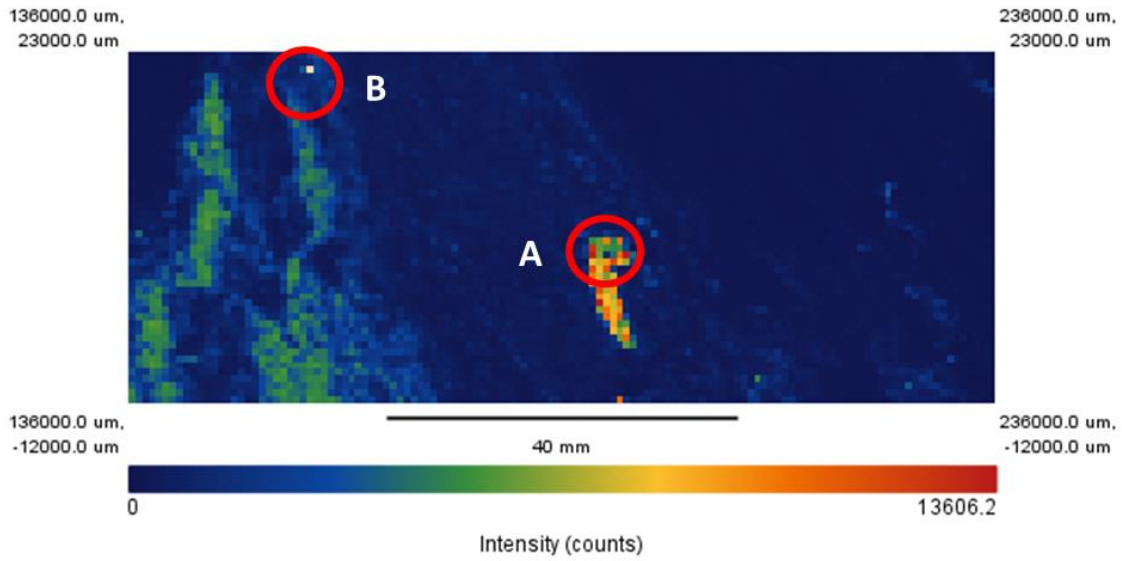
8. Au peak on the As shoulder on the MCA Spectrum, but higher than the shoulder.



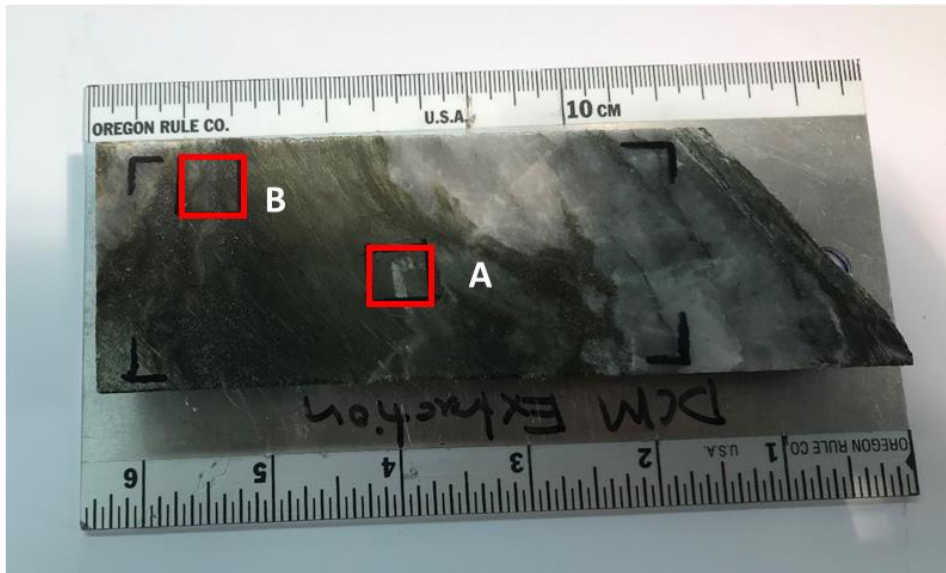
9. Au peak on the As shoulder on the MCA Spectrum, but higher than the shoulder.



2854:



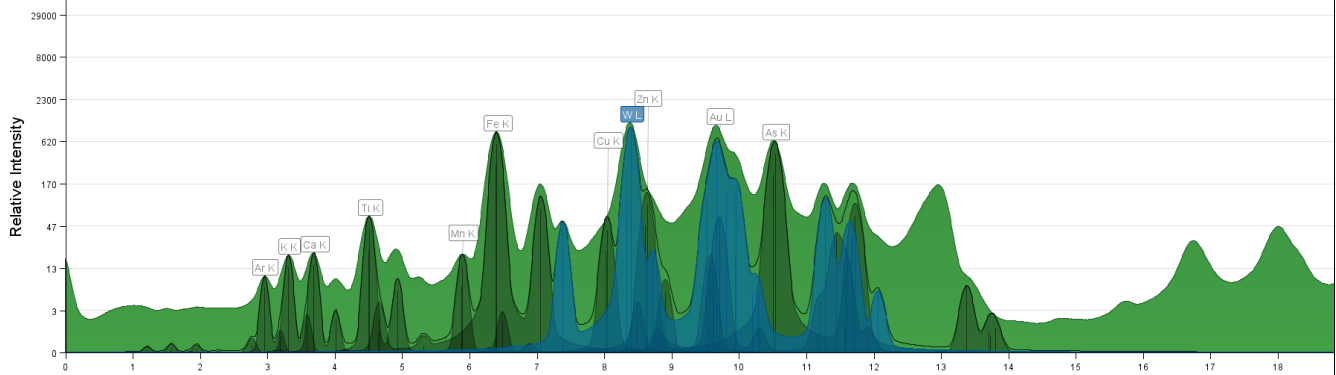
Map of Au L



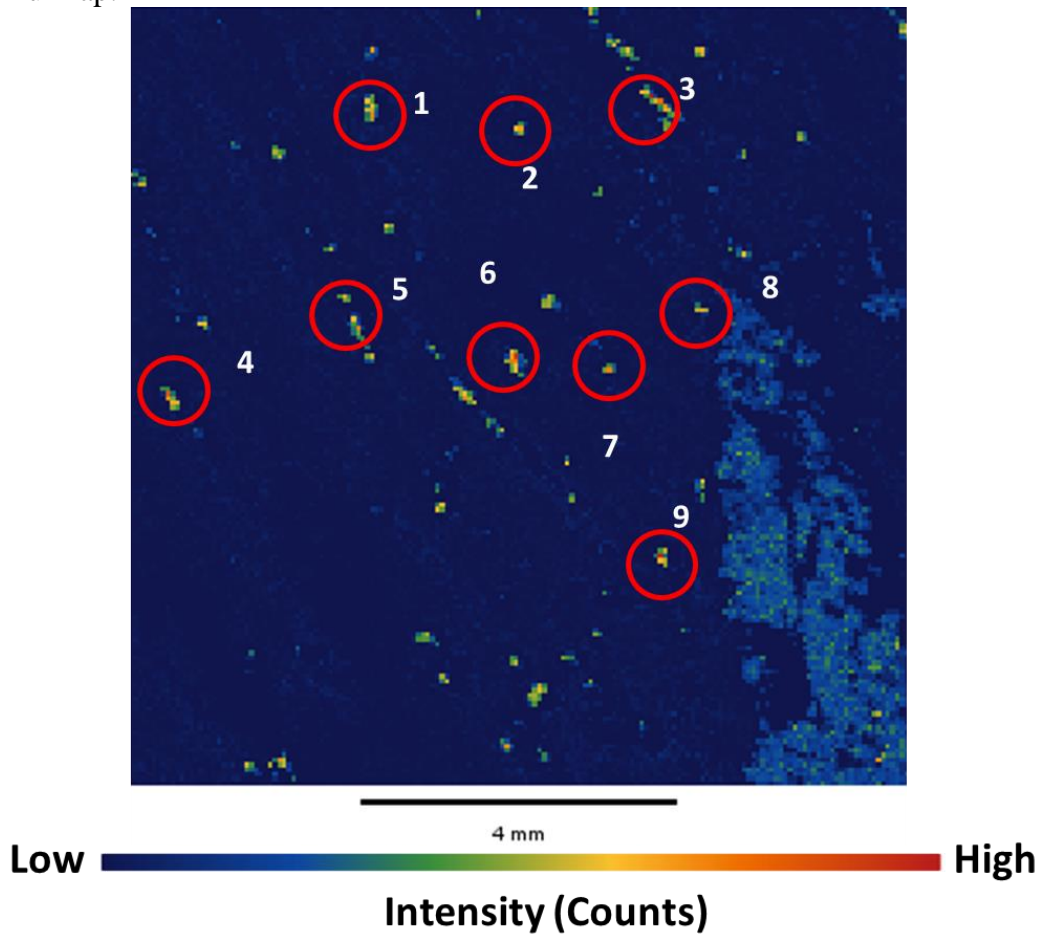
A&B: real Au peak which is much higher than As shoulder.

Sample Number	2854 A	Drill Hole	TL-16-604A	Depth	729.02-729.2m
Lithology	Metavolcanic Tuff	Map Size	1 cm x 1 cm	Gold Grade	10.49 ppm

MCA Spectrum (Full Mapping Area):



SR- μ XRF Au Map:



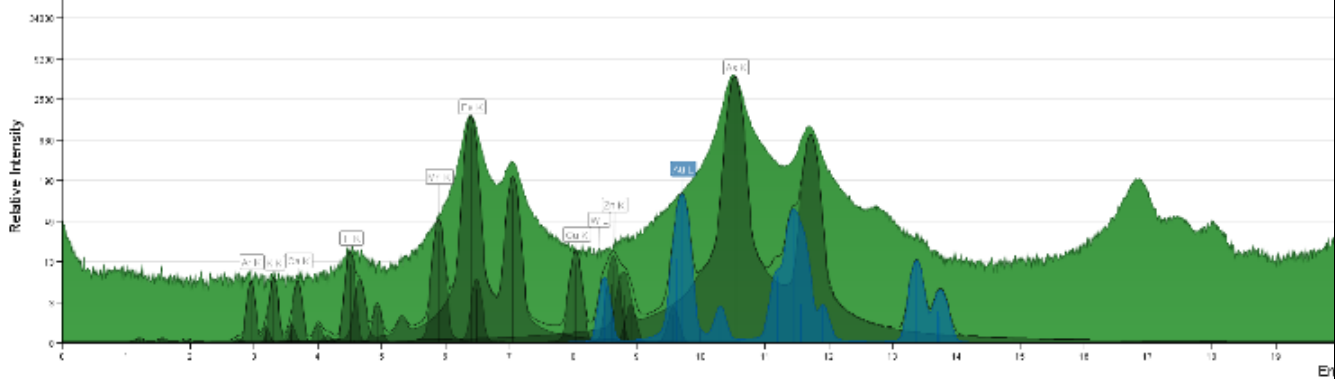
Additional Notes:

Ar intensity (without filter \rightarrow with filter): 399.4 \rightarrow 140

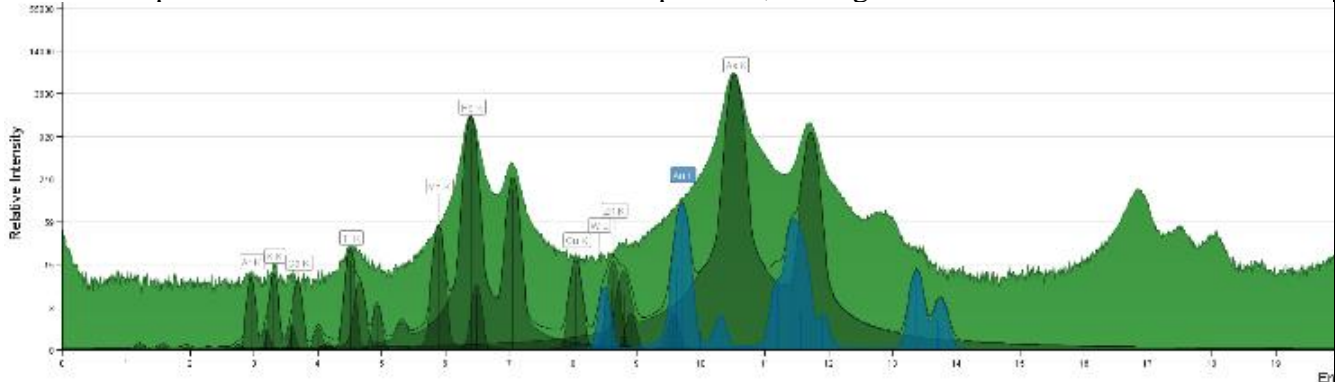
W peak is higher than Au peak and As peak. But W map and Au map are totally different

MCA Spectrum (Au spots):

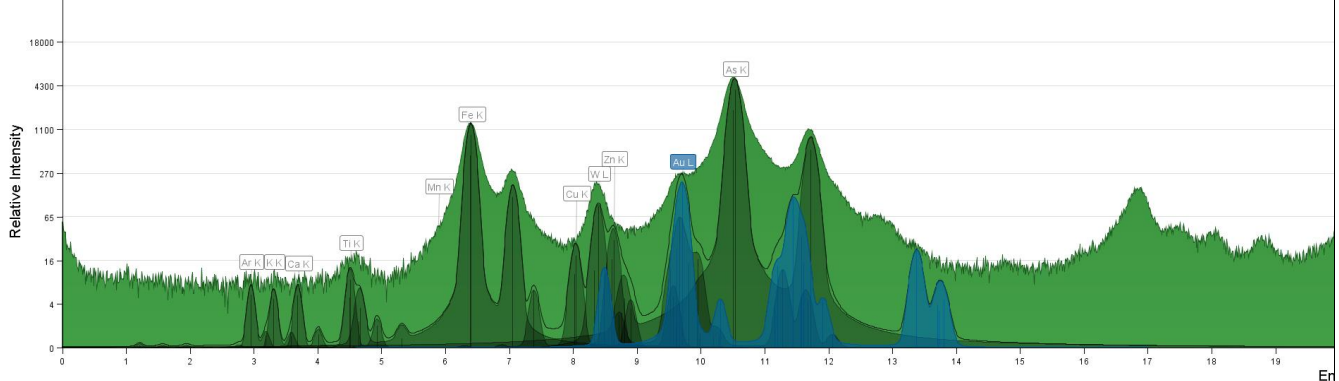
1. Au peak on the As shoulder on the MCA Spectrum, but higher than the shoulder.



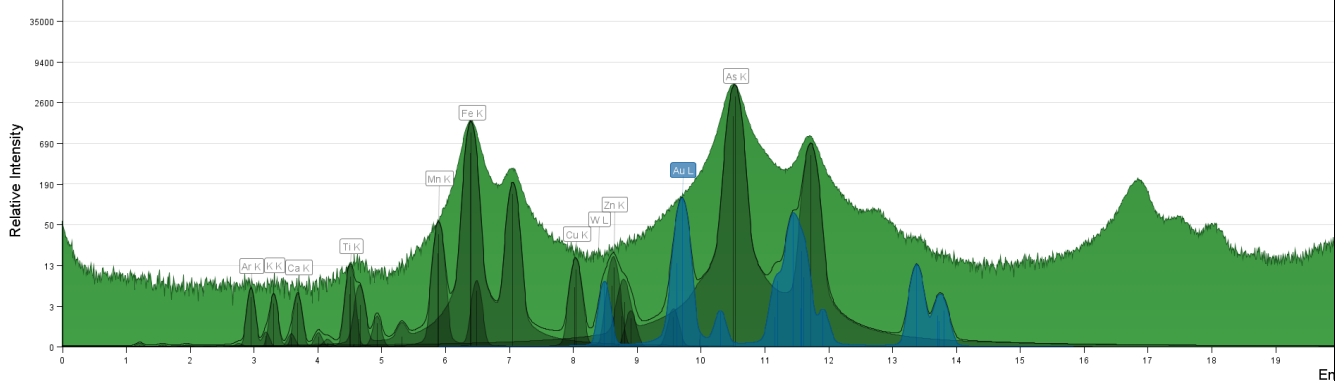
2. Au peak on the As shoulder on the MCA Spectrum, but higher than the shoulder.



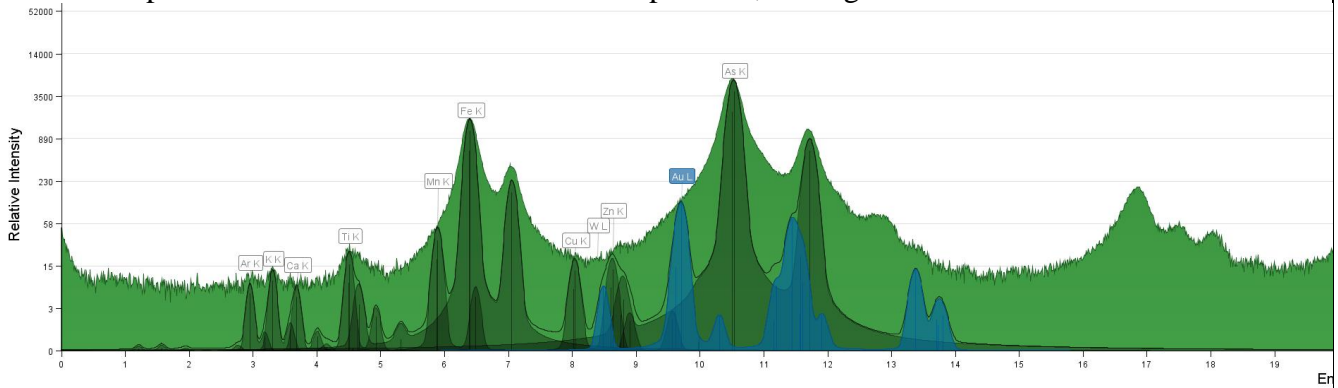
3. Au peak and W peak are overlapped, but Au peak is much higher than As shoulder and W peak.



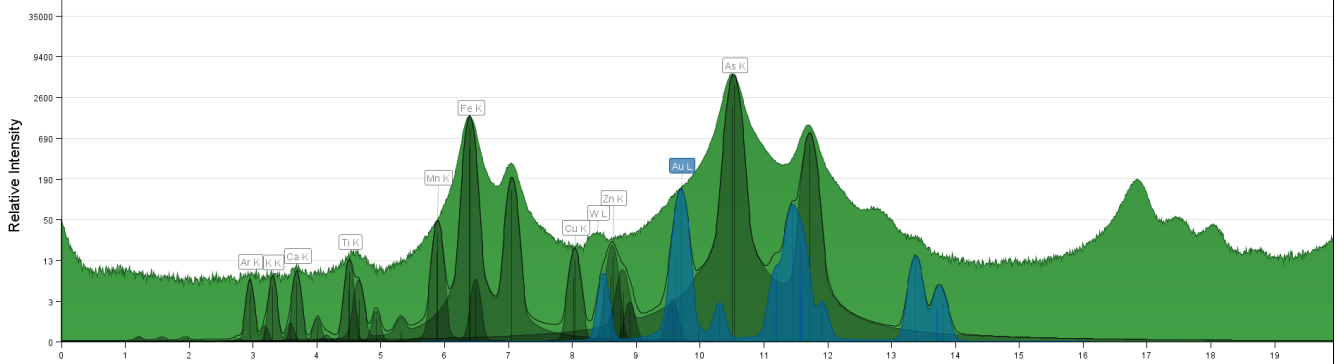
4. Au peak on the As shoulder on the MCA Spectrum, but higher than the shoulder.



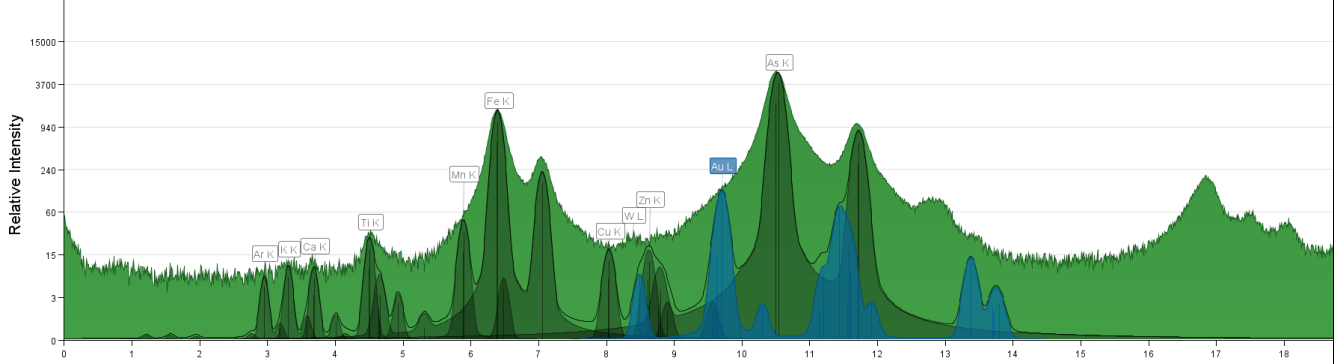
5. Au peak on the As shoulder on the MCA Spectrum, but higher than the shoulder.



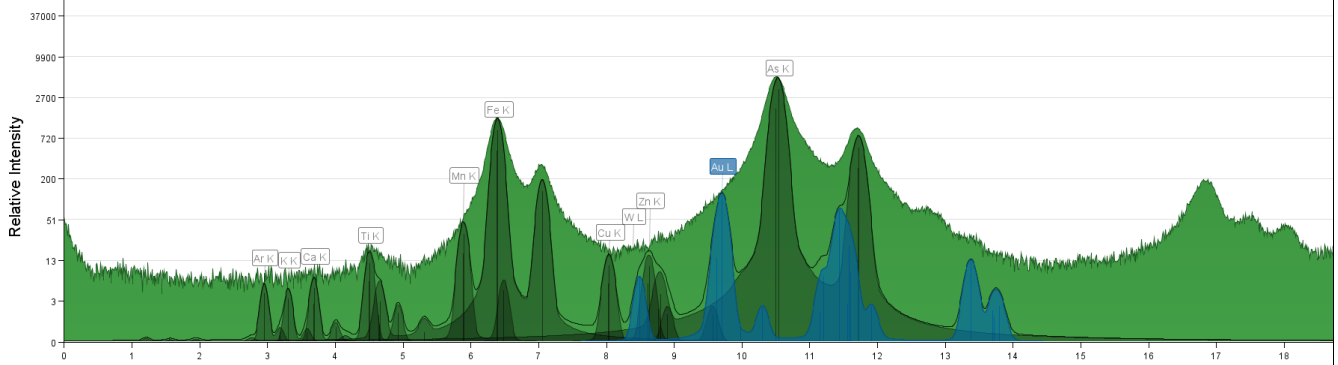
6. Au peak on the As shoulder on the MCA Spectrum, but higher than the shoulder.



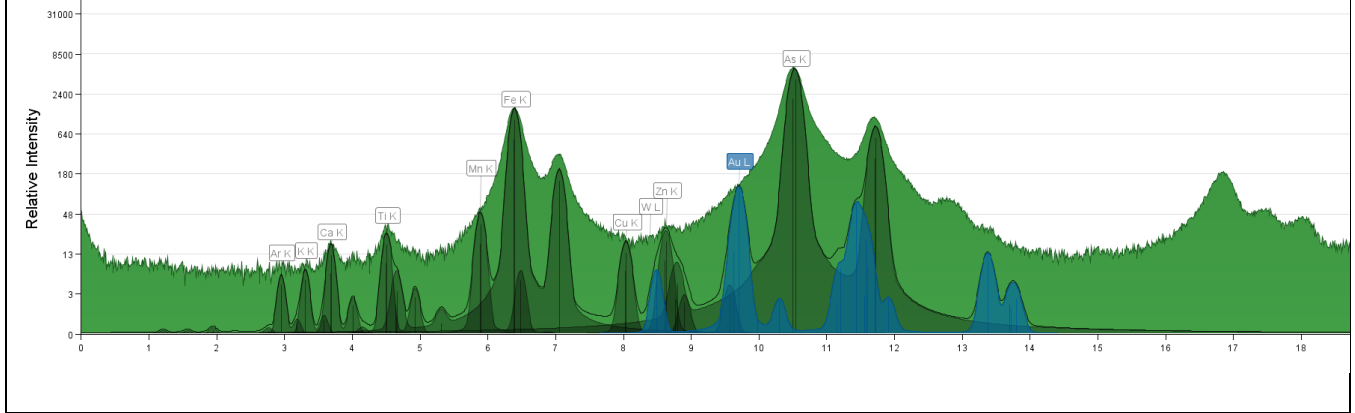
7. Au peak on the As shoulder on the MCA Spectrum, but higher than the shoulder.



8. Au peak on the As shoulder on the MCA Spectrum, but higher than the shoulder.

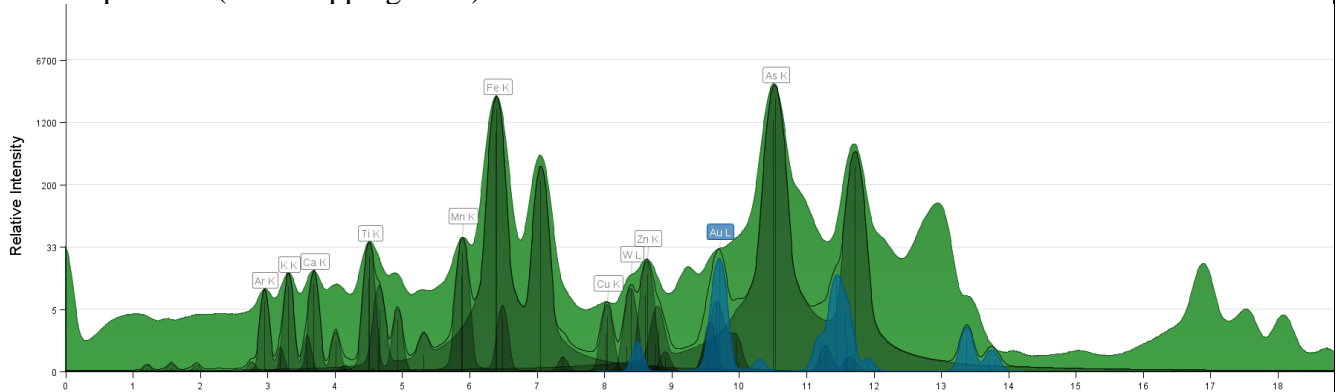


9. Au peak on the As shoulder on the MCA Spectrum, but higher than the shoulder.

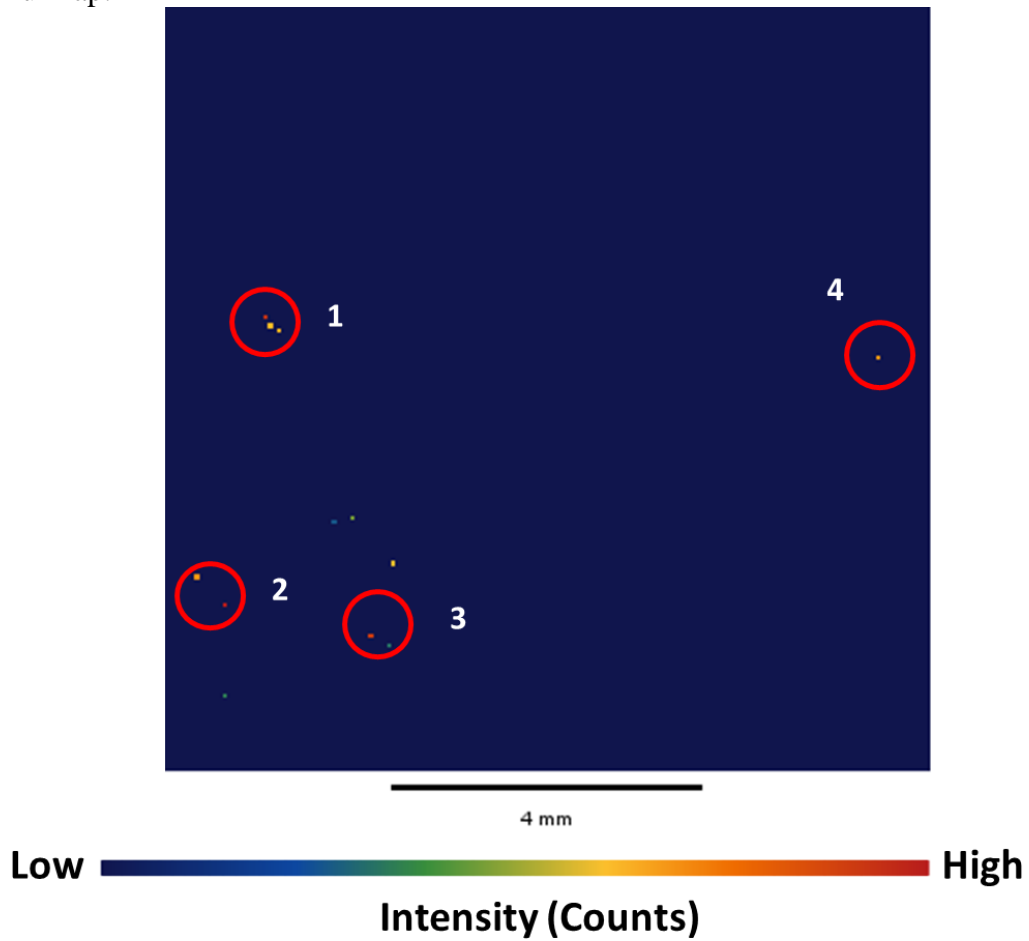


Sample Number	2854 B	Drill Hole	TL-16-604A	Depth	729.02-729.2m
Lithology	Metavolcanic Tuff	Map Size	1 cm x 1 cm	Gold Grade	10.49 ppm

MCA Spectrum (Full Mapping Area):



SR- μ XRF Au Map:

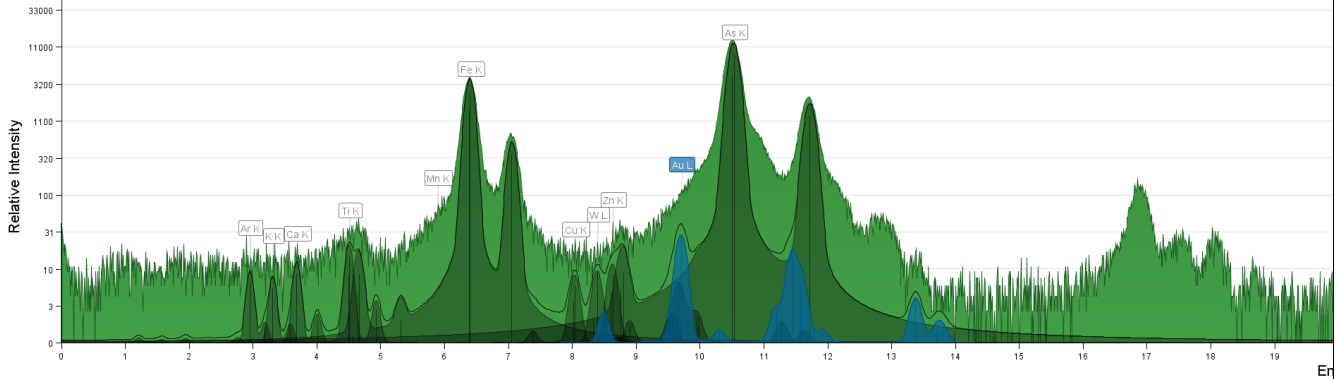


Additional Notes:

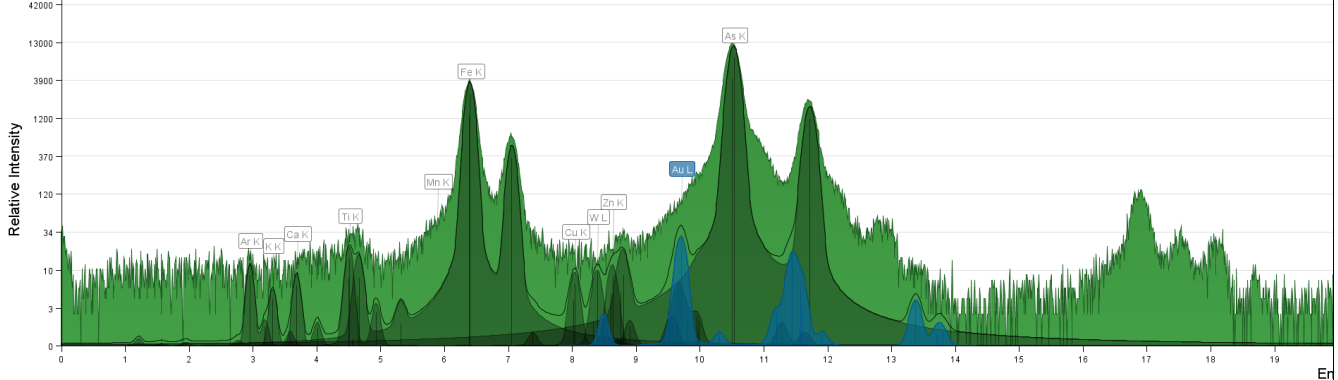
Ar intensity (without filter \rightarrow with filter): 123.7 \rightarrow 139.8

MCA Spectrum (Au spots):

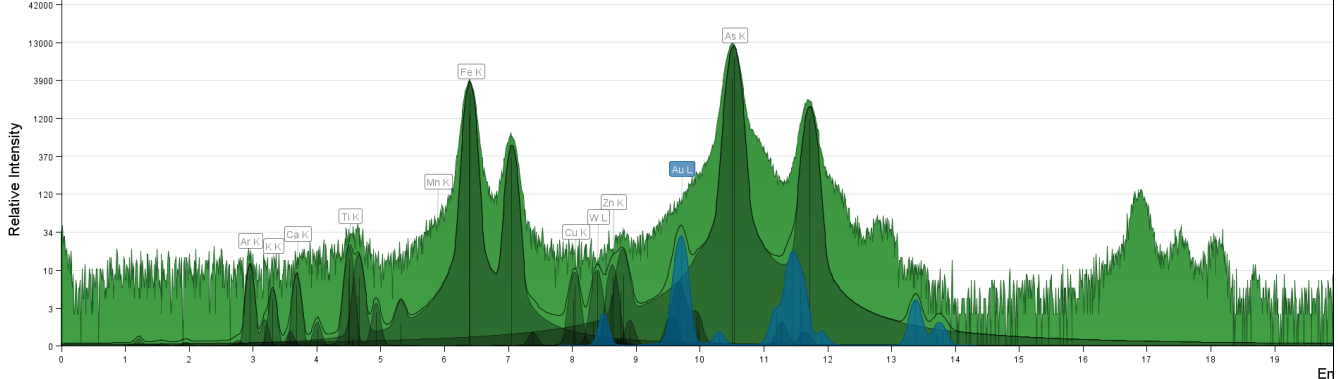
1. Au peak on the As shoulder on the MCA Spectrum, but higher than the shoulder.



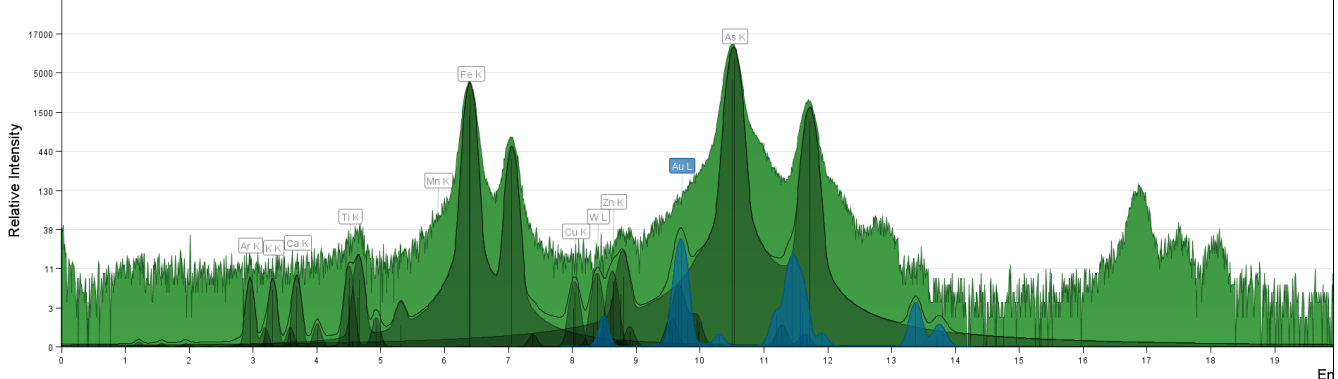
2. Au peak on the As shoulder on the MCA Spectrum, but higher than the shoulder.



3. Au peak on the As shoulder on the MCA Spectrum, but higher than the shoulder.



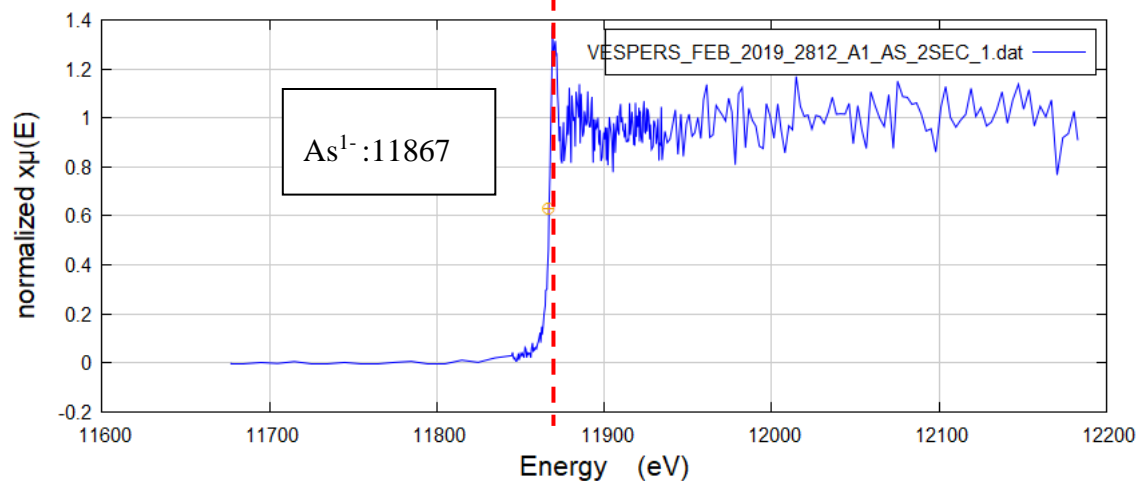
4. Au peak on the As shoulder on the MCA Spectrum, but higher than the shoulder.



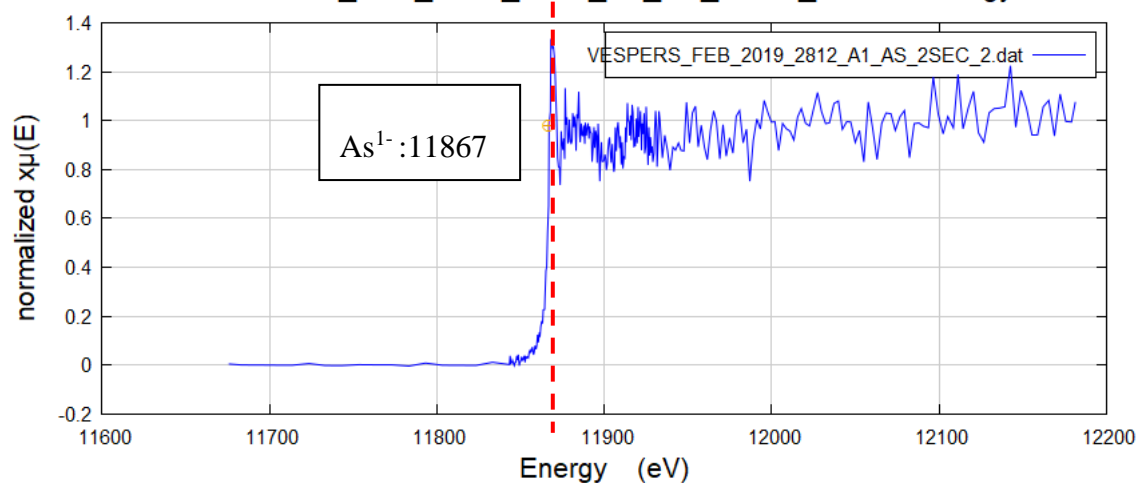
Appendix E: X-ray Absorption Near-edge Structure (XANES) Spectroscopy

Sample Number	2812A	Drill Hole	TL-16-583	Depth	156.11-156.31m
Lithology	QFP	Gold Grade	0.98 ppm	Beamline	CLS-VESPERS
XANES Type	As K-edge Micro-XANES				
Notes	Ran twice and reran twice, found As ¹⁻				

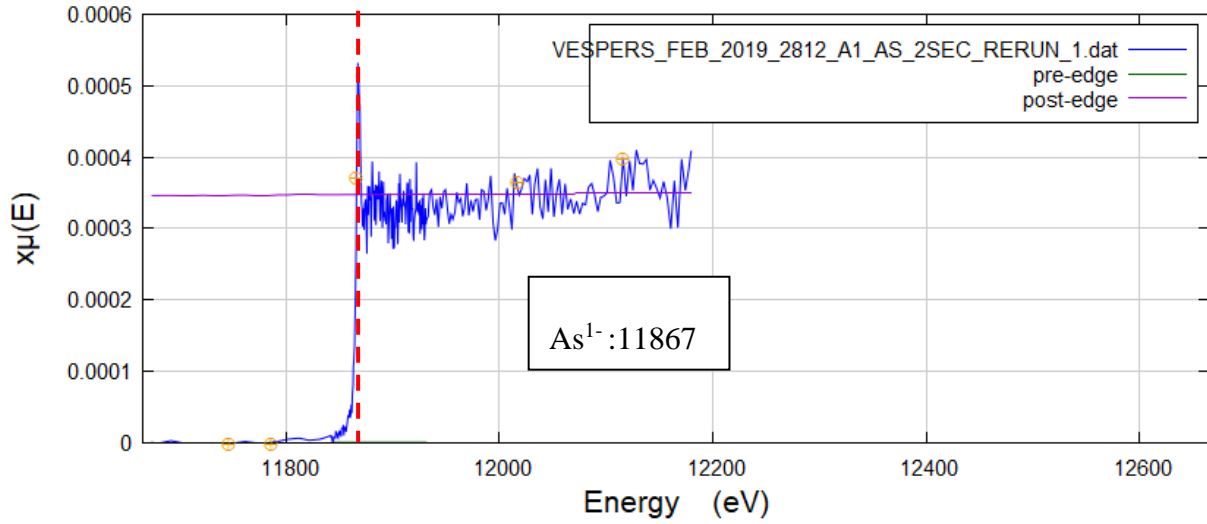
VESPERS_FEB_2019_2812_A1_AS_2SEC_1.dat in energy



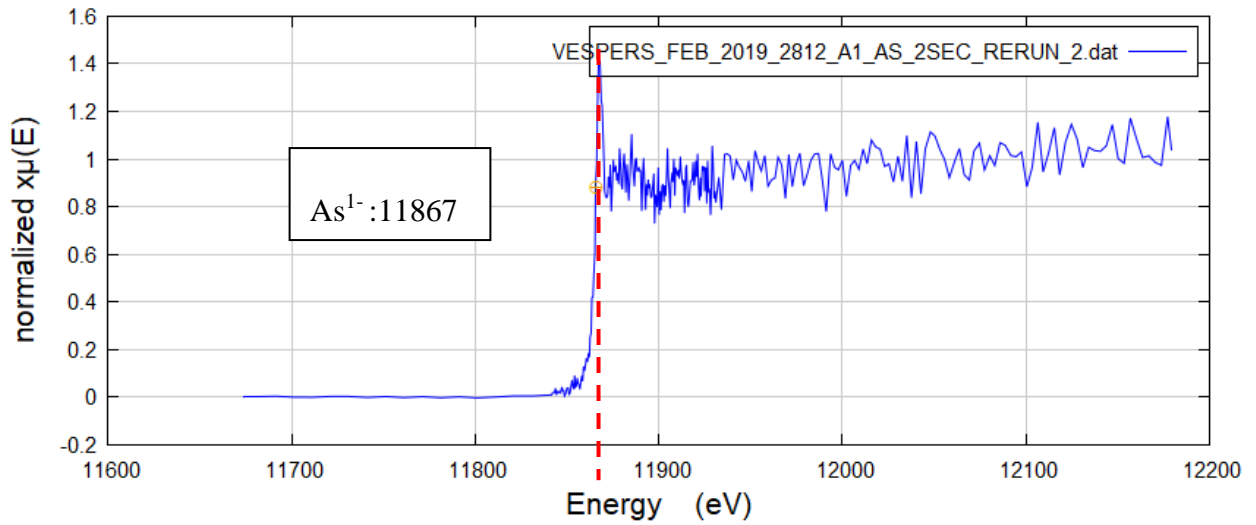
VESPERS_FEB_2019_2812_A1_AS_2SEC_2.dat in energy



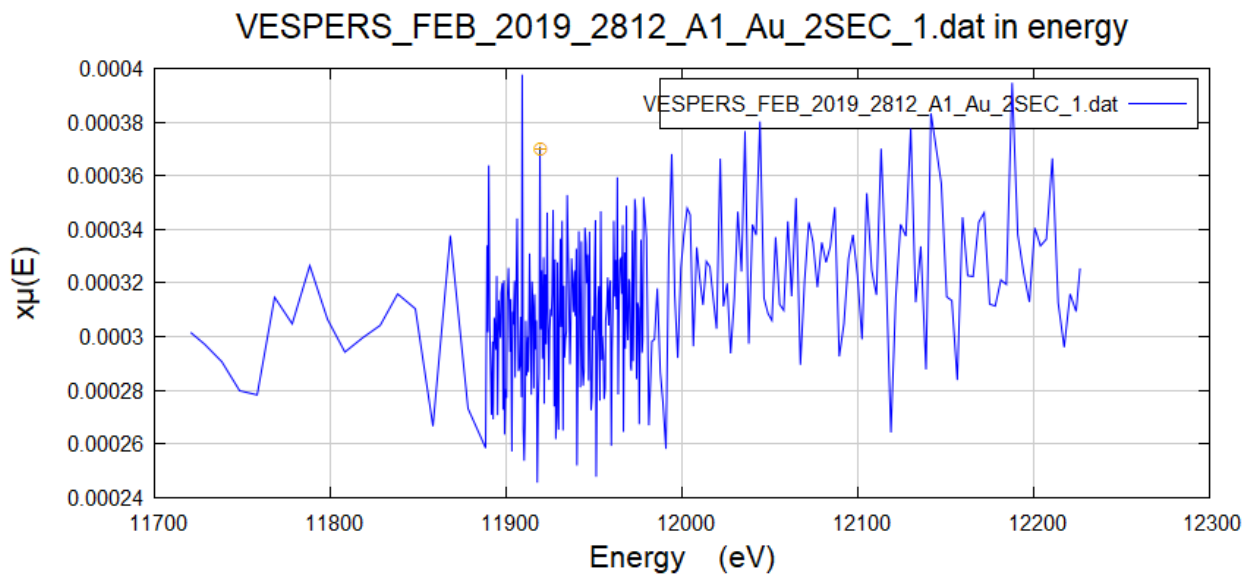
VESPERS_FEB_2019_2812_A1_AS_2SEC_RERUN_1.dat in energy



VESPERS_FEB_2019_2812_A1_AS_2SEC_RERUN_2.dat in energy

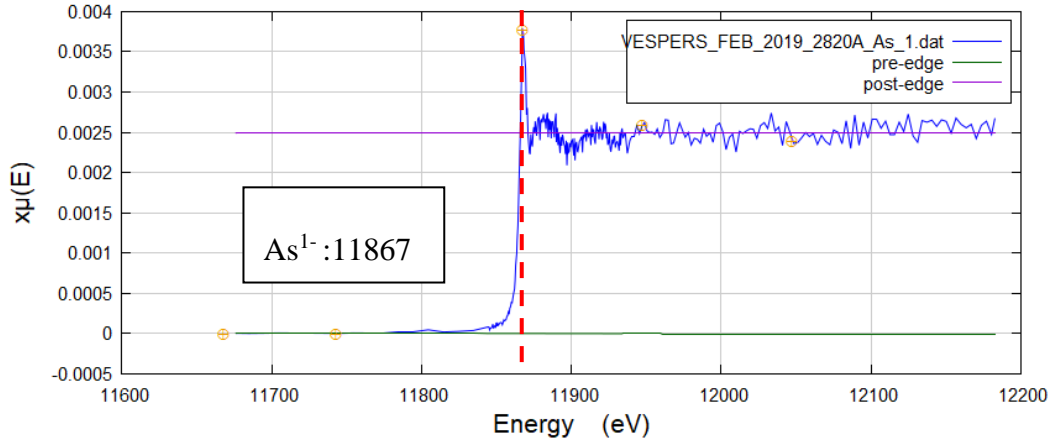


Sample Number	2812A	Drill Hole	TL-16-583	Depth	156.11-156.31m
Lithology	QFP	Gold Grade	0.98 ppm	Beamline	CLS-VESPERS
XANES Type	Au L3-edge Micro-XANES				
Notes	XANES spectra is too noisy and cannot be normalized				

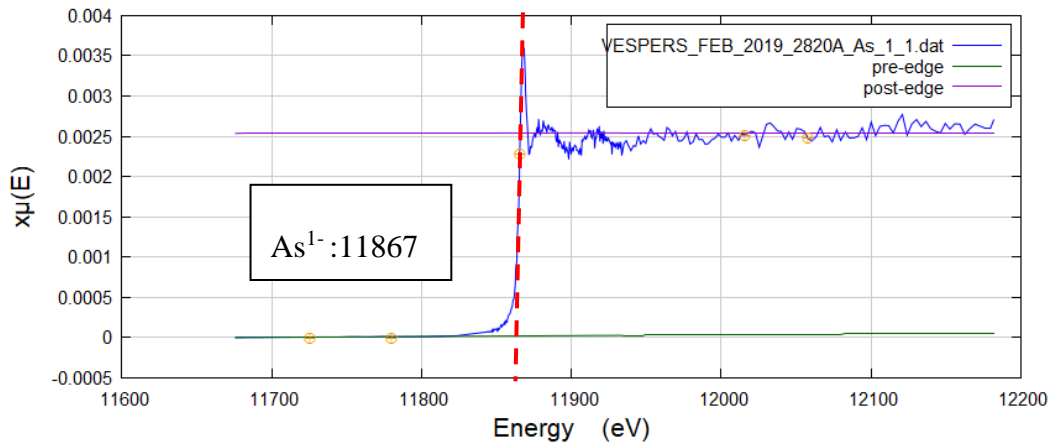


Sample Number	2820A	Drill Hole	TL-16-575	Depth	151.68-151.82m
Lithology	FP	Gold Grade	0.75 ppm	Beamline	CLS-VESPERS
XANES Type	As K-edge Micro-XANES				
Notes	Ran once and reran twice, found As1-				

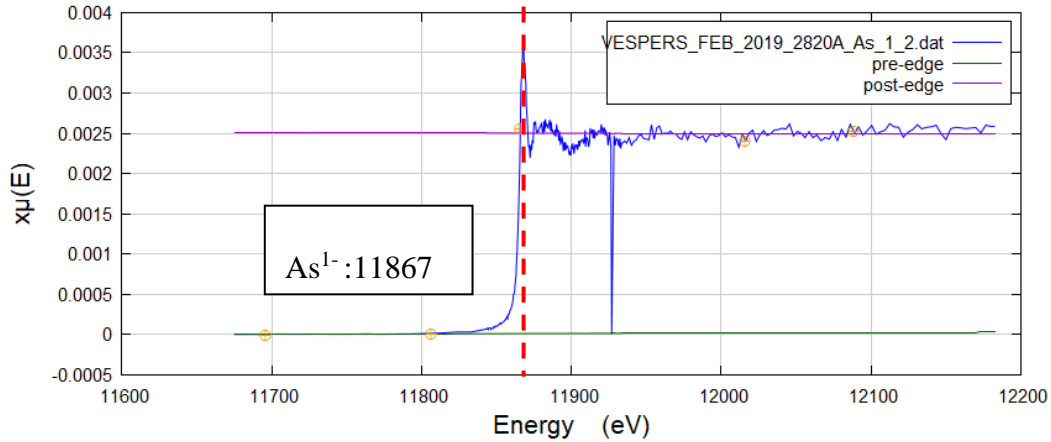
VESPERS_FEB_2019_2820A_As_1.dat in energy



VESPERS_FEB_2019_2820A_As_1_1.dat in energy

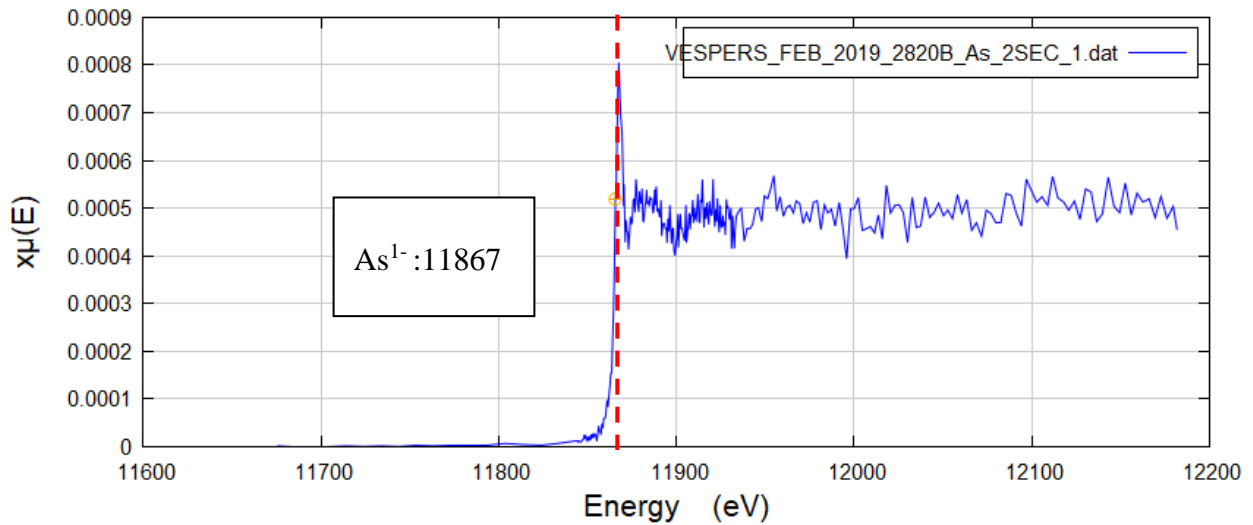


VESPERS_FEB_2019_2820A_As_1_2.dat in energy

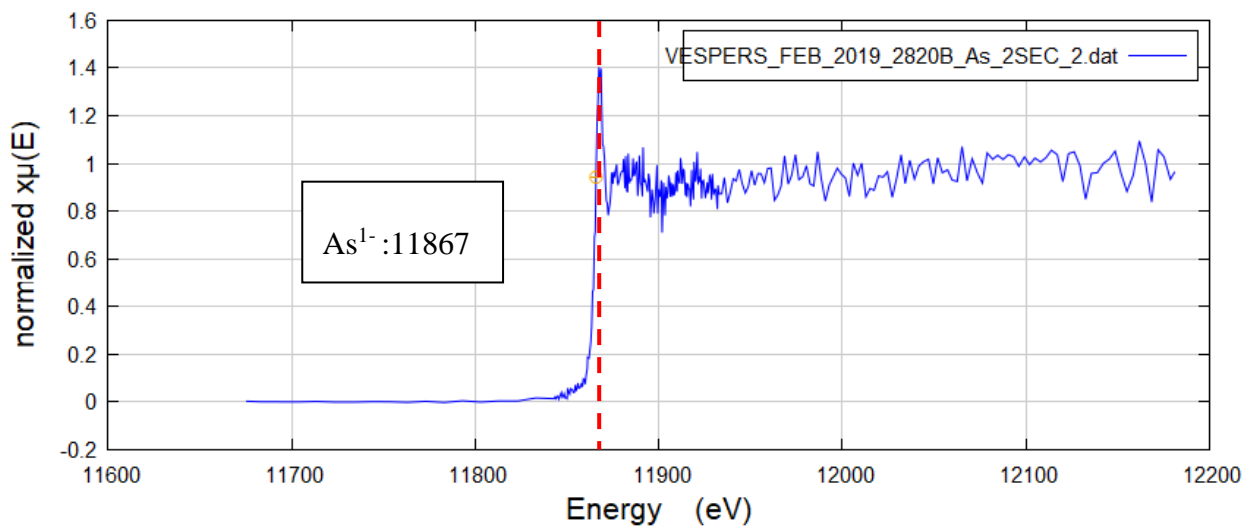


Sample Number	2820B	Drill Hole	TL-16-575	Depth	151.68-151.82m
Lithology	FP	Gold Grade	0.75 ppm	Beamline	CLS-VESPERS
XANES Type	As K-edge Micro-XANES				
Notes	Ran twice, found As ¹⁻				

VESPERS_FEB_2019_2820B_As_2SEC_1.dat in energy

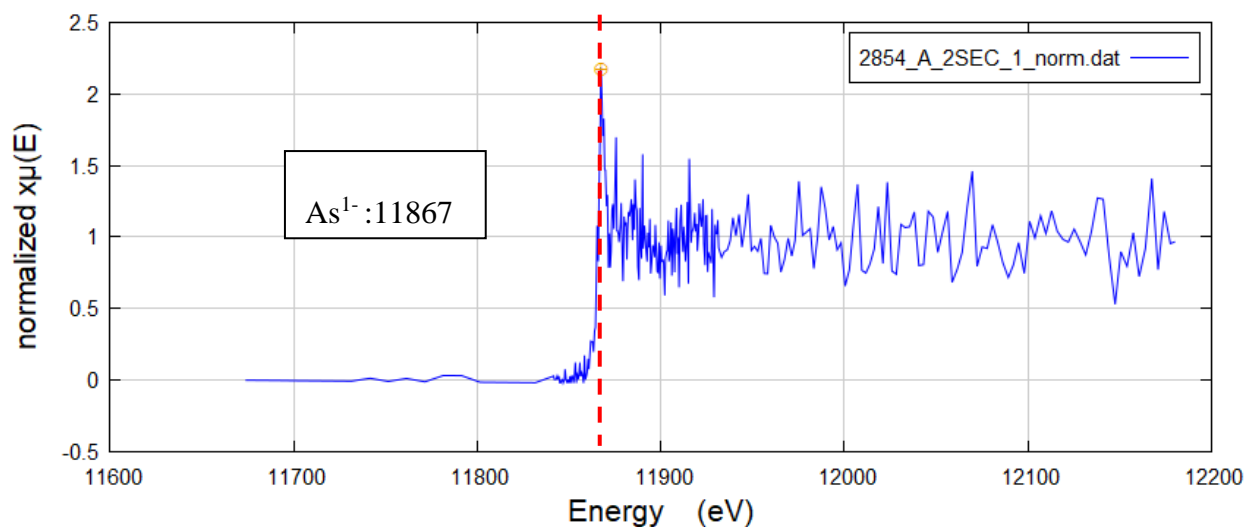


VESPERS_FEB_2019_2820B_As_2SEC_2.dat in energy

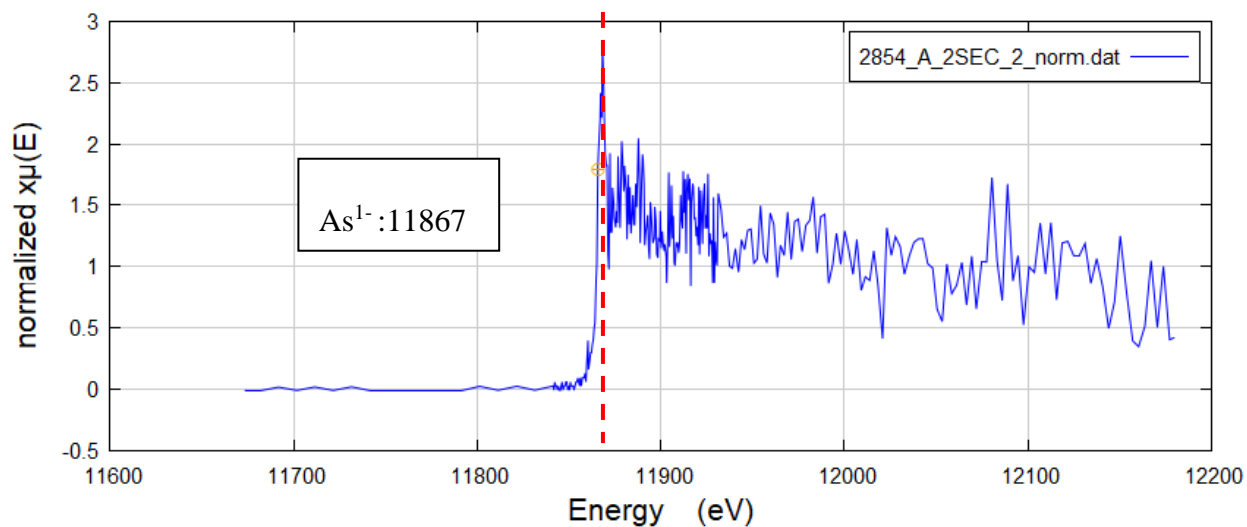


Sample Number	2854	Drill Hole	TL-16-604A	Depth	729.02-729.2 m
Lithology	Felsic Metavolcanics	Gold Grade	10.49 ppm	Beamline	CLS-VESPERS
XANES Type	As K-edge Micro-XANES				
Notes	Ran twice, found As1-				

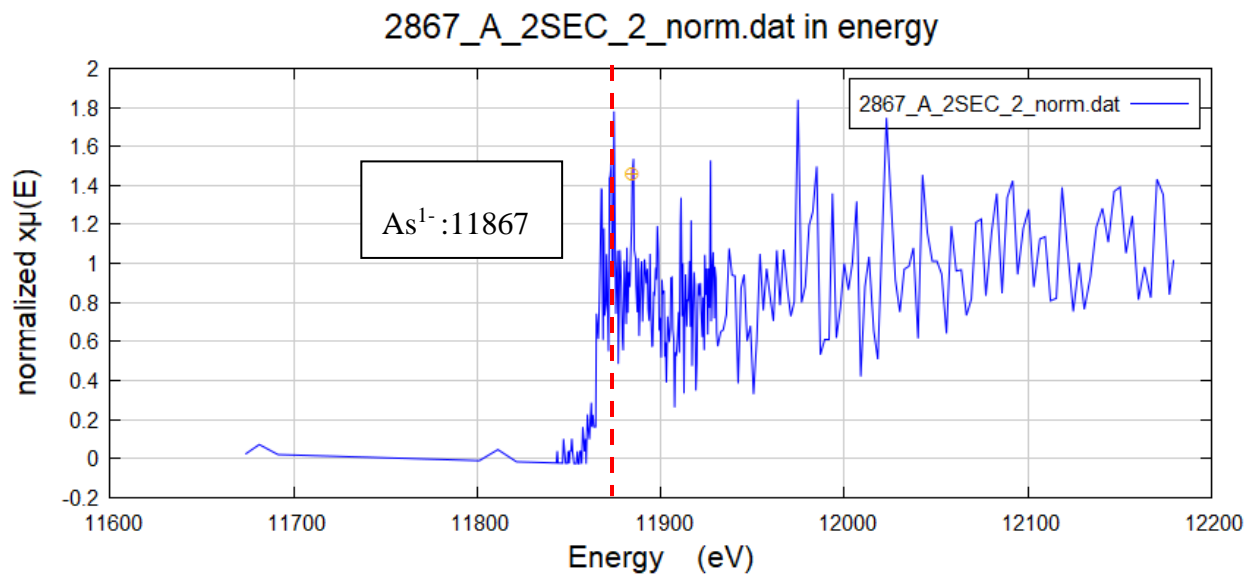
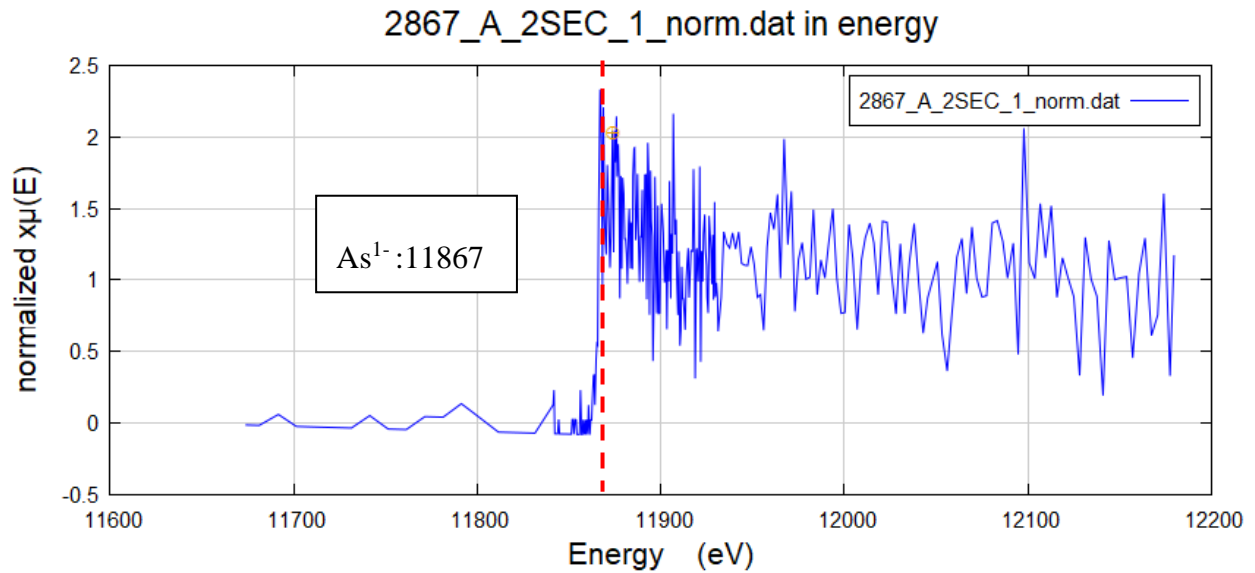
2854_A_2SEC_1_norm.dat in energy



2854_A_2SEC_2_norm.dat in energy

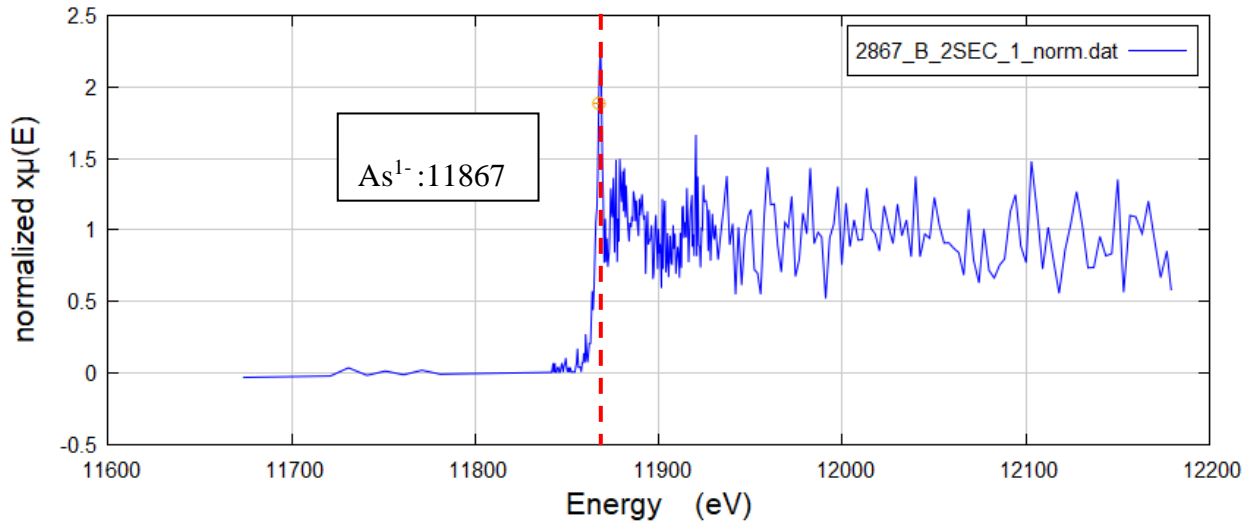


Sample Number	2367A	Drill Hole	TL-06-315	Depth	148.47-148.65 m
Lithology	Metaconglomerate	Gold Grade	0.04 ppm	Beamline	CLS-VESPERS
XANES Type	As K-edge Micro-XANES				
Notes	Ran twice, found As1-				

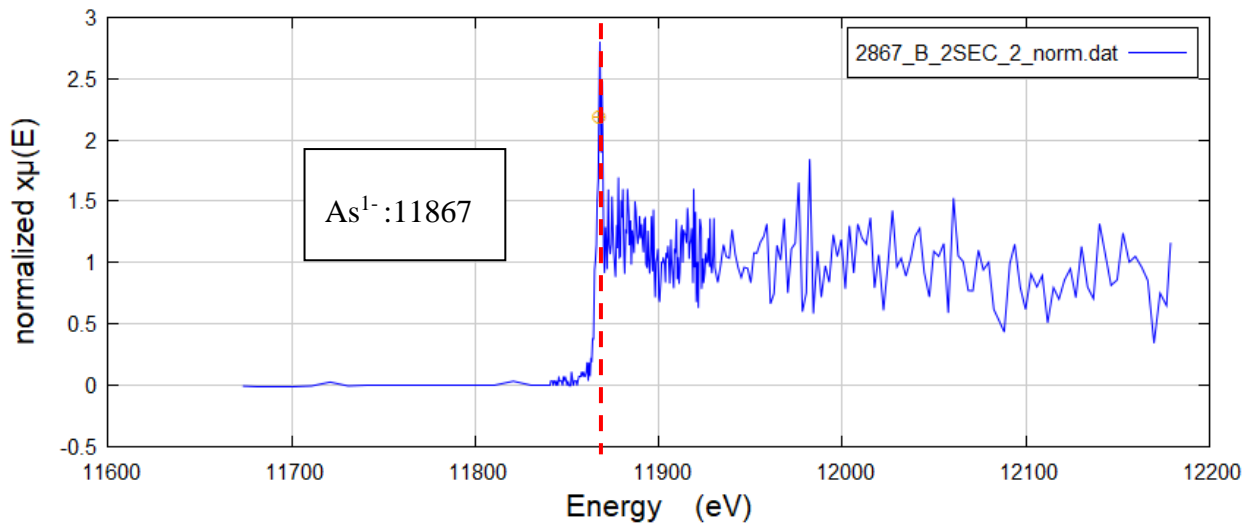


Sample Number	2367B	Drill Hole	TL-06-315	Depth	148.47-148.65 m
Lithology	Metaconglomerate	Gold Grade	0.04 ppm	Beamline	CLS-VESPERS
XANES Type	As K-edge Micro-XANES				
Notes	Ran twice, found As ¹⁻				

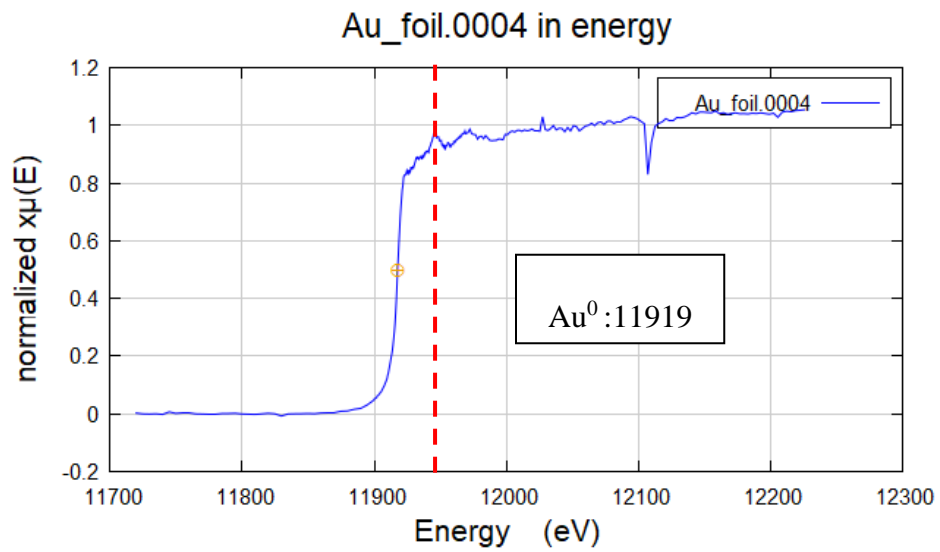
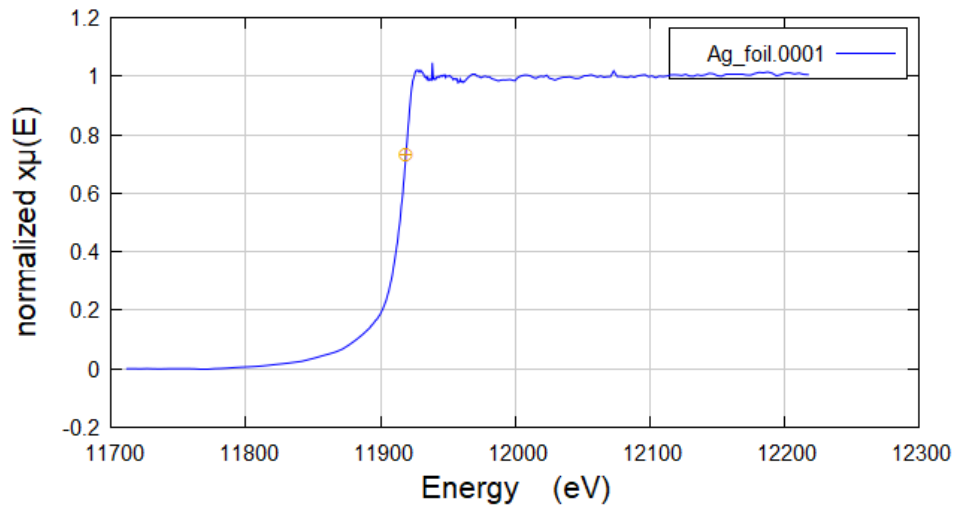
2867_B_2SEC_1_norm.dat in energy



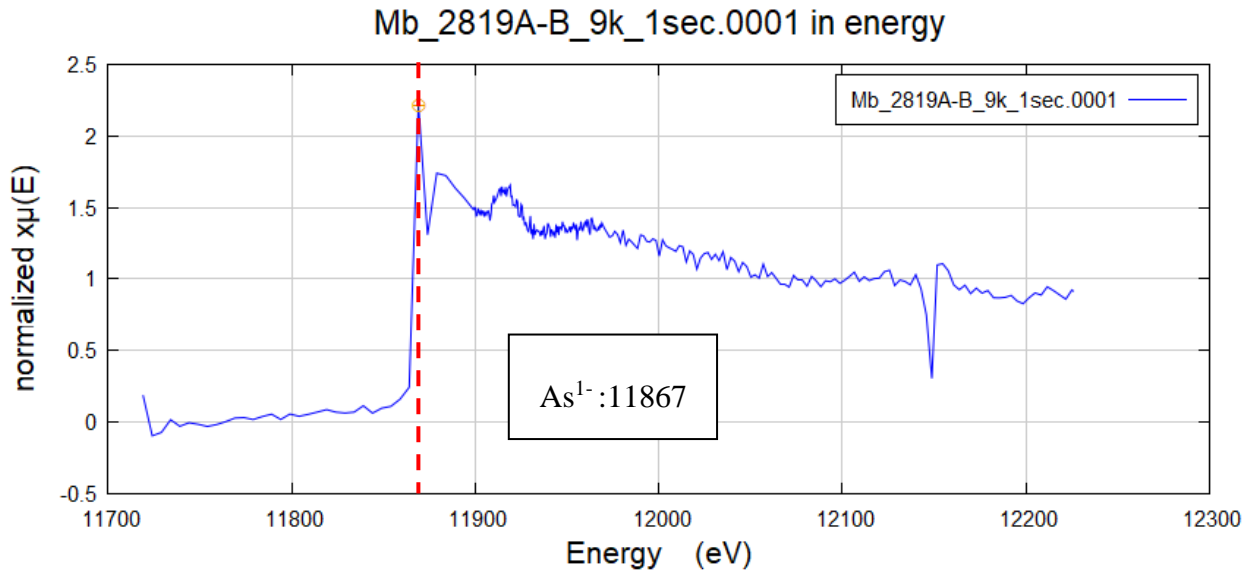
2867_B_2SEC_2_norm.dat in energy



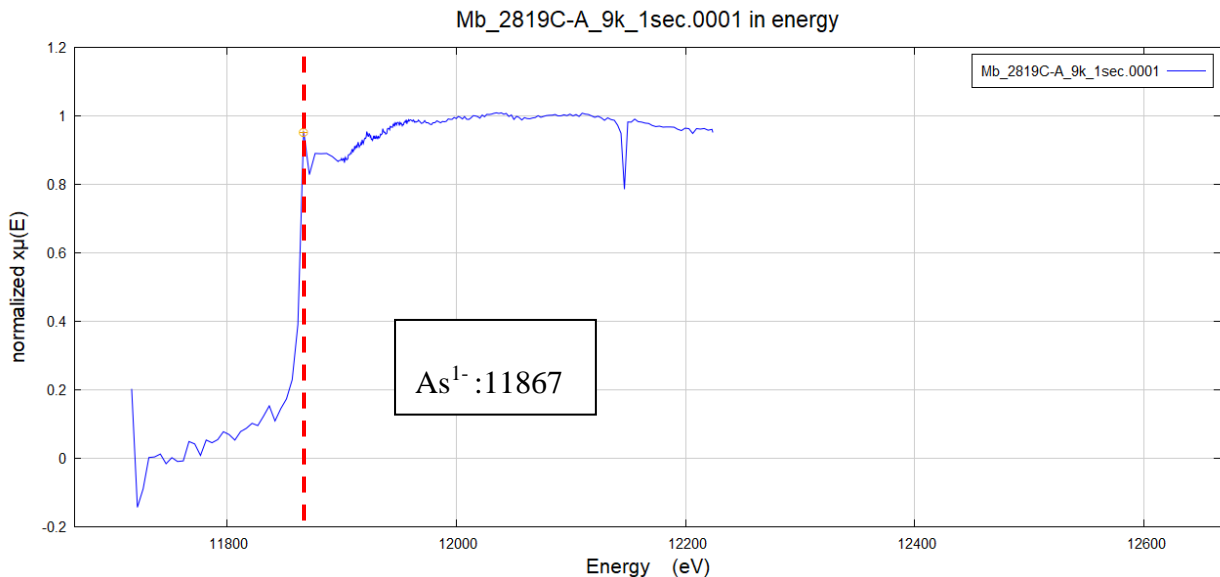
Sample	Gold foil (analyzed twice)	Beamline	APS-20ID
XANES Type	Au L3-edge Micro-XANES		
Notes	The first XANES spectra is too flat and cannot be identified, but the second one is clearer and can be used as a standard of Au ⁰ .		



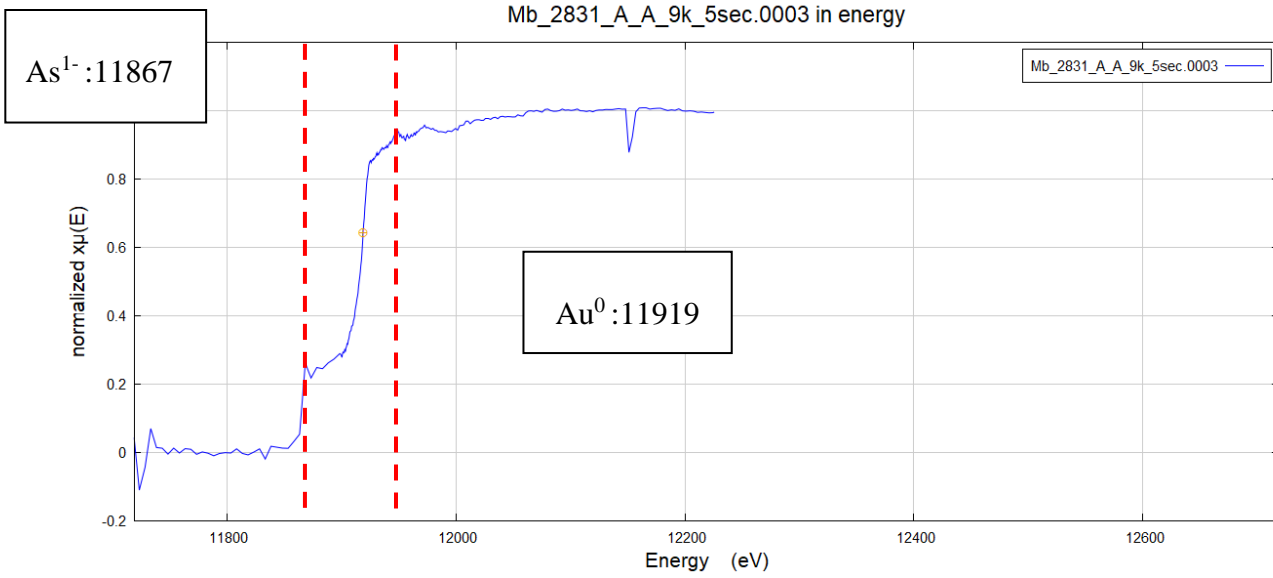
Sample Number	2819A-A	Drill Hole	TL-16-575	Depth	154.1-154.32m
Lithology	FP	Gold Grade	7.21 ppm	Beamline	APS-20ID
XANES Type	Au L3-edge Micro-XANES				
Notes	Ran once. As1- edge is obvious, but Au edge cannot be identified because of the overlaying of As post-edge.				



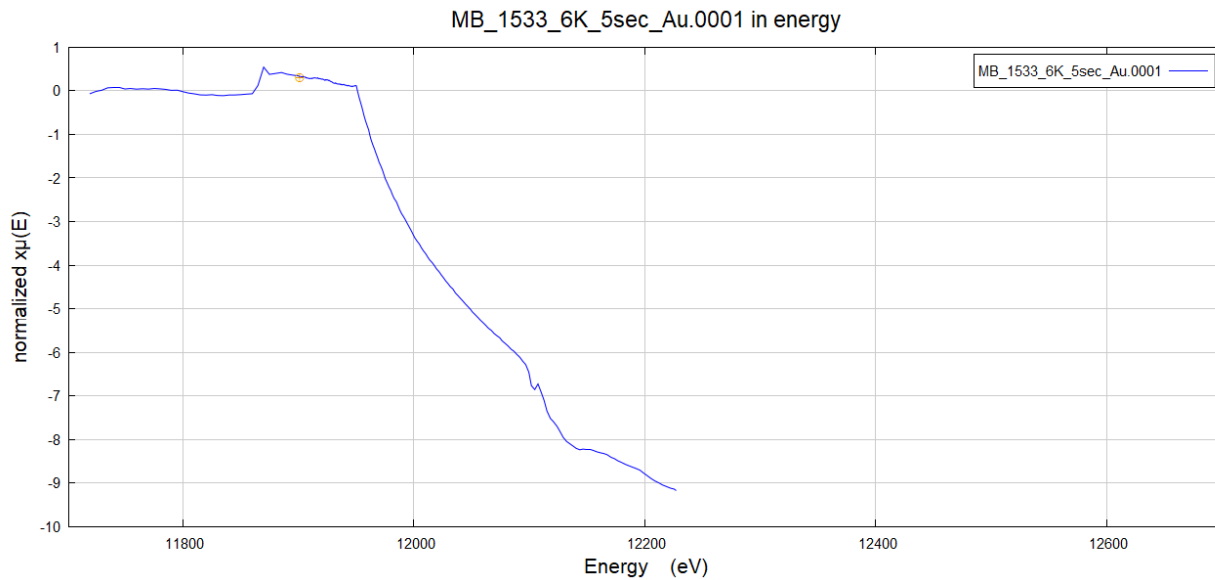
Sample Number	2819C-A	Drill Hole	TL-16-575	Depth	154.1-154.32m
Lithology	FP	Gold Grade	7.21 ppm	Beamline	APS-20ID
XANES Type	Au L3-edge Micro-XANES				
Notes	Ran once. As1- edge is obvious, but Au type cannot be identified because Au edge is the overlapped by As post-edge.				



Sample Number	2831A-A	Drill Hole	TL-15-551	Depth	96.8-97m
Lithology	Metasandstone	Gold Grade	2.26 ppm	Beamline	APS-20ID
XANES Type	Au L3-edge Micro-XANES				
Notes	Ran once. Au ⁰ and As ^I -has been found, Au edge is much higher than As edge.				

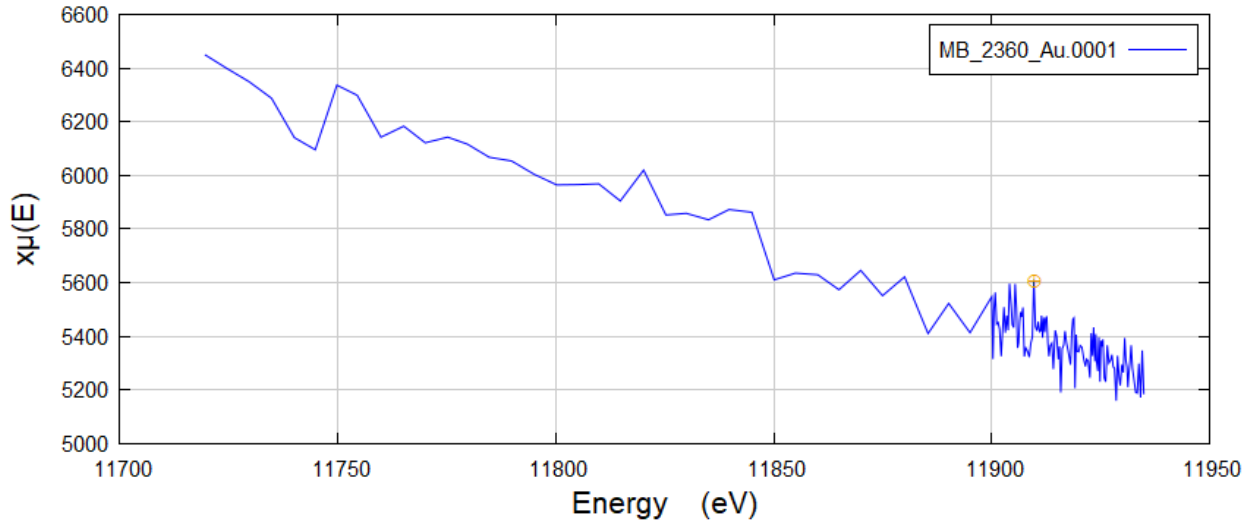


Sample Number	1533	Drill Hole	TL-12-481	Depth	101-102.05m
Lithology	QFP	Gold Grade	13.22 ppm	Beamline	APS-20BM
XANES Type	Au L3-edge Bulk-XANES				
Notes	Ran once. No edge.				



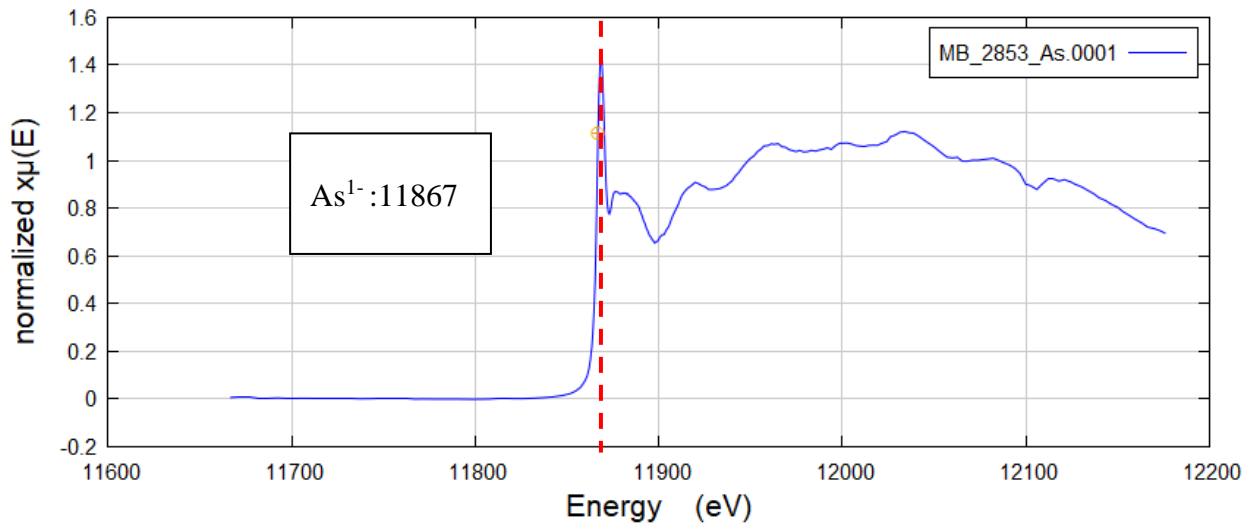
Sample Number	2360	Drill Hole	TL-17-616	Depth	148.6-148.8m
Lithology	Lapilli Tuff	Gold Grade	12-0.01 ppm	Beamline	APS-20BM
XANES Type	Au L3-edge Bulk-XANES				
Notes	Ran once. No edge.				

MB_2360_Au.0001 in energy

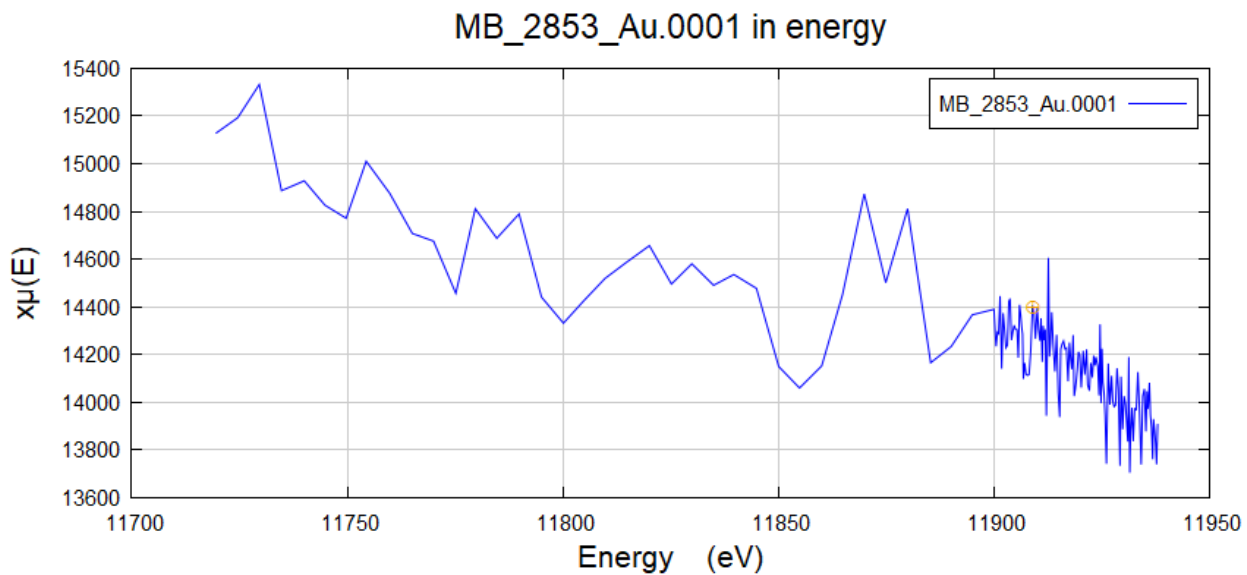


Sample Number	2853	Drill Hole	TL-13-604A	Depth	643.96-644.24m
Lithology	FP	Gold Grade	7.73 ppm	Beamline	APS-20BM
XANES Type	As K-edge Bulk-XANES				
Notes	Ran once. As ¹⁻ found.				

MB_2853_As.0001 in energy

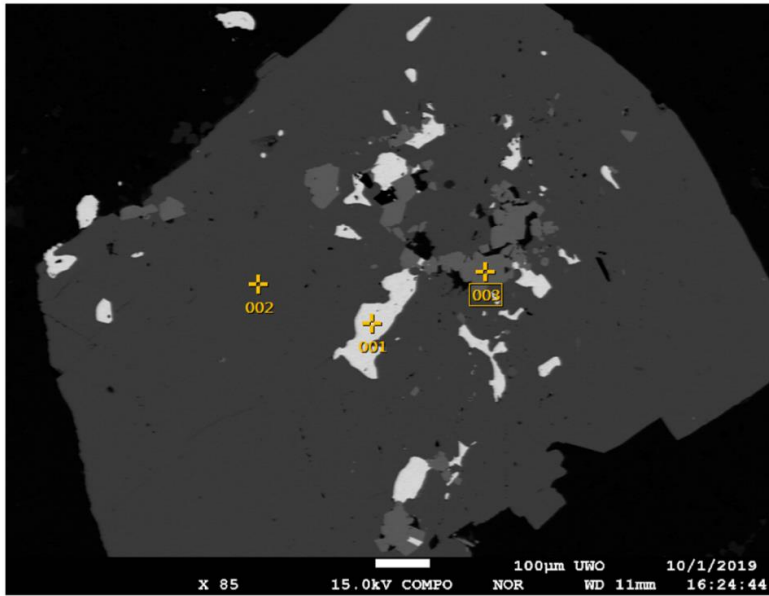


Sample Number	2853	Drill Hole	TL-13-604A	Depth	643.96-644.24m
Lithology	FP	Gold Grade	7.73 ppm	Beamline	APS-20BM
XANES Type	Au L3-edge Bulk-XANES				
Notes	Ran once. No edge.				

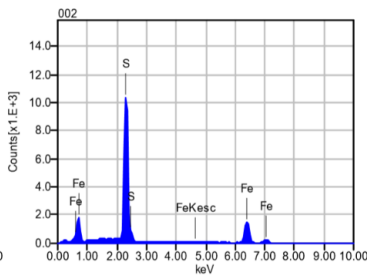
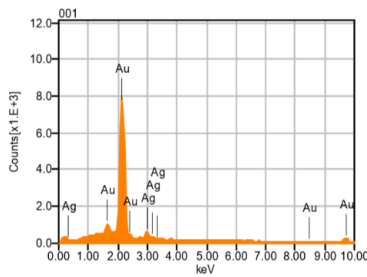


Appendix F: EPMA (EDS Point Analysis & EDS/WDS Element Maps)

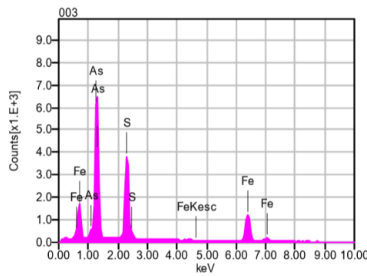
1533A-spot 1-1: Au + Ag grains combined with arsenopyrite inside a corroded euhedral pyrite
 (001: Au + Ag, 002: Pyrite, 003: Arsenopyrite)



Volt : 15.00 kV
 Mag. : x 85
 Date : 2019/10/01
 Pixel : 1280 x 960

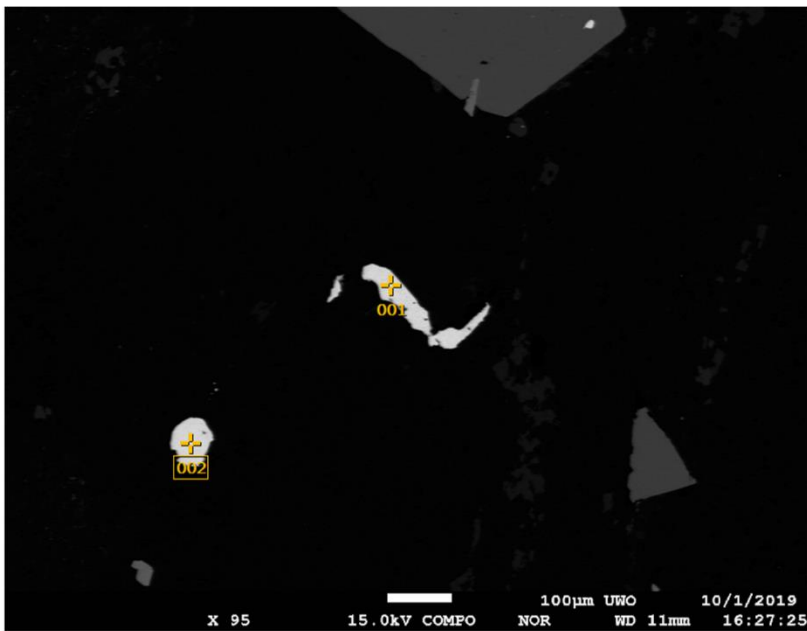


Acquisition Condition
 Instrument : 8530F
 Volt : 15.00 kV
 Current : ---
 Process Time : T2
 Live time : 10.00 sec.
 Real Time : 11.41 sec.
 DeadTime : 12.00 %
 Count Rate : 25245.00 CP

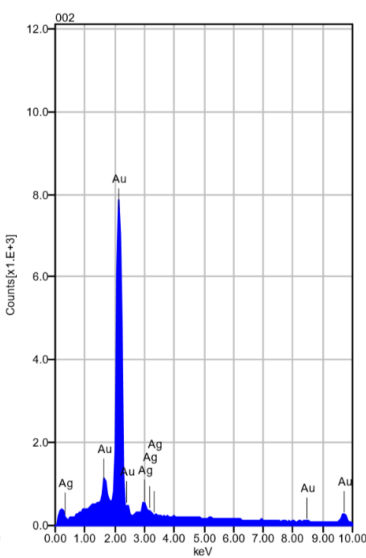
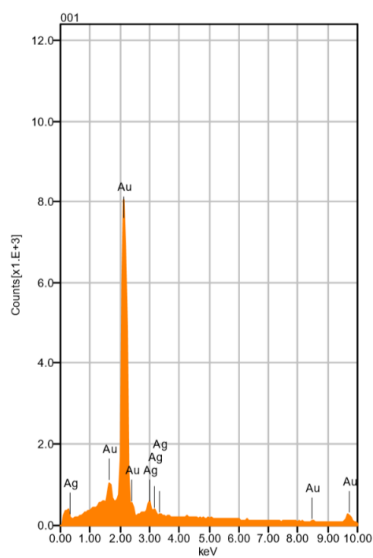


	Fe	Au	Ag	S	As
001		93.63	6.37		
002	51.06			48.94	
003	35.32			18.78	45.90
Average	43.19	93.63	6.37	33.86	45.90
Deviation	11.13	0.00	0.00	21.32	0.00

1533A_spot 1_2: Free gold near euhedral and needle pyrite grains (001&002: Au + Ag)



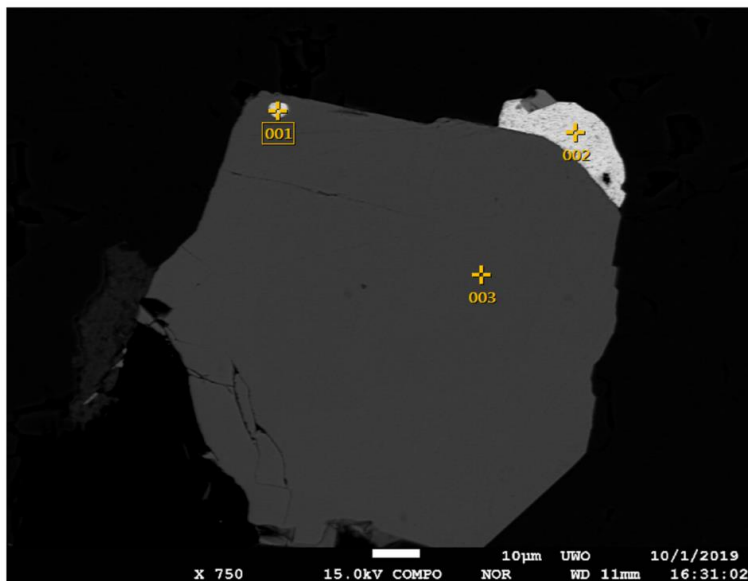
Volt : 15.00 kV
 Mag. : x 95
 Date : 2019/10/01
 Pixel : 1280 x 960



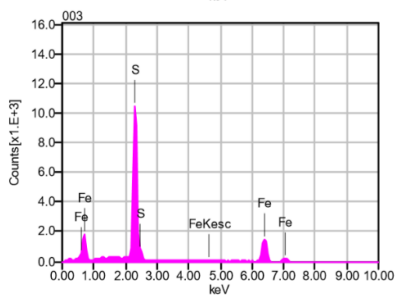
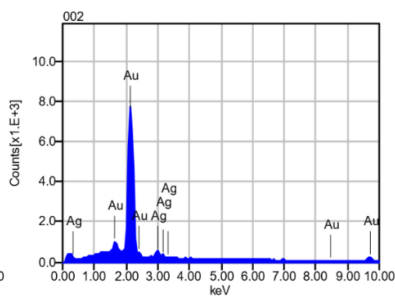
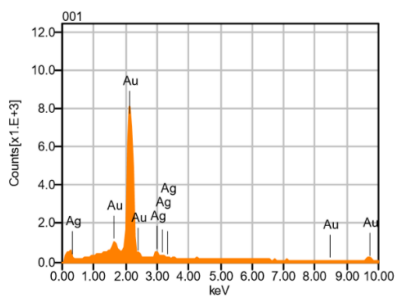
Acquisition Condition
 Instrument : 8530F
 Volt : 15.00 kV
 Current : ---
 Process Time : T2
 Live time : 10.00 sec.
 Real Time : 12.04 sec.
 DeadTime : 17.00 %
 Count Rate : 34720.00 CP

	Au	Ag
001	93.81	6.19
002	94.69	5.31
Average	94.25	5.75
Deviation	0.62	0.62

1533A_spot 1_3: Au + Ag on the edge of subhedral pyrite (001 & 002: Au + Ag, 003: pyrite)



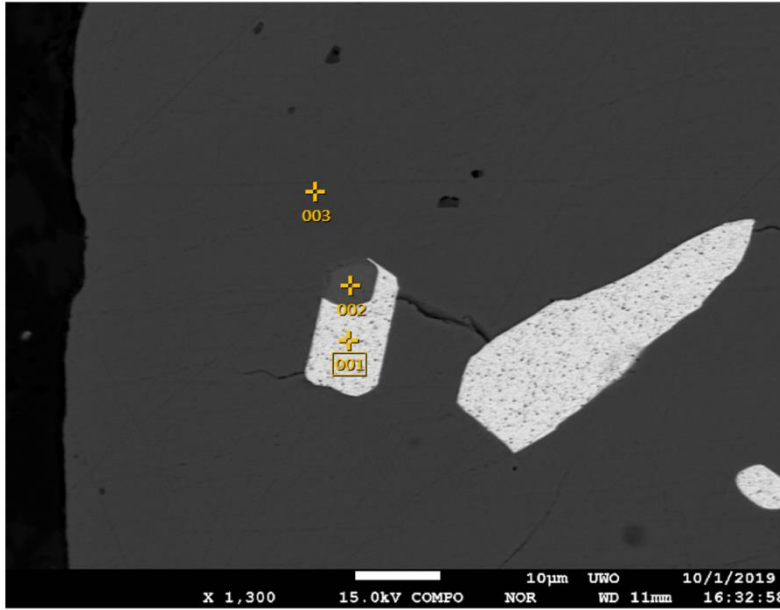
Volt : 15.00 kV
 Mag. : x 750
 Date : 2019/10/01
 Pixel : 1280 x 960



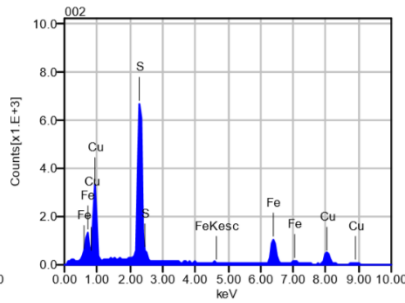
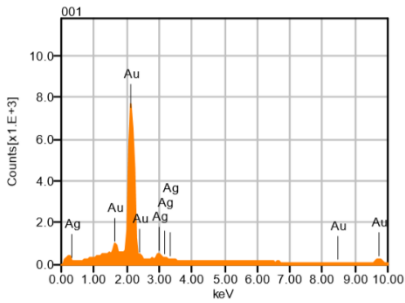
Acquisition Condition
 Instrument : 8530F
 Volt : 15.00 kV
 Current : ---
 Process Time : T2
 Live time : 10.00 sec.
 Real Time : 12.08 sec.
 DeadTime : 17.00 %
 Count Rate : 35032.00 CP

	Fe	Au	Ag	S
001		93.80	6.20	
002		93.98	6.02	
003	50.95			49.05
Average	50.95	93.89	6.11	49.05
Deviation	0.00	0.13	0.13	0.00

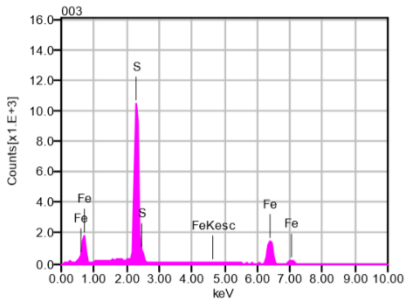
1533A_spot 1_4: Au + Ag grains inside a euhedral pyrite, Combined with chalcopyrite (001: Au + Ag, 002: chalcopyrite, 003: pyrite)



Volt : 15.00 kV
 Mag. : x 1,300
 Date : 2019/10/01
 Pixel : 1280 x 960

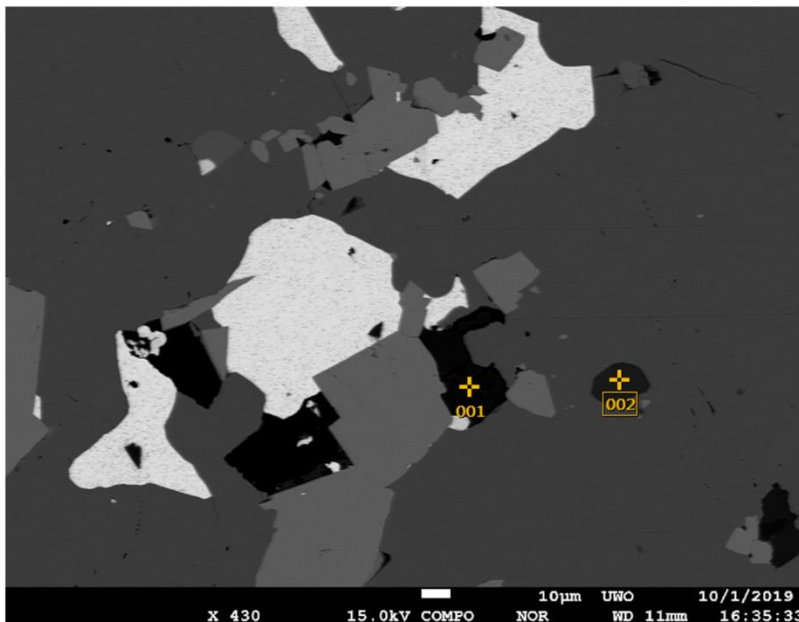


Acquisition Condition
 Instrument : 8530F
 Volt : 15.00 kV
 Current : ---
 Process Time : T2
 Live time : 10.00 sec.
 Real Time : 11.97 sec.
 DeadTime : 16.00 %
 Count Rate : 33165.00 CP

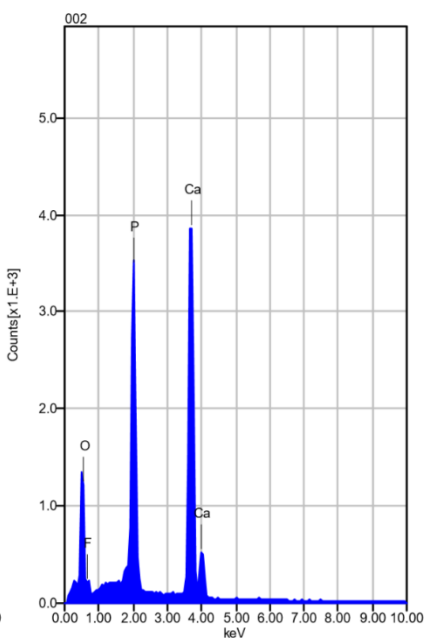
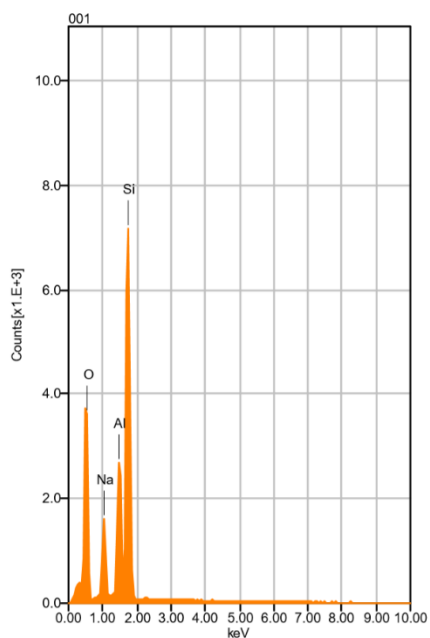


	Fe	Au	Ag	S	Cu
001		94.03	5.97		
002	32.19			32.31	35.51
003	50.86			49.14	
Average	41.52	94.03	5.97	40.72	35.51
Deviation	13.20	0.00	0.00	11.91	0.00

1533A_spot 1_5: Albite (001) and Apatite (002) inclusions in pyrite



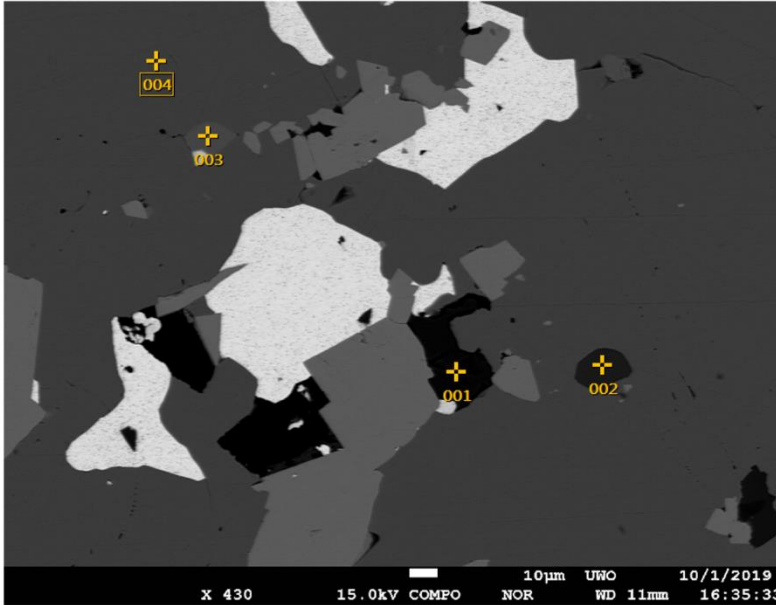
Volt : 15.00 kV
 Mag. : x 430
 Date : 2019/10/01
 Pixel : 1280 x 960



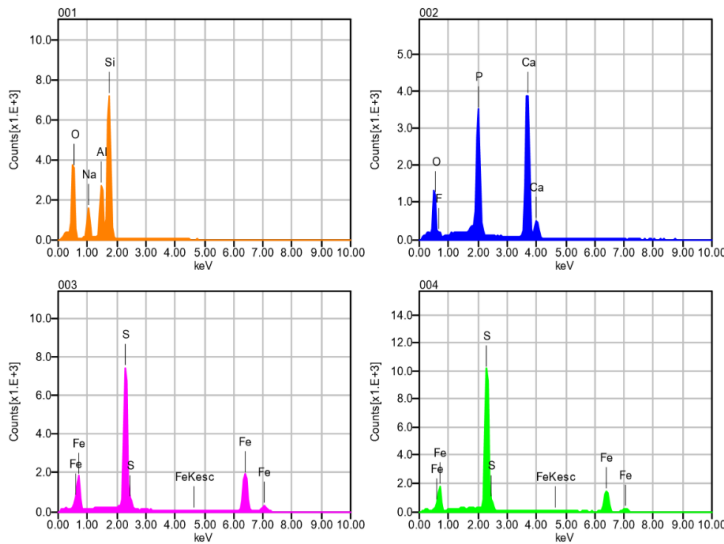
Acquisition Condition
 Instrument : 8530F
 Volt : 15.00 kV
 Current : ---
 Process Time : T2
 Live time : 9.32 sec.
 Real Time : 10.26 sec.
 DeadTime : 9.00 %
 Count Rate : 18331.00 CP

	P	O	F	Na	Al	Si	Ca
001		43.66		7.20	11.44	37.70	
002	19.52	33.36	2.95				44.17
Average	19.52	38.51	2.95	7.20	11.44	37.70	44.17
Deviation	0.00	7.28	0.00	0.00	0.00	0.00	0.00

1533A_spot 1_6: Au +Ag grains with subhedral and needle fractured arsenopyrite inside a corroded euhedral pyrite, with some albite and apatite inclusions. (001: albite, 002: apatite, 003&004: pyrite)



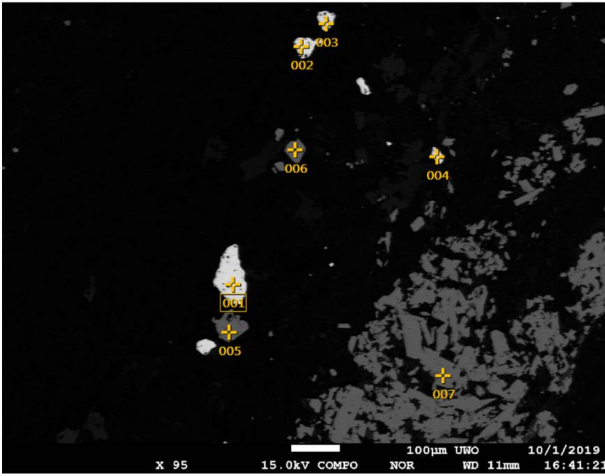
Volt : 15.00 kV
 Mag. : x 430
 Date : 2019/10/01
 Pixel : 1280 x 960



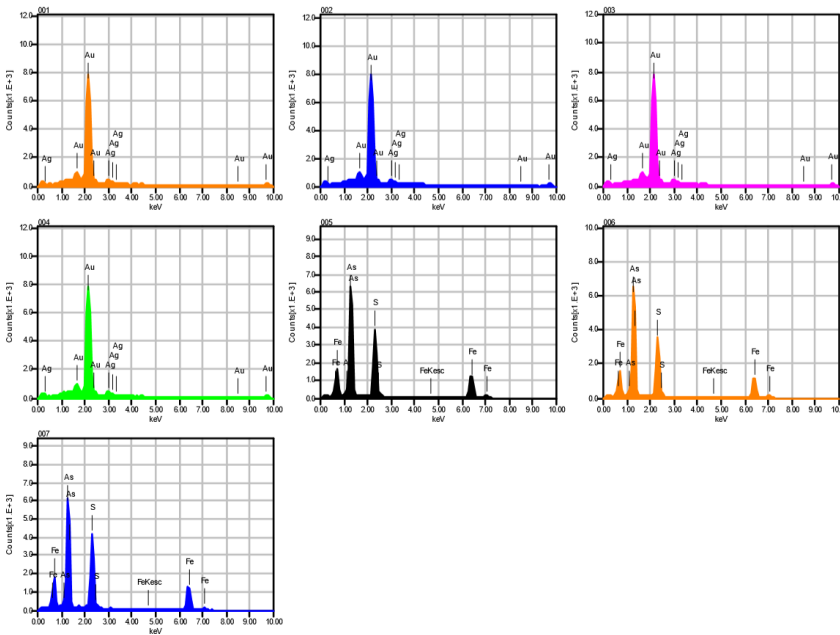
Acquisition Condition
 Instrument : 8530F
 Volt : 15.00 kV
 Current : ---
 Process Time : T2
 Live time : 10.00 sec.
 Real Time : 11.42 sec.
 DeadTime : 13.00 %
 Count Rate : 25422.00 CP

	P	Fe	O	F	Na	Al	Si	S	Ca
001			43.66		7.20	11.44	37.70		
002	19.52		33.36	2.95					44.17
003		64.78						35.22	
004		50.75						49.25	
Average	19.52	57.77	38.51	2.95	7.20	11.44	37.70	42.23	44.17
Deviation	0.00	9.91	7.28	0.00	0.00	0.00	0.00	9.91	0.00

1533A_spot 2_1: Free gold with disseminated Arsenopyrite (001-004: Au + Ag, 005-007: arsenopyrite)



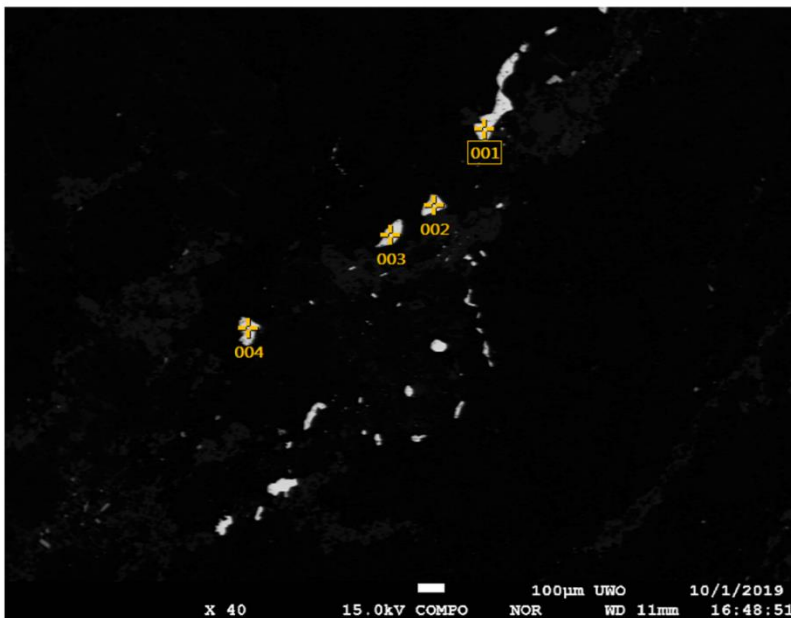
Volt : 15.00 kV
 Mag. : x 95
 Date : 2019/10/01
 Pixel : 1280 x 960



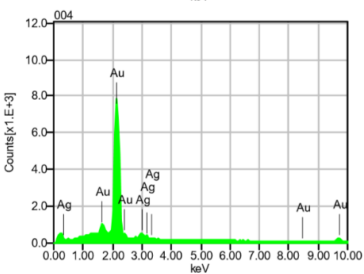
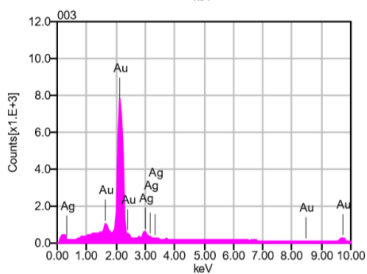
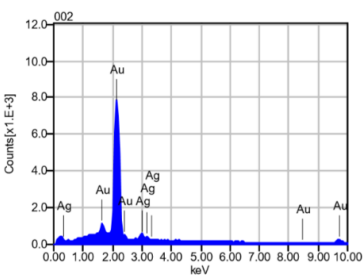
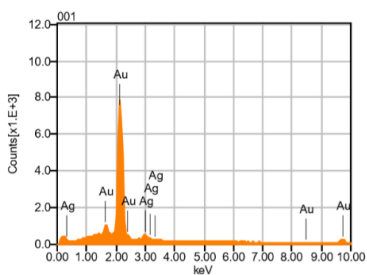
Acquisition Condition
 Instrument : 8530F
 Volt : 15.00 kV
 Current : ---
 Process Time : T2
 Live time : 10.00 sec.
 Real Time : 12.05 sec.
 DeadTime : 17.00 %
 Count Rate : 34591.00 CP

	Fe	Au	Ag	S	As
001		93.70	6.30		
002		94.69	5.31		
003		93.99	6.01		
004		94.02	5.98		
005	36.17			18.80	45.03
006	35.85			17.63	46.53
007	36.63			20.42	42.95
Average	36.21	94.10	5.90	18.95	44.84
Deviation	0.39	0.42	0.42	1.40	1.80

1533A_spot 4_1: Free gold in the groundmass (001-004: Au + Ag)



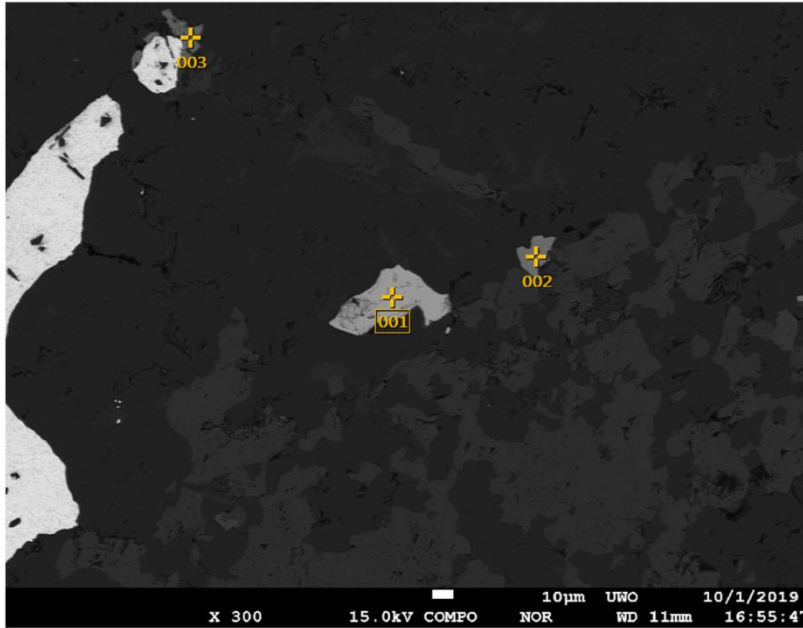
Volt : 15.00 kV
 Mag. : x 40
 Date : 2019/10/01
 Pixel : 1280 x 960



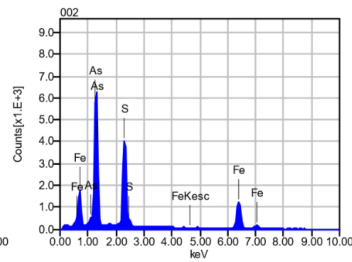
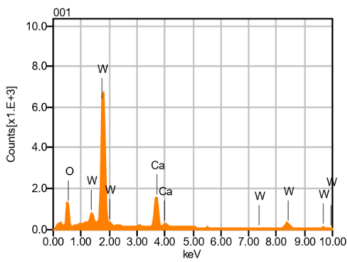
Acquisition Condition
 Instrument : 8530F
 Volt : 15.00 kV
 Current : ---
 Process Time : T2
 Live time : 10.00 sec.
 Real Time : 12.04 sec.
 DeadTime : 17.00 %
 Count Rate : 34523.00 CP

	Au	Ag
001	94.26	5.74
002	93.90	6.10
003	94.29	5.71
004	94.07	5.93
Average	94.13	5.87
Deviation	0.18	0.18

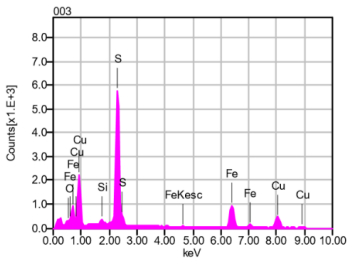
1533A_spot 4_2: Au combined with Chalcopyrite, fine grained anhedral scheelite and arsenopyrite
 (001: scheelite, 002: arsenopyrite, 003: chalcopyrite)



Volt : 15.00 kV
 Mag. : x 300
 Date : 2019/10/01
 Pixel : 1280 x 960

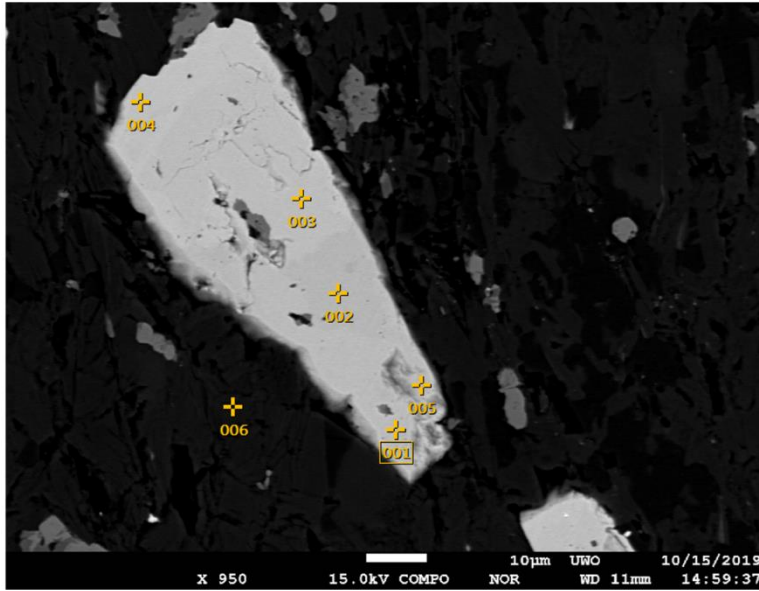


Acquisition Condition
 Instrument : 8530F
 Volt : 15.00 kV
 Current : ---
 Process Time : T2
 Live time : 10.00 sec.
 Real Time : 11.52 sec.
 DeadTime : 13.00 %
 Count Rate : 26250.00 CP

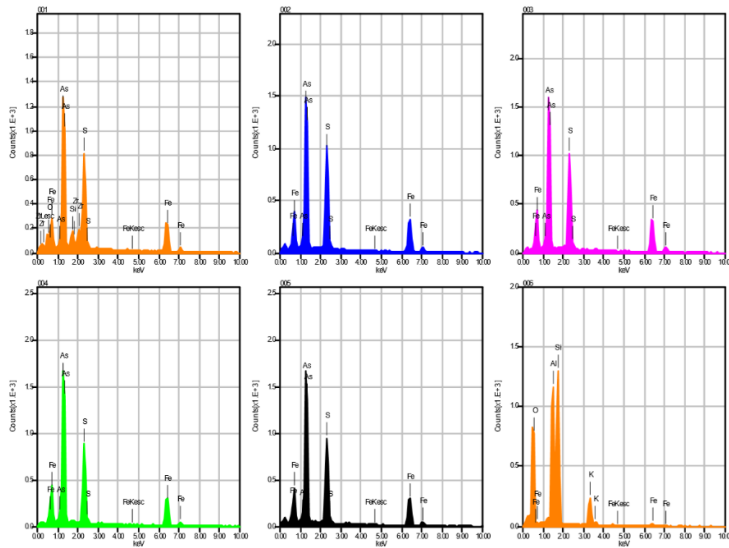


	Fe	O	Si	S	Ca	Cu	As	W
001		16.32			13.74			69.94
002	35.94			19.85			44.21	
003	32.03	1.99	0.82	29.94		35.22		
Average	33.98	9.16	0.82	24.89	13.74	35.22	44.21	69.94
Deviation	2.76	10.14	0.00	7.13	0.00	0.00	0.00	0.00

1533B_spot1_EDS1: Corroded needle arsenopyrite with zircon inclusions in the muscovite groundmass (001: arsenopyrite and zircon, 002-005: arsenopyrite, 006: muscovite)



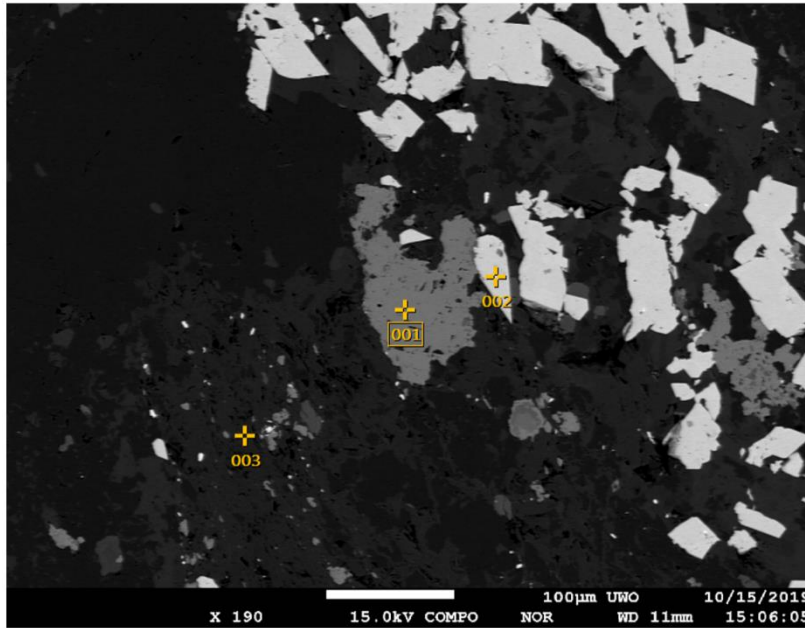
Volt : 15.00 kV
 Mag. : x 950
 Date : 2019/10/15
 Pixel : 1280 x 960



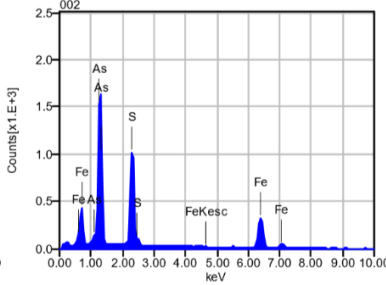
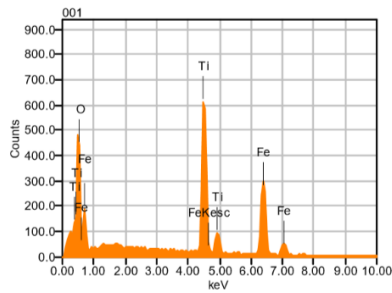
Acquisition Condition
 Instrument : 8530F
 Volt : 15.00 kV
 Current : ---
 Process Time : T2
 Live time : 10.00 sec.
 Real Time : 10.33 sec.
 DeadTime : 3.00 %
 Count Rate : 5952.00 CPS

	Fe	K	O	Al	Si	S	As	Zr
001	30.02		6.54		2.32	16.47	37.48	7.16
002	36.63					20.28	43.09	
003	36.77					18.85	44.38	
004	34.73					18.06	47.21	
005	35.14					18.75	46.11	
006	4.52	9.30	41.83	18.39	25.97			
Average	29.64	9.30	24.19	18.39	14.15	18.48	43.65	7.16
Deviation	12.55	0.00	24.95	0.00	16.72	1.39	3.80	0.00

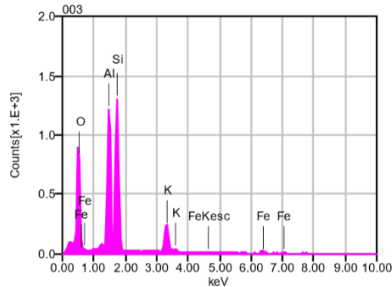
1533B_spot 1_EDS2: Corroded anhedral ilmenite grain and fractured subhedral-euhedral arsenopyrite in the muscovite groundmass (001: ilmenite, 002: arsenopyrite, 003: muscovite)



Volt : 15.00 kV
 Mag. : x 190
 Date : 2019/10/15
 Pixel : 1280 x 960

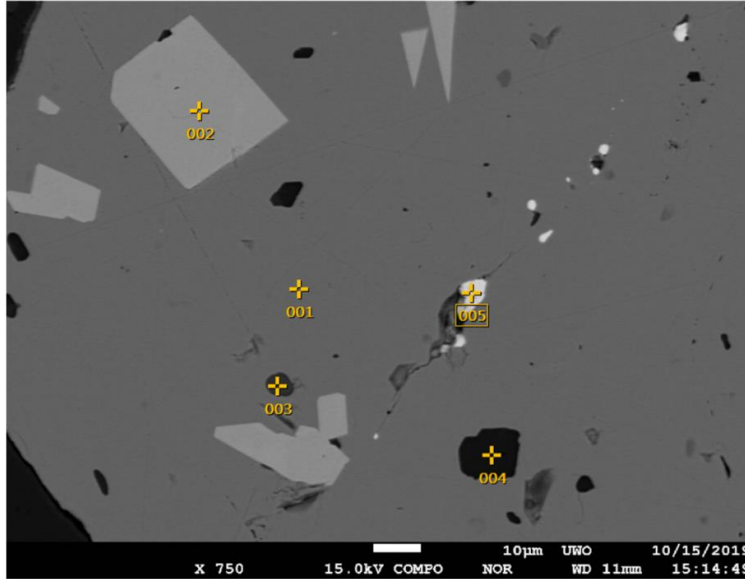


Acquisition Condition
 Instrument : 8530F
 Volt : 15.00 kV
 Current : ---
 Process Time : T2
 Live time : 10.00 sec.
 Real Time : 10.23 sec.
 DeadTime : 2.00 %
 Count Rate : 4236.00 CPS

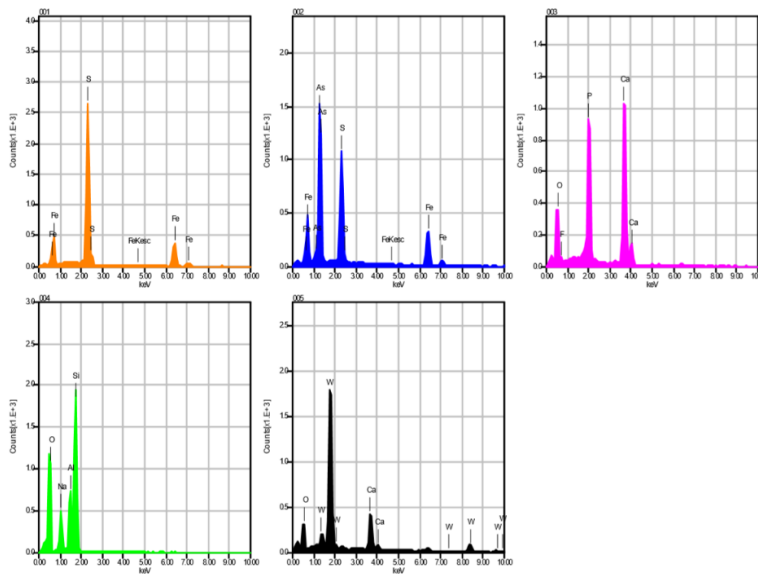


	Fe	K	O	Al	Si	S	Ti	As
001	39.69		26.47				33.84	
002	35.18					19.78		45.04
003	3.04	9.81	43.47	18.84	24.85			
Average	25.97	9.81	34.97	18.84	24.85	19.78	33.84	45.04
Deviation	19.99	0.00	12.02	0.00	0.00	0.00	0.00	0.00

1533B_spot 2_EDS1: Needle and square euhedral arsenopyrite grains, fine grained round scheelite, albite, and apatite inclusions in a corroded euhedral pyrite (001: pyrite, 002: arsenopyrite, 003: apatite, 004: albite, 005: scheelite)



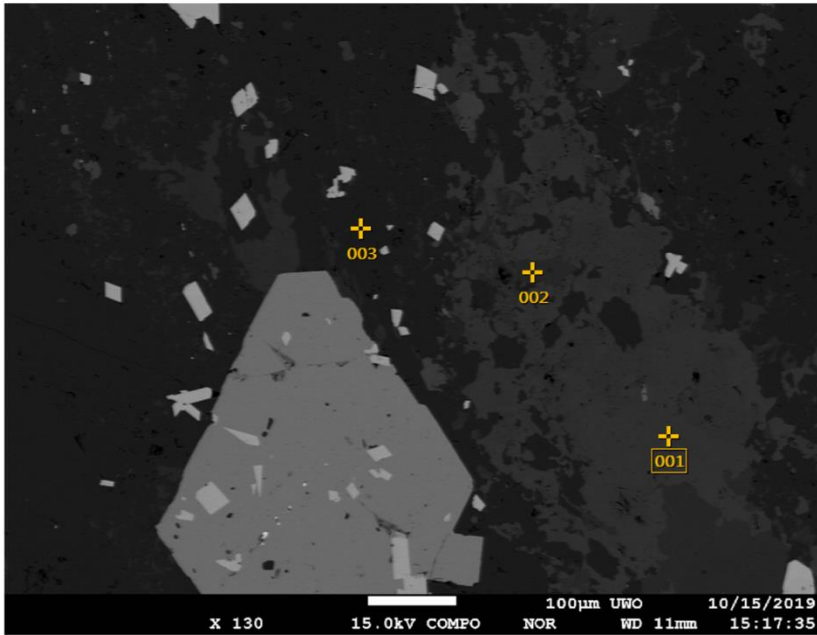
Volt : 15.00 kV
 Mag. : x 750
 Date : 2019/10/15
 Pixel : 1280 x 960



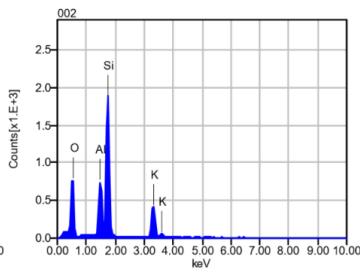
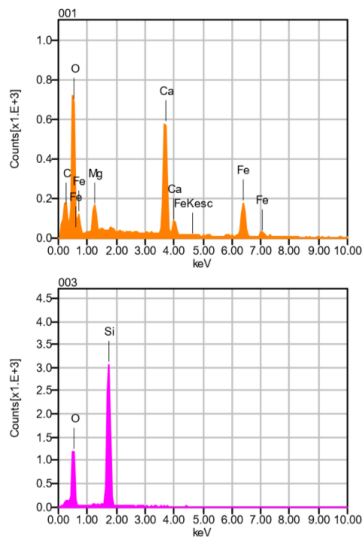
Acquisition Condition
 Instrument : 8530F
 Volt : 15.00 kV
 Current : ---
 Process Time : T2
 Live time : 10.00 sec.
 Real Time : 10.38 sec.
 DeadTime : 4.00 %
 Count Rate : 7099.00 CPS

	P	Fe	O	F	Na	Al	Si	S	Ca	As	W
001		50.21						49.79			
002		36.53						20.45		43.02	
003	19.70		33.57	3.49					43.24		
004			45.84		7.96	11.07	35.12				
005			15.65						13.48		
Average	19.70	43.37	31.69	3.49	7.96	11.07	35.12	35.12	28.36	43.02	
Deviation	0.00	9.68	15.18	0.00	0.00	0.00	0.00	20.75	21.04	0.00	

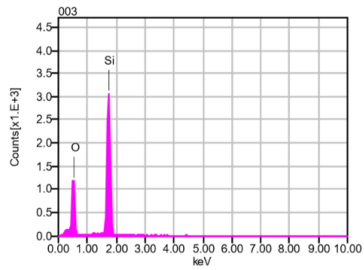
1533B_spot2_EDS2: ankerite, quartz, and K-feldspar groundmass (001: ankerite, 002: K-feldspar, 003: quartz)



Volt : 15.00 kV
 Mag. : x 130
 Date : 2019/10/15
 Pixel : 1280 x 960

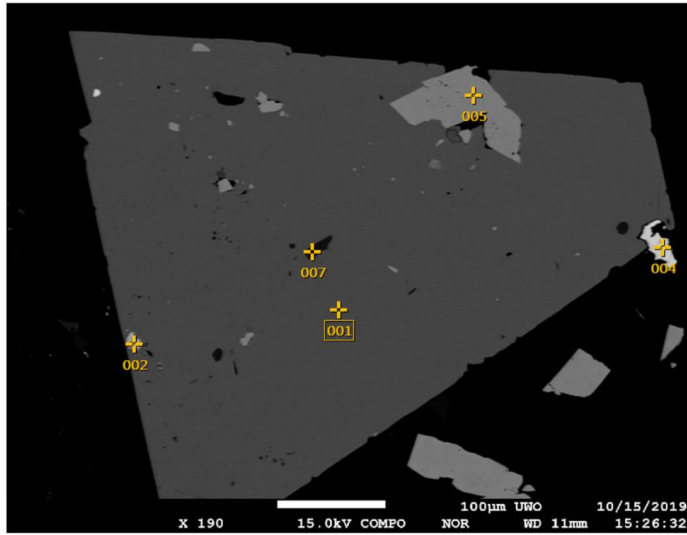


Acquisition Condition
 Instrument : 8530F
 Volt : 15.00 kV
 Current : ---
 Process Time : T2
 Live time : 10.00 sec.
 Real Time : 10.19 sec.
 DeadTime : 2.00 %
 Count Rate : 3745.00 CPS

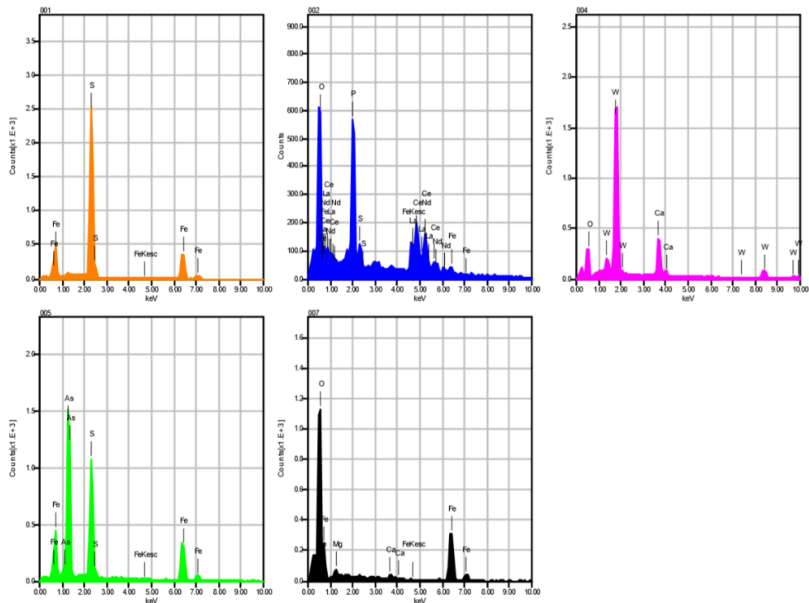


	Fe	K	O	C	Mg	Al	Si	Ca
001	23.74		43.44	7.52	2.49			22.81
002		15.34	42.19			10.29	32.17	
003			50.47				49.53	
Average	23.74	15.34	45.37	7.52	2.49	10.29	40.85	22.81
Deviation	0.00	0.00	4.46	0.00	0.00	0.00	12.27	0.00

1533B_spot3_EDS1: A needle corroded pyrite grain with fine grained anhedral scheelite, medium-fine-grained subhedral arsenopyrite, and fine-grained anhedral hematite and monazite as inclusions. (001: pyrite, 002: monazite, 004: scheelite, 005: arsenopyrite, 007: hematite)



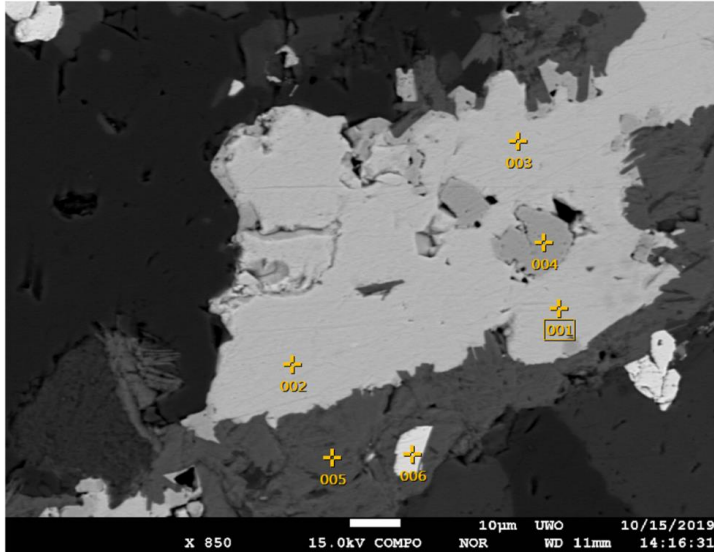
Volt : 15.00 kV
 Mag. : x 190
 Date : 2019/10/15
 Pixel : 1280 x 960



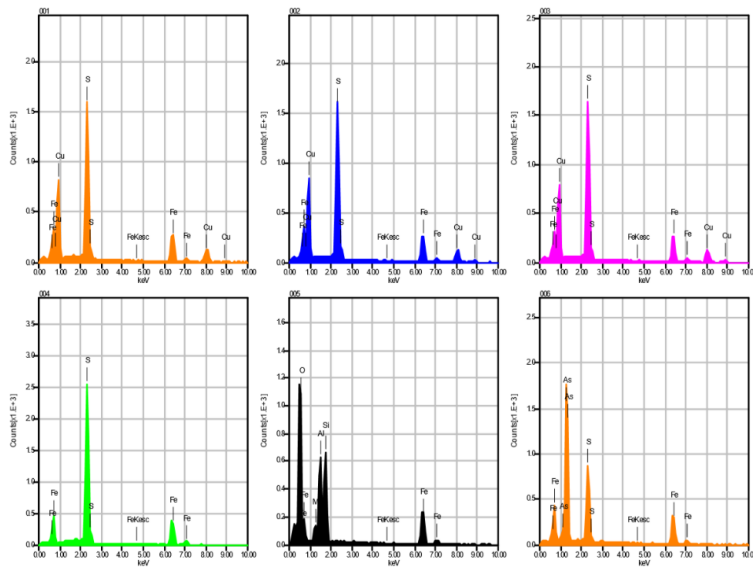
Acquisition Condition
 Instrument : 8530F
 Volt : 15.00 kV
 Current : ---
 Process Time : T2
 Live time : 10.00 sec.
 Real Time : 10.35 sec.
 DeadTime : 4.00 %
 Count Rate : 6670.00 CPS

	P	Fe	O	Mg	S	Ca	As	La	Ce	Nd	W
001		50.10			49.90						
002	12.87	2.36	21.27		2.01			17.33	32.26	11.90	
004			14.73			13.64					
005		37.36			20.37		42.26				
007		58.59	38.58	1.39		1.44					
Average	12.87	37.10	24.86	1.39	24.09	7.54	42.26	17.33	32.26	11.90	
Deviation	0.00	24.75	12.32	0.00	24.16	8.62	0.00	0.00	0.00	0.00	

1539B_spot1_EDS: Corroded anhedral chalcopyrite grain with pyrite inside, and combines with garnet, and fine-grained subhedral arsenopyrite grains are inside chlorite. (001-003: chalcopyrite, 004: pyrite, 005: chlorite, 006: arsenopyrite)



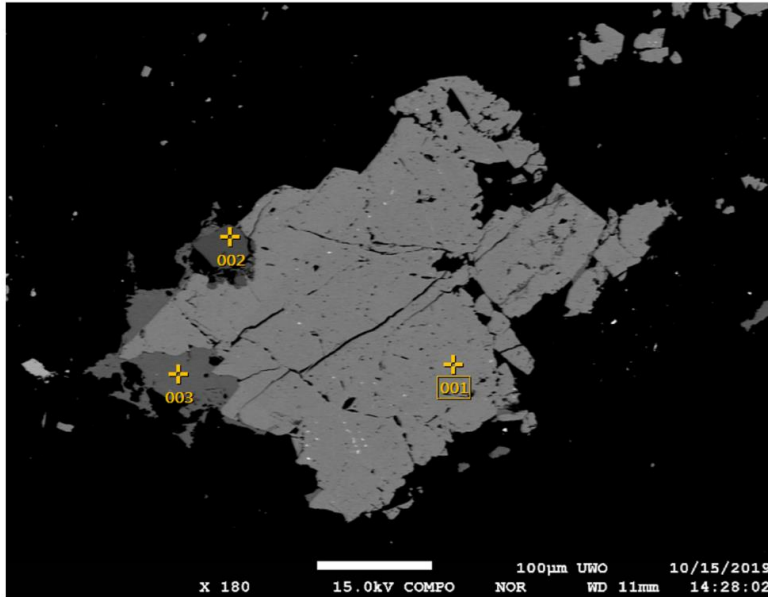
Volt : 15.00 kV
 Mag. : x 850
 Date : 2019/10/15
 Pixel : 1280 x 960



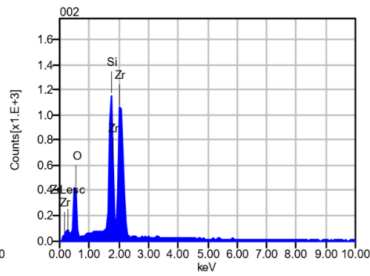
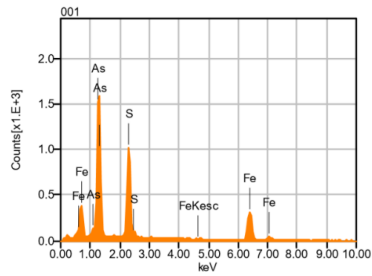
Acquisition Condition
 Instrument : 8530F
 Volt : 15.00 kV
 Current : ---
 Process Time : T2
 Live time : 10.00 sec.
 Real Time : 10.33 sec.
 DeadTime : 3.00 %
 Count Rate : 6203.00 CPS

	Fe	O	Mg	Al	Si	S	Cu	As
001	33.77					32.18	34.04	
002	33.59					31.28	35.12	
003	33.80					31.32	34.88	
004	49.75					50.25		
005	36.93	37.40	2.17	10.75	12.74			
006	35.72					17.00		47.28
Average	37.26	37.40	2.17	10.75	12.74	32.41	34.68	47.28
Deviation	6.26	0.00	0.00	0.00	0.00	11.82	0.57	0.00

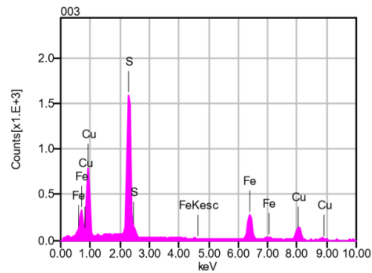
1539B_spot 2_EDS: Fractured subhedral arsenopyrite with zircon as inclusions and chalcopyrite on the edge. Fine-grained pyrite inside. (001: arsenopyrite, 002: zircon, 003: chalcopyrite)



Volt : 15.00 kV
 Mag. : x 180
 Date : 2019/10/15
 Pixel : 1280 x 960

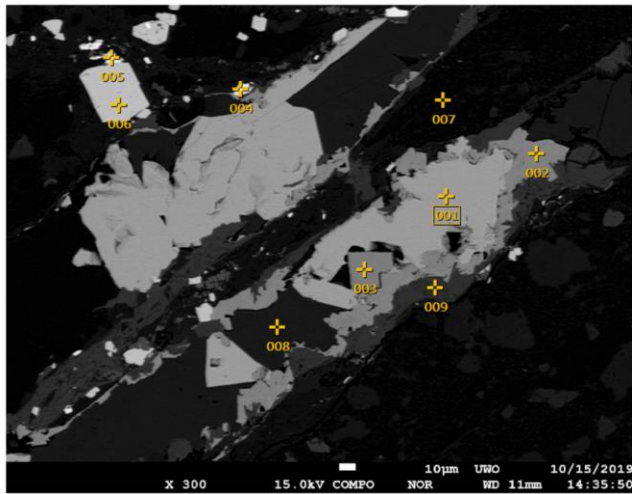


Acquisition Condition
 Instrument : 8530F
 Volt : 15.00 kV
 Current : ---
 Process Time : T2
 Live time : 10.00 sec.
 Real Time : 10.35 sec.
 DeadTime : 3.00 %
 Count Rate : 6638.00 CPS

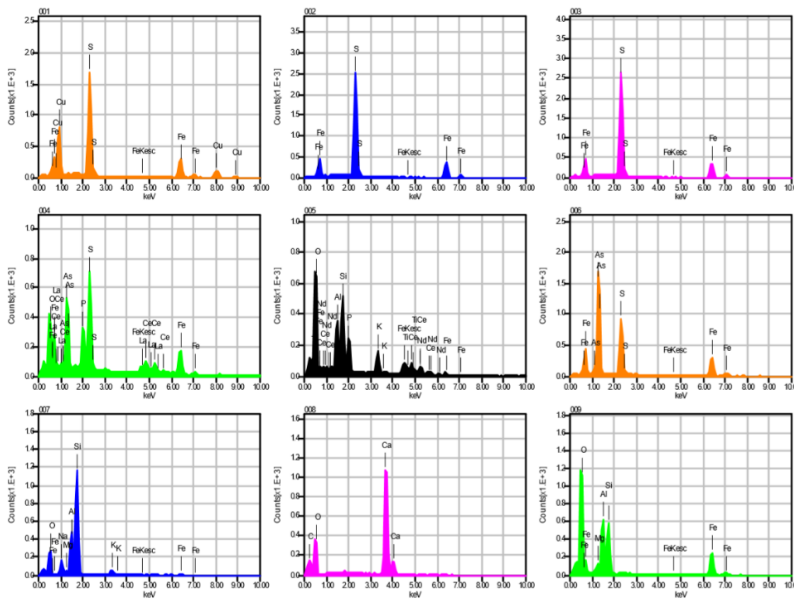


	Fe	O	Si	S	Cu	As	Zr
001	35.43			19.51		45.06	
002		30.28	16.31				53.41
003	32.86			31.60	35.54		
Average	34.15	30.28	16.31	25.56	35.54	45.06	53.41
Deviation	1.81	0.00	0.00	8.55	0.00	0.00	0.00

1539B_spot 3_EDS: Square euhedral arsenopyrite with chlorite, fractured chalcopyrite with fine grained arsenopyrite on the edge, pyrite overgrew outside fractured chalcopyrite and with subhedral arsenopyrite inside and chlorite on the edge; the groundmass is calcite and muscovite. (001: chalcopyrite, 002&003: pyrite, 004&006: arsenopyrite, 005&007: muscovite, 008: calcite, 009: chlorite)



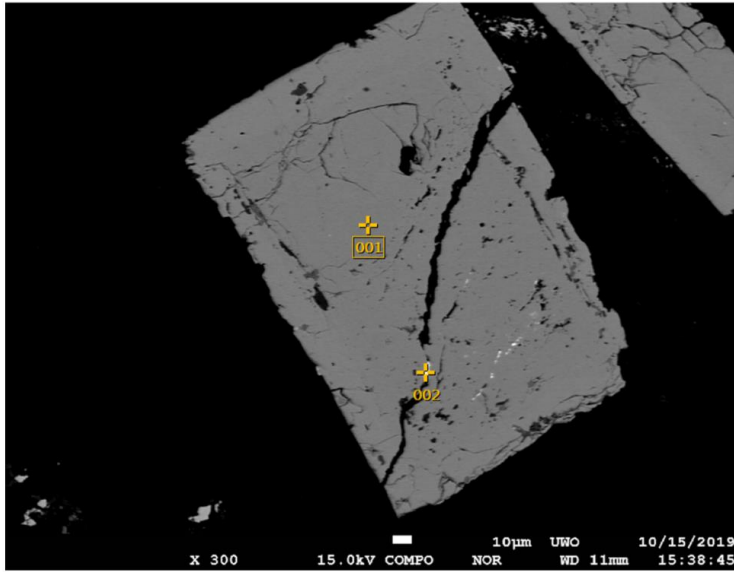
Volt : 15.00 kV
 Mag. : x 300
 Date : 2019/10/15
 Pixel : 1280 x 960



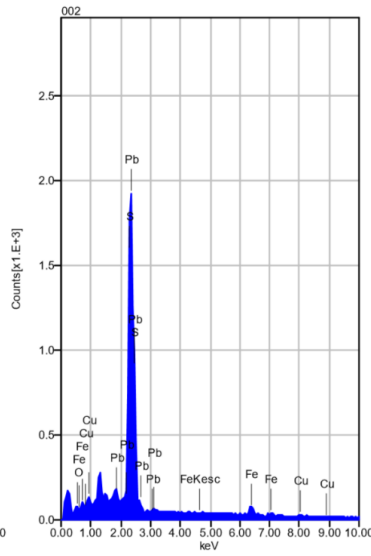
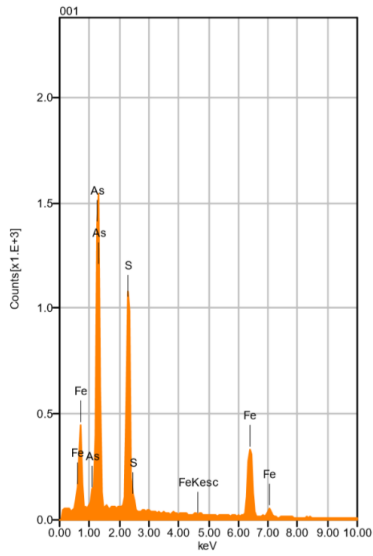
Acquisition Condition
 Instrument : 8530F
 Volt : 15.00 kV
 Current : ---
 Process Time : T2
 Live time : 10.00 sec.
 Real Time : 10.35 sec.
 DeadTime : 3.00 %
 Count Rate : 6287.00 CPS

	P	Fe	K	O	C	Na	Mg	Al	Si	S	Ca	Ti	Cu	As	La	Ce	N
001		33.92								32.95			33.13				
002		49.85								50.15							
003		49.82								50.18							
004	6.64	21.77		14.63						15.14				18.92	7.34	15.56	
005	6.63	3.14	6.06	37.31				7.66	11.99			4.98		47.09		16.10	€
006		34.73								18.18							
007		4.67	4.57	27.53		5.45	1.06	12.74	43.97								
008		37.63		43.79	5.99			2.15	10.59	11.81	50.22						
009		37.63		37.82				1.61	10.33	22.59							
Average	6.63	29.44	5.32	32.22	5.99	5.45	1.61	10.33	22.59	33.32	50.22	4.98	33.13	33.01	7.34	15.83	€
Deviation	0.00	18.17	1.06	11.43	0.00	0.00	0.77	2.55	18.52	16.79	0.00	0.00	0.00	19.92	0.00	0.38	C

2845_spot 1_EDS1: Fractured euhedral arsenopyrite with galena filled in fractures and as inclusions (001: arsenopyrite, 002: galena)



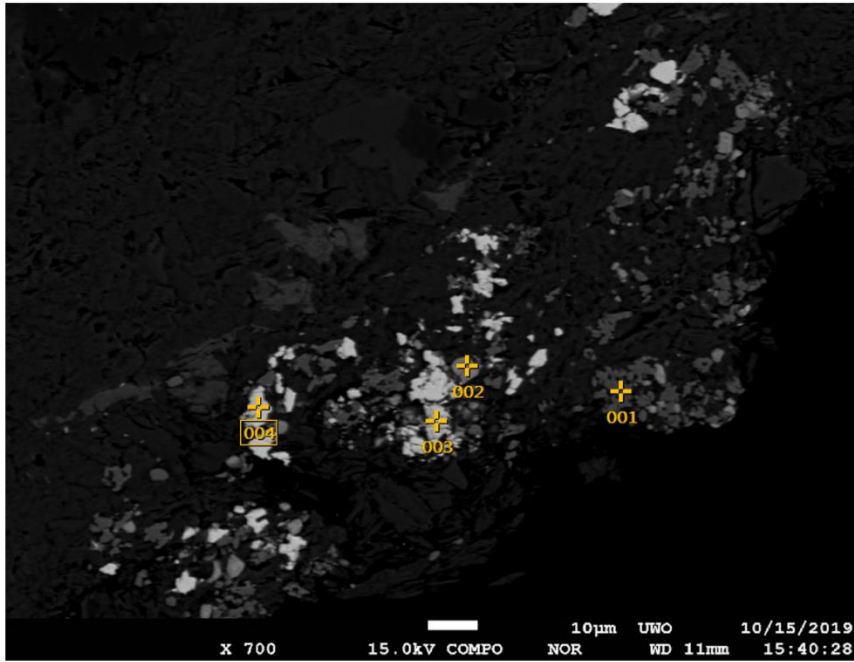
Volt : 15.00 kV
 Mag. : x 300
 Date : 2019/10/15
 Pixel : 1280 x 960



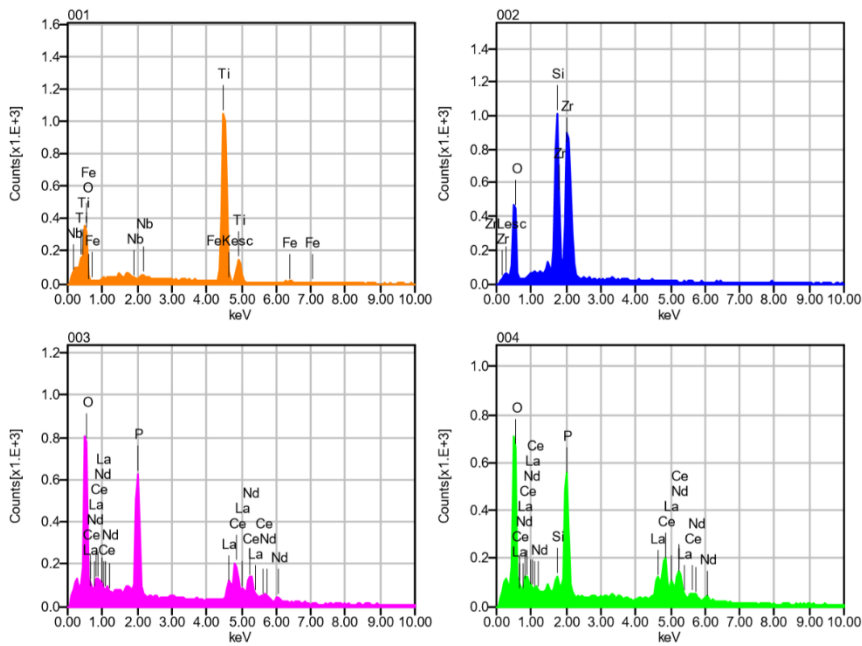
Acquisition Condition
 Instrument : 8530F
 Volt : 15.00 kV
 Current : ---
 Process Time : T2
 Live time : 10.00 sec.
 Real Time : 10.34 sec.
 DeadTime : 3.00 %
 Count Rate : 6548.00 CPS

	Fe	O	Pb	S	Cu	As
001	37.20			20.63		42.17
002	5.95	1.48	75.76	13.69	3.11	
Average	21.58	1.48	75.76	17.16	3.11	42.17
Deviation	22.10	0.00	0.00	4.90	0.00	0.00

2845_spot 1_EDS2: Fine-grained rutile, zircon, and monazite (001: rutile, 002: zircon, 003&004: monazite)



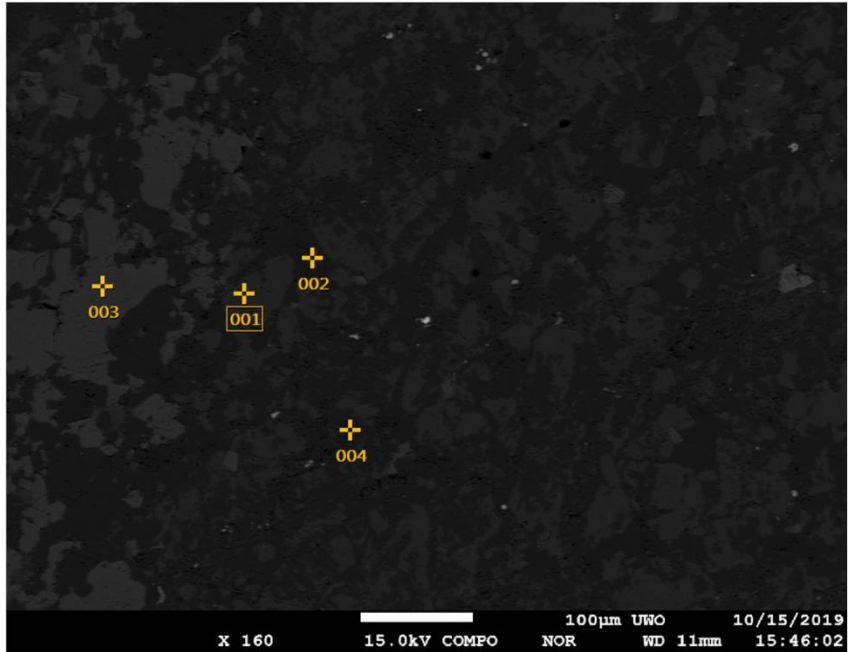
Volt : 15.00 kV
 Mag. : x 700
 Date : 2019/10/15
 Pixel : 1280 x 960



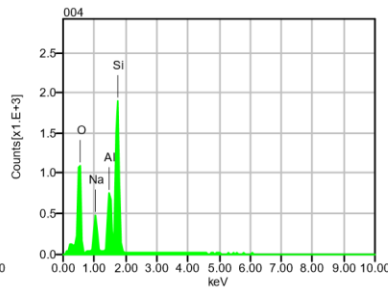
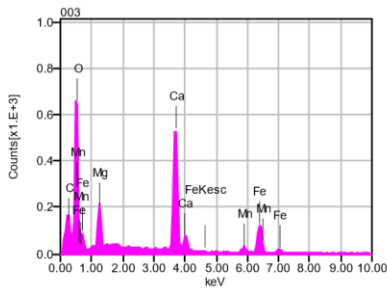
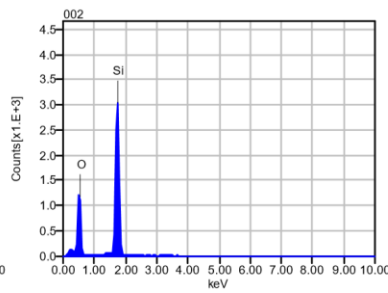
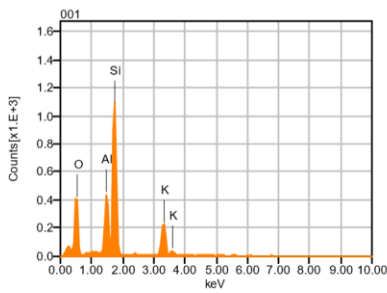
Acquisition Condition
 Instrument : 8530F
 Volt : 15.00 kV
 Current : ---
 Process Time : T2
 Live time : 10.00 sec.
 Real Time : 10.28 sec.
 DeadTime : 3.00 %
 Count Rate : 5381.00 CPS

	P	Fe	O	Si	Ti	Zr	Nb	La	Ce	Nd
001		1.07	34.71		62.96		1.27			
002			35.56	15.36		49.07				
003	15.05		26.46					15.66	31.93	10.91
004	14.07		23.85	1.25				17.39	33.93	9.52
Average	14.56	1.07	30.14	8.30	62.96	49.07	1.27	16.52	32.93	10.21
Deviation	0.70	0.00	5.87	9.98	0.00	0.00	0.00	1.23	1.42	0.98

2845_spot 2_EDS1: K-feldspar (001), quartz (002), ankerite (003), and albite (004) groundmass



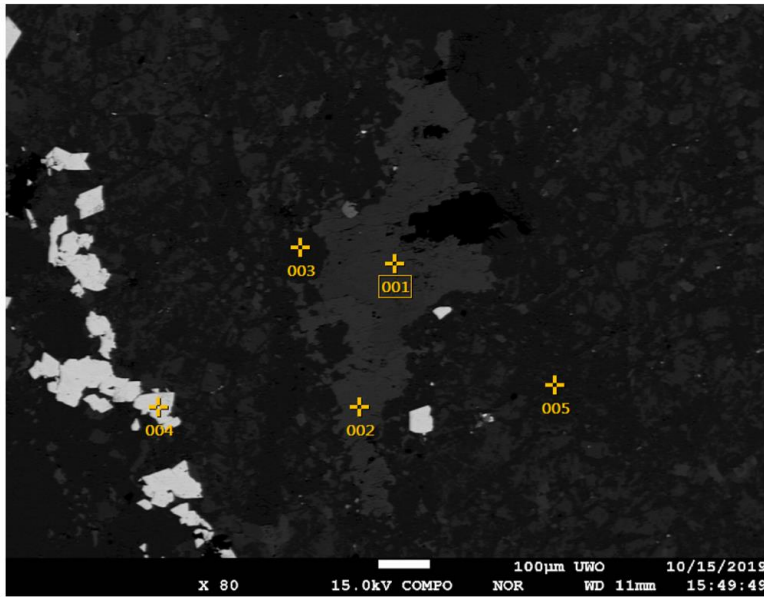
Volt : 15.00 kV
 Mag. : x 160
 Date : 2019/10/15
 Pixel : 1280 x 960



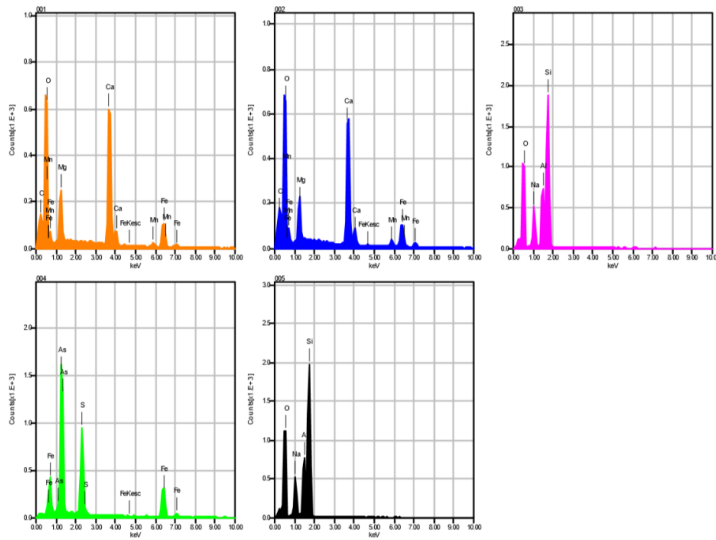
Acquisition Condition
 Instrument : 8530F
 Volt : 15.00 kV
 Current : ---
 Process Time : T2
 Live time : 5.83 sec.
 Real Time : 5.99 sec.
 DeadTime : 3.00 %
 Count Rate : 5241.00 CPS

	Fe	K	O	C	Na	Mg	Al	Si	Ca	Mn
001		15.94	41.16				9.99	32.91		
002			50.14					49.86		
003	20.00		43.18	6.43		3.70			23.44	3.25
004			45.52		7.85		11.53	35.09		
Average	20.00	15.94	45.00	6.43	7.85	3.70	10.76	39.29	23.44	3.25
Deviation	0.00	0.00	3.86	0.00	0.00	0.00	1.09	9.22	0.00	0.00

2845_spot 3_EDS1: Fractured medium grained arsenopyrite in ankerite and albite groundmass
 (001&002: ankerite, 003&005: albite, 004: arsenopyrite)



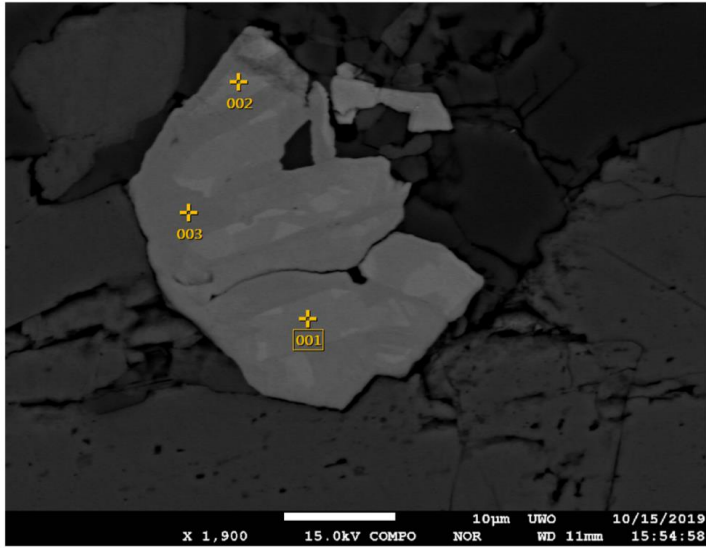
Volt : 15.00 kV
 Mag. : x 80
 Date : 2019/10/15
 Pixel : 1280 x 960



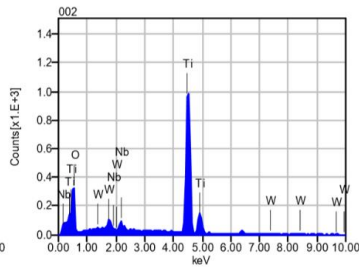
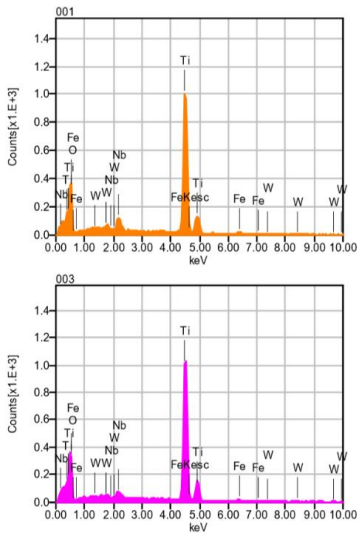
Acquisition Condition
 Instrument : 8530F
 Volt : 15.00 kV
 Current : ---
 Process Time : T2
 Live time : 10.00 sec.
 Real Time : 10.19 sec.
 DeadTime : 2.00 %
 Count Rate : 3686.00 CPS

	Fe	O	C	Na	Mg	Al	Si	S	Ca	Mn	Z
001	17.33	44.70	5.34		4.68				25.67	2.28	?
002	16.88	44.83	7.27		4.00				23.94	3.07	
003		44.07		8.57		11.16	36.20				
004	35.51							18.90			?
005		45.02		8.32		11.09	35.57				
Average	23.24	44.66	6.31	8.44	4.34	11.13	35.88	18.90	24.81	2.68	?
Deviation	10.63	0.41	1.37	0.18	0.48	0.05	0.44	0.00	1.22	0.56	(

2845_spot3_EDS2: rutile (001-003)



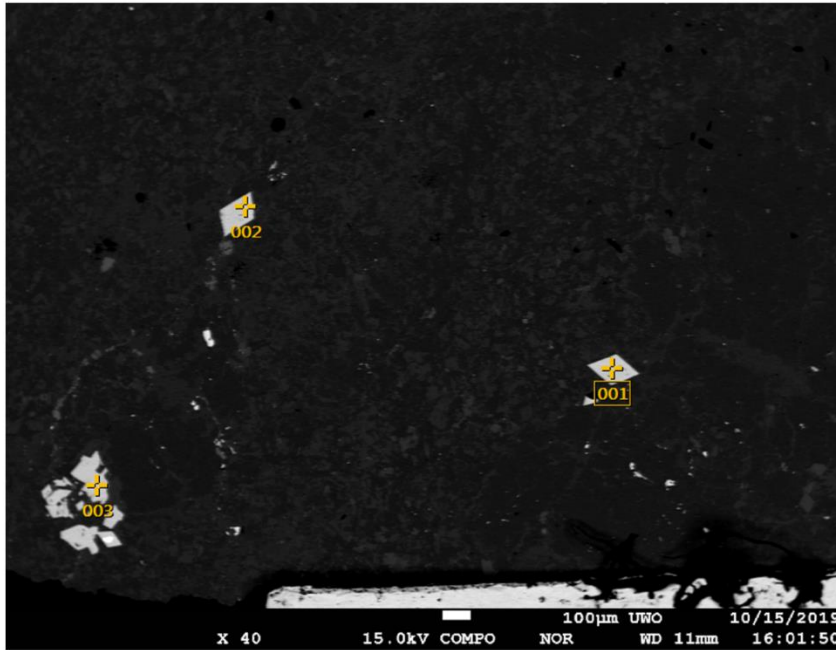
Volt : 15.00 kV
 Mag. : x 1,900
 Date : 2019/10/15
 Pixel : 1280 x 960



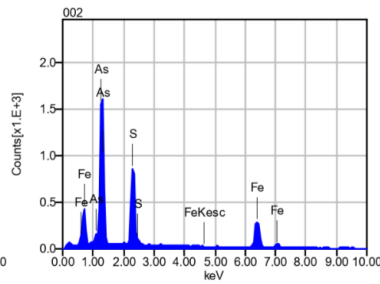
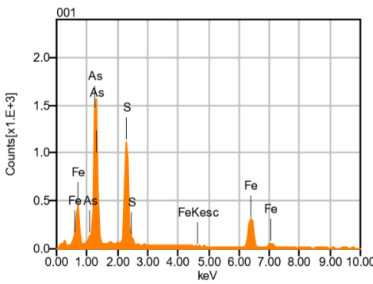
Acquisition Condition
 Instrument : 8530F
 Volt : 15.00 kV
 Current : ---
 Process Time : T2
 Live time : 10.00 sec.
 Real Time : 10.23 sec.
 DeadTime : 2.00 %
 Count Rate : 4266.00 CPS

	Fe	O	Ti	Nb	W
001	2.46	34.51	57.90	3.66	1.46
002		33.32	60.71	2.94	3.04
003	1.82	32.44	62.43	2.34	0.98
Average	2.14	33.43	60.35	2.98	1.82
Deviation	0.45	1.04	2.28	0.66	1.08

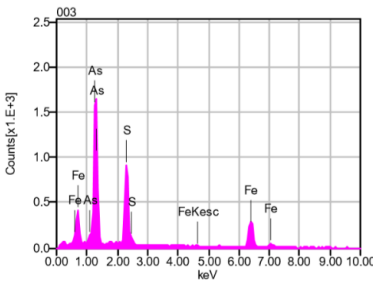
2845_spot4_EDS1: Disseminated fine grained euhedral-subhedral arsenopyrite (001-003)



Volt : 15.00 kV
 Mag. : x 40
 Date : 2019/10/15
 Pixel : 1280 x 960

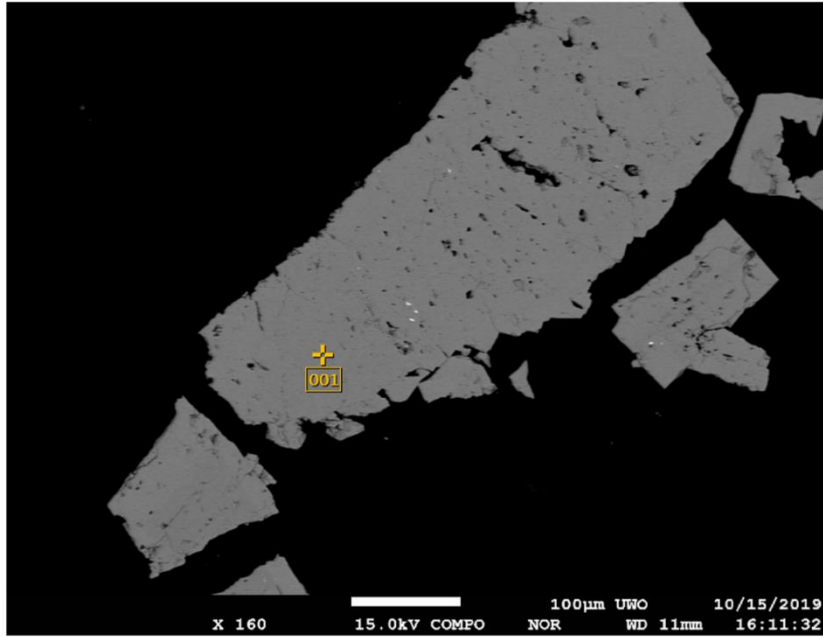


Acquisition Condition
 Instrument : 8530F
 Volt : 15.00 kV
 Current : ---
 Process Time : T2
 Live time : 10.00 sec.
 Real Time : 10.35 sec.
 DeadTime : 4.00 %
 Count Rate : 6726.00 CPS

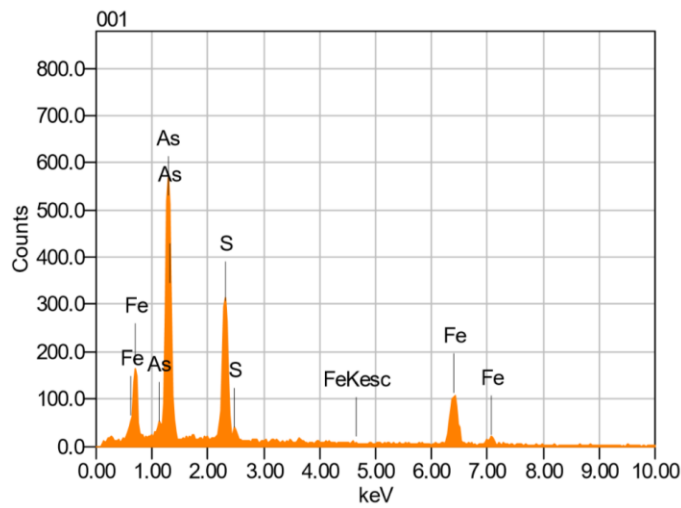


	Fe	S	As
001	35.81	20.55	43.64
002	34.71	17.56	47.73
003	34.16	18.02	47.82
Average	34.89	18.71	46.40
Deviation	0.84	1.61	2.39

2845_spot6_EDS1: corroded arsenopyrite grains (001)



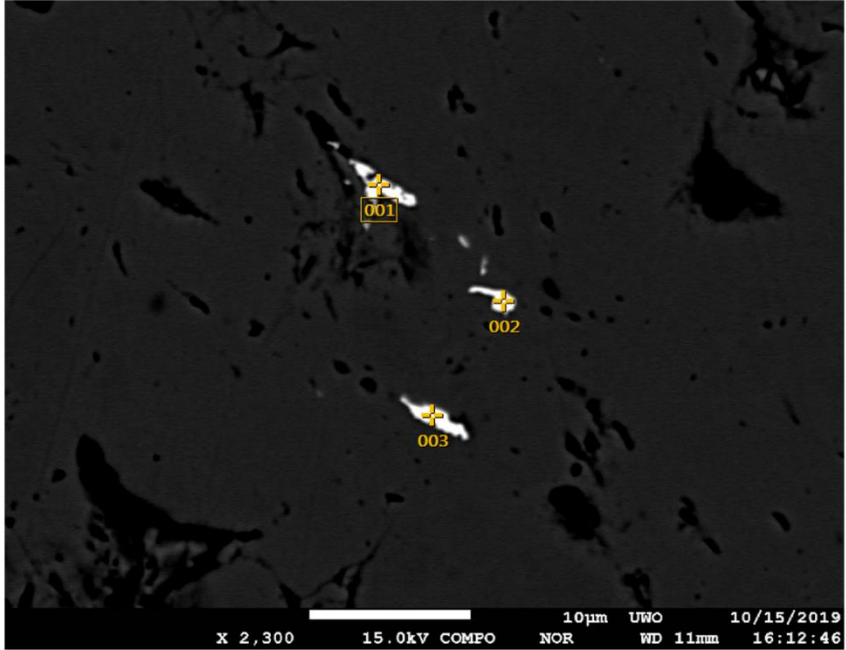
Volt : 15.00 kV
 Mag. : x 160
 Date : 2019/10/15
 Pixel : 1280 x 960



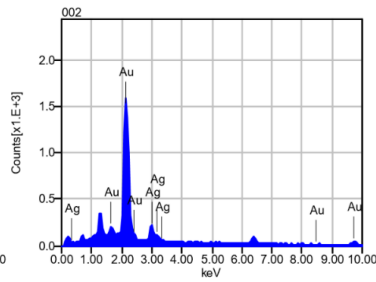
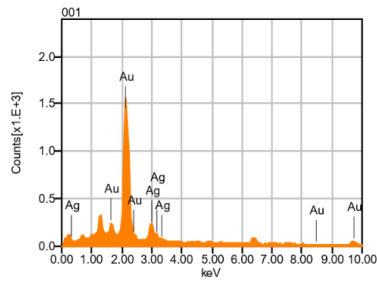
Acquisition Condition
 Instrument : 8530F
 Volt : 15.00 kV
 Current : ---
 Process Time : T2
 Live time : 3.26 sec.
 Real Time : 3.37 sec.
 DeadTime : 3.00 %
 Count Rate : 6791.00 CPS

Formula	mass%	Atom%	Sigma	Net	K ratio	Line
S	18.15	31.10	0.05	103746	3.2501248	K
Fe	35.39	34.82	0.13	56303	7.8717018	K
As*	46.47	34.08	0.16	181827	9.4999641	L
Total	100.00	100.00				

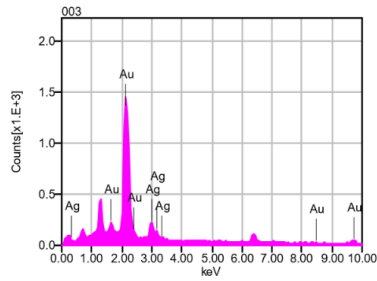
2845_spot 6_EDS2: Au + Ag grains (001-003) within arsenopyrite



Volt : 15.00 kV
 Mag. : x 2,300
 Date : 2019/10/15
 Pixel : 1280 x 960

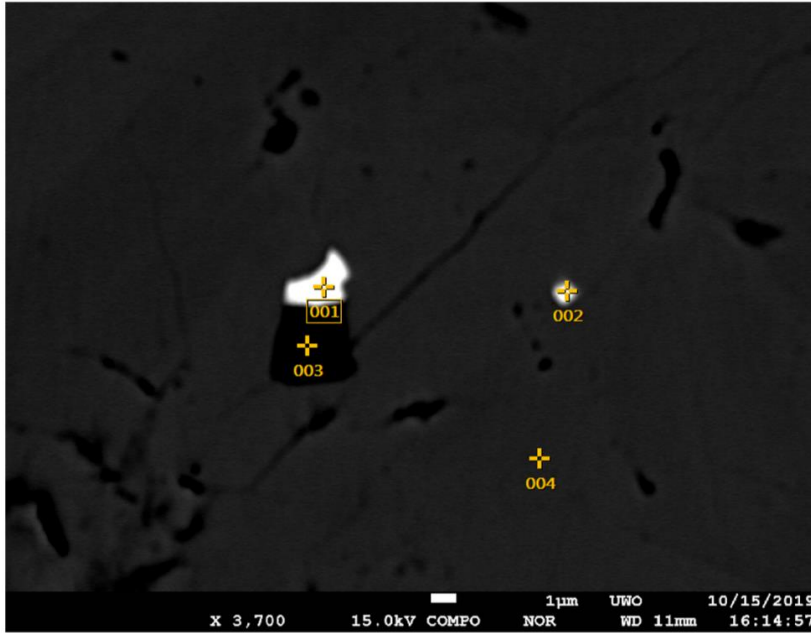


Acquisition Condition
 Instrument : 8530F
 Volt : 15.00 kV
 Current : ---
 Process Time : T2
 Live time : 10.00 sec.
 Real Time : 10.47 sec.
 DeadTime : 4.00 %
 Count Rate : 8414.00 CPS

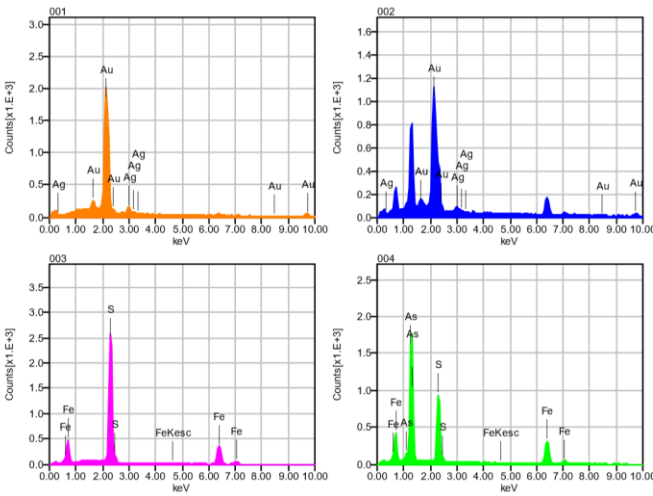


	Au	Ag
001	84.38	15.62
002	86.55	13.45
003	84.55	15.45
Average	85.16	14.84
Deviation	1.20	1.20

2845_spot6_EDS3: Au + Ag grains inside an arsenopyrite + pyrite grain (001&002: Au + Ag, 003: pyrite, 004: arsenopyrite)



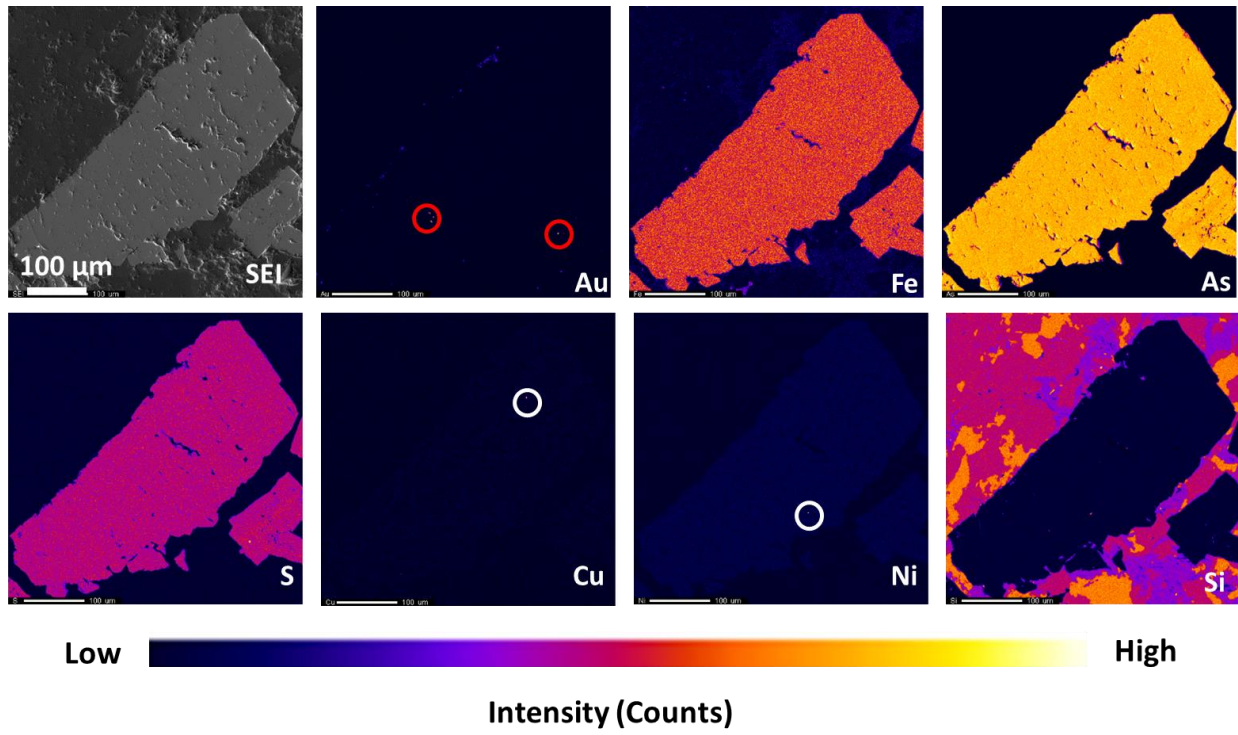
Volt : 15.00 kV
 Mag. : x 3,700
 Date : 2019/10/15
 Pixel : 1280 x 960



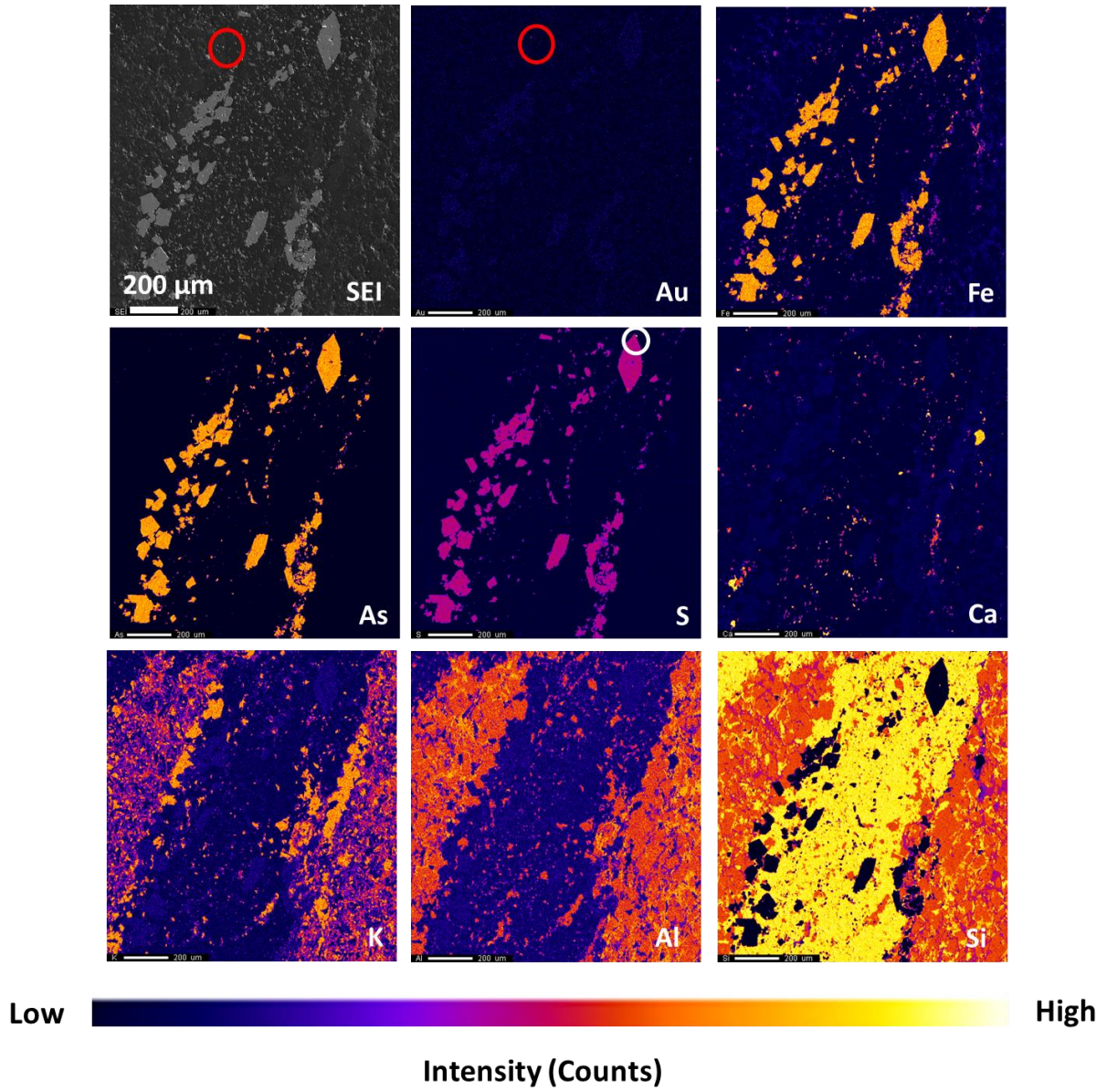
Acquisition Condition
 Instrument : 8530F
 Volt : 15.00 kV
 Current : ---
 Process Time : T2
 Live time : 10.00 sec.
 Real Time : 10.49 sec.
 DeadTime : 5.00 %
 Count Rate : 9071.00 CPS

	Fe	Au	Ag	S	As
001		92.39	7.61		
002		92.67	7.33		
003	50.87			49.13	
004	34.89			18.13	46.98
Average	42.88	92.53	7.47	33.63	46.98
Deviation	11.30	0.20	0.20	21.93	0.00

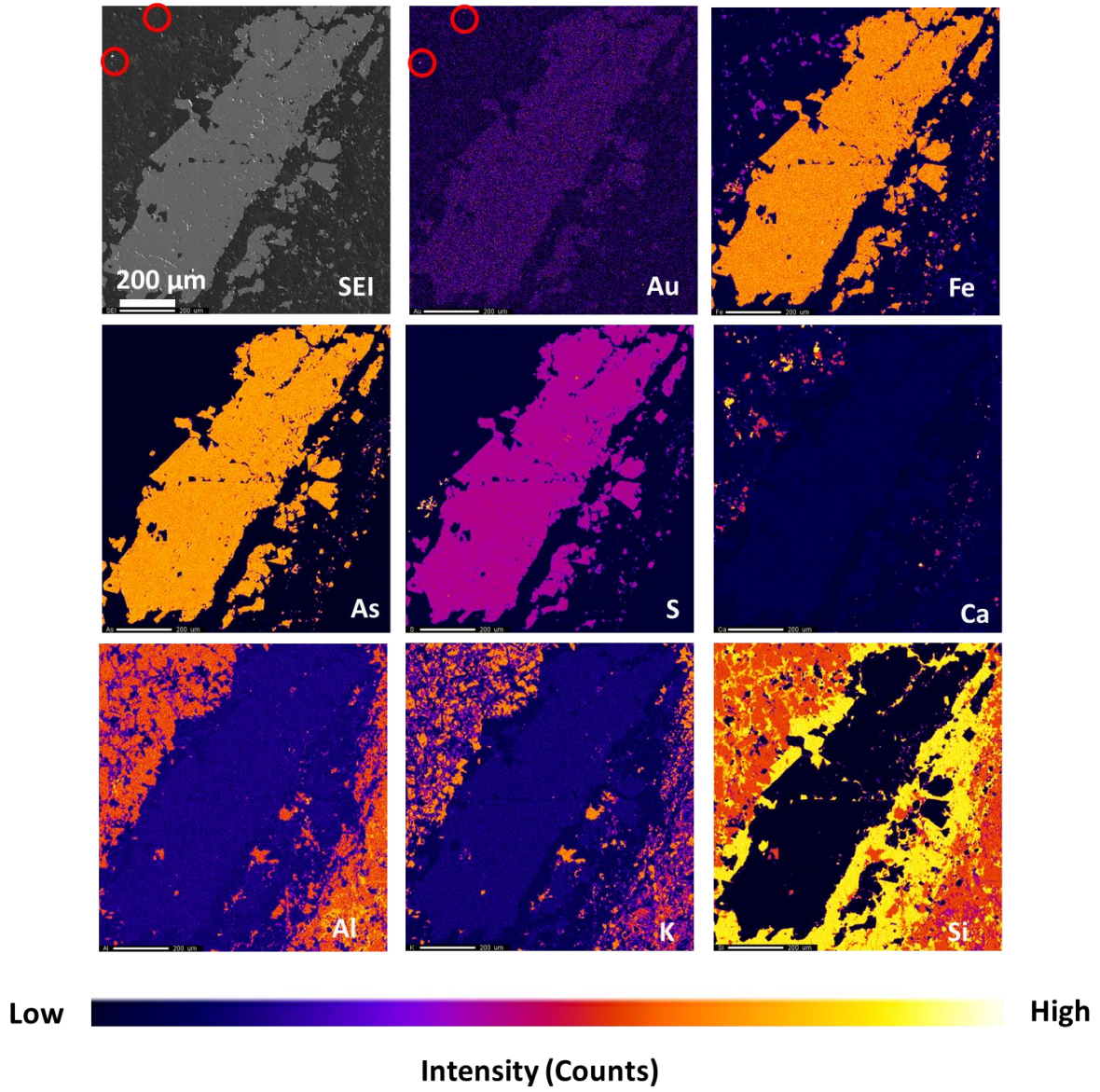
2845_spot6_arsenopyrite_1um_EDS: High intensity gold spots and chalcopyrite and sphalerite inclusions in arsenopyrite.



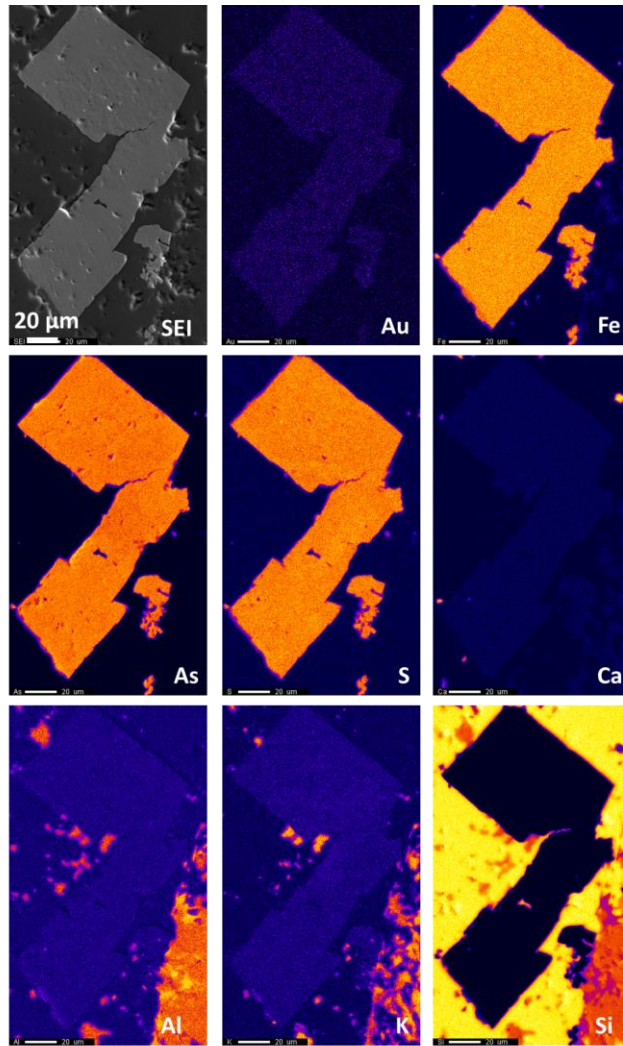
2827_1_3um-EDS/WDS: High intensity gold spot near euhedral arsenopyrite in quartz vein



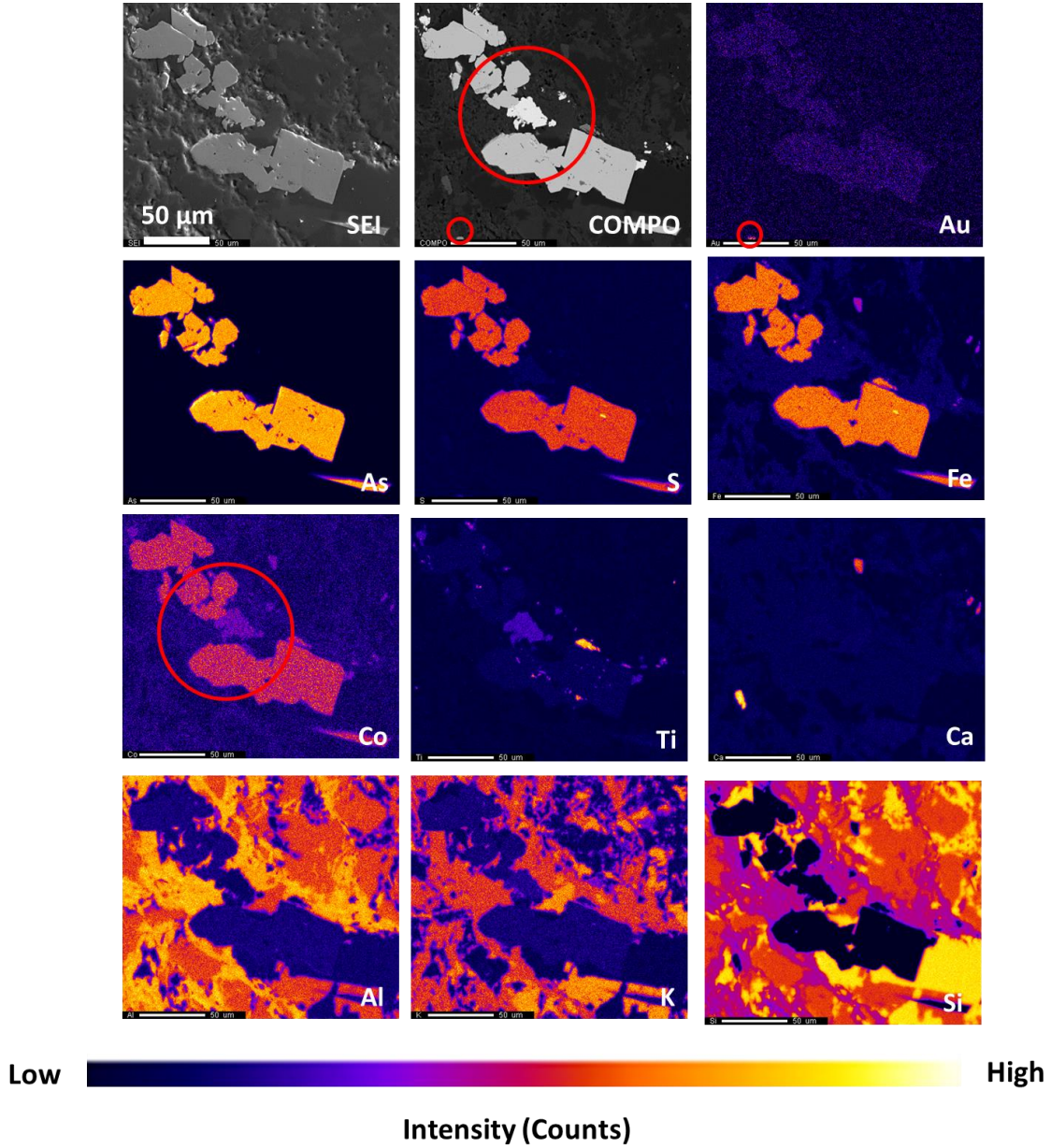
2827_2_2um-EDS/WDS: High intensity gold spots near arsenopyrite filled quartz vein



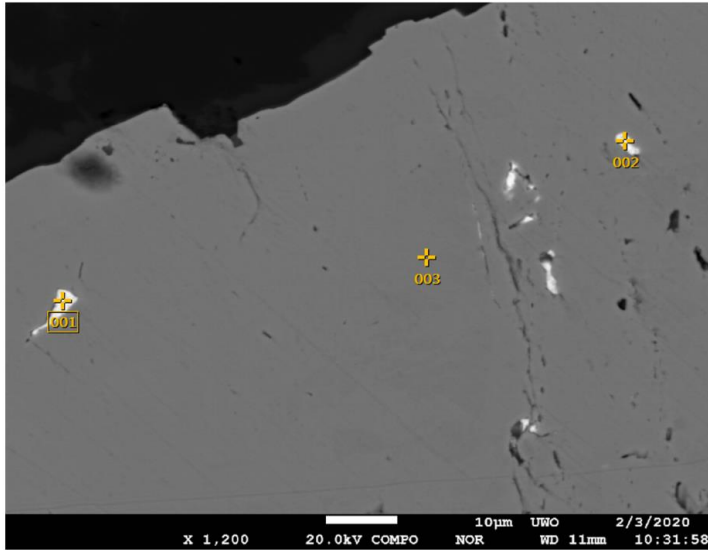
2827_3_4um_EDS/WDS: No gold within euhedral arsenopyrite



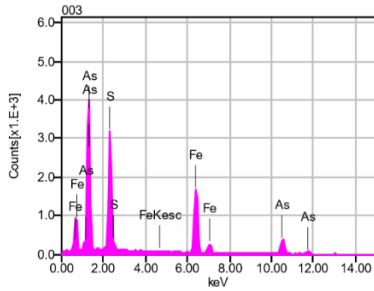
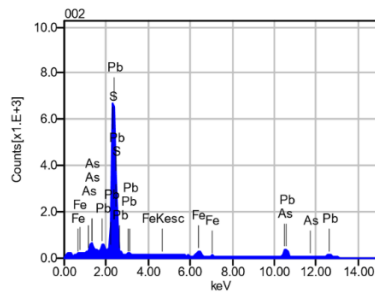
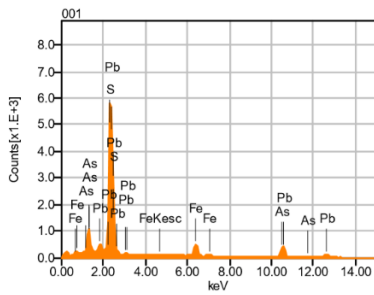
2827_4_5um_EDS/WDS: High intensity gold spots near subhedral arsenopyrite filled. The color difference in arsenopyrite is because the difference in the concentration of Co. Ti map: possible rutile inclusion inside arsenopyrite.



2819_EDS1: arsenopyrite inside galena (001&002: galena, 003: arsenopyrite)



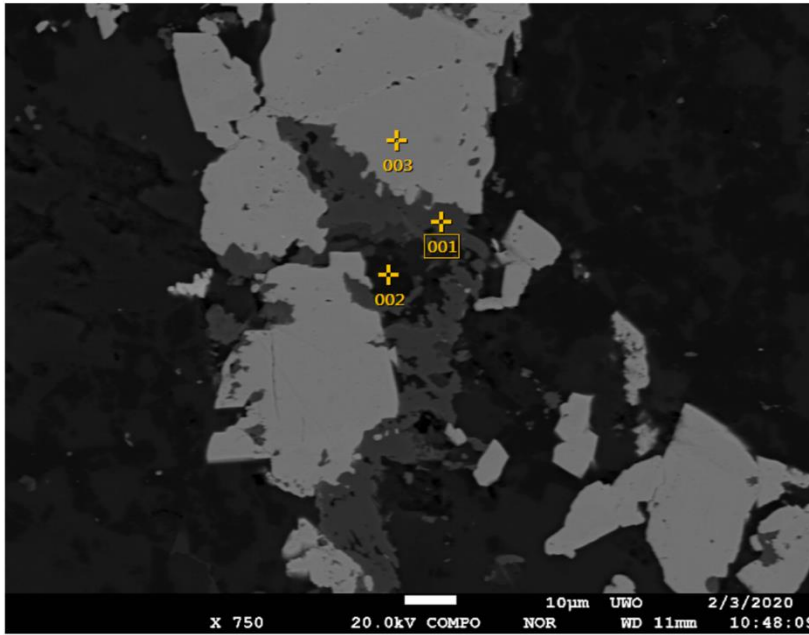
Volt : 20.00 kV
 Mag. : x 1,200
 Date : 2020/02/03
 Pixel : 1280 x 960



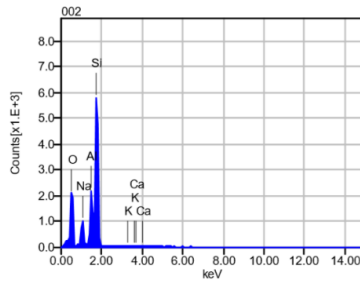
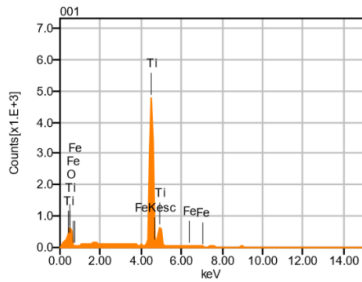
Acquisition Condition
 Instrument : 8530F
 Volt : 20.00 kV
 Current : ---
 Process Time : T2
 Live time : 10.00 sec.
 Real Time : 11.63 sec.
 DeadTime : 14.00 %
 Count Rate : 27352.00 CP

	Fe	Pb	S	As
001	9.55	68.33	11.67	10.45
002	4.43	76.18	11.29	8.09
003	36.79		18.73	44.48
Average	16.93	72.25	13.90	21.01
Deviation	17.40	5.55	4.19	20.36

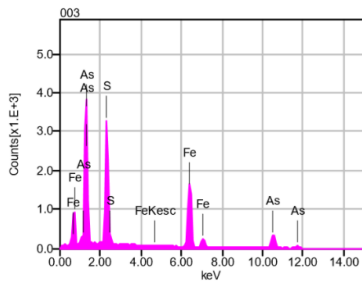
2819_EDS2: fractured arsenopyrite with rutile in albite groundmass (001: rutile, 002: albite, 003: arsenopyrite)



Volt : 20.00 kV
 Mag. : x 750
 Date : 2020/02/03
 Pixel : 1280 x 960

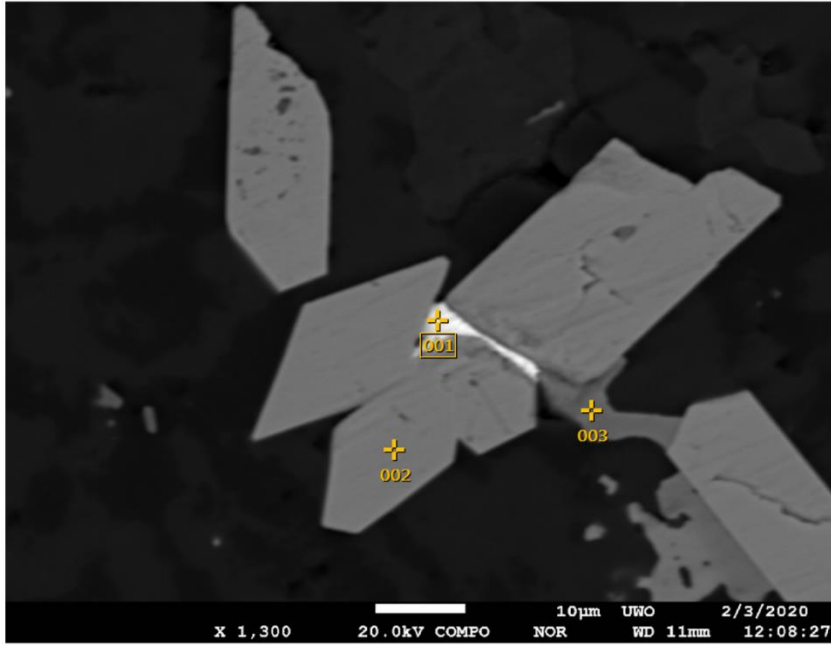


Acquisition Condition
 Instrument : 8530F
 Volt : 20.00 kV
 Current : ---
 Process Time : T2
 Live time : 10.00 sec.
 Real Time : 10.81 sec.
 DeadTime : 7.00 %
 Count Rate : 14370.00 CP

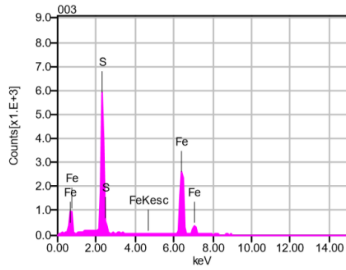
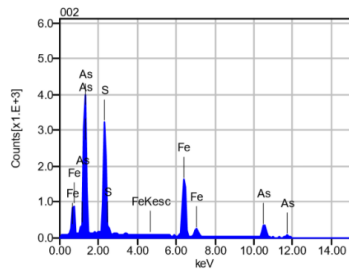
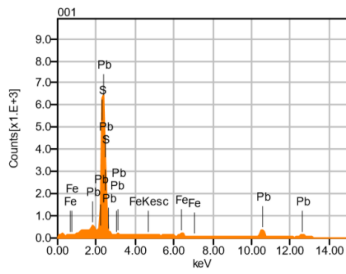


	Fe	K	O	Na	Al	Si	S	Ca	Ti	As
001	1.00		35.23						63.76	
002		0.41	46.52	7.03	10.80	34.79		0.46		
003	37.21						19.99			42.80
Average	19.11	0.41	40.87	7.03	10.80	34.79	19.99	0.46	63.76	42.80
Deviation	25.60	0.00	7.98	0.00	0.00	0.00	0.00	0.00	0.00	0.00

2857_EDS01: euhedral arsenopyrite, with intensive fractured anhedral pyrite, and galena overgrow between arsenopyrite grains (001: galena, 002: arsenopyrite, 003: pyrite)



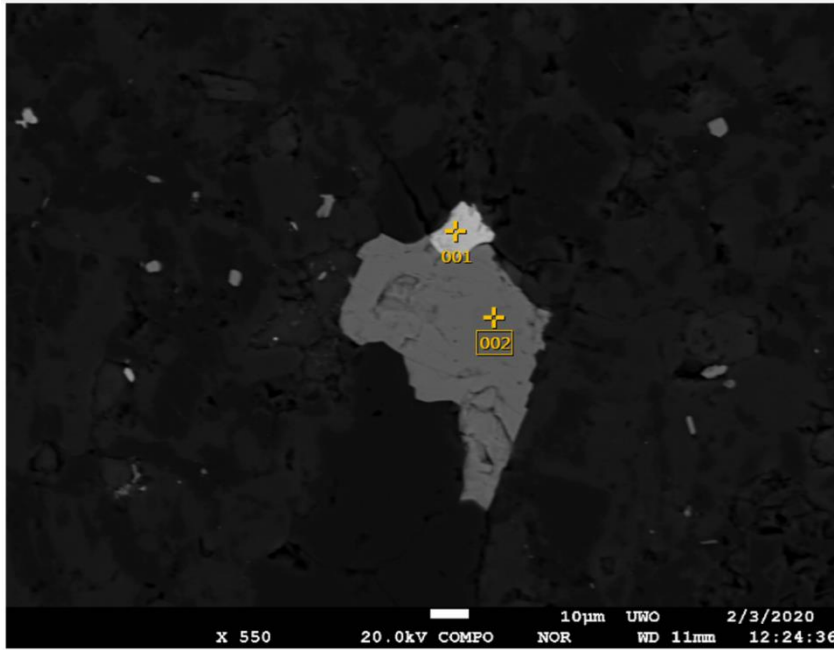
Volt : 20.00 kV
 Mag. : x 1,300
 Date : 2020/02/03
 Pixel : 1280 x 960



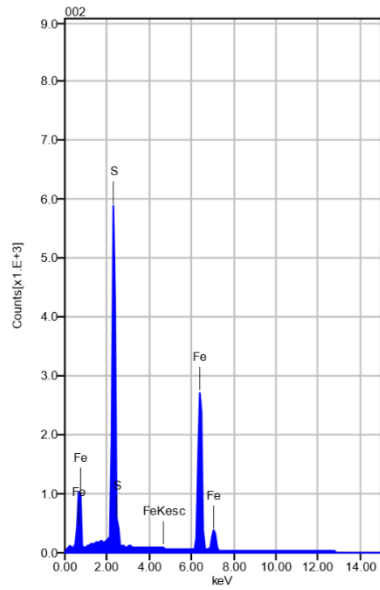
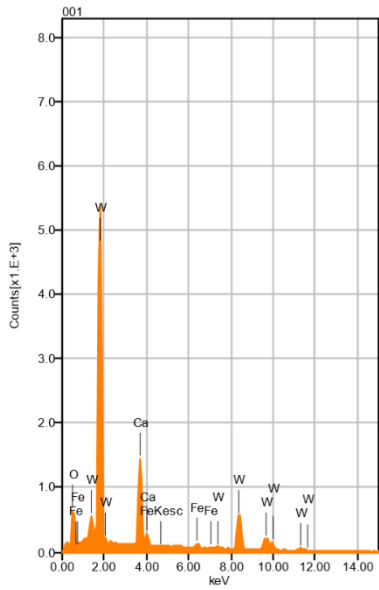
Acquisition Condition
 Instrument : 8530F
 Volt : 20.00 kV
 Current : ---
 Process Time : T2
 Live time : 10.00 sec.
 Real Time : 11.61 sec.
 DeadTime : 14.00 %
 Count Rate : 27550.00 CP

	Fe	Pb	S	As
001	2.99	85.50	11.51	
002	37.05		19.36	43.58
003	67.20		32.80	
Average	35.75	85.50	21.22	43.58
Deviation	32.13	0.00	10.76	0.00

2857_EDS02: scheelite (001) with pyrite (002)



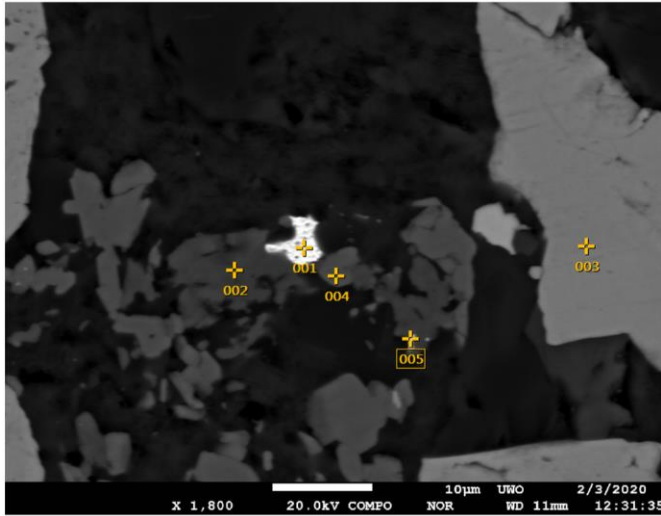
Volt : 20.00 kV
 Mag. : x 550
 Date : 2020/02/03
 Pixel : 1280 x 960



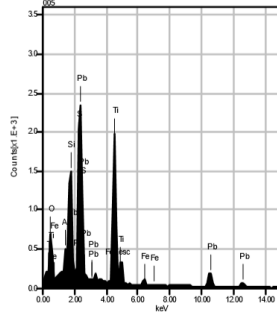
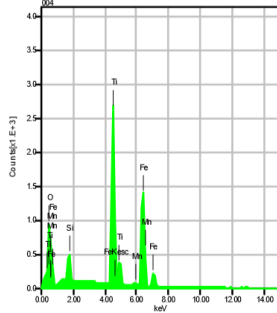
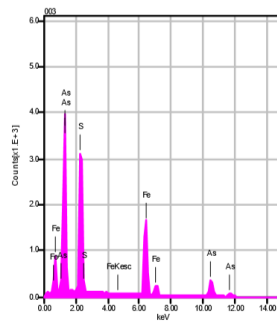
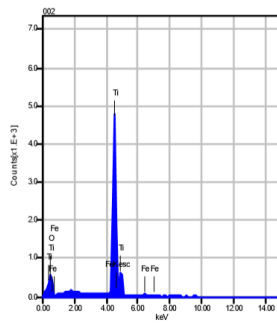
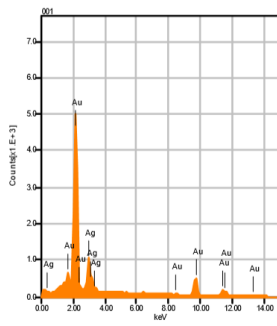
Acquisition Condition
 Instrument : 8530F
 Volt : 20.00 kV
 Current : ---
 Process Time : T2
 Live time : 10.00 sec.
 Real Time : 11.17 sec.
 DeadTime : 10.00 %
 Count Rate : 20721.00 CP

	Fe	O	S	Ca	W
001	1.12	16.61		11.75	70.52
002	67.57		32.43		
Average	34.35	16.61	32.43	11.75	70.52
Deviation	46.99	0.00	0.00	0.00	0.00

2857_EDS03_Au: 001: Au + Ag, 002&004: rutile, 003: arsenopyrite, 004: galena



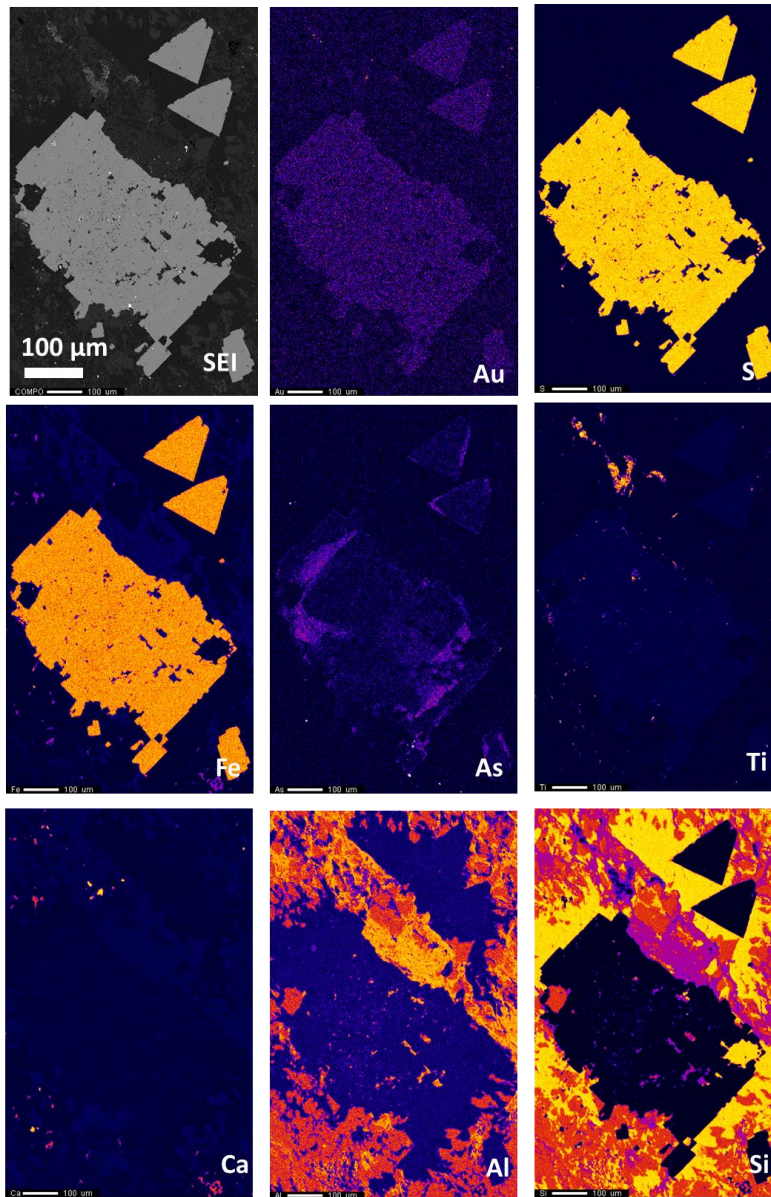
Volt : 20.00 kV
 Mag. : x 1,800
 Date : 2020/02/03
 Pixel : 1280 x 960



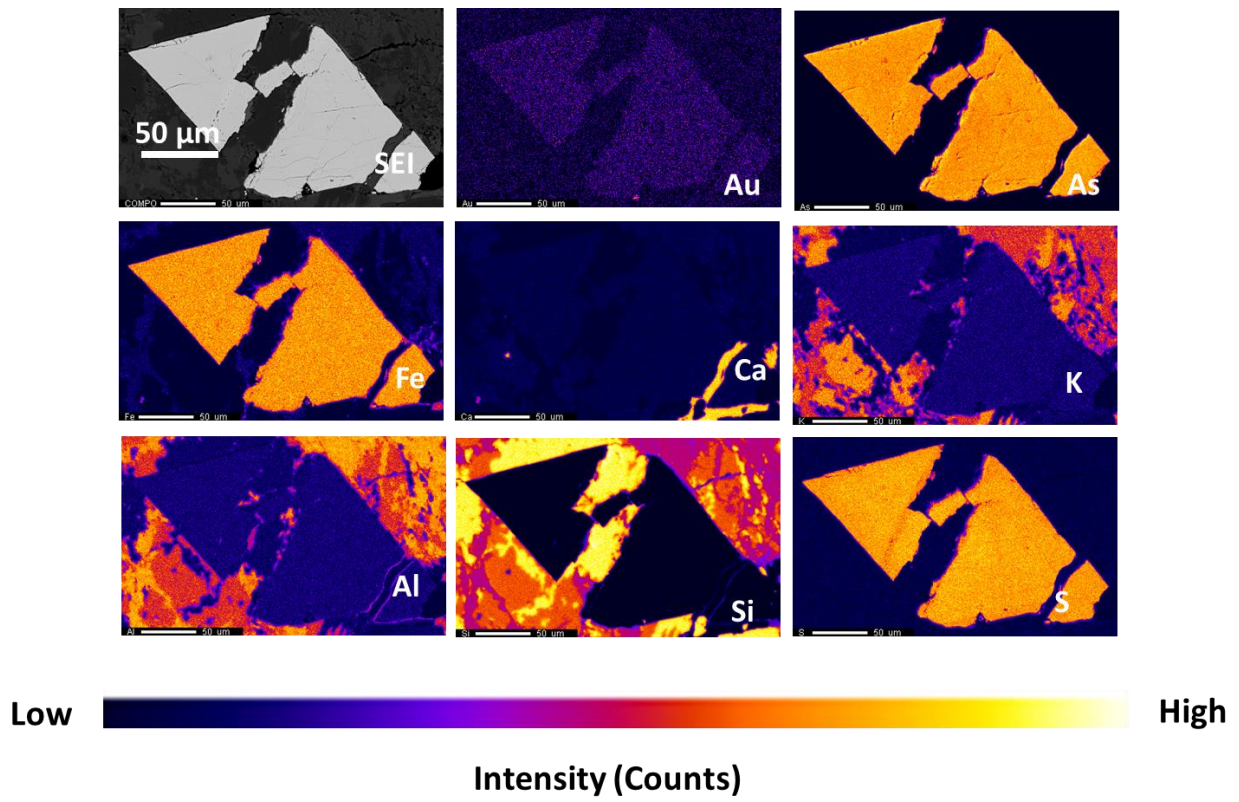
Acquisition Condition
 Instrument : 8530F
 Volt : 20.00 kV
 Current : ---
 Process Time : T2
 Live time : 10.00 sec.
 Real Time : 11.07 sec.
 DeadTime : 10.00 %
 Count Rate : 19242.00 CP

	Fe	O	Pb	Au	Ag	Al	Si	S	Ti	Mn	As
001				80.20	19.80						
002	1.04	35.56							63.40		
003	36.76							19.50			43.74
004	36.60	28.86					1.81		31.69	1.04	
005	1.52	21.91	36.52			1.61	6.29	4.17	27.98		
Average	18.98	28.78	36.52	80.20	19.80	1.61	4.05	11.83	41.02	1.04	43.74
Deviation	20.44	6.83	0.00	0.00	0.00	0.00	3.17	10.83	19.47	0.00	0.00

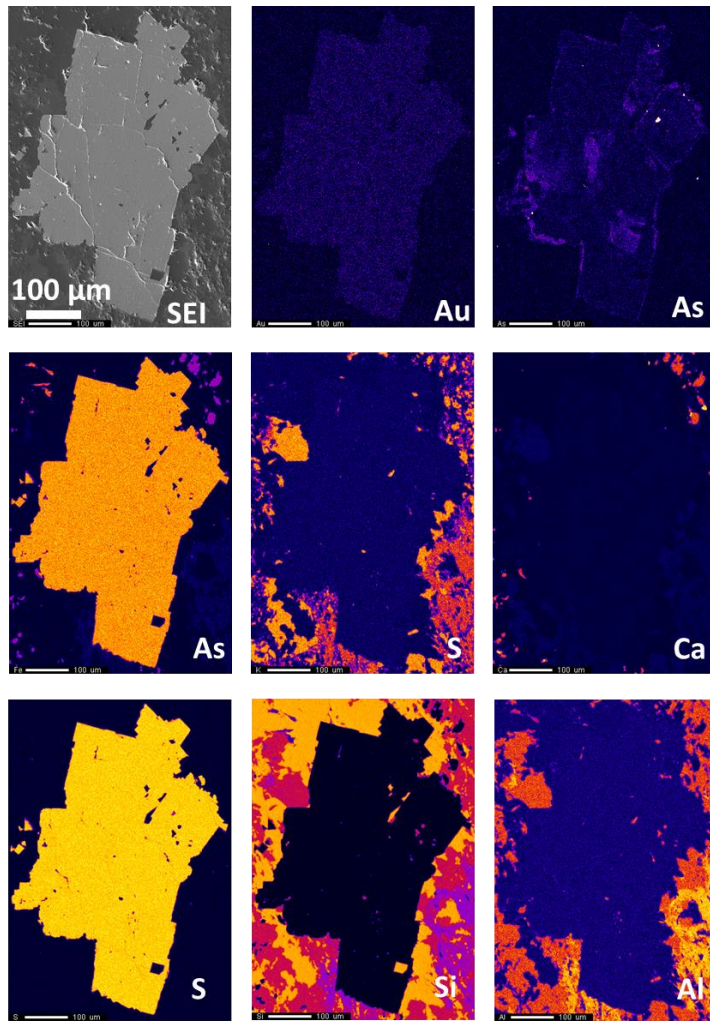
2824_1_2um EDS/WDS Element Maps: Corroded subhedral pyrite and needle-shaped pyrite show zoning texture. No high intensity gold spot.



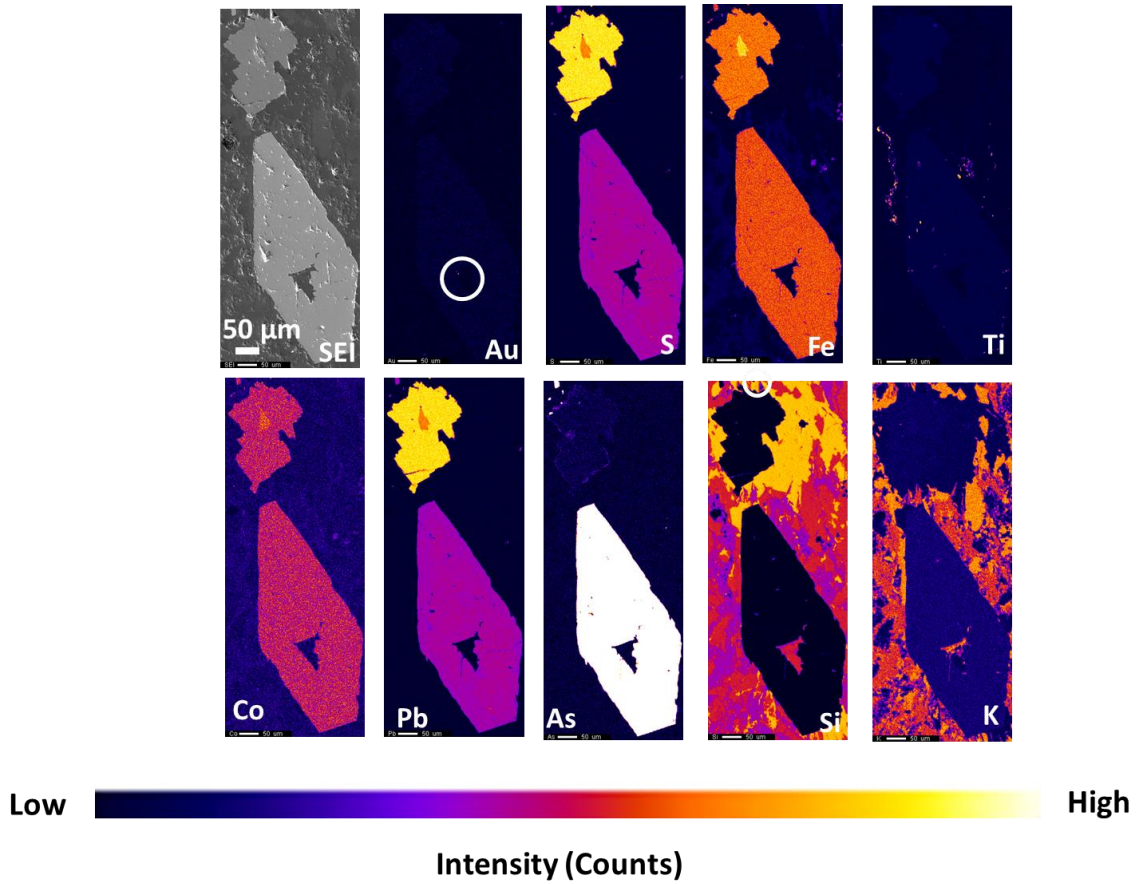
2824_2_7um EDS/WDS Element Maps: Needle arsenopyrite in quartz vein without high intensity gold spot.



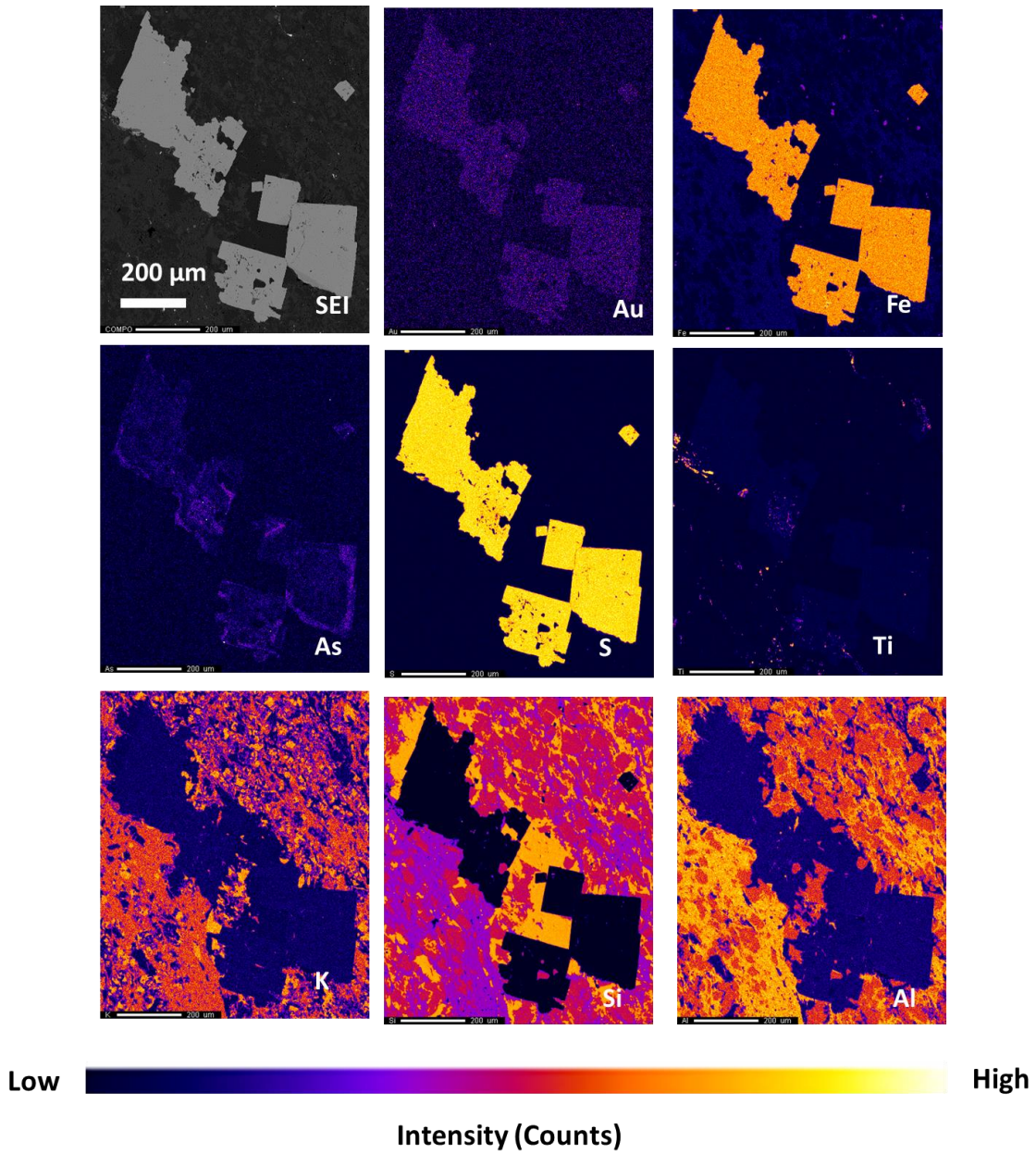
2824_3_5um EDS/WDS Element Maps: Corroded subhedral pyrite shows zoning texture and a few arsenopyrite filled in the fracture. No high intensity gold spot.



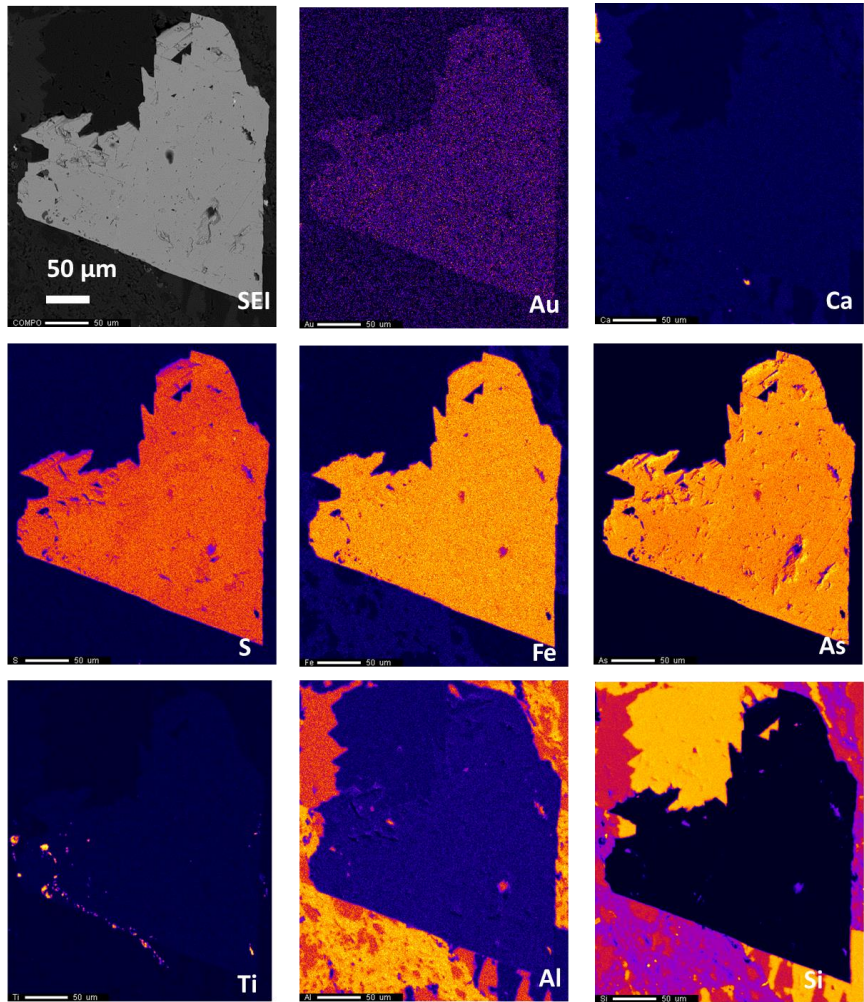
2824_4_5um EDS/WDS Element Maps: Euhedral arsenopyrite with high intensity gold spots in the pit. Anhedral pyrite shows zonation and with Pb&Co-rich inclusion inside (galena).



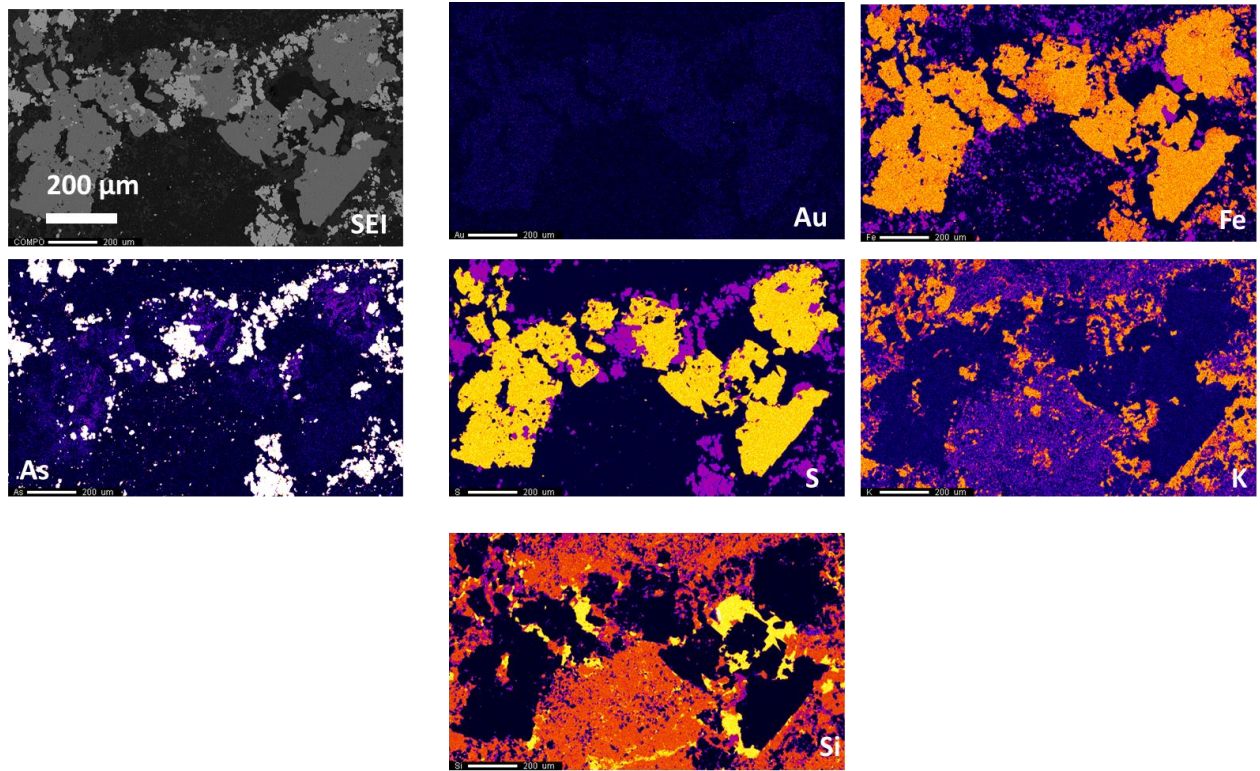
2824_5_2um EDS/WDS Element Maps: Euhedral to subhedral pyrite with zonation in As map.
No high intensity gold spot.



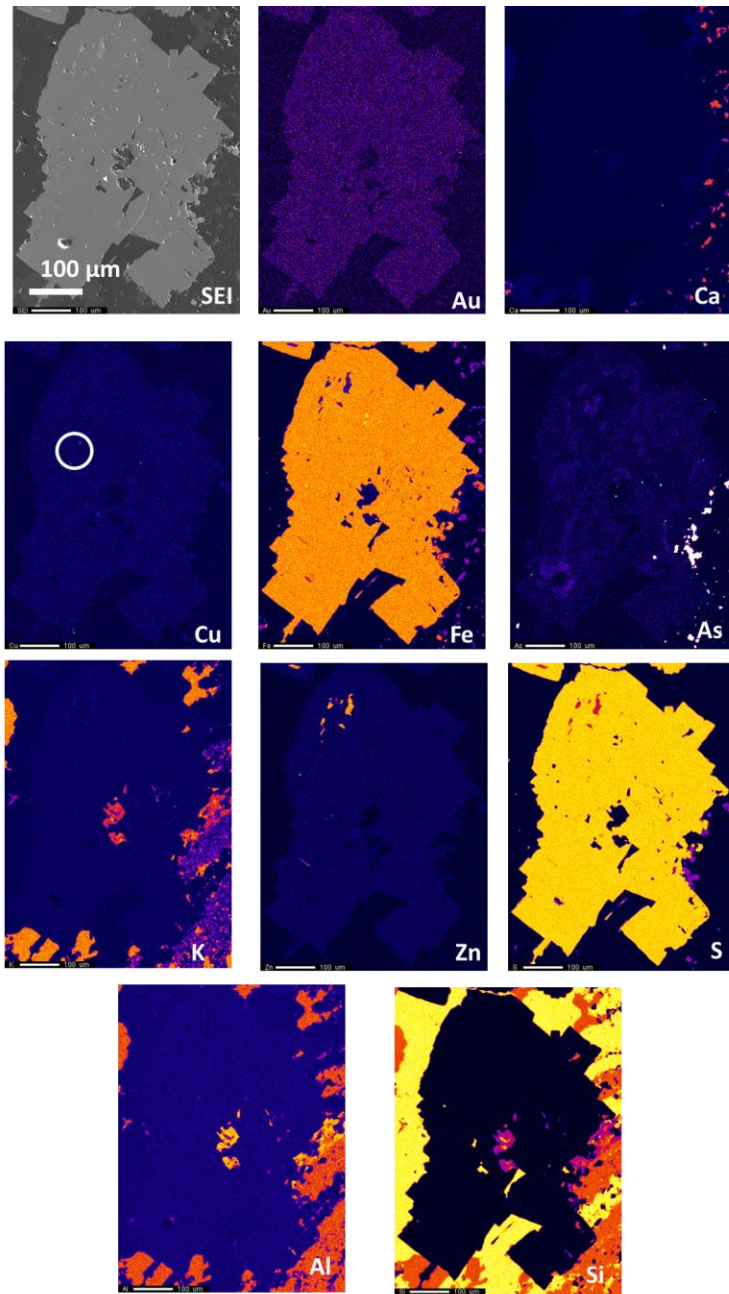
2824_6_8um EDS/WDS Element Maps: Subhedral arsenopyrite without gold.



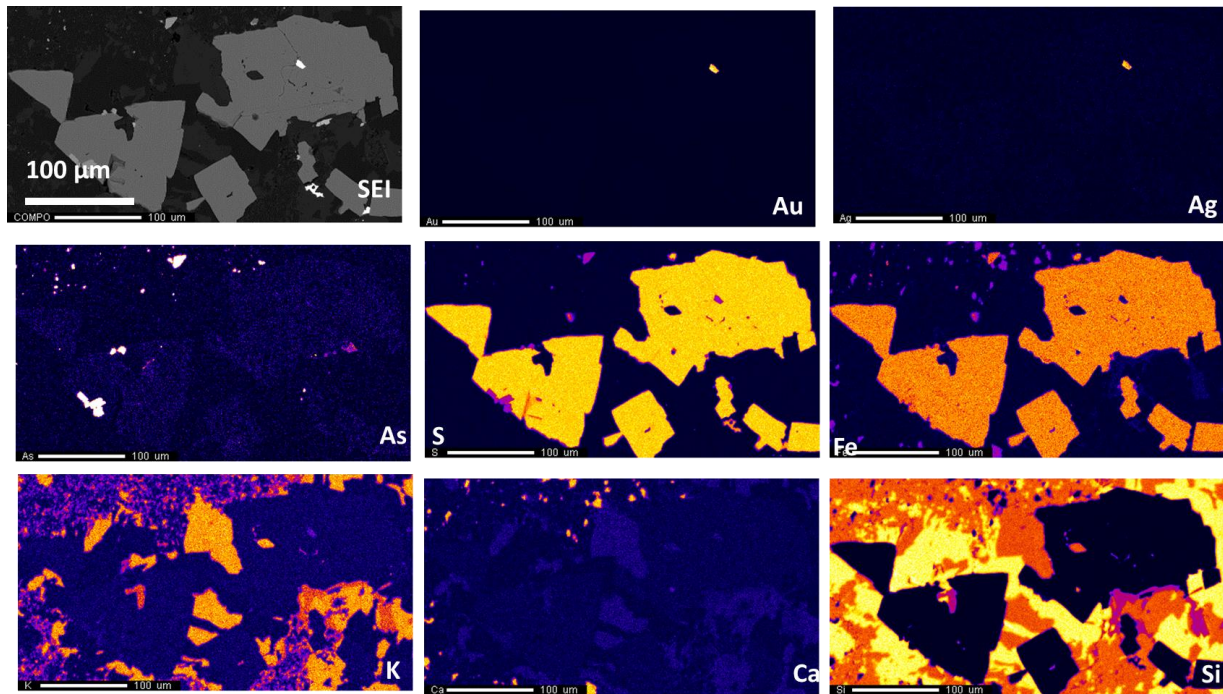
2841_1_3um EDS/WDS Element Maps: The combination of Arsenopyrite and pyrite without gold.



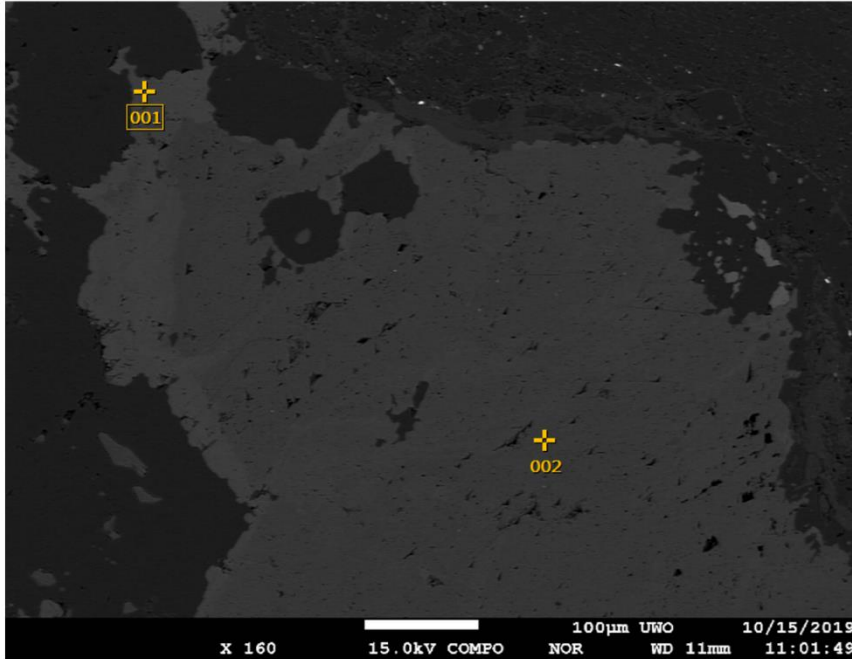
2841_2_5um EDS/WDS Element Maps: Corroded subhedral pyrite with zonation in As map and chalcopyrite and sphalerite inclusions inside. Arsenopyrite are on the edge. No gold.



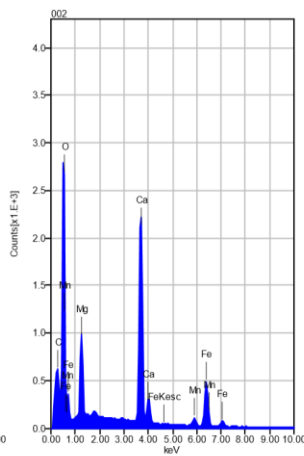
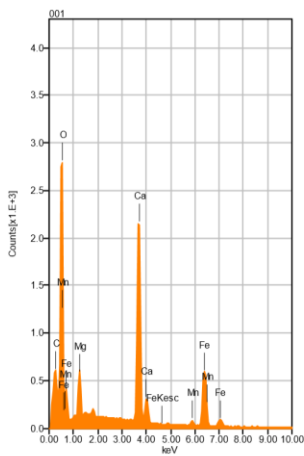
2841_4_1um EDS/WDS Element Maps: Au + Ag inside corroded pyrite, a few fine-grained arsenopyrite grains are on the edge of pyrite.



2834_spot1_carbonate: ankerite (001-002)



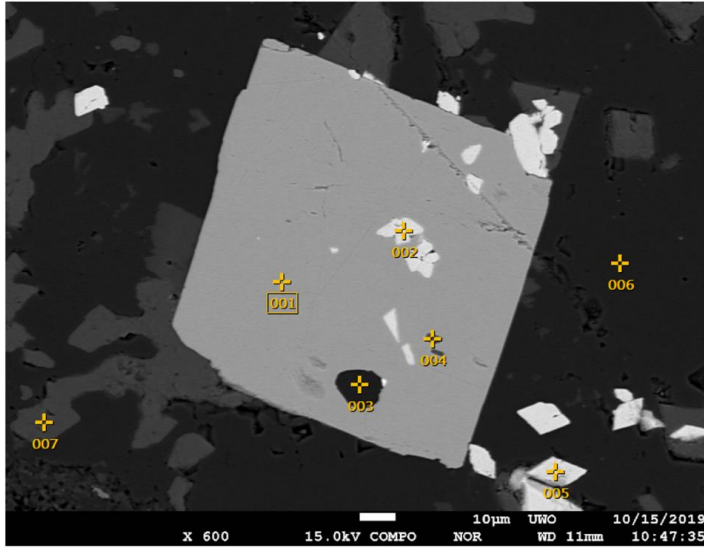
Volt : 15.00 kV
 Mag. : x 160
 Date : 2019/10/15
 Pixel : 1280 x 960



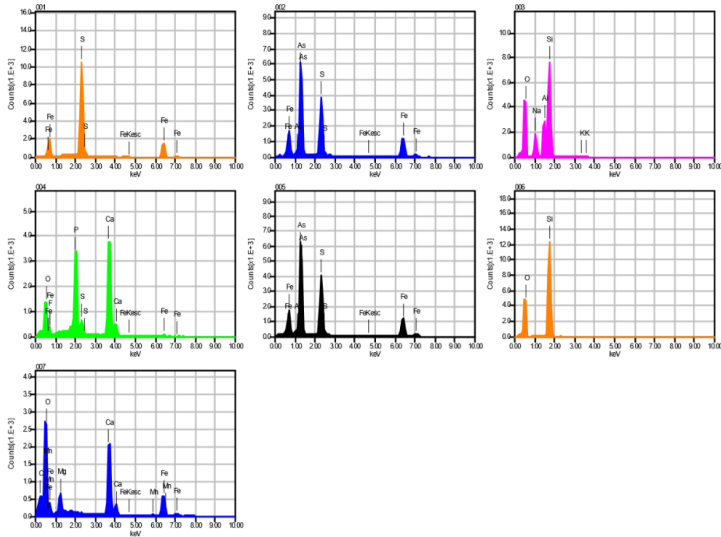
Acquisition Condition
 Instrument : 8530F
 Volt : 15.00 kV
 Current : ---
 Process Time : T2
 Live time : 10.00 sec.
 Real Time : 10.73 sec.
 DeadTime : 7.00 %
 Count Rate : 13941.00 CP

	Fe	O	C	Mg	Ca	Mn
001	24.31	43.13	6.02	2.52	22.54	1.48
002	18.16	45.21	5.68	4.53	23.87	2.54
Average	21.24	44.17	5.85	3.53	23.21	2.01
Deviation	4.35	1.48	0.24	1.42	0.95	0.75

2834_spot1_sulphide: arsenopyrite, apatite, and K-feldspar inclusions in euhedral pyrite grains in quartz + ankerite groundmass (001: pyrite, 002&005: arsenopyrite, 003: K-feldspar, 004: apatite, 006: quartz, 007: albite)



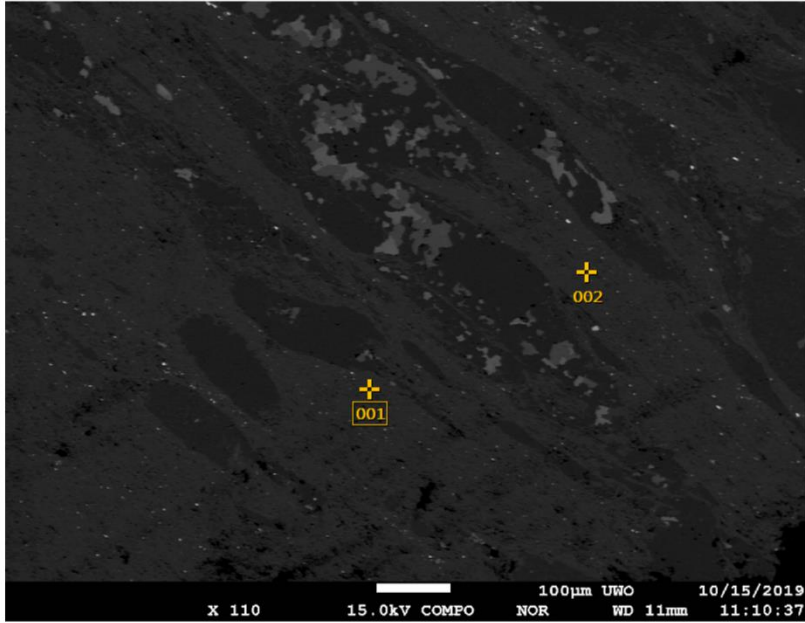
Volt : 15.00 kV
 Mag. : x 600
 Date : 2019/10/15
 Pixel : 1280 x 960



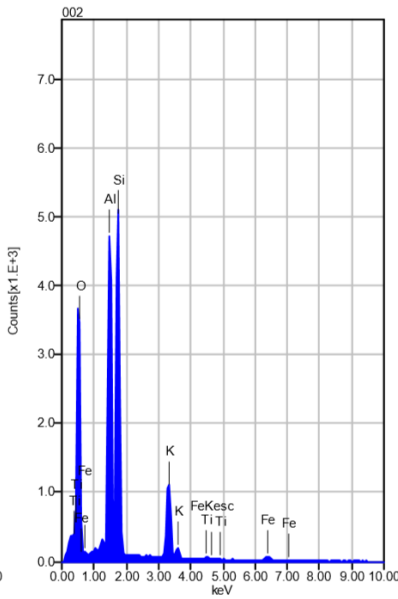
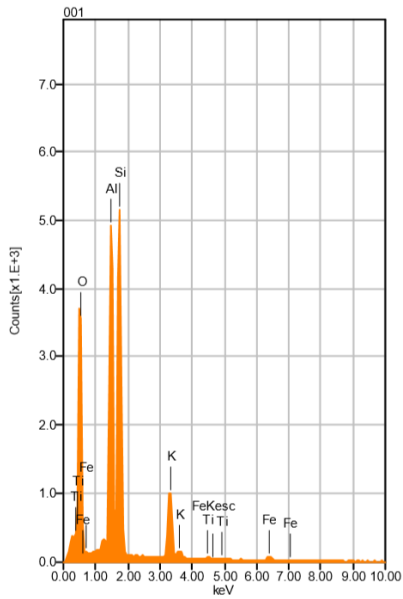
Acquisition Condition
 Instrument : 8530F
 Volt : 15.00 kV
 Current : ---
 Process Time : T2
 Live time : 10.00 sec.
 Real Time : 11.44 sec.
 DeadTime : 12.00 %
 Count Rate : 25684.00 CP

	P	Fe	K	O	C	F	Na	Mg	Al	Si	S	Ca	Mn	As
001		51.10									48.90			
002		36.86									19.16			43.98
003			0.82	46.32			7.79		10.80	34.27				
004	17.75	2.40		31.53		4.58					3.52	40.21		
005		35.50									20.40			44.10
006				51.02						48.98				
007		24.69		43.05	5.54			3.05				22.66	1.01	
Average	17.75	30.11	0.82	42.98	5.54	4.58	7.79	3.05	10.80	41.63	23.00	31.44	1.01	44.04
Deviation	0.00	18.11	0.00	8.31	0.00	0.00	0.00	0.00	0.00	10.41	18.90	12.41	0.00	0.08

2834_spot2_Mica: muscovite (001 & 002)



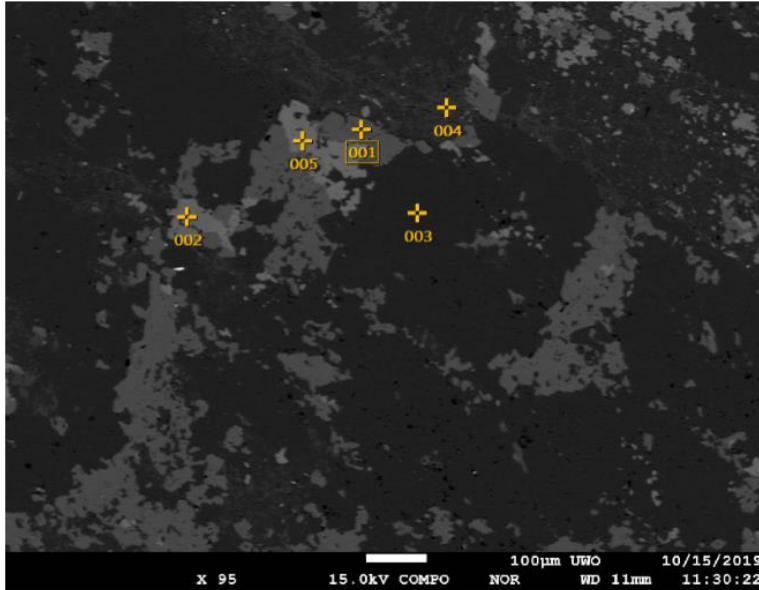
Volt : 15.00 kV
 Mag. : x 110
 Date : 2019/10/15
 Pixel : 1280 x 960



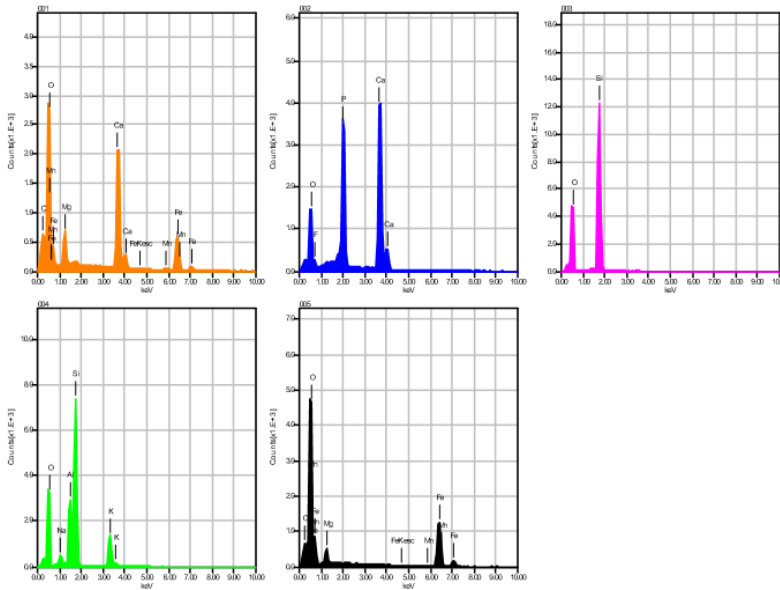
Acquisition Condition
 Instrument : 8530F
 Volt : 15.00 kV
 Current : ---
 Process Time : T2
 Live time : 10.00 sec.
 Real Time : 11.07 sec.
 DeadTime : 10.00 %
 Count Rate : 20008.00 CP

	Fe	K	O	Al	Si	Ti
001	2.38	9.36	44.90	18.46	24.36	0.53
002	2.78	10.42	44.44	17.64	24.16	0.56
Average	2.58	9.89	44.67	18.05	24.26	0.55
Deviation	0.29	0.75	0.32	0.58	0.14	0.02

2834_spot4_carbonate: ankerite (001), apatite (002), quartz (003), muscovite (004), hematite (005)



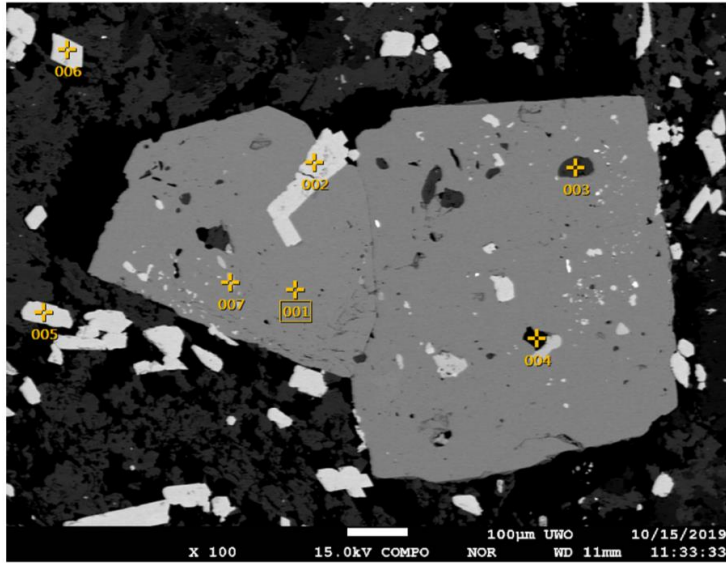
Volt : 15.00 kV
 Mag. : x 95
 Date : 2019/10/15
 Pixel : 1280 x 960



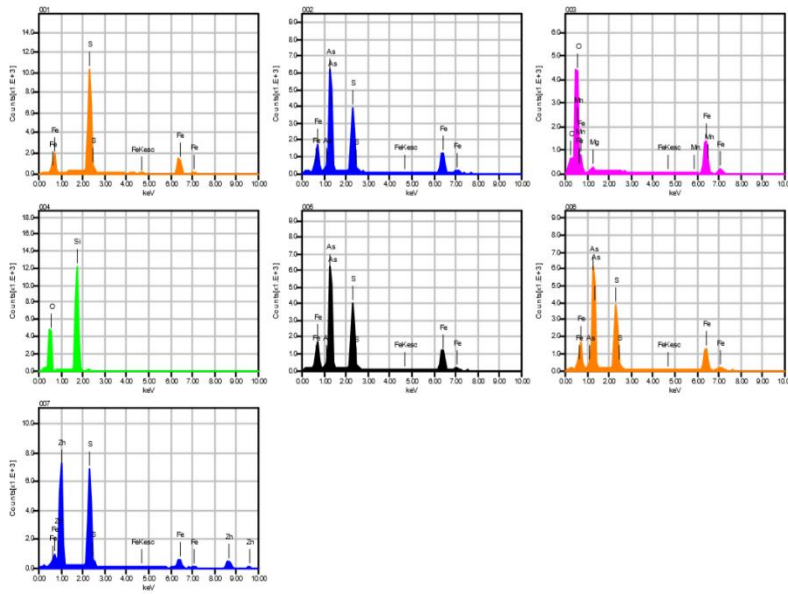
Acquisition Condition
 Instrument : 8530F
 Volt : 15.00 kV
 Current : ---
 Process Time : T2
 Live time : 10.00 sec.
 Real Time : 10.72 sec.
 DeadTime : 7.00 %
 Count Rate : 13775.00 CP

	P	Fe	K	O	C	F	Na	Mg	Al	Si	Ca	Mn
001		23.70		44.06	5.70			3.02			22.48	1.04
002	18.75			34.41		4.50					42.35	
003				50.23						49.77		
004			12.87	43.64			1.75		10.02	31.73		
005		52.13		37.84	6.71			2.47				0.86
Average	18.75	37.91	12.87	42.03	6.20	4.50	1.75	2.75	10.02	40.75	32.41	0.95
Deviation	0.00	20.10	0.00	6.12	0.71	0.00	0.00	0.39	0.00	12.76	14.05	0.13

2834_spot5_EDS: arsenopyrite, quartz, hematite, and sphalerite inclusions in subhedral pyrite grains (001: pyrite, 002, 005, & 006: arsenopyrite, 003: hematite, 004: quartz, 007: sphalerite)



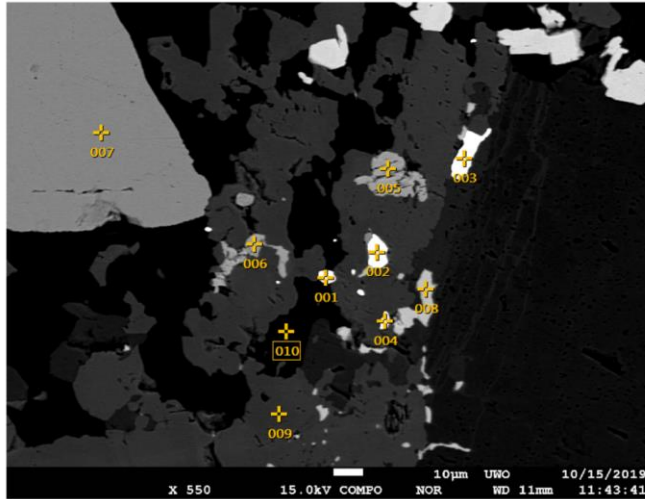
Volt : 15.00 kV
 Mag. : x 100
 Date : 2019/10/15
 Pixel : 1280 x 960



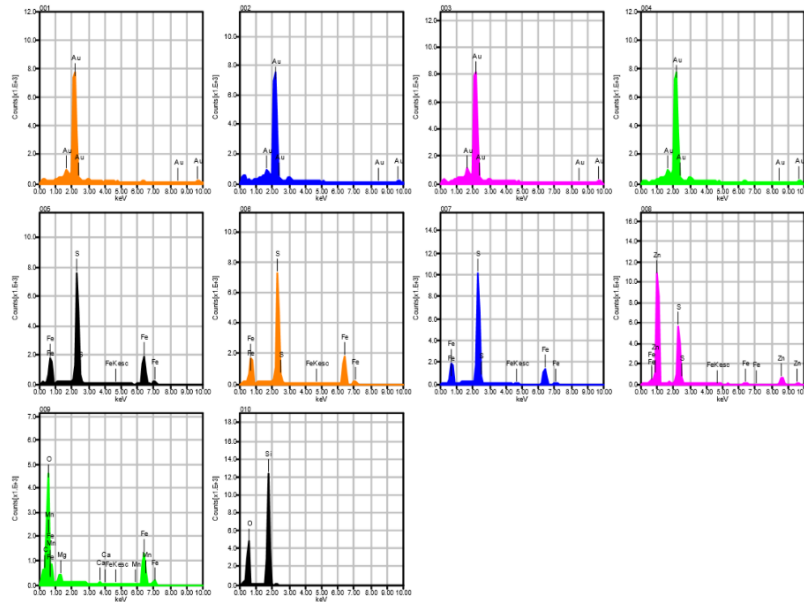
Acquisition Condition
 Instrument : 8530F
 Volt : 15.00 kV
 Current : ---
 Process Time : T2
 Live time : 10.00 sec.
 Real Time : 11.45 sec.
 DeadTime : 13.00 %
 Count Rate : 25640.00 CP

	Fe	O	C	Mg	Si	S	Mn	Zn	As
001	50.44					49.56			
002	36.58					19.53			43.90
003	56.40	35.20	6.14	1.07			1.19		
004		50.54			49.46				
005	36.04					19.51			44.45
006	36.51					19.39			44.10
007	17.05					33.28		49.66	
Average	38.84	42.87	6.14	1.07	49.46	28.25	1.19	49.66	44.15
Deviation	13.68	10.84	0.00	0.00	0.00	13.33	0.00	0.00	0.28

2834_spot6_EDS: Pure free gold near sphalerite, pyrite, and hematite in quartz vein (001-004;
 pure gold, 005-007: pyrite, 008: sphalerite, 009: hematite, 010: quartz)



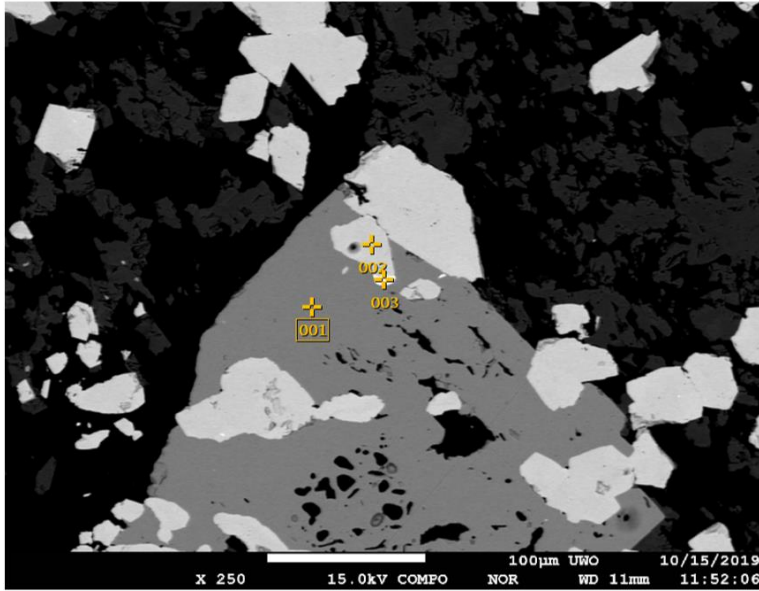
Volt : 15.00 kV
 Mag. : x 550
 Date : 2019/10/15
 Pixel : 1280 x 960



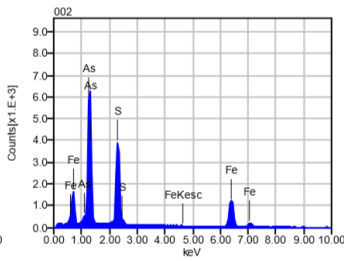
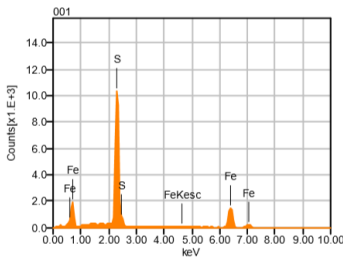
Acquisition Condition
 Instrument : 8530F
 Volt : 15.00 kV
 Current : ---
 Process Time : T2
 Live time : 10.00 sec.
 Real Time : 11.17 sec.
 DeadTime : 10.00 %
 Count Rate : 22135.00 CP

	Fe	O	Au	C	Mg	Si	S	Ca	Mn	Zn
001			100.00							
002			100.00							
003			100.00							
004			100.00							
005	64.27						35.73			
006	64.96						35.04			
007	51.14						48.86			
008	4.53						29.90			65.57
009	52.62	36.30		6.43	2.07			0.51	2.06	
010		50.07				49.93				
Average	47.50	43.19	100.00	6.43	2.07	49.93	37.38	0.51	2.06	65.57
Deviation	24.86	9.73	0.00	0.00	0.00	0.00	8.08	0.00	0.00	0.00

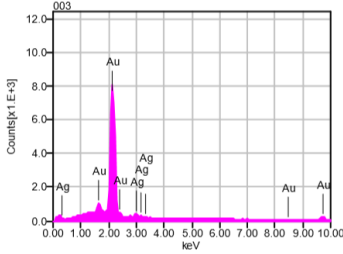
2834_spot7_EDS: gold with arsenopyrite inside corroded pyrite (001: pyrite, 002: arsenopyrite, 003: Au + Ag)



Volt : 15.00 kV
 Mag. : x 250
 Date : 2019/10/15
 Pixel : 1280 x 960

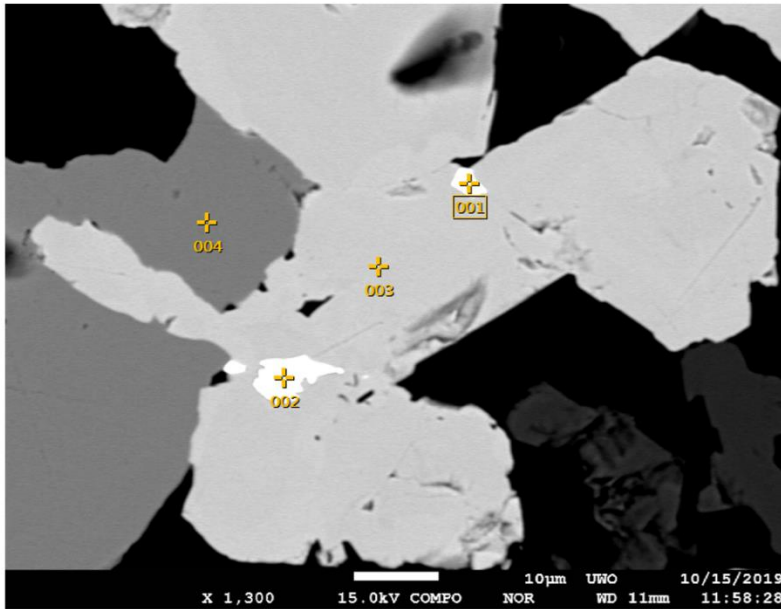


Acquisition Condition
 Instrument : 8530F
 Volt : 15.00 kV
 Current : ---
 Process Time : T2
 Live time : 10.00 sec.
 Real Time : 11.43 sec.
 DeadTime : 12.00 %
 Count Rate : 25525.00 CP

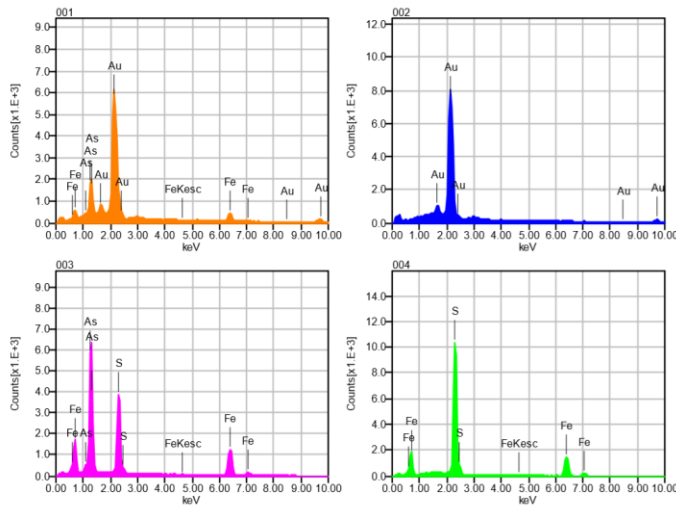


	Fe	Au	Ag	S	As
001	50.38			49.62	
002	36.52			19.00	44.48
003		96.35	3.65		
Average	43.45	96.35	3.65	34.31	44.48
Deviation	9.80	0.00	0.00	21.65	0.00

2834_spot7_EDS2: Pure gold in combinations of pyrite + Arsenopyrite (001-002: pure gold, 003: arsenopyrite, 004: pyrite)



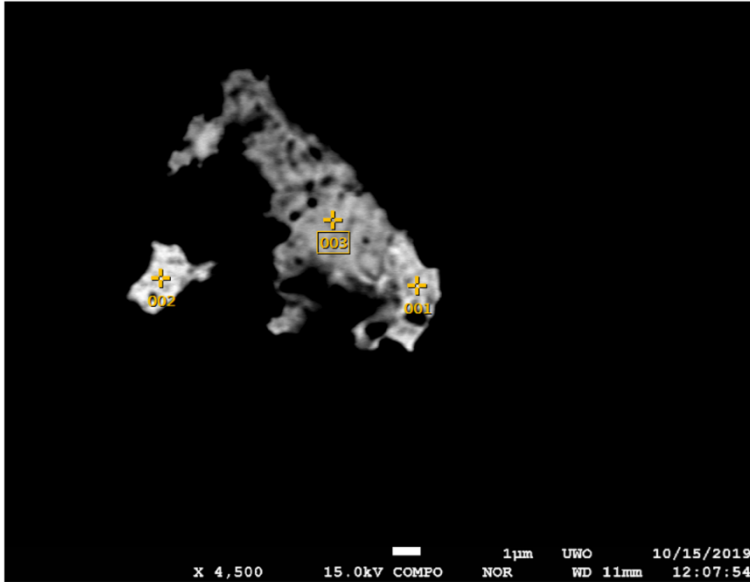
Volt : 15.00 kV
 Mag. : x 1,300
 Date : 2019/10/15
 Pixel : 1280 x 960



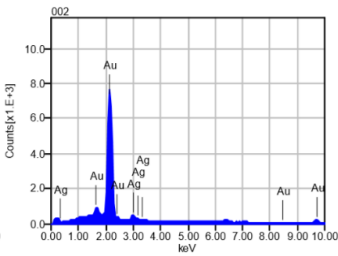
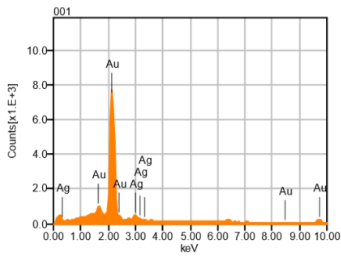
Acquisition Condition
 Instrument : 8530F
 Volt : 15.00 kV
 Current : ---
 Process Time : T2
 Live time : 10.00 sec.
 Real Time : 11.92 sec.
 DeadTime : 16.00 %
 Count Rate : 31665.00 CP

	Fe	Au	S	As
001	10.45	78.24		11.31
002		100.00		
003	36.84		19.02	44.15
004	50.64		49.36	
Average	32.64	89.12	34.19	27.73
Deviation	20.42	15.39	21.46	23.22

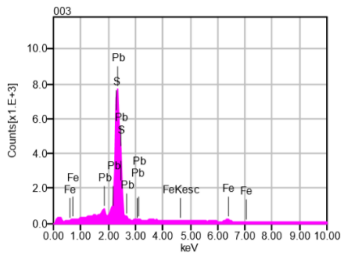
2834_spot8_EDS1: Au + Ag (001&002) in galena (003)



Volt : 15.00 kV
 Mag. : x 4,500
 Date : 2019/10/15
 Pixel : 1280 x 960

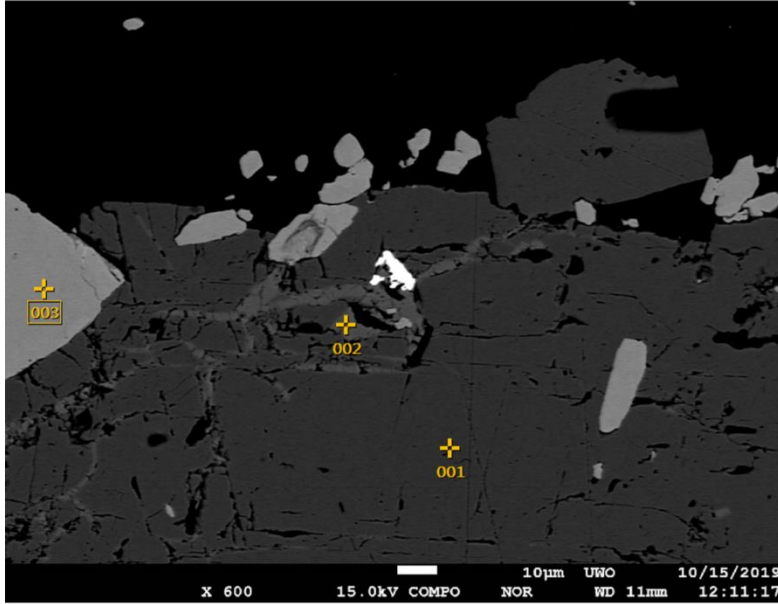


Acquisition Condition
 Instrument : 8530F
 Volt : 15.00 kV
 Current : ---
 Process Time : T2
 Live time : 10.00 sec.
 Real Time : 11.95 sec.
 DeadTime : 16.00 %
 Count Rate : 32942.00 CP

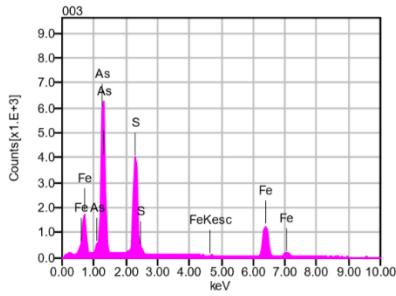
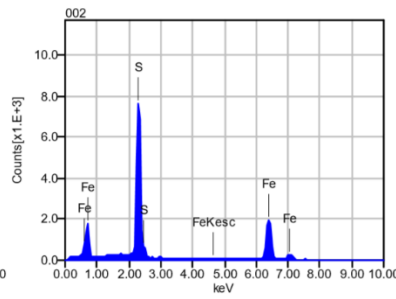
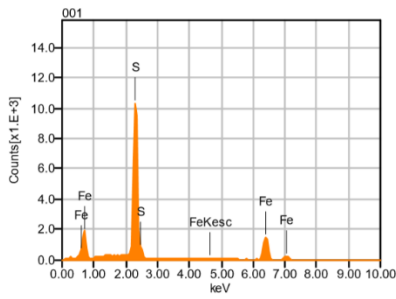


	Fe	Pb	Au	Ag	S
001			94.48	5.52	
002			94.33	5.67	
003	3.45	84.36			12.19
Average	3.45	84.36	94.41	5.59	12.19
Deviation	0.00	0.00	0.11	0.11	0.00

2834_spot8_EDS2: gold and arsenopyrite inside pyrite (001&002: pyrite, 003: arsenopyrite)



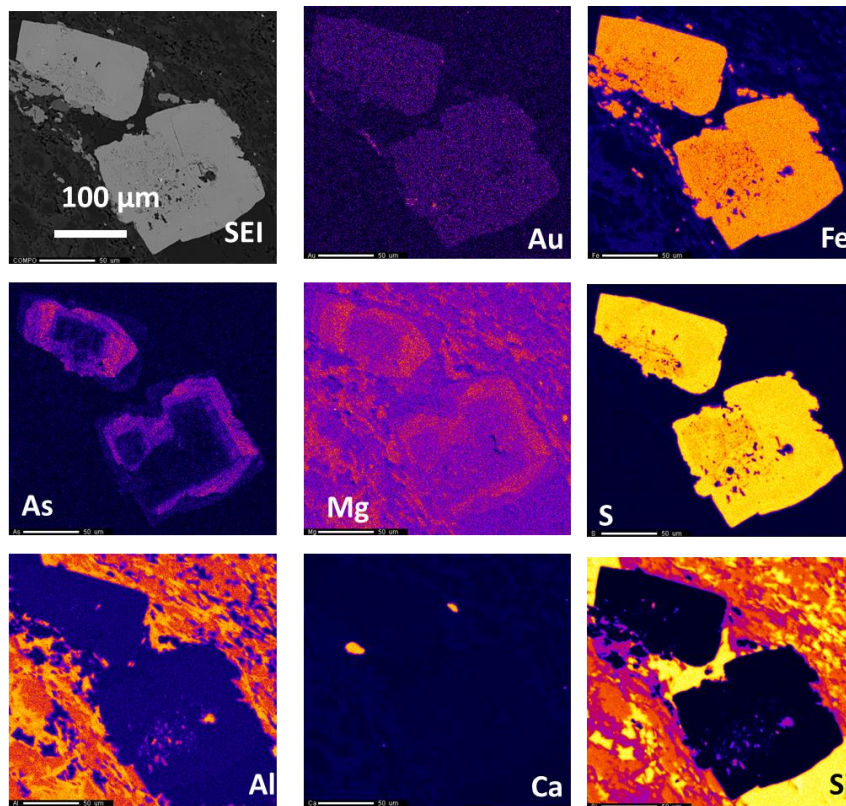
Volt : 15.00 kV
 Mag. : x 600
 Date : 2019/10/15
 Pixel : 1280 x 960



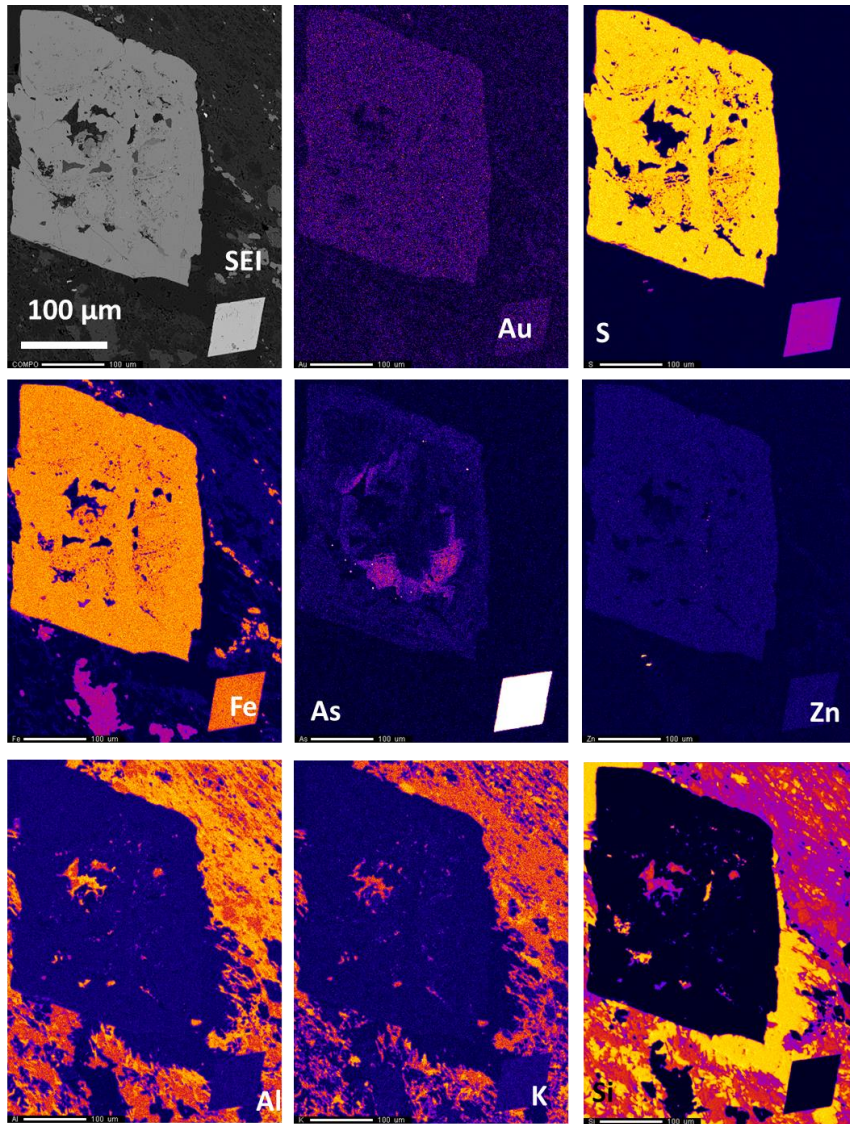
Acquisition Condition
 Instrument : 8530F
 Volt : 15.00 kV
 Current : ---
 Process Time : T2
 Live time : 10.00 sec.
 Real Time : 11.43 sec.
 DeadTime : 13.00 %
 Count Rate : 25283.00 CP

	Fe	S	As
001	50.51	49.49	
002	64.15	35.85	
003	36.56	19.35	44.09
Average	50.41	34.90	44.09
Deviation	13.79	15.09	0.00

2858_1_5um EDS/WDS Element Maps: Pyrite with zonation in Mg and As map with calcite and without gold.



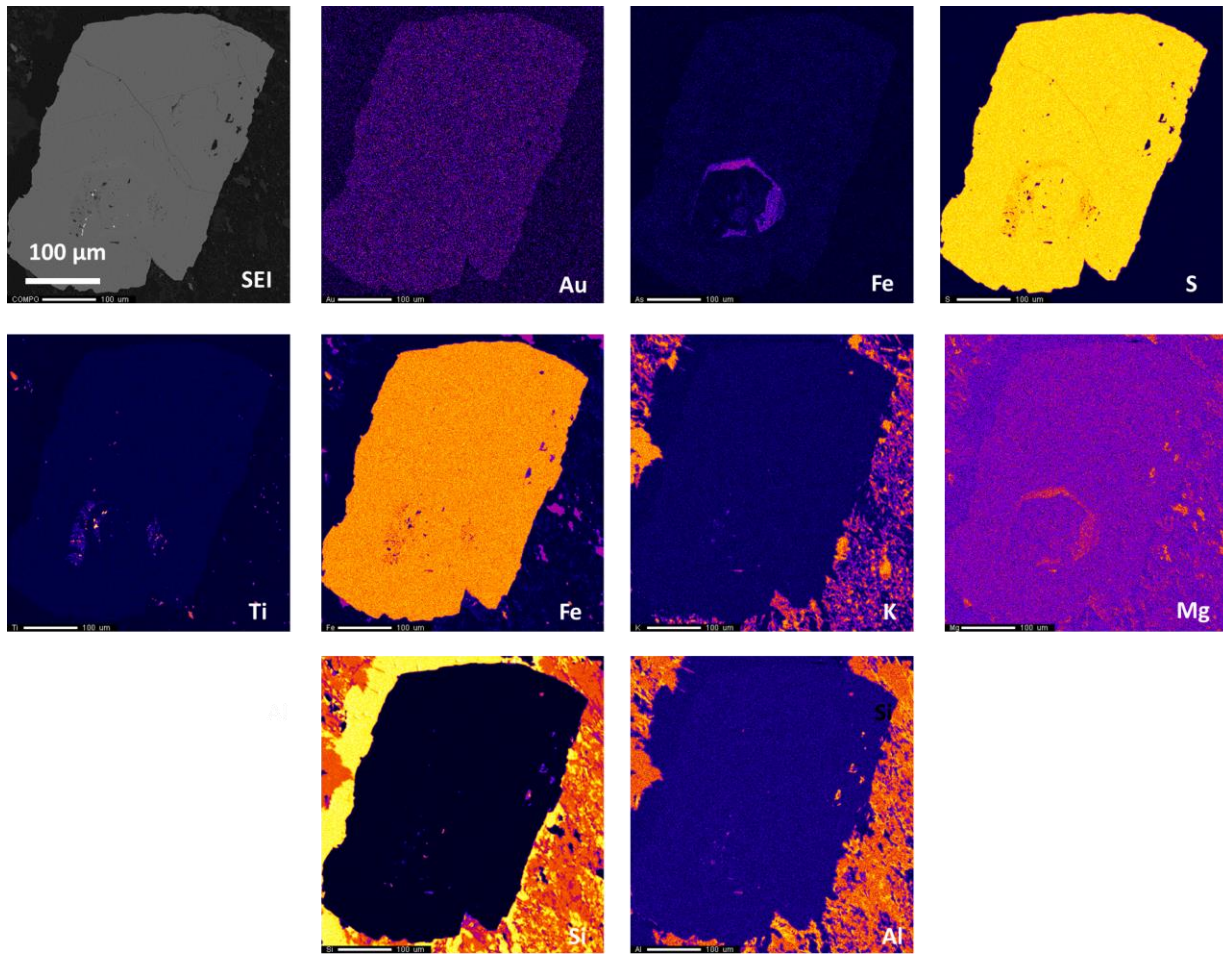
2858_2_1um EDS/WDS Element Maps: euhedral corroded pyrite with euhedral arsenopyrite.



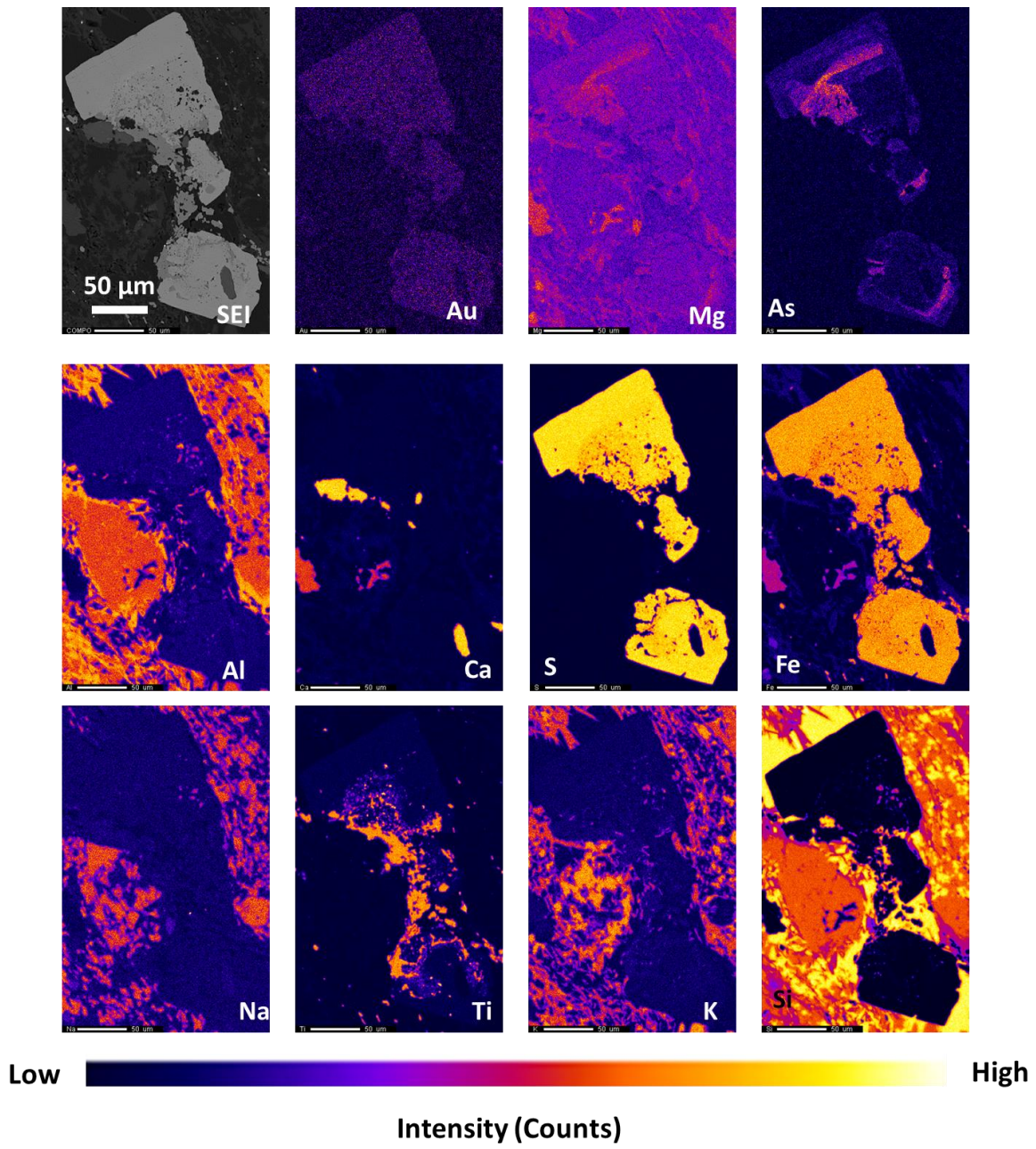
Low  High

Intensity (Counts)

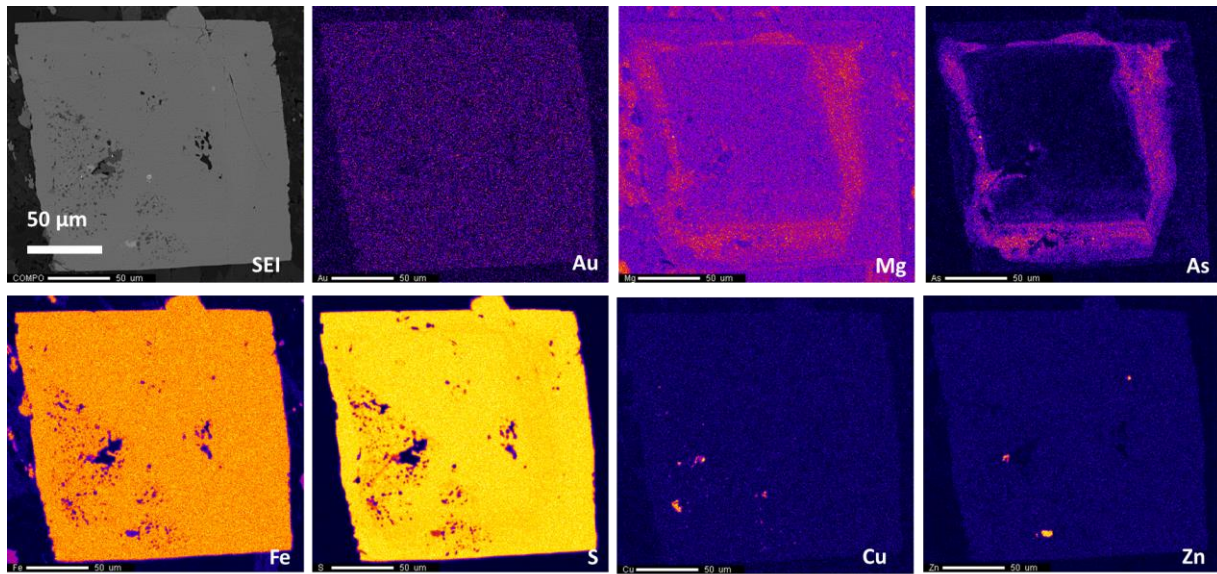
2858_3_1.2um EDS/WDS Element Maps: Euhedral pyrite with zonation in Mg and As map and without gold.



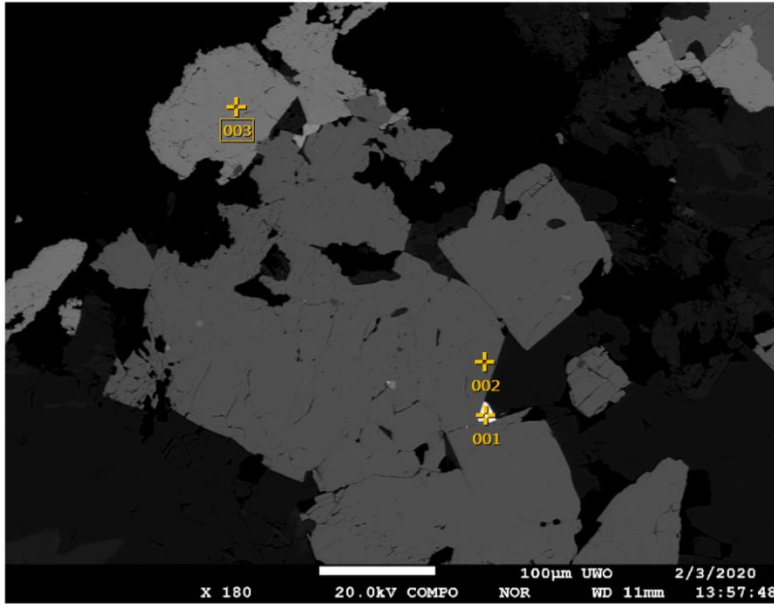
2858_4_0.6um EDS/WDS Element Maps: Corroded pyrite with zonation in Mg and As map and calcite on the edge. No gold.



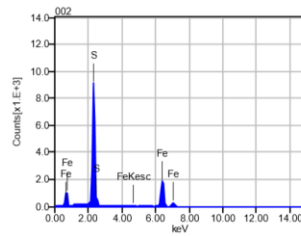
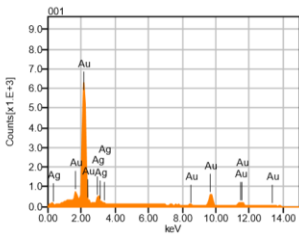
2858_5_0.6um EDS/WDS Element Maps: Euhedral pyrite with zonation in As and Au map and chalcopyrite and sphalerite inclusions inside. No gold.



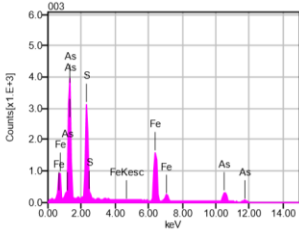
2854EDS06_Au: Au + Ag (001) with pyrite (002) + arsenopyrite (003) grain



Volt : 20.00 kV
 Mag. : x 180
 Date : 2020/02/03
 Pixel : 1280 x 960

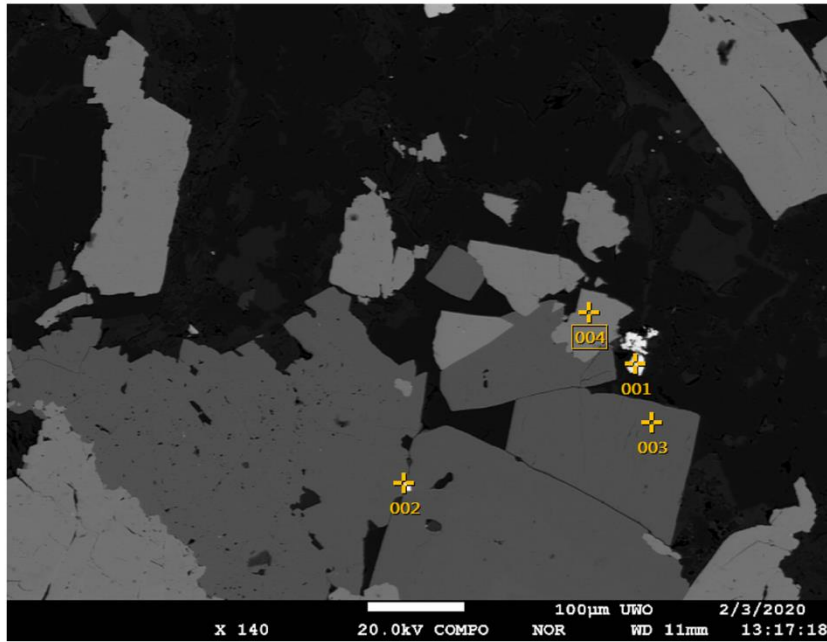


Acquisition Condition
 Instrument : 8530F
 Volt : 20.00 kV
 Current : ---
 Process Time : T2
 Live time : 10.00 sec.
 Real Time : 11.17 sec.
 DeadTime : 10.00 %
 Count Rate : 20671.00 CP

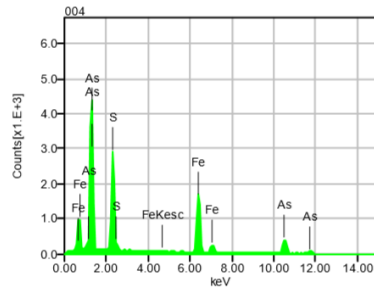
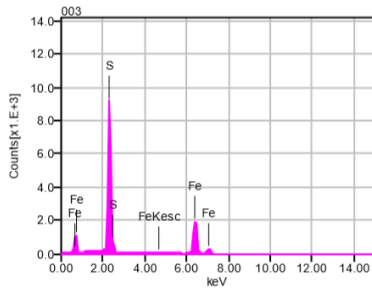
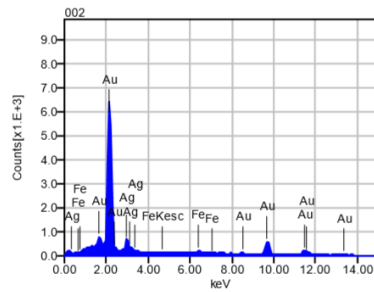
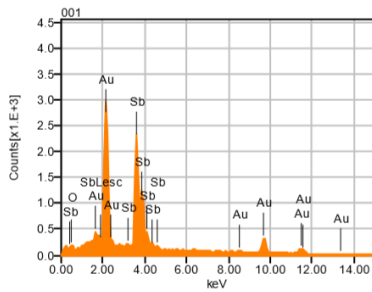


	Fe	Au	Ag	S	As
001		92.21	7.79		
002	50.58			49.42	
003	37.27			20.04	42.69
Average	43.92	92.21	7.79	34.73	42.69
Deviation	9.41	0.00	0.00	20.77	0.00

2854EDS01_Au: Au+Sb (001) and Au + Ag (002) with pyrite (003) + arsenopyrite (004)



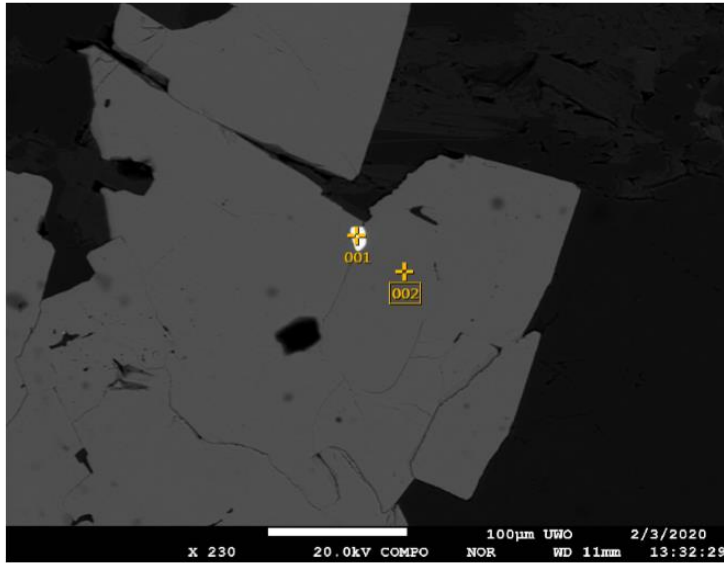
Volt : 20.00 kV
 Mag. : x 140
 Date : 2020/02/03
 Pixel : 1280 x 960



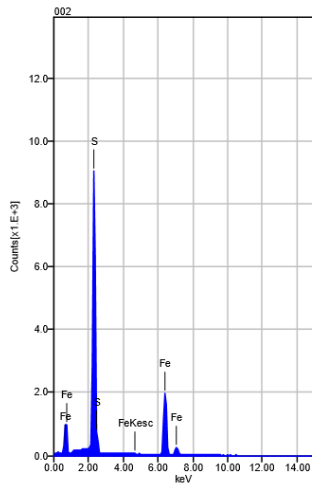
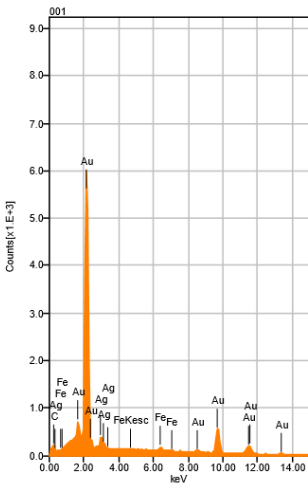
Acquisition Condition
 Instrument : 8530F
 Volt : 20.00 kV
 Current : ---
 Process Time : T2
 Live time : 10.00 sec.
 Real Time : 11.21 sec.
 DeadTime : 11.00 %
 Count Rate : 21485.00 CP

	Fe	O	Au	Ag	S	As	Sb
001		1.66	45.32				53.02
002	1.84		88.39	9.77			
003	50.84				49.16		
004	35.96				17.39	46.65	
Average	29.55	1.66	66.86	9.77	33.28	46.65	53.02
Deviation	25.12	0.00	30.45	0.00	22.46	0.00	0.00

2854EDS02_Au: gold in pyrite (001: Au + Ag, 002: pyrite)



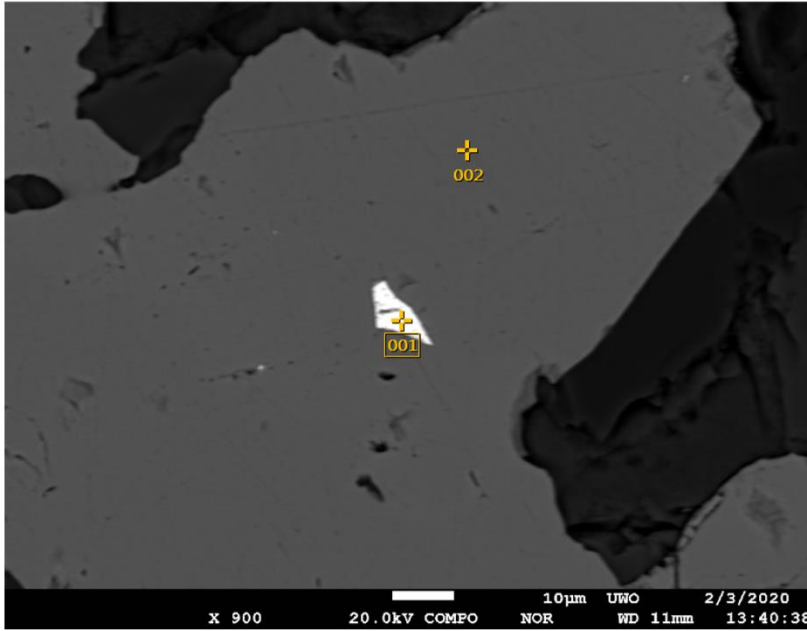
Volt : 20.00 kV
 Mag. : x 230
 Date : 2020/02/03
 Pixel : 1280 x 960



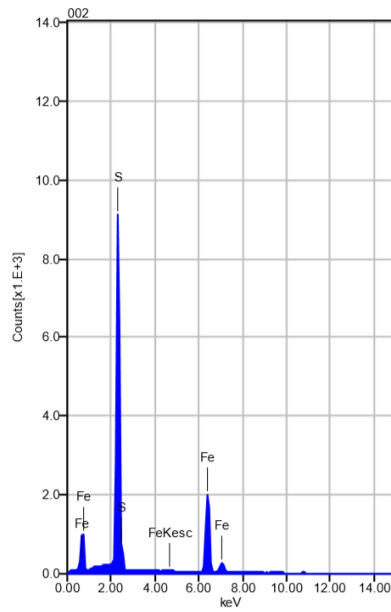
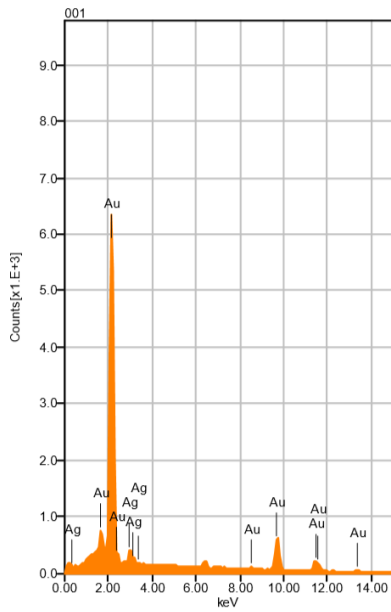
Acquisition Condition
 Instrument : 8530F
 Volt : 20.00 kV
 Current : ---
 Process Time : T2
 Live time : 10.00 sec.
 Real Time : 11.28 sec.
 DeadTime : 11.00 %
 Count Rate : 22704.00 CP

	Fe	Au	Ag	C	S
001	1.23	87.51	4.94	6.31	
002	51.01				48.99
Average	26.12	87.51	4.94	6.31	48.99
Deviation	35.20	0.00	0.00	0.00	0.00

2854EDS03_Au: gold (Au +Ag: 001) in pyrite (002)



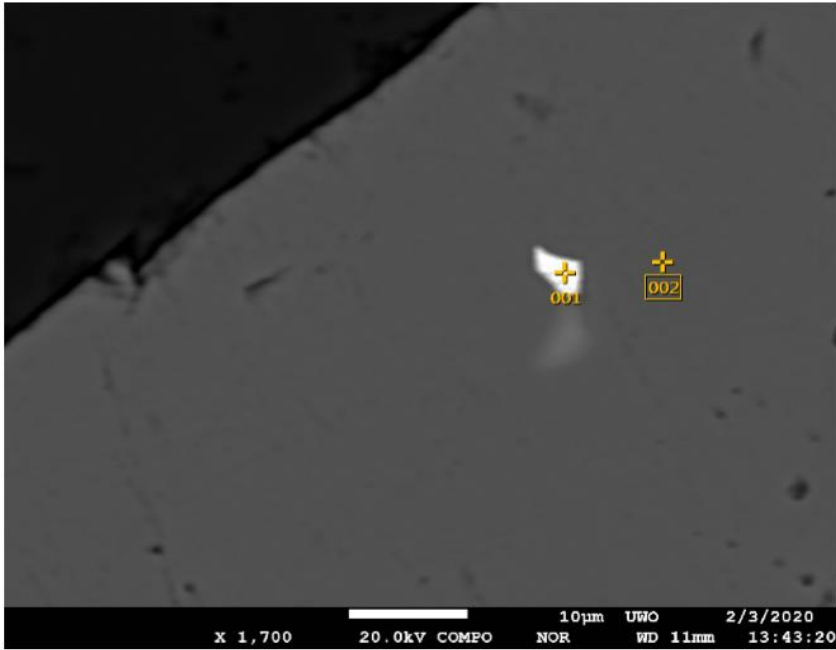
Volt : 20.00 kV
 Mag. : x 900
 Date : 2020/02/03
 Pixel : 1280 x 960



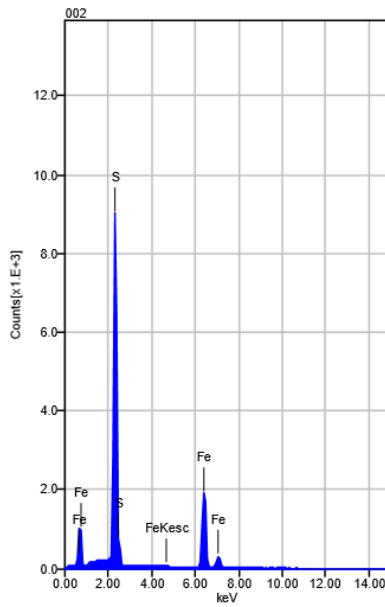
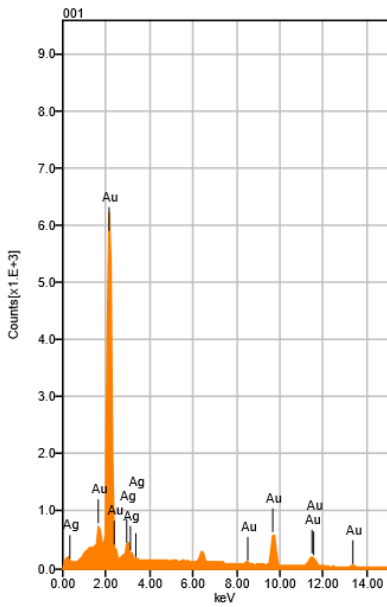
Acquisition Condition
 Instrument : 8530F
 Volt : 20.00 kV
 Current : ---
 Process Time : T2
 Live time : 10.00 sec.
 Real Time : 11.80 sec.
 DeadTime : 15.00 %
 Count Rate : 30267.00 CP

	Fe	Au	Ag	S
001		93.96	6.04	
002	51.04			48.96
Average	51.04	93.96	6.04	48.96
Deviation	0.00	0.00	0.00	0.00

2854EDS04_Au: gold (Au +Ag: 001) in pyrite (002)



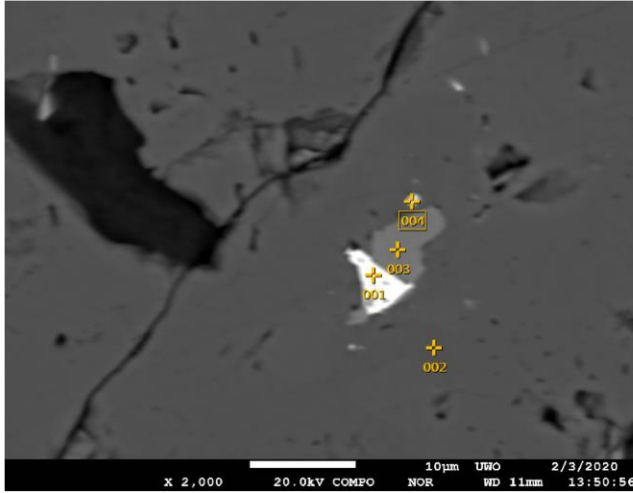
Volt : 20.00 kV
 Mag. : x 1,700
 Date : 2020/02/03
 Pixel : 1280 x 960



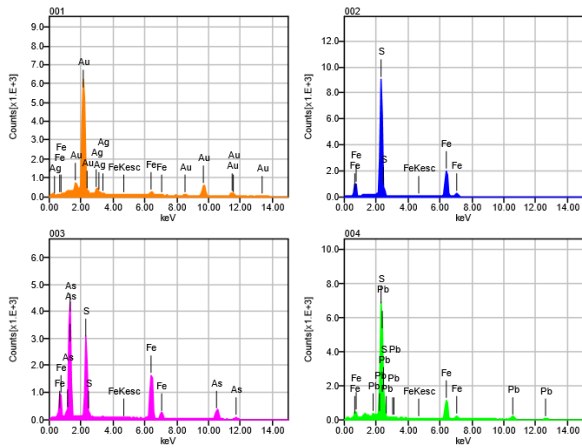
Acquisition Condition
 Instrument : 8530F
 Volt : 20.00 kV
 Current : ---
 Process Time : T2
 Live time : 10.00 sec.
 Real Time : 11.28 sec.
 DeadTime : 12.00 %
 Count Rate : 22688.00 CP

	Fe	Au	Ag	S
001		93.39	6.61	
002	50.81			49.19
Average	50.81	93.39	6.61	49.19
Deviation	0.00	0.00	0.00	0.00

2854EDS05_Au: gold (Au + Ag: 001) , galena (004), arsenopyrite (003) in pyrite (002)



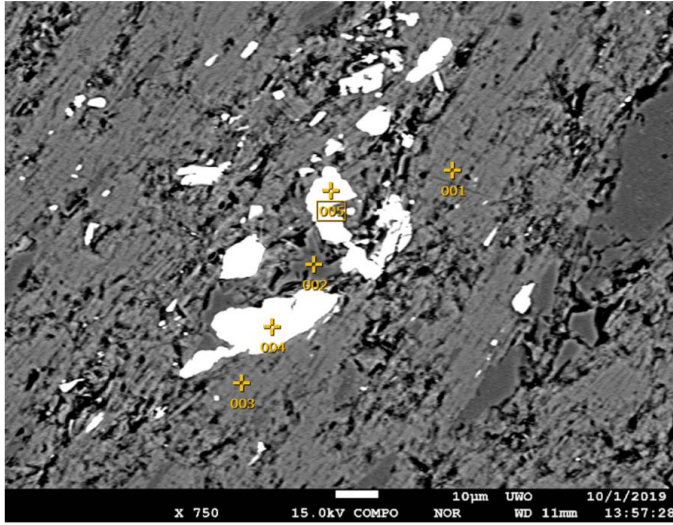
Volt : 20.00 kV
 Mag. : x 2,000
 Date : 2020/02/03
 Pixel : 1280 x 960



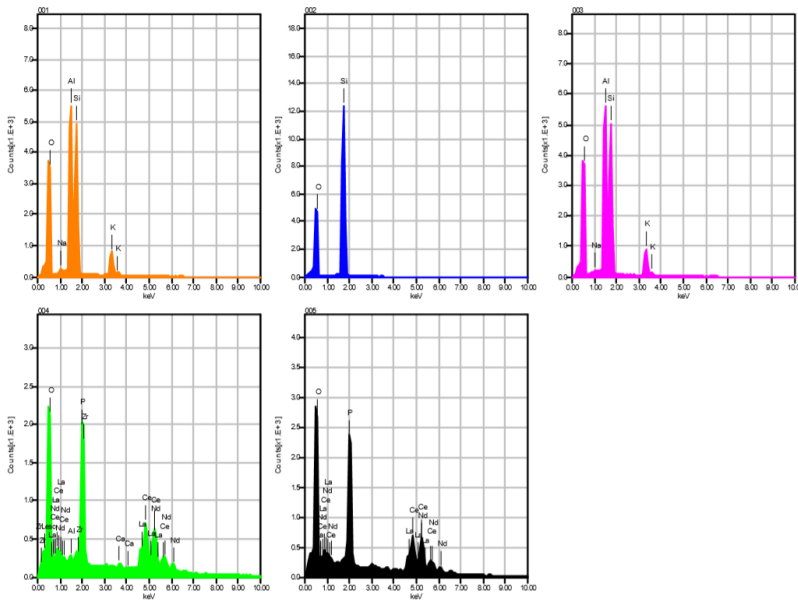
Acquisition Condition
 Instrument : 8530F
 Volt : 20.00 kV
 Current : ---
 Process Time : T2
 Live time : 10.00 sec.
 Real Time : 11.37 sec.
 DeadTime : 12.00 %
 Count Rate : 24030.00 CP

	Fe	Pb	Au	Ag	S	As
001	2.88		90.31	6.82		
002	50.99				49.01	
003	37.78				18.35	43.88
004	27.05	45.26			27.69	
Average	29.67	45.26	90.31	6.82	31.68	43.88
Deviation	20.37	0.00	0.00	0.00	15.72	0.00

2831_Mical-2: muscovite (001&003), quartz (002), monazite + zircon (004), monazite (005)



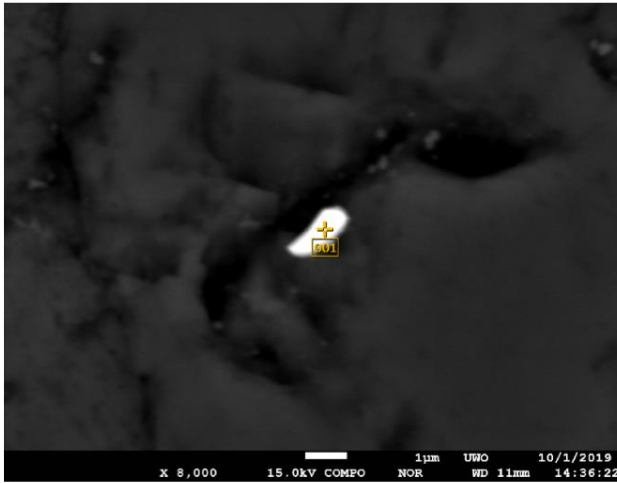
Volt : 15.00 kV
 Mag. : x 750
 Date : 2019/10/01
 Pixel : 1280 x 960



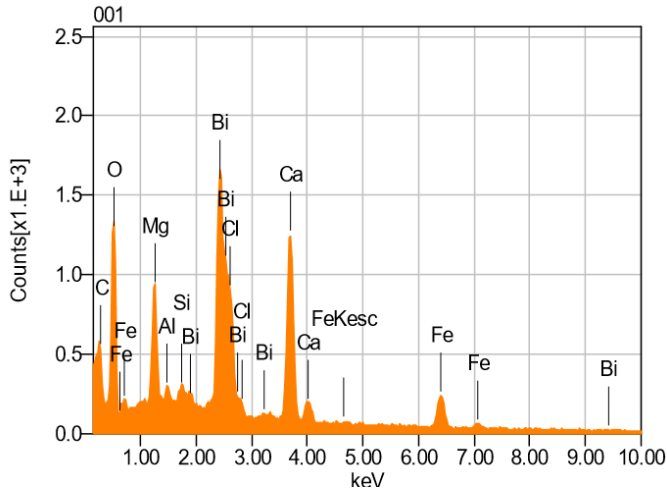
Acquisition Condition
 Instrument : 8530F
 Volt : 15.00 kV
 Current : ---
 Process Time : T2
 Live time : 10.00 sec.
 Real Time : 11.17 sec.
 DeadTime : 11.00 %
 Count Rate : 21293.00 CP

	P	K	O	Na	Al	Si	Ca	Zr	La	Ce	Pr
001		8.39	45.21	0.53	21.22	24.65					
002			50.62			49.38					
003		8.50	45.83	0.47	21.03	24.17					
004	11.62		21.08		0.53		0.70	4.79	13.23	32.29	1
005	14.54		24.43						13.04	31.77	1
Average	13.08	8.44	37.43	0.50	14.26	32.74	0.70	4.79	13.14	32.03	1
Deviation	2.07	0.08	13.62	0.04	11.89	14.42	0.00	0.00	0.14	0.36	0

2831_spot1_Bi: Bismuth in calcite



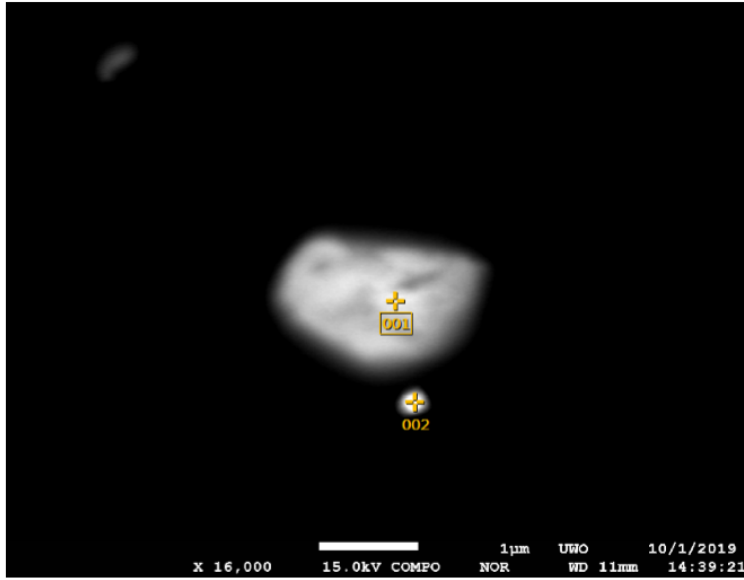
Volt : 15.00 kV
 Mag. : x 8,000
 Date : 2019/10/01
 Pixel : 1280 x 960



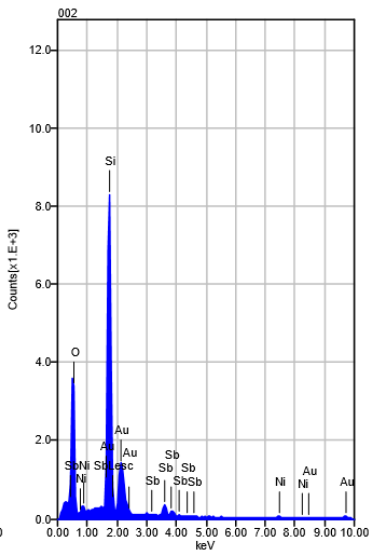
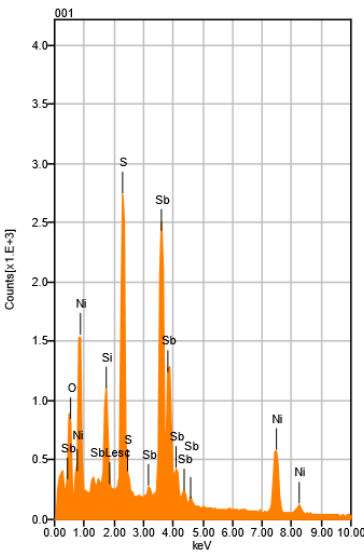
Acquisition Condition
 Instrument : 8530F
 Volt : 15.00 kV
 Current : ---
 Process Time : T2
 Live time : 10.00 sec.
 Real Time : 10.92 sec.
 DeadTime : 8.00 %
 Count Rate : 16941.00 CP

Formula	mass%	Atom%	Sigma	Net	K ratio	Line
C	9.63	25.61	0.06	50882	0.0810245	K
O	20.37	40.68	0.10	258372	1.4816018	K
Mg	3.96	5.20	0.05	189789	0.3549816	K
Al	0.57	0.67	0.04	30555	0.0589675	K
Si	0.46	0.52	0.04	25985	0.0560914	K
Cl	5.21	4.70	0.06	254311	0.7359504	K
Ca	15.10	12.04	0.10	506377	2.2617396	K
Fe	8.93	5.11	0.11	109254	1.2541189	K
Bi	35.78	5.47	0.30	798967	3.5839200	M
Total	100.00	100.00				

2831_spot1_Sb_Au: Stibnite (001) and Au (002) in quartz vein



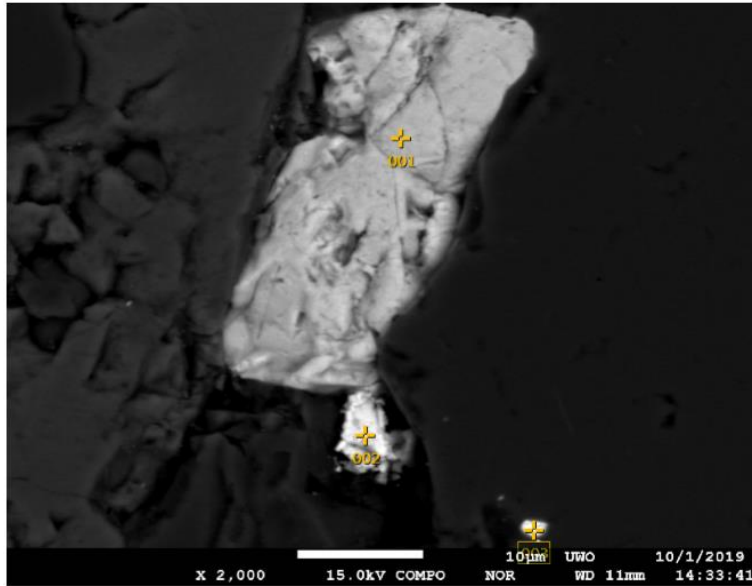
Volt : 15.00 kV
 Mag. : x 16,000
 Date : 2019/10/01
 Pixel : 1280 x 960



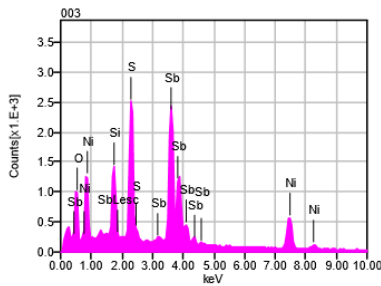
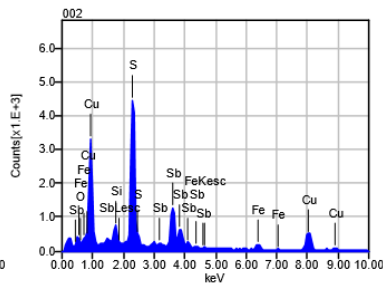
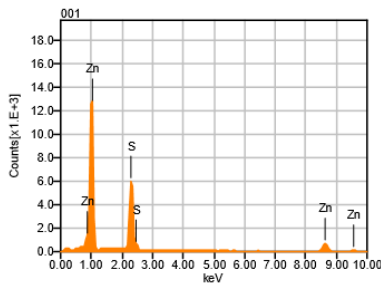
Acquisition Condition
 Instrument : 8530F
 Volt : 15.00 kV
 Current : ---
 Process Time : T2
 Live time : 10.00 sec.
 Real Time : 11.43 sec.
 DeadTime : 13.00 %
 Count Rate : 25241.00 CP

	O	Au	Si	S	Ni	Sb
001	4.68		3.41	11.75	25.97	54.19
002	36.90	22.21	31.36		2.26	7.27
Average	20.79	22.21	17.39	11.75	14.11	30.73
Deviation	22.78	0.00	19.77	0.00	16.76	33.18

2831_spot1_Sph_Sb: sphalerite (001) , chalcopyrite (002), and stibnite (003)



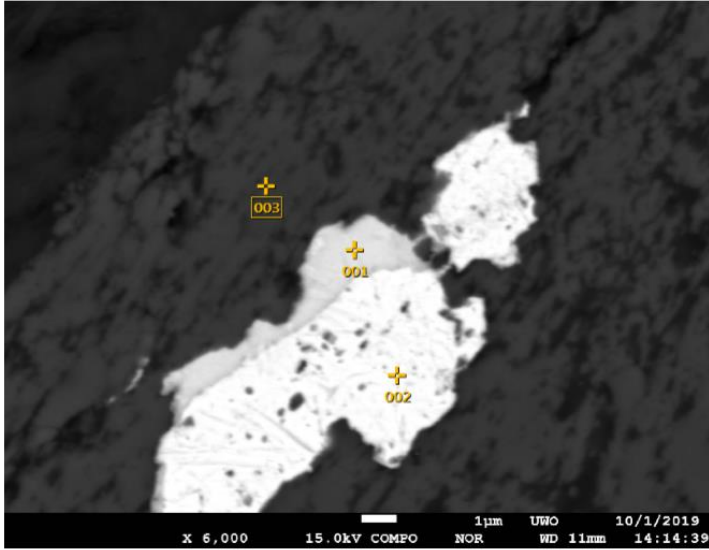
Volt : 15.00 kV
 Mag. : x 2,000
 Date : 2019/10/01
 Pixel : 1280 x 960



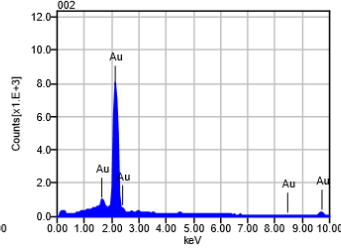
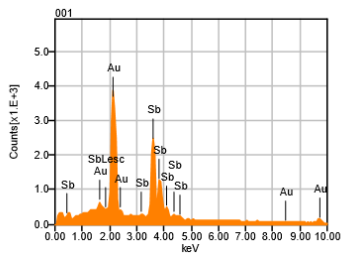
Acquisition Condition
 Instrument : 8530F
 Volt : 15.00 kV
 Current : ---
 Process Time : T2
 Live time : 10.00 sec.
 Real Time : 11.40 sec.
 DeadTime : 12.00 %
 Count Rate : 24531.00 CP

	Fe	O	Si	S	Ni	Cu	Zn	Sb
001				30.79			69.21	
002	5.61	2.35	2.38	21.96		36.83		30.87
003		6.21	4.72	11.11	25.17			52.79
Average	5.61	4.28	3.55	21.29	25.17	36.83	69.21	41.83
Deviation	0.00	2.73	1.65	9.86	0.00	0.00	0.00	15.50

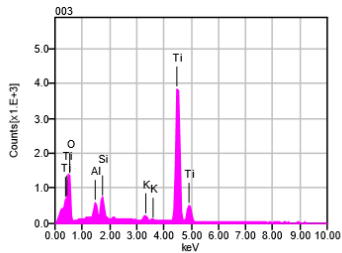
2831_spot2_Au: pure gold (001), Au+Sb (002), Rutile (003)



Volt : 15.00 kV
 Mag. : x 6,000
 Date : 2019/10/01
 Pixel : 1280 x 960

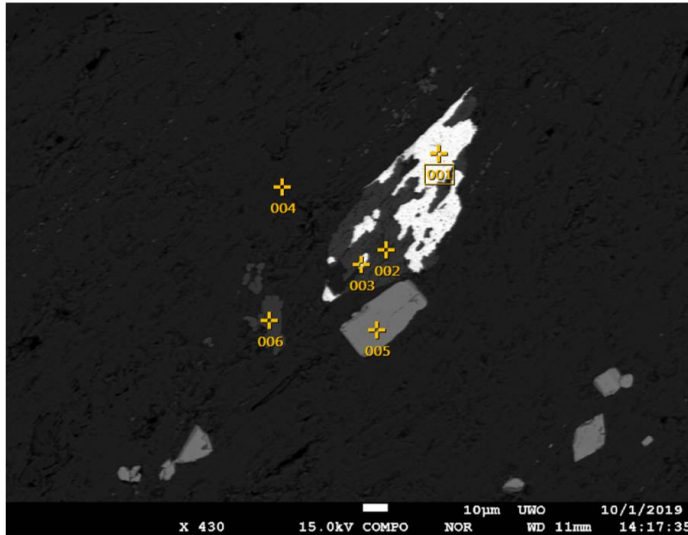


Acquisition Condition
 Instrument : 8530F
 Volt : 15.00 kV
 Current : ---
 Process Time : T2
 Live time : 10.00 sec.
 Real Time : 10.86 sec.
 DeadTime : 8.00 %
 Count Rate : 15861.00 CP

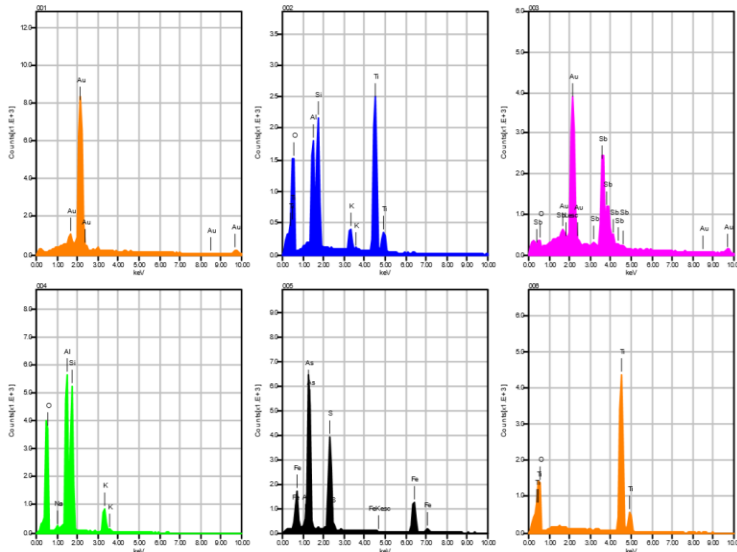


	K	O	Au	Al	Si	Ti	Sb
001			48.32				51.68
002			100.00				
003	1.18	34.72		1.70	2.35	60.04	
Average	1.18	34.72	74.16	1.70	2.35	60.04	51.68
Deviation	0.00	0.00	36.54	0.00	0.00	0.00	0.00

2831_spot2_Au2: pure gold (001), Au+Sb (003), rutile (002&006) near euhedral arsenopyrite (006) in muscovite (002&004) groundmass



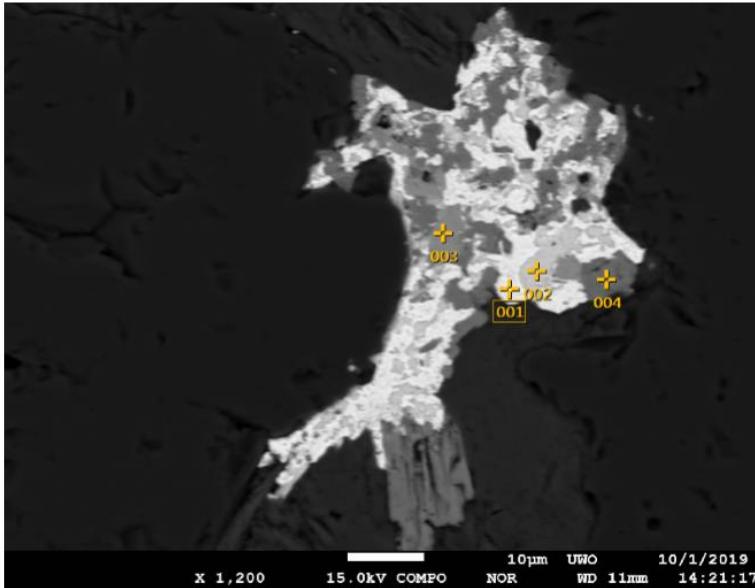
Volt : 15.00 kV
 Mag. : x 430
 Date : 2019/10/01
 Pixel : 1280 x 960



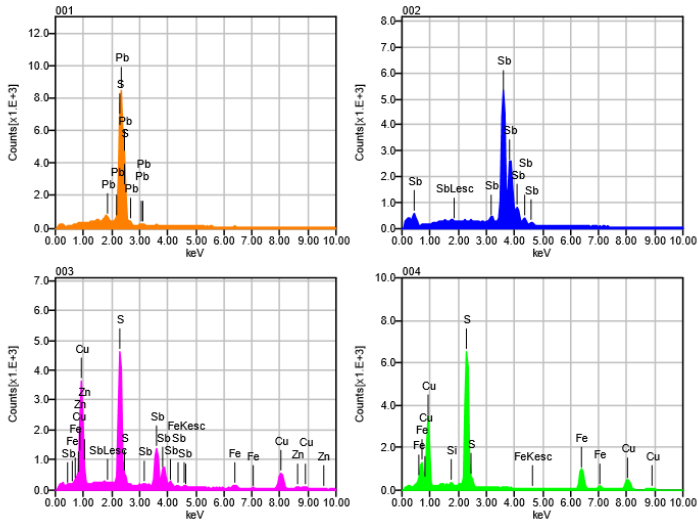
Acquisition Condition
 Instrument : 8530F
 Volt : 15.00 kV
 Current : ---
 Process Time : T2
 Live time : 10.00 sec.
 Real Time : 12.13 sec.
 DeadTime : 17.00 µs
 Count Rate : 35563.00 CP

	Fe	K	O	Au	Na	Al	Si	S	Ti	As	%
001				100.00							100
002		3.20	36.63			7.07	9.38		43.73		100
003			1.58	48.78							100
004		8.11	46.24		0.44	20.61	24.60				100
005	36.36							19.17		44.47	100
006			34.43						65.57		100
Average	36.36	5.65	29.72	74.39	0.44	13.84	16.99	19.17	54.65	44.47	100
Deviation	0.00	3.47	19.45	36.22	0.00	9.58	10.77	0.00	15.45	0.00	100

2831_spot2_Pb_Sb: galena (001)+ Sb (002) + Chalcopyrite (003&004)



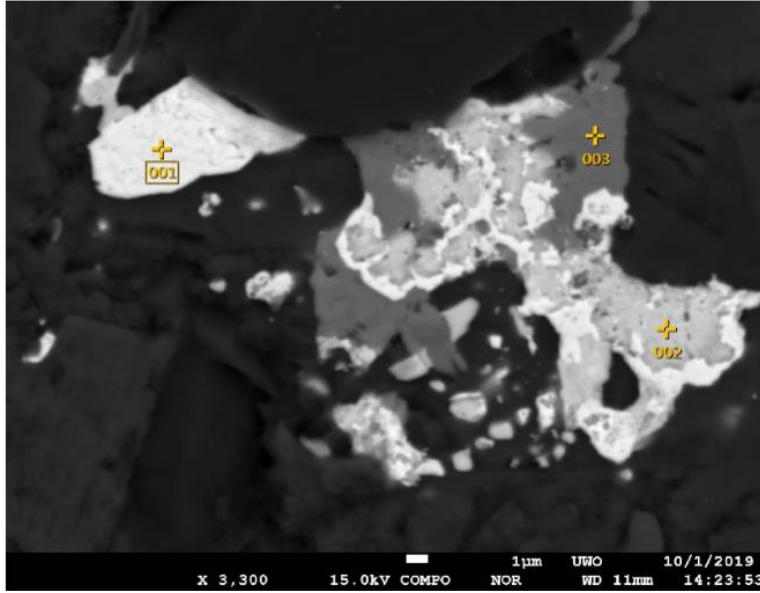
Volt : 15.00 kV
 Mag. : x 1,200
 Date : 2019/10/01
 Pixel : 1280 x 960



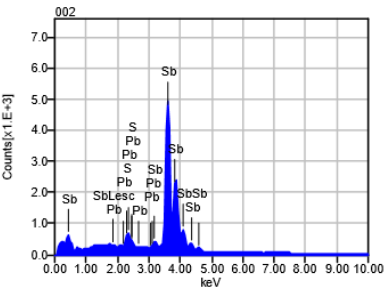
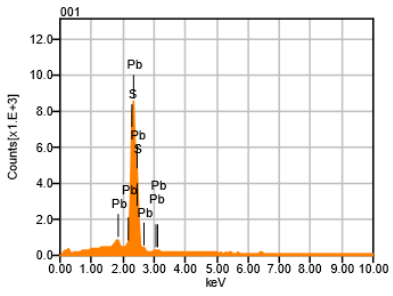
Acquisition Condition
 Instrument : 8530F
 Volt : 15.00 kV
 Current : ---
 Process Time : T2
 Live time : 10.00 sec.
 Real Time : 12.03 sec.
 DeadTime : 17.00 %
 Count Rate : 34403.00 CP

	Fe	Pb	Si	S	Cu	Zn	Sb
001		87.05		12.95			
002							100.00
003	2.71			22.35	37.92	5.59	31.44
004	31.75		0.44	32.43	35.38		
Average	17.23	87.05	0.44	22.57	36.65	5.59	65.72
Deviation	20.54	0.00	0.00	9.74	1.79	0.00	48.48

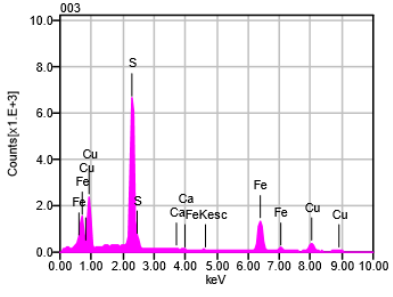
2831_spot2_Pb_Sb2: galena (001&002)+ chalcopyrite (003)



Volt : 15.00 kV
 Mag. : x 3,300
 Date : 2019/10/01
 Pixel : 1280 x 960

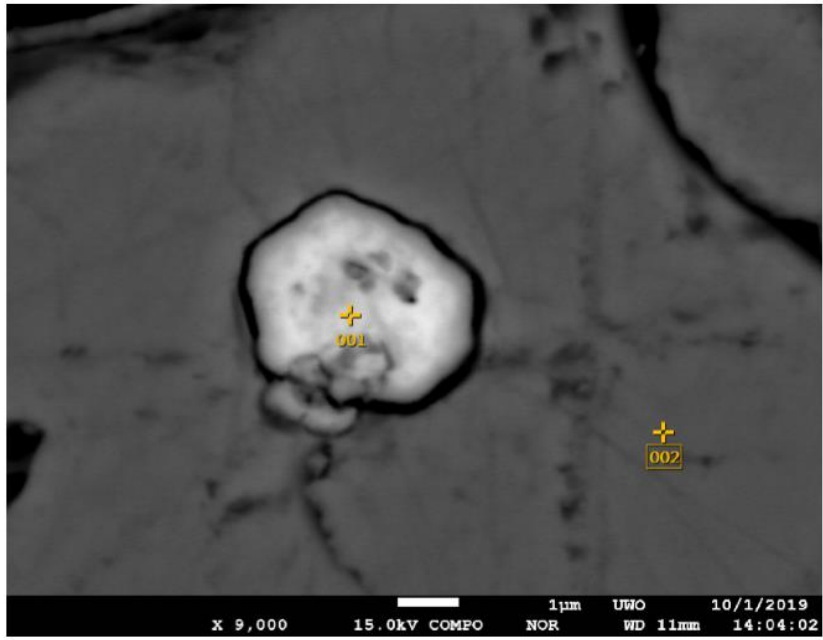


Acquisition Condition
 Instrument : 8530F
 Volt : 15.00 kV
 Current : ---
 Process Time : T2
 Live time : 10.00 sec.
 Real Time : 11.98 sec.
 DeadTime : 17.00 %
 Count Rate : 34161.00 CP

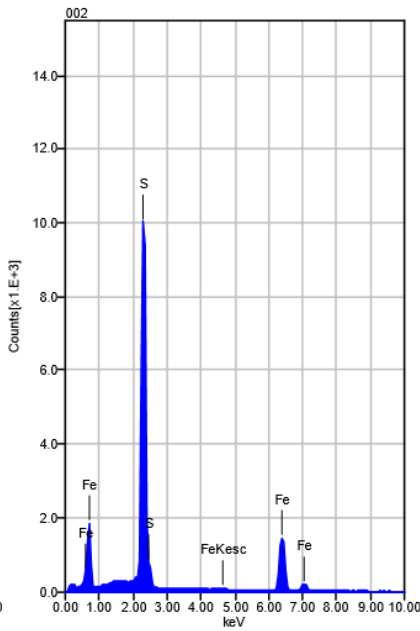
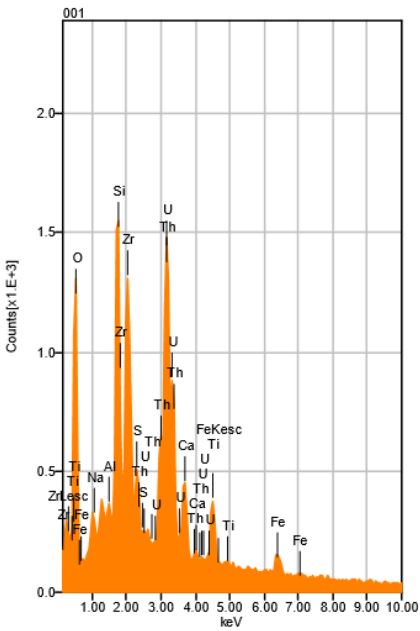


	Fe	Pb	S	Ca	Cu	Sb
001		86.43	13.57			
002		4.99	0.71			94.31
003	41.69		32.99	0.36	24.95	
Average	41.69	45.71	15.76	0.36	24.95	94.31
Deviation	0.00	57.59	16.25	0.00	0.00	0.00

2831_Sulf_inclusion: zircon inclusion (001) in pyrite (002)



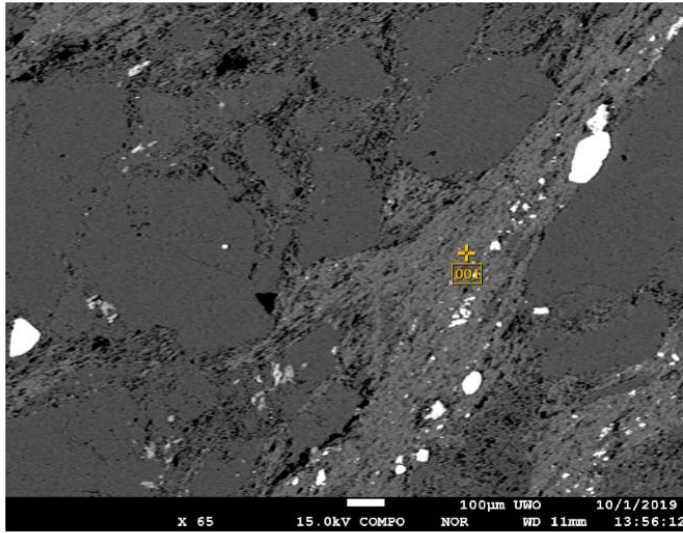
Volt : 15.00 kV
 Mag. : x 9,000
 Date : 2019/10/01
 Pixel : 1280 x 960



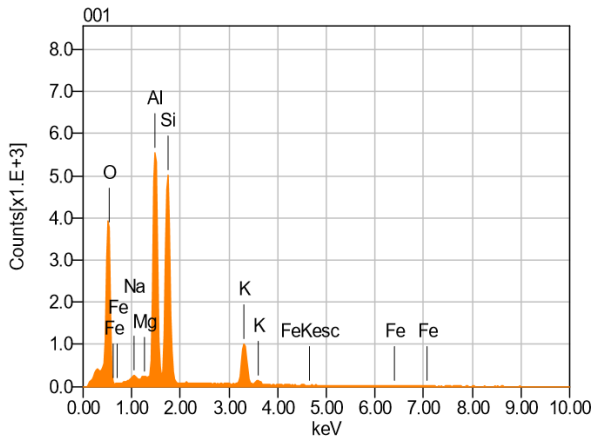
Acquisition Condition
 Instrument : 8530F
 Volt : 15.00 kV
 Current : ---
 Process Time : T2
 Live time : 10.00 sec.
 Real Time : 11.43 sec.
 DeadTime : 12.00 %
 Count Rate : 25135.00 CP

	Fe	O	Na	Al	Si	S	Ca	Ti	Zr	Th	t
001	2.25	13.79	0.40	0.31	4.05	1.12	2.36	3.12	9.46	8.51	!
002	50.38					49.62					!
Average	26.31	13.79	0.40	0.31	4.05	25.37	2.36	3.12	9.46	8.51	!
Deviation	34.03	0.00	0.00	0.00	0.00	34.30	0.00	0.00	0.00	0.00	!

2831_Mical: muscovite (001)



Volt : 15.00 kV
 Mag. : x 65
 Date : 2019/10/01
 Pixel : 1280 x 960



Acquisition Condition
 Instrument : 8530F
 Volt : 15.00 kV
 Current : ---
 Process Time : T2
 Live time : 10.00 sec.
 Real Time : 11.09 sec.
 DeadTime : 10.00 %
 Count Rate : 20478.00 CP

Formula	mass%	Atom%	Sigma	Net	K ratio	Line
O	46.00	60.76	0.12	799073	4.5821795	K
Na	0.46	0.42	0.02	25801	0.0596511	K
Mg*	0.29	0.25	0.02	19715	0.0368750	K
Al	20.10	15.74	0.08	1519127	2.9317474	K
Si	23.42	17.62	0.10	1501967	3.2421476	K
K	9.40	5.08	0.07	399045	1.5665007	K
Fe*	0.32	0.12	0.05	4371	0.0501797	K
Total	100.00	100.00				

Curriculum Vitae

Chunyi Hao

EDUCATION

- **Department of Earth Sciences, University of Western Ontario** 09/2018-12/2020
Master of Science in Geology (thesis-based)
- **Department of Earth Sciences, Guilin University of Technology, China** 09/2014-06/2018
Bachelor of Resources Exploration Engineering (Elite Program)

RESEARCH PROJECTS

- **Master Thesis Project**, Geometallurgy Gold Mineralization at the Monument Bay Deposit, Stull Lake Greenstone Belt, Manitoba, Canada 09/2018- 12/2020
- **Bachelor Research Project**, The Exploration Engineering Design of Napin Gold Deposit in Sanjia Gold Mining Area in Fengshan County, Guangxi, China 09/2017-06/2018
- **Participant**, National-level Research: Huiquan Bay Beach Storm Sedimentation and the Establishment of Levee Cycling Model 05/2015-03/2016
- **Project Leader**, University-level Research: Analysis and Identification of Paleontological Fossils of GLUT Geological Museum 05/2015-03/2016
- **Project Leader**, Province-level Research: Research on the Age and Process of Ocean Floor Spreading in the South China Sea 03/2015-03/2016

Related Work Experience

- **Research Assistant** at University of Western Ontario 09/2018-12/2020
- **Teaching Assistant** at University of Western Ontario 09/2018-12/2020
- **Assistant Geologist** (Long-distance internship) at Shanxi Geological and Mineral Technology Evaluation Center, China 2018-2019
- **Assistant Geologist & Docent** (Internship) at Shanxi Museum of Geology, China 01/2017-02/2017
- **Assistant Geologist** (Internship) at Guangdong Nonferrous Metals Geological Exploration Institution, China 08/2016-09/2016

Conference Attendances

- **Prospectors & Developers Association of Canada Conference**
Academic Poster Presentation | Toronto, Canada | 03/2020
- **Central Canada Mineral Exploration Convention**

- The Monument Bay Project Technical Meeting | Winnipeg, Canada | 11/2019
- **The 10th Summer School on X-ray Science**
Synchrotron Techniques Application Summit | Taiwan, China | 08/2019
- **Responsible Mining Summit**
The Canadian Perspective – Corporate Social Responsibility | Quito, Ecuador | 04/2019
- **Prospectors & Developers Association of Canada Conference**
Academic Poster Presentation | Toronto, Canada | 03/2019

HONORS

- Robert W. Hodder International Geoscience Field Experience Award 2019
- Guilin University of Technology Outstanding Graduates 2018
- Yuan Kuirong Alumnus Scholarship 2017
- First-class Scholarship for Excellent Engineer in China 2016-2017
- Second-class Scholarship for Excellent Engineer in China 2015-2016
- Guilin University of Technology Second-class Scholarship 2015-2016
- First-class Scholarship for Excellent Engineer in China 2014-2015
- Guilin University of Technology First-class Scholarship 2014-2015

Publications

- **Hao, C.**, Casali, J., Ghorbani, Z., Cavallin, H., Van Loon, L., & Banerjee, N. (2020). Multi-scale SR- μ XRF Imaging and Characterization of Gold Mineralization at the Monument Bay Deposit, Stull Lake Greenstone Belt, Manitoba, Canada. *Microscopy and Microanalysis*, 1-4. doi:10.1017/S1431927620017493
- **Hao, C.**, Casali, J., Ghorbani, Z., Cavallin, H., Van Loon, L., & Banerjee, N. (2020). EPMA Characterization of Gold Associated with Different Sulphide Textures at the Monument Bay Deposit, Manitoba, Canada. *Microscopy and Microanalysis*, 1-4. doi:10.1017/S1431927620020723
- Casali, J., **Hao, C.**, Ghorbani, Z., Cavallin, H., Van Loon, L., & Banerjee, N. (2020). Application of Large-scale Synchrotron X-Ray Fluorescence 2D Mapping of Alteration Styles to Understand Gold Mineralization at the Monument Bay Project, Stull Lake Greenstone Belt, Manitoba, Canada. *Microscopy and Microanalysis*, 1-3. doi:10.1017/S1431927620024198
- Ghorbani, Z., Casali, J., **Hao, C.**, Cavallin, H., Van Loon, L., & Banerjee, N. (2020). Biogeochemical Exploration at the Twin Lakes Au Deposit Using Synchrotron Radiation Micro X-ray Fluorescence and X-ray Absorption Near-Edge Structure Spectroscopy. *Microscopy and Microanalysis*, 1-5. doi:10.1017/S1431927620017547